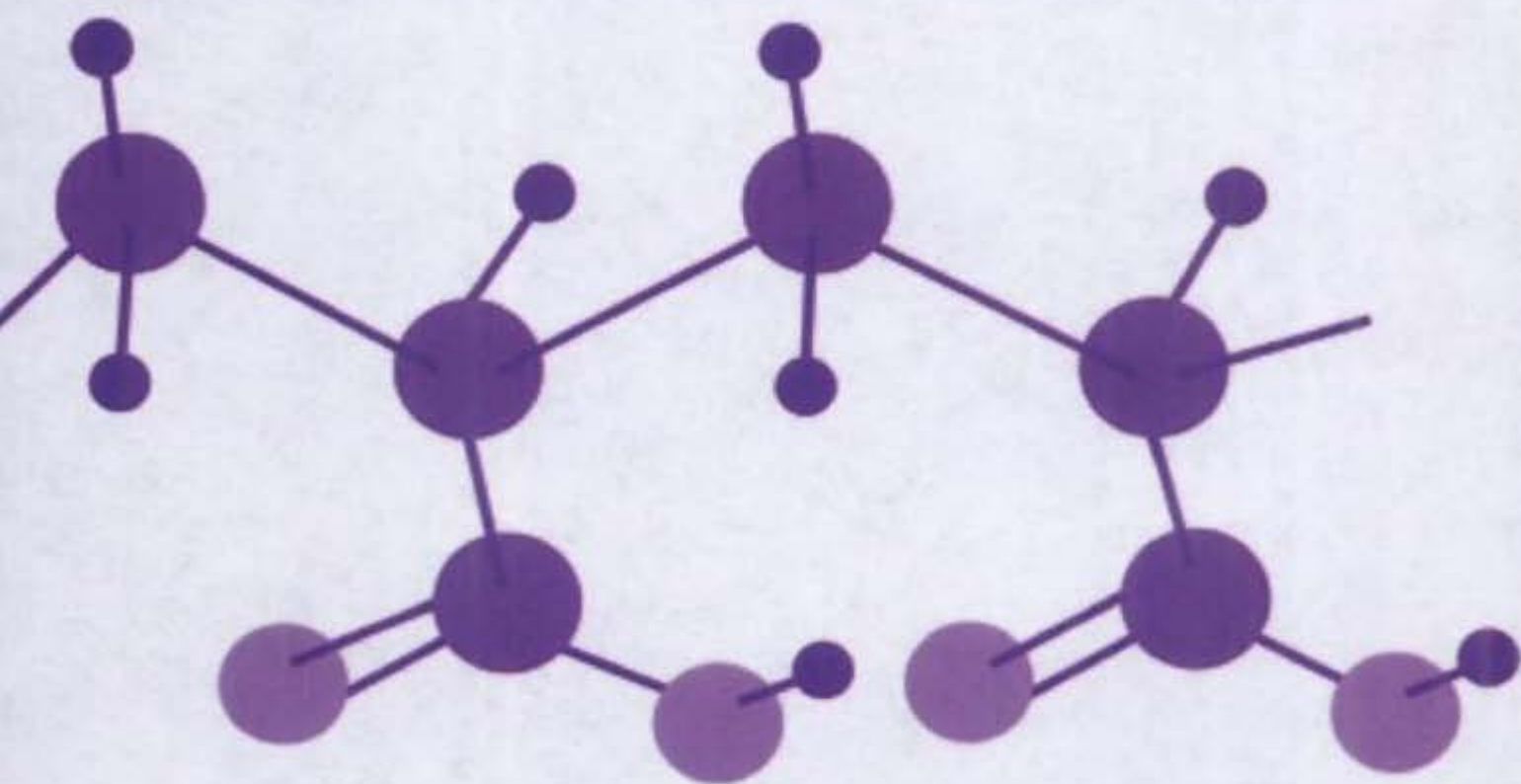


WATER SOLUBLE POLYMERS

Solution Properties
and Applications



Edited by
Zahid Amjad

Water Soluble Polymers

Solution Properties and Applications

Edited by

Zahid Amjad

*The B.F. Goodrich Company
Brecksville, Ohio*

Kluwer Academic Publishers

New York / Boston / Dordrecht / London / Moscow

eBook ISBN: 0-306-46915-4
Print ISBN: 0-306-45931-0

©2002 Kluwer Academic Publishers
New York, Boston, Dordrecht, London, Moscow

All rights reserved

No part of this eBook may be reproduced or transmitted in any form or by any means, electronic, mechanical, recording, or otherwise, without written consent from the Publisher

Created in the United States of America

Visit Kluwer Online at: <http://www.kluweronline.com>
and Kluwer's eBookstore at: <http://www.ebooks.kluweronline.com>

To my wife, Rukhsana, for her patience and encouragement

PREFACE

This volume contains a series of papers originally presented at the symposium on Water Soluble Polymers: Solution Properties and Applications, sponsored by the Division of Colloids and Surface Chemistry of the American Chemical Society.

The symposium took place in Las Vegas City, Nevada on 9 to 11th September, 1997 at the 214th American Chemical Society National Meeting. Recognized experts in their respective fields were invited to speak. There was a strong attendance from academia, government, and industrial research centers. The purpose of the symposium was to present and discuss recent developments in the solution properties of water soluble polymers and their applications in aqueous systems.

Water soluble polymers find applications in a number of fields of which the following may be worth mentioning: cosmetics, detergent, oral care, industrial water treatment, geothermal, wastewater treatment, water purification and reuse, pulp and paper production, sugar refining, and many more. Moreover, water soluble polymers play vital role in the oil industry, especially in enhanced oil recovery. Water soluble polymers are also used in agriculture and controlled release pharmaceutical applications. Therefore, a fundamental knowledge of solution properties of these polymers is essential for most industrial scientists. An understanding of the basic phenomena involved in the application of these polymers, such as adsorption and interaction with different substrates (i.e., tooth enamel, hair, reverse osmosis membrane, heat exchanger surfaces, etc.) is of vital importance in developing high performance formulations for achieving optimum efficiency of the system.

A serious problem encountered in many industrial processes is the build-up of undesirable deposits on the walls of water handling equipment. These deposits, especially on heat transfer surfaces in cooling, boiler, geothermal, and distillation systems, lead to overheating, loss of system efficiency, unscheduled shutdown time, and ultimately heat exchanger failure. These deposits can be categorized into the following four groups: a) mineral scales (i.e., CaCO_3 , $\text{CaSO}_4 \cdot 2\text{H}_2\text{O}$, CaSO_4 , CaF_2 , $\text{Ca}_3(\text{PO}_4)_2$, etc.), b) suspended solids (i.e., mud or silt), c) corrosion products (i.e., Fe_2O_3 , Fe_3O_4 , ZnO , etc.), and d) microbiological mass. In reverse osmosis systems, deposition of unwanted materials may result in poor water quality and premature membrane failure. The development of deposits on heat exchanger and membrane surfaces continues to be a limiting factor in the efficient operation of the systems. Thus, effective operation of industrial water systems continues to depend on the control of deposits in these systems.

In the past few years, polymers have been successfully used by the water treatment industry for numerous functions including scale inhibition, metal ion stabilization, crystal

modification, and dispersancy. Polymers used in water treatment formulations are usually anionic and have molecular weight ranging from 500 to 20,000 daltons. In wastewater treatment, high molecular weight polymer are used as flocculating and coagulating agents. In cosmetics and hair care applications, the industrial chemist depends on the use of water soluble polymers to develop an aesthetically pleasing, functional, and stable product. Polymers also offer unique opportunities in the controlled release of active from the formulated product. In detergents use of polymers as builders is prevalent.

This volume provides an introduction to the use of water soluble polymers in many fields ranging from oral care, cosmetics, detergent, pharmaceutical, to industrial water treatment. A wide range of expertise has been brought together to this book in such a diverse applications. The first four chapters address the solution properties of polymers. The next five chapters examine the growth and inhibition of hydroxyapatite, an important component of teeth, bones, and urinary stones. In the next 8 chapters use of polymers in industrial water and wastewater treatment applications is presented. The final two chapters deal with the use of polymers in hair care and detergent applications.

I hope this book will prove to be a valuable addition to the library of the academic researchers and, even more so, for the technology-focused industrial scientist involved with polymers who are interested in expanding their applications into new fields.

Zahid Amjad
Cleveland, Ohio

ACKNOWLEDGMENTS

I am grateful to all the contributors for their cooperation and hard work in preparing their respective chapters and to all those who made the symposium possible and this volume available. Financial support of the national and international scientists is gratefully acknowledged. Special thanks are extended to the American Chemical Society Division of Colloid and Surface Chemistry, ACS Corporation Associates, Avlon Industries, Colgate-Palmolive Company, and The B.F. Goodrich Company. Their generous assistance contributed substantially to the success of the symposium.

I am thankful to Drs. Michael M. Reddy and Petros G. Koutsoukos for serving as the various session chairmen, and to John Zibrida for his efforts in the selection of industrial speakers. I want to give special thanks to Jeff Pugh for his efficient and organized handling of the considerable correspondence associated with both the symposium and the book. I would like to thank the management of The B.F. Goodrich, in particular Dr. Victoria F. Haynes, for encouragement and support in organizing this symposium and the editing of this volume. Thanks are also extended to the editorial staff of Plenum Publishing Corporation, and especially to Susan Safren, for assistance during all stages of production of this book. Finally, I would to thank my wife for contending with me during the several weekends I was finalizing the manuscript.

ABOUT THE EDITOR

Zahid Amjad is a Research Fellow in the Advanced Technology Group of The B. F. Goodrich Company. A native of Pakistan, he received his M.Sc. in Chemistry from Panjab University and a Ph.D. from Glasgow University, Scotland. Dr. Amjad was a Lecturer at the Institute of Chemistry of Panjab University, and was Assistant Research Professor at the State University of New York at Buffalo. After spending 3 years with Calgon Corporation, he joined The B.F. Goodrich Company where he has served since 1982. Dr. Amjad's current major interests include biological and industrial applications of water soluble and water swellable polymers, interaction of polymers at solid-liquid interface, membrane-based separation processes, and controlled-release of pharmaceuticals.

Dr. Amjad has presented invited lectures at various national and international meetings, contributed to several books, and published numerous papers on the properties and behavior of water soluble and water swellable polymers, as well as on crystal growth and inhibition kinetics, control and removal of foulants from water purification apparatus—particularly membrane-based processes, and controlled release of actives. He is holder of 28 patents and has edited three books. He has been inducted into National Hall of Corporate Inventors, is the recipient of the 1997 EDI Innovation Award, and is a member of several professional organizations. He is also on the Adjunct Faculty in Pharmaceutical Sciences at the School of Pharmacy, Northeast Louisiana University, Monroe, Louisiana.

CONTENTS

1. Kinetics of Adsorption for Hydrophobically Modified Poly(Acrylic Acids) at Cyclohexane/Water Interfaces	1
Christopher Rulison	
2. Effect of Solids Concentration on Polymer Adsorption and Conformation	23
Tsung-yuan Chen, Chidambaram Maltesh, and Ponisseril Somasundaran	
3. Water Solubility Characteristics of Poly(Vinyl Alcohol) and Gels Prepared by Freezing/Thawing Processes	31
Christie M. Hassan, Patrina Trakarnpan, and Nicholas A. Peppas	
4. Enzymatic Modification of Guar Solutions: Viscosity–Molecular Weight Relationships	41
Akash Tayal, Vandita Pai, Robert M. Kelly, and Saad A. Khan	
5. The Influence of Additives and Impurities on Crystallization Kinetics: An Interfacial Tension Approach	51
Wenju Wu and George H. Nancollas	
6. Inhibition of Hydroxyapatite Growth <i>in Vitro</i> by Glycosaminoglycans: The Effect of Size, Sulphation, and Primary Structure	63
Paschalsi Paschalakis, Demitrios H. Vynios, Constantine P. Tsiganos, and Petros G. Koutsoukos	
7. Influence of Humic Compounds on the Crystal Growth of Hydroxyapatite	77
Zahid Amjad and Michael M. Reddy	
8. Crystal Growth of Hydroxyapatite in Vitro and Dental Calculus and Plaque Formation on Human Teeth <i>in Vivo</i>	91
Abdul Gaffar, Edgard C. Moreno, John Afflitto, and Yelloji-Rao K. Mirajkar	
9. Adsorption of Hydroxypropylcellulose on Hydroxyapatite via Formation of Surface Complex with Sodium Dodecylsulfate	105
Saburo Shimabayashi, Sawa Nishine, Tadayuki Uno, and Tomoaki Hino	

10. The Inhibition of Calcium Carbonate Formation by Copolymers Containing Maleic Acid	117
Pavlos G. Klepetsanis, Petros G. Koutsoukos, Gabriele-Charlotte Chitanu, and Adrian Carpov	
11. Kinetic Inhibition of Calcium Carbonate Crystal Growth in the Presence of Natural and Synthetic Organic Inhibitors	131
Zahid Amjad, Jeff Pugh, and Michael M. Reddy	
12. Novel Calcium Phosphate Scale Inhibitor	149
Libardo A. Perez and Stephen M. Kessler	
13. Inhibition of Mineral Scale Precipitation by Polymers	163
Shiliang He, Amy T. Kan, and Mason B. Tomson	
14. Pilot Test Results Utilizing Polymeric Dispersants for Control of Silica	173
Charles W. Smith	
15. Inhibition of Gypsum Scale Formation on Heat Exchanger Surfaces by Polymeric Additives	183
Zahid Amjad	
16. Applications of Structured Cationic Polyelectrolytes in Wastewater Treatments	193
Haunn-Lin T. Chen	
17. Optimization of Cooling Water Treatment Formulations for Use in Recycled Waters	207
Paul J. Forbes	
18. Water-Soluble Polymers in Hair Care: Prevention and Repair of Damage during Hair Relaxing	231
Ali N. Syed, Wagdi W. Habib, and Anna M. Kuhajda	
19. Application of Ultra-High Molecular Weight Amphoteric Acrylamide Copolymers to Detergents	245
Yoshiyuki Hayashi, Danian Lu, and Nobuo Kobayashi	
About the Editor	251
Index	253

KINETICS OF ADSORPTION FOR HYDROPHOBICALLY MODIFIED POLY(ACRYLIC ACIDS) AT CYCLOHEXANE/WATER INTERFACES

Christopher Rulison

Krüss USA
9305B Monroe Road
Charlotte, North Carolina 28720-1488

1. ABSTRACT

Hydrophobically modified poly(acrylic acids) (HMPAA'S) are commonly used as primary, pH sensitive, stabilizers for oil-in-water emulsions. It has been shown that electrosteric stabilization is one of the mechanisms. An important factor in steric stabilization is the breadth of the extension of stabilizing molecules from the discontinuous phase interface into the continuous phase. It must be substantial. This dictates that the stabilizing molecules be of substantial hydrodynamic volume. However, polymers with large hydrodynamic volumes diffuse slowly through solution (Brownian diffusion coefficients on the order of 10^{-12} to 10^{-13} m²/s). This can be a restriction to their use as emulsifiers, since the kinetics of emulsion coalescence begin to compete with the kinetics of interfacial adsorption of the stabilizing species. With these things in mind, we have developed a technique, based on drop volume tensiometry, which can be used to determine the "adsorption/diffusion" coefficients that characterize the kinetics of polymers adsorbing at oil/water interfaces. We have previously used this technique to show that increased hydrophobic content and increased crosslink density enhance adsorption efficiency for HMPAA'S. The current work is a pH dependence study which shows that neutralizing HMPAA in aqueous solution decreases its adsorption efficiency.

2. INTRODUCTION

Hydrophobically modified poly(acrylic acids) (HMPAA's) are commonly used as primary, pH sensitive stabilizers for oil-in-water emulsions.¹⁻⁶ It has been shown that elec-

trosteric stabilization is one of the mechanisms.⁷ The term electrosteric refers to inter-droplet repulsive forces that are caused by osmotic, entropic, and most especially electrical double layer effects, owed to polyelectrolyte molecules adsorbed at the interface between the droplets of an emulsion and the continuous phase.⁸

Figure 1 is a schematic representation of the repulsive forces of electrosteric stabilization. When droplets containing adsorbed polymer diffuse to close proximity (due to Brownian motion), and the continuous phase is dilute in the polymer adsorbed, an unfavorable chemical potential can be developed in the region between the droplets due to an increase in polymer concentration. Osmotic pressure forces develop, which rush continuous phase solvent to this region and subsequently redisperse the droplets. The adsorbed polymer may also become entropically restricted on the surface to avoid overlap with the polymer adsorbed on the neighboring droplet (provided the continuous phase is a good solvent for the portions of the polymer which extend from the droplet's surface). This is thermodynamically unfavorable, and so counteracts van der Waals attractions between the droplets. In situations where these osmotic and entropic effects more than compensate for the van der Waals attractive forces between the droplets, stabilization is effective. These two modes of stabilization (osmotic and entropic) are responsible for classic *steric* stabilization.

With electrosteric stabilization, there is the third mode of stabilization—electrical double layer repulsion.^{9,10} Adsorbed polyelectrolytes, like neutralized HMPAA's, provide for double layers around emulsion droplets by having most of their counterions within a close sphere surrounding the droplet. Such a "sphere" is often referred to as a Debye layer.¹¹ Since these layers repel each other coulombically, as any two droplets approach the droplets are repelled from one another and thus cannot coalesce.

An important factor in both steric and electrosteric stabilization is the breadth of the extension of stabilizing molecules from the discontinuous phase interface into the continuous phase. It must be substantial (minimum 100 Å)^{8,12} if long term stabilization is to result. This dictates that the stabilizing molecules be of substantial hydrodynamic volume. High molecular weight HMPAA's, which contain enough hydrophobic character to adsorb firmly to the oil/water interface, and resist desorption, have substantial breadth of extension from the discontinuous phase interface into the continuous phase.

However, the large hydrodynamic volumes of these polyelectrolytes cause them to diffuse quite slowly through solution. Brownian diffusion coefficients for neutralized HMPAA's in the 1,000,000 g/cm³ molecular weight range are on the order of 10⁻¹² to 10⁻¹³ m²/s (compared to the typical small molecule surfactant emulsifiers which have Brownian diffusion coefficients in the range of 10⁻⁹ to 10⁻¹⁰ m²/s).

The slow diffusion of high molecular weight HMPAA's is an issue for their use as emulsifiers, because during the actual process of forming an oil-in-water emulsion the kinetics of adsorption of the stabilizing emulsifier to developing oil/water interfaces must be favorable relative to the kinetics of unstabilized droplet coalescence. It is conceivable that a polymer could have a high interfacial activity, be capable of firm adsorption to an oil/water interface, have an extension from the surface which is conducive to steric stabilization, and yet still be ineffective as a steric stabilizer simply because the kinetics of its adsorption to oil/water interfaces does not compete favorably with the time frame for natural coalescence of droplets during the emulsion formation process.

Early theory on the coalescence of unstabilized disperse droplets, simply due to random droplet collisions owing to Brownian motion, is reported by Smoluchowski.¹² From Smoluchowski's theory it can be calculated that the half-life for coalescence of an unstabilized emulsion containing 10²² droplets per liter of continuous phase is on the order of 10⁻⁹ seconds. 10²² drops/liter is not an exorbitant number of droplets for a commercial emulsion

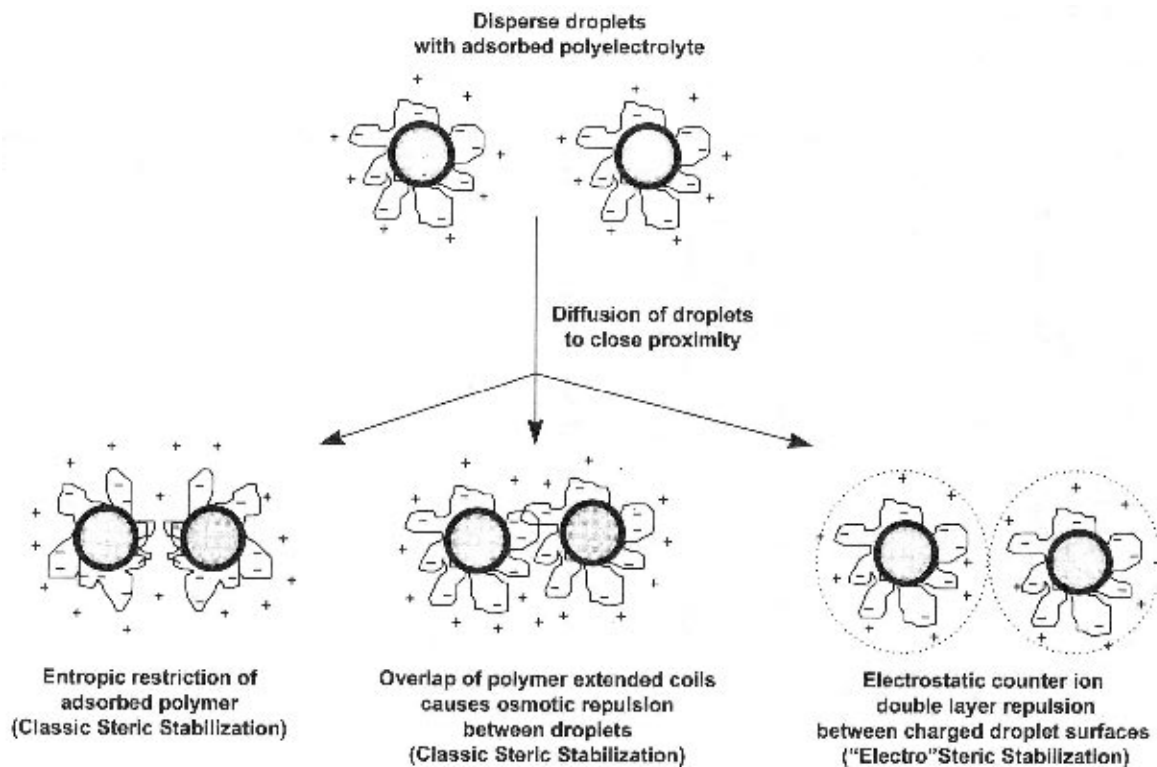


Figure 1. Mechanisms of electrosteric stabilization.

system¹ and the theoretical work of Smoluchowski has been verified to represent experimental findings within a factor of approximately two by Lips,¹³ Honig,¹⁴ and Lichtenbelt.¹⁵ This further justifies the need to explore the kinetics of the process of HMPAA adsorption to oil/water interfaces for purposes of further understanding electrosteric stabilization.

With these things in mind, we have developed a technique, based on drop volume tensiometry, which can be used to determine "adsorption/diffusion" coefficients that characterize the kinetics of neutralized HMPAA's adsorbing to oil/water interfaces from aqueous solution. We have previously used this technique to show that increased hydrophobic content and increased crosslink density enhance adsorption efficiency for HMPAA's.³

The current work is an exploration of the effect of pH on the adsorption kinetics of four well characterized HMPAA model polymers. Each of these polymers exhibits a well defined pH triggered breakdown in its ability to stabilize cyclohexane-in-water emulsions. Each pH trigger is different, and characteristic of the molecular structure of its particular HMPAA. The current kinetic studies confirm the effects of hydrophobe content and crosslink density on the adsorption efficiency of HMPAA's, as reported in the previous work.³ More importantly, however, they show for the first time: (i) that increasing pH decreases the adsorption efficiency (increases the activation energy for adsorption) for HMPAA's, and (ii) that there is a critical adsorption activation energy beyond which HMPAA's will no longer stabilize cyclohexane-in-water emulsions by electrosteric stabilization. This critical adsorption activation energy is reached for each HMPAA at the pH value which corresponds to its particular pH trigger.

3. MATERIALS AND MATERIALS CHARACTERIZATION

The four modified HMPAA's studied are model copolymers which were synthesized by the author in the laboratories of Dr. Robert Lochhead at the University of Southern Mississippi, and characterized as to their precise incorporation of hydrophobic modifica-

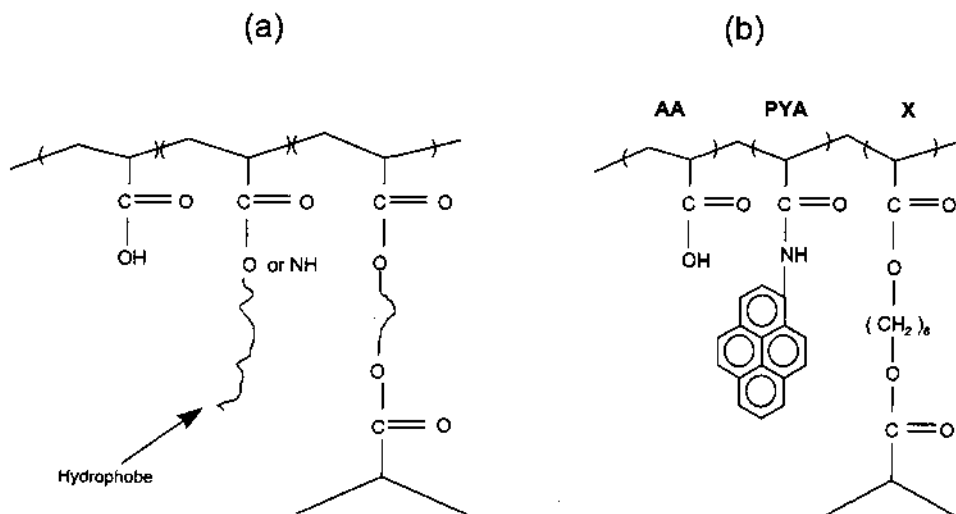


Figure 2. Structures of hydrophobically modified poly(acrylic acid) emulsifiers: (a) general structures, (b) structure of pyrene acrylamide containing polymers.

Table 1. Polymer characteristics

Polymer	Molecular weight (g/mole)	PH*	Critical overlap concentration g/L)*	Average hydrodynamic diameter Å**	D (m ² /s)
PYA/AA 1/340	1.0×10^6	5.5	0.89	1603	3.0×10^{-12}
PYA/AA 1/340	1.0×10^6	7.0	0.69	2085	2.3×10^{-12}
PYA/AA 1/150	1.2×10^6	5.5	0.58	2405	2.0×10^{-12}
PYA/AA 1/150	1.2×10^6	7.0	0.40	3197	1.5×10^{-12}
PYA/X/AA 1/0.9/230	1.2×10^6	5.5	0.67	2009	2.4×10^{-12}
PYA/X/AA 1/0.9/230	1.2×10^6	7.0	0.55	2320	2.1×10^{-12}
PYA/X/AA 1/0.6/150	1.1×10^6	5.5	0.85	1842	2.6×10^{-12}
PYA/X/AA 1/0.6/150	1.1×10^6	7.0	0.71	2105	2.3×10^{-12}

*In aqueous solution neutralized with NaOH.

**In aqueous solution neutralized with NaOH at a concentration = (critical overlap concentration/10).

tion and crosslinking. They are copolymers of pyreneacrylamide (PYA) and acrylic acid (AA). Their general structure is shown in Figure 2. Details of synthesis and general characterization of these copolymers has been reported elsewhere.^{16,17} The PYA units serve as the hydrophobic modification in these copolymers. It has been proven that the PYA units are incorporated in a random fashion into the four copolymers discussed here.¹⁷

Table 1 provides relevant characterization information on the PYA/AA copolymers. The nomenclature used to describe each copolymer is based on the relative molar incorporation's of PYA and AA in the copolymers. For example, copolymer PYA/AA 11340 contains 1 monomeric unit of PYA for every 340 monomeric units of AA. Two of the copolymers (PYA/X/AA 1/0.9/230 and PYA/X/AA 1/0.6/150) are lightly crosslinked with 1,6 hexanediol diacrylate (X). The crosslinked copolymers contain one monomeric unit of X per 250 monomeric units of AA. The nomenclature used for the crosslinked copolymers, however, is analogous to that used for the non-crosslinked copolymers, so that the molar ratio of X reported in the nomenclature is based on unit PYA monomer incorporation. For example, PYA/X/AA 1/0.9/230 is a copolymer which has 1 monomeric unit of PYA for every 0.9 monomeric units of X and 230 monomeric units of AA.

Table 1 shows the approximate molecular weight for each PYA/AA copolymer. These values were determined by viscometry techniques as reported elsewhere.^{4,7,17} The critical overlap concentration (c^*) values for these copolymers (also reported in Table 1) were determined in NaOH-neutralized distilled water at pH = 5.5 and at pH = 7.0 by viscometry experimentation and the formation of Huggins plots. This technique has also been described previously.⁷ The 0.1 % aqueous NaOH solution used for neutralization was prepared from distilled water and Fisher, Scientific grade NaOH pellets.

Dynamic light scattering studies were performed on the copolymers in distilled water at pH = 5.5 and at pH = 7.0, at concentrations of $c^*/10$, to determine average hydrodynamic diameters and Brownian diffusion coefficients (D) for copolymers under dilute conditions. These results are also included in Table 1. A Brookhaven instrument at a scattering angle of 90° was employed. All measurements were made at 25 °C. The distributions in hydrodynamic diameter in each case were found to be Gaussian. Sample preparation included pre-filtration of distilled water through a 0.02 µm inorganic membrane filter (Whatman, Anotop 10), dilution of the copolymer studied in such water, neutralization with a 0.1% NaOH solution which was prepared in similarly prepared water, and filtration of the polymer solution through a 1.2 µm membrane filter (Gelman, low protein binding Acrodisc® brand). The Brookhaven light scattering sample cells used were

washed with aqua regia and rinsed with copious amounts of filtered distilled water prior to use.

Note that the data in Table 1 follows expected trends for neutralized poly(acrylic acid) based polymers in dilute solution at less than neutral pH values. As the solution pH is increased, the number of carboxylic acid units on a poly(acrylic acid) based polymer that are neutralized increases. This makes the polymer more electrolytic (increases the charge density on the polymer chain). Since the charge density of the polymer chain increases, and the ions attached to the chain are all of the same charge (-), the polymer expands in solution (increases in hydrodynamic diameter) to alleviate intra-chain charge/charge repulsion. This causes the polymer chain to be slower diffusing in solution (decreases D) and causes the solution to require less polymer chains to reach its critical overlap concentration (decreases c^*). The increased charge density also makes the polymer less interfacially active toward oil/water interfaces (more water soluble), as will be seen shortly.

Each of the four HMPAA's was characterized for its ability to stabilize 10% cyclohexane-in-water emulsions at a variety of concentrations and pH values. This was done through the preparation of pseudo phase diagrams. A pseudo phase diagram for each HMPAA is included (Figures 3, 4, 5, and 6). Each point, on each of those four diagrams, represents a 10% cyclohexane-in-water emulsion that was prepared and kept for evaluation for one year. Each emulsion sample was prepared by dispersing the required amount of copolymer into distilled water, neutralizing to the required pH with 0.1% aqueous NaOH, adding cyclohexane, and hand shaking the sample vigorously for 30 seconds. The cyclohexane used was Fisher, Certified A.C.S. Scientific grade. This cyclohexane was determined to have a density of $\rho = 0.77392 \text{ g/cm}^3$ using a Paar DMA 58 density meter and an interfacial tension against distilled water of $50.7 \pm 0.1 \text{ mN/m}$ using a Kruss Processor Tensiometer K12 and the DuNouy ring method.

Also plotted on each phase diagram is data for the c^* of the HMPAA as a function of pH. This c^* data was also determined in the manner described above. The c^* data is in-

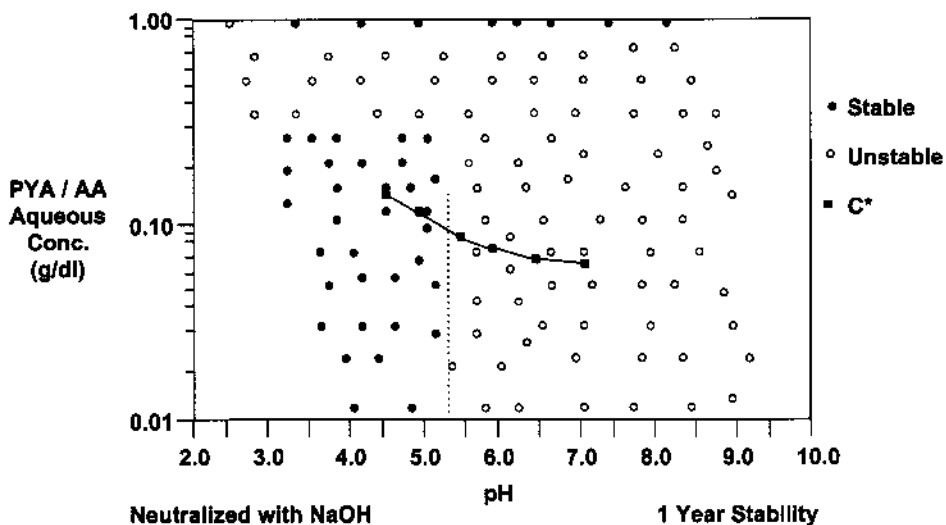


Figure 3. Pseudo phase diagram of emulsion stabilization by PYA/AA (1/340).

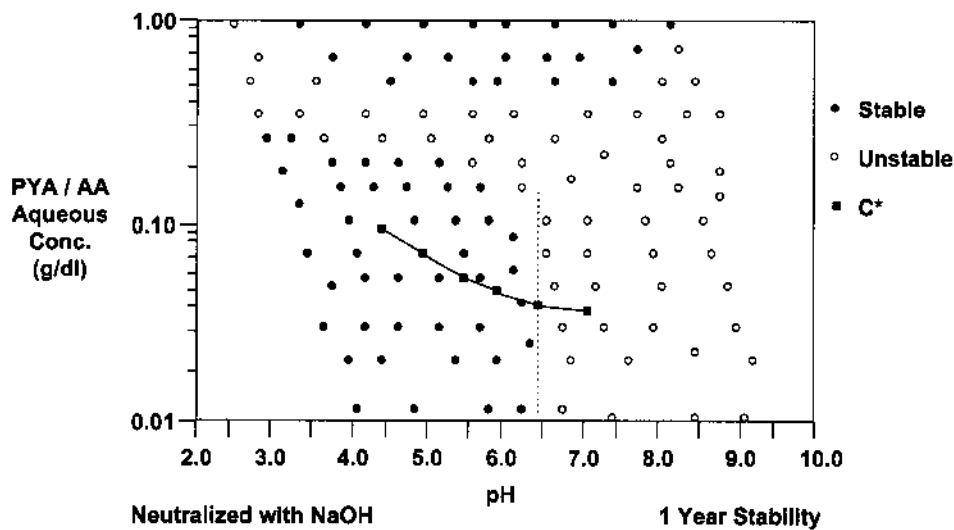


Figure 4. Pseudo phase diagram of emulsion stabilization by PYA/AA (1/150).

cluded here because in evaluating the electrosteric stabilization ability of these HMPAA's we wished to investigate whether the theory of Vincent¹⁸ was applicable. Vincent theory states that the steric stabilization ability of a polymer will break down at concentrations above the c^* , due to the fact that the osmotic and entropic effects described earlier should be greatly diminished. By definition, at c^* for a polymer in solution, the polymer chains overlap on one another (thus diminishing the osmotic effect). The polymer chains will also become entropically restricted to alleviate overlap and maintain chain-solvent interactions (thus diminishing the entropic effect).

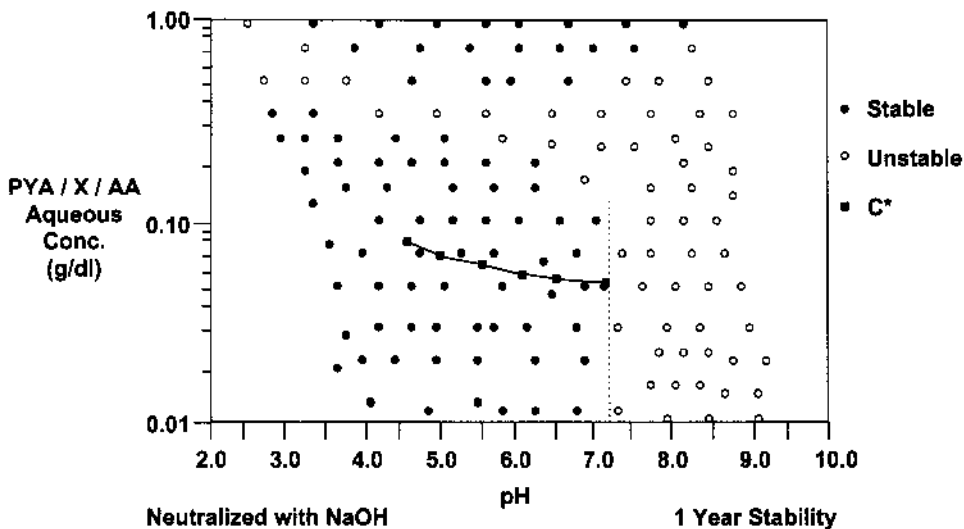


Figure 5. Pseudo phase diagram of emulsion stabilization by PYA/X/AA (1/0.9/230).

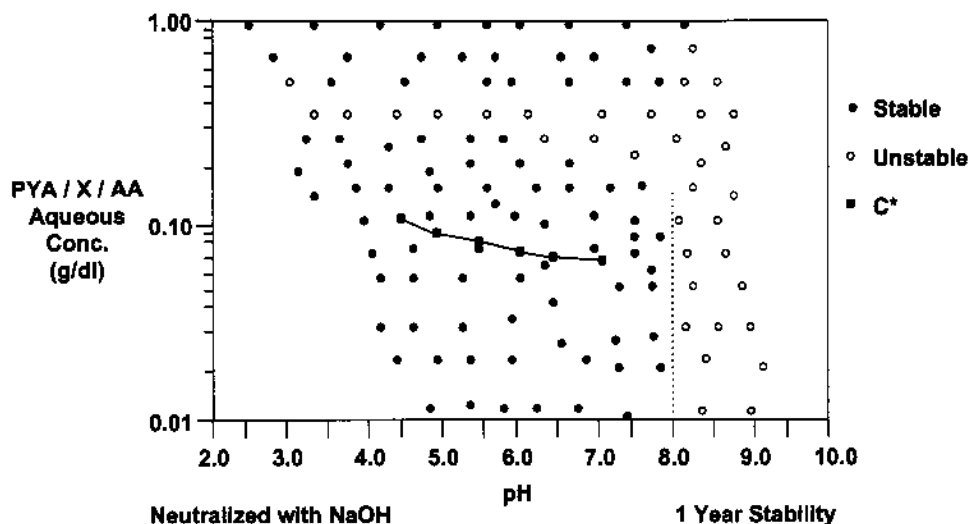


Figure 6. Pseudo phase diagram of emulsion stabilization by PYA/X/AA (1/0.6/150).

From the phase diagrams several things are evident. For each of the polymers studied two distinct regions of stabilization ability are observed. One is a region of stability at low pH values below the critical overlap concentration curve of each polymer. This region extends to concentrations somewhat above the critical overlap concentration curve in each case, but at some higher concentration breaks down. The breadth of this stabilization region indicates that the theory of Vincent is not strictly adhered to for these polymers (stabilization does not break down distinctively at the c^*). However, the fact the region extends, for each polymer, below the c^* strongly suggests that steric (or electrosteric) stabilization is indeed a stabilization mechanism for these polymers. The other possible mechanism of emulsion stabilization by HMPAA's is associative thickening stabilization, in which the hydrophobic portions of the polymer associate with each other and with the hydrophobic dispersed phase to create a network structure which stabilizes the droplets against coalescence by restricting their Brownian diffusion.⁸ Associative thickening stabilization is not possible below the c^* of the polymer in solution, since intermolecular associations are not occurring at these concentrations. The second stabilization region, which occurs for each HMPAA, at concentrations much in excess of the c^* , is believed to be due to associative thickening stabilization.

Concerning the region of electrosteric stabilization for each polymer, note that the stability breaks down at a very distinct pH in each case. This pH trigger is different for each HMPAA studied. For PYA/AA 1/340 the pH trigger is pH = 5.3. For PYA/AA 1/150 the pH trigger is pH = 6.5. For PYA/X/AA 1/0.9/230 the pH trigger is pH = 7.2. And, for PYA/X/AA 1/0.6/150 the pH trigger is pH = 8.0. It is thus the trend that the pH trigger increases with increasing extent of hydrophobic modification and increasing crosslink density.

Given this trend, it is not unreasonable to speculate that the existence of the pH trigger is due to each HMPAA becoming less interfacially active as pH is increased. This would occur because the HMPAA becomes more neutralized, and therefore more water soluble, as pH is increased. At some pH value, which is dependent on molecular structure, the interfacial activity of any particular HMPAA becomes so diminished that the HMPAA is longer effective at adsorbing to the oil/water interface. This is the pH trigger. With this hypothesis,

the trend for the pH triggers as function of HMPAA structure is expected. As hydrophobic incorporation is increased for an HMPAA, the polymer has more hydrophobes for attachment to the oil/water interface. A polymer with more attachment “opportunities” would be expected to tolerate a higher degree of neutralization before its interfacial activity becomes so diminished that it becomes ineffective at interfacial adsorption. Also, as the crosslink density of an HMPAA is increased the polymer becomes more entropically restricted in solution. Adsorption to an interface is also entropically restricting to a polymer chain. Thus, a polymer with more crosslink density would be expected to lose less entropy upon adsorption to an interface than a like polymer with less crosslink density. Therefore, an HMPAA with more crosslink density would be expected to remain interfacially active to a higher degree of neutralization (a higher pH) than a like HMPAA with less crosslink density.

The equilibrium interfacial tension data for the model polymers adsorbing to the cyclohexane/water interface, which is shown in Figures 7 through 10, justifies the above hypotheses. Each HMPAA becomes less interfacially active (diminishes the interfacial tension at the cyclohexane/water interface less) as pH is increased. The non-crosslinked HMPAA's (PYA/AA 1/340 and PYA/AA 1/150) become effectively non-interfacially active at pH = 8.0. The crosslinked HMPAA's (PYA/X/AA 1/0.9/230 and PYA/X/AA 1/0.6/150) are still interfacially active at pH = 8.0. Complete loss of interfacial activity is therefore not essential for a pH triggered breakdown in emulsion stabilization ability to occur. Some diminishment of interfacial activity is sufficient. However, the level of interfacial activity necessary for stabilization seems to be independent of polymer structure. As a justification of this, please note the dashed lines that have been added to Figures 7 through 10 as a visual aid. Each of these lines is placed over the same range of concentrations and the same range of interfacial tensions on each graph (for each HMPAA). Next note that, for all four polymers, if an interfacial tension versus concentration profile for a particular pH falls above this dashed line then that pH is above the pH trigger. If the interfacial tension versus concentration profile for a particular pH falls below this dashed line then that pH is below the pH trigger.

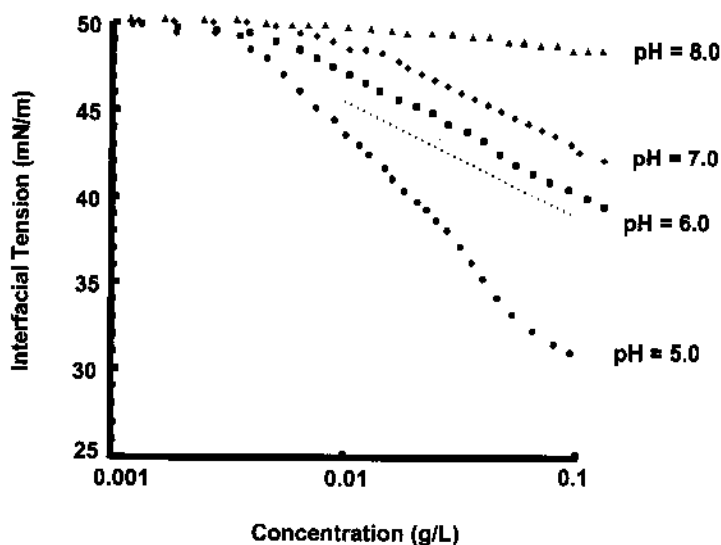


Figure 7. Equilibrium interfacial tension data for PYA/AA (1/340).

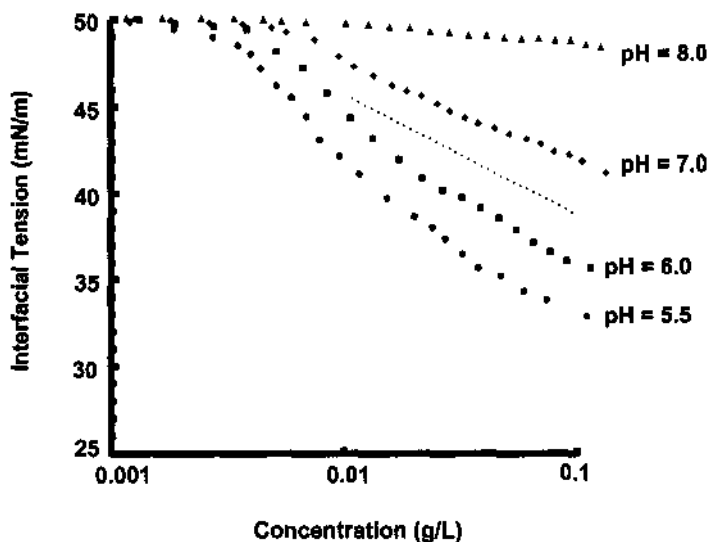


Figure 8. Equilibrium interfacial tension data for PYA/AA (1/150).

Equilibrium interfacial tensions were evaluated using a Kruss Processor Tensiometer K12 which determines interfacial tension by the DuNouy ring method.¹⁹ The process involves filling a sample holder with a known quantity of distilled water (neutralized to the proper pH), covering the distilled water with a layer of oil, and then dosing specific quantities of an aqueous polymer solution (neutralized to the proper pH) into the aqueous layer while measuring the interfacial tension between the two layers. After each dose of polymer solution the polymer obviously takes time to disperse throughout the aqueous layer, as well as to reach equilibrium adsorption at the oil/water interface. The “equilibrium” in-

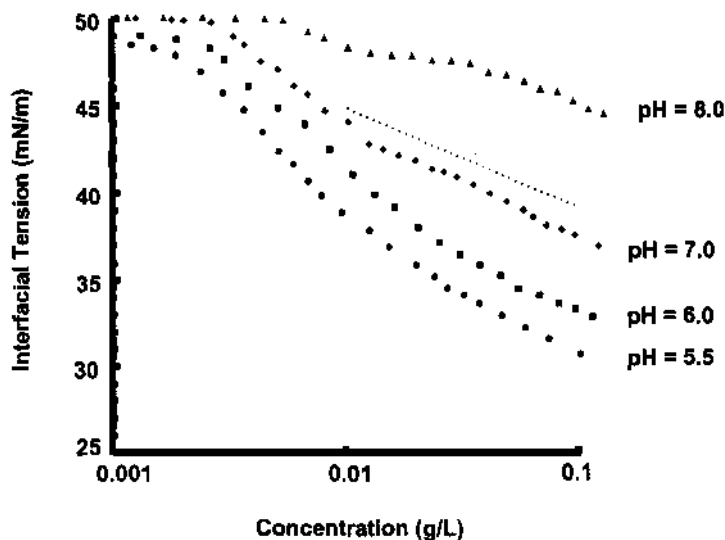


Figure 9. Equilibrium interfacial tension data for PYA/X/AA (1/0.9/230).

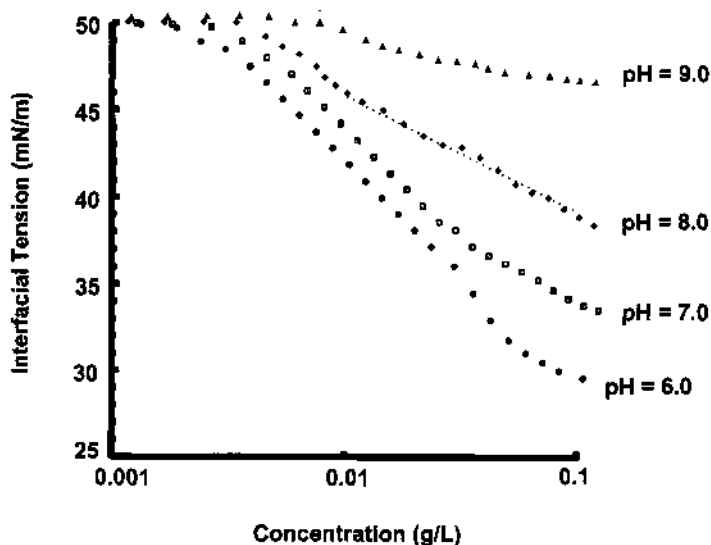


Figure 10. Equilibrium interfacial tension data for PYA/X/AA (1/0.6/150).

terfacial tension must then be defined in some manner. For these studies, the equilibrium interfacial tension is defined at the point in time, after a dose, when five consecutive measurements of interfacial tension, each taking approximately 90 seconds, fall within a standard deviation of 0.01 mN/m. In other words, equilibrium is defined as a situation in which the interfacial tension does not change more than 0.01 mN/m for approximately 450 seconds. Using this criterion, it takes anywhere from two to fifteen hours for an HMPAA to come to equilibrium at the interface once the aqueous phase concentration is altered by a dose of polymer solution.

The general structure, emulsion stabilization, and equilibrium interfacial activity characterization work that has been done on the four model HMPAA's makes them excellent candidates for kinetics of adsorption studies. The characterization work has provided a profile of the interfacial activity of each the polymers under equilibrium conditions. With that background information in hand, a detailed study of adsorption kinetics becomes possible for these polymers.

4. THEORY AND EXPERIMENTAL TECHNIQUES FOR KINETICS OF ADSORPTION STUDIES

In order to study the diffusion of HMPAA's from aqueous solution to the cyclohexane/water interface, we employed drop volume tensiometry. The general procedure for drop volume analysis of interfacial tension between two liquid phases is to form drops of the less dense liquid at the end of a well defined capillary tip which is submerged in the more dense liquid. The forming droplets increase in size until they disconnect themselves from the capillary tip and become droplets in the more dense continuous phase. Tate's law,²⁰ derived from a balance of forces acting on a forming droplet, states that the volume (V) of each droplet, when it disconnects, will be given by:

$$V = \frac{2\pi r\gamma}{\Delta\rho g} \quad (1)$$

where r = the radius of the tube, γ = the interfacial tension between the two phases, $\Delta\rho$ = the difference in density between the two liquids, and g = the force of gravity.

While the drop volume technique certainly provides a means of determining the *equilibrium* interfacially tension between two pure liquids, it also provides the capability of determining *dynamic* interfacial tensions for systems in which one of the liquids contains an interfacially active solute. The concept of why this should be possible is depicted schematically in Figure 11, for the case in which the interfacially active solute is in the less dense of the two liquids. In this schematic, the small squares represent molecules of the interfacially active solute. The tip on which the drops are formed can be connected to a precision pump, so that drops can be formed at precise rates. A droplet formed rapidly will have little time for the interfacially active solute within it to diffuse to and adsorb at the liquid/liquid interface. The result is that the drop will be relatively large on detachment, because the interfacial tension between the two phases will be high(γ_H) and near the interfacial tension between the two pure liquids in the absence of the interfacially active solute. Conversely, if a drop is formed more slowly, the interfacially active material will have time to diffuse to and adsorb at the liquid/liquid interface. As a result, the interfacial tension will be lower (γ_L), as evidenced by smaller droplet size at detachment. In forming a drop over an infinite time frame, with respect to the rate of diffusion and adsorption of the solute to the interface, the interfacial tension realized will be the equilibrium interfacial tension between the solution and the liquid, and would be expected to match this value as determined by ring tensiometry. (In the case of this research, the interfacially active material is the HMPAA, which is actually in the continuous phase. The discussion of drop volume experimentation with the interfacially active solute in the continuous phase is analogous).

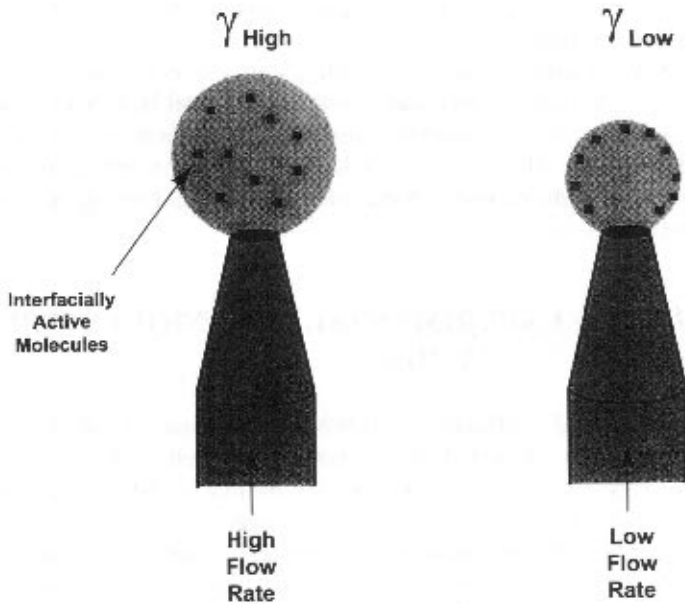


Figure 11. Principle of dynamic interfacial tension.

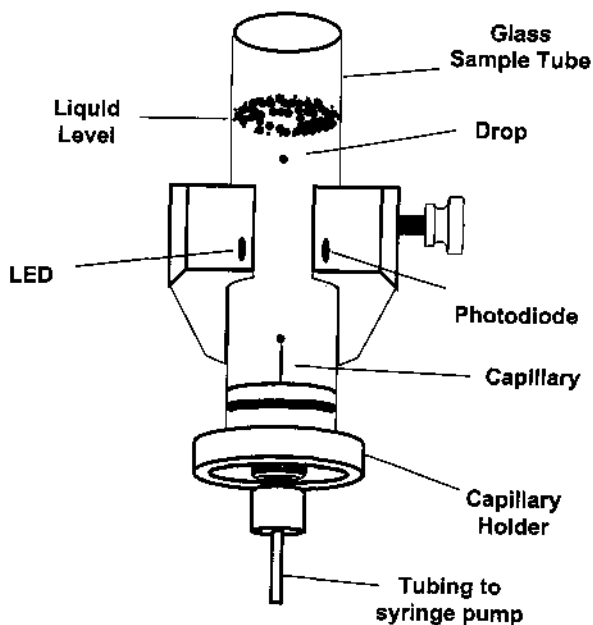


Figure 12. Partial schematic of the interfacial tension apparatus.

The drop volume apparatus used for this work was a Kruss Drop Volume Tensiometer DVT10. The apparatus is depicted in Figure 12. The experiment was designed so that the cyclohexane used formed drops from thin walled tungsten carbide tip with a 254 μm inside diameter, which was submerged in a sample cell containing the aqueous HMPAA solution to be tested. The drop flow rate of the aqueous solution was controlled very accurately with a Harvard[®] syringe pump. The sample cell is fitted with an infrared motion detector so that the time between drops can be detected to the accuracy of 0.01 sec by the Kruss DVT10. The time between drops is converted to drop volume with knowledge of the drop flow rate from the syringe pump. This volume is then used in the Tate's law equation, along with the known radius of the tip, the acceleration due to gravity (taken as 9.806 m/s^2) and the difference in density between the two liquid phases.

With this information, the interfacial tension was determined for the dilute HMPAA solutions against the cyclohexane at a variety of drop rates. The HMPAA solutions were prepared in distilled water and neutralized with 0.01% aqueous NaOH. For all drop volume testing the HMPAA concentration was kept well below the c^* for the polymer in aqueous solution, in order to ensure that the kinetics being studied relate to the diffusion and adsorption of single polymer chains (rather than aggregates).

5. RESULTS AND DISCUSSION

Figure 13 shows the dynamic interfacial tension data obtained for copolymer PYA/AA 1/340 diffusing to the cyclohexane/water interface from aqueous solutions of pH = 5.5 and pH = 7.0. Two different dilute concentrations were studied. Each data point on this diagram represents the average interfacial tension obtained from twenty drops volume at a particular concentration, pH, and rate. Standard deviation error bars are not included on these points, because the standard deviation did not exceed 0.6 mN/m for any of the

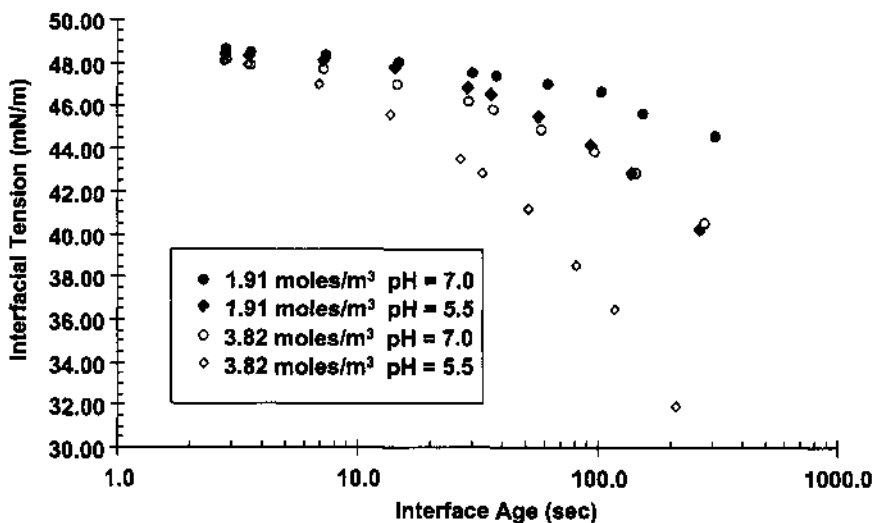


Figure 13. Dynamic interfacial tension data for aqueous (NaOH neutralized) PYA/AA (1/340) against cyclohexane.

data points. The size of the data points themselves is approximately equal to the standard deviation in all cases. The interface ages corresponding to each interfacial tension were calculated from the average drop times according to the method of Joos.²¹

The trends in Figure 13 are as one would expect. As interface age increases, the interfacial tension that the PYA/AA 1/340 imparts on the cyclohexane/water decreases at any given pH and concentration. In other words, the more time the HMPAA has to adsorb at the interface, the more HMPAA adsorbs. As pH is increased, at the same PYA/AA 1/340 concentration and the same interface age, the interfacial tension increases. In other words, HMPAA's become less interfacially active as pH is increased (and they become more neutralized). This was known from the equilibrium work. Also, as the concentration of PYA/AA 1/340 is increased, at the same pH and interface age, the interfacial tension decreases. In other words, if more molecules of HMPAA are available which have the possibility of adsorbing at an interface, then the interface is filled more quickly.

In the majority of drop volume work reported in the literature, observations such as the ones stated in the last paragraph are common. Drop volume is typically performed to study adsorption kinetics, but the results are generally presented qualitatively, based on comparisons of plots similar to those in Figure 13. However, methods have been developed which can be used to quantify the kinetics of interfacial adsorption of solutes, as related to their diffusion properties through the phase in which they are initially contained.

Van Voorst Vader and coworkers²² have proposed that equation 2, a modification of Fick's second law of diffusion, applies to the case of an interfacially active solute diffusing from one bulk phase to a spherically growing interface, based on prior theoretical work by Ward and Tordai²³ (which applied to the same situation, but with an interface that expands as a plane).

$$\frac{\partial C}{\partial t} - \theta z \frac{\partial C}{\partial z} = D \frac{\partial^2 C}{\partial z^2} \quad (2)$$

In equation 2, C = bulk solute concentration, t = time over which the interface expands, z = a coordinate normal to the growing interface, q = dilation ($1/A \, dA/dt$, where A = droplet surface area), and D = the diffusion constant for the interfacially active material. This equation applies directly to drop volume experimentation, in so far as the drops grow spherically, which has been shown by Lando and Oakley²⁴ to be a good assumption. However, Van Voorst Vader never strictly solved the equation for the spherical system.

The solution, only possible under three very important assumptions, is due to Joos and Rillaerts²¹ and is shown below.

$$\Pi = 2RTC_0 \left(\frac{D_{\Delta} t}{\pi} \right)^{1/2} \quad (3)$$

In equation 3, P = interfacial pressure = $\gamma_0 - \gamma$ (where γ_0 is the interfacial tension between the two pure phases considered, and γ is the interfacial tension after adsorption of solute molecules to the interface), C_0 = bulk solute concentration in the phase that contains the solute, t = interface age, D = the diffusion constant of the solute through the bulk phase in which it is contained initially, and R and T have their standard scientific meanings.

Based on equation 3, if dynamic interfacial tension data such as that shown in Figure 13 for PYA/AA 1/340 adsorbing to the cyclohexane/water interface at a specific pH is plotted in the form of interfacial pressure (P) as a function of (bulk concentration (C_0) \times the square root of drop time ($t^{1/2}$)), it would be expected to yield a straight line with a slope = $2RT(D/p)$. A value for D can be calculated from the slope. D is the diffusion coefficient of the solute through the phase in which it is initially dispersed. This is, however, not strictly true, due to the assumptions used in the derivation of equation 3.

The first, and least important assumption, because it has been proven experimentally by McBain and Swain,²⁵ is that interfacial pressure decreases logarithmically with the excess concentration of the solute at the interface relative to the bulk. This is known as the Gibbs adsorption isotherm.¹⁹ The second, more important assumption is that the “sub-interface concentration is zero for all time”.²¹ This is equivalent to assuming that once an interfacially active solute molecule adsorbs at the interface, it “disappears”, or more precisely that the interface is, throughout the experiment, free of barriers to solute adsorption based on possible adsorption sites being pre-filled by the solute molecules that adsorbed at a earlier time. This assumption will be valid only in the initial stages of adsorption (low interfacial pressures), until enough solute is absorbed to the interface that such a barrier to adsorption begins to develop. The work reported here therefore focuses on the low pressure region for each HMPAA studied. The fact that this region alone was studied is clearly shown by Figure 14 (or any other plot of bulk concentration \times the square root of drop time in this paper), since plots of this type are linear over the range of interfacial pressures studied. Once the low interfacial pressure region is exceeded, in terms of interface age or concentration, the plot of bulk concentration \times the square root of drop time will begin to plateau^{3,17} — since at high values of interfacial pressure there must exist barriers to continued solute interfacial adsorption, due to the interface being so saturated with polymer that further adsorption is only possible based on surface rearrangement of the already adsorbed polymer.

The third, and most important assumption in terms of this work, is that adsorption is purely diffusion controlled. In other words, the effectiveness of approaches of the solute to the interface in leading to adsorption is 100%. There is *no* activation energy associated with the adsorption process.

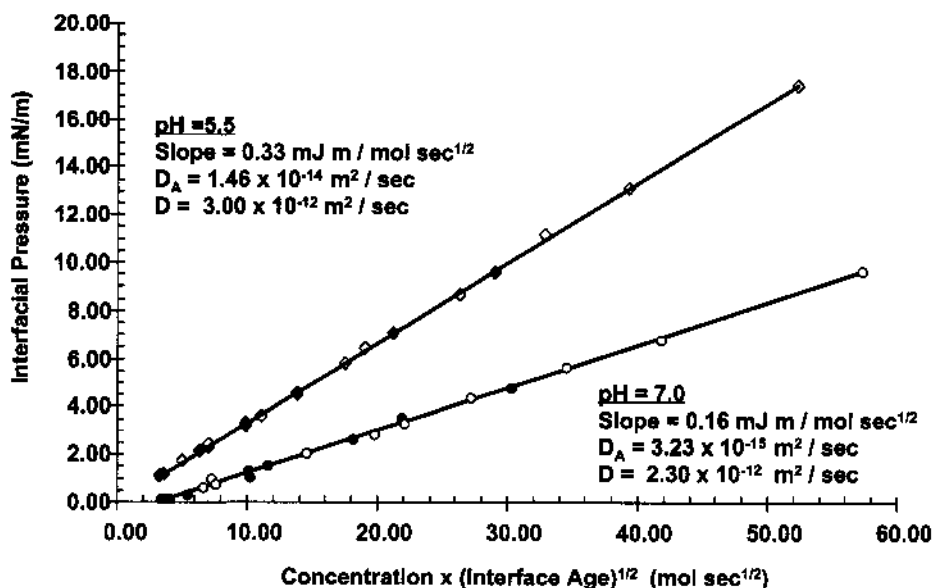


Figure 14. Adsorption diffusion coefficient determination plots for aqueous (NaOH neutralized) PYA/AA (1/340) against cyclohexane.

Under these assumptions, dynamic interfacial tension data can still be evaluated quantitatively using equation 3, and plots of P versus $(C_o * t^{1/2})$ should be found to be linear at low P values. However, the diffusion coefficient calculated from the slope in this region may not equal the Brownian diffusion coefficient of the polymer molecule in solution. Rather, the diffusion coefficient obtained may be lower than the Brownian diffusion coefficient owing to the fact that there may exist an activation energy barrier to adsorption, which is not accounted for in the derivation of equation 3.

The fact that drop volume tensiometry provides a diffusion coefficient for an adsorbing polymer that is complexed with barrier to adsorption effects provides that an opportunity to further study the kinetics of adsorption for the polymer. Consider a hypothetical polymer molecule having a Brownian diffusion coefficient of 2 hypothetical units. Assume an activation energy barrier to this polymer's adsorption exists. The barrier is of a magnitude such that the efficiency of approaches of the polymer to the interface in leading to adsorption is 50%. Under these conditions the diffusion coefficient for the polymer, as calculated by drop volume experimentation, and the theory described above, will be 1 hypothetical unit. To distinguish diffusion coefficients calculated from interfacial tension studies from Brownian diffusion coefficients determined by dynamic light scattering, throughout the remainder of this text, the former will be referred to as "adsorption diffusion coefficients" and signified by " D_A ", and the latter will be signified by their common symbol of " D ". In other words, if a particular polymer had the values $D = 2$ (from light scattering) and $D_A = 1$ (from drop volume tensiometry), then it could be calculated to have an adsorption efficiency of $D_A / D = 50\%$. Correspondingly the number of approaches a polymer makes to an interface for every time it adsorbs can be calculated as D/D_A , which is equal to 2 in this case.

This type of analysis is what has been done with the dynamic interfacial tension data for each of the four model polymers. Figure 14 is the P versus $(C_o * t^{1/2})$ plot based on the data for PYA/AA 1/340 given in Figure 13. In viewing Figure 14 note that there are only

two linear sets of data. All of the data from Figure 13 at pH = 5.5 becomes one data set (both concentrations studied), and all of the data from Figure 13 at pH = 7.0 becomes the other data set (both concentrations studied). This is an important finding, because it indicates that at each pH the adsorption/diffusion coefficient for PYA/AA 1/340 is independent of concentration for the two concentrations studied. This is characteristic of dilute solution conditions having been maintained at both concentrations studied. Had the two concentrations at the same pH yielded different adsorption/diffusion coefficients, one would have had to wonder whether dilute solution was maintained or some pre-c* aggregation had occurred with these polymers. Since the data itself is a justification that dilute solution was maintained, it is valid to use the D_A values obtained for comparison with the Brownian diffusion coefficients for the diffusion of PYA/AA 1/340 at the pH values studied. Such Brownian diffusion coefficients were reported in the materials characterization section of this text, and are again reported on Figure 14.

From the D/D_A data in Figure 14 it can be calculated that PYA/AA 1/340 approaches the cyclohexane/water about 205 times for every 1 adsorption event at pH = 5.5. At pH = 7.0 the PYA/AA 1/340 approaches the cyclohexane/water about 712 times for every 1 adsorption event. Figures 15 through 20 are analogous raw drop volume interfacial tension data and adsorption/diffusion coefficient determination plots for the other model HMPAA's studied. Table 2 summarizes the D/D_A data obtained from all of these studies.

D_A is a diffusion coefficient which is characteristic of actual adsorption events that have occurred. D is a diffusion coefficient which is characteristic of the number of chances an adsorption event has to occur per unit time (since D is characteristic of random Brownian motion). Therefore, the evaluation of adsorption kinetics can be taken one step further. The Arrhenius expression:

$$K = A \exp (-E_a/kT) \quad (4)$$

(where K = the rate of occurrence of an event, A = the number of chances an event has to occur per unit time, E_a = the activation energy necessary for the event to occur, k =

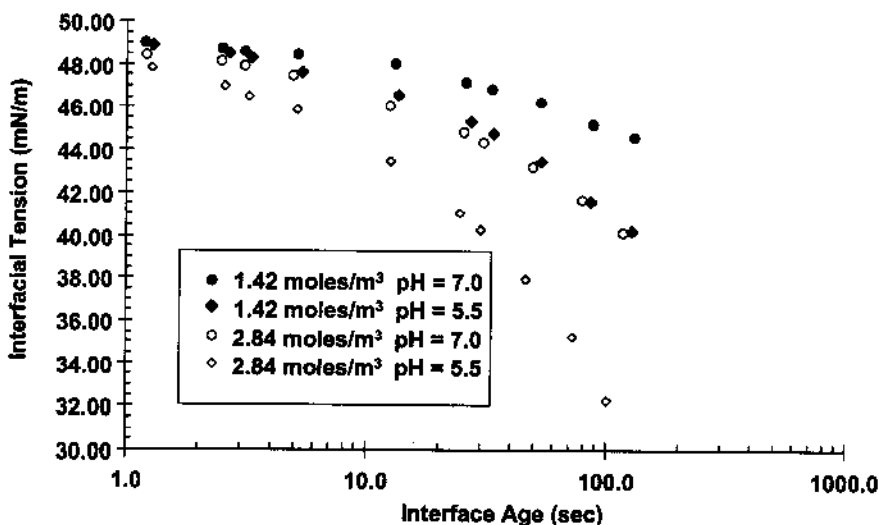


Figure 15. Dynamic interfacial tension data for aqueous (NaOH neutralized) PYA/AA (1/150) against cyclohexane.

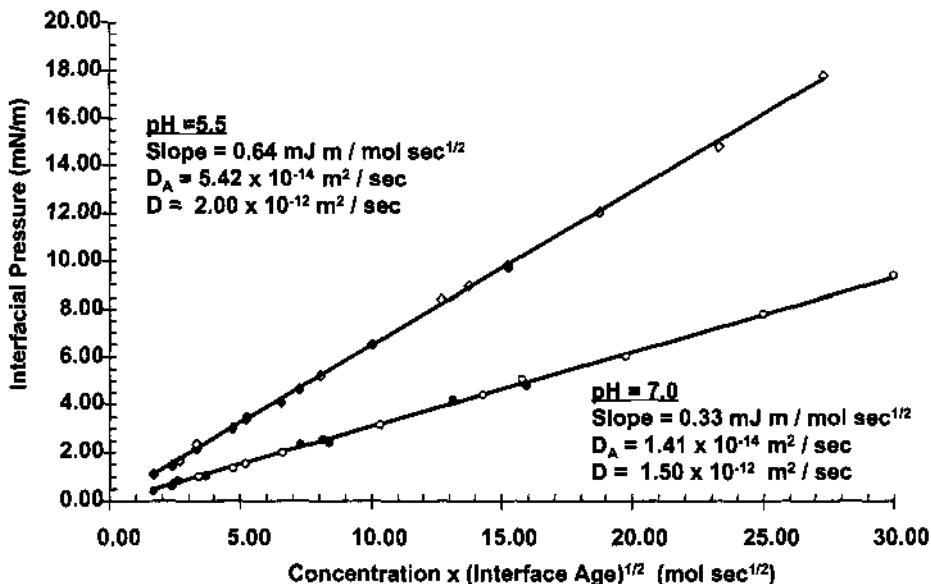


Figure 16. Adsorption diffusion coefficient determination plots for aqueous (NaOH neutralized) PYA/AA (1/150) against cyclohexane.

Boltzmann's constant, and T = temperature) can be applied to the data by allowing that $D_A \propto K$ and $D \propto A$. Therefore, a value of E_a can be calculated for the adsorption of each of the HMPAA's studied at each of the pH's studied. Results of such calculations are also reported in Table 2, along with the pH trigger value for each HMPAA with regard to 10 % cyclohexane-in-water emulsions, as determined by the pseudo phase diagram work discussed previously.

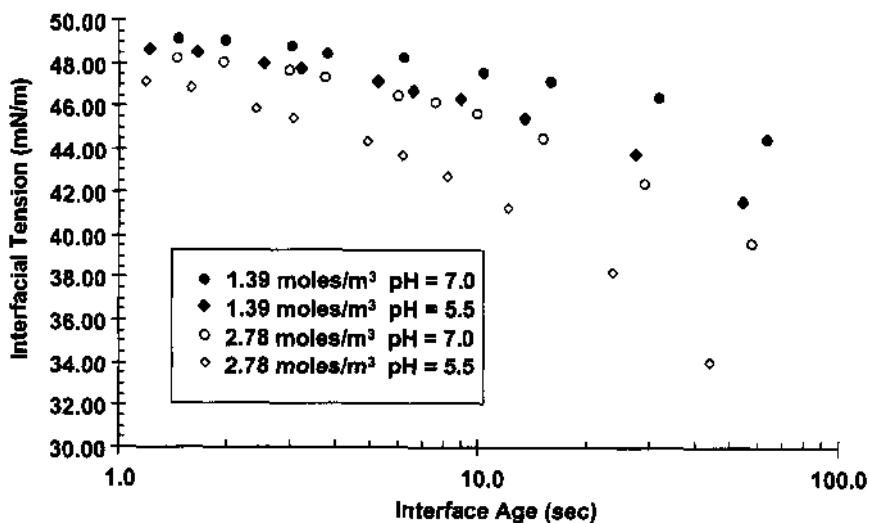


Figure 17. Dynamic interfacial tension data for aqueous (NaOH neutralized) PYA/X/AA (1/0.9/230) against cyclohexane.

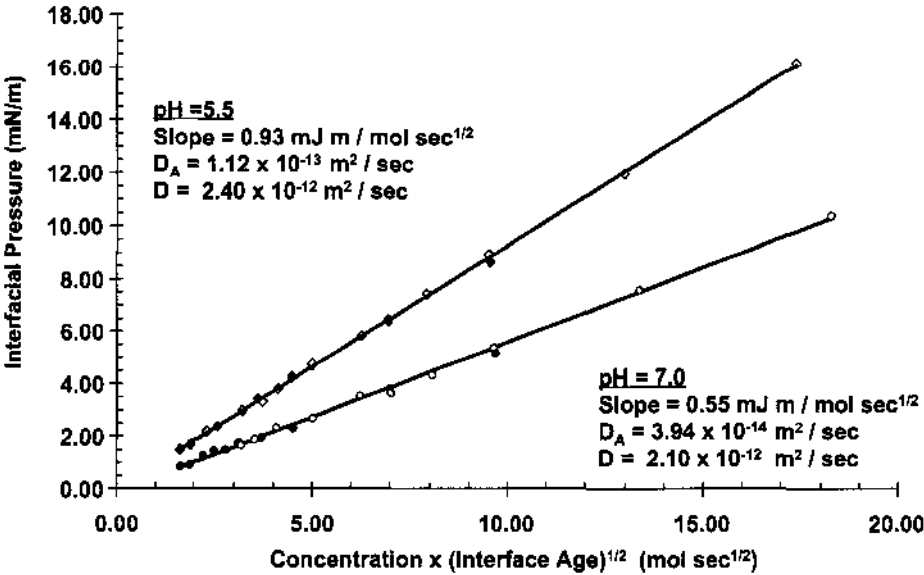


Figure 18. Adsorption diffusion coefficient determination plots for aqueous (NaOH neutralized) PYA/X/AA (1/0.9/230) against cyclohexane.

6. CONCLUSIONS

Four conclusions can be drawn from the data summary in Table 2.

1. For all of the model HMPAA's studied, as solution pH is increased, adsorption efficiency decreases (activation energy for adsorption increases). This is believed to be due to the development of electrostatic resistance to adsorption as

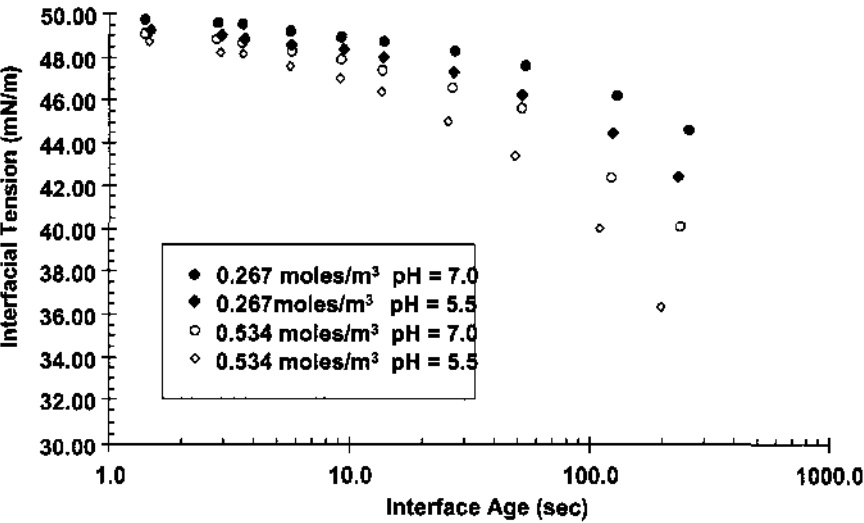


Figure 19. Dynamic interfacial tension data for aqueous (NaOH neutralized) PYAX//AA (1/0.6/150) against cyclohexane.

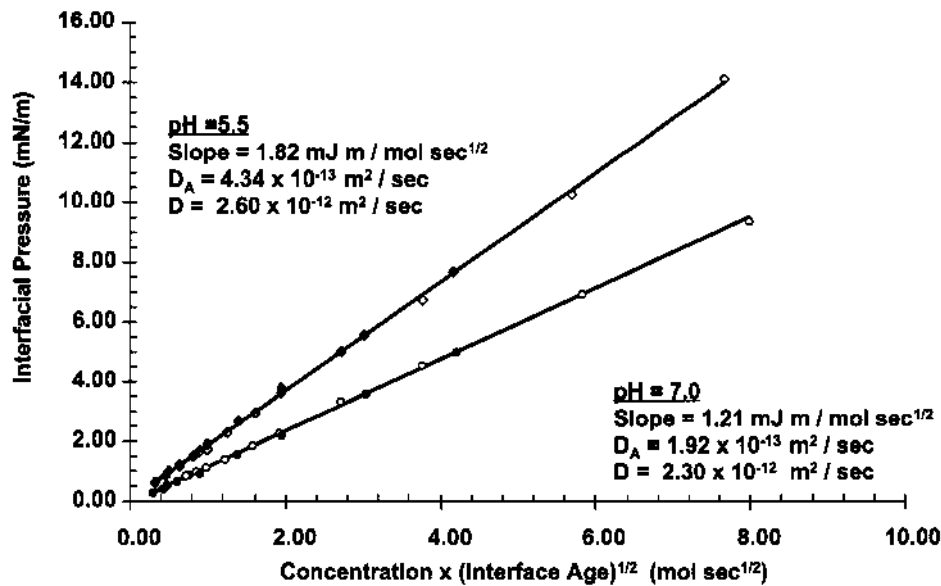


Figure 20. Adsorption diffusion coefficient determination plots for aqueous (NaOH neutralized) PYA/X/AA (1/0.6/150) against cyclohexane.

the cyclohexane/water interface begins to adsorb HMPAA. It has been shown previously³ that when an ionic interfacially active material adsorbs at an interface, charge/charge repulsion between the molecules that adsorb at the interface first and those that diffuse toward the still unsaturated interface at later times causes the kinetics of adsorption to be much less than that of diffusion controlled. As pH is increased HMPAA's become more neutralized. Therefore, electrostatic resistance to their adsorption would also be expected to increase- thus decreasing adsorption efficiency (increasing activation energy for adsorption).

- 2. As crosslink density is increased in the HMPAA's studied, adsorption efficiency increases. This is believed to be due the fact that more highly crosslinked polymers are more entropically restricted in solution. Their efficiency of adsorption is thus increased because adsorption is an entropically restricting event that de-

Table 2. Kinetics of interfacial adsorption data summary

Aqueous system/oil	D/D _A	Ea (kJ/mol)	pH trigger
PYA/AA 1/340 (pH = 5.5)/Cyclohexane	205	1.32	5.3
PYA/AA 1/340 (pH = 7.0)/Cyclohexane	712	1.63	
PYA/AA 1/150 (pH = 5.5)/Cyclohexane	37	0.89	6.5
PYA/AA 1/150 (pH = 7.0)/Cyclohexane	106	1.16	
PYA/X/AA 1/0.9/230 (pH = 5.5)/Cyclohexane	21	0.75	7.2
PYA/X/AA 1/0.9/230 (pH = 7.0)/Cyclohexane	53	0.98	
PYA/X/AA 1/0.6/150 (pH = 5.5)/Cyclohexane	6	0.44	8.0
PYA/X/AA 1/0.6/150 (pH = 7.0)/Cyclohexane	12	0.62	

Polymer diffusion coefficients by dynamic light scattering at conc. = c/10.

creases the overall entropy of a more crosslinked chain less than it does a less crosslinked chain.

3. As hydrophobe content is increased in the HMPAA's studied, adsorption efficiency increases. This is believed to be due to the fact that polymers containing more hydrophobic character are more likely (by random chance) to approach a cyclohexane/water interface with the hydrophobe exposed to the interface for adsorption. If each approach has a better chance of being effective, efficiency is increased.
4. When comparing the E_a values for adsorption of the HMPAA's with the pH triggers that the HMPAA's were found to have, it is apparent that the two follow the same trend over the range of polymers studied. A low pH trigger for emulsion destabilization corresponds to higher values of E_a at both of the pH values studied. Further, considering that the E_a determination experiments were done for each of the polymers at pH = 5.5 and pH = 7.0 (values which are both below the pH trigger for two of the HMPAA's studied, both above the pH trigger for one of the HMPAA's studied, and compassing the pH trigger for one of the HMPAA's), one could speculate from the data that the pH for HMPAA's in general occurs at an E_a for adsorption of approximately 1 kJ/mol.

ACKNOWLEDGMENTS

The author wishes to acknowledge Dr. Robert Lochhead for his guidance during the initial stages of the work reported here, the SC Johnson Foundation for funding of the initial work, Hy Bui for his help with phase diagram work, and Derek Falberg for his efforts on the drop volume interfacial tension studies.

REFERENCES

1. Lochhead RY, "Electrosteric Stabilization of Oil-in-Water Emulsions by Hydrophobically Modified Poly(acrylic acid) Thickeners", In *Polymers as Rheology Modifiers*, ACS Symposium Series 462, E.D. Glass (ed), 1991.
2. Chu KW, Masters Thesis, University of Cincinnati, 1990.
3. Rulison CJ and Lochhead RY, "Kinetic Study of the Adsorption of Nonionic and Anionic Surfactants and Hydrophobically Modified Water-Soluble Polymers to Oil-Water Interfaces" In *Surface Surfactant Adsorption and Surface Solubilization*, R. Sharma (ed.), ACS Symposium Series 615, 1995.
4. Rulison CJ and Lochhead RY, "The Effect of pH and Electrolyte Concentration on the Stability of Polymerically Stabilized Emulsion Systems." *Polymer Preprints*, 1992;33(2).
5. Rulison CJ, Lochhead, R.Y, Bui HS and Pierce TD, "Investigation of the Mechanism of Emulsification by Hydrophobically Modified Hydrogels", *Polymer Preprints*, 1993;34(1).
6. Rulison CJ and Lochhead RY, *Polymer Preprints*, 1993;34(2).
7. Lochhead RY and Rulison CJ, "An Investigation of the Mechanism by which Hydrophobically-Modified Hydrophilic Polymers Act as Primary Emulsifiers for Oil-in-Water Emulsions .1. Polyacrylic Acids and Hydroxyethyl Celluloses", *Colloids and Surfaces A*, 1994;88(1):27.
8. Napper DH, *Polymeric Stabilization of Colloidal Dispersions*, Academic Press, (1983).
9. Overbeek JTG, Kinetics of Flocculation, "Kinetics of Flocculation", In *Colloidal Science*, H.R. Kruyt (ed), 1965.
10. Overbeek JTG, "Electrochemistry of the Double Layer", In *Colloid Science-Irreversible Systems*, H.R. Kruyt (ed), Elsevier, 1952.
11. Debye and Hückel, *Phys. Z.*, 1923;24:185; Debye P, "Osmotische Zustandsgleichung und Aktivität Verdünnter Starker Elektrolyte", *Phys. Z.*, 1924;25:93.
12. Von Smoluchowski M, *Physik Z.*, 1916;17:557-585; 1917;92:129.

13. Lips A, Smart C and Willis E, "Light Scattering Studies on a Coagulating Polystyrene Latex", Trans. Faraday Soc., 1971;67:2979.
14. Honig EP, Roberson GJ, Wiersema PH, "Effect of Hydrodynamic Interaction on the Coagulation Rate of Hydrophobic Colloids", J. Colloid Interface Sci., 1971;36:97.
15. Lichtenbelt JWT, Pathmamohanar C, Wiersema PH, "Rapid Coagulation of Polystyrene Latex in a Stopped-Flow Spectrophotometer", Jour. Colloid Interface Sci., 1974;49:281.
16. Lochhead RY, p. 375 In ACS Symposium Series 213, D.N. Schulz, and J.E. Glass (eds.), American Chemical Society, Washington, DC, 1986.
17. Rulison CJ, "Mechanistic and Kinetic Aspects of the Use of Hydrophobically Modified Hydrophilic Polymers as Primary Emulsifiers", Ph.D. Dissertation, Univ. Of Southern Miss., 1994.
18. Vincent B and Whittington S, In *Colloid and Surface Science*, E. Matigovic (ed), Plenum, 1982.
19. Shaw DJ, *Introduction to Colloid and Surface Chemistry*, Third Edition, 1980.
20. Tate T, "On the Magnitude of a Drop of Liquid Formed Under Different Circumstances", Phil. Mag., 1864;27:176.
21. Joos P and Rillaerts E, "Theory of the Determination of the Dynamic Surface-Tension with the Drop Volume and Maximum Bubble Pressure Methods", J. of Colloid and Interface Science, 1981;79,1:96.
22. Van Voorst Vader F, Erkens TF and Van Den Tempel M, "Measurement of Dilatational Surface Properties", Trans. Faraday Soc., 1964;60:1170.
23. Ward AFH and Tordai L, "Time-Dependence of Boundary Tensions of Solutions"(1.The Role of Diffusion in Time-Effects)", Jour. Chem. Phys., 1946;14,7:453.
24. Lando JL and Oakley HT, "Tabulated Correction Factors for the Drop-Weight-Volume Determination of Surface and Interfacial Tensions", J. Coll. Inter. Sci., 1967;25:526.
25. McBain JW and Swain RC, "Measurements of Adsorption at the Air-Water Interface by the Microtome Method" Proc. Royal Soc., 1936;A154:608.

EFFECT OF SOLIDS CONCENTRATION ON POLYMER ADSORPTION AND CONFORMATION

Tsung-yuan Chen,¹ Chidambaram Maltesh,² and Ponisseril Somasundaran¹

¹Henry Krumb School of Mines
Columbia University
New York, New York 10027

²Nalco Chemical Co.
Naperville, Illinois 60563

1. ABSTRACT

The effect of solids concentration on the adsorption and conformation of polymers at solid/liquid interface was investigated using depletion adsorption and fluorescence techniques. The fluorescence of pyrene labeled polyethylene oxide at silica/water interface as a function of solids concentration revealed a surprisingly measurable change in polymer conformation as the solids content was increased. Adsorption density as well as coiling of the polymers was found to decrease with increase in solids concentration. These changes are correlated with the rheological behavior of the suspensions.

2. INTRODUCTION

Concentrated particulate suspensions are widely used for coatings, paints, electronic pastes, clay and ceramic slurries in many industrial processes. To maintain the stability of these concentrated suspensions and to facilitate the processing, polymers are frequently used for controlling the suspension rheology.¹ Although polymers are currently used for dispersing concentrated suspensions, the role of polymer properties, particularly their conformation and orientation, in stabilization of colloidal particles in concentrated slurries remains unclear.

Recently, we have used fluorescence spectroscopy to estimate the conformation and interaction of polymers at surfaces.²⁻⁴ Information obtained for polymer conformation at solid/liquid interface has been correlated with the flocculation properties of particulate suspensions. In this paper, effects of solids concentration on polymer adsorption and conformation on selected model systems are presented.

3. EXPERIMENTAL

3.1. Materials

AKP50 alumina powder (Sumitomo Chemical, New York) of 0.2 μm diameter and 10.9 m^2/g specific surface area was used for the adsorption study. Particle size distribution measured with Photon Correlation Spectroscopy (Brookhaven Instruments, BI-8000AT), shows a log normal distribution with an average particle size of 0.21 μm (Figure 1). The alumina particles are nonporous as indicated by the scanning electron microscopic examination. Purity of the powders is specified by the manufacturer as 99.9%.

For silica, Geltech powder (Geltech Tech., Florida) of 1.0 μm diameter and 4.2 m^2/g specific surface area was used. This silica powder is manufactured using a sol-gel process and SEM examination showed nonporous spherical shape. Particle size distribution measured using the PCS method indicates the silica to be relatively monodisperse with an average diameter of 0.92 μm (Figure 1). The density of the silica was measured to be 2.1 g/cm^3 and their purity is claimed to be 99.9% by the manufacturer.

Polyacrylic acid polymer of molecular weight 90,000 and polyethylene oxide polymer of molecular weight 6000 ~ 7500 were used for the adsorption study. Both polymers were purchased from Polysciences, Inc. and used as received. Polyethylene oxide polymer with pyrene probes attached on both ends was synthesized by Kumar and Aguilar of University of Florida. The labeling ratio of pyrene molecule on polyethylene oxide polymer was 2 to 1. The attachment of pyrene probes to the polymer was confirmed by NMR measurements. Polyvinyl pyrrolidone polymer of molecular weight 40,000 supplied by Fluka Chemical Company was also used in the adsorption study.

Sodium nitrate (Fisher Scientific) of ACS grade was used for ionic strength control. Water of resistivity 17 MW after distillation and deionization (Barnstead Nanopure System) processes was used for making all solutions.

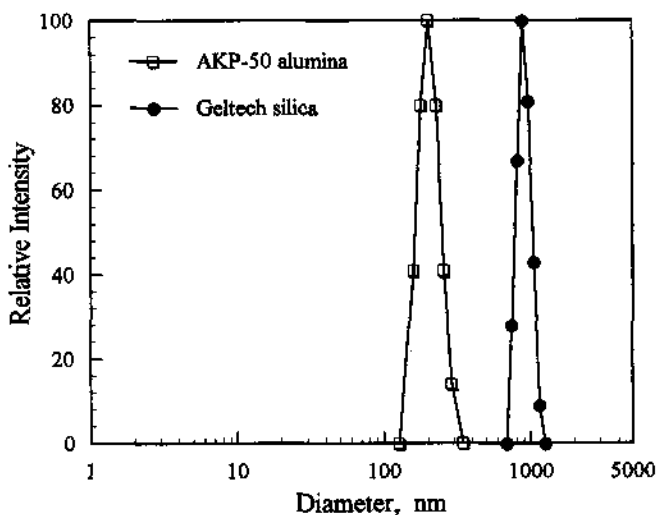


Figure 1. Particle size distribution of AKP50 alumina and Geltech silica powders measured by Photon Correlation Spectroscopy.

3.2. Methods

3.2.1. Polymer Adsorption. Solutions of polymers at desired concentration were prepared in 0.03 M NaNO₃ solution and the solution pH adjusted. 10 ml of each polymer solution was then placed in a 20 ml glass vial and alumina or silica powder was added gradually into above glass vial while the polymer solution was being stirred. The suspensions were then stirred for 30 minutes, pH adjusted, and further stirred for 18 hours for equilibrium adsorption. After adsorption, samples were centrifuged at 2400 rpm for one hour and the supernatants were removed for determination of polymer concentration. Polymer concentration was determined using a DC-90 Total Organic Carbon Analyzer (Dohrmann Instrument). Adsorption density of polymers on the solid surface was calculated from the difference between the initial and residual polymer concentrations.

For the study of polymer conformation at solid/liquid interface, mixtures of pyrene labeled polymer with unlabeled polymer were used.

3.2.2. Polymer Conformation. The conformation of pyrene labeled polyethylene oxide polymers in solution and at solid/liquid interface was monitored using the fluorescence spectrum of the pyrene probe using a LS-1 fluorescence spectrometer (Photon Technology International Inc.). Coiling index, defined as the ratio of intensity of the excimer peak (480 nm) to that of the monomer peak (373 nm) in the pyrene fluorescence spectrum, was used as a measure of the polymer conformation (Figure 2). When the polymer is stretched, the possibility of pyrene excimer formation is low and this yields a low excimer peak, and therefore the coiling index is low. In contrast, when the polymer is coiled, the possibility of excimer formation is high and the coiling index is higher. Thus, the coiling index of pyrene labeled polymers serves as an in-situ measure of the polymer conformation in the solution or at the solid/liquid interface. In all the experiments, suspensions with nearly no residual polymer are used for conformation study to minimize the influence of fluorescence spectra of free polymers in the supernatant.

4. RESULTS AND DISCUSSION

The effect of solids concentration as well as suspension pH on the adsorption of polyacrylic acid on alumina was first studied and the results obtained are shown in Fig-

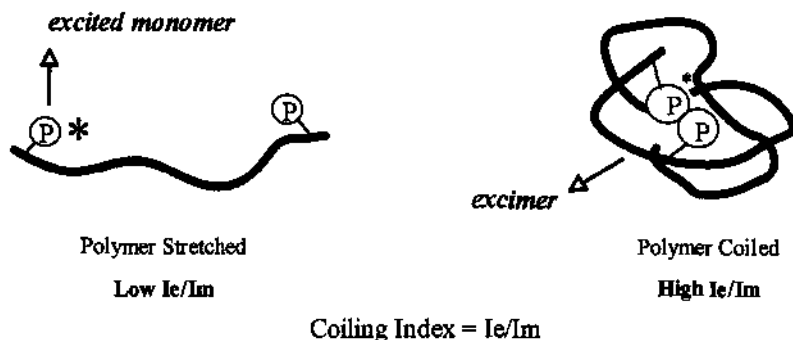


Figure 2. Schematic presentation of coiling index and polymer conformation. I_e and I_m represent the fluorescence intensities of the excited monomers and excimers, respectively. The coiling index is low when the polymer is stretched and high when polymer is coiled.

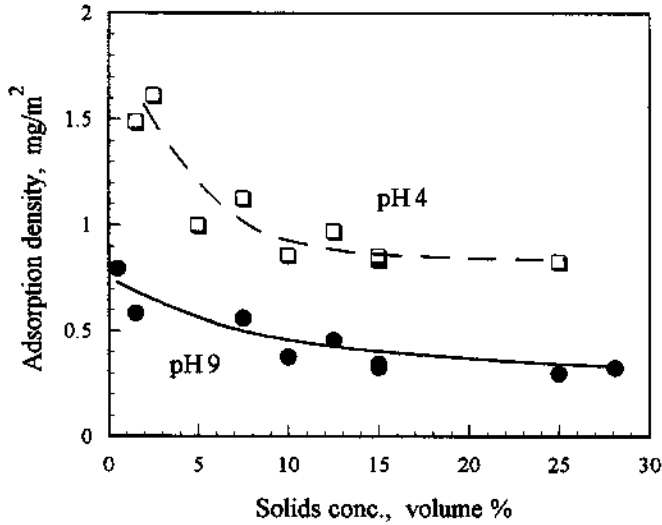


Figure 3. Effect of solids concentration on the adsorption of polyacrylic acid on alumina.

ure 3. Interestingly, the solids content was found to markedly decrease the adsorption when it was increased from 0.5 volume percent to 27 volume percent both at pH 4 and pH 9. Surprisingly, the decrease in adsorption density occurred even in the low solids concentration region when interactions between particles are less than at high concentrations.

The effect of suspension pH on the adsorption of polyacrylic acid on alumina existed in the entire concentration range tested with the adsorption higher at lower pH. Since the adsorption of polyacrylic acid on the alumina surface depends on the population and the ionization status of hydroxyl groups presented on the alumina surface, this suggests the electrostatic interaction between the polymer and alumina surface to play a dominant role in determining the adsorption behavior of polyacrylic acid polymers even when the solids content of system is high.

The marked effect of solids concentration on polymer adsorption was also observed in the case of polyvinyl pyrrolidone–alumina system. When the solids concentration in the suspension increased from 1 volume percent to 20 volume percent, the adsorption density of polyvinyl pyrrolidone on alumina surface dropped a couple of orders of magnitude (Figure 4). Such huge difference in the polymer adsorption due to solids concentration change has not been reported previously to our knowledge.

The effect of solids concentration on the adsorption of polyacrylic acid and polyvinyl pyrrolidone on alumina can best be illustrated by plotting log-log the polymer adsorption density against the available surface area per suspension volume (which will be termed as surface area loading later). Figure 5 shows an inverse correlation between polymer adsorption density and the surface area loading. The slope of this plot between the polymer adsorption density and surface solids loading is an indicator of the effect of solids concentration on polymer adsorption. For the polyvinyl pyrrolidone system the slope is -0.939, while for the polyacrylic acid system the slopes are -0.231 and -0.257 at pH 4 and pH 9, respectively with the higher slope suggesting the stronger dependence of adsorption on solids concentration.

Similar effects of solids concentration on adsorption of polyethylene oxide on silica are illustrated in Figure 6. pH was found to have a measurable effect on polyethylene ox-

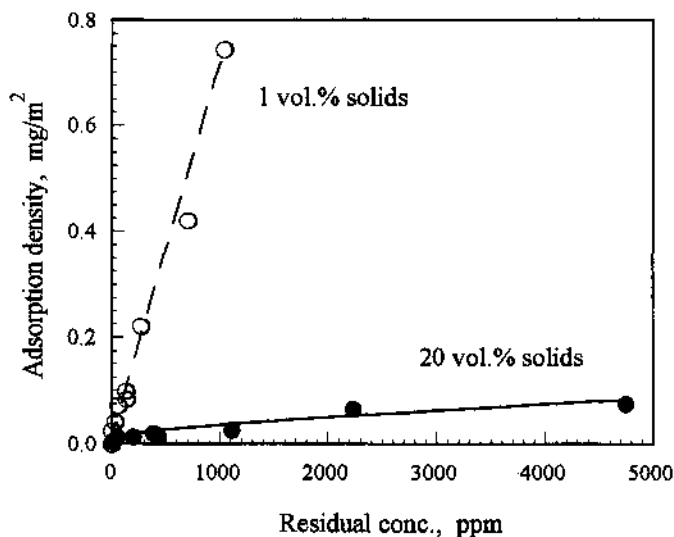


Figure 4. Adsorption of polyvinyl pyrrolidone on alumina surface at low (1 vol.%) and high (20 vol.%) solids loadings.

ide adsorption even though polyethylene oxide is a nonionic polymer. This is attributed to pH dependence of possible hydrogen bonding as a result of the pH dependent ionization of hydroxyl groups on silica.

Solids concentration affects the adsorption of polyethylene oxide on silica at pH 4 at solids loading below 10 volume percent and at pH 9 at solids loading above 25 volume percent. The change in polymer adsorption behavior at high solids content is particularly

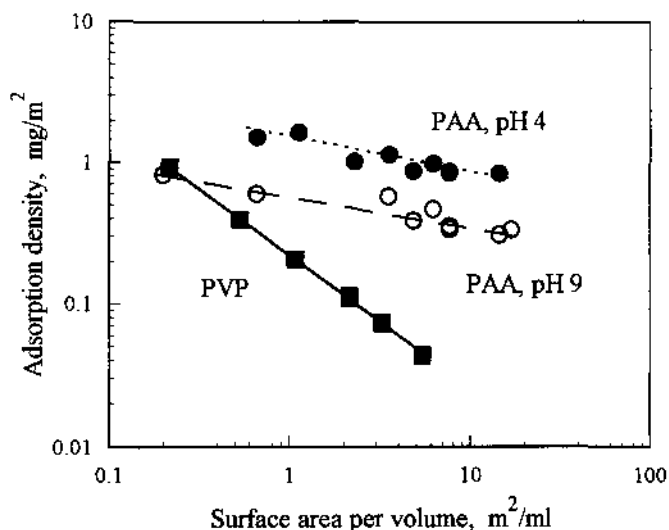


Figure 5. Correlation between the polymer adsorption density and surface area per suspension volume for polyacrylic acid and polyvinyl pyrrolidone/alumina systems.

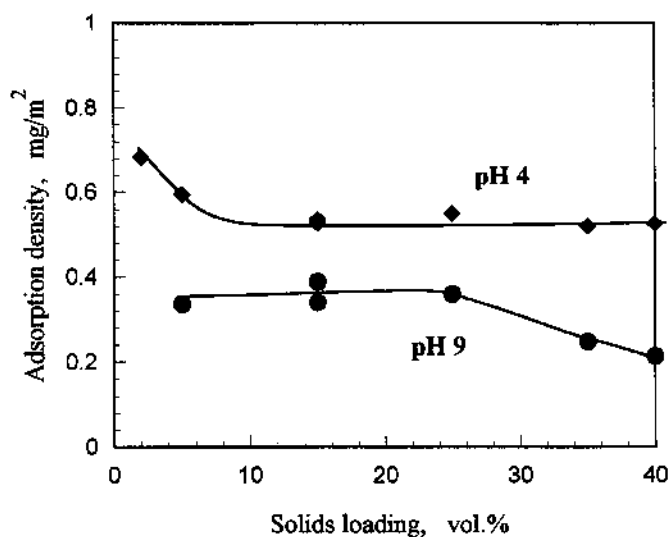


Figure 6. Effects of solids concentration and suspension pH on polyethylene adsorption at silica/water interface.

interesting since most industrial processes use such highly concentrated suspensions. To understand the reasons for the behavior, fluorescence experiments were done with mixtures of pyrene labeled polymers in unlabeled polymers along with their adsorption isotherms. In Figure 7, the coiling index of the adsorbed polymer is plotted against solids loading along with polymer adsorption density. There is a clear correlation between the polymer conformation change and the decrease in polymer adsorption density with the increase in solids concentration. The coiling index of adsorbed polymers drops from 0.75 at 5 volume percent of solids to 0.3 at 35 volume percent solids of concentration. This sug-

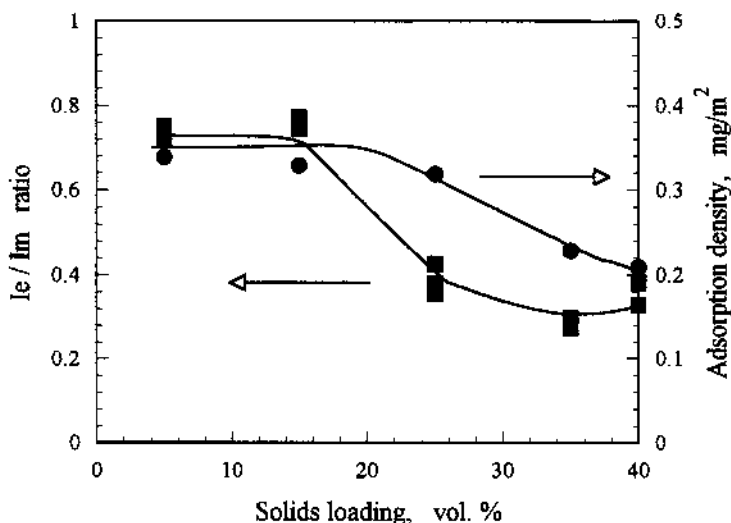


Figure 7. Correlation between polymer conformation and the polymer adsorption density.

gests that polymers become stretched when the solids content is increased above 25 volume percent. Conformational changes correlate well with this change in polymer adsorption density since a stretched polymer will occupy more area on the surface than a coiled polymer. This suggests that the change in polymer adsorption density results primarily from the stretching of polymers at silica surfaces rather than the change in the nature of polymer-surface interaction.

The effect of polymer coverage on conformation of adsorbed polymers at two different solids concentrations is shown in Figure 8. Interestingly, in the complete range of adsorption density, the coiling index of the adsorbed polymer at high solids loading is always lower than that at lower solids loading. The adsorbed polymer is thus more stretched at high solids loading even when the particle surface is not completely covered. The rheology data for silica suspension sheds some lights on the possible reasons for this effect. Zamman et. al.⁵ have reported the relative viscosity of silica suspensions of the same composition but without polymers to show an increase from the value predicted by Batchelor model⁶ when the solids concentration was above 25 volume percent. This suggests a stronger particle-particle interaction than that dictated by the Batchelor model at solids concentration above 25 volume percent. Such interaction can indeed cause the polymer to stretch on the surface. The observed increase in polymer stretching can be accounted for by the enhanced interaction between particles that are closer to each other at high solids loading.

5. SUMMARY

Solids concentration exhibits a marked effect on the adsorption of polyacrylic acid, polyvinyl pyrrolidone, and polyethylene oxide polymers on solids. Adsorption of polyacrylic acid and polyvinyl pyrrolidone on alumina was found to decrease as the solids concentration was increased from 0.5 to 27 volume percent with a logarithmic correlation

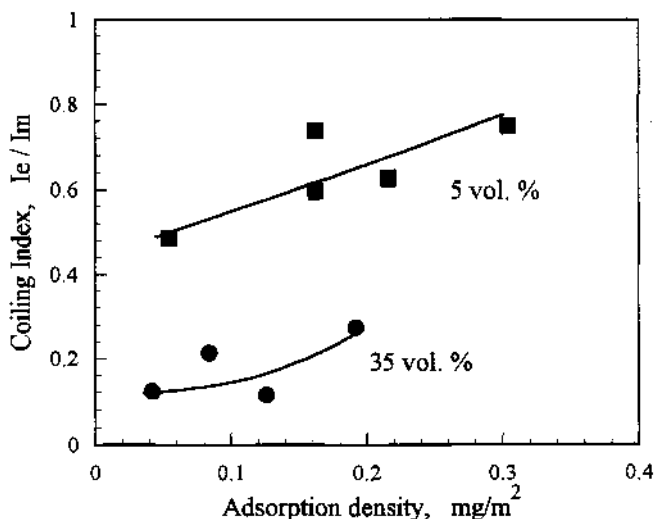


Figure 8. Effects of solids concentration and polymer adsorption density on conformation of adsorbed polyethylene oxide polymers.

of the adsorption with solids surface area loading. The effect of solids concentration on adsorption was measurably higher for polyvinyl pyrrolidone than for polyacrylic acid.

In the case of adsorption of polyethylene oxide on silica at high pH the adsorption density decreased at solids concentration above 25 volume percent. Investigation of the polymer conformation at silica/water interface using fluorescence spectroscopy indicates polymer to become more stretched as the solids loading was increased. The decrease in polymer adsorption density with solids can be accounted for by considering the stretching at high solids concentration. With more stretched polymers on the surface, the area occupied per polymer is larger; and hence the total number of polymer molecules on the surface and hence adsorption density is lower. It was also found that the conformation of the adsorbed polymer at low solids loading is different from that at high solids concentration even at low adsorption densities. This suggests strong influence of particle interaction on adsorbed polymer conformation even when the surface coverage is low. Correlation between the suspension rheology and the polymer adsorption density and conformation change suggests that increased interaction between particles at high solids to be a possible reason for the observed effect of solids loading on polymer conformation and adsorption density.

ACKNOWLEDGMENTS

The authors acknowledge the financial support of the Engineering Research Center (ERC) for Particle Science and Technology at the University of Florida, the National Science Foundation (NSF) grant #EEC-94-02989, and the Industrial Partners of the ERC.

REFERENCES

1. Cesarano III J, and Aksay I A, "Processing of Highly Concentrated Aqueous α -Alumina Suspensions Stabilized with Polyelectrolytes", *J. Am. Ceram. Soc.*, 1988;71(12):1062–1067.
2. Chanar P, Somasundaran P, Tumo NJ, and Waterman KC, "Excimer Fluorescence Determination of Solid-Liquid Interfacial Pyrene-Labeled Poly(acrylic acid) Conformations, *Langmuir*, 1987;3:298–300.
3. Somasundaran P and Krishnakumar S, "In-situ spectroscopic investigations of adsorbed surfactant and polymer layers in aqueous and nonaqueous systems", *Colloids and Surfaces*, 1994;93:79–95.
4. Xiang Yu and Somasundaran P, "Role of Polymer Conformation in Interparticle-Bridging Dominated Flocculation", *Journal of Colloid and Interface Science*, 1996;177:283–287.
5. Zaman AA, Moudgil BM, Fricke AL, and El-Shall H, "Rheological Behavior of Highly Concentrated Aqueous Silica Suspensions in the Presence of Sodium Nitrate and Polyethylene Oxide", *J. Rheology*, 1996;40(6):1191–1210.
6. Batchelor GK, "The Effect of Brownian Motion on the Bulk Stress in a Suspension of Spherical Particles", *J. Fluid Mech.*, 1977;83:97–117.

WATER SOLUBILITY CHARACTERISTICS OF POLY(VINYL ALCOHOL) AND GELS PREPARED BY FREEZING/THAWING PROCESSES

Christie M. Hassan, Patrina Trakampan, and Nicholas A. Peppas

Polymer Science and Engineering Laboratories
School of Chemical Engineering
Purdue University
West Lafayette, Indiana 47907-1283

1. ABSTRACT

Poly(vinyl alcohol) (PVA) is a water soluble polymer whose water solubility depends on its degree of hydrolysis, molecular weight, and tendency to hydrogen bond in aqueous solutions. PVA exhibits both upper and lower critical solubility temperatures and can be readily solubilized in water. For long-term dimensional stability, a new method involving freezing and thawing of aqueous PVA solutions was used to prepare insoluble PVA gels held together by physical crosslinks formed predominantly by crystallites. Solutions containing 15% PVA were frozen at -20 °C for 1, 8, and 18 hours and thawed at room temperature for 30 minutes to 6 hours. These cycles were repeated for up to 10 times. The ensuing gels were analyzed by equilibrium swelling studies. Each cycle led to further crystallization of PVA leading to stable gels. Differential scanning calorimetry was used to analyze the gel morphology. Degrees of crystallinity varied from 4 to 16% on a swollen basis. Upon exposure to swelling temperatures of up to 37 °C, the crystallites of these gels remained remarkably stable for a period of several weeks. However at 60 °C relatively fast crystal melting occurred. The dissolution process was followed using complexation with boric acid.

2. INTRODUCTION

Poly(vinyl alcohol), henceforth designated as PVA, is a widely used hydrophilic polymer that can dissolve in water over a wide range of temperatures. Its solubility has been well characterized by Finch¹ and Peppas.² Typically PVA solubility is a function of

the PVA molecular weight and the degree of hydrolysis of the samples. As PVA is produced by methanolysis of poly(vinyl acetate), a small amount of acetate groups is always present. The characteristic Flory interaction parameter for the PVA-water system has been determined by Peppas and Merrill³ as a function of temperature and concentration.

Aqueous PVA solutions exhibit two critical temperatures, an upper and a lower one,⁴ according to well known thermodynamic characteristics. Long term stability of PVA solutions is rather difficult because of aging, "retrogradation",^{4,5} or hydrogen bonding. Long-term stability can be obtained by treatment of aqueous PVA solutions in the absence of any additives, in order to produce temporary (or sometimes permanent) gel structures by crystallization. These physical hydrogels have a wide range of applications. For example, PVA hydrogels have many characteristics which make them desirable for a wide range of applications. Some of these characteristics include swelling to a high degree in water, high mechanical strength, and high elasticity. For biomedical applications, PVA gels are commonly crosslinked with formaldehyde or glutaraldehyde to yield insoluble networks.² Often, unreacted residue from the crosslinking agent may be eluted slowly over time resulting in the release of toxic agents. This toxicity is undesirable for pharmaceutical applications because the activity of the drug or agent being released could be destroyed. For biomedical applications, the direct release of toxic agents into the body would result in obvious undesirable effects.

A method of solidification by freezing and thawing aqueous solutions of PVA has been developed. This method involves casting dilute, aqueous solutions then cooling to -20 °C and thawing back to room temperature several times. This results in the formation of a stable three-dimensional network held together by crystallites. The stability of the structure is reinforced by an increasing number of freezing/thawing cycles.⁶

3. HEAT-TREATED POLY(VINYL ALCOHOL) GELS

The stabilization of aqueous PVA solutions and the preparation of ultrapure PVA hydrogels using freezing and thawing techniques was first reported by Peppas⁷ in 1975. In this work, aqueous solutions of 2.5 to 15 wt% PVA were frozen at -20 °C and thawed back to room temperature. Turbidimetric studies were performed in which the transmittance of visible light was examined as a function of thawing time. Crystallite formation was found to be a function of time of freezing, time of thawing, and PVA solution concentration. In particular, it was determined that crystallinity increased with increasing freezing time and increasing PVA solution concentration. It was also found that during thawing, the size of crystalline structures initially increased and then decreased due to the breaking down of regions that were not very dense (smaller crystallites).

Nambu⁸ reported a process for the preparation of a freeze-dried PVA hydrogel. The process consisted of preparing a 2.5 to 25 wt% aqueous PVA solution. The average degree of polymerization of the PVA was at least 800. A water-soluble polyhydric alcohol such as ethylene glycol, propylene glycol, or glycerin was added to the PVA solution which was then cooled to -3 °C or lower and then dehydrated. This procedure resulted in the formation of a hydrogel that could be used as a cooling medium.

Ohkura *et al.*⁹ reported interesting features of PVA gels formed from solutions with the addition of organic solvents. A mixture of dimethyl sulfoxide (DMSO) and water was chosen as an appropriate solvent for PVA because it would not freeze until very low temperatures. From their work, it was found that gels obtained below 0 °C were transparent and exhibited high elasticity. It was also shown that higher gelation rates were observed

when compared to aqueous solutions consisting only of PVA and water. The properties were dependent on the DMSO to water ratio. Gelation from the mixture occurred without phase separation at temperatures below 20 °C. However, above this temperature, phase separation played a significant part in the gelation process. Their work also increased interest in the use of wide- and small-angle neutron scattering in order to understand the structure of the gels from a microscopic perspective.

Stauffer and Peppas⁶ investigated PVA gels prepared by freezing and thawing techniques. In this work, hydrogels were prepared by existing aqueous solutions of 10–15 wt % PVA to freezing at -20 °C for 1–24 hours and thawing at 23 °C for up to 24 hours for 5 cycles. It was found that higher PVA concentrations produced strong thermoreversible gels with mechanical integrity. This was specifically observed for gels that were frozen for 24 hours for 5 cycles but thawed for any period of time. Swelling experiments as a function of thawing time and freezing cycles indicated that denser structures were observed after 5 cycles. These results showed that the crystallinity increased with increasing number of freezing/thawing cycles.

Ficek and Peppas¹⁰ investigated PVA microparticles that were prepared by freezing and thawing processes. An aqueous solution of PVA was dispersed in corn oil with 1.25 wt% sodium sulfate as the surfactant. The suspended droplets of PVA solution were solidified by freezing and thawing cycles to produce microparticles with diameter ranging from 150 to 1400 nm. Some of the important parameters in this work were found to be the oil to PVA ratio, and the amount of surfactant added. The microparticles were capable of releasing bovine serum albumin for up to 7 days. In the work of Hickey and Peppas,¹¹ PVA membranes were prepared by freezing and thawing aqueous PVA solutions for up to 10 cycles. The crystalline PVA fraction was determined to be a function of the number of cycles and the duration of each cycle. The volume-based crystalline fraction of PVA on a wet basis varied from 0.052 to 0.116. The equilibrium volume swelling ratios were found to increase from 4.48 to 9.58 as a function of decreasing degree of crystallinity. Diffusion studies with theophylline and FITC-dextran indicated that the transport of solutes was a function of the crystalline PVA fraction and mesh size. Peppas and Mongia¹² examined the bioadhesive behavior of PVA gels prepared by freezing and thawing methods. Adhesion studies showed that the work of fracture, or detachment, decreased with increasing number of freezing/thawing cycles due to the increase in the degree of crystallinity. It was also found from oxprenolol and theophylline delivery studies that the number of freezing and thawing cycles affected drug release behavior. Their results showed that the mucoadhesive characteristics and release behavior could be optimized by controlling the freezing/thawing conditions.

In the present work, we examined the preparation of PVA hydrogels using freezing and thawing techniques. The stability of the gels was examined for different freezing and thawing conditions. In particular, the swelling behavior in water and the dissolution behavior of PVA chains were examined as a function of time for gels that were exposed to varying numbers of freezing and thawing cycles.

4. EXPERIMENTAL

4.1. Synthesis of Poly(Vinyl Alcohol) Hydrogels

Aqueous solutions of 15 wt% PVA were prepared by dissolving PVA (Elvanol® 90–50, E.I. duPont de Nemours, Wilmington, DE, $M_n = 35,740$, polydispersity index =

2.15, degree of hydrolysis = 99.0%) in deionized water for 6 h at 90 °C. The solutions were cast between glass microscope slides with 0.7 mm thick spacers. The samples were then exposed to 3 to 12 cycles of freezing for up to 8 hours at -20 °C and thawing for up to 6 hours at 25 °C.

4.2. Swelling Studies

Equilibrium swelling studies were conducted in deionized water at 37 °C. The PVA films prepared by repeated cycles of freezing and thawing were cut into thin disks of 12 mm diameter using a cork borer. Each disk was initially weighed in air and heptane and then placed in a jar containing 50 ml of deionized water. At specific times during swelling, the samples were blotted and weighed in air and heptane and 5 ml samples were removed from the swelling media.

4.3. Dissolution Studies

The swelling media samples were analyzed for PVA dissolution by complexing each 5 ml sample of aqueous PVA with 2.5 ml of a 0.65M boric acid solution and 0.3 ml of a 0.05M I₂ / 0.15M KI solution and then diluting to 10 ml with deionized water at 25 °C. The absorbance of visible light at 671 nm was then measured with a UV/Vis Spectrometer (Lambda 10 model, Perkin Elmer, Norwalk, CT) to determine the concentration of complexed PVA in solution.

5. RESULTS AND DISCUSSION

5.1. Equilibrium Swelling and Stability

In order to investigate the stability of the PVA solutions after the freezing/thawing process, a series of experimental studies was undertaken whereby 15 wt% PVA solutions were frozen for 8 hours at -20 °C and thawed for 4 hours at 25 °C. Figure 1 shows the volume swelling ratio, Q , as a function of thawing time for samples prepared with 3, 5 and 7 cycles. It can be seen that in all cases the swelling ratio increases with time and passes through a maximum at about 10 to 30 hours. This maximum is followed by a re-equilibration to a lower value. Figure 2 shows the water uptake in the first 50 hours, clearly indicating the nature of that “overshoot”. Eventually, all gels attained a constant volume swelling ratio. The samples treated for 3 cycles showed a much more swollen structure than those treated for 5 or 7 cycles. Evidently, the freezing/thawing process leads to crystal formation. The ensuing physical network seems to be relatively stable. However, the “overshoot” in the volume swelling ratio is a strong indication of some loss of initial crystallinity or, most probably, chain dissolution.

Indeed, using the boric acid technique, we were able to determine that a certain amount of amorphous PVA was dissolved at 37 °C in water over the same period of time (Figure 3). By taking this into consideration, it was possible to calculate the true volume swelling ratio represented in the swelling results (Figures 1 and 2). These results clearly indicate that after an initial loss of PVA chains that were not incorporated in the physical network structure, the gels remained relatively stable as a function of time over a period of approximately 2 months. This stability is not necessarily true for longer periods of time as we will discuss in a future publication from our laboratory.

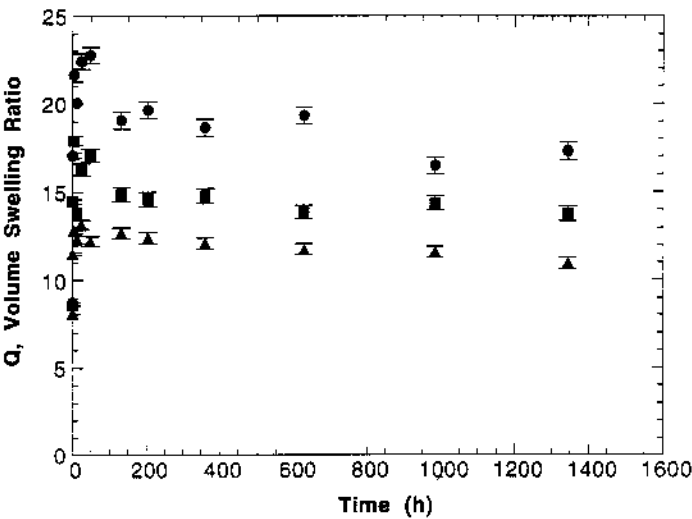


Figure 1. Equilibrium swelling at 37 °C of PVA hydrogels with 3 (●), 5 (■), and 7 (▲) cycles of 8 hour freezing and 4 hour thawing.

5.2. Crystalline Structure of Stable Gels

To further investigate the nature of the crystalline structure, we conducted differential scanning calorimetry experiments on PVA samples. Figure 4 shows a typical thermogram for a PVA sample prepared by freezing for 6 hours followed for thawing for 4 hours, this cycle being repeated 6 times. The first broad peak observed corresponds to water

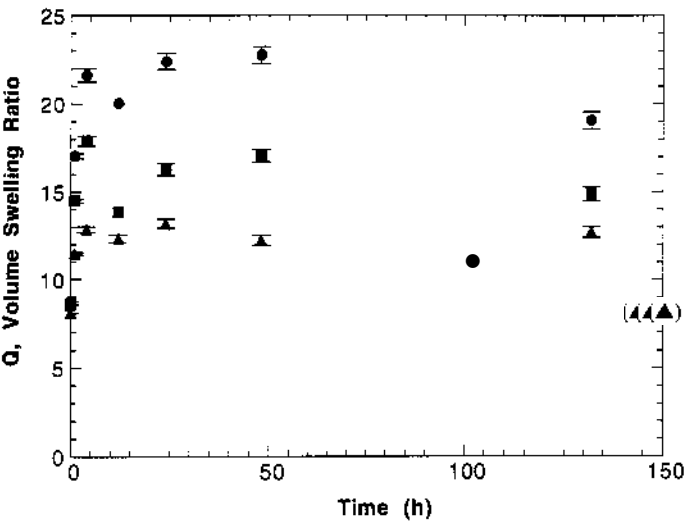


Figure 2. Initial swelling “overshoot” at 37 °C of PVA hydrogels with 3 (●), 5 (■), and 7 (▲) cycles of 8 hour freezing and 4 hour thawing.

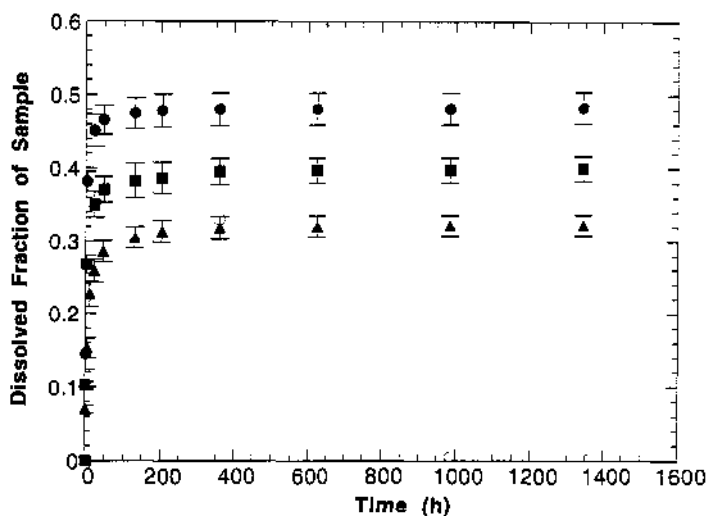


Figure 3. Fractional dissolution in water at 37 °C of PVA samples with 3 (●), 5 (■), and 7(▲) cycles of 8 hour freezing and 4 hour thawing.

evaporation, roughly starting at 85.1 °C. The melting peak of PVA starts at 196.8 °C and exhibits a maximum melting point of 211.6 °C. Based on these studies, the PVA degree of crystallinity on a dry basis was calculated as 32.9%. Taking the equilibrium swelling ratio of this sample into consideration, this degree of crystallinity corresponded to 6.7% on a swollen basis. Similar analysis for all other samples tested indicated that the degrees of

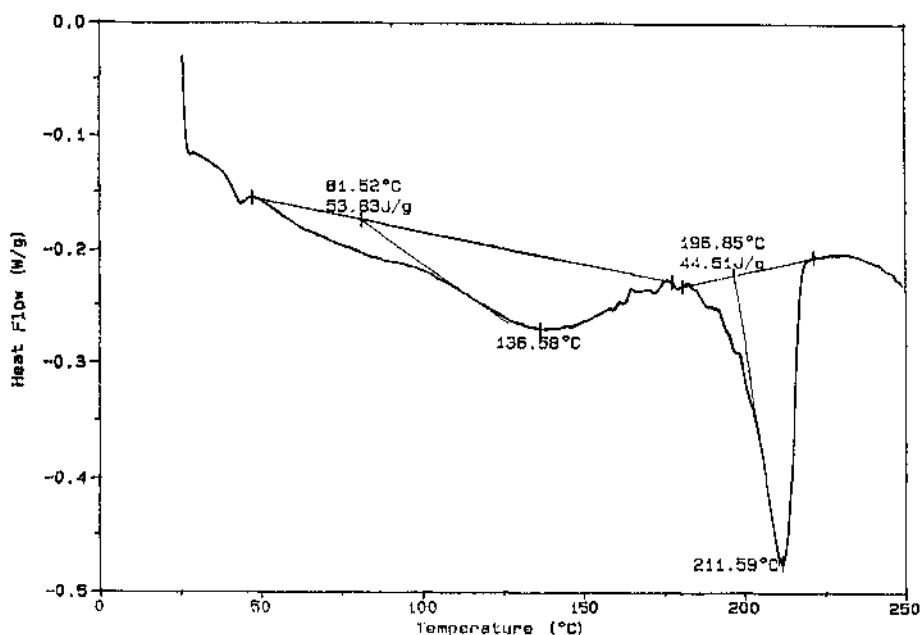


Figure 4. DSC thermogram for a PVA sample exposed to 6 cycles of 6 hour freezing and 4 hour thawing.

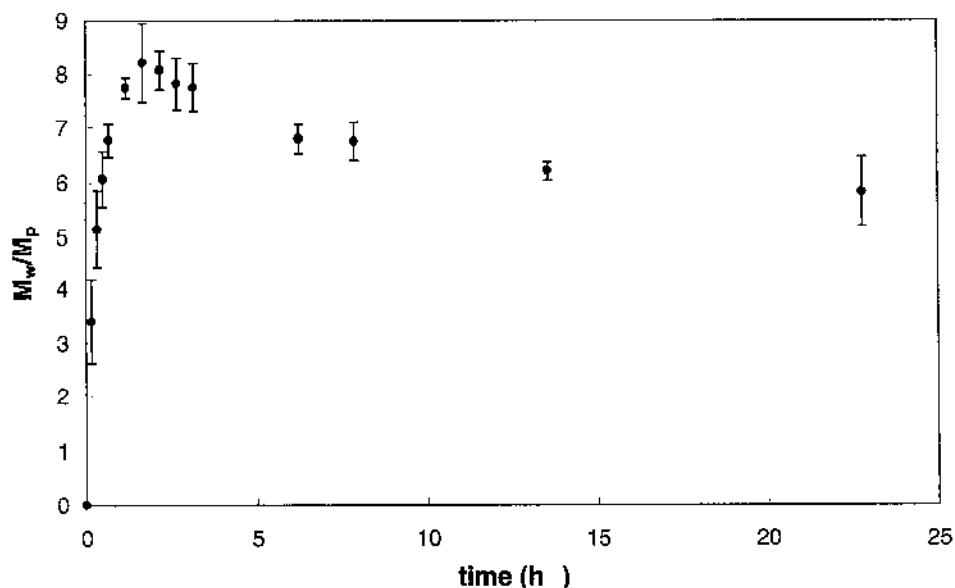


Figure 5. Equilibrium swelling at 37 °C of PVA samples with 6 cycles of 1 hour freezing and 45 minute thawing.

crystallinity on a swollen basis varied from 4 to 16%. Clearly this amount of crystallites was sufficient for the formation of a stable, three-dimensional network of physical crosslinks.

5.3. Gel Stability under Rapid Cycling Conditions

An important consideration in the development of stable PVA gels is the time required for the freezing/thawing cycles. Previous studies have shown that optimal freezing times for the attainment of a significant degree of crystallinity were 4 to 6 hours.

To investigate the possibility of utilizing rapid freeze/thaw cycles, we conducted a six-cycle study shown in Figure 5. These gels were frozen for 1 hour at -20 °C followed by thawing for 45 minutes at 25 °C for six cycles. At the end of the final thawing process, the samples were immersed in water at 37 °C and allowed to swell to equilibrium. The weight uptake of water during this swelling process is expressed as a function of time where the abscissa indicates the weight of water incorporated in the system per weight of the original polymer solution. These results indicate that after a small overshoot associated with the leaching out of any PVA chains that were not incorporated in the crystalline structure, the remaining gel achieved a constant weight after a period of about 20 hours.

Figure 6 shows the swelling behavior of a PVA sample prepared with 10 cycles consisting of freezing for 1 hour followed by thawing for 30 minutes. Again, stable gels were obtained after about 20 hours, although the increased amount of water in the gel was an indication of a less crystalline (therefore, less stable) structure. Further reduction of the freezing time lead to a series of interesting samples. For example, Figure 7 shows the swelling behavior of a PVA sample prepared with 10 cycles of freezing for only 30 minutes and thawing for 45 minutes. Again, the dimensional stability seemed to have been attained after about 15 hours, although the variation in the data is larger than that of samples with longer freezing and thawing times.

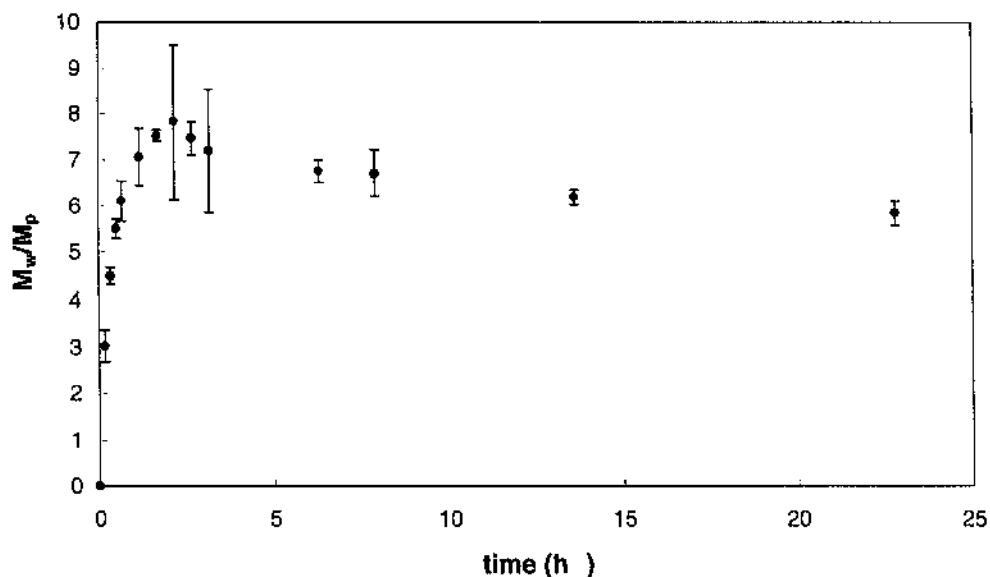


Figure 6. Equilibrium swelling at 37 °C of PVA samples with 10 cycles of 1 hour freezing and 30 minute thawing.

Although shorter-term freezing and thawing processes are possible, one inherent difficulty in these techniques is the very weak mechanical stability of the gels produced. Thus, although mechanical and dimensional stability of PVA solutions can be easily achieved by a rapid freezing process, the ensuing gels are only of theoretical interest. In our own studies, we were able to produce more stable gels with freezing/thawing tech-

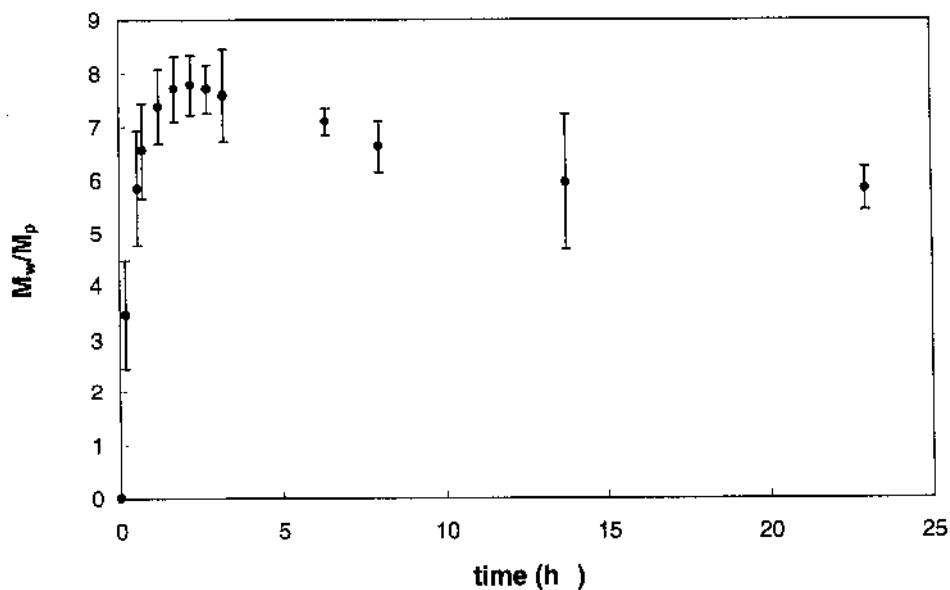


Figure 7. Equilibrium swelling at 37 °C of PVA samples with 10 cycles of 30 minute freezing and 45 minute thawing.

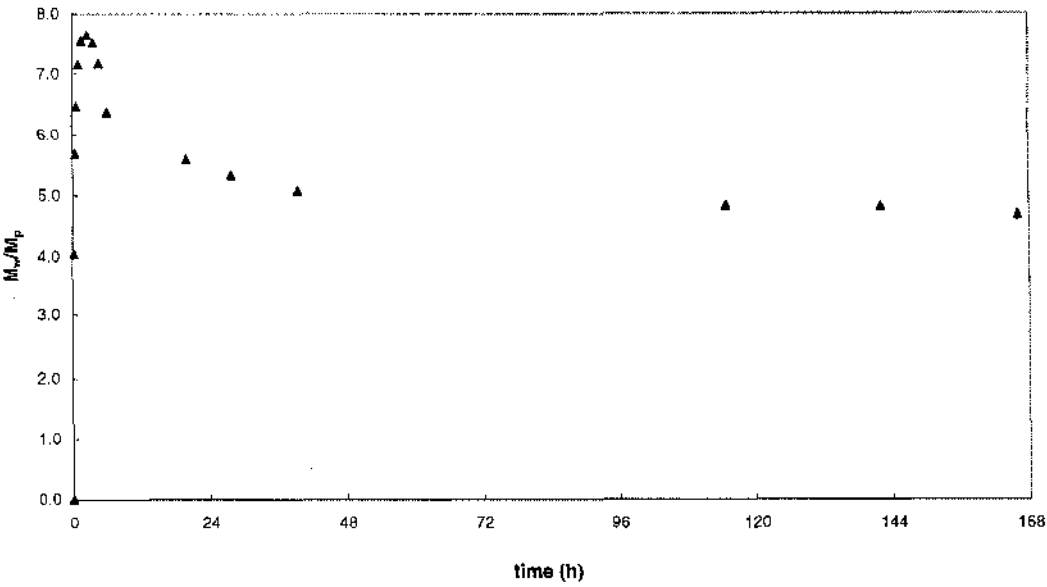


Figure 8. Equilibrium swelling at 37 °C of PVA samples with 7 cycles of 1 hour freezing and 1 hour thawing.

niques using freezing and thawing times of 1 hour each. Figures 8 and 9 show the swelling behavior of two such gels prepared after 7 and 12 cycles, respectively, and then swollen at 37 °C for up to 7 days. These gels have a higher degree of crystallinity (therefore a lower equilibrium swelling) than those previously discussed and seem to attain their equilibrium swelling after about 2 days. Obviously, further experimental studies are needed in order to ascertain the long-term stability of these gels.

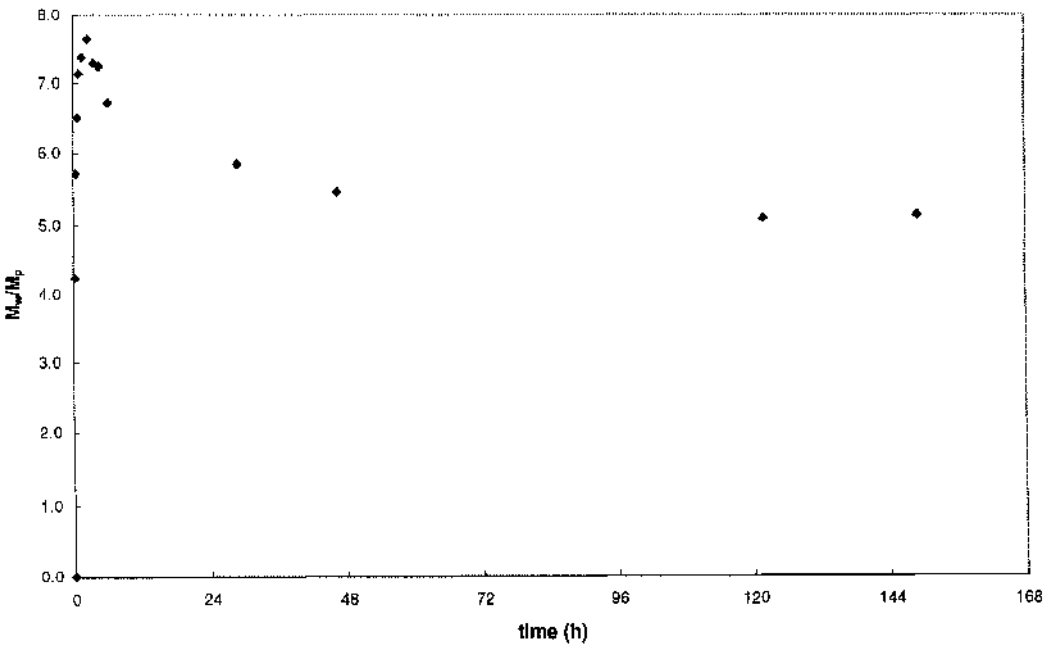


Figure 9. Equilibrium swelling at 37 °C of PVA samples with 12 cycles of 1 hour freezing and 1 hour thawing.

ACKNOWLEDGMENT

This work was supported in part by a grant from the Showalter Trust.

REFERENCES

1. Finch CA, Polyvinyl Alcohol Properties and Applications, Wiley, NY, 1973.
2. Peppas NA, Hydrogels in Medicine and Pharmacy, Vol 2, Polymers, CRC Press, Boca Raton, FL, 1987.
3. Peppas NA and Merrill EW, "Determination of interaction parameter χ_1 for PVA and water in gels crosslinked from solutions", J. Polym. Sci., 1976;14:459.
4. Klenina OV, Klenin VI, and Frenkel S Ya, "Formation and breakdown of supermolecular order in aqueous PVA solutions", Polym Sci USSR, 1970;12:1448.
5. Peppas NA, Merrill EW, "PVA Hydrogels: Reinforcement of radiation-crosslinked networks by crystallization", J. Polym. Sci., 1976;14:441.
6. Stauffer SR, Peppas NA, "Poly(vinyl alcohol) hydrogels prepared by freezing-thawing cyclic processing", Polymer, 1992;33:3932.
7. Peppas NA, "Turbidimetric studies of aqueous PVA solutions", Makromol. Chem. 1975;176:3433.
8. Nambu M, "Freeze-dried poly(vinyl alcohol) gel", US Patent No. 4,472,542. 1984.
9. Ohkura M, Kanaya T, Kaji K, "Gels of poly(vinyl alcohol) from dimethyl sulphoxide/water solutions," Polymer, 1992;33:3686.
10. Ficek BJ, Peppas NA, "Novel Preparation of poly(vinyl alcohol) microparticles without crosslinking agent for controlled drug delivery of proteins." J. Contr. Rel., 1993;27:259.
11. Hickey AS, Peppas NA, "Mesh size and diffusive characteristics of semicrystalline poly(vinyl alcohol) membranes prepared by freezing/thawing techniques," J. Membr. Sci., 1995;107:229.
12. Peppas NA, Mongia NK, "Ultrapure poly(vinyl alcohol) hydrogels with mucoadhesive drug delivery characteristics," Eur. J. Pharm. Biopharm., 1997;43:51.

ENZYMATIC MODIFICATION OF GUAR SOLUTIONS

Viscosity–Molecular Weight Relationships

Akash Tayal, Vandita Pai, Robert M. Kelly, and Saad A. Khan

Department of Chemical Engineering
North Carolina State University
Raleigh, North Carolina 27695-7905

1. ABSTRACT

Structurally modified guar galactomannans find application in food and petroleum industries as rheology modifiers. Enzymes provide a powerful and convenient method to modify guar structure. In this study, the kinetics of enzymatic degradation of guar solutions were investigated using SEC and rheology. Molecular information from SEC reveals the degradation reaction to be zeroth order in guar concentration. Further, the rate constant was proportional to enzyme concentration, demonstrating that the enzyme acts as a true catalyst. The zero shear viscosity was very sensitive to degradation, with several orders of magnitude change being observed over the course of polymer chain scission. A unique correlation was developed between degradation time, guar molecular weight and viscosity. This enables superposition of the viscosity-time profiles for different enzyme concentrations to a master curve; providing for *a priori* prediction of guar solution viscosity as a function of degradation time and enzyme concentration.

2. INTRODUCTION

Water-soluble polymers, such as guar, tara or locust bean, are used extensively in many applications because of their ready availability, low cost compared to other synthetic polymers, and ability to produce high viscosity solutions and gels at low polymer concentrations. In particular, these industrial gums have found a variety of uses in industries ranging from printing and paper to mining, textiles, foods, and, oil/gas production. Guar gum and its derivatives are used in the paper industry in the production of different grades

of paper and paperboard to improve dry strength, formation, drainage and retention properties.¹ In the mining industry, they are used as processing aids in the separation of minerals, such as aluminum and uranium, from their ores¹ with the gums performing two independent functions, flocculation of particles in aqueous suspension and depression of slimes in froth flotation. The textile industry uses guar gum and its derivatives as thickeners for dye liquors to impart desired mobility since they exhibit good electrolyte tolerance, high thickening efficiency and good compatibility with other dye liquors. Gums are also used in flatgoods printing where their greater solubility, easier wash out and lower level of insolubles results in better runnability and improved prints.¹

By far, the two major applications for guar are in oil and gas production and as food additives. In the oil and gas industry, viscous formulations of guar are used to enhance oil or gas production. In this process, known as hydraulic fracturing, metal-crosslinked guar, together with particulate suspensions (sand), are injected at high rates under high pressures through well-bores.² This induces fractures in the rock that propagate hundreds of meters radially outward from the well bore. The fracturing polymer is then degraded (typically using chemicals) and flushed out leaving behind a highly permeable channel of sand for outflow of gas or oil.³ Enzymes offer an efficient and environmentally benign way of degrading the guar gels. More importantly, the use of thermostable enzymes that are active only at high temperatures would allow to tap deeper reservoirs and enhance oil/gas production significantly.⁴

Enzymatically modified guar also has tremendous potential in food applications. Galactomannans such as guar and locust bean gum are widely used in foods such as cheeses, dressings, dairy and bakery products to improve mouthfeel and chewiness, elongate shelf-life through moisture retention and prevent syneresis.⁵ Many of these functions are achieved by mixing galactomannans with other polysaccharides, such as xanthan and carrageenans. Galactomannans have the ability to effect gelation in polysaccharide systems that are otherwise non-gelling, rendering stability, texture and controlled rheological characteristics to food. Locust bean gum forms smooth, firm, elastic synergistic gels with xanthan, κ -carrageenan and agarose, for example. Such synergistic combinations are employed in canned meat products, confectionery products, dips and spreads, acidified milk gels, etc. The supply of locust may dwindle in the future owing to the long maturation period, labor-intensive harvesting and competition from other cash crops.⁶ In comparison, guar is cheaper and readily available which makes it a suitable replacement for locust bean. Hence, it is of commercial interest to see if the structure of guar can be modified to convert it to a material having the desired functional properties of locust bean. Guar and locust bean both have an irregular distribution of galactose side chains along the mannan backbone, with the primary difference being that guar has a higher mannose to galactose ratio (3:2) compared to locust bean (4: 1). This mannose to galactose ratio is critical as the extent of interaction of galactomannans with other polysaccharides depends on the level of substitution of the (1–4)-linked β -D-mannan chain by the (1–6)-linked α -D-galactose side chain.⁷ Enzymes offer a powerful way to selectively clip off the galactose side chains from guar molecules to not only mimic the architecture of locust beans but also provide new materials for making synergistic gels with other polysaccharides.

Guaran, the functional polysaccharide in guar gum is a chain of (1–4)-linked β -D-mannopyranosyl units with single (1–6)-linked α -D-galactopyranosyl units as the side chains. Recent information on the fine structures of guar galactomannan indicate that the galactose distribution is irregular to random.⁷ The molecule is susceptible to enzymatic hydrolysis at three types of sites, namely, the endo- and exo- β -1,4 linkages between the D-mannose sugar units on the backbone and the α -1,6 linkage between the mannose unit

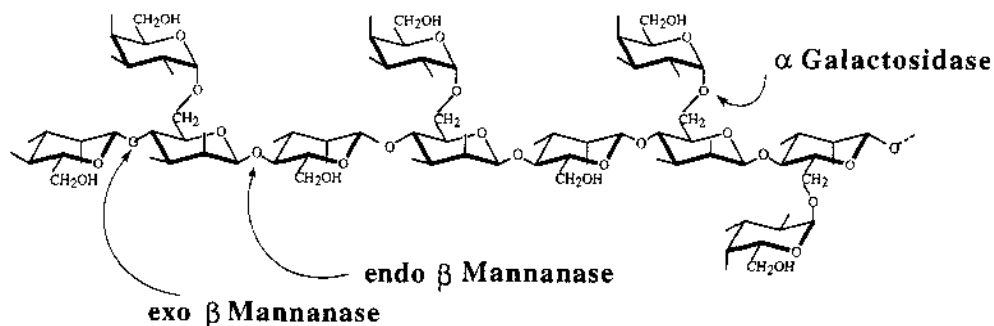


Figure 1. Schematic representation of a guar molecule showing sites susceptible to enzymatic hydrolysis.

on the backbone and the galactose side chain (Figure 1). The enzymes that cleave these bonds are referred to as endo- and exo- β -mannanases and α -galactosidase, respectively. The cleavage of these bonds reduces polymer molecular weight and changes rheological behavior. Our ultimate goal is to understand the relationship between molecular and rheological property changes of guar solutions and gels during the course of enzymatic hydrolysis.

Although there is considerable rheological information on non-degraded guar solutions,^{8,9} not much is known about the rheological characteristics of degraded guar. Tjon-Joe-Pin¹⁰ used viscometry to measure the effectiveness of commercial enzymes in reducing guar viscosity. He proposed a power law model (for viscosity as a function of shear rate) to follow the enzymatic degradation. While this model works fairly well at high shear rates, it greatly overestimates viscosity at low shear rates. Similarly, the thermal degradation of guar has been investigated¹¹ using a slit viscometer at very high shear rates (1000–10,000 sec⁻¹). However, neither of these studies provide any fundamental understanding on the kinetics and mechanisms of enzymatic degradation. To the best of our knowledge, no rheological characterization of gel degradation has been previously reported. Rheological studies of non-degraded guar-borax systems have revealed that it behaves as a temporary gel with solid-like properties at short to intermediate time scales and shows solution-like behavior at long times. The network properties can be correlated to system variables like polymer, cross-linker concentration and changes in temperature and pH.^{12,13}

In this chapter, we focus on the enzymatic degradation of native guar gum solutions. Fundamental understanding of the kinetics and mechanism of enzymatic degradation is important, not only from the standpoint of modifying guar, but also for developing schemes for modifying water soluble polymers in general. In this context, we examine the relationship between molecular structure and rheological properties of guar solutions during enzymatic hydrolysis.

3. EXPERIMENTAL MATERIALS AND METHODS

Food grade guar galactomannan (Jaguar 6003, Rhone-Poulenc, NJ) was purified through Soxhlet extraction with ethanol.¹⁴ Hydrocolloidal dispersions were prepared by dispersing purified guar powder in water containing 0.5M sodium chloride and 0.05M sodium thiosulfate.¹⁵ Additionally, solutions were centrifuged at 20000 \times g for 1.5 hours to

obtain a clarified solution. Unless otherwise specified, enzymatic degradation of the guar solution was performed using Gamanase, a commercial hemicellulosic extract from *Aspergillus niger*, containing primarily a mixture of endo- β -mannanases and α -galactosidase (Novo Nordisk, Bioindustrials Inc., Danbury, CT). All degradation experiments were conducted at 25 °C. Required amounts of enzyme were injected into the equilibrated guar using a microsyringe. After the guar solution had been degraded for the required time period, it was tested on a Rheometrics Dynamic Stress Rheometer, DSR 100. To prevent evaporation of water from the guar solution, a thin layer of a low viscosity silicone oil was spread on the surface of the sample exposed to the atmosphere. Experiments were repeated to ensure that the addition of oil did not affect the rheological data.

Molecular weight (MW) averages and molecular weight distributions (MWD) were determined by GPC on a bank of Ultrahydrogel columns (Ultrahydrogel 2000, 500, and 120, Waters Corporation, Milford, MA). A guard column (Ultrahydrogel Guard Column, Waters) was placed ahead of the column bank. A Shimadzu HPLC system with RID-6A differential refractive index detector was used. The mobile phase was water containing 0.1 M sodium nitrate and 5×10^{-3} M sodium azide; the flow rate was fixed at 0.8 ml/min. and a temperature of 45°C was used. All degraded guar samples were diluted to 0.05%-0.1% (w/v) (to eliminate viscous spreading in the columns) and filtered through 0.45 mm filter prior to analysis. The dilution was made in 4M urea solution which also served to denature the enzyme and stop the degradation reaction. The bank of columns was calibrated using pullulan standards. The MW distributions thus obtained were checked for skewing and symmetrical spreading using ASTM method D3536-91. Both effects were found to be small and were neglected. The molecular weight averages were calculated by numerical integration of the MW distribution curve. The reproducibility in the MW averages was within $\pm 2\%$. Details on all experimental procedures is presented elsewhere.¹⁶

4. RESULTS AND DISCUSSION

Figure 2 shows a representative plot of guar solution viscosity as a function of shear stress for different time periods during enzymatic hydrolysis. For all samples, we observe a Newtonian behavior with viscosity independent of shear stress at low shear stress. At higher shear stresses, we observe a slight shear thinning where the viscosity decreases with shear stress. We also find the viscosity to be significantly affected by the enzymes decreasing by more than two decades in five hours. Viscosity reduces by more than an order of magnitude following one hour of sample incubation with the enzyme. Incubation of the sample for four additional hours results in a further decrease in viscosity by an order of magnitude. These results indicate that viscosity reduction is much more rapid during the early stages of enzymatic hydrolysis than at the latter stages.

In order to further investigate the time-dependent behavior of viscosity, we have focussed only on the Newtonian viscosity plateau referred to as the zero shear viscosity η_0 . Figure 3 shows the zero shear viscosity of a 1% guar solution as a function of degradation time. We observe a sharp decrease in viscosity value by several orders of magnitude in the first 5 hours. At longer times, the viscosity seems to asymptote slowly to a value in the range of ~ 0.1 poise. This long-time asymptote may be due to the actual slow down in the chain scission reaction itself or because the viscosity is no longer sensitive to chain scission and has attained as low a value as it can achieve. Further information on this aspect can only be obtained from molecular weight measurements. It should also be noted here that the enzyme system used in this experiment was a mixture of both endo- β -mannanases and α -

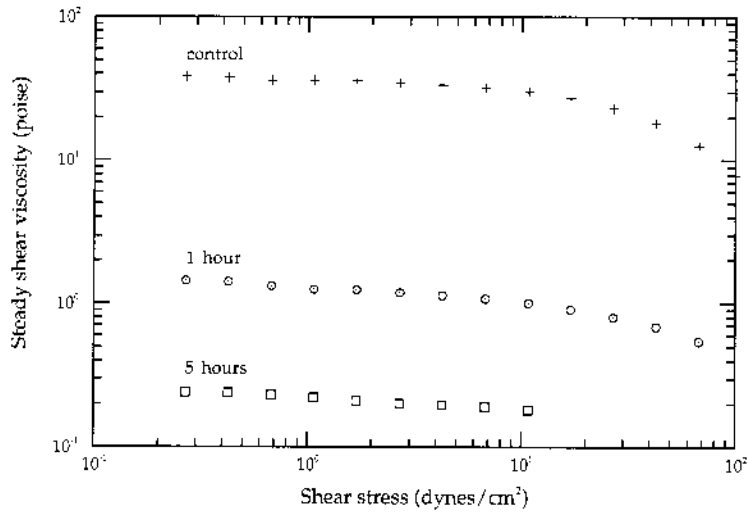


Figure 2. Viscosity as a function of shear stress for a 0.7% (w/v) guar solution shown for three different incubation period with the enzyme Gammanase: 0, 1, and 5 hours. Enzyme concentration was 2×10^{-4} units/ml of guar solution.

galactosidase, the main- and side-chain cleaving enzymes respectively. The relative effect of each of these enzymes in viscosity reduction therefore needs further elucidation.

To isolate the role α -galactosidase, the side-chain cleaving enzyme, plays in viscosity reduction, guar samples were incubated for different time periods with only this enzyme (obtained from Megazyme Corporation, Ireland). Figure 4 shows the viscosity versus shear stress plot of such a samples for two different incubation times. We find the

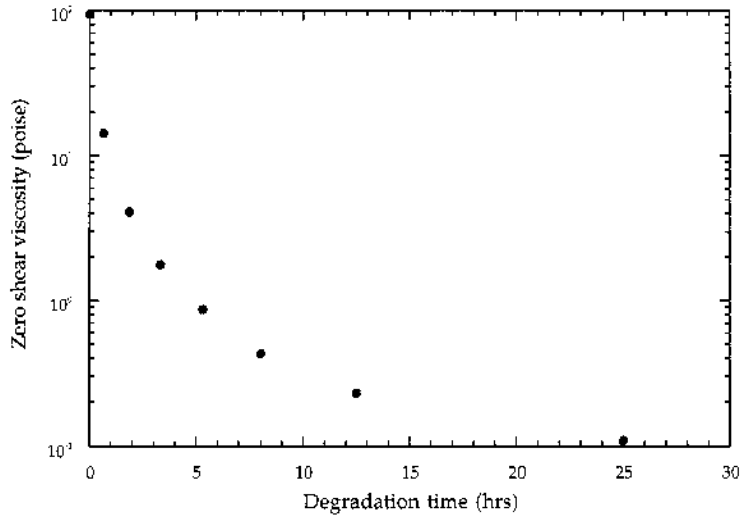


Figure 3. Zero-shear viscosity as a function of enzymatic degradation time for a 1% (w/v) guar solution. Enzyme concentration was 8.3×10^{-4} units/ml of guar solution.

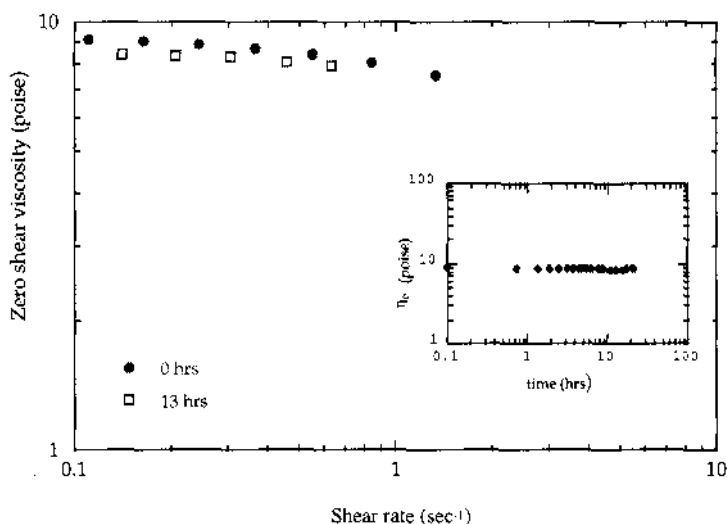


Figure 4. Viscosity versus shear stress plots of a 1 % (w/v) guar solution exposed to different extents (0 hr., 13 hr) of α -galactosidase, the side chain cleaving enzyme. The inset shows zero shear viscosity as a function of degradation time.

viscosity of the samples to be within 5% of each other following 13 hours of exposure to the enzyme. The inset in Figure 4 reveals changes in zero shear viscosity as a function of degradation time during guar hydrolysis with α -galactosidase. We find the viscosity to remain effectively unchanged for 21 hours. These results suggest that any viscosity reduction in guar, observed in Figures 2 and 3, can be attributed to the main-chain cleaving enzyme only. Our trends are also consistent with the work of McCleary⁷ who suggests that removal of galactose side groups causes minimal changes in viscosity except at very long time periods when considerable removal of the galactose sugars causes the guar molecules to precipitate out of the solution.

Figure 5 shows GPC traces of a guar solution for three different degradation times, 0, 2, and 13 hours. Two things are apparent from this figure. First, the peak maximum shifts by two orders of magnitude during the course of enzymatic hydrolysis suggestive of significant reduction in molecular weight. Secondly, the peak broadens considerably with degradation time indicating an increase in molecular weight distribution. Calculation of the polydispersity index (defined as the ratio of the weight average to the number average molecular weight, M_w/M_n) indeed shows it to increase from an initial value of 3.9 to about 12 during the enzymatic hydrolysis process.¹⁶ This is an interesting result as it suggests that the enzyme is possibly breaking the polymer backbone in a random fashion rather than a systematic way, such as cleaving it at the center, in which case the polydispersity index would remain constant or decrease.

The weight- (M_w) and number-average (M_n) molecular weights, obtained from the chromatograms, are shown in Figure 6 as a function of degradation time. We find the molecular weights of the polymer to show a rapid initial decrease followed by an asymptotic behavior, reminiscent of the viscosity trend observed in Figure 3. This seems to suggest that the viscosity kinetics is dictated, at least qualitatively, by the changes in the molecular weight. It is interesting to note that most of the molecular weight changes occur in the first 4–6 hours of the experiment.

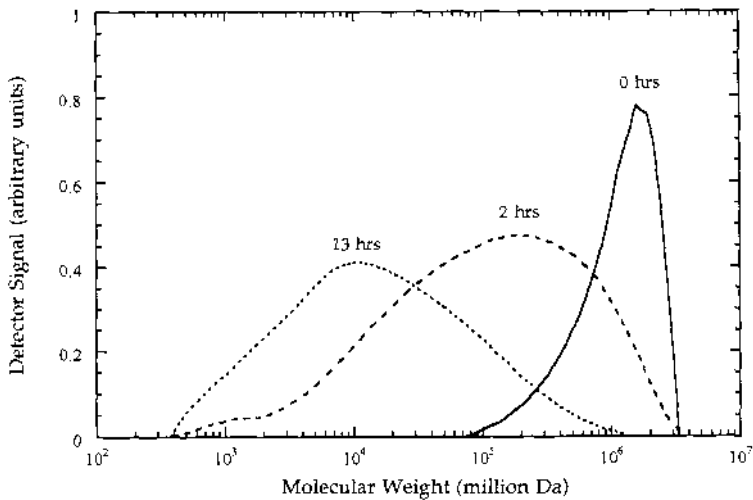


Figure 5. Typical chromatograms of a 1% (w/v) guar solution shown for three different times during enzymatic hydrolysis: 0, 2 and 13 hours. Enzyme concentration was same as that for Figure 3.

The temporal changes in viscosity and molecular weight during enzymatic degradation is correlated in Figure 7 which reveals the dependence of zero shear viscosity on molecular weight. For the entire range of molecular weight shown in this figure, the samples were above the overlap concentration regime.¹⁶ In this range, conventional polymers depict a power-law dependence of viscosity on molecular weight with exponents of 3–3.5.^{9,17} We find guar viscosity to be a very strong function of molecular weight and displaying two different power-law regimes. At lower molecular weights corresponding to the later stages of degradation, viscosity scales with molecular weight with an exponent approxi-

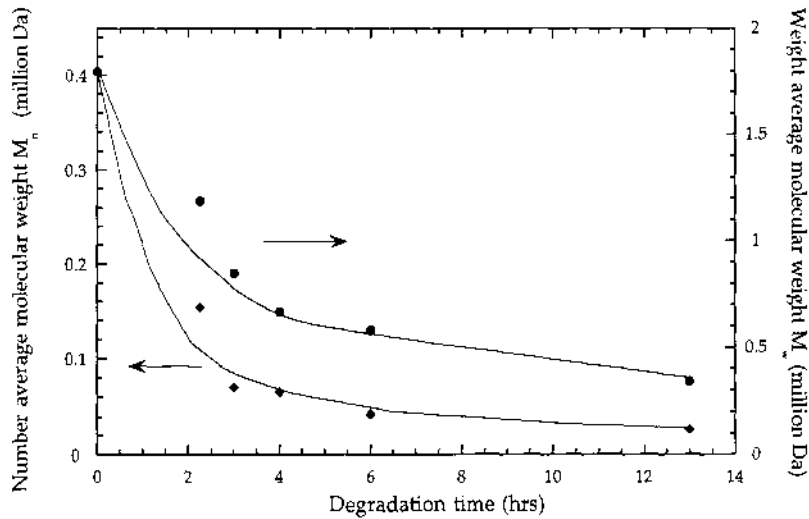


Figure 6. Changes in guar molecular weight during enzymatic degradation. Enzyme concentration was same as that for Figure 3.

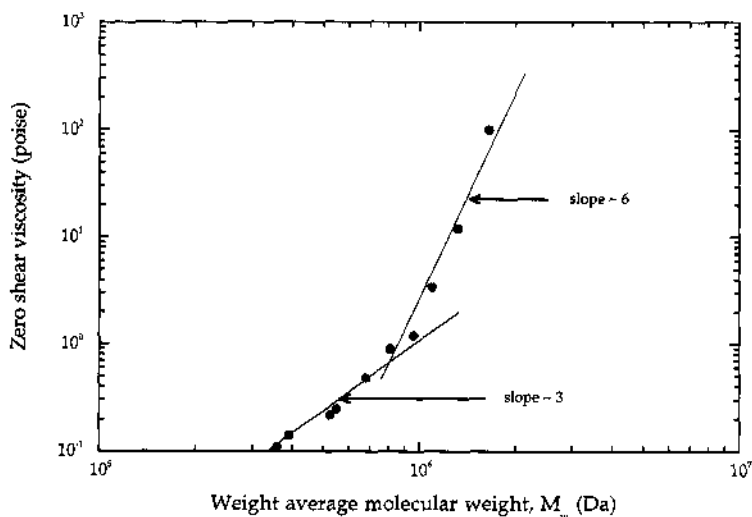


Figure 7. Scaling of zero-shear viscosity with weight average molecular weight during enzymatic hydrolysis of a 1 % (w/v) guar solution. Enzyme concentration was same as that for Figure 3.

ming 3, consistent with traditional polymers. At higher molecular weights during the early stages of degradation, we observe a power-law behavior with an exponent slightly exceeding 6, significantly larger than that observed in conventional polymers. However, high scaling factors (~ 8) are not unusual for associative polymers.¹⁸ The fact that guar forms “hypercanglement”^{8,9} through intermolecular associations could possibly explain the observed behavior. Interestingly, our exponent is slightly higher but well within the range of the exponent (~ 5.3) we calculate using the data of Robinson *et al.*⁹ However, the change in molecular weight dependency of viscosity at lower molecular weights is somewhat surprising. One possible explanation could be that the hyperentanglement effect diminishes in this regime. Work is currently underway to investigate these observations further.

5. CONCLUSION

The viscosity of guar solutions during enzymatic hydrolysis is only affected by endo- β -mannanase, the enzyme that cleaves the polymer back bone. Such an enzyme significantly reduces guar solution viscosity by as much as two orders of magnitude. The viscosity reduction kinetics reveal an initial rapid decrease followed by an asymptotic decay closely resembling the trends observed in the average molecular weight reduction. Correlation of zero shear viscosity with molecular weight reveals viscosity to follow a scaling relation with an unusually high scaling exponent of ~ 6 .

ACKNOWLEDGMENTS

The authors gratefully acknowledge the National Science Foundation and the US Department of Agriculture for funding this research.

REFERENCES

1. Maier H, Anderson M, Karl C and Magnuson K, "Industrial gums: Polysaccharides and their derivatives" In *Guar, locust bean, tara and fenugreek gum*, R.L. Whistler and J.N. BeMiller (eds.), Academic Press, CA, 1993.
2. Prud'homme RK, Constien V, and Knoll S, "Polymers in aqueous media: Performance through association", *ACS Advances in Chemistry* Series 223, 89, J.E. Glass (ed.) Washington D.C., 1989.
3. Borchardt JK, "Oil-Field Chemistry: enhanced recovery and production", In *Chemicals used in oil-field operations*, ACS Symposium Series 396, J.K. Borchardt and T.F. Fun (eds.), 1989.
4. Kelly RM, Khan SA, Leduc P, Tayal A, and Prud'homme RK, "Methods and compositions for fracturing subterranean formations", US Patent 5,421,412. 1995.
5. Moms, ER, "Food Gels" In *Mixed Polymer Gels*, P. Harris (ed.), Elsevier Applied Science., NY, 1990.
6. Bulpin PV, Gidley MJ, Jeffcoat R, Underwood DR, "Development of a biotechnological process for the modification of galactomannan polymers with plant α -galactosidase", *Carbohydrate Polymers* 1990;12:155.
7. McCleary BV, Amado R, Waibel R, Neukom H, "Effect of galactose content on the solution and interaction properties of guar and carob galactomannan", *Carbohydrate Research*, 1981;92:269.
8. Morris ER, Cutler AN, Ross-Murphy SB, Rees DA, and Price J, "Concentration and shear rate dependence of viscosity in random coil polysaccharide solutions", *Carbohydrate Polymers*, 1981;5:1.
9. Robinson G, Ross-Murphy SB, and Morris ER, "Viscosity-molecular weight relationships, intrinsic chain flexibility, and dynamic solution properties of guar galactomannan", *Carbohydrate Research*, 1982;17:107.
10. Tjon-Joe-Pin R, "Enzyme breaker for galactomannan based fracturing fluids", U.S. Pat. No. 5,201,370. 1993.
11. Bradley TD, Ball A, Harding SE, and Mitchell JR, "Thermal degradation of guar gum", *Carbohydrate Polymers*, 1989;10:205.
12. Pezron E, Ricard A, and Leibler L, "Rheology of galactomannan-borax gels", *Journal of Polymer Science: Part B: Polymer Physics*, 1990;28:2445.
13. Kesavan S, "Rheology of aqueous gels", Ph.D. Thesis, Princeton University, 1992.
14. Whitcomb PJ, Gutowski J, and Howland WW, "Rheology of guar solutions", *Journal of Applied Polymer Science*, 1980;25:2815.
15. Tayal A, Kelly RM, Khan SA, "Viscosity reduction of hydraulic fracturing fluids through enzymatic hydrolysis", *SPE Journal*, 1997;2(2):204.
16. Tayal A, "Enzymatic hydrolysis of guar galactomannan solutions and gels: molecular structure and rheology", Ph.D. Thesis, North Carolina State University, 1997.
17. Graessley WW, "Physical Properties of Polymers" In *Viscoelasticity and flow in polymer melts and solutions*, 2nd edition, J.E., Mark (ed.), ACS Publishers, Washington D.C., 1993.
18. English RJ, Gulati HS, Jenkins RD, Khan SA, "Solution rheology of a hydrophobically modified alkali-soluble associative polymer", *J. Rheology*, 1997;41:427.
19. Goycoolea FM, Morris ER, Gidley MJ, "Viscosity of galactomannans at alkaline and neutral pH: evidence of hyperentanglement in solution", *Carbohydrate Polymers*, 1995;27:69.

This page intentionally left blank.

THE INFLUENCE OF ADDITIVES AND IMPURITIES ON CRYSTALLIZATION KINETICS

An Interfacial Tension Approach

Wenju Wu and George H. Nancollas

Department of Chemistry
State University of New York at Buffalo
Buffalo, New York 14260

1. ABSTRACT

Expressions describing the influence of additives and impurities on the kinetics of mineralization and demineralization have been derived from an interfacial tension point of view. In aqueous solution, the Lifshitz-van der Waals interfacial tension component changes very little, but the Lewis base (or electron-donicity) surface tension parameter varies markedly as a function of additive and impurity concentrations. The inhibiting effects of simple cations on crystal growth in solution may result from the increase in interfacial tension accompanying their adsorption on the surfaces. In the case of polymers or macromolecules, the kinetics of crystallization will not only depend upon the substrata but also the surface properties of the additives. Nucleation of calcium phosphate phases was observed only on surfaces having low solid/solution interfacial tension and relatively high electron-donicity of the solid surfaces. Such properties were found for human serum albumin immobilized on polymer solid surfaces of poly(methyl methacrylate) (PMMA) and poly(tetrafluoroethylene-co-hexafluoropropylene) (FEP), and following radiofrequency glow discharge (RFGD) treatment which mimicked the adsorption of impurity OH^- ions on the surfaces.

2. INTRODUCTION

The presence of additives and impurities, ranging from simple ions to small molecules and polymers, including proteins at crystal surfaces, is frequently found to have a profound effect on crystallization properties. Some impurities can suppress growth entirely; others

may actually enhance nucleation and crystal growth. While the effects may be observed at very low concentrations (less than 1 part per million) other additives require much greater concentrations. Although the influence of impurities on the kinetics of crystallization in solution has been extensively studied experimentally,¹⁻²⁰ satisfactory theoretical treatments are generally lacking.²¹⁻²⁶ Proposed mechanisms have been discussed in term of two main factors: 1) strong adsorption and immobilization of the foreign species on the crystal surfaces, thereby impeding the movement of surface steps and resulting in a decreased rate of step generation;²² and 2) poisoning of active growth sites.²³ With these general mechanisms in mind, previous studies of the influence of impurities on the kinetics of mineralization and demineralization have largely focused on their adsorption isotherms at the crystalline surfaces.⁶⁻²⁰ In this work, the influence of impurities on crystallization kinetics is discussed from the point of view of interfacial interactions, and the mechanisms of inhibition and promotion are elucidated using the interfacial tension component theory.

3. THERMODYNAMICS OF CRYSTALLIZATION

3.1. Crystal Growth in Pure Solution

There are three hypothetical steps involving free energy changes for the two-dimensional growth of a crystal on its seeding surfaces.²⁷ First, the transference of n molecules from supersaturated solution having a solute concentration C_B and a chemical potential μ_B , at constant temperature, T , and pressure, P , to a saturated state with corresponding parameters, C_o and μ_o . The free energy change or crystallization driving force is usually expressed by Eq. (1)

$$\Delta G = n(\mu_o - \mu_B) \quad (1)$$

Since

$$\mu = kT \ln(C) \quad (2)$$

Eq. (1) becomes

$$\begin{aligned} \Delta G &= nkT \ln\left(\frac{C_o}{C_B}\right) \\ &= -nkT \ln\left[1 + \frac{C_B - C_o}{C_o}\right] \\ &= -nkT \ln(1 + \sigma) = -nkT \ln S \end{aligned} \quad (3)$$

where k is the Boltzmann's constant, σ , the relative supersaturation ($S-1$), and S , the supersaturation ratio (C_B/C_o). For crystallization reactions involving electrolytes, the concentrations must be replaced by activities, and the supersaturation ratio is expressed by Eq. (4)

$$S = \left(\frac{IP}{K_{so}} \right)^{1/v} \quad (4)$$

where IP is the ionic activity product for the precipitating phase in a solution, K_{so} is its activity solubility product, and v the number of ions in the formula unit.

During the addition of n molecules from saturated solution onto the surface of the crystal, there is no free energy change since the crystal surface is in equilibrium with C_o . As these n molecules are allowed to build up into pillbox-shaped embryos of radius r and height h (Figure 1A), free energy changes involving an isothermal compression are obtained according to Eq. (5)²⁷

$$\Delta G = 2\pi hr\gamma_{LE} \quad (5)$$

where γ_{LE} is the interfacial tension between solution and embryo or nucleus. Thus, the total free energy change to form a nucleus of radius r is given by the sum of Eqs. (3) and (5).

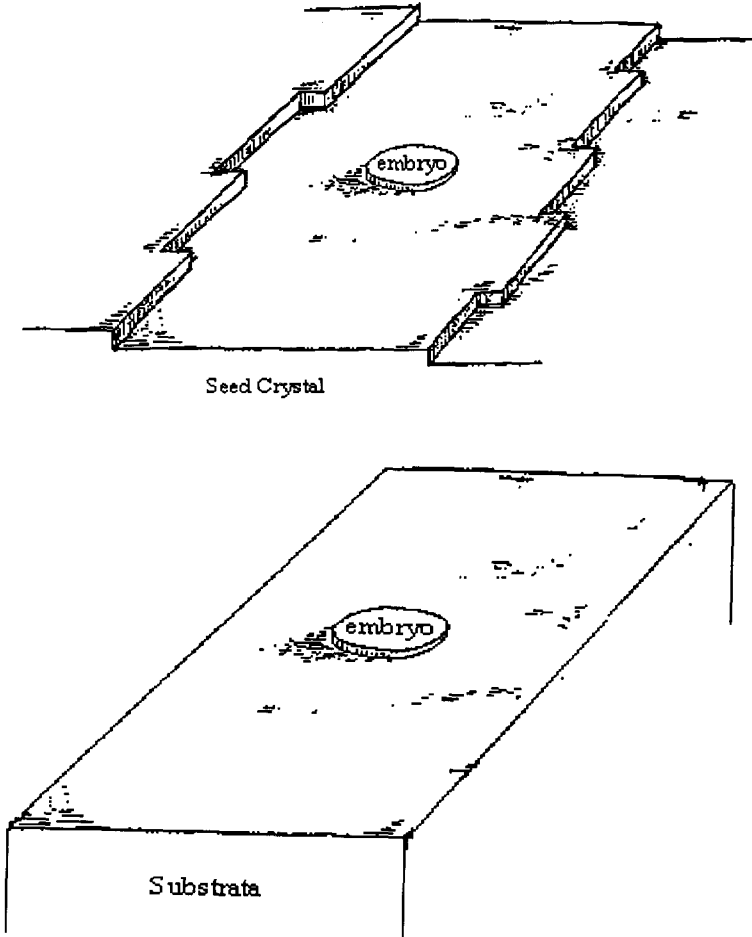


Figure 1.

$$\begin{aligned}
\Delta G &= 2\pi r h \gamma_{LE} - nkT \ln(1 + \sigma) \\
&= 2\pi r h \gamma_{LE} - \left(\frac{\pi r^2 h k T}{V_m} \right) \ln(1 + \sigma)
\end{aligned} \tag{6}$$

where $n = \pi r^2 h / V_m$ and V_m is the molecular volume. Eq.(6) yields the typical free energy/embryo radius relationship for homogeneous nucleation.

3.2. Crystallization in the Presence of Additives and Impurities

It is well-known that an increase in the concentration of inorganic electrolytes in aqueous solution increases the surface tension at the solution/vapor interface while the presence of small amounts of surfactant at the solution surface markedly decreases the surface tension.²⁸ The relationship between adsorption and surface tension-surface energy was established by the Gibbs²⁸ equation (7):

$$\Gamma = - \frac{1}{RT} \left(\frac{d\gamma}{d \ln C} \right)_T \tag{7}$$

where Γ is the surface excess, R , the gas constant, and C , the concentration of solute. Eq. (7) expresses the relationship between surface excess of solute (adsorption) and the surface tension of the interface. In contrast, at solid-gas (air) interfaces, γ is not directly measurable. However, if the amount of adsorbed material can be determined, this may also be related to the reduction of surface free energy through Eq. (7).

During crystallization reactions in the presence of impurities, although the interfacial tensions or free energies at the crystal/solution interfaces are changed through additive or impurity adsorption, it has hitherto been impossible to apply theoretical or experimental techniques to determine the changes, even qualitatively. Since the adsorption of species on a crystal surface essentially results in a completely different surface, equations for qualitatively discussing the influence of additives and impurities on crystallization kinetics are derived, in this paper, by analogy to heterogeneous nucleation processes. The corresponding free energy for heterogeneous nucleation reactions involving the wetting contact angle (θ) of embryos on substrata surfaces has been discussed by Becker and Doring²⁹ and by Volmer.³⁰ However, these models are less meaningful since the contact angle concepts provide little insight into the kinetics of crystallization at foreign surfaces.³¹⁻³³ In the present treatment, the use of contact angle concepts has been avoided in favor of a model involving the formation of island nuclei of height h and radius r .

In heterogeneous nucleation reactions, since the seed crystal surfaces in the corresponding homogeneous processes are replaced by foreign substrata or impurity-poisoned surfaces, the nuclei or embryos must adhere to the substrata quite firmly rather than forming loose deposits. The net free energy change will therefore consists of adhesive (ΔG_{adh}) terms given by Eq. (8) in addition to the free energy for homogeneous nucleation (Figure 1B),

$$\Delta G_{adh} = \pi r^2 (\gamma_{SE} - \gamma_{LE} - \gamma_{SL}) \tag{8}$$

where γ_{SL} is the interfacial tension between the foreign or impurity poisoned surfaces and the solution, and γ_{SE} is the interfacial tension between the foreign surface and embryo.

Therefore, the total free energy change to form a nucleus of radius r on a foreign surface S is given by Eq. (9)

$$\Delta G^{het} = 2\pi r h \gamma_{LE} + \pi r^2 (\gamma_{SE} - \gamma_{LE} - \gamma_{SL}) - \frac{\pi r^2 h k T}{V_m} \ln(1 + \sigma) \quad (9)$$

For a nucleus having critical size,

$$\frac{\partial \Delta G^{het}}{\partial r} = 0 \quad (10)$$

and

$$\frac{\partial \Delta G^{het}}{\partial h} = 0 \quad (11)$$

It follows that the critical nucleus dimensions are given by Eqs. (12) and (13)

$$r^* = \frac{2V_m \gamma_{LE}}{kT \ln(1 + \sigma)} \quad (12)$$

and

$$h^* = \frac{2V_m (\gamma_{SE} - \gamma_{LE} - \gamma_{SL})}{kT \ln(1 + \sigma)} \quad (13)$$

Substitution in Eq. (9) leads to Eq. (14):

$$\Delta G_{het}^* = \frac{4\pi V_m \gamma_{LE}^2}{kT \ln(1 + \sigma)} (\gamma_{SL} + \gamma_{LE} - \gamma_{SE}) \quad (14)$$

The nucleation rate J may be given by Eq. (15)^{29,34,35}

$$J = Z \frac{kT}{h} S^* \exp\left(-\frac{\Delta G_a}{kT}\right) N \exp\left(-\frac{\Delta G_{het}^*}{kT}\right) \quad (15)$$

and, in abbreviated form, as Eq. (16)

$$J = \Omega \exp\left(-\frac{\Delta G_{het}^*}{kT}\right) \quad (16)$$

where Z is the so-called Zeldovich factor, ΔG_a is the activation free energy, and Ω is the pre-exponential factor. By substituting Eq. (14) into Eq. (16), the nucleation rate for heterogeneous nucleation is approximated by Eq. (17)

$$J = \Omega \exp \left[-\frac{4\pi V_m \gamma_{LE}^2}{k^2 T^2 \ell n(1+\sigma)} (\gamma_{SL} + \gamma_{LE} - \gamma_{SE}) \right] \quad (17)$$

In the reverse, dissolution reaction, the free energy change involves a detachment rather than an adhesion free energy, and the corresponding expression is given by Eq. (18)

$$\Delta G_{\text{det}} = \pi r^2 (\gamma_{SL} + \gamma_{LE} - \gamma_{SE}) \quad (18)$$

accordingly, the rate of dissolution in the presence of impurities is given by Eq. (19)

$$J = \Omega \exp \left[-\frac{4\pi V_m \gamma_{LE}^2}{k^2 T^2 \ell n(1+\sigma)} (\gamma_{SE} - \gamma_{SL} - \gamma_{LE}) \right] \quad (19)$$

4. METHODOLOGY

4.1. Kinetics of Crystallization

The constant composition method³⁶ has been used quite extensively to investigate the influence of additives or impurities on the kinetics of crystallization. This technique enables the rates of reaction to be measured over extended time periods while the reaction solution compositions are maintained constant for all species, both additives and crystal lattice ions. In conventional free-drift and potentiostatic seeded growth procedures, the solution supersaturations change during the reactions due to the reduction in concentration of the lattice ions. In some systems, at each stage, the supersaturated solutions may be metastable with respect to different phases which can form and subsequently redissolve as the concentrations decrease. For the calcium phosphates, another problem is associated with the lack of precision of the analytically determined calcium and phosphate concentrations.

These problems were avoided with the development of the constant composition (CC) method,³⁶ in which titrant solutions containing the lattice ions were simultaneously added to the reaction solutions to compensate for their removal during crystal growth. The titrants were prepared having stoichiometries matching those of the growing phases while also accommodating reaction solution dilution changes due to the addition of multiple titrants. A thermostatted cell, a potentiometer incorporating ion selective and reference electrodes, a potentiostat containing an appropriate switching device (impulsomat), and a recorder (computer or dosigraph) completed the instrumentation. During the reactions, the output of the potentiometer was constantly compared with a preset value and the difference, or error, signal was amplified and relayed to an electronic switch. When the error signal exceeded a certain pre-determined threshold value, the switch activated motor-driven titrant burets. The effective titrant concentrations and the number of burets could also be changed in order to ensure optimal titrant addition rates. Thus a constant thermodynamic driving force for crystal growth was maintained during each crystallization experiment. Using the CC method, a relatively large extent of crystallization could be achieved even at very low supersaturation enabling the characterization of newly precipitated phases.

In a typical calcium phosphate crystal growth experiment, a metastable supersaturated solution was prepared in stirred, double-walled Pyrex glass vessels maintained at $37.0 \pm 0.05^\circ\text{C}$, in an atmosphere of nitrogen gas, presaturated with water vapor in order to

exclude carbon dioxide. Sodium chloride or potassium nitrate solution was used to adjust the ionic strength. The solution pH was brought to the desired value by the slow addition of dilute base (usually potassium hydroxide). A pH electrode coupled with a single junction reference electrode along with an Orion pH meter was used to monitor changes in hydrogen ion activities. Once equilibrium of solution was attained, as indicated by a constant electrode potential, a known amount of seed crystals was added to initiate the crystallization. Any changes in the hydrogen ion activities sensed by electrodes triggered the addition of titrants from the stepper motor driven burets and the titrant volumes were recorded as a function of time.

From the CC experiments, the rates of reaction were calculated from the volumes of titrant added, converted to moles of deposited or dissolved material, as a function of time. For CC, the overall reaction rate is simply given by Eq. (20),

$$R = \frac{C_{\text{eff}}}{SSA} \frac{dV}{dt} \quad (20)$$

where (dV/dt) is the slope of the titrant volume-time curve during the reactions, SSA , the specific surface area, and C_{eff} , the number of moles of precipitate formed per unit volume of added titrant.

4.2. Interfacial Tension Determination from Contact Angle Measurements

Direct (advancing) contact angle (θ) measurements on flat surfaces were made using a telescopic goniometer (Gaertner Instruments, Chicago, IL) and Teflon syringes (Gilmont, Barrington, IL) to place liquid drops on the surfaces.³⁷

For the determination of the contact angle formed between a liquid (and air, or vapor) and finely divided powder particles, for which direct contact angle measurements cannot be performed, a thin layer wicking capillary rise method was used.^{38,39} In this method, the measured rate of capillary rise (i.e., the capillary rise h , in a time t) of a liquid L , through a packed column of powder supported on a glass microscope slide, was substituted into the Washburn Eq. (21):⁴⁰

$$h^2 = \frac{t R_{\text{eff}} \gamma_L \cos \theta}{2\eta} \quad (21)$$

where, R_{eff} is the effective interstitial pore radius, and η , the viscosity of the liquid.

The surface tension or surface free energy for a condensed phase i is the sum of Lifshitz-van der Waals or apolar component (γ^{LW}) and Lewis acid-base or polar components (γ^{AB}). The latter forces are always asymmetric since they comprise the Lewis base or electron-donating (γ^-) as well as the Lewis acid or the electron-accepting (γ^+) properties of a surface. γ^{AB} is expressed as Eq. (22)⁴¹

$$\gamma_i^{\text{AB}} = 2\sqrt{\gamma_i^+ \gamma_i^-} \quad (22)$$

The surface tension component and parameters of the solid particles may be calculated by means of the Young's equation (23):^{37,41}

Table 1. Surface tension of various polar and apolar liquids

Liquid	γ_L	γ^{LW}	γ^{AB}	γ^+	γ^-	η
Heptane	20.14	20.14	0	0	0	0.00409
Octane	21.62	21.62	0	0	0	0.00542
Decane	23.83	23.83	0	0	0	0.00907
Dodecane	25.35	25.35	0	0	0	0.01493
Tetradecane	26.56	26.56	0	0	0	0.02322
Hexadecane	27.47	27.47	0	0	0	0.03451
1-Bromonaphthalene	44.4	44.4	0	0	0	0.0489
Diiodomethane	50.8	50.8	0	0	0	0.028
Ethylene Glycol	48.0	29.0	19.0	1.92	47.0	0.199
Formamide	58.0	39.0	19.0	2.28	39.6	0.0455
Glycerol	64.0	34.0	30.0	3.92	57.4	14.9
Water	72.8	21.8	51.0	25.5	25.5	0.01

Total surface tension $\gamma_L = \gamma^{LW} + \gamma^{AB}$, and $\gamma^{AB} = 2(\gamma^+ \gamma^-)^{1/2}$. The values of γ_L , γ^{LW} , γ^{AB} , γ^+ and γ^- and η are from refs. 37, 38.

$$(1 + \cos\theta)\gamma_L = 2\left(\sqrt{\gamma_s^{LW}\gamma_L^{LW}} + \sqrt{\gamma_s^+\gamma_L^-} + \sqrt{\gamma_s^-\gamma_L^+}\right) \quad (23)$$

where θ is the contact angle between the solid (S) and the liquid (L), and γ_L is the liquid surface tension against its vapor. The values of γ_s^{LW} of the crystal surface was determined with α -bromonaphthalene and diiodomethane (Table 1), apolar liquids which form finite contact angles. Finally, the polar parameters, γ_s^+ and γ_s^- , were obtained with polar liquids (formamide, ethylene glycol, and water, see Table 1), using the determined γ_s^{LW} values. The interfacial tensions between solid surfaces and aqueous solutions were calculated from Eq. (24):^{37,41}

$$\gamma_{SL} = \left(\sqrt{\gamma_s^{LW}} - \sqrt{\gamma_L^{LW}}\right)^2 + 2\left(\sqrt{\gamma_s^+\gamma_s^-} + \sqrt{\gamma_L^+\gamma_L^-} - \sqrt{\gamma_s^+\gamma_L^-} - \sqrt{\gamma_s^-\gamma_L^+}\right) \quad (24)$$

5. RESULTS AND DISCUSSION

It can be seen from Eqs. (14) and (17) that the kinetics of nucleation and growth of a crystal are influenced not only by nucleus/solution interfacial free energy γ_{LE} but also by the interfacial tensions (γ_{SL} and γ_{SE}) resulting from additives or impurities adsorbed on the crystal surfaces. An increase (decrease) in the interfacial tension, γ_{SL} , due to adsorption of impurities inhibit (enhance) the nucleation and growth kinetics.

5.1. Crystallization in the Presence of Cations

It has long been known that the presence of traces of foreign cations can suppress nucleation and growth of a crystal in aqueous solution, and certain patterns of behavior are beginning to emerge. For example, the higher the charge of the cations the more powerful the inhibiting effect, e.g., $\text{Cr}^{3+} > \text{Fe}^{3+} > \text{Al}^{3+} > \text{Ni}^{2+} > \text{Na}^+$.⁴² The studies of calcium phosphates mineralization and demineralization kinetics in the presence of zinc and magnesium ions over a range of concentrations have revealed an overall order of inhibiting effectiveness $\text{Zn}^{2+} > \text{Mg}^{2+}$.¹³⁻²⁰ The preceding discussions suggest that these phenomena

may be understood in terms of surface tension component theory.^{37,41,43} Since the Lifshitz-van der Waals interactions are related to electrodynamic interactions mainly resulting from bulk properties such as dielectric permeability,⁴⁴ they will be unlikely to be influenced by the adsorption of trace impurities on crystal surfaces. Therefore, the value of the Lifshitz-van der Waals interfacial tension in Eq. (24) remains small and almost constant since the values of γ^{LW} for most inorganic solids under ambient condition range approximately from 30 to 50 mJ m⁻².^{45,46} The Lewis base parameter can markedly decrease following the adsorption of cations, but since latter are hydrated, they would not be expected to significantly increase the electron-accepting character of the surfaces.^{46,47,48} The higher the cation valence, the greater the reduction in the electron-donicity of the surface. It can be seen from Eq. (24) that a decrease in the Lewis basicity increases the interfacial tension or free energy and results in inhibition of crystal growth. Eq. (17) indicates that the extent of the rate of crystallization retardation is exponentially proportional to $(\gamma_{SL}/\gamma_{LE})$ but not to the square or the cube of the individual free energy terms (γ_{LS} or γ_{LE}) as has been suggested by other workers.^{27,29,30}

5.2. Nucleation on Polymer Surfaces

Poly(methyl methacrylate) (PMMA), silicone rubber and poly(tetrafluoroethylene-co-hexafluoropropylene) (FEP) have relatively high aqueous interfacial tension values; γ_{SL} = 19.0, 38.9 and 40.9 mJ m⁻²,³³ respectively. In attempts to nucleate of calcium phosphate on these polymer surfaces, no mineral phases were detectable in the scanning electron microscope (Hitachi S800 field emission microscope). However, following radiofrequency glow discharge (RFGD) treatment of these surfaces and exposure to calcium phosphate supersaturated solutions, these mineral phases were found to nucleate on the RFGD-PMMA and RFGD-FEP but not on the RFGD-silicone surfaces. These observations suggest a direct causal relationship between the low interfacial tension values resulting from RFGD-treatment of the polymer surfaces and their abilities to nucleate at a given mineral supersaturation. The values of γ_{SL} , following RFGD treatment were -8.5 and 3.7 mJ m⁻², respectively, for PMMA and FEP. However, RFGD-silicone surfaces still retained their relatively high interfacial value with $\gamma_{SL} \sim 21$ mJ m⁻². The action of RFGD simulates the adsorption of impurity OH⁻ ions at the polymer surfaces, which increases their electron-donating properties. It can be seen from Eqs. (17) and (24) that an increase in electron-donicity of surface will be expected to decrease the interfacial tension and promote nucleation.

5.3. Mineralization in the Presence of Macromolecules

Although the adsorption of water-soluble macromolecules on crystal surfaces is probably able to decrease the interfacial tension due to the large electron-donicity, γ^- , from 20 to 60 mJ m⁻², on their surfaces,³⁷ it is difficult to predict their interfacial behavior since the configuration of the macromolecules often changes depending on factors such as solid surface properties and solution pH. It is therefore not surprising that proteins may play a dual role both as crystal inhibitors in solution and as crystal nucleators on immobilized surfaces.¹⁶

The extent of adsorption of human serum albumin (HSA) on PMMA was tested by treating the surfaces with 0.1% (w/v) HSA followed by extensive washing and examination by ESCA. The ESCA surface spectrum of the resulting PMMA showed a significant nitrogen 1s photoelectron peak at a binding energy of ~ 400.0 eV, indicating the presence

of HSA. When PMMA and HSA-treated surfaces were exposed to calcium phosphate solutions, supersaturated with respect to hydroxyapatite (HAP), mineralization of calcium phosphate was observed only on the HSA-PMMA surfaces. It has been suggested that HSA hydrates extend to two water layers with resultant surface tension values $\gamma^{LW} = 26.8 \text{ mJ m}^{-2}$, $\gamma^+ = 6.3 \text{ mJ m}^{-2}$ and $\gamma^- = 60 \text{ mJ m}^{-2}$.³⁷ The contact angle of water on HSA-PMMA decreased to 58° from the 70° for untreated PMMA surfaces, and HSA adsorption resulted in an increase in γ from 12 to 25 mJ m^{-2} , reflecting a decrease in the interfacial tension, γ_{SL} , from 19 to 3 mJ m^{-2} .³³

The adsorption of HSA at PMMA surfaces probably resulted from hydrophobic attractions between the polymer and the hydrophobic moieties of HSA.^{37,49} This would result in most of the HSA hydrophilic groups being directed away from the HSA-PMMA surfaces, with hydrophobic moieties of the HSA surfaces facing towards the PMMA, leading to a decrease in the interfacial tension. However, the configurations of HSA adsorbed on charged surfaces such as HAP are probably quite different from those on hydrophobic PMMA surfaces. The attraction energy would mainly result from electrostatic interactions between the charged HAP surfaces and the charged moieties of the HSA surfaces, with the charged groups of the HSA surface facing toward the HSA-HAP surface. Hydrophobic groups of the HSA would face out from the surfaces, and increase the measured interfacial tension. This postulation may also account for the increase in the water contact angle on HAP surfaces in the presence of HSA (from 68° to 80°). Such a model might explain the results recently reported in studies such as those of Nicholov et al.⁵⁰ Using electron spin resonance spectroscopy, these workers showed that the conformational status of HSA adsorbed onto glass surfaces differs from that of HSA adsorbed onto polystyrene in buffer solution at pH 7.0.

In general, Eq. (7) is applicable at concentrations of adsorbed additives or impurities below that corresponding to the plateau of the Langmuir adsorption isotherm curves. Higher concentrations of impurities may complicate our understanding of interactions at an interface, especially in the case of macromolecules.

ACKNOWLEDGMENT

We thank the National Institute of Dental Research for support of this work (DE 03223).

REFERENCES

1. Buckley, H.E. (1951) *Crystal Growth*, John Wiley & Sons, New York, pp. 339–387.
2. Mullin, J.W. and Amatavivadhana, A., 1967, Growth Kinetics of ammonium and potassium dihydrogen phosphate crystal. *J. Applied Chem.*, 17:151–278.
3. Davey, R. J. and Mullin, J. W., 1974, Growth of the {100} faces of ammonium dihydrogen phosphate crystals in the presence of ionic species, *J. Crystal Growth*, 26:45–51.
4. Davey, R. J., 1976, The effect of impurity adsorption on the kinetics of crystal from solution, *J. Crystal Growth*, 34: 109–119.
5. Davey, R.J. and Mullin, J.W., 1976, A mechanism for the habit modification of ADP crystal in the presence of ionic species in aqueous solution. *Kristall und Technik*, 11 : 229–233.
6. Leung, W. H. and Nancollas, G. H., 1978, Nitritoltri (methylenephosphonic acid) adsorption on barium sulfate crystal and its influence on crystal growth, *J. Crystal Growth*, 44: 163–167.
7. Nancollas, G. H. (1979) The growth of crystals in solution, *Adv. Colloid Interface Sci.* 215–252.

8. Amjad, Z.; Koutsoukos, P.G. and Nancollas, G. H. (1984) The crystallization of hydroxyapatite and fluorapatite in the presence of magnesium ions, *J. Colloid Interface Sci.*, 101:250–256.
9. Nancollas, G.H. and Zawacki, S. J.,1984, In: Industrial Crystallization 84 (9th Symposium, Hague), S. J. Jancic and E.J. de Jonn (eds.), Elsevier, Amsterdam, pp. 51–60.
10. Kubota, N.; Uchiyama, I. Nakai, K.; Shimizu, K. and Mullin, J.W. (1988) Change of solubility of K_2SO_4 in water by trace of Cr(III). *Industrial and Engineering Chemistry Research*, 27:390–394.
11. Black, S.N.; Davey, R.J. and Halcrow, M. (1986) The kinetics of crystal growth in the presence of the tailor-made additives, *J. Crystal Growth*, 79: 765–774.
12. Black, S. N. and Davey, R. J. (1988) Crystallization of Amino Acids, *J. Crystal Growth*, 90:136–144.
13. Ebrahimpour, A. (1990) Kinetics of Dissolution, Growth and Transformation of Calcium Salts and The Development of Spectroscopic and Dual Constant Composition Methods, Ph.D. dissertation, State University of New York at Buffalo, New York.
14. Chin, K. O. (1992) A constant composition kinetics study of the dissolution of fluorapatite and other synthetic and natural calcium phosphates. Influence of inorganic ions and salivary macromolecules, Ph.D. dissertation, State University of New York at Buffalo, New York.
15. Paschalis, E.P. (1993) Physiochemical Studies of Biologically Important Calcium Phosphates, Ph.D. dissertation, State University of New York at Buffalo, New York.
16. Tsortos, A. (1993) The Role of Macromolecules as Inhibitors and Nucleators of Calcium Phosphate Phases, Ph.D. dissertation, State University of New York at Buffalo, New York.
17. Tan, J. (1995) The Mineralization and Demineralization Kinetics of Synthetic Hydroxyapatite and Human Dentin, Ph.D. dissertation, State University of New York at Buffalo, New York.
18. Burke, E. M. (1996) Kinetic Studies Involving Octacalcium Phosphate and hydroxyapatite: Model Crystals For Biomineralization, Ph.D. dissertation, State University of New York at Buffalo, New York.
19. Fuierer, T.A. (1996) A Dual Constant Composition Study of the Mineralization Kinetics of Hydroxyapatite and Human Dental Enamel: The Influence of Biologically Relevant Additives. Ph.D. dissertation, State University of New York at Buffalo, New York.
20. Liu, Y. (1996) Surface Properties and Mineralization Kinetics of Calcium Phosphates and Calcium Sulfates, Ph.D. dissertation, State University of New York at Buffalo, New York.
21. Bunn, C.W., 1933, Adsorption, oriented overgrowth and mixed crystal formation. *Proceedings of the Royal Society*, 141: 567–593.
22. Cabrera, N. and Vermilyea, D.A.,1958, in: Growth and Perfection of Crystal, Doremus, R.H.; Roberts, B.W. and Turnbull, D. (eds), John Wiley & Sons, New York, pp. 391–410.
23. Sears, G.W., 1958, in: Growth and Perfection of Crystal, Doremus, R.H.; Roberts, B.W. and Turnbull, D. (eds), John Wiley & Sons, New York. pp. 441–445.
24. Lacman, R. and Sampson, M. J., 1958, in: Growth and Perfection of Crystal, Doremus, R.H.; Roberts, B.W. and Turnbull, D. (eds), John Wiley & Sons, New York, pp. 427–439.
25. Chernov, A. A., 1965, Some aspects of the theory on crystal growth forms in the presence of impurities. In *Kern* (1965), 1–13.
26. Boistelle, R.,1982. in: Industrial Crystallization (6th Symposium, Usti nad Labem). Mullin, J.W. (ed) 203–214, Plenum Press, New York.
27. Ohara, M. and Reid, R. C. (1973) Modeling Crystal Growth Rates From Solution, Prentice-Hall, Inc. Englewood Cliffs, N.J.
28. Adamson, A.W. (1990) Physical Chemistry of Surfaces, Wiley-Interscience, New York.
29. Becker, R. and Doring, W.,1935, Kinetische Behandlung der Keimbildung in übersatigen Dämpfen, *Annalen der Physik*, 24:719–752.
30. Volmer, M. (1939) Kinetic der Phasenbildung, Steinkopff, Leipzig, German.
31. Walton, A. G.,1969, in: Nucleation, Zettlemoyer, A.C. (ed.), Marcel Dekker, New York. p.225.
32. Wu, W. and Nancollas, G. H., 1996, Interfacial free energies and crystallization in aqueous media, *J. Colloid Interface Sci.* 182:365–373.
33. Wu, W.; Zhuang, H.Z. and Nancollas, G.H. (1997) Heterogeneous nucleation of calcium phosphates on solid surfaces in aqueous solution. *J. Biomedical Materials Research*, 35: 93–99.
34. Frenkel, J. (1946) Kinetic theory of liquids, Oxford at the Clarendon Press.
35. Zeldovich, J.B. (1943) Acta Physiocochem. URSS, 18, 17 (see also re. 34).
36. Tomson, M.B. and Nancollas, G.H.,1978, Mineralization kinetics: A Constant Composition Approach, *Science*, 200:1059–1060.
37. Van Oss, C. J. (1994) Interfacial Forces in Aqueous Media, Marcel Dekker, New York.
38. Van Oss, C.J.; Giese, R.F.; Li, Z.; Murphy, K; Norris, J.; Chaudhury, M. K. and Good, R. J.,1992, Determination of contact angles and pore sizes of porous media by column and thin layer wicking, *J. Adhes. Sci. Tech.*, 6: 413–428.

39. Wu, W. and Nancollas, G.H., 1997, Nucleation and crystal growth of octacalcium Phosphate on titanium oxide surfaces, *Langmuir*, 13: 861–865.
40. Washburn, E.W., 1921, The dynamics of capillary flow, *Phys. Rev.* 17: 273–283.
41. Van Oss, C. J.; Chaudhury, M.K. and Good, R. J., 1988, Interfacial Lifshitz-van der Waals and polar interactions in macroscopic systems, *Chem. Rev.* 88: 927–941.
42. Mullin, J.W. (1993) Crystallization, Butterworth-Heinemann Ltd, London.
43. Fowkes, F.M. (1978) *J. Adhesion Sci. Tech.* 1, 7.
44. Mahanty, J. and Ninham, B.W. (1976) Dispersion Forces, Academic Press, New York.
45. Ross, S. and Morrison, I.D. (1988) Colloidal Systems and Interfaces, John Wiley & Sons, New York.
46. Giese, R.F.; Wu, W. and Van Oss, C.J., 1996, Surface and electronkinetic properties of clays and other mineral particles, untreated and treated with organic or inorganic cations, *J. Dispersion Sci. Tech.* 17: 527–547.
47. Wu, W.; Giese, R.F. and Van Oss, C.J., 1994, Linkage between ζ -potential and electron donicity of charged polar surfaces, *Colloids & Surfaces A*: 89: 241–252.
48. Van Oss, C.J.; Giese, R.F. and Wu, W., 1997, On the predominant electro-donicity of polar solid surfaces, *J. Adhesion*, 63: 71–88.
49. Van Oss, C. J.; Wu, W. and Giese, R.F., 1995, in: Proteins at Interfaces II, Horbett, T.A. and Brash, J.L., ACS Symposium Series 602. American Chemical Society, Washington, D.C. pp. 80–91.
50. Nicholov, R.; Lum, N.; Veregin, R.P.N. and DiCosmo, F., 1995, in: Proteins at Interfaces II, Horbett, T.A. and Brash, J.L., ACS Symposium Series 602 American Chemical Society, Washington, D.C. pp. 281–295.

INHIBITION OF HYDROXYAPATITE GROWTH IN VITRO BY GLYCOSAMINOGLYCANS

The Effect of Size, Sulphation, and Primary Structure

Paschalsi Paschalakis,¹ Demitrios H. Vynios,¹ Constantine P. Tsiganos,¹ and
Petros G. Koutsoukos²

¹Laboratory of Biochemistry
Department of Chemistry
University of Patras
Patras 261 00, Greece

²FORTH/ICEHT and Department of Chemical Engineering
University of Patras
Patras 265 00, Greece

1. ABSTRACT

Hydroxyapatite (HAP) crystal growth was found to be inhibited by glycosaminoglycans *in vitro*. The major effect was produced by hyaluronan and of the sulphated glycosaminoglycans by chondroitin-4-sulphate. Chondroitin-6-sulphate did have a minor effect, while oversulphated chondroitin did not inhibit growth of HAP crystals. Chemically desulphated chondroitin sulphate still retains its inhibitory ability. Fragmented glycosaminoglycans by testicular hyaluronidase behaved in a manner similar to the respective intact molecules, even in the case in which the size of the fragments was in the tetrasaccharide range. Constituents of the monosaccharide of the glycosaminoglycans, were also examined with respect to their effect on HAP crystal growth; N-acetylglucosamine being the most potent inhibitor. The results clearly suggest that the chemical structure of the glycosaminoglycans determines their behavior in inhibiting HAP crystal growth. The presence of N-acetylglucosamine, and of only one sulphate ester group in the axial position, seemed to be the most prominent.

2. INTRODUCTION

Ion deposition in vertebrate tissues, in general, takes place through the formation of hydroxyapatite (HAP). This event, in endochondral ossification, follows a number of ul-

trastructural tissue changes involving chondrocyte proliferation, differentiation and hypertrophy and matrix calcification, which prepare the cartilage for replacement by bone.¹ The morphological changes are accompanied by changes in chondrocyte phenotype and several biochemical events such as: synthesis of type X collagen,^{2,3} accumulation of C-propeptide of type II collagen,⁴ increasing activity of alkaline phosphatase⁵ and qualitative and/or quantitative modifications of proteoglycans. The modifications of proteoglycans still remain in confusion for a number of reasons. Evidence from various laboratories suggests that degradation of aggrecan occurs in calcifying cartilage affecting its aggregation with hyaluronan,⁶⁻⁸ although other studies have shown that there is no change in its size nor in its aggregability.⁹⁻¹⁰ Furthermore, it has been found that increase in the chondroitin-6-sulphate content occurs as cartilage ossifies¹¹⁻¹³ whereas an increase in the chondroitin-4-sulphate content¹⁴ has also been reported. Proteoglycans have been highly suspected to have a critical role during ossification of cartilage. Accumulated data from *in vitro* experiments suggest that proteoglycans inhibit hydroxyapatite crystal growth, the extent of the inhibition depending on their size and sulphation.¹⁵⁻¹⁹ Recent data from our laboratory indicate that proteoglycan aggregates are stronger inhibitors than the monomers.²⁰ This was attributed mainly to the high inhibitory effect of hyaluronan; the proteoglycan subunit enhancing the inhibitory effect through steric hindrance. The inhibitory effect of proteoglycan subunits alone, of whatever magnitude, is expected to be due to the presence of the glycosaminoglycan chains, since it has been reported that they alone inhibit HAP crystal growth.^{18,21}

In order to elucidate the structure of a glycosaminoglycan molecule needed for the inhibition of hydroxyapatite growth, we have examined the effect of size, degree of sulphation, position of sulphate ester groups and chemical structure of four naturally occurring glycosaminoglycans in the crystal growth of hydroxyapatite by the constant supersaturation procedure.^{20,22,23}

3. MATERIALS AND METHODS

3.1. Analytical Methods

Uronic acid was determined by the borate-carbazole reaction.²⁴ Calcium was analyzed by atomic absorption and phosphate by the reaction with vanadomolybdate.²⁵ The position of sulphate ester groups in glycosaminoglycans was determined after digestion by chondroitinase ABC²⁶ and HPLC separation of the produced Δ -disaccharides.²⁷

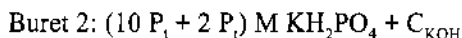
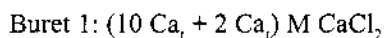
3.2. Materials

Hydroxyapatite ($\text{Ca}_5(\text{PO}_4)_3$, HAP) was prepared as described elsewhere.²³ The synthetic crystals displayed the characteristic powder x-ray diffraction pattern and the IR spectrum of stoichiometric hydroxyapatite. The molar ratio of Ca^{2+} to PO_4^{3-} was found to be 1.67 ± 0.01 and the specific surface area (SSA) was $34.6 \text{ m}^2/\text{g}$, as determined by a multiple point nitrogen adsorption B.E.T. method. Hyaluronan from rooster comb was isolated as described by Tsiganos *et al.*²⁸ Hyaluronan from *Streptomyces* ($M_r > 2 \times 10^6$), chondroitin-6-sulphate (C-6S, M_r 45,000), testicular hyaluronidase (type VI) and chondroitinase ABC were purchased from Sigma Chemical Co. Chondroitin-4-sulphate (C-4S, M_r 15,000) was isolated from pig laryngeal cartilage proteoglycans after β -elimination and DEAE-Sephacel ion exchange chromatography. In brief, tissue proteoglycans were ex-

tracted with 4M GdnHCl / 0.05M CH₃COONa pH 5.8 containing proteinase inhibitors,²⁹ and precipitated in 66% ethanol by volume. The dry powder was suspended in 1M NaBH₄ / 0.05M NaOH (20 ml / g) for 48h at 45 °C under N₂ atmosphere. Then, the suspension was clarified by centrifugation, and the glycosaminoglycans were precipitated in 50% ethanol by volume. The precipitate was dissolved (2 mg / ml) in 0.05M NaCl and applied on a DEAE-Sephacel column (0.5 mg / ml gel), eluted with 0.05M, 0.5M and 2M NaCl, the last fraction containing pure chondroitin-4-sulphate. Chondroitin sulphate E (4,6-disulphated) (M_r 150,000) was isolated from squid cranial cartilage as described previously.²⁶ Chemical desulphation of chondroitin-4- and -6-sulphate was performed as described by Nagasawa and Inoue.³⁰ The extent of desulphation was calculated by HPLC analysis of the Δ -disaccharides after digestion of the glycosaminoglycans with chondroitinase ABC. Glycosaminoglycan fragments of M_r 30,000 and 1,000 were obtained after limited and total digestion with testicular hyaluronidase and gel chromatography of the digests on Sepharose CL-6B and BioGel P-2, respectively. For total digestion, 5 mg of the substrate in 2 ml of 0.15M NaCl-0.05M CH₃COONa pH 5.3 were incubated for 18 h at 37 °C with 500 units of the enzyme. For limited digestion, one fifth of the enzyme was used and the incubation period was decreased to 5 h.

3.3. Hydroxyapatite Crystal Growth

The procedure described by Tomson and Nancollas²² was used which in brief is as follows. The experimental system consists of a double wall reaction vessel in which a glass/SCE electrode (Metrohm) connected to a pH-stat is immersed and two burettes from which calcium and phosphates are added to maintain the composition constant and the volume is recorded. The reaction vessel (200 ml) contained metastable supersaturated solution of calcium phosphate prepared by mixing equal volumes of 1 mM CaCl₂ and 0.6 mM KH₂PO₄ stock solutions and adjusting its pH value to 7.4 with KOH and maintained at 37°C under N₂ atmosphere. The final salt concentration was adjusted to 0.15 M by adding the appropriate amounts of NaCl. The compound under investigation was added and the system allowed to equilibrate for 2 h. Next, well-characterized HAP seed crystals (20 mg) were added for the initiation of the crystal growth process. Hydroxyapatite crystal growth started immediately without any induction period. The crystal growth process was monitored by the proton release resulting from the formation of HAP. pH changes as small as 0.005 pH units triggered the addition of titrant solutions from the mechanically coupled burets of the appropriate concentrations so that the solution supersaturation was kept constant. The concentration of the titrant solutions was as follows:



with molar ratios of Ca_t:P_t:OH = 5:3:1, where Ca_i and P_i are the initial total concentrations of calcium and phosphate in the working solution, respectively and C_{KOH} the concentration of sodium hydroxide needed for the precipitation of hydroxyapatite according to the salt stoichiometry and for the working solution pH adjustment. The rate of crystal growth in the presence (R_i) and absence (R_o) of each type of macromolecules was calculated from the slope of the respective curves, i.e., from the plots of volume of titrants added as a function of time, obtained directly from an electronic device recording the pulses sent to the motor from the impulsomat. During the crystallization process, samples were with-

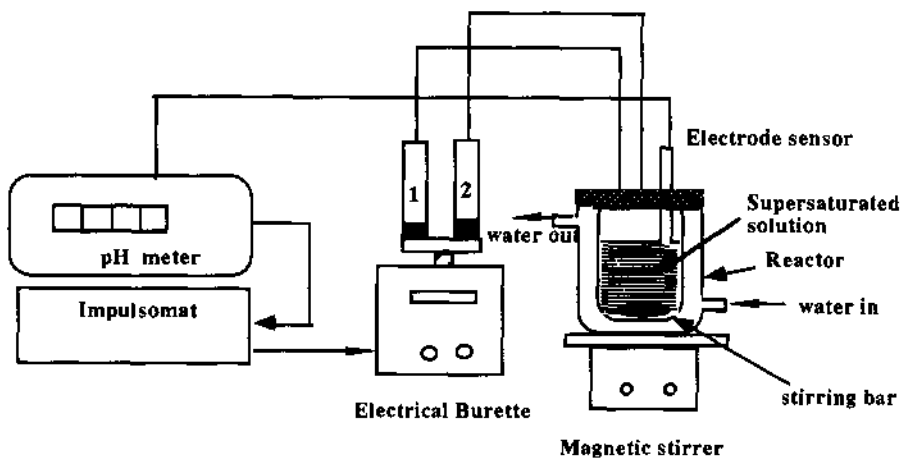


Figure 1. Experimental set-up for the crystallization experiments of hydroxyapatite crystal growth.

drawn, filtered through a membrane filter (Sartorius, 0.2 μm) and the filtrates were analyzed for calcium and phosphate in order to ensure that the supersaturation was kept constant throughout the experiments. The solid phase was examined by FTIR spectroscopy and powder x-ray diffraction. The experimental set-up for the crystal growth experiments at constant supersaturation is shown in Figure 1.

3.4. Adsorption Isotherms

In order to determine the amounts of the macromolecules adsorbed on the hydroxyapatite crystals, the appropriate amounts of the macromolecules dissolved in water were added to 10 mg lots of hydroxyapatite (0.346 m^2) in plastic vials, the volume adjusted to 10 ml with a NaCl solution of the appropriate ionic strength and the crystals were dispersed by vigorous shaking. The pH of the suspensions was adjusted to 7.4, the vials were rotated over a period of 24 h at 37°C. This time period was sufficient for the equilibration of the solid with the aqueous phase as determined from preliminary experiments. Following equilibration the suspension pH was recorded, the suspensions were centrifuged at $5,000 \times g$, the supernatants were separated from the solids and they were analyzed for their uronic acid content. In all cases, the final pH was never lower than 6.5. The hydroxyapatite residues were washed repeatedly with a NaCl solution of the same ionic strength as the adsorption medium, freeze dried, dissolved in 85% H_2SO_4 and analyzed for their uronic acid content. From the difference between the equilibrium concentration (C_{eq}) and the initial concentration (C_i), the surface excess, Γ , of the adsorbed macromolecules was calculated from equation 1 :

$$\Gamma = \frac{(C_i - C_{\text{eq}})V}{wS} \quad (1)$$

where V is the volume of the solution in which adsorption took place, w the amount of hydroxyapatite suspended in the macromolecules containing solutions and S its SSA.

4. RESULTS

4.1. Inhibition of Hydroxyapatite Crystal Growth

The effect of the various glycosaminoglycans on the rate of HAP crystal growth was studied at constant supersaturation. Their effect was examined over a wide range of concentrations (0.01–1 mg/ml). It should be noted that at the concentration levels investigated the glycosaminoglycans did not significantly affect the supersaturation of the solution due to calcium complex formation with the negatively charged groups^{31,32} as ascertained by potentiometric titrations. Formation of HAP was verified by characterizing the solids separated from the supersaturated solutions after crystal growth by FTIR and x-ray powder diffraction. As may be seen in Figure 2, the rate of HAP crystal growth decreased in the presence of the glycosaminoglycans as a function of their concentration reaching a plateau past a limiting concentration.

Comparison of the effect of two glycosaminoglycans which differ with respect to the position of the sulphate group [C-4S,C-6S], suggested that the spatial orientation of these charged groups was important in determining the inhibitory activities of the chain. It is interesting to note that C-6S was a less effective inhibitor in comparison with C-4s and at low concentrations was by a factor of three. The presence of an extra sulphate group on galactosamine, as in the case of CSE, resulted in a considerable reduction of the inhibition

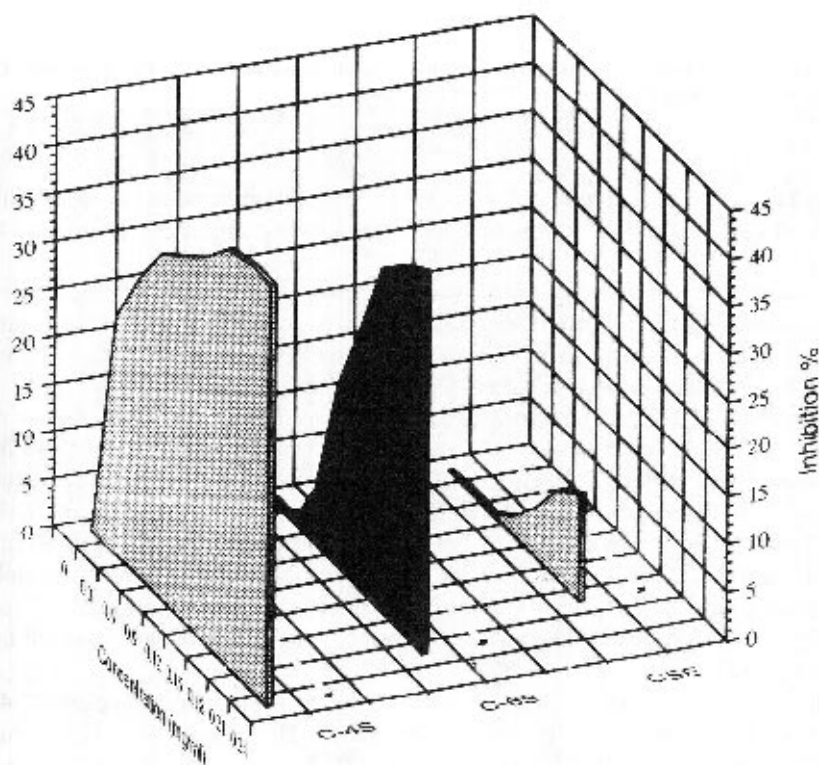


Figure 2. Inhibition of seeded crystal growth of HAP at constant supersaturation by glycosaminoglycans, C-4S, C-6S and CSE; pH 7.40, 37°C, 0.15M NaCl.

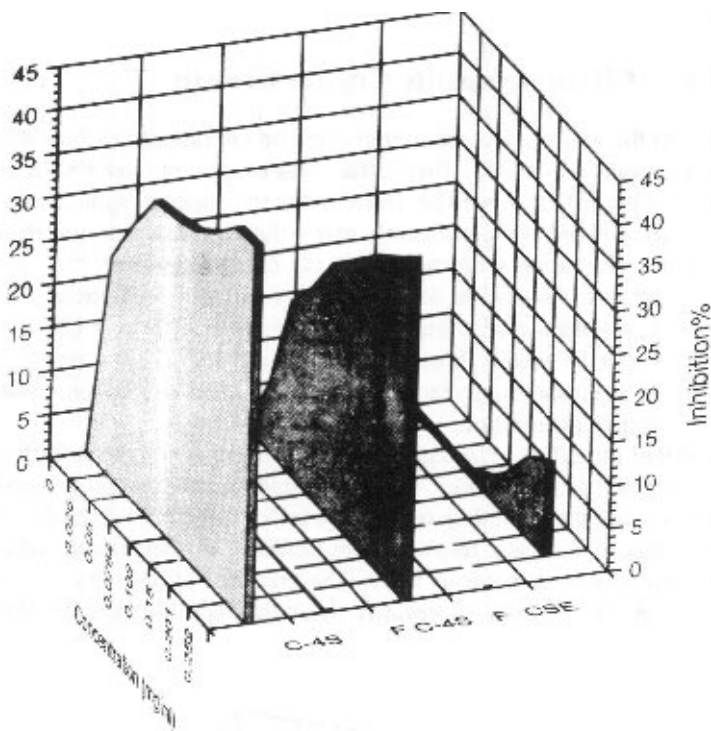


Figure 3. Inhibition of hydroxyapatite crystal growth by chondroitin-4-sulphate (C-4S), fragmented C-4S (F C-4S) and fragmented CSE (F CSE); pH 7.40, 37°C, 0.15M NaCl.

of the HAP crystal growth rates (Figure 2). The inhibition expected to occur due to the sulphate on C-4 was almost completely suppressed by the presence of a second anion on C-6.

It was also examined if the observed differences were due to the molecular size of the glycosaminoglycans. Partially degraded CSE was isolated after a brief treatment with testicular hyaluronidase and its inhibitory activity on HAP crystal growth was studied. As shown in Figure 3, the molecular size of CSE did not affect its properties.

Fragments of CSE of size comparable to that of C-4S exhibited the same effect on the crystal growth of HAP as the whole molecule. Even totally degraded C-4S and C-6S by testicular hyaluronidase inhibited HAP crystal growth to almost the same extent as the intact molecule (Figure 3). These findings suggested that the inhibition of HAP crystal growth was not affected by the size of the additives but mainly by the position of the sulphate ester groups. It is known that considerable portions of C-6S chains are sulphated on C-4 of galactosamine. The preparation used in this study was found by HPLC to contain about 40% of C-4S disaccharides, which might be responsible for the observed inhibition of C-6S chains.

Moreover, the effect of chemically desulphated glycosaminoglycans (C-4S, C-6S and CSE) on HAP seed crystal growth was examined. The extent of sulphate removal was measured by HPLC and it was found to exceed 98%. The effect of chemically desulphated glycosaminoglycans on HAP crystallization was also compared with that of the naturally occurring non-sulphated glycosaminoglycan, hyaluronan, which differs in that it contains

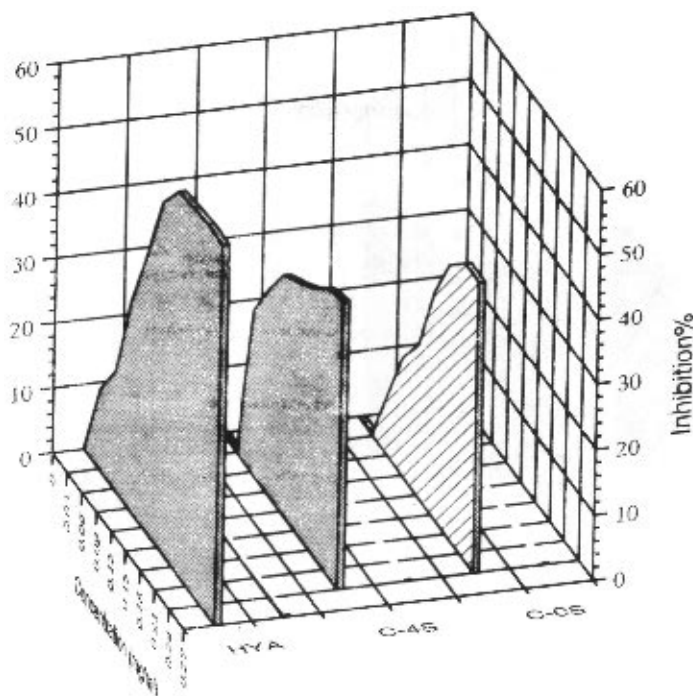


Figure 4. Inhibition of hydroxyapatite crystal growth by hyaluronan (HYA), chondroitin-4-sulphate (C-4S) and desulphated chondroitin sulphate (C-0S) ; pH 7.40, 37°C, 0.15M NaCl.

glucosamine (N-acetylated) instead of galactosamine (N-acetylated). As shown in Figure 4, C-0S had a strong inhibitory effect on HAP crystal growth, comparable to that of C-4S.

All of the desulphated glycosaminoglycans (C-0S) inhibited HAP crystal growth to the same extent, thus the negative behavior (i.e., accelerating effect) even of CSE can be eliminated after its desulphation. Hyaluronan, on the other hand, which bears the same charged group as the desulphated glycosaminoglycans, i.e., carboxyl groups, was a comparatively stronger inhibitor of HAP crystal growth as reported earlier.²⁰ The presence of hyaluronan in the aqueous supersaturated solutions decreased HAP crystal growth rate almost two times more than the other glycosaminoglycans even at concentrations corresponding to the plateau values (Figure 4). Of interest is also the effect of hyaluronan size on the HAP crystal growth. As shown in Figure 5, hyaluronan of $M_r > 2 \times 10^6$, hyaluronan oligosaccharides of $M_r \sim 30,000$ and hyaluronan tetrasaccharides inhibited HAP crystal growth to almost the same extent, suggesting, once more, that the size of glycosaminoglycans did not affect significantly their effect on the kinetics of hydroxyapatite crystal growth.

The difference in the inhibition of HAP crystal growth between hyaluronan and the desulphated glycosaminoglycans is therefore expected to be due to their difference in the primary structure (i.e. glucosamine/galactosamine). In order to elucidate this hypothesis, the effect of glucuronic acid, N-acetylglucosamine and N-acetylgalactosamine in HAP crystal growth rates was examined. As shown in Figure 6, using low concentrations of the monosaccharides (0.0–0.08 mg/ml), we were able to measure differences in their behavior as inhibitors of HAP crystal growth. N-acetylglucosamine had the strongest effect, while

glucuronic acid and N-acetylgalactosamine inhibited HAP crystal growth to a similar extent. The effect of N-acetylglucosamine remained higher than that of the other two monosaccharides even at significantly higher concentrations.

4.2. Adsorption Experiments

It is now well documented that crystal growth of HAP in aqueous supersaturated solutions is a surface diffusion controlled process. Adsorption therefore of foreign additives on the growing solid surfaces, resulting possibly to the blocking of the centers active for crystal growth is expected to influence directly the crystal growth process. The determination therefore of the adsorption isotherms of the various glycosaminoglycans would help to explain the observed differences in reducing the rate of hydroxyapatite seed crystal growth. The adsorption isotherms obtained for C-4S, C-6S, CSE, hyaluronan and C-0S in 0.15 M NaCl and pH 7.4 are shown in Figure 7.

Small amounts of desulphated chondroitin sulphate seemed to adsorb onto hydroxyapatite under such conditions. The amounts of hyaluronan and C-6S adsorbed were similar and about two times higher than the desulphated chondroitin sulphate. The highest adsorption was measured in the case of CSE. It should be noticed that, in both CSE and C-4S, the adsorption isotherms did not reach a discrete plateau value, even at high initial concentration of the additives. As it was expected, the number of charged groups per disaccharide unit influenced adsorption, which was also affected by the position of the sulphate group. Adsorption seemed also to be affected by the primary structure of the additives i.e., the presence of glucosamine or galactosamine.

5. DISCUSSION

The experimental work presented here showed that glycosaminoglycans inhibited HAP crystal growth *in vitro*. The extent of the observed inhibition could not be related to reduction of the supersaturation of the working medium due to complexation of calcium ions by the glycosaminoglycans, since all experiments were carried out in the presence of 0.15 M NaCl which would suppress the extent of calcium–glycosaminoglycans complexation. Potentiometric titrations of macromolecule solutions in the presence of calcium ions

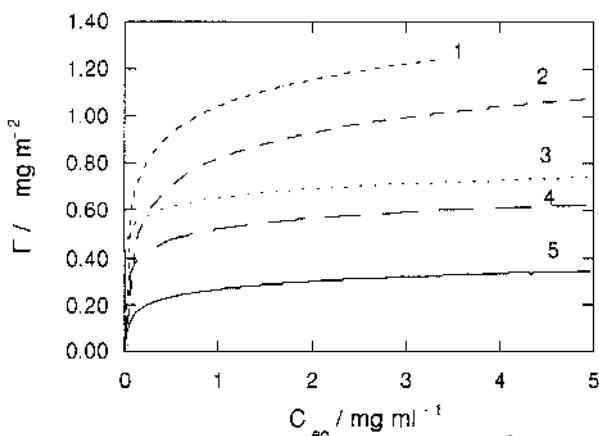


Figure 7. Adsorption isotherms of glycosaminoglycans on hydroxyapatite. Surface excess as a function of the equilibrium concentration of the glycosaminoglycans: 1: CSE; 2: C-4S; 3: C-6S; 4: HYA; 5: C-0S; 37°C, 0.15M NaCl, initial pH 7.40.

confirmed this assumption. Furthermore, substantial inhibition at very low concentrations of glycosaminoglycans (~ 0.01 mg/ml) were measured. At these conditions the amounts of calcium available for complex formation (assuming 1:1 complexes) were in the μmol range whereas the concentration of Ca^{2+} in the working solution was 0.5 mM.

The inhibition measured in the present work was different for each glycosaminoglycan. CSE, a disulphated glycosaminoglycan found in squid cranial cartilage, inhibited HAP crystal growth very little and only at relatively high concentration values. However, CSE was adsorbed very strongly on the hydroxyapatite surface as confirmed by the adsorption measurements and the corresponding isotherms. This result suggested that, in the case of glycosaminoglycans, adsorption on the hydroxyapatite crystals did not result in the inhibition of HAP crystal growth. Similar conclusions may be obtained from the comparison of the inhibition and the adsorption properties of the remaining glycosaminoglycan species. Desulphated chondroitin sulphate, the less adsorbed molecule, appeared to be a rather strong inhibitor of HAP crystal growth. On the other hand, hyaluronan, the strongest inhibitor of HAP crystal growth, was adsorbed onto hydroxyapatite less than the mono- or the disulphated chondroitin sulphate. From the results of the adsorption experiments, it may be concluded that the number of charged groups per disaccharide residue influenced the adsorptivity of the glycosaminoglycans on the hydroxyapatite crystals. The amounts adsorbed were also affected by the chemical structure of the molecules, such as the position of sulphate ester groups (hydroxyapatite adsorbed C-4S more than C-6S) and by the presence of N-acetylglucosamine instead of N-acetylgalactosamine (HAP adsorbed hyaluronan more than C-0S). The M_r of the molecules seemed to play a minor or no role in their adsorption properties.

The effect of the various glycosaminoglycans examined in the present study in reducing the rate of HAP crystal growth was measured with respect to their molecular weight, charge and primary structure. It appears that the size of the macromolecules has no significant effect on HAP crystal. Published data by other investigators,^{17,18} suggest that there is a correlation between the extent of the inhibition of HAP crystal growth and the degree of sulphation of polyanions. The results presented here do not support such an effect. Disulphated chondroitin (CSE), had the lowest inhibitory effect that the mono- and non-sulphated chondroitin. More important appears to be the position of the sulphate group. Thus, removal of the sulphate from C-4S reduced the effect but not below that of the C-6S suggesting that the substituents at C-4 of the galactosamine influence the degree of inhibition of HAP crystal growth; the sulphate being more effective than the hydroxyl group. The significance of the substituents at C-4 and C-6 of galactosamine rather than the macromolecular structure and the degree of sulphation of the glycosaminoglycans on the inhibition efficiency of HAP crystallization, was corroborated by the fact that oligosaccharides, mainly tetrasaccharides from the various glycosaminoglycans exhibited approximately the same inhibitory effect as the respective intact chains. Thus, it is not only the presence of sulphate ester group that might add to the inhibition properties of glycosaminoglycans but also, its position on galactosamine.

The presence of glucosamine instead of galactosamine in the glycosaminoglycan chain is another important parameter. Hyaluronan, regardless of size, caused higher inhibition of HAP crystal growth than C-4S and C-0S, strengthening the notion that it is the orientation of hydroxyl group at C-4 the factor which mainly determines the inhibition properties of the glycosaminoglycans. Since hyaluronan fragments of $M_r \sim 30,000$ differ from C-0S only with respect to the hexosamine, it becomes apparent that the primary structure is a determining factor for the inhibition. The high inhibitory effect of N-acetylglucosamine compared to that of both N-acetylgalactosamine and glucuronic acid pro-

vides conclusive evidence for the high inhibition property of hyaluronan over the other glycosaminoglycans widely present in cartilage and other tissues.

The glycosaminoglycans, with the exception of hyaluronan, do not appear as free chains in cartilage, but in proteoglycan form. Their properties differ from that of the proteoglycan monomer, since the latter is an effective inhibitor of HAP crystal growth at very high concentrations.²⁰ During endochondral ossification of growth plate cartilage, degradation of proteoglycans has been proposed to occur.⁶⁻⁸ This degradation is initiated from the liberation of proteoglycan monomers and proceeds with the liberation of chondroitin sulphate clusters and free chains by proteolytic attack. The relative concentrations of proteoglycan monomers and free glycosaminoglycan chains may regulate the rate of ossification, since these molecules reduce the rate of HAP crystal growth to a different extent. It has been reported that hypertrophic cartilage is richer in C-6S compared to non-ossifying cartilage.¹¹⁻¹³ This phenomenon accompanied with a decrease in C-4S content would act favorably for local ossification. *In vitro* incorporation of ³⁵S,⁷ suggest higher sulphate incorporation in the hypertrophic zone than in the resting zone of the growth plate, possibly resulting to oversulphation of chondroitin sulphate chains. This being true, in the light of our results with CSE, would also favor ossification in the hypertrophic zone.

It is known that cartilage from aged animals contain increased amounts of C-6S compared to newborn.³³⁻³⁶ Moreover, it is also known that increased degradation of proteoglycans occurred in older cartilages of all anatomical sites.³⁷⁻⁴² Since the calcium content of articular cartilage (23 mmol Ca / kg wet weight) is close to that of growth plate (35 mmol Ca / kg wet weight) and therefore favors calcification, the observed mineralization may be due to a decrease in aggregates content (the main inhibitor of hydroxyapatite growth) and an increase in free chondroitin-6-sulphate chains which are weak inhibitors of HAP formation.

ACKNOWLEDGMENTS

The partial financial support of this work by the General Secretariat of Research and Technology (GSRT) through the PENED97 program is gratefully acknowledged. The authors wish also to extend their thanks to Prof. E. Dalas (Chemistry Department) for providing laboratory facilities for the crystal growth experiments.

REFERENCES

1. Caplan AI, In *Cell and Molecular Biology of Vertebrate Hard Tissues*, Wiley, Chichester, Ciba Foundation Symposium 136, 1988.
2. Schmid TM and Conrad HE, "A unique low mol. weight collagen secreted by cultured chick embryo chondrocytes", *J. Biol. Chem.*, 1982;257: 12444.
3. Schmid TM and Linsenmayer TF, In *Structure and Function of Collagen Types*, R. Mayne and R.E. Burgeson, (eds.), Academic Press, London, 1987.
4. Hinek A, Reiner A and Poole AR, "The calcification of cartilage matrix in chondrocyte culture: studies of the C-propeptide of type II collagen (chondrocalcin)", *J. Cell Biol.* 1987;104: 1435.
5. Fell HB and Robison R, "Effect of vitamin D metabolites on the expression of alkaline phosphatase activity by epiphyseal hypertrophic chondrocytes in primary cell culture", *Biochem. J.*, 1934;28:2243.
6. Buckwalter JA, Rosenberg LC and Ungar R, "Changes in proteoglycan aggregates during cartilage mineralization", *Calcif. Tissue Int.*, 1987;41:228.
7. Campo RD and Romano JE, "Changes in cartilage proteoglycans associated with calcification", *Calcif. Tissue Int.*, 1986;39: 175.

8. Shapses SA, Sandell LJ and Ratcliffe A, "Differential rates of aggrecan synthesis and breakdown in different zones of the bovine growth plate", *Matrix Biol.*, 199; 14:77.
9. Buckwalter JA and Rosenberg LC, "Structural Changes in the reassembled Growth Plate aggregates", *J. Orthop. Res.*, 1986;4: 1-9.
10. Matsui Y, Alini M, Webber C and Poole AR, "Characterization of Aggregating Proteoglycans from the Proliferative, Maturing Hypertrophic and Calcifying Zones of the Cartilaginous Physis", *J. Bone Joint Surg. (Am)*, 1991;73:1064.
11. Byers S, Caterson B, Hopwood JJ and Foster BK, "Immunolocation analysis of glycosaminoglycans in the human growth plate", *J. Histochem. Cytochem.*, 1992;40:275.
12. Deutsch AJ, Midura RJ and Plaas AH, "Structure of chondroitin sulfate on aggrecan isolated from bovine tibial and costochondral growth plates", *J. Orthop. Res.*, 1995; 13:230.
13. Mourao PA, "Distribution of chondroitin-4-sulfate and chondroitin-6-sulfate in human articular and growth cartilage", *Arthritis Rheum.*, 1988;31: 1028.
14. Hagiwara H, Aoki T and Yoshimi T, "Immunoelectron microscopic analysis of chondroitin sulfates during calcification in the rat growth plate cartilage", *Histochem. Cell Biol.*, 1995;103:213.
15. Blumenthal NC, Posner AS, Silverman LD and Rosenberg LC, "Effect of Proteoglycans on in Vitro Hydroxyapatite Formation", *Calcif. Tissue Int.*, 1979;27:75.
16. Boskey AL, "Hydroxyapatite Formation in a Dynamic Collagen Gel System: Effects of Type I Collagen, Lipids, and Proteoglycans", *J. Phys. Chem.*, 1989;93: 1628.
17. Boskey AL, Maresca M, Wikstrom B and Hjerpe A, "Hydroxyapatite Formation in the Presence of Proteoglycans of Reduced Sulfate Content: Studies in the Brachymorphic Mice", *Calcif. Tissue Int.*, 1991 ;49:389.
18. Chen C-C and Boskey AL, "Mechanisms of Proteoglycan Inhibition by Hydroxyapatite Growth", *Calcif. Tissue Int.*, 1985;37:395.
19. Chen C-C, Boskey AL and Rosenberg LC, "The Inhibitory Effects of cartilage Proteoglycans on Hydroxyapatite growth", *Calcif. Tissue Int.*, 1984;36:285.
20. Paschalakis P, Vynios DH, Tsiganos CP, Dalas E, Maniatis C and Koutsoukos PG, "Effect of proteoglycans on Hydroxyapatite growth in vitro: The Role of Hyaluronan", *Biochim. Biophys. Acta*, 1993;1158: 129.
21. Hunter GK, Allen BL, Grynblas MD and Cheng P-T, "Inhibition of Hydroxyapatite Formation in Collagen Gels by Chondroitin Sulfate", *Biochem. J.*, 1985;228:463.
22. Tomson MB and Nancollas GH, "Crystallization of Octacalcium I'phosphate at Constant Composition", *Science*, 1978;200:1059.
23. Koutsoukos PG, Amjad ZH, Tomson MB and Nancollas GH, "Crystallization of Calcium Phosphates. A Constant Composition Approach", *J. Am. Chem. Soc.*, 1980;102: 1553.
24. Bitter T and Muir H, "A Modified Uronic Acid Carbazole Reaction", *Anal. Biochem.*, 1962;4:3330
25. Murphy J and Riley JP, "A Modified Single Solution Method for the Determination of Phosphate in Natural Waters", *Anal. Chim. Acta*, 1962;27:3 1.
26. Hjerpe A, Engfeldt B, Tsegienidis T, Antonopoulos CA, Vynios DH and Tsiganos CP, "Analysis of the acid polysaccharides from squid cranial cartilage and examination of a novel polysaccharide", *Biochim. Biophys. Acta*, 1983;757:85.
27. Hjerpe A, Antonopoulos CA and Engfeldt B, "Determination of sulphated disacchades from chondroitin sulphates by high performance liquid chromatography", *J. Chromatogr.* 1979; 171:339.
28. Tsiganos CP, Vynios DH and Kalpaxis DL, "Rooster comb hyaluronate-pprotein, a non-covalently linked complex", *Biochem. J.* 1986;235:117.
29. Aletras AJ and Tsiganos CP, "In Situ Interaction of Cartilage Proteoglycans with Matrix Proteins", *Biochim. Biophys. Acta*, 1985;840: 170.
30. Nagasawa K Inoue Y and Tokuyatsu T, "An Improved Method for the Preparation of Chondroitin by Solvolytic Desulfation of Chondroitin Sulfates", *J. Biochem.(Tokyo)*, 1979;86: 1323-1329 Hunter GK, "An Ion Exchange Mechanism of Cartilage Calcification", *Connect. Tissue Res.*, 1987;16: 11 1.
31. Maroudas A, Weinberg PD, Parker KH and Winlove CP, "The Distributions and Diffusivities of Small Ions in Chondroitin Sulphate, Hyaluronate and Some Proteoglycan Solutions", *Biophys. Chem.*, 1988;32:257.
32. Carney SL and Muir H, "The structure and function of cartilage proteoglycans", *Physiol. Rev.*, 1988;68:858.
33. Eguch, M, Saita YSH, Matsumoto S and Nishio A, "The glycosaminoglycans of Articular Cartilage in relation to age and osteoarthritis", *Calcif. Tissue Res.*, 1974; 15: 169.
34. Hjertquist S-O and Lemperg R, "Identification and concentration of the glycosaminoglycans of hyman articular cartilage inrelation to age and osteoarthritis", *Calcif. Tissue Res.*, 1972; 10:223.
35. Murata K and Bjelle AO, "Age-Dependent Constitution of Chondroitin Sulphate Isomers in Cartilage Proteoglycans under Associative Conditions", *J. Biochem.*, 1979;85:371.

36. Bayliss MT and Ali YS, "Age Related Changes in the Composition and Structure of Human Articular-Cartilage Proteoglycans", *Biochem. J.*, 1978;176:683.
37. Hardingham TE and Bayliss MT, "Proteoglycans of articular cartilage: Changes in aging and in joint disease, *Seminars in Arthritis and Rheumatism*, 1990;20 (suppl. 3): 12.
38. Inerot S and Heinegård D, "Bovine tracheal cartilage proteoglycans. Variations in structure and composition with age", *Collagen Rel. Res.*, 1983;3:245.
39. McDevitt CA and Muir H, "Gel Electrophoresis of proteoglycans and Glycosaminoglycans on Large-Pore Composite polyacrylamide-Agarose gels", *Anal. Biochem.*, 1972;44:612.
40. Roughley PJ and White RJ, "Age-related changes in the structure of the proteoglycan subunits from human articular cartilage", *J. Biol. Chem.*, 1980;255:217.
41. Simunek Z and Muir H, "Changes in the protein-polysaccharides of Pig Articular Cartilage during prenatal life, Development and Old Age", *Biochem. J.*, 1972;126:515.

This page intentionally left blank.

INFLUENCE OF HUMIC COMPOUNDS ON THE CRYSTAL GROWTH OF HYDROXYAPATITE

Zahid Amjad¹ and Michael M. Reddy²

¹The Advanced Technology Group
The BFGoodrich Company
9921 Brecksville Road
Brecksville, Ohio 44141

²U. S. Geological Survey
3215 Marine Street
Boulder, Colorado 80303

1. ABSTRACT

The influence of several natural and synthetic additives containing hydroxy and/or carboxyl groups on the kinetics of crystal growth of hydroxyapatite (HAP) at sustained supersaturation has been investigated using the constant composition method. Addition of low levels (0.25 to 5 parts per million) of fulvic acid, tannic acid, benzene hexacarboxylic acid, and poly(acrylic acid) to supersaturated calcium phosphate solutions has an inhibitory influence upon the rate of crystal growth of HAP. Salicyclic acid, under similar experimental conditions, is an ineffective HAP growth inhibitor. Kinetic analysis suggests Langmuir-type adsorption of added ions on the HAP surfaces with a relatively high affinity for the substrate in the concentration range investigated.

2. INTRODUCTION

The influence of inhibitors on the crystallization of hydroxyapatite ($\text{Ca}_5(\text{PO}_4)_3\text{OH}$, HAP) has been extensively studied in relation to calcification in biological systems and mineral scale formation in industrial water systems. HAP, a mineral prototype for teeth and bones, is also encountered as a deposit on heat exchanger surfaces in industrial applications (cooling, boiler, pulp and paper) where alkaline pH accelerates the conversion of initially precipitated amorphous calcium phosphate to HAP. Results of previous investigations using both seeded growth and spontaneous precipitation techniques have shown that

both pyrophosphate and organophosphonates are effective crystal growth inhibitors for di-calcium phosphate dihydrate (DCPD) ($\text{CaHPO}_4 \cdot 2\text{H}_2\text{O}$) and HAP phases.¹⁻⁴

Several studies have been reported pertaining to the influence of di-, tri-, and hexacarboxylic acids on the crystal growth of HAP. Nancollas et al.⁵ investigated the influence of tricarboxylic acids on calcium phosphate precipitation using the seeded growth method. Comparison of the effect of citric acid, isocitric acid, and tricarboxylic acid suggests that the hydroxyl group in the molecular backbone plays a key role in the effectiveness of two of these tricarboxylate ions. A study on the influence of benzene hexacarboxylic acid, benzene tricarboxylic acid, glycolic acid, malic acid, and malonic acid as crystal growth inhibitors for HAP reported that the inhibitory power of these additives strongly depends on the ionic charge (or the number of carboxyl and/or hydroxyl groups) of the inhibitor.^{6,7} Effects of additives containing hydroxy, phosphonic, and carboxylic group as HAP and DCPD crystal growth inhibitors have recently been reported. Results of these studies reveal that additives containing both phosphono and carboxy groups exhibit stronger inhibitory activity than those containing hydroxy and/or carboxy groups.^{7,8}

The influence of polymeric inhibitors (e.g., poly(acrylic acid), poly(maleic acid), and acrylic acid-based copolymers) as crystal growth inhibitors for sparingly soluble salts has attracted the attention of several researchers. Smith and Alexander⁹ have reported that calcium sulfate crystal growth is inhibited by poly(acrylic acid), poly(methacrylic acid), and carboxycellulose. Amjad¹⁰⁻¹³ has reported that the effectiveness of a polymer as a crystal growth inhibitor for sparingly soluble salts (e.g., HAP, DCPD, BaSO_4 , CaF_2), is inversely proportional to its molecular weight. In addition, it has also been reported that substituting the carboxyl group with bulky groups (for example, hydroxyl propylacrylate, tertiary butyl acrylamide, 2-acrylamido-2-methyl propane sulfonic acid) results in increased inhibitory power of the copolymer in preventing the precipitation of calcium phosphates.¹⁴ A study of water-soluble polymers¹⁵ reported phosphorylated polyvinyl alcohol and sulfated polyvinylalcohol retarded transformation of amorphous calcium phosphate to hydroxyapatite. The adsorption of citrate (CA) and phosphocitrate (PC) ions by HAP surfaces and their influence on constant-composition growth kinetics have been reported. According to Williams et al.,¹⁶ PC was strongly adsorbed to HAP and inhibited crystal growth and the two additives, PC and CA, behaved synergistically in their HAP crystal growth inhibition.

Humic and fulvic acids, commonly found in the natural environment, are polymeric molecules whose molecular weights range from several hundred to several thousand. They mostly contain carboxylic and phenolic acid functionalities, and can behave as negatively charged colloids or anionic polyelectrolytes in surface waters. Nystrom et al.¹⁷ in their study on the filtration of process waters containing humic acid by membrane-based filtration procedures reported that humic acid forms a gel-like layer on the filter and blocks the pores of the filter. Recently, using a constant-composition method, Lacout et al.¹⁸ reported that low levels of fulvic acid markedly inhibit DCPD crystal growth.

In our laboratory, several studies have been conducted on the effect of synthetic polymers containing a variety of functional groups (including hydroxyl, carboxyl, ester, sulfonic) on the precipitation of sparingly soluble salts using the constant composition (CC) technique. It has been found that the overall efficacy of the polymer as a crystal growth inhibitor strongly depends on ionic charge, polymer composition, and molecular weight. Humic and fulvic acids commonly present in many surface waters are known to affect the efficiency of industrial water systems (cooling, boiler, desalination) and agricultural fertilization. To understand humic substance interactions with various scale-forming salts, we examined fulvic acid growth inhibition effectiveness on HAP crystals. This study

also presents results on the effect of tannic acid and salicylic acid on the crystal growth of HAP at constant supersaturation. For performance comparison, crystal growth experiments were also carried out in the presence of low molecular weight poly(acrylic acid) and benzene polycarboxylic acids.

3. EXPERIMENTAL

Solutions were prepared using reagent grade chemicals with deionized, distilled, CO₂-free water. Calcium ion concentrations were determined by atomic absorption spectroscopy and phosphate solutions were analyzed spectrophotometrically. Fulvic acid used in this study was characterized as described previously.¹⁹ Tannic acid was obtained from Fisher Scientific and was used without further purification. Benzene hexacarboxylic acid and benzene-1,3,5-tricarboxylic acid were obtained from Sigma Chemical Company. Poly(acrylic acid) was a commercial sample from the BFGoodrich Company (the use of trade names in this report is for identification purposes only and does not constitute endorsement by the USGS).

HAP seed crystals were prepared and characterized as described previously.¹⁰ All experiments were conducted at 37 ± 0.1 °C in doubled-walled, water-jacketed, Pyrex cells (Figure 1). The crystal growth experiments were made at constant supersaturation as described previously.¹⁰ Hydrogen ion activity measurements were made with a glass/Ag - AgCl electrode pair equilibrated at 37 °C. The electrode pair was standardized before each experiment. In a typical crystal growth experiment, the stable supersaturated solution of calcium phosphate with a calcium to phosphate molar ratio of 1.67 was prepared by adjusting the premixed subsaturated solution of calcium phosphate to a pH of 7.40 by the slow addition of 0.10 M potassium hydroxide. The supersaturated calcium phosphate solutions were continuously stirred while nitrogen gas presaturated with water was bubbled through the solution to exclude carbon dioxide.

After the pH adjustment and a waiting period of about 45 minutes, the crystallization was initiated by the addition of well-characterized HAP seed crystals. To investigate the effect of inhibitors, stock solutions were diluted to the desired concentrations in the working solutions. In all cases, the precipitation reaction started immediately following the introduction of the seed crystals in the crystallization medium. During HAP forma-

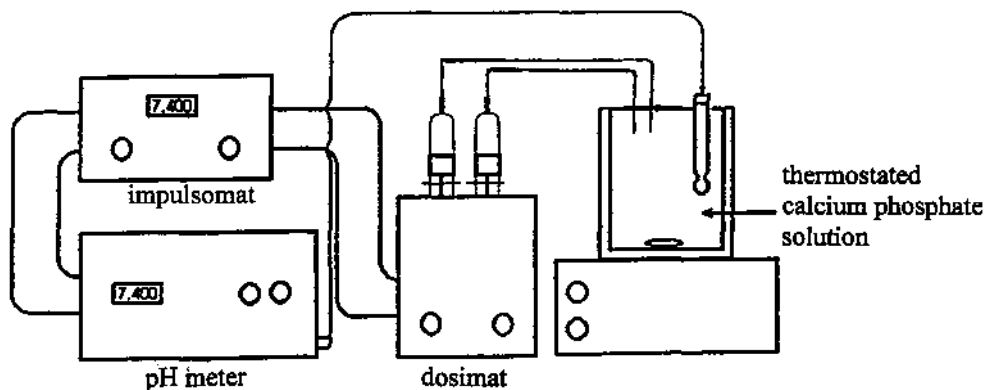


Figure 1. Constant composition experimental apparatus.

Table 1. Substances evaluated for inhibition of HAP crystal growth onto HAP seed crystals at constant supersaturation

Inhibitor	Acronym
Fulvic acid	FA
Tannic acid	TA
Salicylic acid	SA
Benzene Hexacarboxylic Acid	BHCA
Benzene-1, 3, 5-Tricarboxylic acid	BTCA
Poly (Acrylic acid)	PAA

tion, protons are released in the solution thus offering a very sensitive means of monitoring its crystallization process. This increase in hydrogen ion activity accompanying crystallization, was sensed by the pH electrode, which triggered an automatic titrator potentiostat (Brinkmann Instruments, Westbury, NY) to add titrant solutions of calcium chloride, potassium phosphate, potassium hydroxide, and inhibitor. The molar concentration ratios of the titrants corresponded to the stoichiometry of the HAP phase. Potassium chloride was added to calcium phosphate supersaturated solutions to maintain constant ionic strength. Periodically, aliquots of the reaction mixtures were filtered (0.22 micrometer, Millipore Corporation, MA) and the filtrate analyzed for calcium and phosphate ions to verify the constancy (within 1%) of the concentrations. Crystallization rates were determined from the rates of addition of mixed titrants and corrected for surface area changes.¹⁰ Table 1 lists the additives studied in this investigation.

4. RESULTS AND DISCUSSION

The solution supersaturation was computed by accounting for the mass balance equations for total calcium and phosphate and electroneutrality conditions by successive approximations for ionic strength using the method described previously.¹⁰ The driving force for the crystallization of HAP is the change in Gibbs free energy (ΔG) for going from the supersaturated solution to equilibrium:

$$\Delta G = - (RT/n) \ln (IP/K_{so}) \quad (1)$$

where IP is the ionic activity product, K_{so} the value of IP at equilibrium, and R, T, and n are the ideal gas constant, absolute temperature, and the number of ions in the unit formula of the calcium phosphate phases (for HAP $n = 9$), respectively. The ΔG values obtained using Equation 1 for various calcium phosphate phases indicate the thermodynamic stability of the experimental solutions compared to solutions in thermodynamic equilibrium with that particular phase. Positive ΔG values represent undersaturated solutions and negative ΔG values represent solutions supersaturated with respect to the solid phase under consideration. Table 2 summarizes the experimental conditions used and the results of typical crystal growth experiments made in the presence and absence of inhibitors.

By conducting a series of crystal growth experiments in the presence of varying concentrations of FA, it is possible to describe the concentration--performance relationship for FA (Figure 2). HAP growth rate decreases with increasing fulvic acid concentration.

Table 2. Crystallization of HAP on HAP seed crystals in the presence of inhibitors

Exp	Inhibitor	Inhibitor conc., PPm	Rate of HAP crystal growth x 10 ⁶ mole min ⁻¹ m ⁻²
10.	none	0.0	14.3
12.	none	0.0	13.6
13.	none	0.0	14.9
14.	FA	0.25	11.5
15.	FA	0.33	10.6
16.	FA	0.50	9.4
17.	EA	0.50	8.7
18.	FA	0.70	6.5
19.	FA	1.00	4.0
20.	FA	1.25	2.8
27.	TA	0.50	11.8
28.	TA	1.0	8.9
29.	TA	2.0	4.5
30.	TA	3.0	2.5
31.	TA	4.0	1.6
32.	SA	1.0	13.8
33.	SA	5.0	14.5
34.	BHCA	0.50	8.0
35.	BTCA	1.00	14.2
36.	BTCA	5.00	14.8
37.	PAA	0.25	8.0
38.	PAA	0.33	6.1
39.	PAA	0.50	3.5
40.	PAA	0.60	1.2
41.	PAA	1.00	0.7

*Initial conditions : T_{Ca} (total solution calcium concentration) = 0.500 mM, T_{phos} (total solution phosphate concentration) = 0.300 mM, pH 7.40, 37 °C

KCl = 7.00 mM. Titrant 1: CaCl₂ = 8.00 mM. Titrant 2 : KH₂PO₄ = 4.80 mM + KOH = 9.91 mM. ΔG (kJ mol⁻¹) HAP, - 52.6; OCP, -10.2; DCPD +4.02

Interestingly, a fulvic acid concentration as low as 0.25 ppm significantly reduces the crystal growth rate of HAP. The rate data in Figure 2 also show that increasing the FA concentration from 0.25 to 1 ppm results in a significant decrease in growth rate, respectively. It is worth noting that a further increase in the inhibitor concentration to 1.25 ppm decreased the growth rate by about 80%.

In view of the above results indicating that fulvic acid exhibits strong inhibitory activity for HAP crystal growth, additional experiments were performed with TA (Table 2). The marked inhibition of HAP crystallization by TA is clearly seen in the plots of moles of HAP grown as a function of time during several of these experiments (Figure 3). For example, in the presence of 1 ppm TA, the rate of HAP growth rate is reduced by 38% and increasing the concentration by a factor of four results in 89% reduction in growth rate. The kinetic data on FA and TA (Table 2) show that FA exhibits stronger inhibitory power than TA in reducing the crystal growth of HAP (under similar growth conditions).

To evaluate the effect of hydroxyl and/or carboxyl groups present in the inhibitors, several HAP growth experiments were carried out in the presence of BHCA (benzene hexacarboxylic acid), BTCA (benzene-1,3,5-tricarboxylic acid), salicylic acid and low mo-

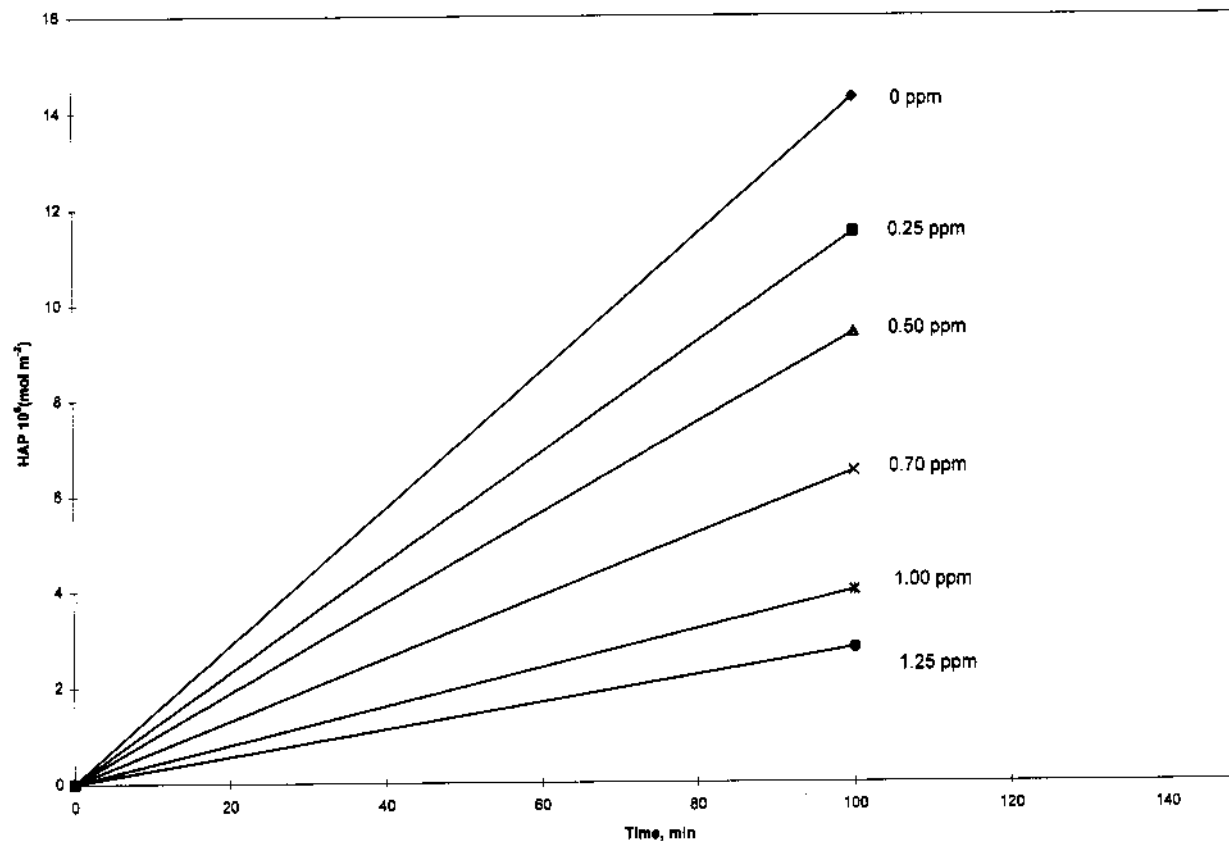


Figure 2. Crystal growth of hydroxyapatite onto hydroxyapatite seed crystals at constant supersaturation. Plots of amount of hydroxyapatite formed as a function of time in the presence of various concentrations of fulvic acid (FA).

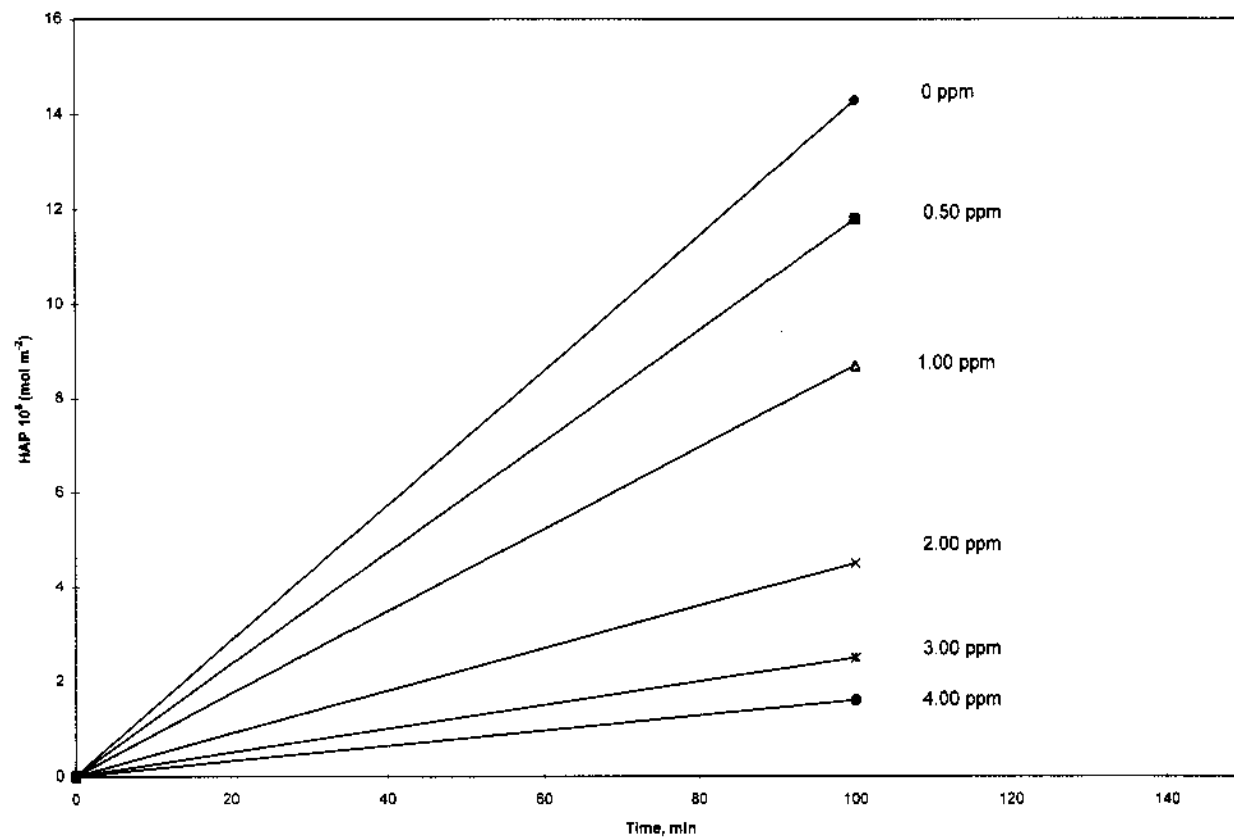


Figure 3. Crystal growth of hydroxyapatite onto hydroxyapatite seed crystals at constant supersaturation in the presence of varying concentrations of tannic acid (TA).

lular weight poly(acrylic acid). The results of these experiments are summarized in Table 2. Amounts of HAP formed in solutions of constant supersaturation versus time profiles for varying concentrations of poly(acrylic acid), PAA, are shown in Figure 4. The data shown in Figure 4 indicates that PAA is an effective HAP growth inhibitor. Figure 5 shows the competitive inhibition data for SA, TA, FA, and BHCA at 0.5 ppm. The data indicates that BHCA (highly anionic compound) exhibits superior performance compared to SA, TA, and FA. Growth rates obtained in the presence of 1 ppm inhibitor concentration for PAA, BHCA, FA, and TA are $\ll 1$, 2.9, 6.8, and 10.4 ($10^8 \text{ mole min}^{-1} \text{ m}^{-2}$), respectively. It is worth noting that, under similar experimental conditions, BTCA did not exhibit any inhibitory activity (Table 2). Based on this inhibition data (Table 2 and Figure 6), the ranking in terms of inhibitor efficacy is:

$$\text{PAA} > \text{BHCA} > \text{FA} > \text{TA} \gg \text{BTCA}, \text{SA} = \text{control (no additive)}.$$

The kinetic data clearly suggests that overall ionic charge of the additive plays a key role in influencing the growth rate. This is consistent with previous observations that the best inhibitors for BaSO_4 precipitation were those that imparted the most negative electrophoretic mobility to the BaSO_4 particles.²⁰ Similar observations have been reported in kinetic studies involving the effect of polycarboxylic acids on the crystallization of dicalcium phosphate dihydrate²¹ and calcium carbonate.²²

Polymeric and non-polymeric inhibitors play an important role in several industrial and biological processes where precipitation of sparingly soluble salts must be prevented. To explain the influence of inhibitors on the crystal growth and dissolution of sparingly soluble salts, various mechanisms have been proposed, including: a) inhibitor absorption on the crystal surface, either generally or at the active sites, b) inhibitor formation of stable solution complexes with calcium, thus reducing solution supersaturation, and c) supersaturation decrease due to increased solubility resulting from increased ionic strength. Under the experimental conditions employed in the present study, however, the decrease in rate of crystallization must be attributed to surface adsorption rather than to an increase in ionic strength of the supersaturated solution in the presence of inhibitor. Inhibitors concentration is orders of magnitude smaller than a concentration that would give rise to significant changes in ionic strength or to simple calcium-inhibitor complex formation. The percentage of calcium complexed, even at the highest inhibitor concentration, accounts for less than 4% of total calcium concentration in solution (M. Reddy, unpublished results).

Previous investigations of the influence of both polymeric and non-polymeric inhibitors have shown that the reduction in the rates of crystal growth and dissolution of sparingly soluble salts by inhibitory anions follow a Langmuir adsorption model. If the adsorbed inhibitor at concentration $[B]$ covers a fraction (A) of the total available surface, then the rate of adsorption may be expressed as $k_1 [B](1-A)$ and the rate of desorption as $k_2 A$, where k_1 and k_2 are the corresponding rate constants. At equilibrium, then:

$$R / (R - R_i) = 1 + (k_2 / k_1) [B] \quad (2)$$

where R and R_i are the growth rate constants in the absence and presence of inhibitors, respectively. According to Equation 2, a plot of $R / (R - R_i)$ against $[B]^{-1}$ should give a straight line. Such plots for fulvic acid and tannic acid are shown in Figure 7. The data in Figure 7 suggest that crystal growth of HAP is completely inhibited, i.e., ~ 1 at a concentration of 1.3 and 3.9 ppm for FA and TA, respectively, which may be compared with 0.65 ppm obtained for PAA. Table 3 summarizes the concentrations needed for complete inhi-

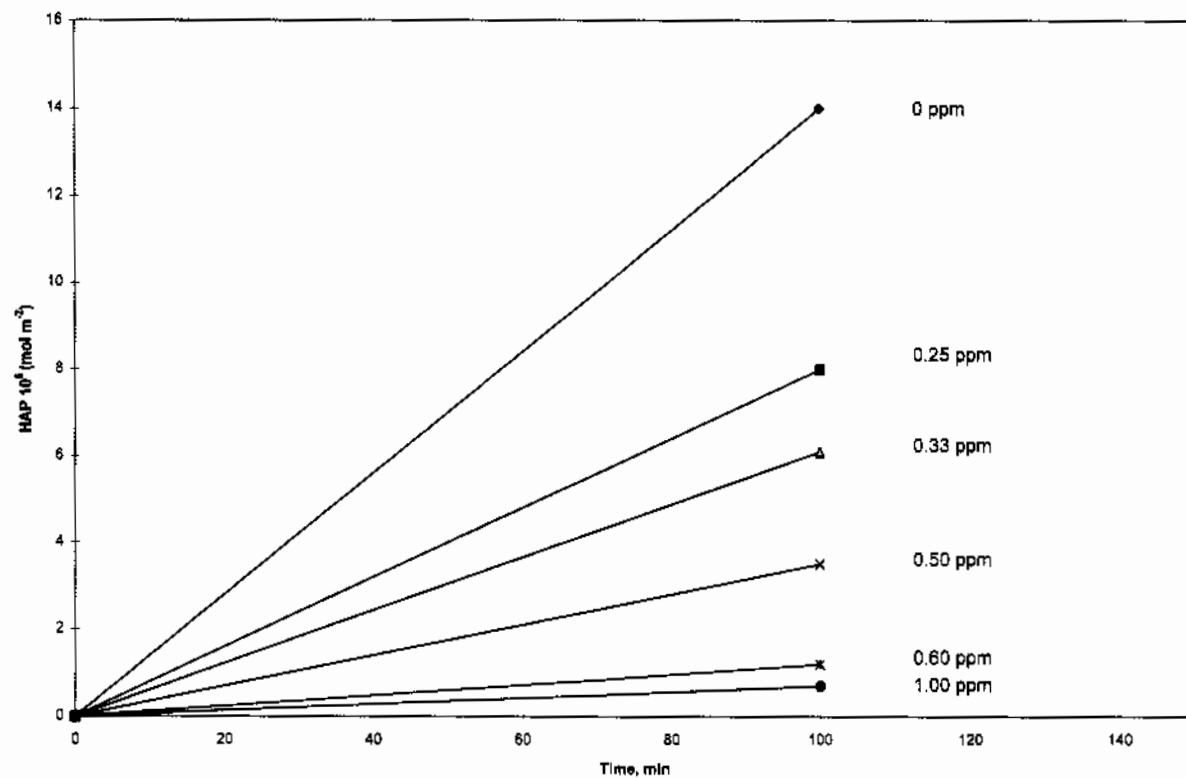


Figure 4. Hydroxyapatite crystal growth onto hydroxyapatite seed crystals at constant supersaturation in the presence of various additives at 0.5 ppm concentration.

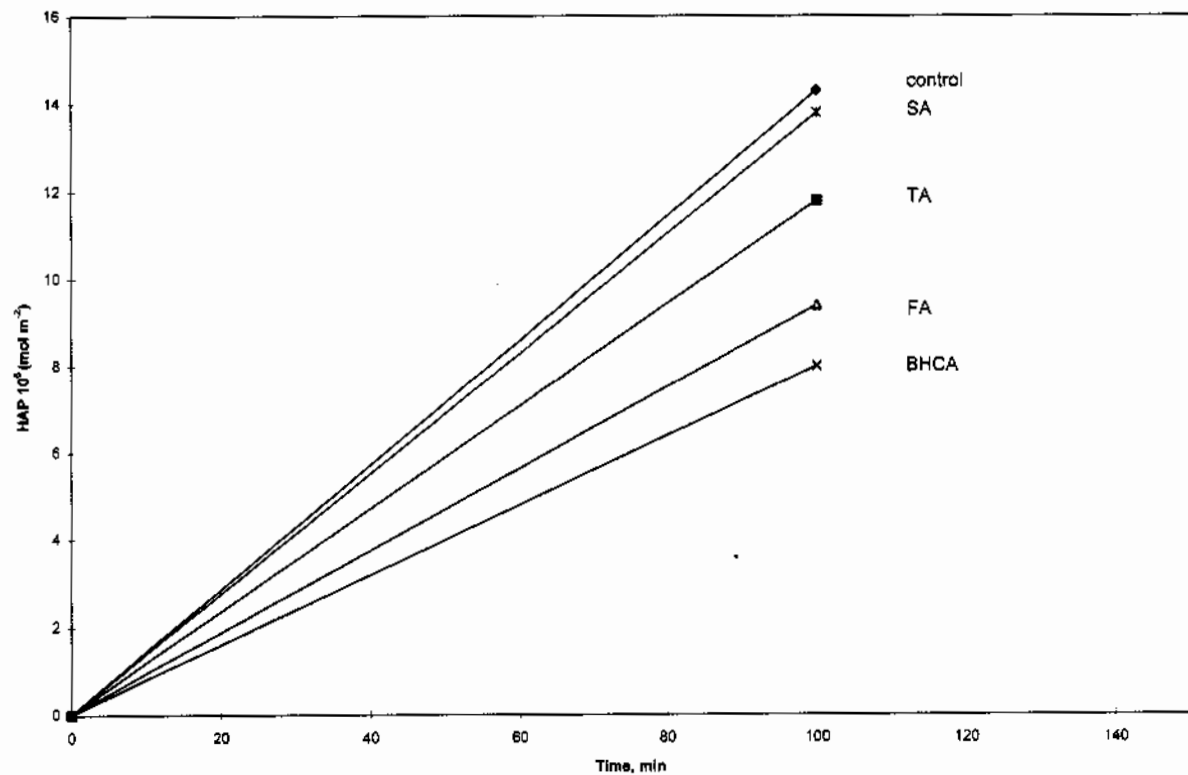


Figure 5. Hydroxyapatite crystal growth onto hydroxyapatite seed crystals at constant supersaturation in the presence of various additives and poly (acrylic acid) (PAC), (SA concentration = 1 ppm, all others are 0.5 ppm).

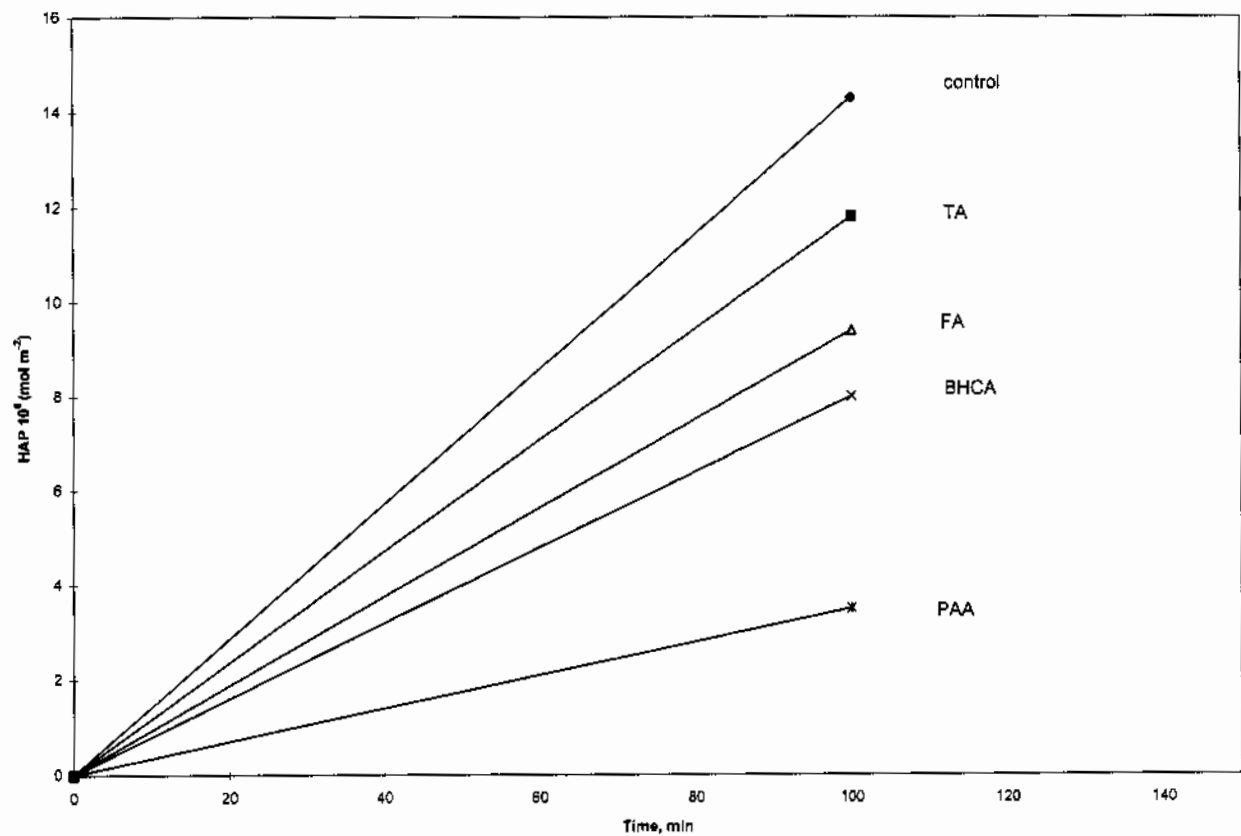


Figure 6. Hydroxyapatite crystal growth onto hydroxyapatite seed crystal at constant supersaturation in the presence of varying concentrations of poly (acrylic acid) (PAA).

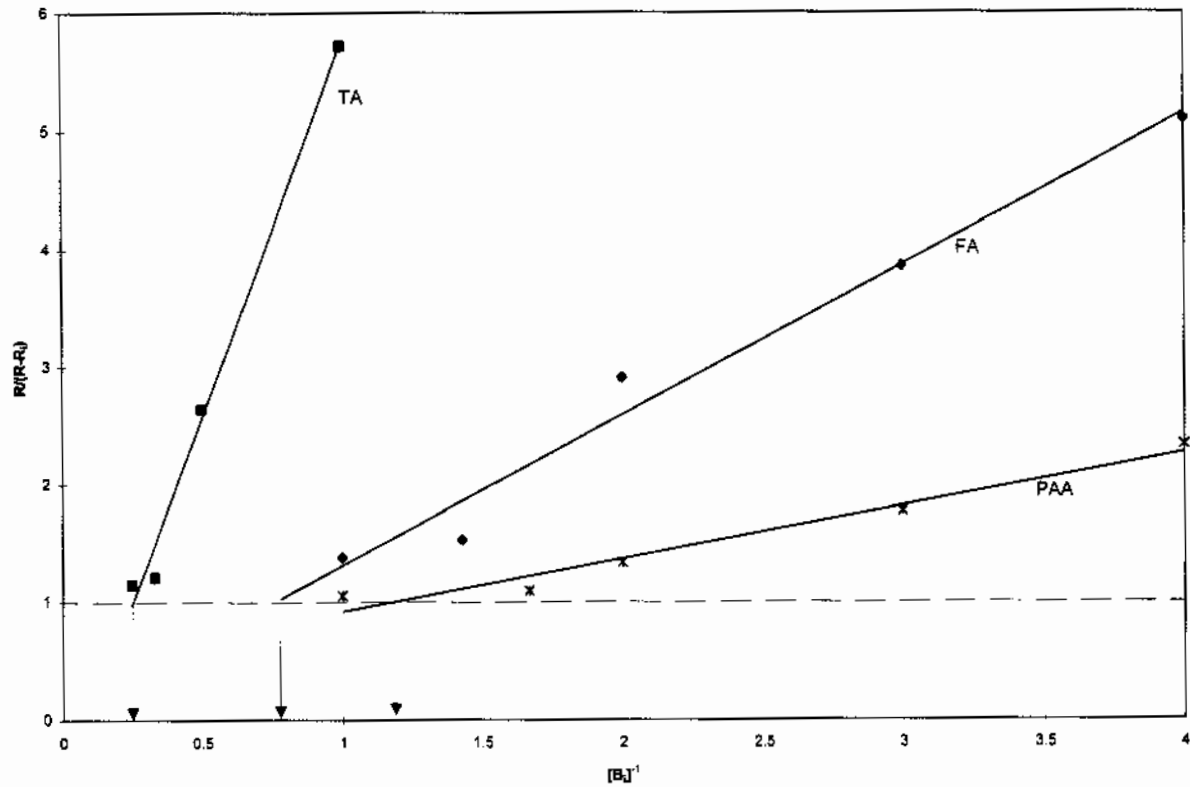


Figure 7. The Langmuir rate function for hydroxyapatite crystal growth onto hydroxyapatite seed crystals at constant supersaturation plotted as a function of the reciprocal fulvic acid (FA), tannic acid (TA), and poly(acrylic acid) (PAA) inhibitor concentrations.

Table 3. Comparative growth rate data on inhibitor performance as indicated by the inhibitor concentration needed to reduce the growth by 50% in the absence of inhibitor for HAP, DCPD, and calcite

System	Inhibitor conc, ppm			Ref.
	FA	TA	PAA	
HAP	1.3	3.9	0.65	this study
DCPD	0.52	0.83	0.021	submitted for publication
Calcite	0.45	1.1		submitted for publication

bition for HAP, DCPD, and calcite for FA, TA, and PAA. It is interesting to note that for all these systems the order of inhibitor effectiveness is the same, i.e., PAA > FA > TA.

The inverse of the slope of the straight line (Figure 7) is a measure of the sorption “affinity constant” of the inhibitor for HAP and may be useful for comparing the effect of various inhibitors. Because molecular weights of fulvic and tannic acids are not available for comparing the performance of various inhibitors, an arbitrary criterion was selected to determine the concentration of inhibitor that results in 50% reduction in growth rate ($R_{0.5}$). Table 4 lists the concentration of a variety of inhibitors for HAP system taken from this report and other published investigations.

Comparison of $R_{0.5}$ for various carboxyl- and/or hydroxy-containing additives reveals that the most effective inhibitor among these additives is poly(acrylic acid) and the additive which exhibits the least effectiveness is glycolic acid. This ranking of performance suggests that the inhibitory power strongly depends upon the ionic charge of the additive.

Among the phosphorus-containing additives, the best performance is observed for HEDP and PBTC. Phytic acid showed the poorest performance (by a factor of 50 less effective than HEDP).

Regarding the influence of metal ions, zinc ions are ten times more effective in inhibiting HAP crystal growth than magnesium ions. It is interesting to note that the inhibitory power of zinc is comparable to phosphonates which are considered to be the best inhibitors for HAP.

Table 4. Inhibitor concentration that reduces HAP growth rate onto HAP seed crystals at constant supersaturation to one half the inhibitor-free value (i.e., $R_{0.5}$)

Inhibitor	Acronym	Inhibitor Conc, ppm	Ref.
Fulvic acid	FA	1.3	this study
Tannic acid	TA	3.9	this study
Mellitic acid	MA	1.9	6
Citric acid	CA	11	4
Glycolic acid	GLA	38	7
Poly(acrylic acid)	PAA	0.65	this study
Pyrophosphate	PYP	0.18	4
Phytic acid	PA	5.8	23
Nitrilotri(methylene phosphonic acid)	NTMP	0.4	4
1-Hydroxyethylidine-1,1-diphosphonic acid	HEDP	0.12	4
2-phosphonobutane-1,2,4-tricarboxylic acid	PBTC	0.11	7
Hydroxyphosphono acetic acid	HPA	0.22	7
Magnesium	Mg	1.3	24
Zinc	Zn	0.13	25
Glucose	GL	5.9	26

REFERENCES

1. Gaffar A and Moreno EC, "Evaluation of 2-Phosphono- in butane 1,2,4-Tricarboxylate as a Crystal Growth Inhibitor *in vitro* and *in vivo*", J Den Res, 1985;64:6-11.
2. Amjad Z, "Constant Composition Study of the Crystal Growth of Dicalcium Phosphate Dihydrate. The Influence of Polyphosphates, phosphonates, and Phytate", Can J Chem, 1988;66:2 181-2187.
3. Meyer JL and Nancollas GH, "The Influence of Multidentate Organic Phosphonates on the Crystal Growth of Hydroxyapatite", J Crystal Growth, 1973;13:295-303.
4. Amjad Z, "The Influence of Polyphosphates, Phosphonates, and Poly(carboxylic acids) on the Crystal Growth of Hydroxyapatite", Langmuir 1987;3: 1063 -1069.
5. Nancollas GH and Tomson MB, "The Precipitation of Biological Minerals", Faraday Discussion Chem Soc, 1976;61:176-183.
6. Amjad Z, "The Influence of Mellitic Acid on the Crystal Growth of Hydroxyapatite" In *Adsorption on and Surface Chemistry of Hydroxyapatite*, D.N. Misra (Ed.) Plenum Press, New York, 1984.
7. Amjad Z, "Inhibition of Hydroxyapatite Crystal Growth by Phosphonated Hydroxy Carboxylic Acids, Non-Phosphonates Hydroxy Carboxylic Acids, and Poly (Acrylic Acid)", Phos Res Bull, 1997;7: 1-16.
8. Amjad Z, "Evaluation of Phosphono-, Alpha hydroxy Carboxylic, and Polycarboxylic acids as Dicalcium Phosphate Dihydrate Crystal Growth", In *Mineral Scale Formation and Inhibition*, Z.Amjad (Ed.), Plenum Press, New York, 1995.
9. Smith BR and Alexander AE, "The Effect of Additives on the Process of Crystallization. II. Further Studies on Calcium Sulfate", J Colloid Interface Sci, 1970;34:81-90.
10. Amjad Z, "Performance of Polymeric Additives as Hydroxyapatite Crystal Growth Inhibitors", Phos Res Bull, 1995;5:1-12.
11. Amjad Z, "Constant Composition Study of Dicalcium Phosphate Dihydrate Crystal Growth in the Presence of Poly(acrylic acids)", Langmuir, 1989;5: 1222-1 225.
12. Amjad Z, "Inhibition of Barium Sulfate Precipitation: Effects of Additives, Solution pH, and Supersaturation", Water Treatment, 1994;9:47-56.
13. Amjad Z, "Inhibition of Calcium Fluoride Crystal Growth by Polyelectrolytes", Langmuir, 1991;7:2405-2408.
14. Amjad Z, Pugh J, Zibrida J and Zuhl R, "Polymer Performance in Cooling Water: The Influence of Process Variables", Materials Performance, 1997;36(1):32-38.
15. Shimabayashi S, Hashimoto N, Kawamura H and Uno T, "Formation of Hydroxyapatite in the Presence of Phosphorylated and Sulfated polymer in an Aqueous Phase", In *Mineral Scale Formation and Inhibition*, Z. Amjad (Ed.), Plenum Press, New York, 1995.
16. Williams G and Sallis JD, "Structural Factors Influencing the Ability of Compounds to Inhibit Hydroxyapatite Formation", Calcif Tissue Int, 1982;34: 169-177.
17. Nystrom M, Ruohomaki K and Kaipia L, "Humic Acid as a Fouling Agent in Filtration", Desalination, 1996;106:79-87.
18. Lacout JL, Koutsoukos PG, Rouquet N, and Freche M, "Effect of Humic Compounds on the Crystal Growth of Dicalcium Phosphate Dihydrate", Agrochimica, 1992;36:500-510.
19. Leenheer JA, Wershaw RL, and Reddy MM, "Strong Acid, Carboxyl-Group Structures in Fulvic Acid from the Suwannee River, Georgia. I. Minor Structures". Envir. Sci. Tech., 1995;29:393-398.
20. Coffey MD, Paper No. SPE 5302, Inter. Symp. Oilfield, Soc. Pet. Eng., Dallas, Texas, 1975.
21. Amjad Z, "The Inhibition of Dicalcium Phosphate Dihydrate Crystal Growth by Polycarboxylic Acids", J. Colloid Interface Science, 1987;117:98-103.
22. Amjad Z, "Kinetic Study of the Seeded Growth of Calcium Carbonate in the Presence of Benzene Polycarboxylic Acids", Langmuir, 1987;3:224-228.
23. Koutsoukos PG, Amjad Z, and Nancollas GH, "The influence of Phytate and Phosphonate on the Crystal Growth of Fluorapatite and Hydroxyapatite", J. Colloid Interface Science, 1981;83:599-605.
24. Amjad Z, Koutsoukos PG and Nancollas GH, "The Crystallization of Hydroxyapatite and Fluorapatite in the Presence of Magnesium Ions", J. Colloid Interface Science, 1984;101:250-256.
25. Dalpi M, Karayianni E and Koutsoukos PG, "Inhibition of Hydroxyapatite Formation in Aqueous solutions by Zinc and 1,2-Dihydroxy- 1,2-bis(dihydroxyphosphonyl)ethane", J. Chem. Soc. Farady Trans., 1993; 89:965-969.
26. Dalas E and Koutsoukos PG, "The Effect of Glucose on the Crystallization of Hydroxyapatite in Aqueous Solutions", J. Chem. Soc. Farady Trans., 1989;85:2465-2472.

CRYSTAL GROWTH OF HYDROXYAPATITE IN VITRO AND DENTAL CALCULUS AND PLAQUE FORMATION ON HUMAN TEETH IN VIVO

Abdul Gaffar,¹ Edgard C. Moreno,² John Afflitto,¹ and Yelloji-Rao K. Mirajkar¹

¹Colgate-Palmolive Company

909 River Road

Piscataway, New Jersey 08855

²Department of Physical Chemistry

Forsyth Dental Center

Boston, Massachusetts 02115

1. ABSTRACT

Sodium polyvinylphosphonic acid (SPVPA) was synthesized using vinyl phosphonyl dichloride and azobisisobutyronitrile (AIBN) as a radical initiator. The homopolymer obtained was characterized by molecular weight, purity and impurities by using gel permeation chromatography and NMR. The pure polymer was used to assess the influence on crystal growth kinetics of hydroxyapatite (HAP) in vitro. Briefly, the experimental solution supersaturated with respect to hydroxyapatite (HAP) was prepared from stock solutions of CaCl_2 , K_2HPO_4 , KH_2PO_4 , and NaCl . The crystal growth was initiated by adding pure seeds of HAP at 37 °C. The precipitation kinetics was followed using a pH-stat and measuring calcium phosphate in the solution. The effect of the polymer on the crystal growth kinetics was assessed, and it was found that the polymer inhibited the growth at 10^{-5} M. The inhibitory effect of the polymer was related to its adsorption onto the growing crystals. The adsorption parameters were derived from an adsorption isotherm-yielding a K value of 1,950 ml/mM and the N value of 0.038 mM/m². A topical application of 1% solution of the polymer onto teeth was effective in reducing calculus formation by 18% in rat model system. SPVPA was also very effective in reducing adsorption (>90%) of radio-labelled bacteria, *Streptococcus mutans*, and *Actinomyces viscosus*, onto saliva-coated hydroxyapatite beads and disks. The polymer was also tested in short-term human clinical studies and showed that 1% and 3% solutions significantly ($P = 0.05$) reduced bacterial plaque film on teeth by 21 to 36%, respectively. Collectively, the data indicated that the

sodium polyvinylphosphonic acid has the potential to prevent soft and hard dental deposits on teeth.

2. INTRODUCTION

Dental plaque and calculus formation are the two processes that occur either subgingivally or supragingivally. If not removed or prevented, dental calculus and plaque tend to accumulate, initially prominent at the gingival margin and with time could cover an entire tooth. If these deposits are allowed to persist, they promote the development of oral diseases such as gingivitis and periodontitis leading to the loss of teeth.¹ Oral hygiene practices such as brushing and rinsing can remove plaque to a certain extent, but these methods either practiced at home or in dental offices are time consuming, painful and expensive. Another approach would be to develop chemical agents which provide dual effect to inhibit dental plaque and calculus formation. Inhibitory effects on crystal growth both in vitro and in vivo have been reported earlier for several carboxyphosphonates.² Similarly, studies carried out in the past 5 years have shown anticalculus effects of PVM/MA copolymer both in vitro and in vivo.

The aim of this research was to develop compounds that could inhibit formation of both calculus and plaque. Sodium polyvinylphosphonic acid (SPVPA), a homopolymer, is one of the compounds which has been studied extensively. In this paper, the results of the high molecular weight copolymer sodium polyvinylphosphonic acid (SPVPA) are presented. Various aspects tested with this copolymer include inhibitory effects on the formation of calculus minerals, adsorption of polymer to model tooth surfaces and oral bacteria, and its impact on the formation of dental plaque and calculus in vivo. Attempts have been made to understand the mechanisms associated with the processes inhibiting the formation of both plaque and calculus.

3. MATERIALS AND METHODS

3.1. Synthesis of SPVPA

Sodium polyvinylphosphonic acid (SPVPA) was synthesized using vinyl phosphonyl dichloride and Azobisisobutyronitrile (AIBN) as a radical initiator. Detailed procedures of polymer synthesis and characterization is reported elsewhere.² Briefly, after synthesis polymer sample was dialyzed overnight using a dialysis membrane having a 3500 Dalton cut off and recovered by lyophilization. The ³¹P NMR solution spectrum in D₂O showed a major peak at 2239 Hz (Varion FT 80A, carrier frequency 32.198 MHz) characteristic of this polymer. The molecular weight of the polymer estimated by the light scattering method was 12,000.

Synthesis of ¹⁴C-SPVPA, used as tracer in adsorption studies, was prepared as described elsewhere.⁶ The product had specific activity of 5 mCi/mg and radiochemical purity over 99%.

3.2. Seeded Crystal Growth

The supersaturated solution used was prepared from the stock solutions of CaCl₂, K₂HPO₄, KH₂PO₄ and NaCl. The two phosphate solutions were mixed in appropriate pro-

portions to obtain an initial pH of 7.4. The nominal concentrations of calcium and phosphate were 1.06 and 0.63 mM, respectively, with 50 mM NaCl as a background electrolyte. Although the supersaturated solution did not produce any spontaneous precipitation over a period of several days, fresh solutions were prepared and thermostated at 37 ± 0.02 °C prior to each experiment. A stock solution of SPVPA was prepared by dissolving the polymer in distilled, deionized water containing 50 mM NaCl (as a background electrolyte). The pH of the stock solution of polymer was adjusted to 7.4 using NaOH and stored at 4 °C. In all the experiments, aliquots of the inhibitor solutions were added to the supersaturated solution to provide predetermined original concentrations.

Details of the experimental procedure and preparation of the seed slurry were the same as previously described.⁷ Briefly, the experimental solution (250 ml) was maintained at 37 °C in a water bath and stirred with a Teflon coated magnetic stir-bar at a constant rate. The solution pH, monitored using low-flow reference and glass electrodes, was recorded continuously as a function of time. After the solution reached thermal equilibrium and constant pH reading, the precipitation reaction was initiated by adding a slurry of hydroxyapatite seeds. The time course of the seeded crystal growth was followed by a continuous pH reading and by removing 3 ml aliquots of well-stirred experimental solution before seeding and at specified intervals throughout the experimental period (5 hr, unless otherwise specified). These aliquots were quickly filtered through Millipore filters (0.33 mM), and analyzed for calcium and total phosphorus concentrations. Calcium concentrations were determined using atomic adsorption spectrophotometer and phosphorus concentrations by colorimeter.

3.3. Adsorption of SPVPA to the Hydroxyapatite Crystal

The adsorption of SPVPA was determined at 25 °C using two different solutions; one with 1×10^{-6} M SPVPA and 50 mM NaCl, and the other with 1×10^{-6} M SPVPA and solution used for crystal growth studies (0.65 mM total phosphate, 1.07 mM Ca and 50 mM NaCl). The initial pH was adjusted to 7.4 in both solutions. To avoid any precipitation of calcium-PVPA during the preparation of experimental solutions, calcium was introduced simultaneously with the adsorbent into the solution. Before introducing the adsorbent into the solution, 50 ml of ¹⁴C-SPVPA (1.4 mCi) was added to the well-stirred (using Teflon coated magnetic stir-bar) solution and then 100 ml of the solution was withdrawn to determine the initial counts of radioactivity.

Hydroxyapatite crystals used as adsorbent were with specific surface area of 10.6 m²/g. Accurately weighed HAP (30 mg) was dispersed with a vortex in 1 ml of 50 mM NaCl or 100 mM CaCl₂ solution (to yield a concentration of 1 mM calcium in the experimental solutions). The slurry was then introduced into the well-stirred adsorbate solution. Starting from zero, aliquots of 250 ml were withdrawn at different time points and each sample was centrifuged at 3000 rpm for 1 min. (37 °C). An aliquot of 100 ml of the supernatant was transferred to a vial and mixed with a scintillation cocktail (Aquasol-2, New England Nuclear). The radioactivity of each sample was counted for 5 min. using a liquid scintillation spectrometer (Packard Instruments Co., Model TRICARB 2000).

Adsorption of SPVPA onto hydroxyapatite as a function of polymer concentration was conducted as follows. Different concentrations of cold-SPVPA ranging from 10^{-4} to 10^{-6} M were prepared containing 50 mM NaCl (as background electrolyte with final pH of 7.4 adjusted using NaOH). Two of these solutions were transferred to 6 ml polystyrene test tube (with a tight cap) and the radiolabelled SPVPA (5×10^{-2} mCi) was added as a tracer to the above solutions. Accurately weighed HAP crystals (5 mg to 200 mg) were

added to the solutions. The resulting slurry was shaken vigorously in a water bath maintained at 37 °C. In all the measurements, a control solution containing equal amount of radiolabelled SPVPA without adsorbent were also included. After 3 hr. of shaking, the slurry (and the blank) was centrifuged as described above and then an aliquot of 100 ml was withdrawn from the supernatant for measuring radioactivity remaining in the solution. The final concentration of SPVPA in the equilibrium solution C ml/ml was calculated according to

$$C = C_o \times \text{CPMf/CPMi} \quad (1)$$

where C_o is the initial concentration of SPVPA, CPMf and CPMi are the counts per minute in equilibrated and blank solutions, respectively. The amounts of SPVPA adsorbed onto HAP, Q (mM/m²), was also calculated based on the mass balance of the SPVPA molecule in the system concerned

$$Q = C_o (1 - \text{CPMf/CPMi}) V/S \quad (2)$$

where V = solution volume (2 ml in this case) and S = total surface area of the adsorbent (m²).

3.4. Bacterial Cultures and Culture Conditions

Bacterial strains *A. viscosus* (T14V), *A. viscosus* (LY7), *S. Sobrinus* (6715–41), *S. mutans* (MT3) and *S. mutans* (JBP) were obtained from the culture collection of the Forsyth Dental Center, Boston, MA. They were grown overnight from the frozen state in Trypticase soy media without glucose (BBL Cockesville, MD) (composition given in Table 1). The next day cells were counted and 1.0×10^6 cells/ml were added to the above media containing 0.2% glucose and 5 mCi [³H]thymidine (New England Nuclear Corp., Boston, MA - sp. act 73.6 Ci/mM). The cells were incubated anaerobically for 22 hr. at 37 °C. After incubation, the cells were washed twice with 50 mM sodium phosphate buffer (pH 7.0) and resuspended in the same buffer to a concentration of 1.0×10^9 cells/ml. The cells were dispensed in cryo tubes (Nunc, Denmark) in 1 ml quantities and frozen at -70 °C.

Prior to attachment tests, frozen cells with [³H] thymidine were thawed slowly in warm water and washed three times with adsorption buffer to remove any extracellular radioactivity. After the last wash, the bacterial pellet was resuspended in a small amount of buffer and sonicated using a Kontes micro-ultrasonic cell disrupter. Sonication was performed using 5–8 short pulses to achieve a uniform suspension without damaging the bac-

Table 1. Chemical composition of Trypticase labeling media

Compound	Concentration, mM
Trypticase (BBL)	2.0
NaCl	0.2
KH ₂ PO ₄	0.4
Na ₂ HPO ₄	0.2
K ₂ CO ₃	0.1
MgSO ₄	0.012
MnSO ₄	0.0015
Adjusted to pH 7.0	

terial membrane. A final concentration of 10^8 cells/ml was made using adsorption buffer containing 25 mg/ml human serum albumin (Sigma, Fraction V). Previous experiments have shown that the human serum albumin at the above concentration prevents non-specific adsorption of bacteria to the tubes without altering the adsorption of the bacteria to the disks.^{8,9}

3.5. Bacterial Attachment Assay

3.5.1. Adhesion to Saliva Coated Hydroxyapatite (SCHAP) Beads. Bacterial attachment to saliva coated beads was determined by a technique described previously.¹⁰ Briefly, samples of whole stimulated saliva, collected from an adult donor in containers chilled in ice, were clarified by centrifugation at $10,000 \times g$ for 10 min. Samples (30 mg) of spheroidal HAP beads (BDH Biochemical Ltd., Poole, England) equilibrated with buffered KCl, incubated with 1 ml clarified saliva for 1 hour and washed with buffered KCl to remove the saliva not adsorbed. The beads were then treated with different concentrations of SPVPA for 1 hour and washed with buffered KCl as described above. The ability of bacteria to attach to the treated and untreated SCHAP beads was determined as described previously.¹⁰ The mixtures (1.0 ml) contained 5×10^7 [^3H]thymidine-labelled bacteria and 30 mg of saliva treated HAP beads in buffered KCl. All assays were run in duplicate.

3.5.2. Adhesion to Saliva Coated Hydroxyapatite (SCHAP) Disks. The adsorption of [^3H] thymidine-labelled bacteria to saliva coated hydroxyapatite disks was measured as follows. HAP disks were prepared by compressing 250 mg of well-characterized HAP powder (Monsanto, St. Louis, MO) in a KBr die at 600 C for 4 hr. This treatment reduced the porosity. The cooled disks were coated with 1 ml of clarified saliva for 1 hr. The excess saliva was aspirated and the disks were washed with sterile 0.05 M sodium phosphate buffer (pH 7.0) containing 0.6% yeast extract. This buffer was used because buffered KCl significantly affected cell viability. The coated disks were then incubated with a standardized, washed suspension of [^3H] thymidine-labelled bacteria at 37 °C for 90 min. under agitation. The bacterial cell density was measured by ATP content¹¹ after extraction with 0.02 M Tris (pH 7.5) at 110 °C. The net loss was about 20%, based on standard ATP solution. The appropriate corrections were made for the loss. ATP contents of oral bacteria used were standardized via plate and direct microscopic counts. ATP was measured by the firefly luciferase-luciferin reaction with the DuPont Bioluminescence test kit. The ATP contents were converted into the viable cell counts obtained from a standardized suspension of bacteria plated onto Trypticase soy agar.¹¹

3.6. Effect of SPVPA on Calculus Formation in Rats

The topical effect of SPVPA on calculus formation was conducted in a two cell study, each treatment cell (group) containing 10 Osborne-Mendel rats. The rats were fed with a calculogenic diet consisting of the diet 580F, as described previously¹² supplemented with 0.2% P as Na_2HPO_4 . On day 20, the animals were randomly distributed among two treatment groups (two rats per stainless steel, screen bottom cage) and began receiving calculogenic diet and tap water ad libitum. On days 21 and 22, the rats were inoculated twice daily with a heavy suspension of *Actinomyces viscosus* OMZ-105-Ny1. From day 23 on, 100 ml of a 1% solution of SPVPA was applied twice daily with disposable syringes; water was used as a control. The treatments were delivered at 9:00 and 15:00 hr. during the 30 day experimental period. The animals were weighed at the begin-

ning and end of the study. Calculus formation was assessed by the procedure described¹² by Regolati *et al.* The data from the studies was analyzed by an analysis of variance followed by the Student-Newman-Keul's test.

3.7. Effect of SPVPA on Short Term Plaque Formation

A short-term clinical study on humans investigated the impact of SPVPA, used as a mouthrinse, on the plaque formation. The study was conducted as follows. Ten subjects identified as normal plaque formers (Panel I) and six subjects considered heavy plaque formers (Panel II) volunteered for the clinical trial. The teeth of the participants were thoroughly cleaned prior to each period. Sucrose enhanced plaque accumulations were assessed after 4 days of twice daily mouthrinses with 10 ml test agent, during which period no mechanical oral hygiene was performed (Plaque Index, P.I. Silness and Loe). The study design involved a three cell crossover for Panel I and a two cell crossover for Panel II. Each subject in Panel I used each of the three test rinses; 1) deionized water (a negative control), 2) aqueous solution of 1% SPVPA (pH 7) and 3) 0.55 mM chlorhexidine (a positive control). Each participant in Panel II used each of the two test rinses: 1) deionized water and 2) a solution of 3% SPVPA (pH 7). In between each treatment crossover period, at least 10 days was allowed as washout time. Wilcoxon's test for paired comparisons was applied for statistical analyses of the data, using the frequency of the respective P.I. score as test parameter.¹³

4. RESULTS AND DISCUSSIONS

4.1. Crystal Growth Kinetics of Hydroxyapatite in Vitro

The effects of varying concentrations of SPVPA on seeded crystal growth kinetics in the supersaturated solution are shown in Figures 1 to 3, in terms of pH, calcium and phosphorus, respectively, as a function of experimental time (*t*) after seeding at time zero. The

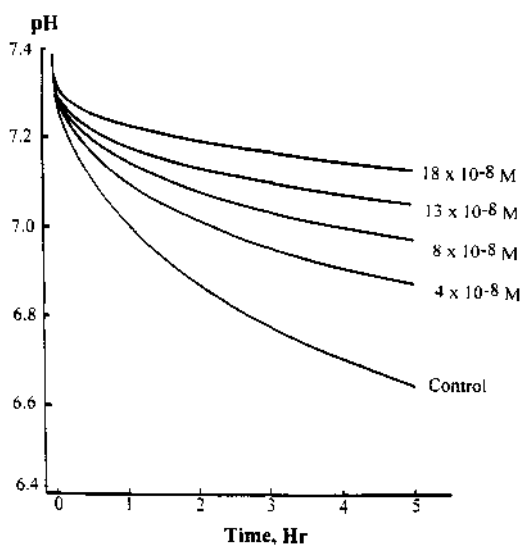


Figure 1. Solution pH vs. time after the addition of hydroxyapatite seeds to the supersaturated solution containing sodium polyvinylphosphonic acid.

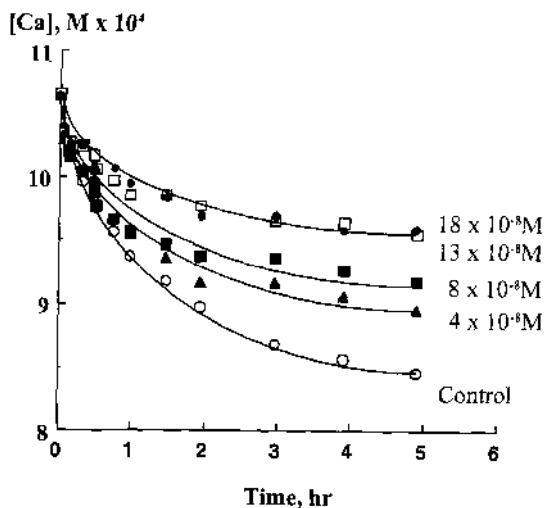


Figure 2. Concentration of calcium in solution vs. time after the addition of hydroxyapatite seeds to the supersaturated solution containing sodium polyvinylphosphonic acid.

corresponding precipitation reaction without inhibitors is also shown as control in all the Figures. The precipitation rates or the seeded crystal growth decreased with increasing concentrations of the polymer in a dose response manner. Complete inhibition of the crystal growth occurred at 0.02 mM of SPVPA. The corresponding value reported for pyrophosphate¹⁴ is 5.7 mM suggesting that SPVPA inhibits crystal growth at a very low concentration.

4.2. Adsorption of SPVPA to the Hydroxyapatite Beads

In order to understand the reasons for inhibition on seeded crystal growth of hydroxyapatite, the adsorption behavior of the polymer onto hydroxyapatite crystals was tested. Preliminary studies were carried out to estimate the equilibration time for the adsorption of polymer. Results of SPVPA adsorption, measured in terms of radioactivity, is

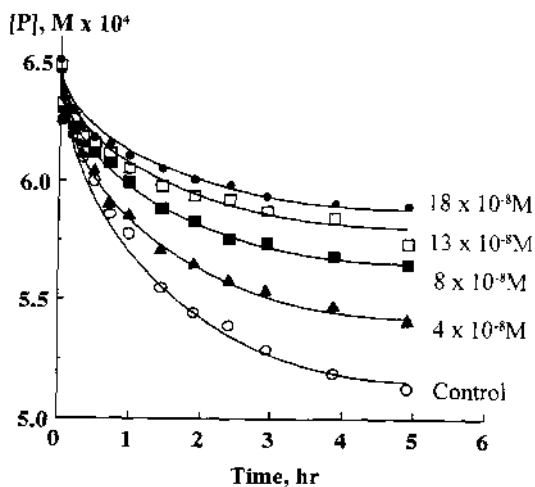


Figure 3. Concentration of phosphate in solution vs. time after the addition of hydroxyapatite seeds to the supersaturated solution containing sodium polyvinylphosphonic acid.

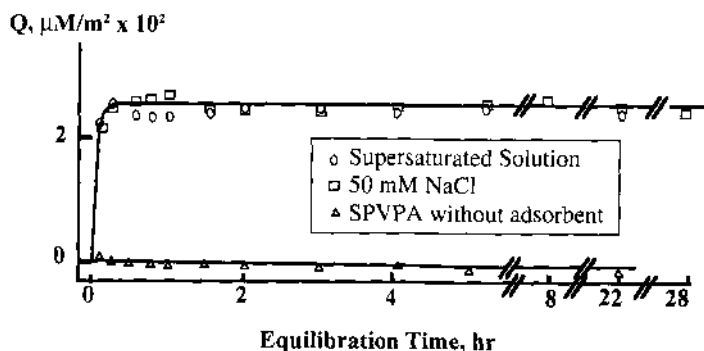


Figure 4. Adsorption of sodium polyvinylphosphonic acid (10^{-6} M) onto hydroxyapatite as a function of equilibrating time after addition of the adsorbent.

shown in Figure 4 as a function of time for the two solutions containing polymer with 1) background electrolyte only and 2) supersaturated solution. In both the cases, the radioactivity of the adsorbate solution decreased rapidly and reached a plateau (adsorption equilibrium) around 30 min. after the addition of HAP crystals. Also shown is the corresponding radioactivity of the control SPVPA solution without the adsorbent. This did not show any changes over the time studied indicating no precipitation of Ca-PVPA in the solution tested and that the decrease in radioactivity observed in the presence of adsorbent is due to the polymer adsorption. From these results, an equilibration time of 3 hr was used in all the subsequent adsorption measurements.

The adsorption isotherm in terms of C/Q vs. C is plotted and shown in Figure 5. The adsorption appears to follow a typical L-shape isotherm. This shape of the curve indicates that the isotherm obtained can be expressed by the Langmuir model, $C/Q = C/N + 1/KN$ ($r = 0.998$). The adsorption parameters N (affinity constant) and K (maximum number of adsorption sites) were obtained by a non-linear least square procedure applied to the expression $Q = NKC/(1+KC)$ using the experimental values of C and Q . The resultant plot is shown in Figure 6 and the values of adsorption parameters are shown below.

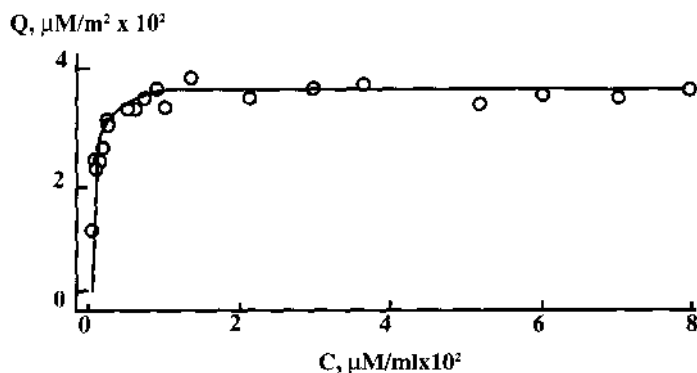


Figure 5. Adsorption isotherm of sodium polyvinylphosphonic acid onto hydroxyapatite at 37 °C.

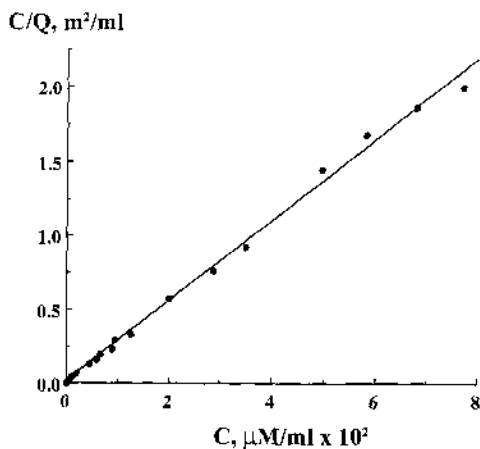


Figure 6. Linearized form adsorption isotherm of sodium polyvinylphosphonic acid onto hydroxyapatite.

Maximum number of adsorption sites

$$K = 1,950 \text{ ml/mM}$$

Affinity constant

$$N = 0.038 \text{ mM/m}^2.$$

4.3. Bacterial Attachment Assay

4.3.1. Adhesion to Saliva Coated Hydroxyapatite (SCHAP) Beads. Bacterial attachment to saliva coated hydroxyapatite beads (SCHAP) was examined by two different methods. In the first method, the ability of bacteria to attach onto SCHAP pretreated with different concentrations of SPVPA. In the other method, the bacteria were pretreated with different concentrations of SPVPA and then tested for their ability to attach onto SCHAP. Control tests of attachment were carried out in buffered KC1 medium. Table 2 shows the results of pretreating saliva coated hydroxyapatite beads with sodium polyvinylphosphonic acid on the subsequent attachment of two oral bacteria *Streptococcus mutans* MT3 and *A. viscosus* LY7. As could be seen, the number of bacteria that could adsorb onto the beads decreased with increasing concentrations of SPVPA used for pretreating. Also, the extent of inhibition to attach to a similar surface differs among bacteria. In this case, inhibition of about 48% with *A. viscosus* and 64% with *S. mutans* was observed. On the other hand, initial pretreatment of the bacteria with sodium polyvinylphosphonic acid reduced their attachment profoundly (Table 3). For example, in the case with *S. mutans* MT3, the attachment reduced by about 94% while those of *A. viscosus* LY7 by about 96%. This clearly suggests that pretreatment with SPVPA significantly alters the attachment characteristics of oral bacteria. These results are significant suggesting the polymer SPVPA could function as an antiplaque agent.

4.3.2. Adhesion to Saliva Coated Hydroxyapatite (SCHAP) Disks. The impact of SPVPA pretreatment on the bacterial attachment onto SCHAP disks was also tested. The rationale in testing this substrate is to represent a low surface-to-volume model, similar to that of the oral environment. In this study also, the effect of pretreatment was carried out

Table 2. Effect of pretreating saliva coated Hydroxyapatite beads (30 mg) with sodium polyvinylphosphonic acid on the subsequent attachment of oral bacteria *Streptococcus mutans* MT3 and *A. viscosus* LY7

Compound treated	<i>S. mutans</i> MT3		<i>A. viscosus</i> LY7	
	Adsorbed ($\times 10^6$)/ 30 mg HAP beads	% Relative to buffer	Adsorbed ($\times 10^6$)/ 30 mg HAP beads	% Relative to buffer
Buffered KCl	5.9 (0.4)	100	39.7 (0.4)	100
0.01% PVPA	4.6 (0.6)	77	35.1 (1.1)	88
0.10% PVPA	3.4 (5.4)	58	31.9 (1.0)	80
1.00% PVPA	3.1 (0.1)	52	14.6 (0.1)	36

either on bacteria or SCHAP prior to the attachment studies. Table 4 shows the effect of pretreating saliva coated hydroxyapatite disks with sodium polyvinylphosphonic acid on the subsequent attachment of three different species of oral bacteria. All the species examined experienced different levels of inhibition in their attachment, more so with *S. mutans* and least in the case of *S. sobrinus* species. The dose response of SPVPA pretreatment was further tested on *A. viscosus* (T14V) species and the results are shown in Table 5. Although pretreatment with 0.01% of SPVPA did not provide any inhibition, such treatment with 0.1 % and above provided increased inhibition. These results clearly suggest that SPVPA polymer, by adsorption onto the oral surfaces, can provide significant inhibition to the bacterial deposition process.

4.4. Effect of PVPA on Calculus Formation in Rats

Sodium polyvinylphosphonic acid (SPVPA) was shown to inhibit not only seeded crystal growth but also bacterial deposition in vitro onto tooth like surfaces. The crystal growth inhibition was further studied in a rat model to test whether in vitro results can translate into in vivo efficacy. The results are given in Table 6 and show a 16% reduction in calculus formation due to topical application of 1% SPVPA when compared to a water control. This suggests the potentiality of the SPVPA as an effective anticalculus agent.

4.5. In Vivo Effect on Plaque Formation in Humans

Sodium polyvinylphosphonic acid (SPVPA) showed promising results in vitro as an effective agent to inhibit bacterial attachment to model tooth surfaces. This concept was fur-

Table 3. Effect of pretreating oral bacteria *Streptococcus mutans* MT3 and *A. viscosus* LY7 with Sodium Polyvinylphosphonic acid on their subsequent adsorption to saliva coated Hydroxyapatite beads

Compound treated	<i>S. mutans</i> MT3		<i>A. viscosus</i> LY7	
	Adsorbed ($\times 10^6$)/ 30 mg HAP beads	% relative to buffer	Adsorbed ($\times 10^6$)/ 30 mg HAP beads	% relative to buffer
Buffered KCl	5.03	100	22.1	100
0.01% PVPA	0.84	17	20.2	91
0.10% PVPA	0.24	5	17.8	81
1.00 % PVPA	0.28	6	0.96	4

Table 4. Effect of pretreating saliva coated Hydroxyapatite disks with Sodium Polyvinylphosphonic acid (1 %) on the subsequent attachment of different oral bacteria

Bacteria	% Inhibition
<i>A. Viscosus (T14V)</i>	65.0
<i>A. viscosus (LY7)</i>	50.3
<i>S. Sobrinus (6715-41)</i>	22.9
<i>S. mutans (JBP)</i>	71.3

Table 5. Effect of pretreating saliva coated Hydroxyapatite disks with Sodium Polyvinylphosphonic acid on the subsequent attachment of oral bacteria *A. viscosus (LY7)*

Compound treated	<i>A. viscosus LY7</i>	
	Cells adsorbed ($\times 10^6$)/disk	% relative to buffer
Buffered KCl	9.7	100.0
0.01% PVPA	10.2	104.0
0.10% PVPA	3.0	30.1
1.00% PVPA	3.9	40.5

ther tested in a short term (4-day) human clinical study using SPVPA as a mouthrinse. As mentioned earlier, the performance was compared against a negative control (water) and a positive control (chlorhexidine). In the case with panelists involving heavy plaque formers, only a two cell study, 3% PVPA and water control, was carried out. The results from the study involving Panel-I are shown in Figure 7 and for Panel-II are shown in Figure 8. Frequency distributions of P1.I. scores 0, 1, 2+3 for each test agent are also shown in the respective Figures. The bars represent the mean number of surfaces, given in percent, with the respective P1.I. score. SPVPA decreased plaque accumulations significantly compared to control, but was significantly less effective than chlorhexidine (Figure 7). The number of surfaces with P1.I. 1 increased at the expense of scores 2+3, with 1% SPVPA (Figure 7). However, SPVPA at 3% gave increased numbers of both scores 0 and 1 (absence or low plaque score) (Figure 8). P1.I. score of 3 (high plaque score) was never recorded with chlorhexidine or 3% SPVPA. No adverse reactions were observed after SPVPA rinses.

Additional analyses of the data from Panel I showed that 22% of all surfaces with P1.I. 1, and 6% of all surfaces with scores 2+3 after water rinses, were recorded as plaque-

Table 6. Effect of topically applied SPVPA on calculus formation in rats

Treatment	n	Mean plaque (S.D)	% Reduction	Significance
Water	15	30.8 (4.0)	—	—
1% SPVPA	15	26.0 (5.3)	16.0	P = 0.05

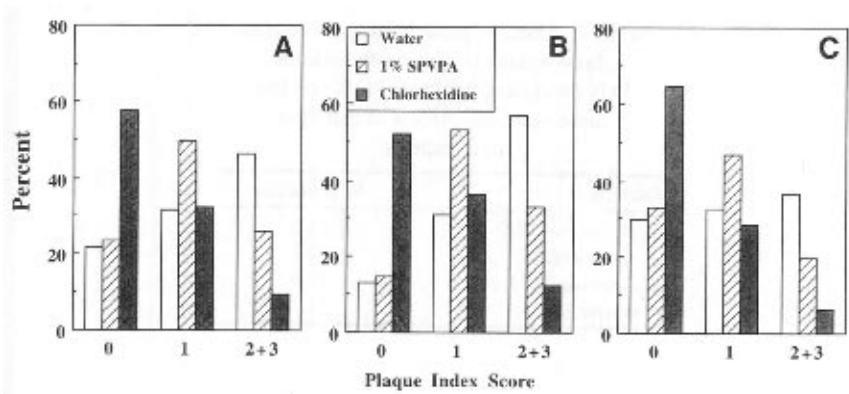


Figure 7. Plaque score index in panel-I. A) all surfaces; B) approximal surfaces and C) smooth (facial and lingual) surfaces ($P < 0.02$).

free with 1% SPVPA. 52% of all surfaces with scores 2+3 after water rinses, decreases to P.I. 1 with 1% SPVPA. Similar analysis of the data from Panel II showed that 25% of all surfaces with P.I. 1, and 8% of all surfaces with scores 2+3 after water rinses, were recorded as plaque-free with 3% SPVPA. Also, 58% of all surfaces with scores 2+3 after water rinses, decreased to P.I. 1 with 3% SPVPA. It is speculated that the SPVPA adsorbs to the enamel through the charged phosphonic groups. PVPA may thus compete with bacteria for attachment sites on the tooth surface and thereby reduce bacterial adhesion. Binding of the polymer to plaque components may also interfere with cohesion of plaque microorganisms. PVPA appears to work as a non-antibacterial agent to reduce plaque accumulation *in vivo*. All these results clearly show that the polymer SPVPA is an effective agent to inhibit the plaque formation.

Mean plaque scores, shown in Table 7, with 1% SPVPA rinse reduced plaque by about 21 % while similar rinse with 3% polymer reduced plaque by about 36%. Considering the nature of the panelists, application of 3% polymer to normal plaque formers could provide more pronounced reductions compared to a placebo. SPVPA molecule has the capacity to adsorb to the enamel through the charged phosphonic groups. Such adsorption

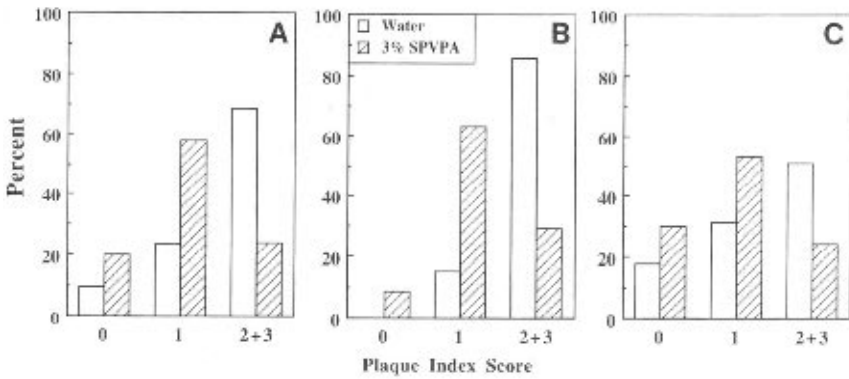


Figure 8. Plaque score index in panel-II. A) all surfaces; B) approximal surfaces and C) smooth (facial and lingual) surfaces ($P < 0.02$).

Table 7. Effect of SPVPA on plaque formation in humans

Treatment	Mean plaque (S.D)	% reduction*
A. Panel I (n = 10)		
Placebo	1.30 (0.39)	—
1% SPVPA	1.03 (0.40)	–21
B. Panel II (n =6)		
Placebo	1.62 (0.21)	—
3% SPVPA	1.04 (0.20)	–36

*P (value based on a paired “t” test) = 0.05

sites can compete with bacterial attachment and thereby reduce plaque formation. Binding of the polymer to plaque bacteria and other components could also similarly interfere with cohesion of plaque microorganisms.

5. SUMMARY

Sodium polyvinylphosphonic acid (SPVPA), a homopolymer, has been examined as an agent with anticalculus and antiplaque properties. In vitro tests show the polymer as an effective inhibitor for seeded hydroxyapatite crystal growth. Adsorption of polymer to hydroxyapatite, both onto crystals and in a low surface-to-volume model, appear to follow a Langmuir model. Attachment of oral bacteria onto hydroxyapatite surface decreased significantly due to the pretreatment with SPVPA. This has been proposed to be due to the ability of the polymer to adsorb onto both the model tooth surfaces and the bacterial surfaces. The solution chemistry of phosphate and the current adsorption data support the proposed hypothesis. An in vivo rat model further showed that topical application of polymer reduces calculus formation. A human study showed the polymer to prevent plaque formation both in normal plaque formers and heavy plaque formers. The polymer has dual effect both inhibiting adsorption of bacteria onto teeth and reducing hard dental deposits, calculus.

ACKNOWLEDGMENTS

The authors would like to thank Ms. S. Herles, Mr. A. Esposito for their excellent assistance in carrying out this work. We acknowledge the help from O. Stringer and A. Charig for their help in the preparation of radiolabelled polymer samples.

REFERENCES

1. Listgarten MA, “The role of dental plaque in gingivitis and periodontitis”, *J. Clin. Periodontol.*, 1988;15:485–487.
2. Gaffar A, Aoba T, Afflitto A, Esposito A and Moreno EC, “Structure-activity relationship between in vitro inhibition of HA crystal growth and in vivo anticalculus effects”. In *Recent advances in the study of Dental calculus*, J.M. ten Cate (ed.), IRL Press, Oxford University Press, 1989.
3. Gaffar A, Esposito A and Afflitto J, “In vitro and in vivo anticalculus effects of a triclosan/copolymer system”. *Am. J. Dentistry, Sp. Iss.*, 1990;3:S37-S42.
4. Schiff T, Cohen S, Volpe AR and Petrone ME, “Effects of two fluoride dentifrices containing triclosan and a copolymer on calculus formation”. *Am. J. Dentistry, Sp. Iss.*, 1990;3:S43-S45.

5. Lobene RR, Battista GW, Petrone DM, Volpe AR and Petrone ME, "Anticalculus effect of a fluoride dentifrice containing triclosan and a copolymer", *Am. J. Dentistry, Sp. Iss.*, 1990;3:S47-S49.
6. Stringer O and Charig A, "Synthesis and characterization of [¹⁴C] polyvinylphosphonic acid", *Journal of Compounds and Radiochemicals*, 1989;27:647-652.
7. Moreno EC, Zahradnik RT, Glazman A and Hwu R, "Precipitation of hydroxyapatite from dilute solution upon seeding", *Calcif. Tissue Res.*, 1977;24:47-57.
8. Hattingh J, "Albumins in saliva: What concentrations?", *S. African Journal of Science*, 1970;75:184-186.
9. Gibbons RJ, Moreno EC and Spinell DM, "Model delineating the Effects of a salivary pellicle on the adsorption of *Streptococcus miteor* on hydroxyapatite", *Infection and Immunity*, 1976; 14: 1109-1112.
10. Gibbons RJ, Van Houte J, In *Bacterial Adherence, Receptors and Recognition*, series B, Vol. 6; E.H. Beachey (Ed.), Chapman and Hall, London, 1980.
11. Gaffar A, Coleman EJ, Esposito A, Niles H and Gibbons RJ, "Nonbactericidal approach to reduce colonization of Plaque Microflora on teeth in vitro and in vivo", *Journal of Pharmaceutical Sciences*, 1985;74:1228-1232.
12. Regolati B, Schmid R and Muhlemann HR, "The effects of diphosphonate, pyrophosphate and sodium fluoride on drinking habits of Osborne-Mendel Rats", *Helv. Odont. Octa.*, 1970; 14:34-36.
13. Lehmann EL and D'Abrera HJM, *Nonparametrics: Statistical Methods Based on Ranks*, McGraw-Hill, New York, 1975.
14. Moreno EC, Aoba T and Margolis HC, "Pyrophosphate adsorption onto hydroxyapatite and its inhibition of crystal growth", *Comp. Cont. Ed. Dent. Suppl.* 1987;8:S256-S266.

ADSORPTION OF HYDROXYPROPYLCELLULOSE ON HYDROXYAPATITE VIA FORMATION OF SURFACE COMPLEX WITH SODIUM DODECYLSULFATE

Saburo Shimabayashi, Sawa Nishine, Tadayuki Uno, and Tomoaki Hino

The University of Tokushima
Faculty of Pharmaceutical Sciences
Department of Physical Pharmacy
Sho-machi 1-78-1, Tokushima
Tokushima 770, Japan

1. ABSTRACT

Adsorption of hydroxypropylcellulose (HPC) on hydroxyapatite (HAP) in the presence of sodium dodecylsulfate (SDS) and its effect on stability of the HAP suspension were studied. Although the adsorption amount of HPC was low in the absence of SDS, it increased with the amount of SDS after the formation of the intermolecular complex between them on the surface of HAP. The adsorption of SDS by HAP is due to electrostatic attractive force between dodecylsulfate anion (DS^-) and Ca^{2+} on the surface and due to isomorphous substitution of the sulfate group of DS^- for the surface phosphate ion. Formation of the surface complex is by virtue of hydrophobic interaction between hydrophobic groups of DS^- thus adsorbed and those of HPC captured from the bulk solution. Adsorption of SDS by HAP was reversible with respect to dilution with its solvent (a NaCl solution). As for HPC, however, the desorption was rather complicated, depending on the dilution procedure whether with water or with an aqueous solution of a given concentration of SDS. This observation suggests that the adsorbed SDS is offering the adsorption sites for HPC on the surface after implantation of the hydrophobic groups on the surface. Mean diameter (d) of the secondary particles of HAP was determined by means of a Coulter counter as a function of concentrations of SDS and HPC. The d -value decreased after attaining a maximum with an HPC concentration when an SDS concentration was kept constant. This result suggests that an SDS-HPC complex plays a role of a dispersing/flocculating agent against the HAP suspension. In fact, the behavior of the complex is quite similar to that of a polyelectrolyte as a dispersing/flocculating agent.

2. INTRODUCTION

Polymer adsorption on particles in an aqueous phase has been extensively studied.¹ A polymer in an aqueous solution is adsorbed on particles through various mechanisms such as (a) electrostatic force, (b) hydrogen bonding, (c) van der Waals force, (d) hydrophobic interaction, (e) ion exchange, (f) isomorphous substitution, etc. The polymer adsorption makes the suspension unstable due to the interparticle bridging effect when the amount of adsorption is low. This bridging flocculation is often observed in the presence of a high molecular weight polymer in a good solvent. However, the suspension becomes stable by virtue of steric hindrance due to the repulsion of loops and tails of the adsorbed polymers when the adsorption amount is high. In the case of polyelectrolyte, in addition to the above, the effect of the electrostatic repulsion among charged groups of the adsorbed polymer plays an important role in the dispersion stability. When a nonionic/hydrophobic polymer on the solid particle captures surfactant ions through a hydrophobic interaction, the intermolecular complex is formed on the surface, of which behavior is quite similar to that of an adsorbed polyelectrolyte. It is known that an intermolecular complex is formed between hydroxypropylcellulose (HPC) and sodium dodecylsulfate (SDS) both on the kaolinite surface and in an aqueous phase,^{1,2} while that of polyvinylpyrrolidone (PVP) with SDS is also formed both in an aqueous phase and on the surface of hydroxyapatite (HAP).^{1,3,4}

In this chapter, we present results of study of the formation of intermolecular complex between HPC and SDS on the surface of HAP. This study includes the effects of several factors (a) the complex formation between HPC and SDS on the surface of HAP, (b) the effect of SDS on the adsorption amount of HPC, (c) the effect of HPC on the adsorption amount of SDS, and (d) the effect of surface complex of SDS-HPC on dispersion/flocculation of an HAP suspension. Though these effects are interrelated, we will discuss them separately and then in combination.

In our previous studies,⁵⁻⁸ it was concluded that SDS, or dodecylsulfate anion (DS^-), was easily adsorbed to the surface of HAP by the mechanisms of isomorphous substitution for a phosphate ion on the surface and of electrostatic attractive force toward a calcium ion on the surface.^{5,6} Size of the sulfate group is quite similar to that of the phosphate ion and both of them are tetrahedral oxoacidic groups. Therefore, the sulfate group can easily substitute for the surface phosphate ion, resulting in the adsorption of SDS to the surface.^{7,8} After the adsorption, the hydrophobic group of SDS is protruding to an aqueous phase or lying on the surface phase of HAP. The surface becomes more hydrophobic (i.e., the surface is modified), and one can expect that hydrophobic groups of the adsorbed SDS might easily interact with hydrophobic group of a polymer, such as HPC and PVP.^{3,4} In the present study, HPC was used as the adsorbant. This polymer is water soluble but has hydrophobic groups in its structure. Figure 1 shows schematically the adsorptions of SDS and HPC by HAP.

3. EXPERIMENTAL

3.1. Materials

HAP ($\text{Ca}_{10}(\text{PO}_4)_6(\text{OH})_2$) was obtained from Nakarai Chemicals, Ltd (Kyoto, Japan). Its specific surface area was estimated as 56.0 m^2/g by the N_2 gas adsorption, while its molar ratio of calcium/phosphorous in the bulk was determined as 1.67 mole/mole after chemical analysis. SDS ($\text{C}_{12}\text{H}_{25}\text{SO}_4\text{Na}$) was of the analaR grade of BDH, Ltd (England).

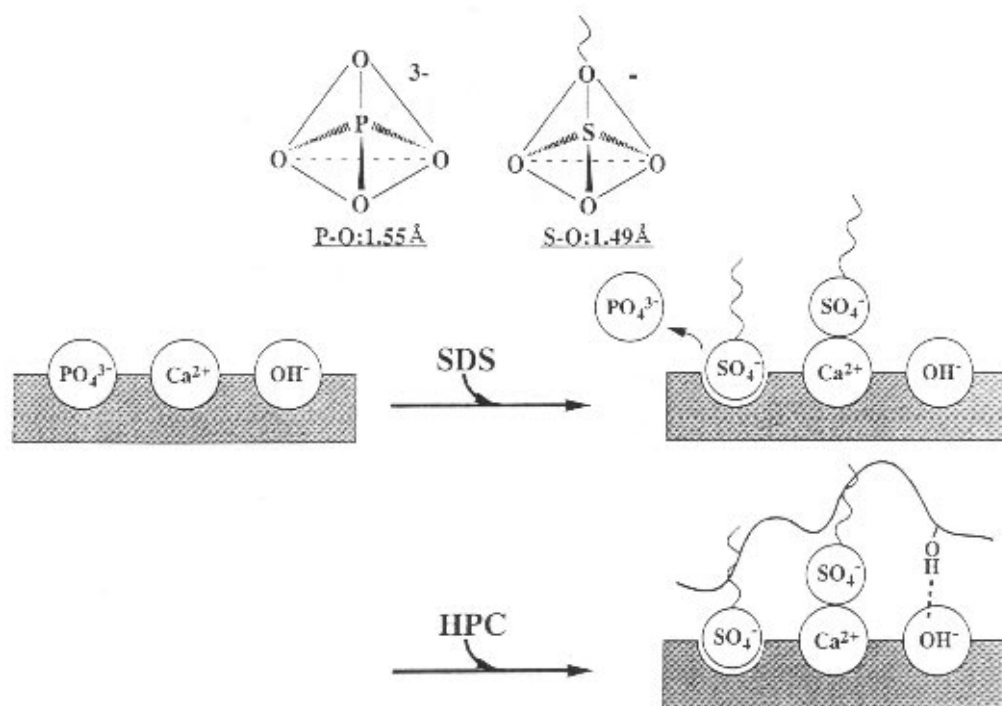


Figure 1. Schematic illustration of the adsorption of SDS and HPC on the surface of HAP. Phosphate ion, calcium ion, and hydroxyl ions are exposed on the surface of HAP. The OH^- group of HPC might interact with the OH^- ion of HAP through the hydrogen bonding.

HPC (average M.W. = $11\text{--}15 \times 10^5$ daltons) is a product of Tokyo Kasei, Ltd. (Tokyo, Japan). According to the report from the manufacturer, the average amount of additional hydroxy-propoxyl groups was about 3.4 moles per mole of sugar.

3.2. Analytical Methods

Total concentration of SDS in an aqueous phase was determined by Epton method (methylene blue diphasic titration method) in the absence of HPC. In the presence, however, it interfered with the SDS determination. Therefore, only the concentration of SDS free from HPC was determined with the assistance of a dialysis equilibrium method, as shown later (Figure 2). Concentration of HPC was determined by colorimetry at 620 nm by the anthrone-sulfuric acid method in the presence and absence of SDS. Adsorption amounts of SDS and HPC on HAP at 30 °C were obtained from the difference in concentrations in the supernatant before and after the adsorption. Mean diameter of the secondary particles of HAP was obtained by a Coulter counter (TAII, Coulter Electronics, Inc.) at room temperature.

3.3. Dialysis Equilibrium Method

Ten ml of an aqueous solution of SDS in the compartment II was separated with a dialyzing membrane (cellulose tubing, Wako, Ltd. Osaka, Japan) against 10 ml of an aque-

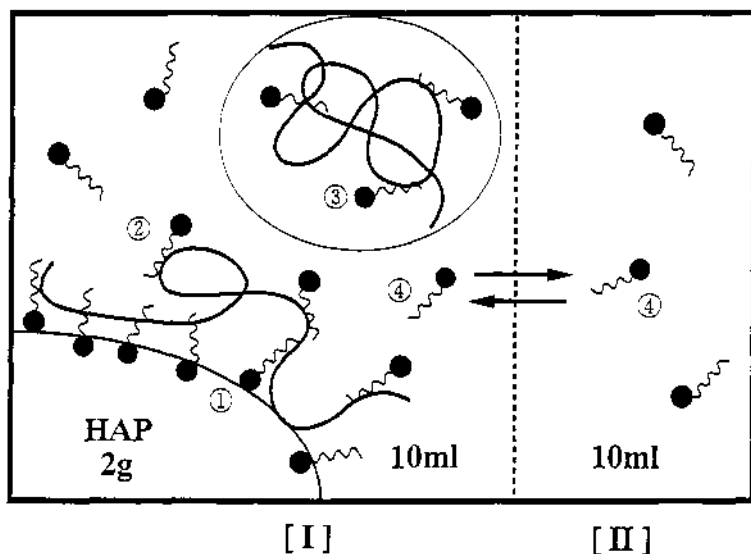


Figure 2. Schematic illustration of the dialyzing system at 30 °C. There are four kinds of the SDS situations (a-d) in the system.

ous solution of SDS containing 2 g of HAP and a known amount of HPC in the compartment I, as shown in Figure 2. After attaining the equilibria at 30 °C with respect to the binding of SDS to HPC and adsorptions of SDS and HPC to HAP in the compartment II, and after attaining the membrane equilibrium between the compartments I and II, the concentration of SDS in the compartment II was determined by the Epton method.

It should be recognized that there are four SDS modes in the system, as shown in Figure 2, that is, (a) SDS adsorbed directly onto the surface of HAP, (b) SDS bound to HPC which is adsorbed to the surface of HAP, (c) SDS bound to HPC which is free from the surface, and (d) SDS that is free from both HAP and HPC. Only the SDS(d) in compartments I and II is permeable to a dialyzing membrane. The concentration is easily determined by means of the Epton method because of the absence of HPC in compartment II. The concentration of SDS(c) in compartment I was indirectly determined² through the combination of the polymer concentration free from the HAP in compartment I and the binding isotherm of SDS to HPC. Total amount of SDS adsorbed by HAP (SDS(a) + SDS(b)) was obtained by subtraction of the amount of SDS(c) + SDS(d) from a total amount of SDS in to the whole system (compartments I+II).

4. RESULTS AND DISCUSSION

The following section presents discussion of the binary systems of HAP-SDS, SDS-HPC, and HPC-HAP, followed by the ternary system of HAP-SDS-HPC.

4.1. Adsorption of SDS on HAP

As shown previously,^{5,6,8} adsorption amount of SDS (or an adsorption isotherm) sigmoidally increased with the concentration of free SDS and attains a maximum around its

cmc (critical micellization concentration). The adsorption amount decreased with an increase in SDS concentration above the cmc. The fact that there is a maximum in the adsorption amount of SDS suggests that the micellization in an aqueous phase is more stable than the aggregate formation of SDS on the HAP surface. The adsorption mechanism of SDS by HAP has been previously discussed in the introduction (Figure 1) and elsewhere.^{5,6}

4.2. Binding of SDS by HPC

Binding of SDS to HPC is due to the mutual hydrophobic interaction between their hydrophobic moiety.^{1,2} Although two kinds of HPC differing in molecular weight were used (higher = $11\text{--}15 \times 10^4$ dalton and lower = $5.5\text{--}7.0 \times 10^4$ dalton), the binding ratios of SDS/HPC were almost the same. With an increase in the concentration of SDS, the binding isotherm decreased after attaining a maximum, at which the concentration of free SDS was approximately its cmc. This behavior is quite similar to that observed in the adsorption isotherm of SDS by HAP, mentioned above. The behavior of the isotherm (i.e., low binding at low concentration while acceleration in the binding at high concentration) suggests that the binding of SDS to HPC is hydrophobic/cooperative.

4.3. Adsorption of HPC to HAP

The adsorption amount of HPC by HAP is shown in Figure 3 as a function of a concentration of added HPC. Dotted line is a theoretical curve which was obtained after assuming that all of the added HPC was adsorbed by HAP. In the absence of SDS, however, the adsorbed amount of HPC was about 20% of the theoretical value. HPC is adsorbed

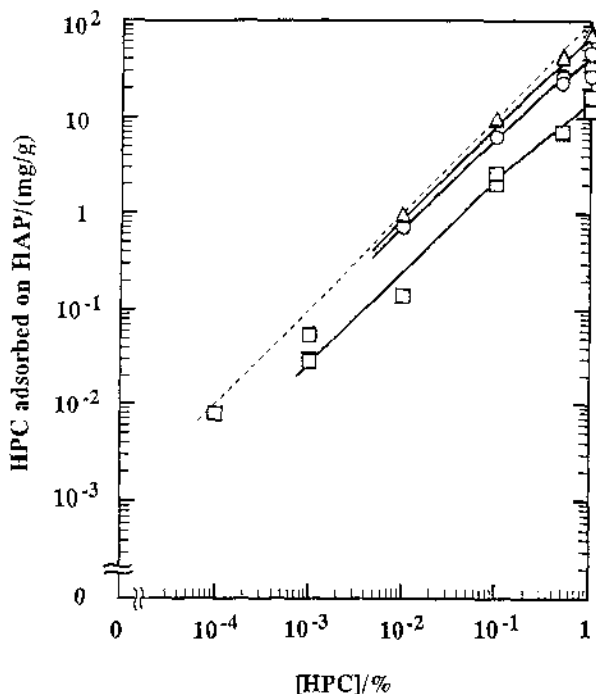


Figure 3. Relationship between concentration of added HPC and the amount of adsorbed HPC by HAP at 30 °C. [SDS]/(mmol/l) = 0 (square), 1 (circle), and 4 (tri-angle). [HAP] = 100 g/l. [NaCl] = 0.9 %. Dotted line is a hypothetical one which shows that all of the added polymer is consumed by the HAP particle.

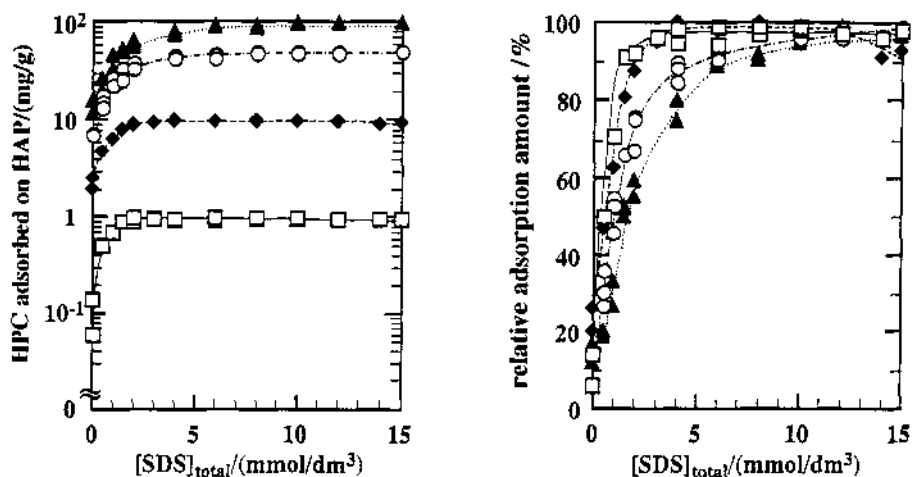


Figure 4. HPC adsorption as a function of the concentration of added SDS, where the HPC concentration was kept constant at 10^{-2} g/dl (open square), 10^{-1} g/dl (closed diamond), 5 g/l (open circle), and 10 g/l (closed triangle). [HAP] = 100 g/l. [NaCl] = 0.9 %.

probably due to van der Waals interaction and hydrogen bonding between OH⁻ groups of HPC and OH⁻ anion on the surface of HAP (Figure 1). The HPC adsorption amount increased with an SDS concentration (Figure 3).

The adsorption amount of HPC is shown in Figure 4 as a function of a concentration of added SDS, where the concentration of added HPC was kept constant. The left side shows the adsorption amount in the unit of mg/g, while the right side shows the adsorption amount relative to the total amount of the added HPC shown as a percentage (%).

As shown in Figure 4, when the concentration of HPC was low, the adsorption amount slightly decreased after attaining a maximum at the higher concentrations of SDS. These trends are quite similar to those previously reported in the system of SDS-PVP-HAP.⁴ This is because the complex is more stable in an aqueous phase than on the surface phase when a high enough concentration of SDS is added to the system. The initial slopes in Figure 4 declines with a given concentration of HPC. This observation suggests that the adsorption sites for HPC on HAP are provided by the SDS adsorption.

4.4. Desorption after Dilution

Time dependence of desorption of SDS and HPC from the surface of HAP was studied after the ten fold dilution with respective solvents (Figure 5). The right side of the Figure shows the desorption behavior of SDS after the dilution with an aqueous solution of 0.9 % NaCl. As illustrated in Figure 5, SDS is easily desorbed in a short period and attains the new equilibrium value, which coincides with the value expected from the adsorption isotherm obtained elsewhere⁶ suggesting the adsorption is reversible.

Contrarily, the desorption behavior of HPC is rather complicated, depending on a dilution method, as shown in the left side of Figure 5. When the suspension is diluted ten fold with 0.9 % NaCl solution not containing SDS, the polymer desorption was observed. As shown in Figure 5, it took at least 6 hours to complete the desorption and to achieve a new equilibrium value, in contrast to the SDS-HAP system discussed above. The new ad-

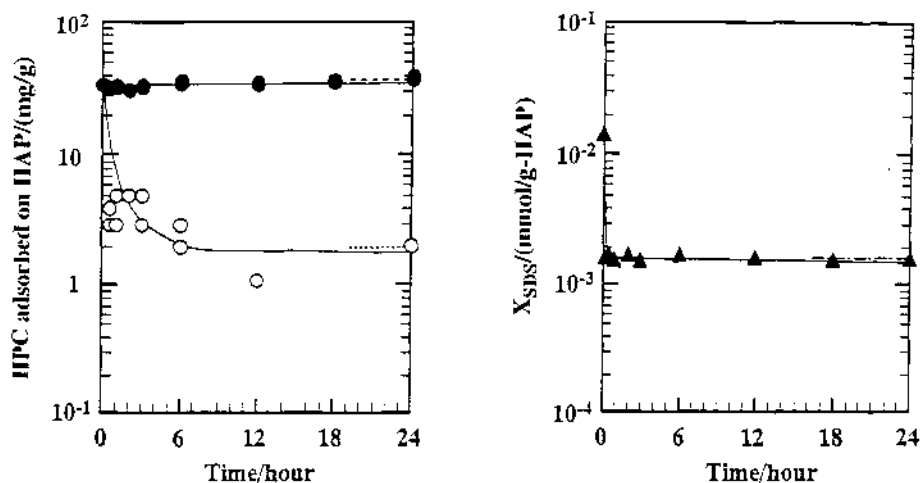


Figure 5. Time-dependence of desorption of SDS (right) and HPC (left) after the ten fold dilution with respective solvents. Initial conditions for the adsorption before the dilution is $[HAP] = 1 \text{ g/10 ml}$, $[NaCl] = 0.9 \%$, and $[SDS] = 2 \text{ mmol/l}$ in common. (Right) Closed triangle: after the ten-time dilution with a 0.9% NaCl solution in the absence of HPC. The broken bar shows the amount of adsorbed SDS at the condition of $[SDS] = 0.2 \text{ mmol/l}$, $[NaCl] = 0.9 \%$, and $[HAP] = 1 \text{ g/100 ml}$ for the reference after the dilution. This data was quoted from a literature.⁶ (Left) The initial concentration of HPC is 5 g/l in common. Open circle: after the dilution with a 0.9% NaCl solution in the absence of SDS. The dotted bar shows the adsorption amount of HPC at the condition of $[HPC] = 5 \times 10^{-2} \text{ g/dl}$, $[SDS] = 0.2 \text{ mmol/l}$, and $[HAP] = 1 \text{ g/100 ml}$ for the reference after the dilution. Closed circle: after the dilution with the 0.9% NaCl aqueous solution containing 2 mmol/l SDS. The broken bar shows the adsorption amount of HPC at the condition of $[HPC] = 5 \text{ g/l}$, $[SDS] = 2 \text{ mmol/l}$, and $[HAP] = 1 \text{ g/100 ml}$ for the reference after the dilution. The reference values were determined independently.

sorption amount was as expected from the direct adsorption of HPC to HAP in the same medium.

Desorption was hardly observed when the suspension was diluted with 0.9% NaCl solution containing 2 mmol/l SDS. The adsorption amount after a ten fold dilution was almost the same as that of the direct adsorption of HPC to HAP at the same concentration. Because the concentration of total SDS in the system was kept constant, the number of the adsorption sites for HPC for each gram of HAP was approximately kept constant also. Therefore, the desorption of HPC by the dilution was not observed but the adsorption amount was almost kept constant even after the solution was diluted with respect to HPC and HAP. These facts are quite similar to those often observed in the adsorption to and desorption from the solid particles of synthetic polymers of random coil in common, generally referred to as the irreversible adsorption of polymer with respect to the dilution.

4.5. Formation of the Surface Complex

Adsorption amounts of SDS by HAP in the presence or absence of HPC are shown in Figure 6. The adsorbed amount of SDS in the presence of HPC, which are regarded as a sum of the bound SDS designated by SDS(a) and SDS(b) in Figure 2, is apparently higher than that in the absence of HPC, which is the adsorption isotherm of SDS in the absence of the polymer. The difference in the adsorption amount is due to the adsorbed polymer which forms a complex with SDS on the surface.

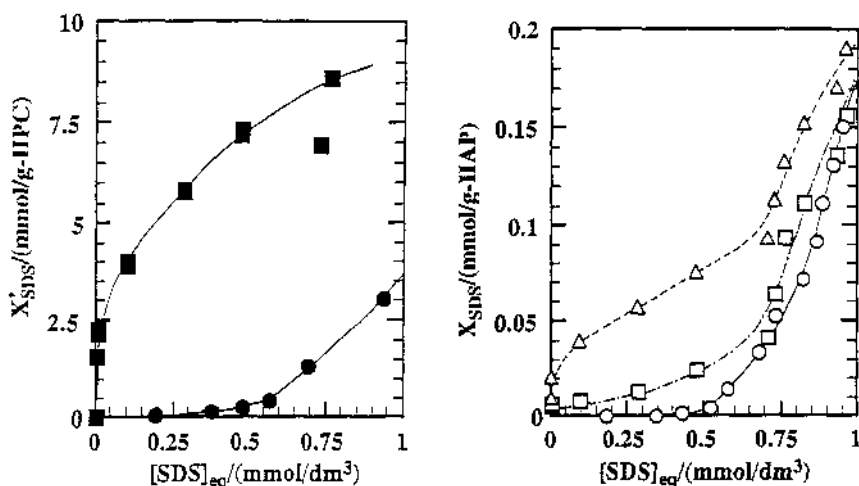


Figure 6. Formation of the surface complex in the presence of 1 g/l HAP and 0.9 % NaCl. (Right) relationship between the binding ratio of SDS/HAP, X_{SDS} , and the concentration of SDS free from both HAP and HPC, $[SDS]_{eq}$. Open circle: adsorption isotherm of SDS to HAP in the absence of HPC, open triangle: the total amount of adsorbed SDS (= SDS (a+b)) in the presence of 1 g/l HPC, open square: hypothetical amount of SDS adsorbed directly to the surface of HAP in the presence of HPC, which was obtained on the assumption that the binding ratio of SDS/HPC on the surface is the same as that in an aqueous phase. (Left) relationship between the binding ratio of SDS/HPC, X'_{SDS} , and concentration of SDS free from both HAP and HPC, $[SDS]_{eq}$. Closed circle: binding isotherm of SDS/HPC in the absence of HAP, Closed square: hypothetical binding ratio of SDS/HPC on the surface, estimated by assuming that the direct adsorption amount of SDS to HAP are not affected in the presence of the polymer, HPC.

We estimated the apparent amount of SDS directly adsorbed onto HAP in the presence of HPC, assuming that the binding ratio of SDS to HPC on the surface is the same as that in an aqueous phase. The apparent amounts were obtained by subtraction of the amount of bound SDS(b) from the adsorbed amount of the total SDS(a+b). The estimated amount of direct adsorption is apparently larger than that obtained from the adsorption isotherm in the absence of HPC. This suggests that the effective binding ratio of SDS/HPC on the surface phase might be larger than that in an aqueous phase.

The left side of Figure 6 shows two kinds of the binding ratio of SDS/HPC, one is an apparent ratio on the surface, and the other the binding isotherm in an aqueous phase for reference. The former was obtained by subtracting the amount SDS directly adsorbed to the surface (SDS(a)) from which the adsorbed amount was estimated from the adsorption isotherm of SDS/HAP from the total amount of SDS adsorbed on the surface (SDS (a+b)). The binding ratio of SDS to HPC on the surface, thus obtained, is remarkably larger than that of the binding isotherm in an aqueous phase in the absence of HAP. This suggests again that the cooperativity between SDS and HPC is larger on the surface than in an aqueous phase.

4.6. Effect of Surface Complex on Dispersion Stability of HAP Particles

Effect of formation of the surface complex on dispersion/flocculation of the HAP suspension was studied by means of a Coulter counter. When primary particles of HAP are repulsive, mean diameter of the secondary particles is small. Conversely, when the particles are attractive, the mean diameter increases, resulting in flocculation. Figure 7 shows

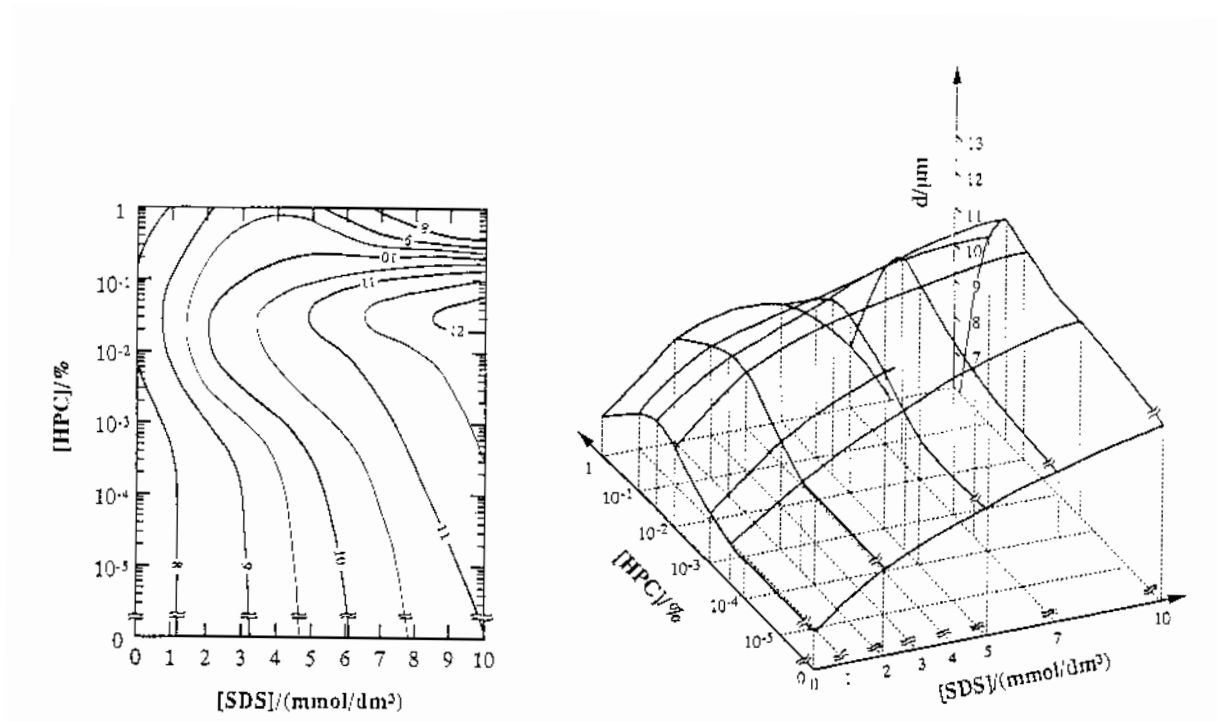


Figure 7. Mean diameter, d , of secondary particles of HAP as a function of concentrations of SDS and HPC. (Right) three dimensional contour plot, (Left) two dimensional projection with contour lines. The digit on each curve represents the mean diameter in the unit of micrometer.

the mean diameter as a function of the concentrations of added SDS and HPC. The right side of this Figure is the three dimensional representation while the left side is the two dimensional projection.

As shown in Figure 7, while in the absence of both SDS and HPC, the mean diameter, d , was approximately 7 μm , an increase in the concentration of SDS in the absence of HPC caused the mean diameter to increase. The mean particle diameter decreased after attaining a maximum with increased polymer concentration in the absence of SDS. When both components, SDS and HPC, are added in small amounts the mean diameter increases with their concentrations, attaining a maximum at about 0.03 % HPC irrespective of the SDS concentration. When both the concentrations of SDS and HPC were high enough (1 % HPC and 10 mmol/l SDS, for example) the mean diameter remarkably and steeply decreased.

Hydrophobic tail of the adsorbed SDS is protruding from or lying on the HAP surface. The tails on the neighboring particles interact with each other by hydrophobic effect, resulting in aggregation of HAP particles. Therefore, the mean diameter increases with an increase in the concentration of SDS even in the absence of the polymer. In the case of HPC at low concentrations, the adsorbed polymer bridges between the HAP particles resulting in flocculation or increase in the mean particle diameter. On the other hand, when the concentration of HPC is high, interparticle repulsion becomes dominant due to the loops and tails of the adsorbed polymer resulting in the dispersion of the particles. This flocculation/dispersion phenomena as a function of polymer concentration is quite common in suspensions based on the polymer's adsorption.

When both HPC and SDS are added together to the system, the complex is formed on the surface of the HAP particle. At low concentrations of the polymer, the bridged complex between the particles resulting in an increase in the mean diameter and the degree of aggregation/flocculation of the particles. When a high enough concentration of SDS and HPC is added, interparticle repulsion becomes dominant mainly to the loops and tails of the surface complex, resulting in the dispersion. Because the surface complex behaves just like a polyelectrolyte and expands its polymer coil much more with the binding ratio of SDS/HAP (i.e., electric charges along the polymer chain), the effect of the HPC complex on the dispersion and flocculation becomes more pronounced than that of the simple HPC alone. Figure 8 schematically shows the mechanism of the bridging and repulsion of the surface complex, where the polymer chains of the complex, consisting of loops and tails, are expanded.

4.7. Biological Significance of the Surface Complex Formation, (A Simple Model for Mammalian Hard Tissues)

The hydrophobic interaction of SDS with HPC on the surface of HAP after the surface modification by SDS is an important factor in understanding of the mechanism of the formation of mammalian hard tissues.^{1,7,8} Teeth and bones are regarded as a composite material of HAP crystallites and organic compounds. The results mentioned above suggest that nonionic and hydrophobic compounds (such as HPC), of which there is hardly any direct adsorption onto the surface of HAP, still contributes to the formation of biological hard tissues through hydrophobic interaction and complex formation with ionic and amphiphilic compounds (such as SDS), which are easily bound to the biological HAP by electrostatic interaction of their charged head-groups with oppositely charged sites on the HAP crystallite. Thus, the space between fine particles of HAP is filled with organic compounds and the particles are bridged with each other, forming a composite texture which has both hardness and elasticity due to the HAP and the organic compounds, respectively.

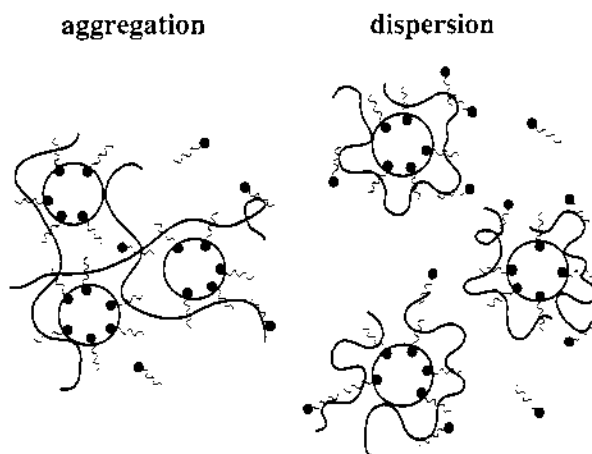


Figure 8. Schematic illustration of the aggregation/disposition effect of the surface complex on the HAP suspension.

5. CONCLUSIONS

The following conclusions may be drawn from the results presented here:

- SDS was adsorbed on the HAP surface by the mechanism of isomorphous substitution and electrostatic attraction.
- Modification of hydrophobic surfaces by SDS and formation of surface complexes through hydrophobic interaction resulted in an increase in the amount of adsorption of HPC.
- The degree of adsorption of SDS also increased in the presence of HPC by virtue of the cooperative adsorption between HPC and SDS on the HAP surface.
- Dispersion/aggregation of HAP particles were accelerated after formation of the surface complex.
- The system of HAP/SDS/HPC may be considered to be a simplified model for biological hard tissues which forms a composite texture.

REFERENCES

1. Shimabayashi S, Umo T, and Nakagaki M, "Formation of surface complex between polymer and surfactant and its effect on the dispersion of solid particles", *Colloids and Surfaces-A*, 1997;123-124:283-295.
2. Shimabayashi S, Uno T, Oouchi Y, and Komatsu E, "Interaction between hydroxypropylcellulose and surfactant and its effect on dispersion stability of kaolinite suspension in aqueous phase", *Progress in Colloid and Polymer Sci.*, in press, 1997.
3. Shimabayashi S, Nishine S, and Uno T, "Formation of inter-molecular complex between polyvinylpyrrolidone and sodium dodecyl-sulfate through hydrophobic interaction on the surface of hydroxy-apatite in an aqueous phase—Flocculation of the HAP particles by the surface complex", *Phosphorus Research Bulletin*, 1996;6:229-232.
4. Shimabayashi S, Yoshida Y, Arima K, and Uno T, "Complex formation through hydrophobic interaction between polyvinylpyrrolidone and sodium dodecylsulfate on the surface of hydroxyapatite—Modification to hydrophobic surface by the adsorption of SDS", *Phosphorus Research Bulletin*, 1994;4:89-94.

5. Shimabayashi S, Tanaka H, and Nakagaki M, "Effect of added salt on the adsorption of dodecylsulfate ion and concurrent release of phosphate and calcium ions at the surface of hydroxyapatite", *Chem.Pharm.Bull.*, 1987;35:2171–2176.
6. Shimabayashi S and Matsumoto M, "Effect of sulfate ion and dodecylsulfate ion on non-stoichiometric dissolution of hydroxyapatite", *J. of the Chem. Soc. of Jap.*, 1994:26–30.
7. Shimabayashi S, Hashimoto N, Kawamura H, and Uno T, "Formation of hydroxyapatite in the presence of phosphorylated and sulfated polymer in an aqueous phase", In *Mineral Scale Formation and Inhibition*, Amjad Zahid (ed.), Plenum Press, New York, 1995.
8. Shimabayashi S and Uno T, "Hydroxyapatite-polymer interaction", In *Polymeric Materials Encyclopedia*, vol.5, Joseph C. Salamone, (ed.), CRC Press, Boca Raton, 1996.

THE INHIBITION OF CALCIUM CARBONATE FORMATION BY COPOLYMERS CONTAINING MALEIC ACID

Pavlos G. Klepetsanis,^{1,3} Petros G. Koutsoukos,^{1,2}
Gabriele-Charlotte Chitanu,⁴ and Adrian Carpov⁴

¹Institute of Chemical Engineering and High Temperature Chemical Processes
P.O. Box 1414

Patras, GR-26500, Greece

²Department of Chemical Engineering

³Department of Pharmacy

University of Patras

Patras, GR-26500, Greece

⁴Academia Romana

Institutue de Chimie Macromoleculara "Petru Poni" Filiala IASI

Lab. Polimeri Bioactivi Si Biocompatibily

IASI, Romania

1. ABSTRACT

Calcium carbonate scale formation in geothermal wells and other industrial processes is a persistent problem. Remediation of this problem may be achieved through the addition of water soluble polymers which may influence nucleation, crystal growth and the particle characteristics of the precipitated calcium carbonate. In the present work we have investigated the effect of water soluble copolymers of maleic acid with N-Vinyl Pyrrolidone, Vinyl Acetate, Methyl Methacrylate and Styrene groups on the kinetics of calcium carbonate crystal growth. The effectiveness of the polymers tested on the kinetics of calcium carbonate scale formation was evaluated using the constant supersaturation methodology. The water soluble copolymers tested, were all found to be effective inhibitors of calcium carbonate formation at concentration levels lower than 1 ppm. The crystal growth rates of calcite showed a drastic decrease, while for inhibitor concentrations exceeding 0.25 ppm crystal growth was completely suppressed. It is suggested that the activity of the inhibitors is due mainly to the presence of the maleic acid entity in the copolymer, which promoted the adsorption of the copolymer onto the growing solid par-

ticles. Kinetics analysis of the rates measured in the presence and in the absence of the polymers, provided additional evidence that adsorption of the macromolecules on the active growth sites of calcite seed crystals was responsible for the inhibition of crystal growth.

2. INTRODUCTION

The formation of sparingly soluble salts is a serious problem in industrial installations,¹ where natural waters and/or seawater are used without any pretreatment for processes such as secondary oil recovery, geothermal energy production, water cooling by heat exchangers, cooling towers, potable water production with reverse osmosis, etc. Scale minerals form tenaciously adherent encrustations which restrict fluid flow, enhance corrosion probability and reduce the heat transfer across the metal-fluid boundary because of their low thermal conductivity. The chemical composition and the characteristics of the formed encrustations depend on a number of parameters, including chemical composition (concentrations of lattice forming ions, pH and ionic strength), flow properties, temperature and pressure of the aqueous fluid phase.² As a consequence the frequent cleaning of the installations involved is necessary to maintain their performance in acceptable levels. In severe scaling cases, plant shut down is often needed thus increasing further the operational costs of the equipment used. One of the most commonly encountered sparingly soluble salts, is calcium carbonate. Calcium carbonate is found in the three crystalline polymorphs: vaterite, aragonite and calcite in the order of decreasing solubility. Calcite is the thermodynamically most stable form of calcium carbonate. Three methods for the prevention of calcium carbonate formation are commonly employed:³

1. Decrease of aqueous media pH by the controlled addition of acid.
2. Addition of chelating agents, causing decrease of supersaturation because of their complexation with cations forming sparingly soluble salts, and
3. Addition of water soluble polymeric compounds, which have the ability to suppress scale formation even at very low concentrations.

The first method increases the probability for corrosion of the metallic parts. In the second method, a large amount of chelating agent is needed for satisfactory results leading to higher cost. The third method has been increasingly used because it has several important advantages.^{4,5,6,7} The water soluble additive compounds give satisfactory results even at very low concentrations (normally up to concentrations less than 1/100 of the total calcium concentration present in the water treated). In several cases, the presence of additives may cause modifications of the crystal habit of the calcite particles formed reducing their ability to adhere on the surfaces.

In the present work, we have studied the effect of maleic acid copolymers on the precipitation of calcium carbonate. The presence of various groups in maleic acid copolymers affect their performance as scale inhibitors. The purpose of synthesis of maleic acid copolymers with various groups is the development of inhibitors with multiple action as scale inhibitors, as corrosion inhibitors and as bacteriocides. The presence of carboxylic, aromatic and heterocyclic groups in synthetic copolymers, readily soluble in water was tested. For the quantitative assessment of the effectiveness of the inhibitors crystal growth experiments were done by the seeded growth method at constant supersaturation which gives most reliable and reproducible results.

3. EXPERIMENTAL

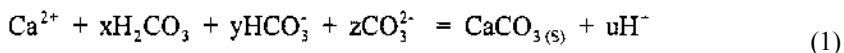
3.1. Calcium Carbonate Crystal Growth at Constant Supersaturation

All experiments were done at $25.0 \pm 0.1^\circ\text{C}$ in a 600 ml double walled pyrex vessel thermostated by water circulating through a constant temperature bath. The stock solutions were prepared from crystalline, reagent grade chemicals (Merck, pro analysi), dissolved in triply distilled water and were filtered through membrane filters ($0.2\ \mu\text{m}$, Millipore). Calcium nitrate and sodium nitrate stock solutions were standardized by ion-exchange liquid chromatography (Metrohm, IC 690, with conductivity detector). The sodium bicarbonate and sodium carbonate solutions were prepared fresh for each experiment by exact weighing the amounts of the respective solids (dried at 105°C overnight) followed by dissolution in triply distilled water.

The preparation of calcite seed crystals was done by slow mixing of calcium chloride and sodium carbonate solutions at 70°C .⁸ The crystalline solid was aged for one week under continuous stirring, filtered, washed with saturated calcium carbonate solution and dried. The final solid was characterized by physicochemical methods including powder x-ray diffraction (XRD, Philips 1840/30), scanning electron microscopy (SEM, JEOL JSM 5200) and specific surface area measurements (multiple point, nitrogen adsorption BET). The powder x-ray diffraction pattern of the crystalline calcite preparation coincided with that of the reference material.⁹ The specific surface area of the seed crystals was $3.5\ \text{m}^2\text{g}^{-1}$.

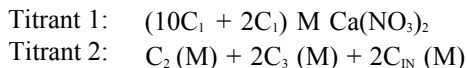
The supersaturated solutions volume totalling 500 ml were prepared in the reaction vessel by carefully mixing simultaneously equal volumes (250 ml) of calcium nitrate and sodium bicarbonate solutions. The ionic strength of the supersaturated solutions was adjusted by the addition of appropriate volume of sodium nitrate stock solution. For the crystal growth experiments in the presence of additives the appropriate volume of additive stock solution was added in the working solution. Next, the solution pH was adjusted to 8.50 by the addition of 0.100M standard sodium hydroxide solution (Merck, Titrisol). The solution pH was measured by a combination pH electrode (Ingold), standardized before and after each experiment with NBS buffer solutions (7.413 and 9.180 at 25°C).¹⁰ The working solutions were stirred by a magnetic stirrer with a teflon coated stirring bar.

The working solutions employed were stable for periods exceeding 24h and were supersaturated with respect to all calcium carbonate polymorphs. After the pH adjustment in the working solutions, a precisely weighted amount of calcite seed crystals (ca. 20mg) was introduced in the supersaturated solutions. As precipitation started, the solution pH decreased. The decrease of pH was due to the proton release concomitant with the solid formation according to the reaction :



A pH drop as small as 0.005 pH units triggered the addition of titrant solutions from two mechanically coupled syringes of a computer controlled titrator through the appropriate software. The titrant solutions in the two burettes consisted of calcium nitrate (titrant 1) and mixture of sodium carbonate, sodium bicarbonate and additive as appropriate (titrant 2). The supersaturated working solution contained sufficient concentration of inert electrolyte (sodium nitrate) so as to maintain the solution ionic strength, which would oth-

erwise change, due to the release of nitrate and sodium ions from the precipitating calcium and carbonate ions respectively. The titrant solutions were prepared as follows:



where C_1 and C_3 are the total calcium and total sodium bicarbonate concentrations in the working solution, C_2 is the sodium carbonate concentration equal to $10C_1$ and C_{IN} is the concentration of additive tested, in the working supersaturated solution. The concentration of the additive included in titrant 2 was twice its concentration in the supersaturated solution account for the dilution effect caused by the titrant addition. The amounts of total calcium and total carbonate in the titrant solutions were calculated according to the stoichiometry (1:1) of the precipitating calcium carbonate.

During the course of the crystal growth experiments samples were withdrawn and filtered through membrane filters (0.2 μm Millipore). The filtrates were analyzed for calcium by atomic absorption spectroscopy (Perkin Elmer 305A) in order to confirm the constancy of the solution composition. In all experiments the analysis showed that the calcium concentration remained constant to within $\pm 2\%$. The working solutions at the end of the experiments were filtered as previously described and the solids were dried overnight at 80 $^\circ\text{C}$ and were analyzed further by XRD and SEM.

Throughout the course of the experiments the pH of the working solution and the added volume of titrants as a function of time were recorded and stored in the computer for further analysis. The precipitation rates (in the presence and in the absence of additives) were determined from the traces of titrant volume added as a function of a time, using curve fitting software. The rates of calcium carbonate formation on the inoculating seed crystals, R_g , were calculated as :

$$R_g = \frac{dV}{dt} \frac{C_t}{A_t} \text{ (mol} \cdot \text{min}^{-1} \cdot \text{m}^{-2}\text{)} \quad (2)$$

where dV/dt is the rate of addition of titrants of concentration C_t ($\text{mol} \cdot \text{l}^{-1}$) ($=10C_1$) and A_t is the total surface area of the added seed crystals.

3.2. Polyelectrolytes Used in Crystal Growth Experiments

The polymers used in this work were water soluble maleic acid copolymers chosen from several copolymers which were examined as scale inhibitors. They were obtained from maleic anhydride copolymers synthesized according to our methods by free radical copolymerization in solution-suspension, followed by extraction in a Soxhlet apparatus.¹¹

The chemical composition of the copolymers was determined by conductometric titrations in acetone:water mixture (1:1 v/v) with aqueous 0.1N NaOH.¹² All copolymers had a 1:1 molar ratio and could be considered as alternating. The molecular weight of copolymers was estimated from viscometric measurements in acetone at 30 $^\circ\text{C}$ using the corresponding Mark-Houwink-Sakurada parameters.^{13,14} The maleic anhydride copolymers were hydrolyzed with water at room temperature, then neutralized with ammonium or sodium hydroxide or with triethanolamine. The maleic polyelectrolytes obtained are presented in Table 1. They were stored as aqueous solutions with concentrations between 13 and 25% (wt).

Table 1. Maleic polyelectrolytes used as crystallization inhibitors

Code	Chemical Formula	Molecular Weight
AV 142.1	$\begin{array}{c} \text{---}(\text{---CH---CH---CH}_2\text{---CH---})_n\text{---} \\ \quad \quad \\ \text{COO}^- \text{COO}^- \text{OCOCH}_3 \\ \text{NH}_4^+ \text{NH}_4^+ \end{array}$	103000
AP 28.2	$\begin{array}{c} \text{---}(\text{---CH---CH---CH}_2\text{---CH---})_n\text{---} \\ \quad \quad \\ \text{COO}^- \text{COO}^- \text{O} \\ \quad \quad \\ \text{Na}^+ \text{Na}^+ \text{N} \\ \quad \\ \text{O} \end{array}$	15000
AP 28.52.1	$\begin{array}{c} \text{---}(\text{---CH---CH---CH}_2\text{---CH---})_n\text{---} \\ \quad \quad \\ \text{COO}^- \text{COO}^- \text{O} \\ \quad \quad \\ (\text{Na}^+, \text{Zn}^{2+}) \text{Na}^+ \text{N} \\ \quad \\ \text{O} \end{array}$	60000
AS 11.2	$\begin{array}{c} \text{---}(\text{---CH---CH---CH}_2\text{---CH---})_n\text{---} \\ \quad \quad \\ \text{COO}^- \text{COO}^- \text{C}_6\text{H}_5 \\ \quad \\ \text{Na}^+ \text{Na}^+ \end{array}$	145000
AM 76.2	$\begin{array}{c} \text{CH}_3 \\ \\ \text{---}(\text{---CH---CH---CH}_2\text{---C---})_n\text{---} \\ \quad \quad \\ \text{COO}^- \text{COO}^- \text{O} \\ \quad \quad \\ \text{Na}^+ \text{Na}^+ \text{C} \\ \quad \\ \text{O} \text{OCH}_3 \end{array}$	-
ATP 6.2	$\begin{array}{c} \text{---}(\text{---CH---CH---})_m\text{---}(\text{CH}_2\text{---CH---})_n\text{---}(\text{CH}_2\text{---CH---})_p\text{---} \\ \quad \quad \quad \\ \text{COO}^- \text{COO}^- \text{O} \text{OCOCH}_3 \\ \quad \quad \\ \text{Na}^+ \text{Na}^+ \text{N} \end{array}$	-

where $m:n:p = 1:0.83:0.19$ and the ratio $\text{Na}^+/\text{Zn}^{2+}$ in AP28.52.1 is 9:1.

4. RESULTS AND DISCUSSION

The experimental conditions were selected so that no change was observed in the supersaturated solutions until the seed crystals were introduced. In all experiments, calcite was exclusively formed on the inoculating calcite seed crystals as it was confirmed by XRD. The spectra of initial seed crystals and the seed crystals after the overgrowth of calcium carbonate are shown in Figures 1a and 1b respectively. Calcite is the thermodynamically most stable polymorph of calcium carbonate and its formation is favored in our experimental conditions. Scanning electron micrographs of the calcite crystals formed in the absence and in the presence of additives are shown in Figures 2a and 2b respectively. As may be seen, the calcite crystals grown in the presence of additives showed a change in their morphology. The crystals growing in their presence showing an increased roundness of their edges. A similar effect has been reported for the growth of calcite crystals in the presence of other maleic acid copolymers.⁷

The assessment of the effectiveness of the water soluble polymers tested with respect to their capability to inhibit crystal growth of calcium carbonate was done by crystal growth experiments at one or two supersaturation levels over a wide range of additives

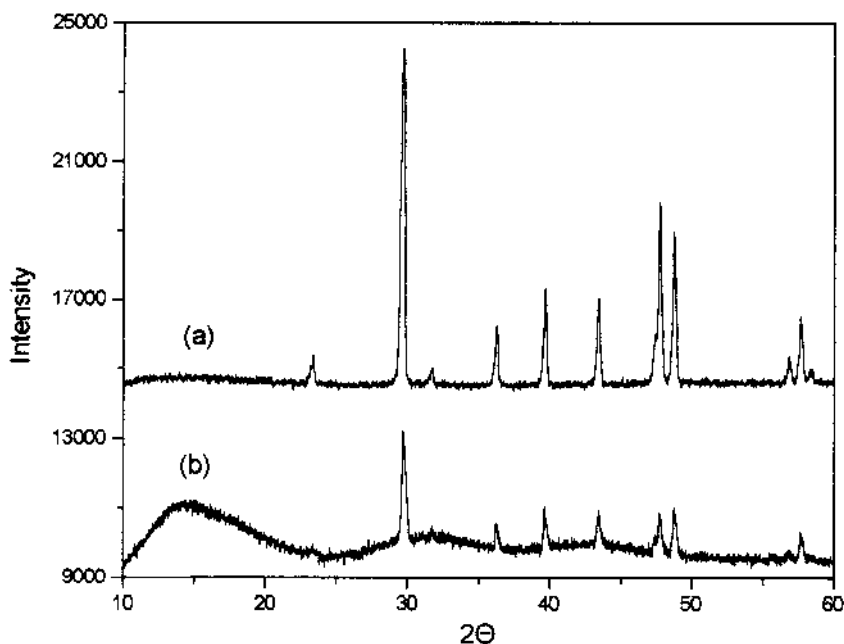


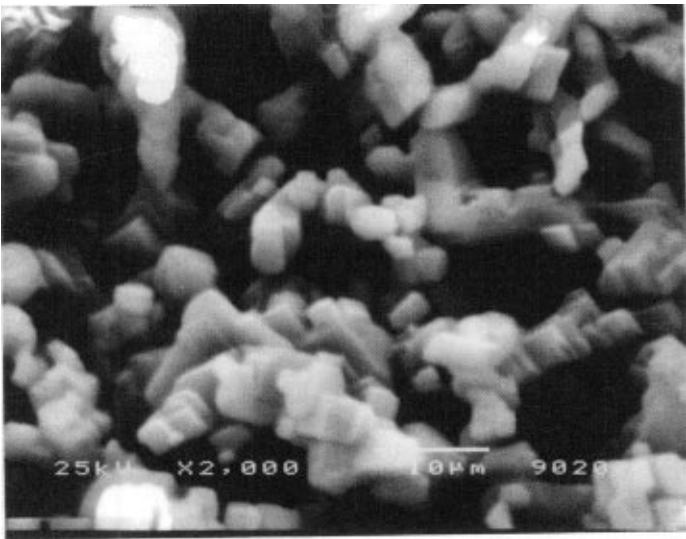
Figure 1. Powder x-ray diffraction spectra for (a) calcite seed crystals and (b) calcite grown on calcite seed crystals (20% growth with respect to inoculating seeds).

concentrations. All additives tested suppressed significantly the rates of calcium carbonate crystal growth. The inhibition of the crystal growth rates relatively to the uninhibited system, was expressed by the % relative inhibition defined as:

$$\text{Relative Inhibition (\%)} = \frac{R_0 - R_i}{R_0} \times 100\% \quad (3)$$

where R_0 and R_i are the calcite crystal growth rates measured in the absence and in the presence of the additives respectively. The experimental conditions for the calcite seeded growth experiments, the kinetics results obtained both in the absence (blank) and in the presence of inhibitors are summarized in Table 2.

The relative decrease of the precipitation rate (R_i/R_0) in the presence of the additives tested as a function of their concentration is shown graphically in Figure 3. The percent inhibition of each additive was found to depend strongly on the respective additive concentration. Typical plots showing the dependence of the relative inhibition of calcite growth on the additive concentration are shown in Figure 4. It is interesting to note that for inhibitor concentrations of up to 0.1 ppm there is a tendency for linear increase of the effectiveness of the additives, while at higher concentrations there is a tendency to attain a plateau for the relative inhibition. The calcite crystals are grown in the absence of additives at similar initial conditions with a screw dislocation mechanism (BCF theory).¹⁵ Crystal growth rates reduction was in all cases examined proportional to the additive concentration while as may be seen from the data in Table 2, in all cases a limiting inhibitor concentration was found in which the crystal growth of the calcite seed crystals was to-



(a)

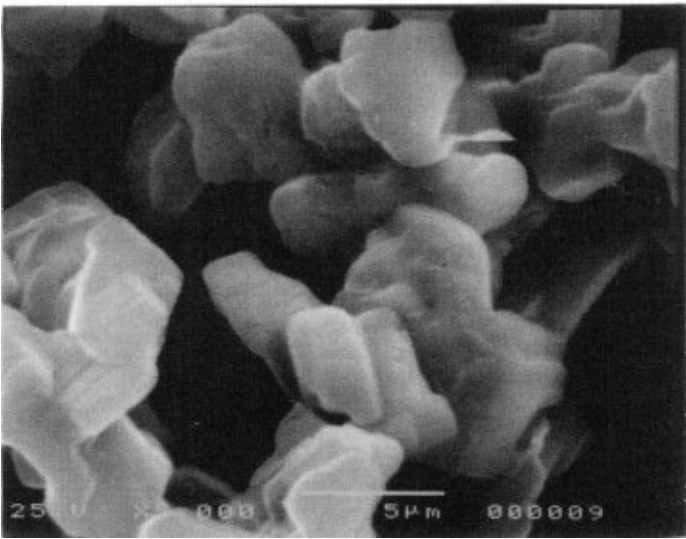


Figure 2. Scanning electron micrographs of calcite (a) seed crystals and (b) past crystal growth in the presence of Maleic Anhydride - Methyl Methacrylate copolymer at constant supersaturation. Exp # 9.

tally suppressed. This additive concentration limit was found to depend on the chemical structure of the polymeric additives.

The dependence of the crystal growth rate of calcite growth on calcite seed on the relative supersaturation is shown in Figure 5. According to the BCF theory, crystal growth in moderately supersaturated solutions proceeds through a repetitive screw dislocation mechanism that continuously creates active sites. The molecules of additives may be ad-

Table 2. Crystal growth of calcite on calcite seed crystals in the presence of maleic acid copolymers at 25°C and pH = 8.50. Initial conditions and kinetic results

Exp. #	Additive	Con/tion ppm	Precipitation rate mmol.l ⁻¹ .min ⁻¹	Relative inhibition
1	Blank-1	0	1.6E-3	–
2	ATP 6.2	0.05	1.1E-3	29
3	ATP 6.2	0.015	4.4E-4	72
4	ATP 6.2	0.10	1.8E-4	88
5	ATP 6.2	0.125	4.8E-5	91
6	ATP 6.2	0.15	complete inhibition	100
1	AM 16.2	0.05	1.5E-3	2
8	AM 16.2	0.015	1.4E-3	12
9	AM 16.2	0.10	8.5E-4	46
10	AM 16.2	0.125	8.0E-4	49
11	AM 16.2	0.15	6.2E-4	60
12	AM 16.2	0.20	3.6E-4	77
13	AM 16.2	0.50	complete inhibition	100
14	Blank-2	0	11.8E-4	–
15	AP28.52.1	0.10	6.5E-4	45
16	AP28.52.1	0.15	4.38E-4	63
17	AP28.52.1	0.20	9.4E-5	92
18	AP28.52.1	0.25	complete inhibition	100
19	AS 11.2	0.05	10.1E-4	14
20	AS 11.2	0.10	5.3E-4	55
21	AS 11.2	0.20	1.6E-4	86
22	AS 11.2	0.50	complete inhibition	100
23	AP 28.2	0.05	10.9E-4	7
24	AP 28.2	0.10	6.8E-4	42
25	AP 28.2	0.15	5.4E-4	54
26	AP 28.2	0.20	1.9E-4	83
27	AP 28.2	0.25	complete inhibition	100
28	AV 142.1	0.01	10.1E-4	14
29	AV 142.1	0.05	6.8E-4	42
30	AV 142.1	0.10	2.5E-4	19
31	AV 142.1	0.20	complete inhibition	100

Blank-1 : Total Calcium = Total Carbonate = 3.00×10^{-3} M, Total Sodium Nitrate = 3.00×10^{-2} M.

Blank-2 : Total Calcium = Total Carbonate = 2.50×10^{-3} M, Total Sodium Nitrate = 2.50×10^{-2} M.

sorbed at the active sites on crystal surfaces, restricting or blocking further growth of the crystals. Blocking of the active growth sites may result in delaying the onset of the crystal growth processes, reduction of the crystal growth rate and change of the crystal size and habit. The changes in crystal size and habit are caused by the preferential growth of crystal faces with a lower surface coverage by the additive molecules. The uncovered part of the crystal surface grow faster resulting in morphological and crystal size variations. Moreover, it should be noted that the additives tested were efficient at substoichiometric proportions with respect to the total calcium concentration in solution. This fact suggested that the inhibition was due to preferential adsorption of the molecules of the polymeric compounds on the active growth sites of calcite crystals rather than to a decrease of supersaturation through sequestration of the calcium ions. The same behaviour has been reported for other water soluble polymeric compounds^{7,16} and for organophosphorus compounds.¹⁷

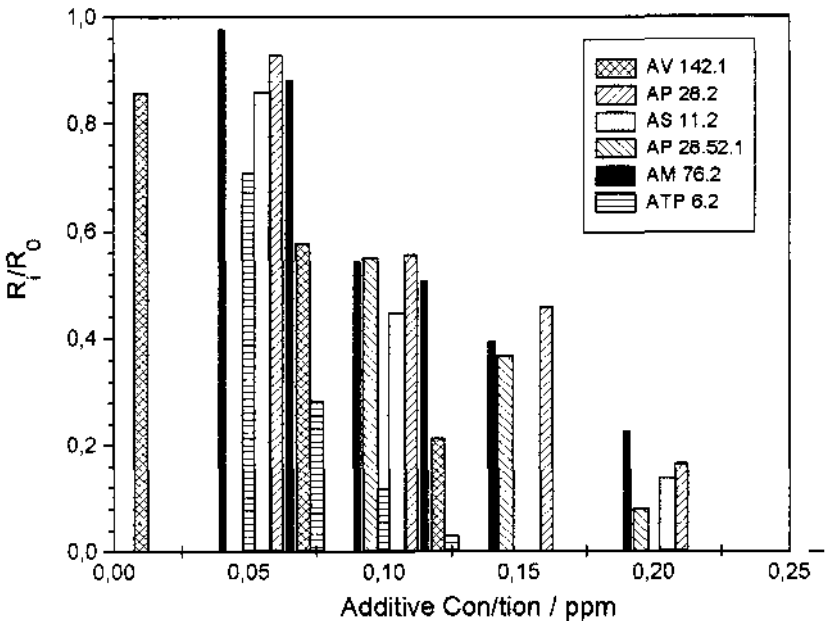


Figure 3. Plot of relative inhibition of the crystal growth of calcite as a function of the additive concentration in the presence of Maleic Acid copolymers.

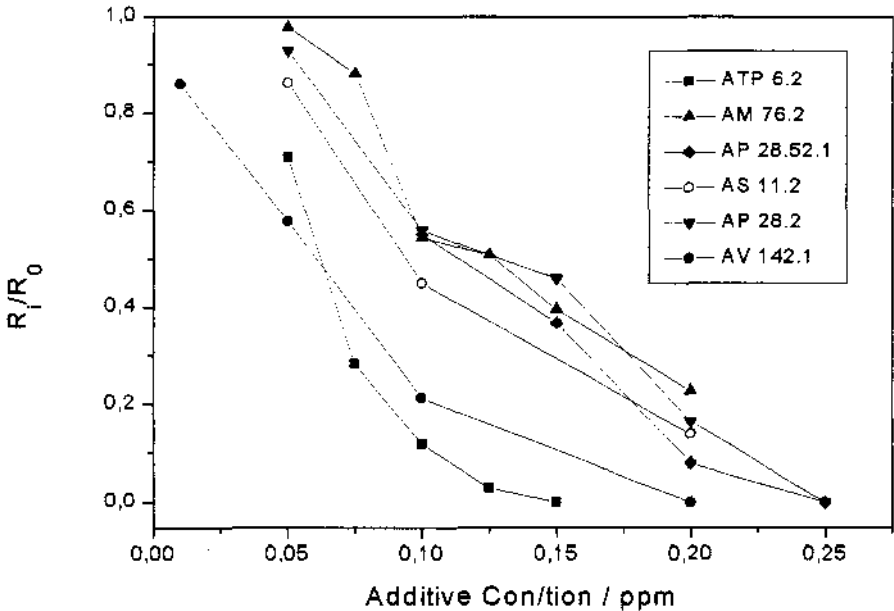


Figure 4. Dependence of the relative inhibition on the additive concentration.

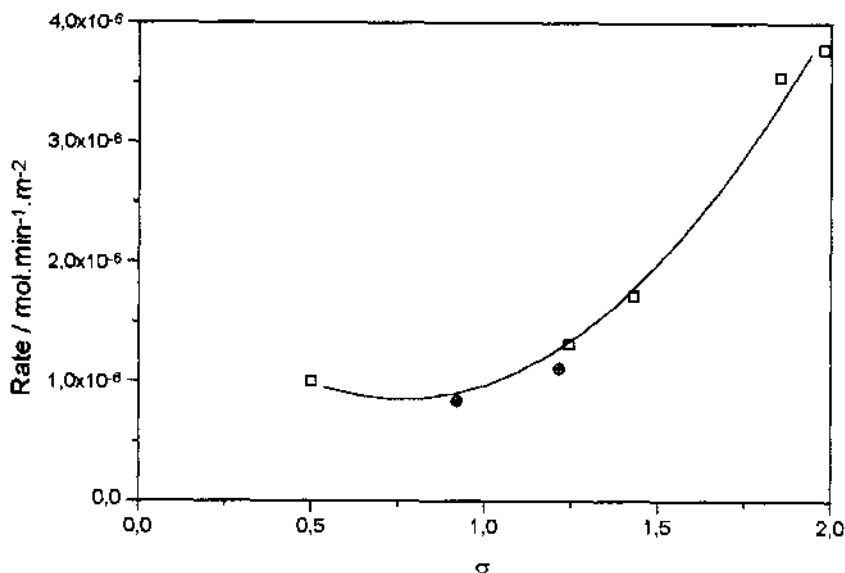


Figure 5. Dependence of the crystal growth of calcite on calcite seed crystals; 25°C, pH 8.50; (□) Data from ref. 15; (●) this work.

Assuming that kinetic inhibition was due to adsorption we have tried to fit the kinetics results to a model in which it is assumed that the reduction of the rates of crystal growth is proportional to the coverage of the surface area of the seed crystals by the additive molecules which are adsorbed as predicted by the Langmuir adsorption model.¹⁸ The relationship between the rates of crystal growth in the presence and in the absence of additives with the additive concentration is given by eq. (4):

$$\frac{R_0}{R_0 - R_i} = 1 + \frac{1}{bC} \quad (4)$$

where C is the additive concentration and b is the affinity constant for the additive and crystal surface. According to eq. (4) a linear relationship between the ratio $R_0/(R_0 - R_i)$ and the inverse of additive concentration, C , is predicted. The analysis of the kinetics data obtained from the crystallization of calcite seed crystals in the presence of AM 76.2 according to eq. (4) is shown in Figure 6.

Similar behaviour was found for the other copolymers of maleic acid tested. It should be noted that according to the model predicted by eq. (4) the intercept is unity. For all additives tested in the present work the value of the intercept was <1 . This value suggested complete inhibition at concentrations below the concentration corresponding to complete coverage of crystal surface with a monolayer of additive molecules.¹⁹ The same behaviour has been quoted in the literature for the organophosphorus compounds, for several insoluble salts of the alkaline earth metals.²⁰ The values of the affinity constant as calculated from kinetic analysis according to the model of eq. (4) for the copolymers tested are summarized in the Table 3.

As may be seen in Table 3, the affinity constants of maleic acid copolymers were significantly larger in comparison with the corresponding values for other inhibitors re-

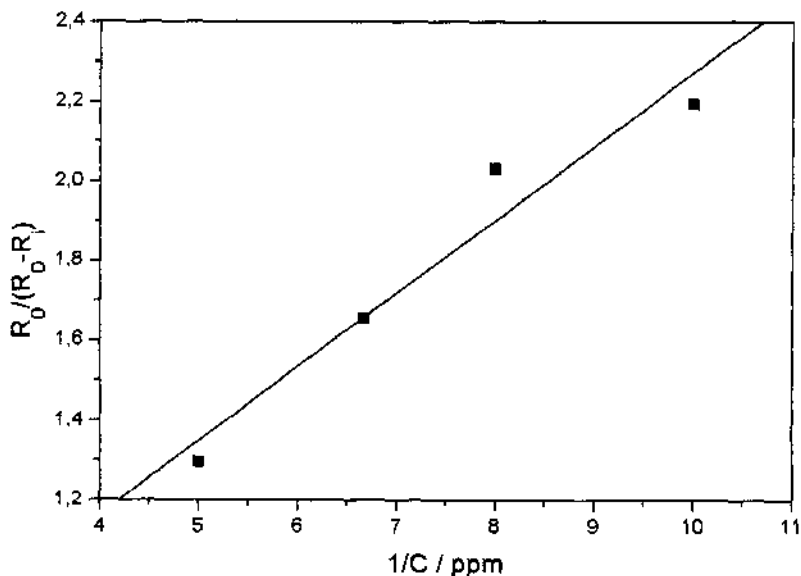


Figure 6. Fit of the kinetics results for the crystal growth of calcite seed crystals in aqueous supersaturated solutions in the presence of AM 76.2; pH 8.50, 25°C.

ported in the literature. This is probably due to the high number of carboxylic groups of the tested copolymers which are extensively ionized at pH = 8.50. The maleic acid copolymer molecules contain a large number of charged carboxylic groups, which may interact strongly with the calcium ions at the calcite surface and may therefore be strongly adsorbed onto active growth sites. It should be noted however that the other inhibitors of which the affinity constants values are shown in Table 3 have also ionizable groups but their molecular sizes are smaller in comparison with the molecular size of maleic acid copolymers. Thus, one molecule of maleic acid copolymer may occupy more than one active

Table 3. Affinity constants for the additive-calcite interface calculated from kinetics of crystal growth data according to eq. (4)

Additive	Affinity constant
AP 28.2	6.71×10^8
AP 28.52.1	2.68×10^9
AS 11.2	3.44×10^9
AV142.1	1.66×10^{10}
Mellitic acid	2×10^6 ⁽²¹⁾
Phosphate	5.84×10^7 ⁽²²⁾
DHHPA	1.35×10^7 ⁽²³⁾
BPDMI	1.59×10^7 ⁽²³⁾
ETMPA	1×10^7 ⁽²⁷⁾

DHHPA: 2-Dihydroxyphosphonyl-2-hydroxy-propionic acid,
 BPDMI: 1,3-Bis[(1-phenyl-1-dihydroxyphosphonyl)methyl]-
 2-imidazolidinone,
 ETMPA: Ethylenediamine-tetra-bis-methylene phosphonic
 acid

growth site in comparison with the molecules of other inhibitors and as a result lower concentrations are needed for the same crystal growth rate reduction. This suggestion, may also explain the fact that complete inhibition was observed at concentrations as low as 0.20 ppm, which is considerably lower than the concentration levels of the other inhibitors needed to achieve complete inhibition (several ppm). This suggestion is corroborated by the fact that at low concentrations, below those corresponding to monolayer coverage, polymers are likely to adsorb "side-on", thus blocking a larger number of active growth sites per molecule.

As may be seen in Table 3, the value of the affinity constant is indicative of the effectiveness of the inhibitors tested. Thus, the compound which caused complete inhibition at the lowest concentration gave the highest value of the affinity constant. The presence of various groups in the maleic acid copolymers affect the performance of the inhibitors for scale formation. Thus, the additives tested may be arranged in the following order with respect to the inhibitory efficiency:

$$AV\ 142.1 > AS\ 11.2 > AP28.52.1 > AP28.2$$

The decrease in inhibition efficiency of maleic acid copolymers may be due to the presence of groups with different hydrophobic character and size. These parameters may affect strongly the adsorption processes of the molecules on the charged crystal surface. The styrene and N-vinyl pyrrolidone groups have larger size and are more hydrophobic in comparison with vinyl acetate group. Thus, the AV 142.1 (MA-VA) additive seems to adsorb to a larger extent than the other maleic acid copolymers and gave stronger inhibition at lower concentrations as may be seen from the data in Table 2. The molecular weight of the copolymers tested is another parameter which is of importance for the adsorption process. The decrease of copolymer molecular weight was accompanied with decrease in its inhibitory efficiency, except for AS 11.2 which contained styrene groups. The same inhibitory effect with AV 142.1 was observed for ATP 6.2, although it contained both N-vinyl pyrrolidone and styrene groups. This is probably due to the structure, flexibility and molecular weight of this copolymer. It is not possible at present to explain this behaviour since a complete physicochemical characterization of the polymeric molecules in aqueous solutions is needed. The kinetics results obtained however, suggested that understanding of the inhibitory action of macromolecules is influenced strongly by the conformation of the polymers at the calcite/water interface.

5. CONCLUSIONS

In the present work it has been shown that the presence of maleic acid copolymers at very low concentrations (below 0.25 ppm) can strongly inhibit the crystal growth of calcite from calcium carbonate supersaturated solutions. This inhibitory effect may be explained by the absorption of the molecules of maleic acid copolymers at the active growth sites. In all cases, high affinity constants for calcite were calculated. The presence of functional groups with different hydrophobic character and size affected the inhibitory efficiency of maleic anhydride copolymers. The presence of the compounds tested did not affect the nature of the phase forming which in all cases it was calcite. The presence of the macromolecules in the supersaturated solutions had a smoothing effect on the edges of the calcite crystals grown.

REFERENCES

1. Cowan JC and Weintritt DJ, *Water Formed Scale Deposits*, Gulf Publishing, Houston, 1976.
2. Hays GF, Thomas PA and Libutti BL, Proc. Engineering Found, Conf. Pennsylvania, Engineering Foundation, New York, 1982.
3. Glater J, York JL and Campbell KS, "Scale Formation and Prevention", In *Principles of Desalination*, K.S. Spiegler and A.D.K. Laird (Eds.), Academic Press, 1980, 627.
4. Weijnen MPC and van Rosmalen GM, "The influence of various polyelectrolytes on the precipitation of Gypsum", *Desalination*, 1985;54:239.
5. Vetter OJ, "An Evaluation of Scale Inhibitors", *J.Pet.Techn.*, 1972;997.
6. Amjad Z, "Calcium Sulfate Dihydrate (Gypsum) Scale Formation on Heat Exchanger Surfaces: The Influence of scale Inhibitors", *J. Colloid Interface Sci.* 1988; 123:523.
7. Carrier AM and Standish ML, "Polymer Mediated Crystal Habit Modification", In *Mineral Scale Formation and Prevention*, Z. Amjad (ed.), Plenum, New York, 1995.
8. Reddy MM and Nancollas GH, "The crystallization of Calcium Carbonate II. Calcite growth mechanism", *J. Colloid Interface Sci.* 1971;37:824.
9. JCPDS ASTM Card No 24-0027
10. Bates RG, *Determination of pH, Theory and practice*, 2nd ed., J.Wiley, New York, 1973.
11. Carpov, A.A., Chitanu, G.C., Maftai, M. and Zamfir, A., "Process of synthesis of carboxylic polyelectrolytes", Romanian Patent 70120/1979 and Chitanu, G.C. and Angelescu-Dogaru, A.G., "Process of preparation of binary or tertiary copolymers of Maleic Anhydride and N-Vinyl Pyrrolidone", Romanian Patent Appl. CO104/1996.
12. Caze C and Loucheux C, "Determination de la composition de copolymeres ethylene anhydride maleique", *J. Macromol. Sci. Chem*, 1973;7:991.
13. Hiroshi A, Takeo Y and Akihiro M, "Dilute solution properties of maleic anhydride-vinyl acetate copolymer", *Fukui Daigaku Kogakubu Keukyu Hokoku*, 1969; 16: 103.
14. Csakvar E, Azor M and Tudos F, "Physicochemical studies of polymeric carriers. Hydrolysis and fractionation of copolymer N-Vinyl pyrrolidone and maleic anhydride", *Polym. Bull. (Berlin)*, 1981;5:413.
15. Xyla AG, Giannimaras EK and Koutsoukos PG, "The precipitation of Calcium Carbonate in aqueous solutions", *Colloids and Surfaces*, 1991 ;53:241.
16. Weijnen MPC, "The influence of additives on the Crystallization of Gypsum", Ph.D. Thesis, University of Delft, 1984.
17. Austin AE, Miller JF, Vaughan DA and Kircher JF, "Chemical Additives for Calcium Sulfate scale control", *Desalination*, 1975; 16:345.
18. Davies CW and Nancollas GH, "The precipitation of Silver Chloride from Aqueous Solutions. Part III. Temperature Coefficients of Growth and Solutions", *Trans.Faraday.Soc.*, 1955;51:818.
19. Nancollas GH and Zawacki SJ, "Inhibitors of Crystallization and Dissolution", In *Industrial Crystallization 84*, S.J. Jancic, and E.J. de Jong, (ed.), Elsevier Science Publishers B.V., 1984.
20. Leung WH and Nancollas GH, "Nitrilotri(methylenephosphonic acid) adsorption on Barium Sulfate crystals and its influence on crystal growth", *J.Crystal Growth*, 1978;44: 163.
21. Amjad Z, "Kinetic study of the seeded growth of Calcium Carbonate in the presence of Benzene polycarboxylic acids", *Langmuir* 1987;3:224.
22. Giannimaras EK and Koutsoukos PG, "The crystallization of Calcite in the presence of Orthophosphate", *J. Colloid Interface Sci.* 1987;116:423.
23. Xyla AG, Mikroyannidis J and Koutsoukos PG, "The inhibition of Calcium Carbonate precipitation in aqueous media by Organophosphorus compounds", *J. Colloid Interface Sci.* 1992; 153:537.
24. Reddy MM, "Kinetic inhibition of Calcium Carbonate formation by wastewater constituents", In *Chemistry of Wastewater Technology*, A.J.Rubin (Ed.), Ann Arbor Science Pub., Ann Arbor, Mich., 1978.

KINETIC INHIBITION OF CALCIUM CARBONATE CRYSTAL GROWTH IN THE PRESENCE OF NATURAL AND SYNTHETIC ORGANIC INHIBITORS

Zahid Amjad,¹ Jeff Pugh,¹ and Michael M. Reddy²

¹Advanced Technology Group
BFGoodrich Company
9921 Brecksville Road
Brecksville, Ohio 44141

²U. S. Geological Survey
3215 Marine Street
Boulder, Colorado 80303

1. ABSTRACT

Addition of carboxylate-containing polymeric materials to a metastable supersaturated calcium carbonate solution greatly reduced calcite crystal growth rates at constant supersaturation and pH = 8.5. Calcite crystallization rates were decreased to half their value in pure solutions by a tannic acid concentration of about 0.3 ppm (parts per million); a fulvic acid concentration of about 0.2 ppm; and a poly(acrylic acid) concentration of about 0.0175 ppm. An equation relating the calcite crystallization rate and the additive concentration follows an expression based on a Langmuir adsorption model. However, the Langmuir isotherm plot has two linear segments suggesting that these polyelectrolyte inhibitors may selectively adsorb initially at the fastest growing crystal faces. This relation between polyelectrolyte concentration and calcite growth rates implies inhibition by carboxylate-containing polymeric materials involves blockage of crystal growth sites on the calcite surface.

2. INTRODUCTION

Formation of mineral scales on heat exchangers and reverse osmosis membranes is a common problem in water treatment processes. Mineral scale forms because of the composi-

tion and hardness of feed water available for industrial applications and because of the presence of scale constituents such as calcium ion and bicarbonate ion. Other industrial processes impacted by mineral scale formation problems include oil and gas production, geothermal power production, sugar refining, pulp and paper fabrication, and laundry applications.

Calcium carbonate formation in natural waters is also a topic of research interest. Natural mineralization processes can be modified by the presence of dissolved organic polyelectrolytes, such as humic and fulvic acids. Dissolved organic carbon (DOC) concentrations are proportional to the concentrations of humic substances in water. DOC concentrations can vary from less than 1 ppm in groundwater to more than 100 ppm in sediment pore water. Often water with high DOC concentrations is supersaturated with calcium carbonate minerals. This persistent supersaturation is attributed to the presence of natural organic polymeric inhibitors. Surface waters precipitate calcium carbonate by physical and chemical processes including: temperature increases, carbon dioxide loss, and photosynthetic utilization of carbon dioxide by algae. Natural organic crystallization inhibitors in water may modify these important biological processes.

Calcite, the thermodynamically stable calcium carbonate polymorph, is the most common scale forming mineral (Polymorphism refers to two or more crystal forms that each has the same chemical composition but different properties and solubility). Calcite coatings form tenacious, hard mineral deposits, and are the most widely studied mineral scale among the sparingly soluble alkaline earth metal salts. Formation of a polymorph other than calcite is facilitated by solution conditions such as pH, temperature, and the presence of crystal growth inhibitors.¹ Spontaneous precipitation studies of calcium carbonate at moderate temperatures often show the calcium carbonate polymorph vaterite to be the first phase to form in solution. Above ambient temperature, the unstable polymorph aragonite has been reported to be the first phase to precipitate.²

During the last two decades investigations of additives to prevent or retard calcium carbonate scaling have attracted the attention of academic and industrial scientists. Common inhibitors of carbonate mineral scales include polyphosphates, phosphonates, and synthetic polymeric inhibitors such as poly(acrylic acid), poly(maleic acid), and copolymers containing acrylic or maleic acid. Investigations of these and several other mineral scale inhibitors suggest that inhibitor effectiveness depends on the functional groups in the inhibitor molecule, polymer composition, and molecular weight.³⁻⁷ In addition, during spontaneous precipitation, the scale composition is influenced by the inhibitor.^{8,9}

The effectiveness of non-polymeric additives as calcium carbonate inhibitors has been the subject of numerous investigations. For example, phosphate, oxalate, glycerophosphate, and benzene polycarboxylic acids are effective inhibitors at low solution concentration. A Langmuir-type adsorption model describes the inhibition of calcium carbonate crystal growth by these ions.¹⁰⁻¹²

Organophosphonates, an important class of crystallization and scale formation inhibitors, have been successfully used to inhibit calcium carbonate scale formation in a number of applications.¹³ However, these compounds may decompose at elevated temperatures, releasing phosphate ion. Elevated phosphate ion concentrations may cause the formation of calcium phosphate scale. Moreover, high concentrations of phosphonates may lead to the deposition of calcium-phosphonate scale on heat exchangers and reverse osmosis membrane surfaces.^{14,15}

Low metal ion concentrations (i.e., iron, zinc, copper, etc.), present as impurities in water supplies, have been reported to influence the precipitation of calcium carbonate, calcium sulfate, and calcium phosphates.^{16,17} Katz and Parsiegl¹⁸ reported that ferrous, ferric, copper, and zinc ions inhibit the crystal growth of calcium carbonate.

Natural organic compounds (i.e., humic substances) are commonly encountered in surface water and groundwater used for water supply. Humic substances are mixtures of natural products with a complex structure and chemistry. Isolation and characterization of humic substances from surface water and groundwater is an ongoing area of research interest.¹⁹ At present the best-characterized humic material is that isolated from the Suwannee River, Georgia.²⁰⁻²³

Nystrom et al.²⁴ examining membrane filtration of water containing humic substances, reported that humic acid forms a gel-like layer on filters and blocks filter pores. Recently, Freche et al.²⁵ examined the influence of humic substances on the crystal growth of dicalcium phosphate dihydrate (DCPD) and found that humic substances reduced crystal growth rates of DCPD. A Langmuir-adsorption process at surface growth sites was proposed to explain the inhibitory effect of humic substances.

The constant composition (CC) technique is used in the study reported here to better understand the influence of humic material on calcium carbonate crystallization rates. This technique provides kinetic information at supersaturations that are low and stable, conditions unattainable by conventional seeded growth methods. Figure 1 shows a schematic representation of a typical CC experiment. A detailed discussion of the CC experiment appears elsewhere.¹³ Calcium carbonate crystal growth inhibitors tested include Suwannee River fulvic acid (FA), tannic acid (TA), poly(acrylic acid) (PAC), benzene hexacarboxylic acid (BHCA), benzene-1,3,5-tricarboxylic acid (BTCA) and salicylic acid (SA).

3. EXPERIMENTAL

Experiments were carried out in a double-walled, water-jacketed Pyrex glass cell, thermostatically controlled at 30 ± 0.1 °C. Supersaturated solutions were magnetically

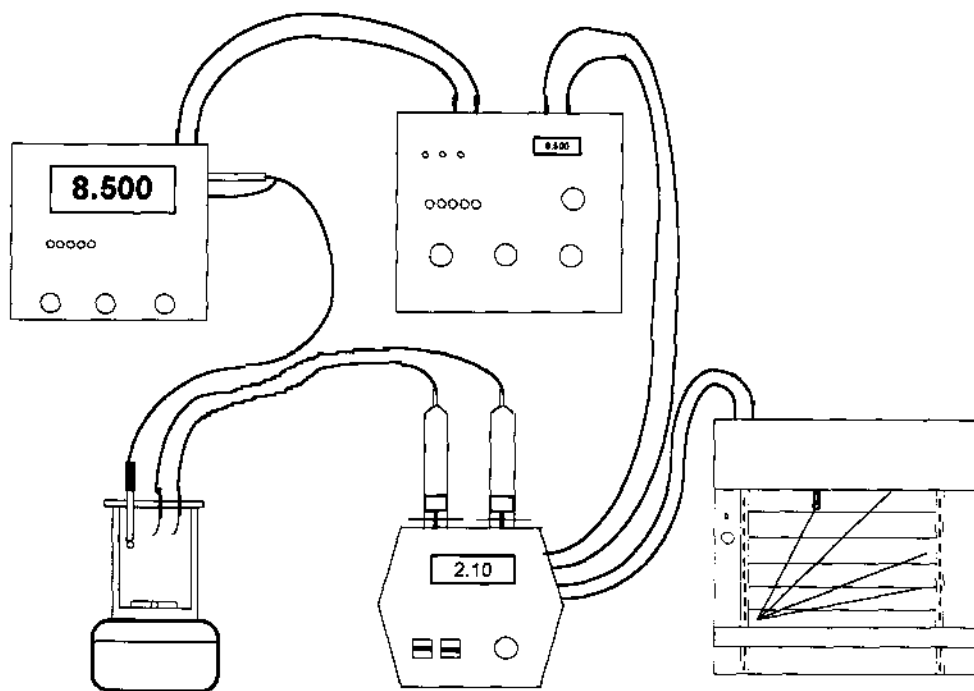
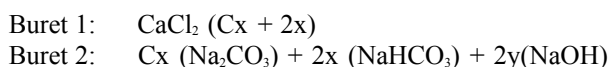


Figure 1. Constant composition experimental apparatus.

stirred by a Teflon coated stirring bar to ensure homogeneity of the solutions and of the seed suspension contained in the cell. Stock solutions of calcium chloride, sodium carbonate, sodium bicarbonate, and sodium chloride were prepared from the respective reagent grade chemicals using distilled, carbon dioxide free water. Calcite seed crystals were prepared and characterized by the method described previously and were stored as dry seed material.¹³ Poly(acrylic acid) solutions were prepared from commercial samples (GOODRITE K-732, 5100 Dalton, BFGoodrich). Salicylic acid and tannic acids used in the present study were obtained from the Sigma-Aldrich Corporation. Suwannee River fulvic acid used in this investigation was isolated by Leenheer *et al.*²¹ and has been extensively studied.²⁰⁻²³

Stable calcium carbonate supersaturated solutions were prepared by placing known volumes of calcium chloride and sodium bicarbonate solutions in the 600-ml cell, the latter addition being made slowly over a period of several minutes. Supersaturated solutions are stable for at least four hours. The mixed solutions were brought to pH=8.5 by the controlled addition of sodium hydroxide. Hydrogen ion measurements were made with a pH combination electrode equilibrated at 30 °C. Supersaturated solution stability was verified by a constant pH reading for at least 45 minutes prior to each experiment. A solution aliquot was taken immediately before the addition of the seed slurry, prepared prior to use by adding a known volume (2 ml) of saturated calcium carbonate to the weighed seed crystals. The suspension was sonicated for 1 minute and then added to the reaction flask. Following the addition of seed crystals, the onset of growth resulted in a solution pH decrease, which was immediately restored to its preset value by the simultaneous addition of two titrant solutions from mechanically coupled 10 ml buret mounted on a modified pH stat (Metrohm, Model 614). The two burettes contained calcium chloride and sodium carbonate at the molar stoichiometry dictated by the precipitating calcite. Calcite growth inhibition experiments were performed by adding inhibitor solution to the bicarbonate solution before the addition of the calcium solution. Titrant solution composition was adjusted to avoid dilution of the working solution. pH control was provided by an amount of sodium hydroxide required for correct pH adjustment of the working solution. More explicitly, the concentration of the titrant in the two burets was calculated as follows:



where x is the molar concentration of calcium chloride or sodium carbonate in the working solution and y the amount of sodium hydroxide required for the pH adjustment in the working solution. For maintenance of constant ionic strength, the amount 2C of inert electrolyte (sodium chloride) was added in the working solution where C is a constant (expressing how many times more concentrated the titrants are than the working solution). In the investigation of the crystal growth in the presence of inhibitor, to avoid dilution of the inhibitor in the working solution, the appropriate amount of inhibitor was added to the carbonate containing buret.

During the crystal growth reaction, samples were withdrawn from the cell, filtered through membrane filters and the filtrate analyzed for calcium, to ensure a constant solution composition. The solids on the filters were characterized by infrared spectroscopy, powder x-ray diffraction, and by scanning electron microscopy.

The uptake of titrant solutions with time were traced on a chart recorder and the rates calculated (as mole of CaCO_3 precipitated per minute) as described previously.²⁶ Figure 2 shows the structures of synthetic inhibitors evaluated in this study.

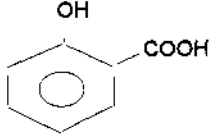
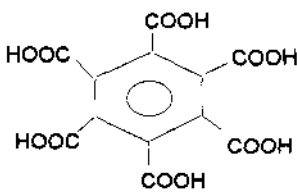
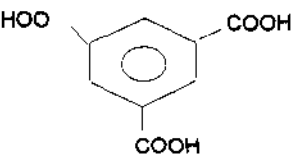
Inhibitor	Acronym	Structure
fulvic acid	FA	-----
tannic acid	TA	-----
salicylic acid	SA	
benzene hexacarboxylic acid	BHCA	
benzene 1,3,5 tricarboxylic acid	BTCA	
poly (acrylic acid)	PAC	$\text{---}(\text{CH}_2\text{---}\underset{\text{COOH}}{\text{CH}})\text{---}$

Figure 2. Inhibitor structures.

4. RESULTS AND DISCUSSION

Solution species concentrations were calculated by using mass balance, proton dissociation, electroneutrality, and equilibrium constants involving calcium ion with inhibitors, by an iterative procedure described previously.²⁶ Experimental conditions and crystal growth rates for each experiment are given in Table 1. Reproducibility of crystal growth rates among different experiments is satisfactory with a mean of 40.15 ± 1.05 ($\pm 2.6\%$) moles of calcium carbonate per (square meter per minute) ($\text{mole m}^{-2} \text{min}^{-1}$) (experiments 1 and 2 in Table 1).

The amount of calcium carbonate formed during reaction (Figure 3) is proportional to the volume of titrant added to maintain constant supersaturation. Calcite crystallization rate is calculated as the slope of the amount of calcium carbonate formed versus time plot. Figure 3 illustrates the change in crystallization rate with varying amount of inoculating seed. Growth rates, R , ($\text{mole m}^{-2} \text{min}^{-1}$) normalized for the initial surface area of inoculating seed (Table 1, expts 1–5) are constant, confirming that crystallization takes place on added calcite seed crystals.

Calcite growth experiments in the presence of varying concentrations of fulvic acid (FA) demonstrate the concentration-inhibition relationship for FA (Figure 4). Fulvic acid

Table 1. Crystallization of calcite on calcite crystals in the presence of inhibitors

Experiment	Inhibitor	Conc., ppm	$10^6 R$, mole $m^{-2} min^{-1}$
1	none	—	39.1
2	none	—	41.2
3	none	—	38.8 ^b
4	none	—	40.4 ^c
5	none	—	38.2 ^d
6	FA	0.125	27.7
7	FA	0.150	24.5
8	FA	0.20	20.5
9	FA	0.25	17.1
10	FA	0.25	18.2
11	FA	0.35	6.9
12	FA	0.50	2.1
13	FA	1.00	0.3 ^c
14	TA	0.15	29.0
15	TA	0.25	24.6
16	TA	0.50	14.5
17	TA	0.75	9.5
18	TA	1.0	2.4
19	TA	1.5	1.5
20	PAC	0.015	25.7
21	PAC	0.0175	21.1
22	PAC	0.020	9.8
23	PAC	0.025	4.2
24	PAC	0.05	0.5 ^c
25	SA	1.00	39.5
26	SA	5.00	38.2
27	BHCA	0.25	15.5
28	BTCA	0.50	39.1

$CaCl_2$, = 2 mM, $NaHCO_3$ = 1 mM, $NaCl$ = 10 mM, pH = 8.5, calcite supersaturation = 0.29, 30°C

^a 100 mg seed crystals

^b 131 mg seed crystals

^c 55 mg seed crystals

^d 34 mg seed crystals

^e Rate calculated based on initial rate

concentration as low as 0.125 ppm reduces the crystallization rate by ~ 30% (Figure 4 curve B); at 0.35 ppm, a rate reduction of ~ 80% is observed. As illustrated in Figure 4 (curves B,C,D,E, F, and G), increasing the concentration from 0.125 to 0.50 ppm resulted in rate reduction of 30 to >90% and, at 1.0 ppm, the precipitation is almost completely inhibited for at least 100 minutes.

Calcite crystal growth reduction by tannic acid (TA) (Table 1 and Figure 5) indicates that TA is an effective calcite growth inhibitor at relatively low solution concentrations. For example, the calcite crystallization rates in the presence of 0.15, 0.50, 1.0, and 1.5 ppm are 29.0, 14.5, 2.4, and 1.5 $\times 10^{-6}$ mole $m^{-2} min^{-1}$ respectively, compared to 39.1 $\times 10^{-6}$ mole $m^{-2} min^{-1}$ obtained in the absence of TA (Table 1).

Constant composition experimental results demonstrate the effectiveness of synthetic polymeric inhibitor materials, such as poly(acrylic acid) (PAC), as calcite growth inhibitor (Table 1 and Figure 6). Poly(acrylic acid) at very low concentration (i.e., 0.015

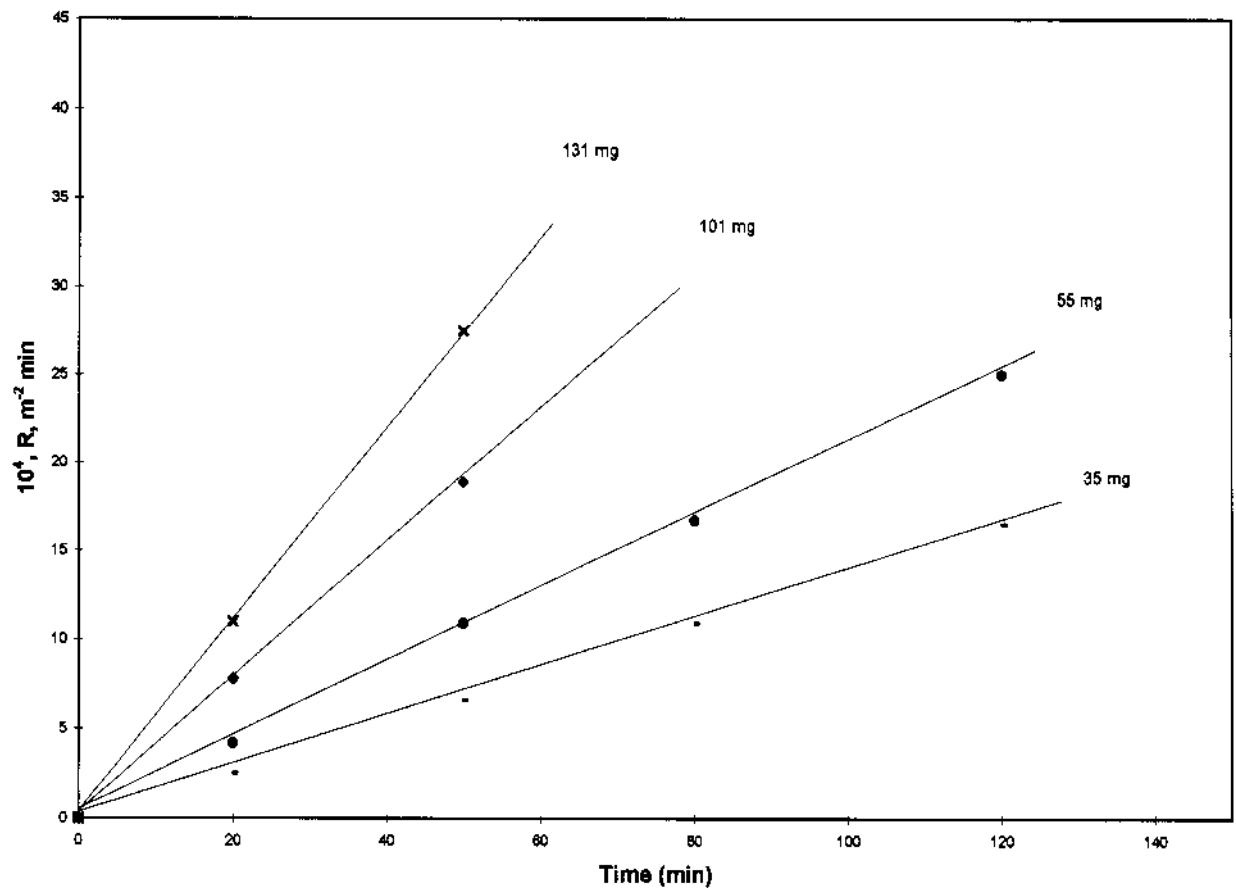


Figure 3. Effect of seed concentration on calcite crystal growth. Plots of calcite growth as a function of time.

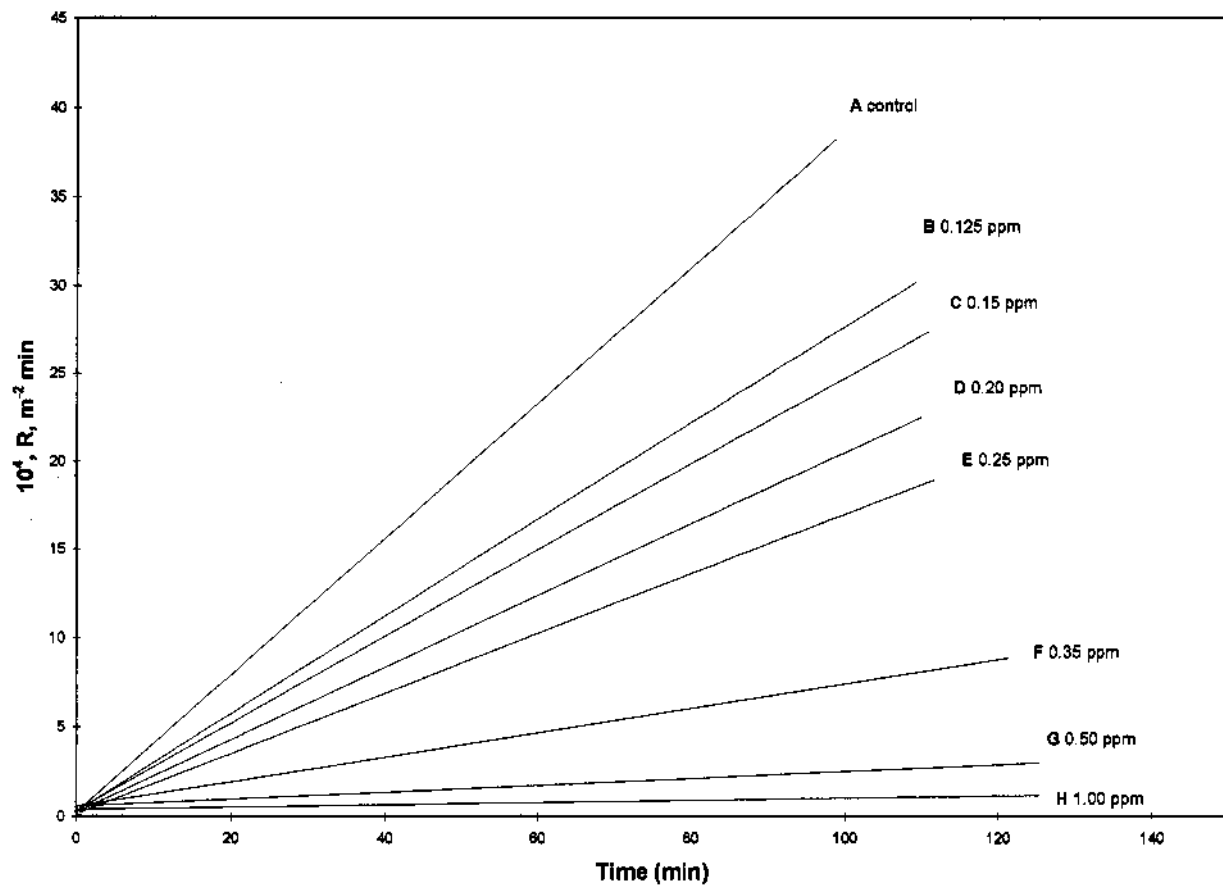


Figure 4. Crystal growth of calcite at constant supersaturation. Amount of calcite growth as a function of time in the presence of fulvic acid.

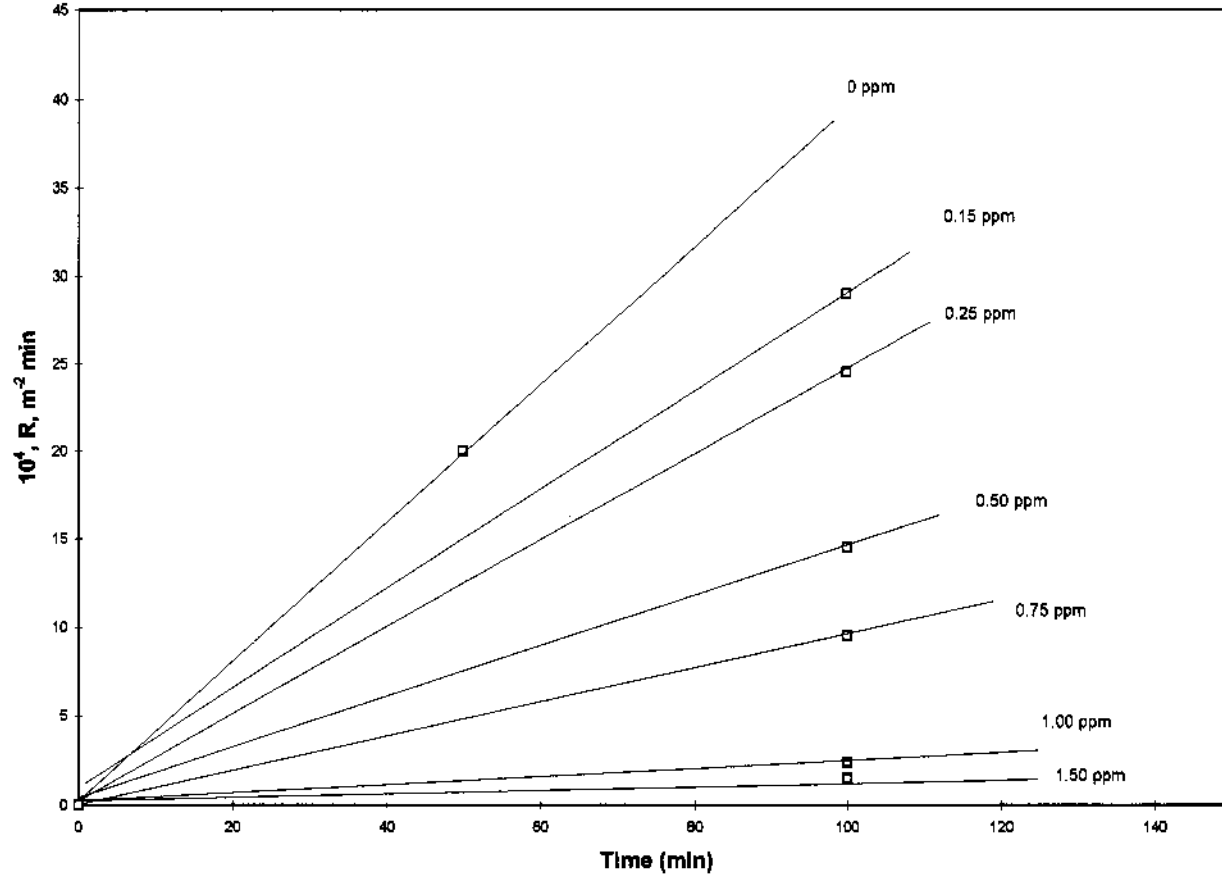


Figure 5. Crystal growth of calcite at constant supersaturation in the presence of varying concentrations of tannic acid.

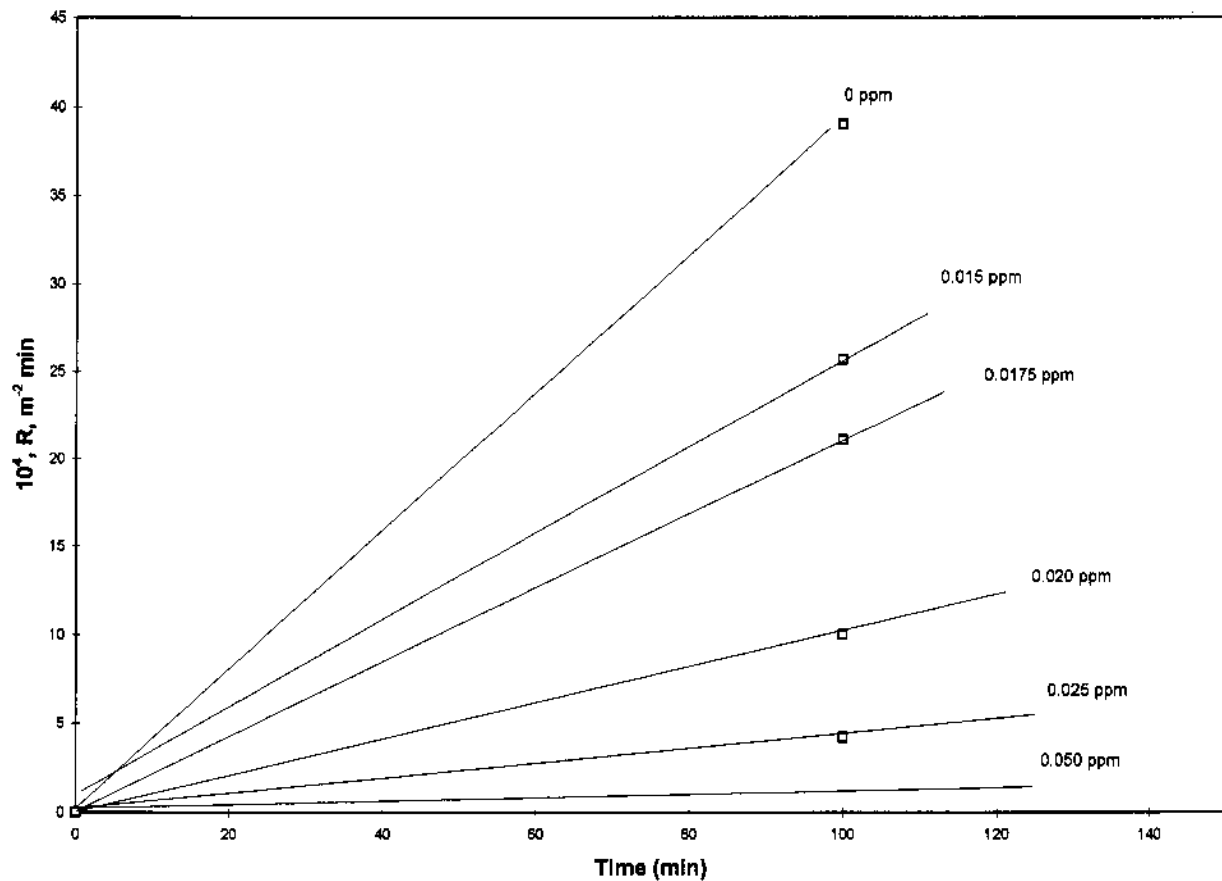


Figure 6. Crystal growth of calcite at constant supersaturation in the presence of poly (acrylic) acid at varying concentrations.

ppm) has a marked inhibitory effect on calcite growth. Calcite growth rates in the presence of 0.015, 0.020, and 0.05 ppm of PAC are 25.7, 9.8, and 0.5×10^{-6} moles $\text{CaCO}_3 \text{ m}^{-2} \text{ min}^{-1}$ respectively, compared to 39.5×10^{-6} mole $\text{m}^{-2} \text{ min}^{-1}$ obtained in the absence of inhibitor (Table 1).

To study the influence of hydroxyl and carboxyl functional groups present in the same molecule, crystal growth experiments were conducted at varying concentrations of salicylic acid (SA). The kinetic data on the inhibition effectiveness of SA (Table 1) demonstrate that SA at concentrations as high as 5.00 ppm does not significantly reduce the growth rate. The inhibition effectiveness of several synthetic compounds containing carboxyl, and both hydroxyl and carboxyl groups (i.e., BHCA, BTCA, and SA) under similar growth conditions is illustrated in Figure 7.

For experiments with solution inhibitor concentration of 0.25 ppm, BHCA exhibits much stronger inhibitor activity than higher concentrations of BTCA (0.5 ppm) and SA (5 ppm). The greater inhibitory effect of BHCA compared to BTCA and SA indicates that inhibitor ionic charge and total number of ionizable groups determines inhibitor effectiveness. The importance of inhibitor charge has been reported in studies involving the crystal growth rate reduction for growth reaction of other sparingly soluble salts. Growth rates (10^{-6} mole $\text{m}^{-2} \text{ min}^{-1}$) obtained at fixed inhibitor concentration (0.25 ppm) in the presence of BHCA are 15.5 compared to 17.1 and 24.6 obtained for FA and TA, respectively. At low concentrations the FA is nearly as effective as BHCA in reducing calcite crystallization rates.

Results of the CC experiments illustrate the effectiveness of natural and synthetic compounds as crystal growth inhibitors (Table 1 and Figure 8). Inhibition effectiveness of FA, TA, SA, BHCA, and PAC at 0.25 ppm concentration of each inhibitor present initially in supersaturated solutions illustrates that the synthetic materials are more effective than the natural polyelectrolytes. Tannic acid (Figure 8) is a less effective growth inhibitor than BHCA and PAC (Figure 8). Inhibitor effectiveness (from most effective inhibitor to least effective inhibitor) for compounds containing hydroxyl and/or carboxyl groups is : PAC >> BHCA ~ FA > TA >> BTCA ~ SA ~ control (no inhibitor).

For many sparingly soluble salts, the mechanism of crystal growth rate inhibition can be described as an adsorption process at crystal growth sites on the mineral surface. Chelating anions may be adsorbed at cationic sites on the crystal surface and inhibit the growth when present at very low concentrations. In addition, inhibitors having large binding constants may also form ion pairs with calcium ions present in the calcium carbonate supersaturated solution, decreasing supersaturation. However, under the experimental conditions employed in the present investigation the decrease in the rate of crystallization must be attributed to the surface adsorption rather than simple calcium-inhibitor complex formation. Inhibitor concentration is much lower than that of calcium ion. The percent of calcium ion complexed to fulvic acid at the highest FA concentration is less than 5%. (M. M. Reddy, unpublished results, 1997).

The adsorption process and its influence on the crystal growth rate can often be interpreted in terms of a Langmuir-type isotherm^{7,15,20,23} represented by the following equation:

$$R_0/(R_0 - R) = 1 + (K_a C)^{-1} \quad (1)$$

where R and R_0 are the rates of crystal growth in the presence and absence of inhibitors respectively, K_a is the adsorption affinity constant of the substrate for the inhibitor ion, and C is the inhibitor concentration. Langmuir function plots for FA and TA according to equation 1 (Figure 9) illustrate that inhibitor adsorption on calcite crystals deviates from

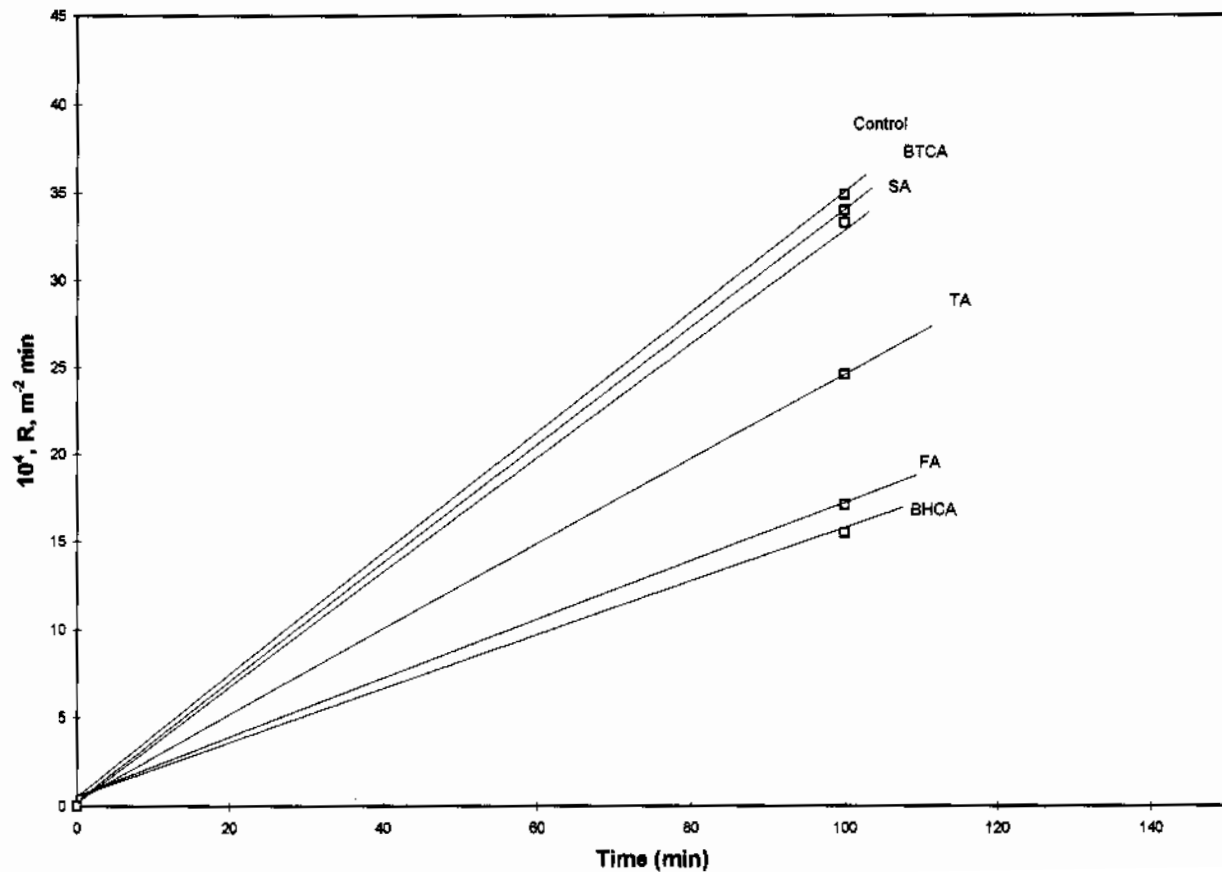


Figure 7. Calcite crystal growth in the presence of various additives at constant supersaturation.

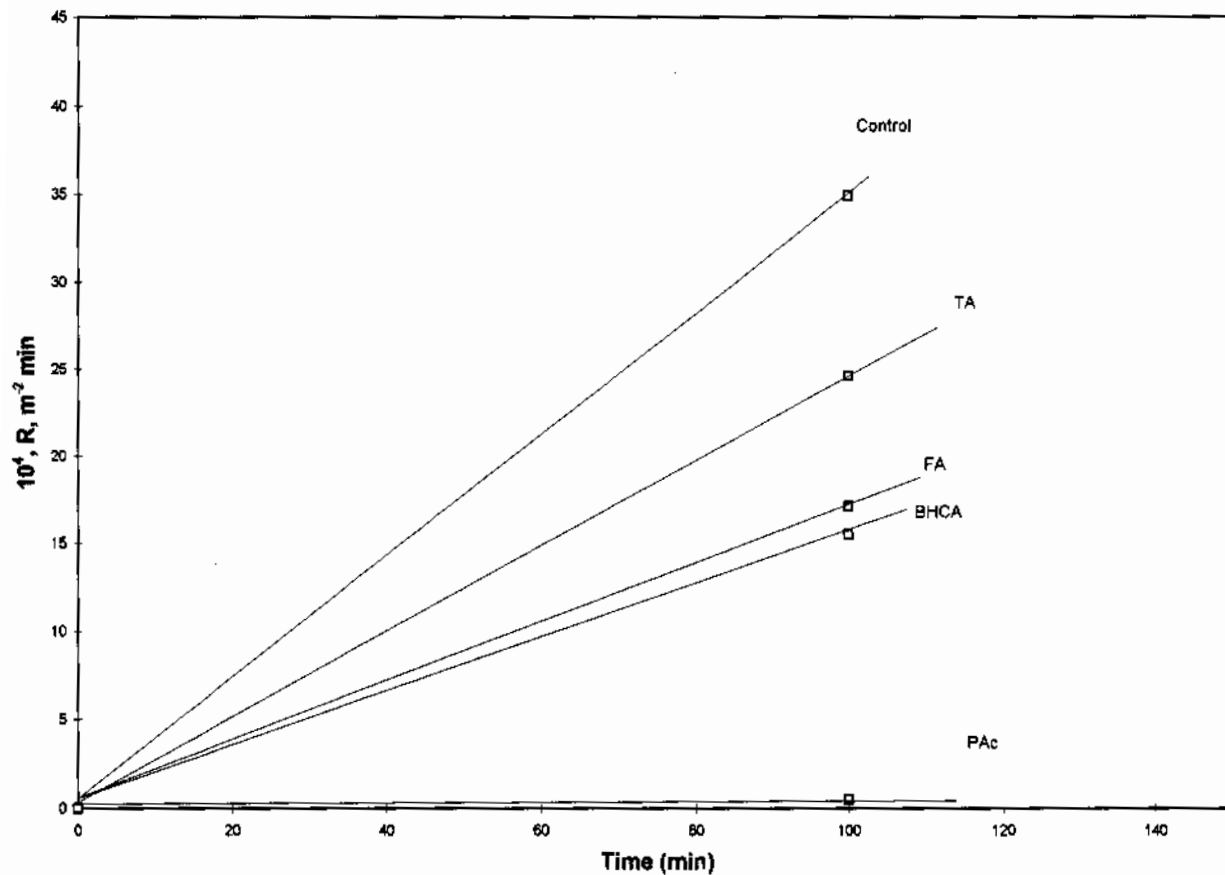


Figure 8. Calcite crystal growth in the presence of various additives and poly (acrylic acid) at constant supersaturation.

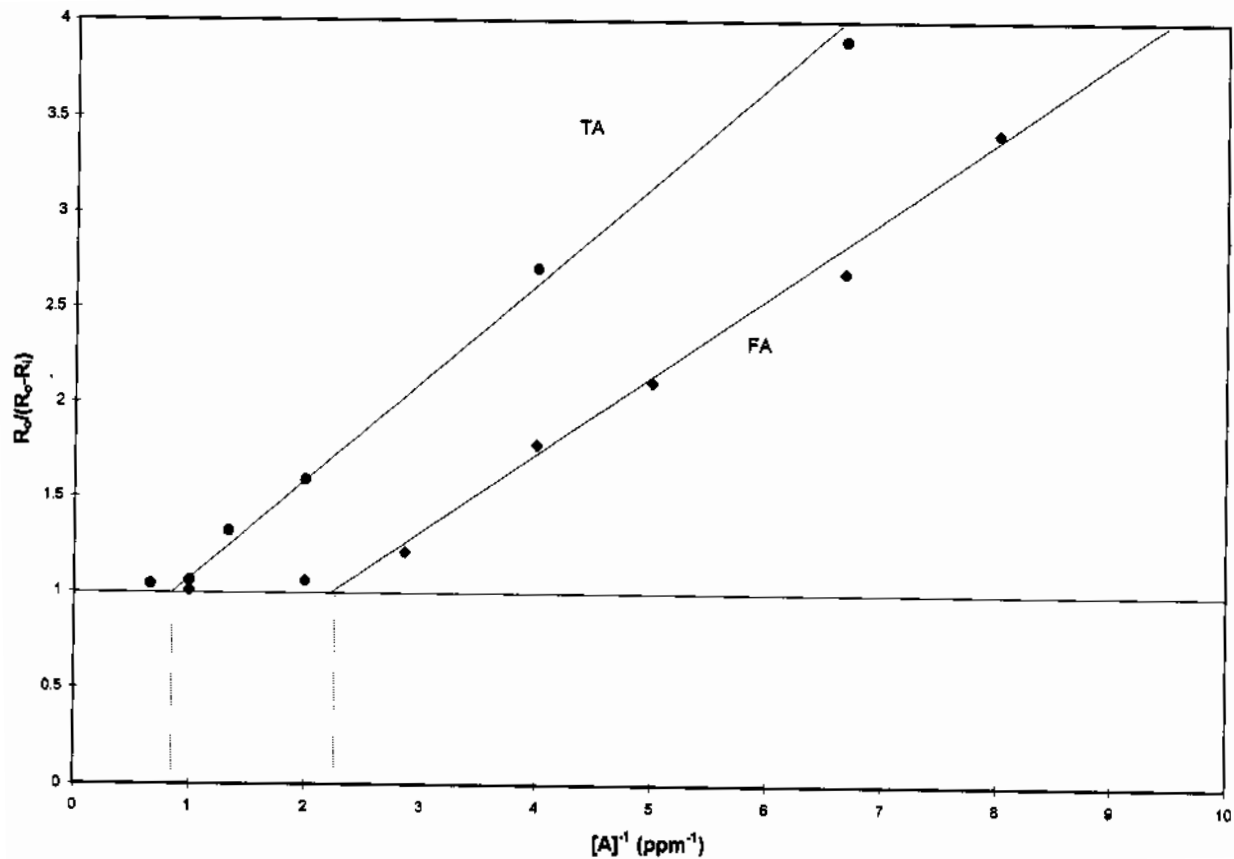


Figure 9. Plots of the rate of calcite formation as a function of the reciprocal of the tannic or fulvic acid concentration,

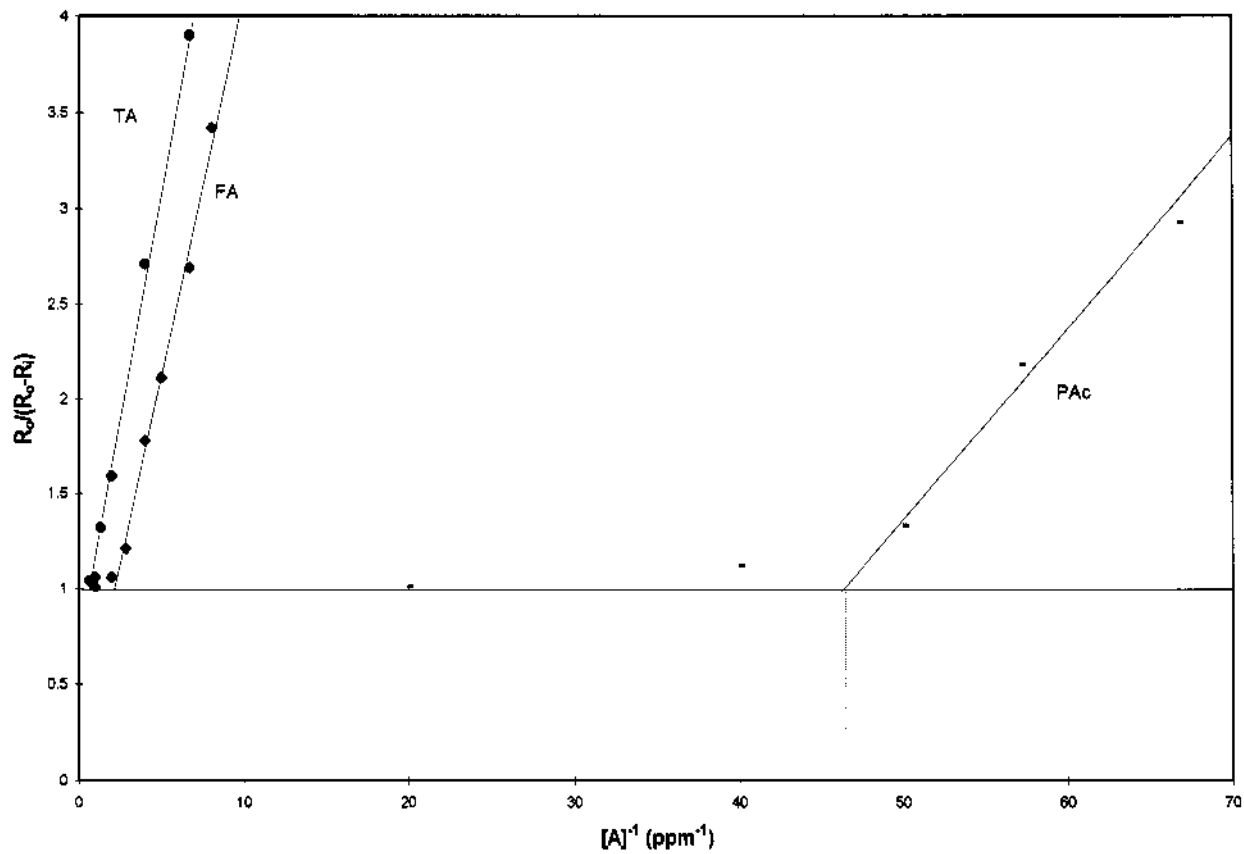


Figure 10. Plots of the rate of calcite formation as a function of the reciprocal of the inhibitor concentration for poly(acrylic acid) as well as TA and FA.

the simple adsorption model—there are two linear segments instead of one predicted by equation 1.

The line corresponding to growth inhibition at low additive concentration (high reciprocal additive concentrations) does not extrapolate to the value of unity at high additive concentrations (Figure 9) expected from equation 1. The appearance of two linear portions in this plot could be due to the failure of the Langmuir-adsorption model assumptions: 1) uniform adsorption sites and 2) absence of interactions between adsorbent molecules. Calcite growth is almost completely inhibited i.e., $R_0/(R_0-R) \sim 1$, at 0.45 ppm for FA, and 1.15 ppm TA (Figure 9). Polyacrylic acid exhibits a more pronounced segmented Langmuir function plot than FA or TA (Figure 10).

A detailed discussion of calcite growth inhibition mechanisms by simple ionic substances has been presented elsewhere.²⁶ Simple ionic inhibitors, which follow a Langmuir model, generally adsorb upon all growing crystal faces equally. This adsorption and blockage of growth sites reduces the crystal growth rate to zero at a characteristic minimum inhibitor concentration. These inhibitors follow a Langmuir function that is linear with an intercept of unity. Moreover, the smallest measurable rate has a Langmuir function value close to unity.

This regular Langmuir function behavior is also observed for simple polyvalent ions such as HCBA.²⁷ However, complex or polymeric inhibitor ions preferentially adsorb on more rapidly growing crystal faces. This adsorption behavior may lead to marked changes in crystal habit and morphology at inhibitor concentrations less than those needed to prevent growth. If polyelectrolyte inhibitor adsorption is greatest on those calcite crystal faces with the highest kink density, then growth for those faces will decrease to a value very close to zero. Other more slowly growing faces will continue to grow until their growth sites are blocked by inhibitor ions. This two-stage inhibition process leads to two linear segments in the Langmuir function plot as observed for the polyelectrolyte inhibitors examined here.

5. SUMMARY

Several natural and synthetic carboxylate-containing polymeric compounds have been shown to greatly reduce the calcite crystal growth rate at a fixed calcite supersaturation and pH=8.5. These synthetic and natural inhibitors seem well suited for use as scale inhibitors in a range of commercial applications. Further work characterizing the crystal growth inhibition process of natural and synthetic carboxylate-containing polymeric compounds under actual industrial conditions seems appropriate.

ACKNOWLEDGMENTS

Any use of trade names in this paper is for descriptive purposes only and does not constitute endorsement by the US. Geological Survey.

REFERENCES

1. Cowan JC and Weintritt DJ, (Eds.), *Water-Formed Scale Deposits*, Gulf Publishing Company, Book division, Houston, Texas, 1976.

2. Dalas E and Koutsoukos PG, "Calcium Carbonate Scale Formation Heated Metal Surfaces", *Geothermics*, 1989;18:83.
3. Wilson D, "Influence of Molecular Weight on Selection and Application of Polymeric Scale Inhibitors", *CORROSION/94*, Paper No. 48, NACE, Houston, Texas, 1994.
4. Amjad Z, "Influence of Calcium Fluoride Crystal Growth by Polyelectrolytes", *Langmuir*, 1991 ;7:2405.
5. Sullivan PJ, O'Brien F, and Ferguson RJ, "A Multifunctional Additive for Deposit Control", *CORROSION/96*, Paper No. 158, NACE, Houston, Texas, 1996.
6. Amjad Z, "Constant Composition Study of Dicalcium Phosphate Dihydrate Crystal Growth in the Presence of Poly(acrylic acids)", *Langmuir*, 1989;5: 1222.
7. Amjad Z, "Performance of Polymeric Additives as Hydroxyapatite Crystal Growth Inhibitor", *Phosphorus Research Bulletin*, 1995;5:1.
8. Manne JS, Biala N, Smith AD, and Gryte CC, "The Effect of Anionic Polyelectrolytes on the Crystallization of Calcium Oxalate Hydrates", *J. Crystal Growth*, 1990; 100:627.
9. Amjad Z, "Effect of Polyelectrolytes on the Spontaneous Precipitation of Calcium Carbonate", in preparation.
10. Giannimaras EK and Koutsoukos PG, "The Crystallization of Calcite in the Presence of Orthophosphate", *J. Colloid Interface Sci.*, 1987; 116:423.
11. Falini G, Gazzano M, and Ripanonti A, "Crystallization of Calcium Carbonate in Presence of Magnesium and Polyelectrolytes", *J. Crystal Growth*, 1994; 137:577.
12. Reddy MM, "Kinetic Inhibition of Calcium Carbonate Formation by Wastewater Constituents", In *Chemistry of Wastewater Technology*, A.J. Rubin, (ed.), Ann Arbor Science, Ann Arbor, Michigan, 1978.
13. Nancollas GH, Kazmierczak TF, and Schuttringer E, "A Controlled Composition Study of Calcium Carbonate Crystal Growth: The Influence of Scale Inhibitors", *CORROSION/80*, Paper No. 226, NACE, Houston, Texas, 1980.
14. Amjad Z, "Performance of Polymers as Precipitation Inhibitors for Calcium Phosphonates", *Tenside*, 1997;34:102.
15. Butt FH, Rahman F, and Baduruthamal U, "Identification of Scale Deposits through Membrane Autopsy", *Desalination*, 1995;101:219.
16. Amjad Z, Pugh J, Zibrida J, and Zuhl R, "Polymer Performance in Cooling Water: The Influence of Process Variable", *Materials Performance*, 1997;36:32.
17. Hamdona SK, Nassim RB, and Hamza SM, "Spontaneous precipitation of Calcium Sulfate Dihydrate in the Presence of some Metal Ions", *Desalination*, 1993;94:69.
18. Katz JL and Parsiegla KI, "Calcite Growth Inhibition by Ferrous and Ferric Ions", In *Mineral Scale Formation and inhibition*, Z. Amjad (ed.), Plenum Press, New York, New York, 1995.
19. Aiken GR, McKnight DM, Wershaw RL and MacCarthy P, (eds.), *Humic Substances in Soil, Sediment and Water- Geochemistry, Isolation and Characterization*, John Wiley and Sons, NY, 1985.
20. Averett RC, Leenheer JA, McKnight DM and Thorn KA, (eds), *Humic Substances in the Suwannee River, Georgia: Interactions, Properties and Proposed Structures*, US. Geological Survey Open-File Report 87-557, 1987.
21. Leenheer JA, Brown PA, Noyes TI, "Implications of Mixture Characteristics on Humic Substance Chemistry", in *Aquatic Humic Substances: Influences on the Fate and Transport of Pollutants*, *Advances in Chemistry Series 219*, American Chemical Society, Washington, D.C., 1989.
22. Leenheer JA, Wershaw RL, and Reddy MM, "Strong-acid, carboxyl-group structures in fulvic acid from the Suwannee River, Georgia. 1. Minor structures", *Environmental Science and Technology*, 1995;29:393.
23. Leenheer JA, Wershaw RL, and Reddy MM, "Strong-acid, carboxyl-group structures in fulvic acid from the Suwannee River, Georgia. 2. Major structures", *Environmental Science and Technology*, 1995;29:399.
24. Nystrom M, Ruohomaiki K and Kaipia L, 1996, *Humic Acid as a Fouling Agent in Filtration*, *Desalination*, 106,79
25. Freche M, Rouquet N, Koutsoukos P, and Lacout JL, *Effect of Humic Compounds on the Crystal Growth of Dicalcium Phosphate Dihydrate*, 1992, *Agrochimica*, 36, 500
26. Kazmierczak TF, Tomson MB, Nancollas GH, 1992, *Crystal Growth of Calcium Carbonate. A Controlled Composition Kinetics Study*, *J. Phys. Chem.*, 86, 103-107
27. Amjad Z, 1987, *Kinetic Study of the Seeded Growth of Calcium Carbonate in the Presence of Benzene-polycarboxylic Acids*, *Langmuir*, 3,224

NOVEL CALCIUM PHOSPHATE SCALE INHIBITOR

Libardo A. Perez and Stephen M. Kessler

BetzDearborn, Inc.
Water Management Group
4636 Somerton Road
Trevose, Pennsylvania 19053

1. ABSTRACT

Phosphate based chemical treatment programs are used in several industrial applications in order to control corrosion on low carbon steel metal surfaces. In cooling systems, for example, phosphates are added to the cooling water to prevent corrosion on low carbon steel heat exchangers and pipes. Because there is a tendency to run cooling systems at higher cycles and process operation at higher temperatures, calcium phosphate scale has become more common in cooling water systems. A new terpolymer able to provide calcium phosphate scale control and dispersion of suspended solids has been developed. The inhibitor has been shown to be effective in highly cycled cooling water and at relatively high temperatures. The efficacy of the new terpolymer at different monomer ratios and molecular weight was also established.

2. INTRODUCTION

After calcium carbonate, calcium phosphate is the most common scale found in cooling systems. In most cases, the relatively high phosphate concentration found in cooling systems is caused by the addition of inorganic phosphates to control corrosion on Low Carbon Steel (LCS) surfaces present in the cooling system (heat exchangers, pipes, and water boxes). The problem has increased in the last ten years because of the tendency to operate cooling systems at higher cycles of concentration due to water conservation, and, in some cases, the higher temperatures for process optimization.¹ Operating cooling systems under these most drastic conditions dramatically increases the potential for calcium phosphate scale formation, even at the relatively low phosphate concentrations found naturally occurring in waters.

Polymers have been used extensively as calcium phosphate scale inhibitors for several decades.² Their efficacy, however, may be affected by the cooling system operating conditions, i.e., temperature, pH, and relative supersaturation of the water with respect to the possible calcium phosphate phases that may form during the precipitation process.³ Operating cooling systems under the conditions described above has increased the need for better calcium phosphate inhibitors that could provide not only scale control under these most drastic conditions, but also be efficient for dispersion of any solid suspended in the water and without being affected by the presence of iron and other possible corrosion byproducts present in the water.

It is believed that ortho-phosphate provides corrosion inhibition on LCS surfaces by forming a protective film that may be composed of calcium, iron, and phosphate.^{4,5} Surface characterization of the film formed, as well as an understanding of the role played by the calcium phosphate inhibiting polymer is important to elucidate both the corrosion inhibition mechanism and the scale prevention mechanism.

In this study, results on calcium phosphate scale inhibition testing conducted with a new terpolymer are presented. This new terpolymer provides better scale control than other more traditional calcium phosphate scale inhibitors at normal and at higher temperature conditions usually found in cooling systems. The terpolymer is also minimally affected by the presence of iron in the cooling water.

3. EXPERIMENTAL

All solutions were prepared by using reagent grade calcium chloride dihydrate, sodium bicarbonate, sodium carbonate, magnesium sulfate heptahydrate, sodium silicate nonahydrate, sodium phosphate dodecahydrate, iron (II) chloride (all from Fisher Scientific Co.), and double distilled water. Calcium and magnesium concentrations were determined by standard EDTA colorimetric titrations and by Inductively Coupled Plasma atomic emission spectroscopy (ICP). Silica, phosphate, and other ions were also determined by ICP or by colorimetric methods. Deposits were analyzed by infrared spectroscopy (Perkin Elmer System 2000 FTIR), scanning electron microscopy (Amray 1700 scanning electron microscope) and energy dispersive x-ray analysis (Tracor Northen 5500). Heat exchanger surfaces were analyzed by ESCA and diffuse reflectance FTIR.

Two types of tests were conducted to determine the efficacy of calcium phosphate inhibitors. One is a Static Beaker Test. This involved the addition of the treatment to solutions containing calcium and phosphate ions at the pH studied. The beakers were incubated in a water bath at 70 °C for 18 hours. A portion of the hot solution was filtered and the phosphate concentration measured by ICP. Percent inhibition was calculated from the phosphate contained in the treated, stock, and control solutions.

The second test performed utilized a Dynamic Recirculating Test Rig. This test evaluates the efficacy of the treatment as a scale control agent for cooling water systems. The recirculating units used for these tests, are designed to provide a realistic measure of the ability of a treatment to prevent corrosion and scale formation under heat transfer and flow conditions⁶ Testing is typically conducted by feeding a synthetic cooling water to the unit sump at a fixed rate with the appropriate treatment under evaluation. With blowdown also being regulated, a system retention time can be maintained. Temperature and pH are controlled to mimic the desired cooling tower condition. Cooling water flow is then diverted at a fixed velocity across numerous coupon specimens as well as a heated surface. Corrosion and deposit analysis are conducted on all metallurgy in order to ascertain treatment effectiveness.

The ability of a polymer to disperse solids suspended in the water is also an important property. Dispersion tests were conducted by using a Dynamic Dispersion Testing Unit (DDTU). This unit allows the screening of dispersant agents under solution dynamics similar to those found in cooling systems. The treated water containing the suspended solids is circulated through a dispersion column that provides the solution dynamic simulation. Temperature and pH are automatically controlled. The unit permits the water velocity to be controlled. Turbidity is measured on-line during the test. The dispersion efficacy of the treatment is measured by the change in turbidity with respect to its initial value. Figure 1 shows a schematic representation of the DDTU.

4. RESULTS AND DISCUSSION

Polymers have been extensively used as scale control agents for several decades. Most of them are acrylic acid based copolymers that have proven to be effective under most typical cooling water conditions. At the present time, however, the efficacy of these copolymers have been limited by the current trend toward operating cooling systems under more severe conditions to increase process efficacy, safety, and water conservation. We will discuss here the development of a new terpolymer that allows the operation of cooling systems under both standard and stressed cooling water conditions.

The new terpolymer has Acrylic Acid, Allyl propyl Hydroxy Propyl Sulfonate Ether, and PolyEthylene Glycol Allyl Ether as the building blocks. In addition to scale control, this new terpolymer, hereafter AA/AHPSE/PEGAE, was shown to be an effective dispersant agent.

4.1. Terpolymer Optimization

Monomer ratio and molecular weight are two important parameters that must be considered in the optimization of a scale inhibitor. Beaker tests, conducted under the con-

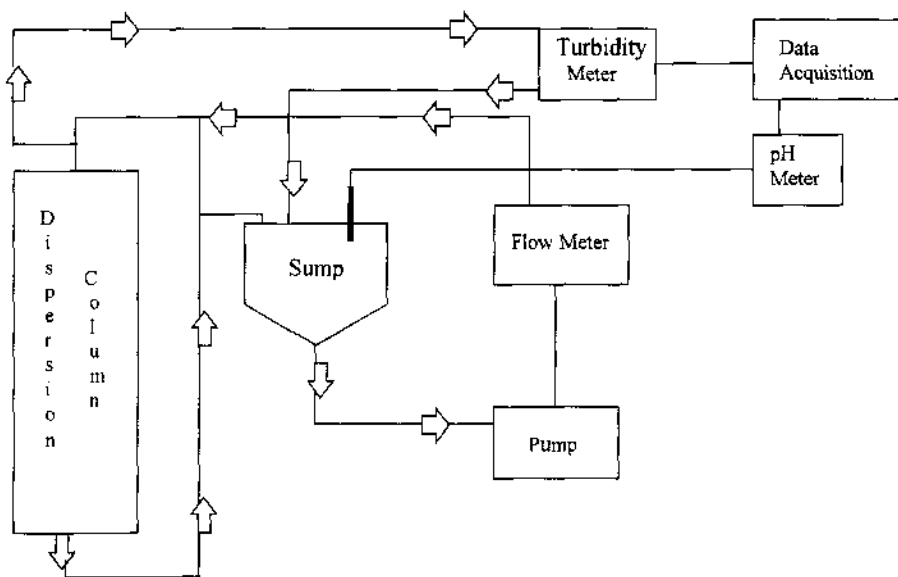


Figure 1. Schematic representation of a Dynamic Dispersion Testing Unit (DDTU).

Table 1. Beaker test experimental conditions

400 ppm Ca as CaCO ₃
100 ppm Mg as CaCO ₃
50 ppm Alkalinity as CaCO ₃
10ppm PO ₄ ³⁻
pH 8.2 at 70°C
Test duration: 18 hours

ditions given in Table 1, were performed with terpolymers having different monomer ratios and with terpolymers having the same monomer ratio but different molecular weight.

The ratio of the monomers forming the polymer chain has a paramount effect on the efficacy of the inhibitor. As illustrated in Figure 2, the terpolymer efficacy was dramatically changed when the ratio of the AA/AHPSE/PEGAE was changed from 10/1/1 to 3/1/1. This effect is perhaps the result of a needed orientation and separation of the functional groups in order to adsorb at the surface of the forming particle. Once adsorbed at the surface, the polymer may inhibit the further growth of the forming particle and may also prevent the phase transformation of an initially formed metastable phase into the most stable one which will reduce the probability for scale formation.

To study the effect of the molecular weight on the polymer performance, terpolymers with the same monomer ratio but with different molecular weights were synthesized. Terpolymers having a viscosity in the range of 11.4 to 19.8 cps were tested. Figure 3 shows the molecular weight effect (given as a function of the viscosity) on the inhibitor for calcium phosphate scale control. As can be seen, the terpolymer having a viscosity of 15.9 gave the best performance in this test at an active concentration of 10 mg/L. The efficacy of the terpolymers decreased at molecular weights higher or lower than the 15.9 cps.

Although to a lesser degree, tests conducted at a higher concentration also showed a similar efficacy distribution. This is illustrated in Figure 4.

The effect of the molecular weight on the performance of the polymer as a scale inhibitor may be attributed to a required size for the terpolymer to accommodate at the active sites of the forming particles.

4.2. Polymer Testing under Simulated Cooling Conditions

Dynamic Recirculating tests were conducted in order to evaluate the new terpolymer under conditions that simulate those found in open recirculating cooling water systems. The performance of the terpolymer was compared against a copolymer of acrylic acid with 2-Acrylamido-2-Methyl-Propane Sulfonic acid (AA/AMPS), which has been widely used in the cooling industry as a calcium phosphate scale inhibitor for more than 15 years. The tests were conducted with recirculating waters having the conditions given in Table 2. Four (4) ppm active polymer were used in all tests in which 13 ppm ortho-phosphate, 2 ppm pyro-phosphate and 1.5 ppm of a commercially available phosphonate were used as the source of phosphate to prevent corrosion on the LCS heat exchanger and coupon surfaces. Since both mild steel and admiralty (ADM) coupons were also utilized in these experiments, yellow metal corrosion was controlled by using 1.5 ppm of tolyltriazole. The recirculating test parameters are given in Table 3. These parameters represent typical conditions found in industrial cooling systems.

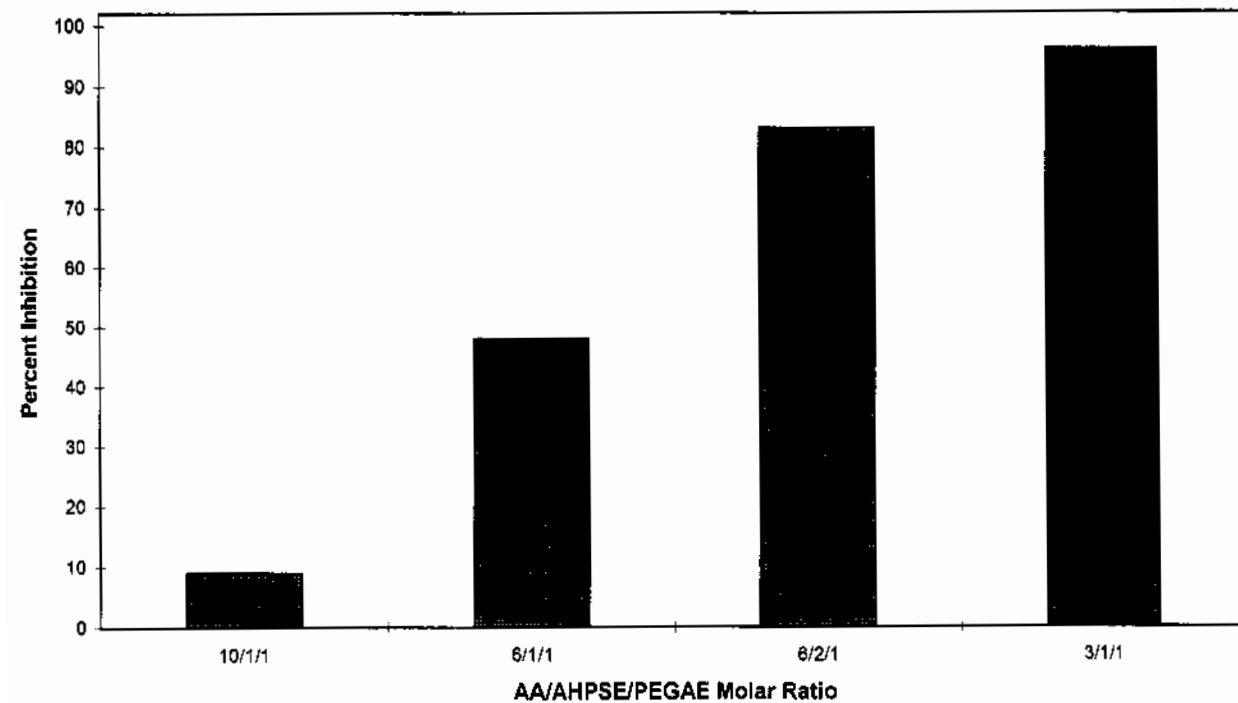


Figure 2. Effect of the monomer ratio on the efficacy of the terpolymer.

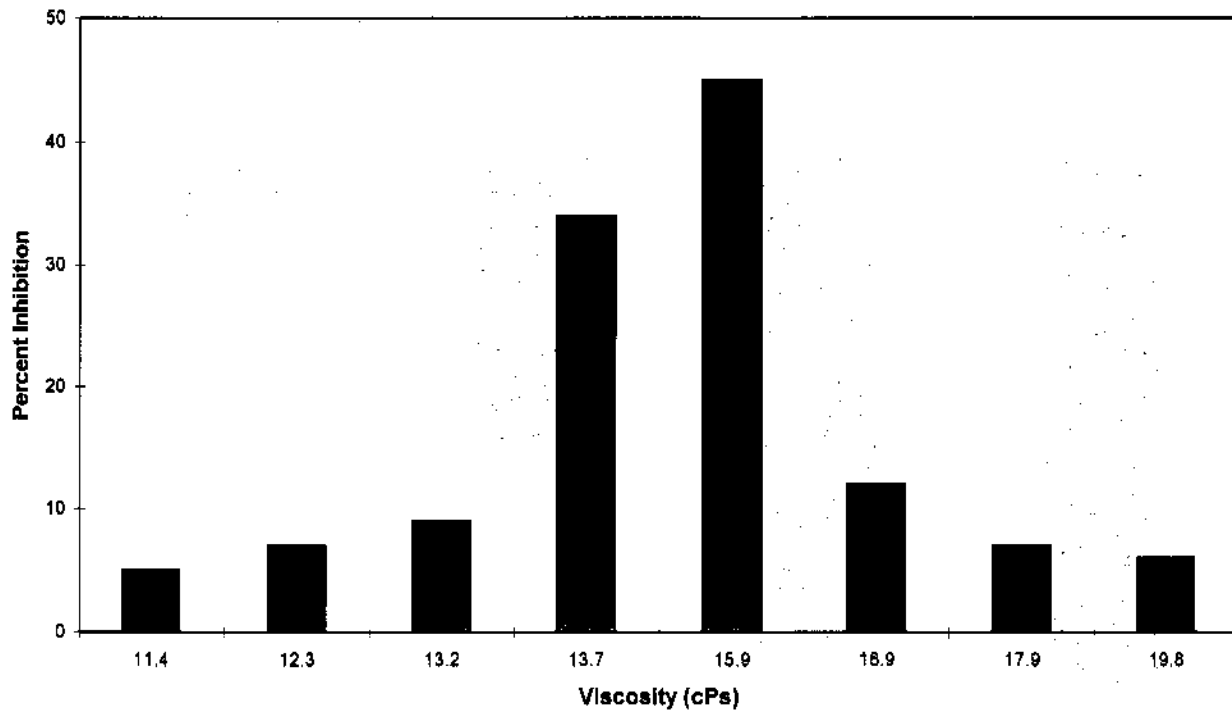


Figure 3. Effect of molecular weight on terpolymer performance.

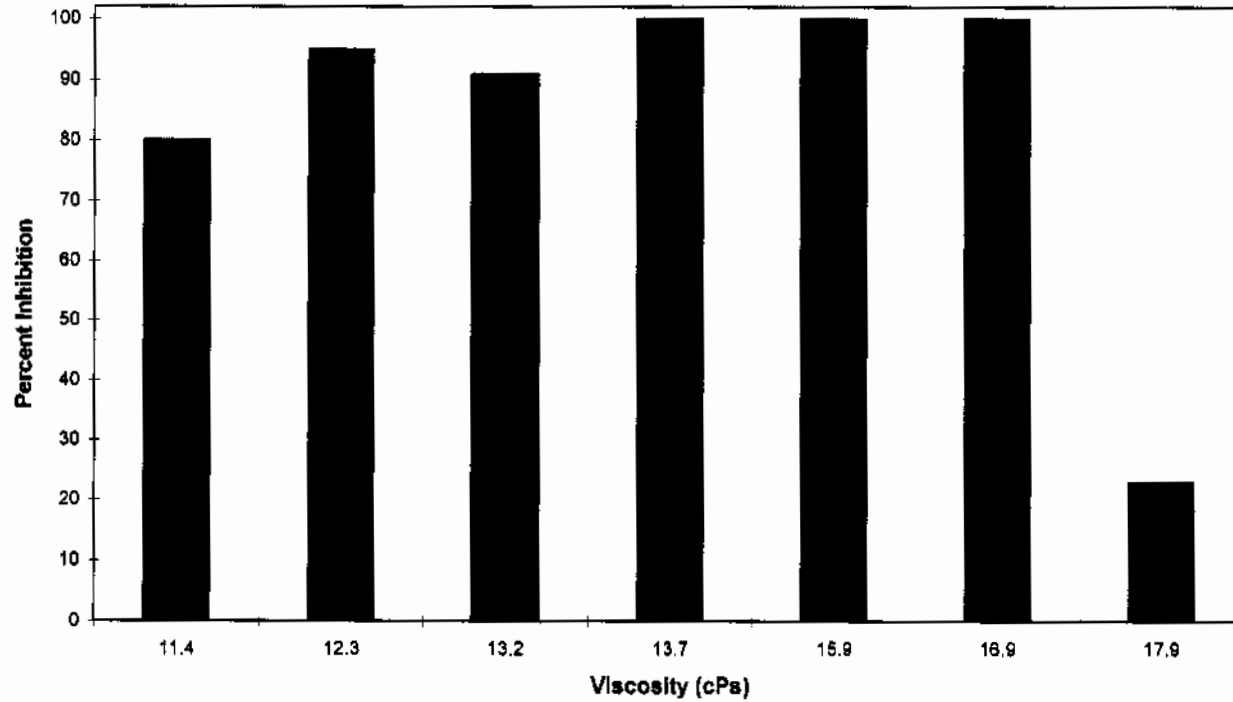


Figure 4. Effect of molecular weight at higher terpolymer concentration.

Table 2. Water conditions and corrosion treatment concentration

Water	600 ppm Ca, 300 ppm Mg, 50 ppm M-alk (all as CaCO ₃), 2200 umhos, pH 7.2
Treatment	13 ppm ortho, 2 ppm pyro, 1.5 ppm phosphonate, 3 ppm azole, 4 ppm active polymer

Table 3. Recirculating test parameters

Bulk temperature	120°F
Skin temperature	135°F
Water velocity	2.8 ft/sec
Retention time (75% depletion)	1.4 days
Test duration	7 days
Metallurgy	
Coupons	LCS/ADM
Heat exchanger	LCS

Under these conditions, the 4 ppm active concentration of the AA/AHPSE/PEGAE terpolymer was able to control scale, maintain a clean heat exchanger surface, and keep corrosion at an acceptable level (0.8 mpy for LCS surface and 0.1 mpy for ADM metal). The AA/AMPS copolymer, however, was not able to keep a clean surface. Very slight to slight deposition was observed on the heat exchanger tube. Comparative results are shown in Table 4. Figure 5 shows the photographs of the heat exchanger tubes at the end of the experiments performed with AA/AHPSE/PEGAE and with AA/AMPS.

While the filtered and unfiltered phosphate analysis was quite similar between the two polymers, the better performance of the terpolymer was demonstrated by the very low water turbidity maintained during the seven day experiment (0.3 NTU). As shown by the analytical results in Table 5, AA/AMPS was not able to keep similarly low turbidity values, i.e., a 0.9 NTU value was measured at the end of the AA/AMPS experiment.

The corrosion protecting film developed on the visible clean heat transfer surface was characterized by using x-ray photoelectron spectroscopy and diffuse reflectance FTIR. The x-ray photoelectron spectrograph showed the presence in the film of calcium, ortho-phosphate, iron, and the terpolymer. The presence of the terpolymer was concluded

Table 4. Polymer comparison

Standard Conditions

(4 ppm active polymer)

AA/AMPS	very slight/slight heat transfer surface deposition Corrosion: LCS = 0.7 ADM = 0.2 (mpy)
AA/AHPSE/PEGAE	clean heat transfer surface Corrosion: LCS = 0.8 ADM = 0.1 (mpy)

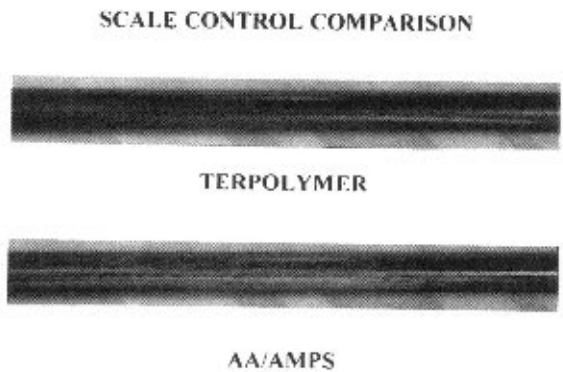


Figure 5. Photographs of heat exchanger surfaces at the end of experiments.

by the presence of the corresponding carboxylic and sulfonic groups. The FTIR analysis showed very weak intensity peaks typical of ortho-phosphate and carboxylic groups.

As mentioned previously, a tendency in industry today is to run processes at higher temperature as a mean of increasing process efficiency. However, this also increases the potential for corrosion and the potential for calcium phosphate deposition due to the inverse solubility presented by the different calcium phosphate phases. As a result, in order to prevent calcium phosphate scale inhibition at higher temperatures, relatively high dosages of the traditional calcium phosphate inhibitors have to be used. This is not the case with the new terpolymer. This material was tested at a higher bulk water temperature (140 °F) and a higher heat transfer surface temperature (155 °F). At the 4 ppm active treatment level, the terpolymer was still able to keep the heat transfer surface free of deposition. The AA/AMPS copolymer, however, was not able to control scale and slight deposition took place on the heat transfer surface. The turbidity was higher during the AA/AMPS evaluation with the phosphate analysis also indicating lower levels being maintained throughout this simulation due to the fouling condition. Experimental results for this comparison are presented in Tables 6 and 7.

Polymer performance is greatly affected by the presence of iron in cooling streams. In these cases, the polymer must not only prevent calcium phosphate scale formation but must also act as a very good dispersant of iron oxide particles which inevitably form. Deposition of these oxides on the heat transfer surface and other surfaces present in the system must be minimized since they can also lead to under-deposit corrosion and in-

Table 5. Polymer comparison

Standard Conditions				
(4 ppm active polymer)				
	Turbidity (ntu)	-----ppm as PO ₄ -----		
		ortho	TIP	TP
AA/AMPS	0.9	14.0/14.2	14.6/15.8	14.4/16.1
AA/AHPSE/PEGAE	0.3	13.4/13.9	14.7/15.6	14.8/15.6

Table 6. Polymer comparison at elevated temperatures
(4 ppm active polymer; 140° F bulk/155° F skin)

AA/AMPS	slight heat transfer deposition Corrosion. LCS = 0.6; ADM = 0.2 (mpy)
AA/AHPSE/PEGAE	clean heat transfer surface Corrosion: LCS = 0.4; ADM = 0.1 (mpy)

Table 7. Polymer comparison at elevated temperatures
(4 ppm active polymer;1400° F bulk/1550° F skin)

	Turbidity (ntu)	-----ppm as PO ₄ -----		
		ortho	TIP	TP
AA/AMPS	0.8	12.9/13.2	14.0/14.5	14.0/14.5
AA/AHPSE/PEGAE	0.5	12.6/13.0	14.5/15.3	15.5/15.8

creased pitting. To simulate conditions of iron contamination, standard testing was again conducted but with a feed of Fe⁺² to the test sump. Initially the system was charged with 0.5 ppm iron and maintained at this level using a syringe pump based on make-up and blow down. Under these stressful conditions, the AA/AHPSE/PEGAE terpolymer also showed superior performance in controlling scale when compared to the AA/AMPS copolymer (Table 8). As shown in Table 9, the terpolymer was able to provide better dispersion of the iron oxide particles, as can be concluded from the higher turbidity data. While significant phosphate loss was noted with both polymers, the terpolymer kept the solids more dispersed in the bulk water (3.8 NTU with the copolymer compared to 6.2 NTU with the terpolymer). Figure 6 shows the extent of deposition that took place in the experiment with the AA/AMPS copolymer and how performance compared with the almost clean sur-

Table 8. Effect of iron
(4 ppm active polymer; continous iron feed at 0.5 ppm)

AA/AMPS	moderate deposition Corrosion: LCS = 0.7; ADM = 0.0 (mpy)
AA/AHPSE/PEGAE	slight deposition Corrosion: LCS = 0.6; ADM = 0.1 (mpy)

Table 9. Effect of iron
(4 ppm active polymer)

	Turbidity (ntu)	-----ppm as PO ₄ -----		
		ortho	TIP	TP
AA/AMPS	3.8	11.5/12.8	11.9/13.3	12.4/13.7
AA/AHP/SE/PEGAE	6.2	11.7/12.7	11.4/14.2	11.6/14.1

face which was the result of the test with AA/AHPSE/PEGAE The terpolymer was superior with regard to both calcium phosphate scale inhibition and iron oxide dispersion.

4.3. Test of AA/AHPSE/PEGAE as a Clay Dispersant Agent

Dispersion of suspended solids such as clay, silt and mud is also very important in preventing deposition on a cooling systems surfaces, Dynamic dispersion testing of the optimized polymer was conducted by using a DDT unit. As it can be seen in Figure 7, the optimized polymer showed better dispersion properties than a polyacrylic acid with a similar molecular weight. It was also superior to other terpolymers with the same monomer ratio composition but lower molecular weight than the optimized AA/AHPSE/PEGAE. These results indicate that this new terpolymer can function in a cooling program as both a calcium phosphate scale inhibitor and as a dispersant of particles suspended in the water.

5. CONCLUSIONS

The newly developed terpolymer (AA/AHPSE/PAGAE) has been shown to be a very effective scale inhibitor for calcium phosphates under laboratory conditions. The inhibitor showed better performance than the traditionally used AA/AMPS under both normal and stressed conditions, i.e., under elevated temperatures and in the presence of iron contamination. The terpolymer also showed very good dispersion properties for suspended clay.

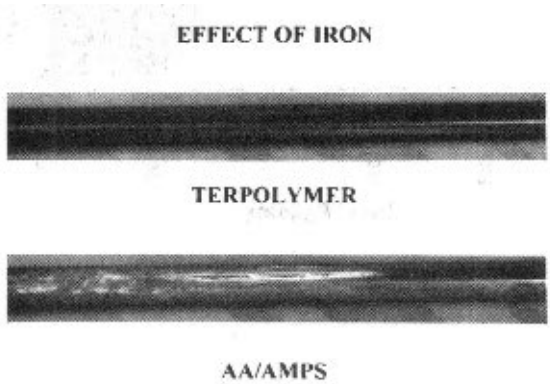


Figure 6. Photograph of the heat exchanger surfaces at the end of the experiments.

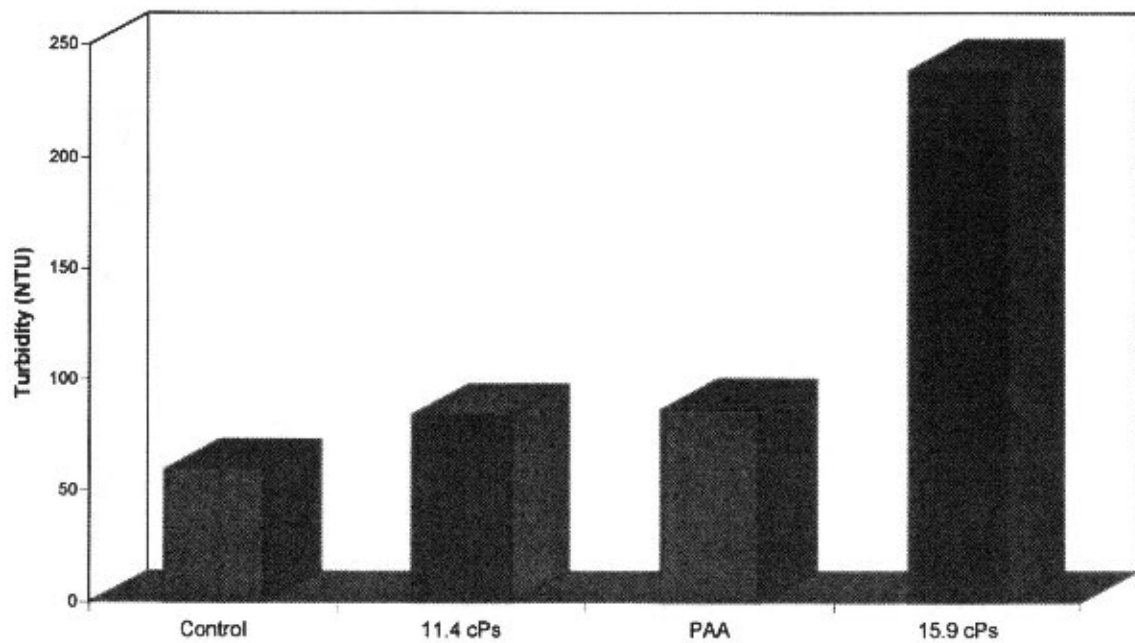


Figure 7. Dispersion capabilities of the optimized AA/AHPSE/PEGAE.

Optimization of the polymer with respect to monomer ratio and molecular weight was also achieved. This is an important step to consider in the development of new polymeric materials to be used as scale inhibitors.

ACKNOWLEDGMENTS

The authors wish to acknowledge the technical assistance of K.A. Whitaker, J. R. Baron, W. G. Fabry, and P. A. Popowich in the publication of this article.

REFERENCES

1. Perez LA and Freese DT, "Scale Prevention at High LSI, High Cycles, and High pH without the Need for Acid Feed", Corrosion 97, Paper No 174, New Orleans, 1997.
2. Perez LA, "Mechanism of Calcium Phosphate Scale Formation and Inhibition in Cooling Systems", In *Calcium Phosphate in Industrial, Environmental, and Biological Systems*, Z. Amjad (ed.), Kluwer Academic Publishers, New York, 1997.
3. Imai T, Uchida T, Ano S, and Tsuneki T, "A Newly Developed Polymer to Inhibit Scale in Cooling Water Systems", Material Performance, 1989;28:4-44.
4. Nancollas GH, "Phosphate Precipitation in Corrosion Protection: Reaction Mechanism", Corrosion, 1983;38:77-82.
5. May RC, Geiger GE, and Bauer DA, "A New Non-chromate Cooling Water Treatment Utilizes High Ortho-phosphate Levels without Calcium Phosphate Fouling", Material Performance, 1981;20: 17-25.
6. Perez LA and Zidovec DF, "Scale Control by Using a New Non-phosphorus, Environmentally Friendly Scale Inhibitor", In *Mineral Scale Formation and Inhibition*, Z. Amjad (ed.), Plenum Press, 1995.

This page intentionally left blank.

INHIBITION OF MINERAL SCALE PRECIPITATION BY POLYMERS

Shiliang He, Amy T. Kan, and Mason B. Tomson

Department of Environmental Science and Engineering
Rice University
6100 Main Street
Houston, Texas 77005-1892

1. ABSTRACT

The inhibitory efficiency of polymeric inhibitors against the precipitation of common mineral scales in industrial processes could be described quantitatively using a semi-empirical model based on nucleation theory and laboratory experimental observations. The minimum effective inhibitor concentration (C_{inh} , mg/l) which is needed to prevent precipitation at a given degree of supersaturation can be estimated by: $C_{inh} = (1/b_{inh}) \log (f_s t_p / t_0)$, where b_{inh} is the efficiency of the inhibitor (l/mg), t_p is the inhibition time or protection time needed for the system (seconds), t_0 is the nucleation induction period for the mineral at a given condition in seconds, and f_s is the safety factor (e.g., 2). Model parameters have been measured for typical scale minerals such as calcite and barite with eight scale inhibitors which have been commonly used in industrial processes, including polyacrylates and their derivatives (PAA, SPA, and PPCA) and poly-phosphonates (HEDP, NTMP, HDTMP, DTPMP, and BHPMP). This semi-empirical model has been demonstrated to be accurate in predicting the minimum effective inhibitor concentrations needed to protect a system from scaling comparing to both laboratory experimental simulation results using a high-temperature/high-pressure flow-through apparatus and preliminary observations in oil and gas production systems.

2. INTRODUCTION

Formation of mineral scale deposits on equipment and pipe surfaces is a common industrial problem where water is either used or produced. Deposits occur in a wide range of processes and conditions such as municipal water supply, evaporative cooling water sys-

tems, boilers, paper making, mineral processing, water and wastewater treatment, energy production, and geothermal drilling.^{1,2} Common problems associated with scale deposits include blockage of fluid flow in pipes, mechanical failure of equipment due to heterogeneous heat transfer, and environmental or healthy effect with co-precipitated naturally-occurring radioactive materials (NORM).³ Among many types of scale deposits, carbonates (calcite in particular) and alkaline earth metal sulfates (e.g., barite, celestite, hemihydrate, anhydrite, and gypsum) are the most common. Scale and corrosion-related problems have been estimated to cost over hundreds of million dollars in the U.S. energy industry alone.²

The most common, economical, and efficient method to control and prevent scale deposits is chemical inhibition using threshold specialty chemicals (inhibitors) at the substoichiometric levels, commonly below 10 mg/l. Typically, scale inhibitors contain at least one of the following functional groups: phosphoric acid [PO(OH)₃], phosphate ester [R-O-PO(OH)₂], phosphonic acid [R-PO(OH)₂], carboxylic acid (R-COOH), and sulfonic acid (R-SO₃H). Polyphosphonates, polyacrylates, polysulfonates, and their derivatives are the most common inhibitors for inorganic mineral scales. The molecular weight of effective polymeric inhibitors is often below 10,000.

Although numerous studies have been conducted to examine the inhibition of precipitation and many hypotheses are proposed to interpret the behavior of inhibitors,⁴⁻⁸ little is known about the mechanistic aspects of inhibition, especially at the molecular level. Therefore, the use of scale inhibitors remains empirical. In addition, most studies have concentrated on the inhibition of crystal growth on well characterized seed materials in relatively low supersaturated solutions. Spontaneous precipitation and nucleation remain unpredictable.

Recently, we have systematically investigated the nucleation rate of carbonate and sulfate minerals in terms of induction periods in the absence and presence of inhibitors over a wide range of supersaturations, temperatures, inhibitors and inhibitor concentrations, and solution composition.⁸⁻¹³ Based on these experimental data, we have developed a novel mathematical model for scale inhibition in moderately to highly supersaturated solutions for calcite and barite.^{12,13} This model is based on the classic nucleation equations and experimental observations in terms of the induction period and metastability of supersaturated solutions in the presence and absence of inhibitor additives. The proposed model can be used to predict the efficiency of various inhibitors under a wide range of conditions (i.e., SI, T, pH, and solution composition). This chapter generalizes this semi-empirical model for scale minerals and reports model parameters for calcite and barite with eight inhibitors including polymers and polyphosphonates.

3. MECHANISTIC ASPECTS OF PRECIPITATION INHIBITION

Both mineral nucleation and inhibition of nucleation are complex interfacial chemical processes involving the formation of clusters and the stability of nuclei on the order of a few angstrom to tens of angstrom which are too large to be treated by individual atomistic concepts but they are also too small to be characterized using macroscopic thermodynamic parameters and analytical instrument.¹⁴ Generally, the action of threshold inhibitors in the precipitation processes at substoichiometric concentrations (i.e., 0.1 to 10 mg/l, or on 10⁻⁷ to 10⁻⁵ M at 1000 molecular weight) is thought to be specific interactions at the interface between the organic inhibitor ionic species and the scale particle surface.¹² In seeded growth processes, the interaction is probably by adsorption of inhibitor species on the active growth sites on the seed materials, such as steps and kinks. Two hypotheses have been used to explain the adsorption of inhibitors. In the Langmuir-Volmer model, a

reversible adsorption of additives on specific surface sites, terraces, steps, or kinks, is assumed and the reduction in the growth rate is proportional to the surface coverage and the additive concentration. In Cabrera and Vermilyea model, an immobile, i.e., irreversible, adsorption of additives on the terrace, is assumed and advancing steps get caught by the additives, while they grow on between them. The reduction in the growth rate constants is thus related to the ratio of the radius of the critical nucleus divided by the radius of the curvature due to irreversible adsorption.

For nucleation processes, the influence of inhibitors on the formation and the stability of nuclei has to be understood, in addition to the effect on the growth of nuclei. With respect to nucleation inhibition, Walton¹⁴ pointed out that probably the inhibitors inhibit nucleation by adsorption on to the active sites on impurity particles or heterogeneous substrates, which serve as the interface and catalyze the nucleation. It is generally observed that in seeded growth experiments, the addition of scale inhibitors in slightly supersaturated solutions will result in occurrence of an induction period which does not exist in the absence of inhibitor^{15,16} In the case of nucleation experiments in moderately to highly supersaturated solutions, a prolongation in the length of induction period has been observed.^{6,9–11,17} For a given inhibitor and supersaturation, the magnitude of the prolongation in induction period increases with inhibitor concentration. The classic nucleation theory states that the induction period of nucleation is proportional to the surface energy [G_{surface}] and inversely proportional to the thermodynamic driving force [degree of supersaturation (SI)] and temperature (T).¹⁴ According to experimental observations and classic nucleation theory, we proposed that the inhibitors in the threshold concentrations increase the surface energy of nuclei formation and thus raise the metastability limit to a higher level.⁸

4. SEMI-EMPIRICAL INHIBITION MODEL

Based on the classical nucleation equation (Gibbs-Kelvin equation), the logarithm of induction period (t_{ind}) is proposed to be inversely proportional to the degree of supersaturation (SI) and temperature (T) as in Eq.1:

$$\log t_{\text{ind}} = \frac{\beta \sigma^3 V_m^2 N_A f(\theta)}{(2.303RT)^3 \text{SI}^2} - C$$

where β is the geometric shape factor ($4S^3/27V^2$ where S and V are the surface area and volume of the nucleus, e.g., $16\pi/3$ for spherical nucleus), σ is the interfacial tension between the nuclei and the aqueous solution (J m^{-2}), V_m is the molar volume of the scale mineral (i.e., $3.7 \times 10^{-5} \text{ m}^3 \text{ mol}^{-1}$ for calcite and $5.21 \times 10^{-5} \text{ m}^3 \text{ mol}^{-1}$ for barite), N_A is the Avogadro's number ($6.023 \times 10^{23} \text{ mol}^{-1}$), $f(\theta)$ is the correction factor for heterogeneous nucleation (θ is the contact/wetting angle between the nuclei and foreign surface), R is the gas constant ($8.314 \text{ J K}^{-1} \text{ mol}^{-1}$), SI is the saturation index defined as the 10-based logarithm of the lattice ion activity products divided by the thermodynamic solubility product (i.e., $\text{SI} = \log \{(\text{Ca}^{2+})(\text{CO}_3^{2-})/K_{\text{sp}}\}$ for calcite), T is the absolute temperature (in K), and C is a constant. The induction period will be very long in low supersaturation levels until a critical supersaturation where nuclei formed become stable in these moderate to high supersaturation levels and will grow into particles of detectable size.

The induction period in the presence of scale inhibitor additives can be described by the same equation (Eq. 1) with different parameters associated with surface energy of nu-

clei which can be modified by inhibitors. These parameters are the nuclei’s physio-chemical properties, such as σ , β , and θ . Therefore, the inhibition in terms of reduction in reaction rates or increase in the induction period can be expressed as:

$$\log\left(\frac{t_{inh}}{t_0}\right) = \frac{N_A V_m^2}{(2.303RT)^3 SI^2} \Delta\{\beta\sigma^3 f(\theta)\} \tag{2}$$

where Δ is the difference between the surface energy in the presence and absence of inhibitors. The presence of scale inhibitors tends to increase the surface energy of nuclei forming and thus prolong the nucleation induction period.⁸ The proportional constant $\{N_A V_m^2/(2.303RT)^3/SI^2\}$ is a function of both supersaturation and temperature as well as the molar volume.

Based on our experimental data,⁸ as shown in Table 1 and Figure 1 for the inhibition of barite by HEDP (refer to Table 2 for the chemical name and molecular weight of inhibitors) and the inhibition of gypsum by HDTMP, the change in the surface energy can be approximated as a linear function of inhibitor concentration C_{inh} as in Eq. 3:

$$\Delta\{\beta\sigma^3 f(\theta)\} = k C_{inh} \tag{3}$$

where k is a constant. Therefore, the nucleation inhibition can be simplified as a linear function of inhibitor concentration as in Eq. 4.

$$\log\left(\frac{t_{inh}^{mineral}}{t_0^{mineral}}\right) = b_{inh}^{mineral} C_{inh} \tag{4}$$

where $b_{inh}^{mineral}$ (1/mg) is the inhibitor efficiency which is specific for the interaction between individual inhibitor and the scaling mineral. Larger values of $b_{inh}^{mineral}$ correspond to more efficient inhibition, Practically, which inhibitor to use under a given condition will be decided based upon the value of $b_{inh}^{mineral}$ under the given condition.

The minimum effective inhibitor concentration needed for a system can be derived from Eq. 4, adding a safety factor (f_s) to account for factors not considered in laboratory experiments such as changes in production practice, equipment changes, turbulence and micro-particles in natural and industrial waters, as in Eq. 5.

Table 1. The effect of inhibitor concentrations on the surface energy of barite and gypsum nuclei at 25 °C. The surface energies in the absence and presence of inhibitors were calculated from experimental data based on He et al. (1994)

HEDP (mg/l)	$\beta\sigma^3 f(\theta)$ - Barite (J m ⁻²) ³	HDTMP (mg/l)	$\beta\sigma^3 f(\theta)$ - Gypsum (J m ⁻²) ³
0.0	0.001426	0.0	4.76E-5
0.5	0.002592	1.0	6.098-5
1.0	0.003064	5.0	8.64E-5
5.0	0.005774	10.0	1.728-4
10.0	0.007895		

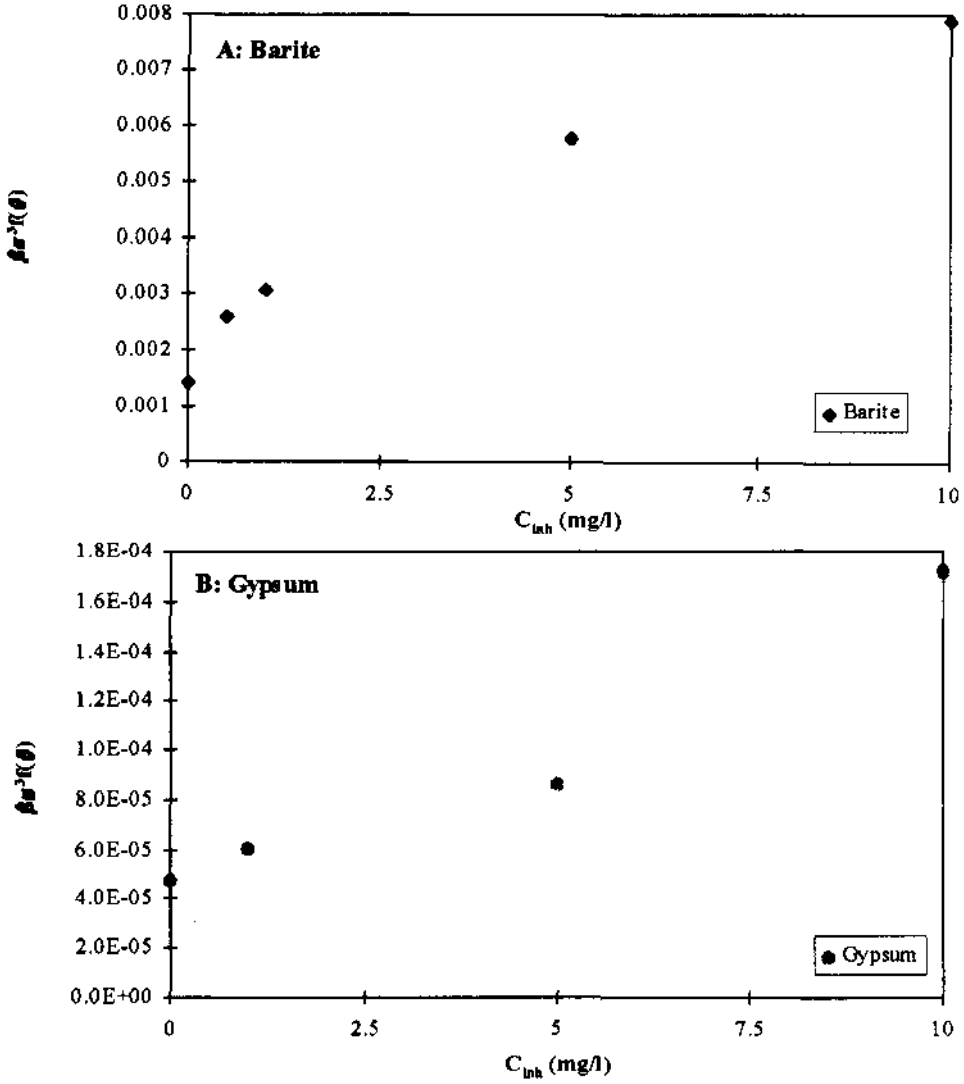


Figure 1. The dependence of the surface energy $\{\beta\sigma^3 f(\theta)$, ($J\ m^{-2}\ s^3$) of nuclei on the inhibitor concentration at 25C. The inhibitors used are HEDP for barite (A) and HDTMP for gypsum (B).

$$C_{inh} = \frac{1}{b_{inh}^{mineral}} \log \left(\frac{f_s t_p}{t_0^{mineral}} \right) \quad (5)$$

where t_p is the time needed to protect the system from scaling. Typically the protection time is the residence or detention time of the fluids in the system. Protection time in oil and gas production systems ranges from a few minutes to several hours depending on the well depth, tubing size, and production rates.¹² In this model, $t_0^{mineral}$ for calcite and barite can be readily calculated from experimental data over a wide range of supersaturations and temperatures⁹⁻¹¹ as in Eq. 6:

Table 2. List of scale inhibitors and their molecular weight considered in this study

Inhibitor	Chemical name	Molecular weight
HEDP	1-hydroxyethylidene-1,1-diphosphonic acid	206
NTMP	nitrolo tri(methylene phosphonic) acid	299
HDTMP	hexamethylene diamine-tetra(methylene phosphonic) acid	492
DTPMP	diethylen triamine-penta(methylene phosphonic) acid	513
BHPMP	bis-hexamethylene triamine-penta(methylene phosphonic) acid	685
PAA	polyacrylic acid	3500
SPA	sulfonated polyacrylic acid	3000
PPCA	phosphinopolycarboxylic acid	1800-3800

$$\log t_0^{\text{mineral}} = \alpha_0 + \frac{\alpha_1}{\text{SI}} + \frac{\alpha_2}{T} + \frac{\alpha_3}{\text{SI} \cdot T} \tag{6}$$

where t_0^{mineral} is in second and a cross-term is added to account the effect of SI at different temperatures. Coefficients $\alpha_0, \alpha_1, \alpha_2$, and α_3 are listed in Table 3 for calcite and barite.

Commonly scales form in a wide range of scaling conditions, such as different SI, T, and solution composition, even in a single process such as oil production. It was suggested that both SI and T influence inhibitor efficiency as shown in Eq. 2. In addition, it has been commonly observed that the solution pH is an important factor in affecting inhibitor performance, possibly because the active concentration of the inhibitor species depends on the solution pH and due to multiple proton dissociation. Also, we have observed that the solution stoichiometry, in terms of the ratio of lattice cations to lattice anions (M/M) has a profound influence on the inhibitor’s efficiency.⁸ This is probably related to the surface charge property of nuclei in non-stoichiometric solutions. Generally as the ratio of lattice cation/lattice anion, R, increases, the inhibitor’s efficiency increases. This is probably because in a lattice-cation dominated solution, the nuclei formed tend to be positively charged because there are more lattice cations in the neighborhood of the nuclei comparing to lattice anions. Positively charged nuclei will be attractive to negatively charged anion inhibitors. This effect has been observed for all scale minerals and inhibitors we have studied, including minerals such as calcite, gypsum, celestite, and barite in case of both phosphonate and other polymer inhibitors.^{8,10–12}

Based on the reasoning above, the inhibitors’ efficiency is expressed as a conditional constant depending on SI, T, pH, and R as in Eq. 7:

$$\log b_{\text{inh}}^{\text{mineral}} = \beta_0 + \beta_1 \cdot \text{SI} + \frac{\beta_2}{T} + \beta_3 \cdot \text{pH} + \beta_4 \cdot \log R \tag{7}$$

where coefficients β_0 to β_4 are curved-fitted using a nonlinear regression analysis software (Systat). These coefficients are listed in Table 4A for calcite and 4B for barite. The β_3 co-

Table 3. List of coefficients to calculate induction periods for scale minerals in the absence of inhibitors (Eq. 6)

Mineral	α_0	α_1	α_2	α_3
Calcite	4.22	−13.8	−1876.4	6259.6
Barite	1.83	−12.1	−885.8	5460.3

Table 4. List of coefficients to calculate inhibitor efficiencies (Eq. 7) for calcite (A) and barite (B)

Inhibitors	β_0	β_1	β_2	β_3^*	β_4
A: Calcite					
HEDP	-1.19	-1.69	1082.0	(0.2)	0.14
NTMP	-1.95	-1.61	1226.0	(0.2)	0.13
HDTMP	-4.57	-1.22	1813.1	(0.2)	0.27
DTPMP	-2.95	-1.63	1396.4	(0.2)	0.29
BHPMP	-4.63	-1.45	1918.7	(0.2)	0.27
PAA	-2.54	-1.55	1734.6	(0.0)	0.27
SPA	-2.96	-1.59	1768.8	(0.0)	0.20
PPCA	-3.04	-1.41	1745.3	(0.0)	0.33
B: Barite					
HEDP	-1.40	-1.05	639.5	0.29	0.18
NTMP	-3.23	-1.13	1254.8	0.34	0.23
HDTMP	-0.01	-1.40	968.6	0.10	0.14
DTPMP	-0.11	-1.76	1076.7	0.15	0.09
BHPMP	-1.00	-1.28	1143.3	0.13	0.11
PAA	0.65	-1.53	1051.1	0.00	0.10
SPA	0.78	-1.76	1068.7	0.00	0.07
PPCA	0.37	-1.58	1131.9	0.00	0.08

*The pH dependence for calcite inhibition is assumed to be similar to barite inhibition. See text for details.
**The pH dependence for polymers have been experimentally found to be negligible.

efficients for the pH dependence of barite inhibition using polymeric inhibitors (PAA, SPA, and PPCA) have been experimentally determined and found to be negligible in the pH range from 4 to 8. The β_3 coefficients for calcite in Table 4A have not yet been completed, but they are expected to be similar to these coefficients for barite listed in Table 4B. Therefore, an average value of 0.2 can be used for phosphonates and 0.0 for polymers.

5. DISCUSSION AND INDUSTRIAL APPLICATIONS

Mechanistically, the influence of scale inhibitors on the nucleation induction period is interpreted as a result of elevation in the surface energy of the nuclei forming and extended metastability limit, either through 1) increase in the interfacial tension between the nuclei and solution (σ), 2) increase in the geometric shape factor (β) by modifying the nuclei's morphology into less regular shapes, or 3) by increase the wetting angle (θ) between the nuclei and heterogeneous substrate through adsorption. This semi-empirical nucleation inhibition model presented above is based on experimental observations and classic nucleation theory. It has been applied to systematically correlate experimental data of inhibition efficiency of threshold inhibitors for a variety of scale minerals. Within the model, the nucleation is separated from nucleation inhibition which allows inhibitors to be evaluated separately.

In coupling with a speciation model to calculate the supersaturation of aqueous solutions, such as ScaleSoft™¹⁸ developed at our laboratory, this model can be applied to a variety of industrial processes for selecting inhibitors among many options and predicting the minimum effective dosage for a given system. It has been demonstrated¹² that the pre-

Table 5. Comparison of predicted inhibitor needs with field observations in oil and gas production systems

Well name	Scale type	Inhibitor	Observed (mg/l)	Predicted (mg/l)
Gladys McCall	Calcite	NTMP	0.1	0.1 to 1.6
Pleasant Bayou	Calcite	NTMP	0.1	0.2 to 0.9
O'Daniel	Calcite	NTMP	< 0.8	0.21
Huff A	Calcite	NTMP	< 0.6	0.14
S. Brae A 16	Barite	PVS/SPA*	150	132

*PVS is the inhibitor used in this well and SPA is the inhibitor having similar properties whose inhibition parameters have been determined in this study.

dicted minimum effective inhibitor concentrations of BHPMP to protect a test loop from barite scaling over a wide range of supersaturations (SI from 1.7 to 2.7 at 70 °C) were within the experimental errors comparing to the experimental data obtained in a dynamic flow-through inhibitor apparatus¹⁹ using synthetic oilfield brines. In addition, this model has been tested against a variety of oil and gas production systems in field conditions recently. Examples are given in Table 5 where the predicted dosage is compared to the actual field observations. Calcite scales in these cases are mainly the result of CO₂ degassing and resultant pH raise during pressure drops as the fluid flows from the reservoir formation to the surface, as in four wells in Table 5. In the case of barite, mixing of incompatible waters is the major cause for high supersaturation and thus high dosage of inhibitor needs, as in South Brae Field A-16 well in North Sea where the breakthrough of seawater caused the mixing and scale problem.²⁰

Considering the complexities and uncertainties in estimating the degree of supersaturation in oil and gas production systems involving multi-phase equilibria among gas, liquid, and solid and measurement of residual inhibitor concentrations in oilfield brines, the agreement is very good. In addition, this model can be extended to other industrial processes such as cooling water systems and boilers with little or no modifications.

6. CONCLUSIONS

A semi-empirical mathematical model is presented for the inhibition of scale mineral formation by chemical inhibitors including phosphonates and polymers. Model parameters are measured for eight inhibitors (three polymers and five phosphonates) for calcite and barite scales. This model can be applied to predict the efficiency of scale inhibitors and the minimum effective concentrations for scale control in a wide range of conditions, such as supersaturation, temperature, and solution composition. Model predictions are in good agreement with both experimental data and field observations in oil and gas production systems.

ACKNOWLEDGMENTS

This work was supported financially by the Brine Chemistry Consortium at Rice University including Amoco, Aramco, Baker Petrolite, Champion Technologies, Chevron, Conoco, Shell, Texaco, and Unichem/BJ Services, but in no way does this constitute an endorsement by these companies of any products or views contained herein.

REFERENCES

1. Cowan JC and Weintritt DJ, *Water-formed Scale Deposits*, Gulf Publishing Co., Houston, TX, 1976.
2. Tomson MB and Oddo JE, *Handbook for Calcite Scale Control*, 1997.
3. Tomson MB, et al. (ed.), 1996, 1995 API/GRI Naturally-occurring Radioactive Material Conference, Houston, TX.
4. Naono H and Miura M, "The effect of sodium triphosphate on the nucleation of strontium sulfate", *Bulletin Chem. Soc. Jpn.*, 1965;38(1):80.
5. Sarig S and Raphael M, "The Inhibiting Effect of Polyphosphates on the Crystallization of Strontium Sulfate", *J. Crystal Growth*, 1972; 16:23.
6. Liu ST and Nancollas GH, J. "Crystal-Growth and Dissolution of Barium Sulfate in Presence of Additives", *Colloid Interface Sci.*, 1975;52:582.
7. Tomson MB, "Effect of Precipitation Inhibitors on Calcium-Carbonate Scale Formation", *J. Crystal Growth*, 1983;62:106.
8. He SL, Oddo JE and Tomson MB, "The Inhibition of Gypsum and Barite Nucleation in NaCl Brines at Temperatures from 25-degrees-C to 90-degrees-C", *App. Geochem.*, 1994;9, 561.
9. He SL, Oddo JE and Tomson MB, "The Nucleation Kinetics of Calcium-Sulfate Dihydrate in NaCl Solutions up to 6-M and 90-degrees-C", *J. Colloid Interface Sci.*, 1994;162:297.
10. He SL, Oddo JE and Tomson MB, "The Nucleation Kinethics of Barium-Sulfate in NaCl Solutions up to 6-M and 90-degrees-C", *J. Colloid Interface Sci.*, 1995;174:3 19.
11. He SL, Oddo JE and Tomson MB, "The Nucleation Kinethics of Barium-Sulfate in NaCl Solutions up to 6-M and 90-degrees-C", *J. Colloid Interface Sci.*, 1995;174:327.
12. He SL, Kan AT and Tomson MB, "Mathematical Inhibitor Model for Barium-Sulfate Scale Control", *Langmuir*, 1996;12:1901.
13. He SL, Kan AT and Tomson MB, "Inhibition of calcium carbonate precipitation in NaCl brines from 25 to 90 °C", 1997 *Applied Geochemistry*, (In press), 1998.
14. Walton AG, *The Formation and Properties of Precipitates*, Interscience Publishers, New York, 1967.
15. Nancollas GH, "The growth of crystals in solution", *Adv. Colloid Interface Sci.*, 1979;10:215.
16. Amjad Z and Hooley JP, "Influence of Poly-Electrolytes on the Crystal-Growth of Calcium-Sulfate Dihydrate", *J. Colloid Interface Sci.*, 1986;111:496.
17. Klepetsanis PG and Koutsoukos PG, "Precipitation of Calcium-Sulfate Dihydrate at Constant Calcium Activity", *J. Crystal Growth*, 1989;98:480.
18. He SL, Kan AT, Tomson MB, Hunter MA, Fu GM, and Oddo JE, "Effectiveness of Chemically Enhanced Solubilization of Hydrocarbons", *SPE Paper # 38801*, 1997;12, N3:153-157.
19. Oddo JE, Sloan KM, and Tomson MB, "Inhibition of CaCO₃ Precipitation from Brine Solutions—A New Flow System for High-Temperature and High-pressure Studies", *J. Petroleum Technology*, 1983;34:2409.
20. Hardy JA, Barthorpe RT, Plummer MA, and Rhudy JS, "Scale Control in the South Brae Field", *SPE Production & Facilities*, 1994;May: 127.

This page intentionally left blank.

PILOT TEST RESULTS UTILIZING POLYMERIC DISPERSANTS FOR CONTROL OF SILICA

Charles W. Smith

Mitco Water Laboratories, Inc.
Post Office Box 1699
Winter Haven, Florida 33882-1699

1. ABSTRACT

Waters containing high levels of silica can result in severe fouling of a water treatment system. In certain cases, high silica levels may become the limiting factor as to the level of RO recovery achievable. The recent usage of polymeric antiscalants has resulted in the attainment of silica levels far in excess of the generally recognized maximum of 150 parts per million (ppm) as SiO_2 . The results of comparative tests incorporating the usage of two polymeric antiscalants for control of silica deposition in reverse osmosis (RO) systems are presented.

2. CHEMISTRY OF SILICA

Silica is one of the most abundant elements found in nature. As such, it is not surprising that it exists in numerous forms. The three most common forms found in RO feedwaters are monomeric, polymeric, and silicate salts. Monomeric silica or silicic acid, $(\text{Si}(\text{OH})_4)$, is often described as “dissolved” or “reactive” silica. This is the form of silica which will react with molybdate to give the characteristic heteropoly blue color used in analytical tests. Polymeric silica results from polymerization of silicic acid. The two most common forms of polymeric silica encountered in water treatment systems are gellular and colloidal. Silicate salts result from precipitation of either monomeric or polymeric silica with various cations, one of the most common being magnesium.¹⁻³

The solubility of silica in water systems is dependent on several factors including pH, temperature, other ions present, and the form in which the silica is present. The solubility of silica increases with pH varying from 120 ppm at a pH of 6 to 140 ppm at a pH of 9. The temperature effect on silica solubility depends on the form in which it is present.

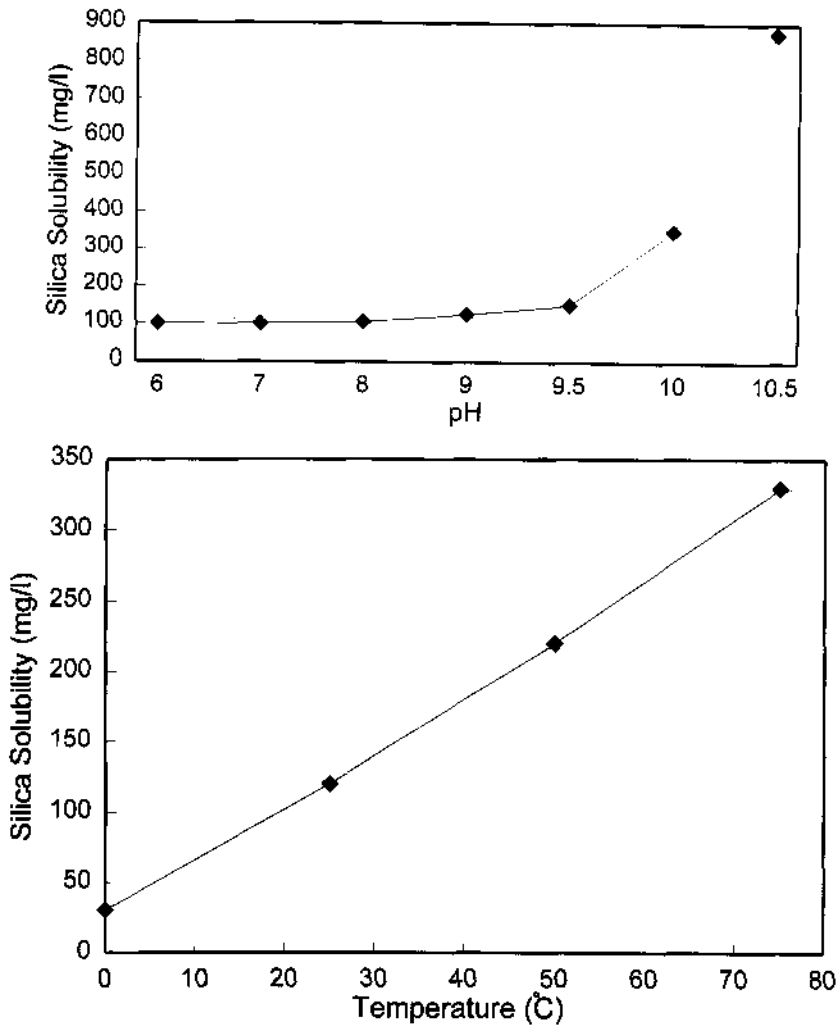
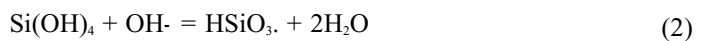


Figure 1. a) Silica solubility as a function of pH. b) Silica solubility as a function of temperature.

Unlike certain silicate salts such as magnesium silicate that becomes less soluble as the temperature increases, silica itself increases in solubility as the temperature increases. The solubility of silica, as a function of solution pH and temperature, is shown in Figures 1a and 1b, respectively.

The form in which silica exists, monomeric or polymeric, is dependent on the pH of the system. Four reactions which silica can undergo in water treatment systems are given in equations one through four.





As outlined in equations one through four, at the pH range of 6 to 9 silica is capable of undergoing a polymerization reaction. The first step involves the formation of silicic acid. In equations 2 and 3, silicic acid is converted to a dimeric silicate anion ($\text{Si}_2\text{O}_5^{2-}$) via the intermediate formation of monomeric silicate anion (HSiO_3^-). Once the dimeric silicate anion is formed it can quickly undergo further polymerization reactions leading to the formation of silica based deposits. Alternatively, the intermediate monomeric anion can react with hydroxide (OH^-) leading to the formation of a silicate dianion (SiO_3^{2-}) as shown in equation 4 which can readily react with various cations to form silicate salt deposits.⁴⁻⁶

3. PROBLEMS WITH SILICA

Water treatment systems are prone to many types of deposits. Unfortunately, deposits tend to form in the most important areas of the equipment. This leads to inhibition of heat transfer, restriction of water flow, fouling of membrane surfaces, and eventual shut-down of the equipment for cleaning. Severe deposition can also lead to overheating and failure of high temperature equipment.

Some of the most difficult deposits encountered in water treatment systems are those comprised of silica. As stated previously, silica can be present in several different forms, each capable of forming its own unique type of deposit. The deposit that ultimately forms is dependent on several factors including pH, temperature, the type of silica present, and other ions present in the system. Several mechanisms for silica scale formation have been reported in the literature such as reactions of monomeric silicate anion or polymeric silica with various ions. Another mechanism involves polymerization of silicic acid leading to the formation of amorphous silica deposits.⁷

Magnesium silicate (MgSiO_3) is one of the more troublesome silica scales. It is a dense scale that is very difficult to remove. The precipitation of magnesium silicate strongly depends on solution pH and temperature. In RO systems operating above a pH of 9, magnesium silicate is very likely to form due to the presence of magnesium hydroxide and silicate ions. Although commonly referred to as MgSiO_3 , magnesium silicate is thought to be present in water treatment systems as a result of a multistep process resulting in a mixture of a variety of chemical species containing magnesium and silica. The first step is the formation of magnesium hydroxide (Mg(OH)_2). The hydroxide salt reacts with monomeric silicate anion and/or polymeric silica to form magnesium silicate. Other hydroxide salts such as calcium, strontium, potassium, and sodium are also capable of undergoing this reaction with silica but the resulting product is much more soluble and hence less likely to foul the membrane.

Another type of silica deposit commonly encountered in water treatment systems is comprised solely of polymeric or amorphous silica. Unlike magnesium silicate, polymeric silica's solubility in water increases with increasing temperature. Hence, it tends to precipitate out in the coolest regions of an RO system. The two major classifications of amorphous silica deposits are colloidal and gellular. The membrane surfaces and feed channel spacers of reverse osmosis (RO) systems are particularly susceptible to fouling by polymeric silica. In RO systems, silica levels in excess of 150 ppm as SiO_2 are readily attainable with high silica feedwater given the fact that the rejection rate is typically greater than 90 %. Furthermore, once formed, these deposits are easily coagulated by small amounts of cations such as calcium, iron, aluminum, and magnesium.

4. SILICA ANTISCALANTS

Silica deposits, once formed, are very difficult to remove. Numerous methods have been developed to keep silica deposition from occurring.^{8,9} One of the simplest methods involves keeping the constituents such as silica and magnesium below the critical concentration levels necessary for precipitation. In the pH range of 6 to 9 most often encountered in water treatment systems, this means that silica levels must be kept below 150 ppm. Moreover, if magnesium is present, the product of magnesium as (CaCO_3) and silica as (SiO_2) should not be allowed to exceed 20,000 ppm.

Various chemical treatment programs have been developed which allow significantly higher levels of silica and/or magnesium than those listed above to be maintained in a water treatment system.^{6,10-15} Most of these programs rely on dispersants that keep the silica particles at a size small enough to preclude deposition. Polymers have been used successfully for many years by the water treatment industry for numerous functions including dispersancy. Polymers used as dispersants are usually anionic and have molecular weights ranging from one to twenty thousand. Anionic polymeric dispersants function by forming a negatively charged complex with the particle being dispersed. Particles successfully kept dispersed in the past using anionic polymers include carbonate, sulfate, and phosphate salts.

Numerous research efforts have focused on expanding the usage of polymers to either disperse silica particles and/or minimize silica polymerization.¹⁶⁻²¹ Since most silica deposits consist of amorphous silica and/or magnesium silicate, the ideal dispersant must have two distinct properties. It must be able to disperse both polymeric silica particles and magnesium silicate particles prior to their growth to sizes capable of deposition. In addition, it must also be capable of dispersing particles such as calcium carbonate that can act as nuclei on which the silicate deposits can form. Another highly desirable feature of a polymeric silica antiscalant would be to minimize or control the effect of silica polymerization.

Various polymers have been tested for these properties by numerous research groups, including our own. The test results from pilot field testing of two particular polymers that have shown to be very promising will be discussed.

5. EXPERIMENTAL

The pilot RO system in operation for this study contained a spiral wound, polyamide, 2.5" \times 40" membrane, model FT30 manufactured by Filmtec®. The pH of the concentrate stream was controlled via the addition of acid. The feedwater was cycled up achieving an average silica concentration in excess of 500 ppm as SiO_2 for the duration of the test. This was achieved by holding the permeate and concentrate flow rate constant respectively while monitoring the pressure of the system. All experimental results reported are on a 100% active inhibitor basis for comparative purposes.

If the membrane feed pressure increased by 10% or more at constant flow, it was determined that the membrane had become fouled with silica. If no pressure drop was observed, then it was apparent that an ample concentration of polymer had been dosed into the feedwater to prevent deposition. A software program was used to create normalized permeate flow versus time graphs for each test. In the tests which fouled with silica, the normalized permeate flow dropped off by at least 10% over the typical test, whereas no significant drop-off was observed in the successful test runs.

In those cases in which the membrane fouled due to silica scaling, a 2% ammonium bifluoride / hydrochloric acid solution was used to clean the membrane. These cleanings were done off-line by isolating the membrane for approximately 30 minutes, followed by a water rinse for at least 10 to 15 minutes. WARNING: Great care must be taken in this process, since the resulting hydrofluoric acid solution can be extremely corrosive to any skin with which it comes into contact.

6. RESULTS

Two commercial polymers, A and B,²² were selected for pilot RO testing based upon a combination of bench top screening test results, discussion with polymer manufacturers, and prior investigations. Both polymers were cited by their respective manufacturers as being silica antiscalants. Multiple tests were run using polymer A and B at varying ratios of silica to active polymer ranging from 0 to 120. In each of the tests in which no polymer was dosed, the RO membrane became fouled within several hours, apparent by the greater than 10% increase in feed pressure necessary to maintain a constant flow rate. In those tests, the silica was concentrated to an average of 530 ppm (SiO_2) at a concentrate pH of approximately 7.25. These “control” tests proved to us that silica would indeed foul a membrane under our experimental conditions.

Comparative tests were obtained using the two polymeric antiscalants in which the ratio of silica to active polymer was gradually increased. Initial tests were conducted at a ratio of 7.5 ppm of silica (SiO_2) per ppm of active polymer. The maximum ratio of silica to polymer concentration was found to be 75 for polymer A; at this ratio the RO membrane did not scale. The RO concentrate stream had an average Langlier Saturation Index (LSI) of 1.26 and a pH of 7.30. The average silica concentration was 524 ppm as SiO_2 . All test runs made at higher ratios resulted in fouling of the membrane.

Using polymer B, the polymer to silica ratio was increased to 120 without experiencing any signs of fouling throughout the test. The RO concentrate stream had an average LSI of 1.73 and a pH of 7.10 at an average silica concentration of 556 ppm as SiO_2 . Some of the results of these test runs are summarized in Table 1.

Based on the above results, it was decided to repeat two prior tests using new, “virgin”, membranes which could be evaluated for autopsy and foulant analysis. As before, silica waters were concentrated by RO to significant silica supersaturation (more than 500

Table 1. Summary of pilot RO test results

Polymer	Feed polymer	Feed SiO_2	SiO_2 /polymer	Concentrate SiO_2	Membrane fouled
None	0	110	—	525	Yes
A	16.8	128	7.6	476	No
A	2.83	102	36	531	No
A	1.94	107	55	566	No
A	1.48	111	75	591	No
A	1.31	121	92	540	Yes
B	16.1	138	8.6	546	No
B	2.78	106	38	554	No
B	1.60	112	70	582	No
B	1.11	105	95	549	No
B	0.92	110	120	565	No

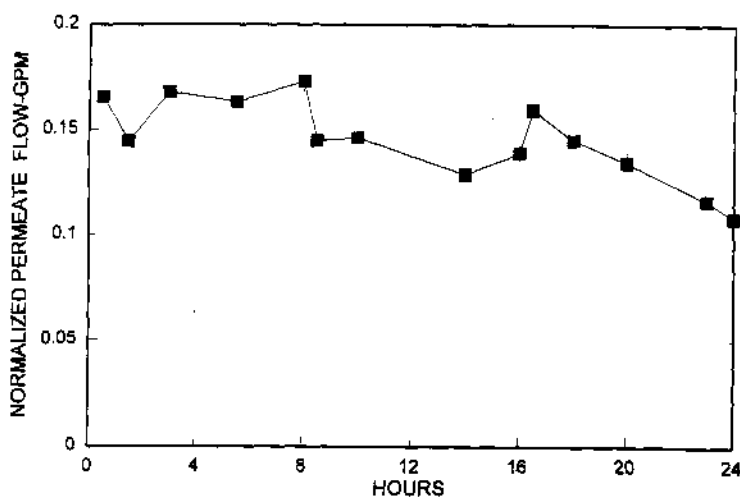
Table 2. RO concentrate water analysis

Hydrogen ion (pH)	6.81
Conductivity (MM)	7600
Total hardness (CaCO ₃)	3800
Total alkalinity (CaCO ₃)	152
Chloride (NaCl)	1120
Silica (SiO ₂)	544
Total org. carbon (TOC)	49.6
Pressure (PSI)	158
Temperature (°F)	91

ppm SO₂). Natural waters were again used in the tests so that the results would most resemble, and could be directly applied to, actual use conditions. A brief elemental description of a typical concentrate stream sample from the RO is shown in Table 2. The pilot unit was fitted with Dow Filmtec FT30 membranes and was designed to operate in a manner comparable to full size units. The pilot unit was started without any inhibitor until such time as the unit began to foul. The normalized permeate flow data (given in Figure 2) shows that the membrane began to foul in a matter of hours under these accelerated conditions. The system was shut down after undergoing a 26% loss in normalized permeate flow and the membrane was removed for autopsy and detailed foulant analysis.

New membranes were installed and the unit was restarted with polymer B. Polymer B dosage was regulated to maintain 1 ppm active inhibitor for each 120 ppm silica (SiO₂) in the concentrate stream. This test was stopped after the same number of hours of run time so that the membranes could be directly compared to the control. The normalized permeate flow data for the system showed no significant signs of performance deterioration (Figure 3).

Both membranes were returned to the laboratory for autopsy and foulant analysis. The control membrane (no inhibitor) was completely coated with a light powdery substance that could be removed by touch. Representative swatches of the membrane were

**Figure 2.** Normalized permeate flow in the absence of polymer B.

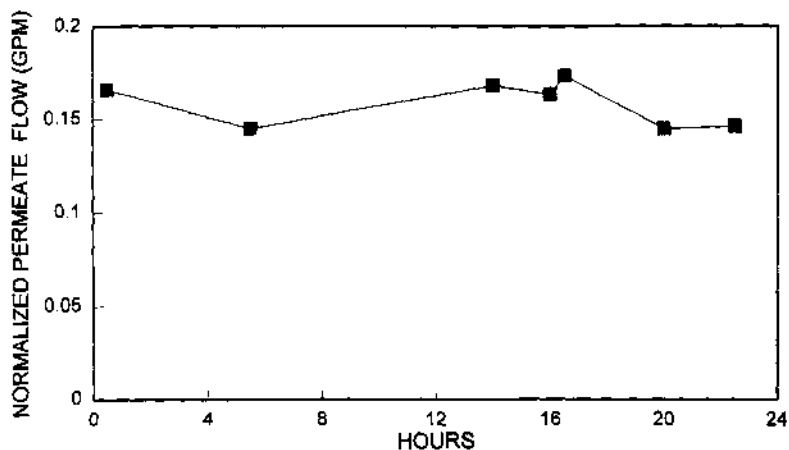


Figure 3. Permeate flow in the presence of polymer B.

cut for elemental analysis. Figure 4 is an electron micrograph of the material on the concentrate end of the membrane. This material is predominantly silicon though there is a mixture of polyvalent ions present in the mixture as determined by Energy Dispersive X-Ray (EDX) spectroscopy which is shown in Figure 5. Elemental analysis of the foulants showed that the silicon peak in the control membrane (Figure 5) dominates the field.

The membrane from the test run with silica inhibitor polymer B was also autopsied. The leaves of the membrane showed no visible signs of fouling (i.e., appearance was as a virgin membrane). Scraping the membrane did not remove any material and rubbing the surface did not remove any powdery material. Samples of the membrane were taken and

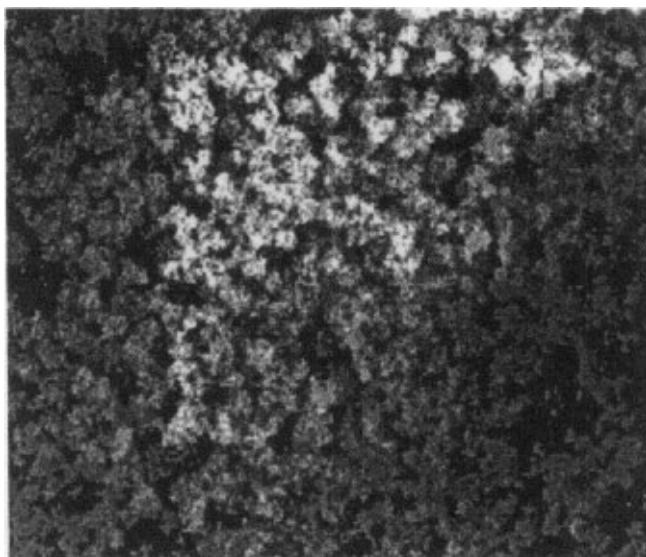


Figure 4. Electron micrograph of RO membrane in the absence of polymer B.

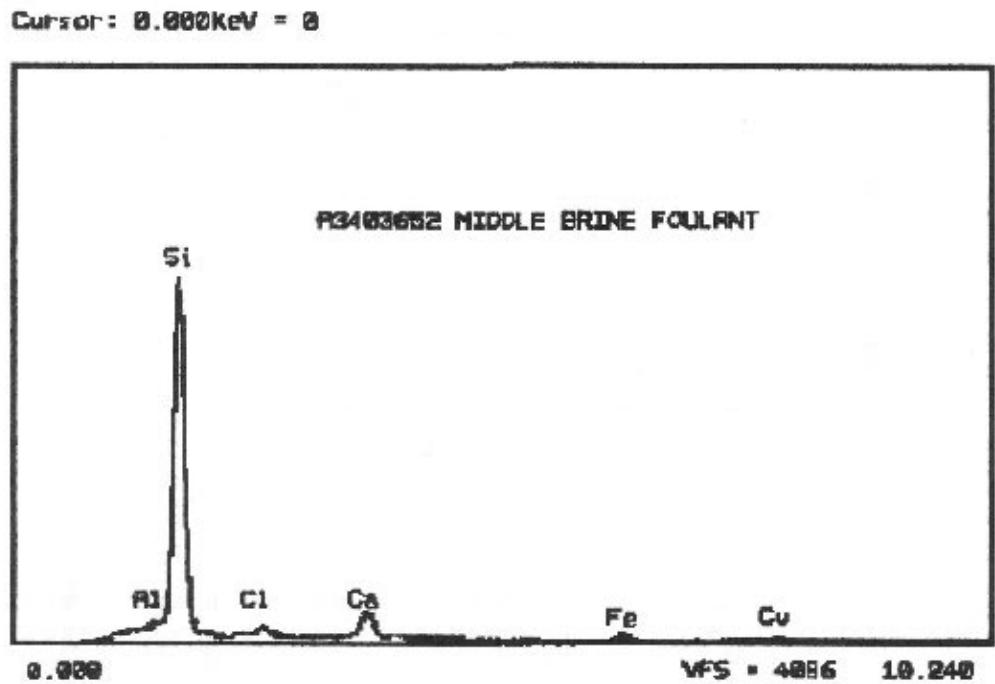


Figure 5. Energy dispersive X-ray spectrograph of fouled membrane.

submitted for analysis. Figure 6 is a photomicrograph of the membrane surface at the concentrate end. The EDX spectrograph of the area (Figure 7) shows low levels of silicon based foulant. However, the silicon found on the polymer B test run membrane (Figure 7) is insignificant compared to the sulfur peak from the polysulfone support material of the

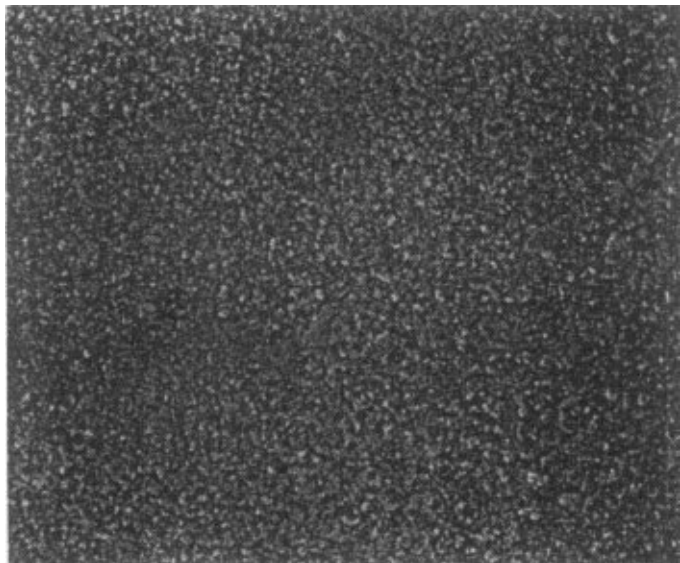


Figure6. Electron micrograph of RO membrane in the presence of polymer B.

Cursor: 0.000keV = 0

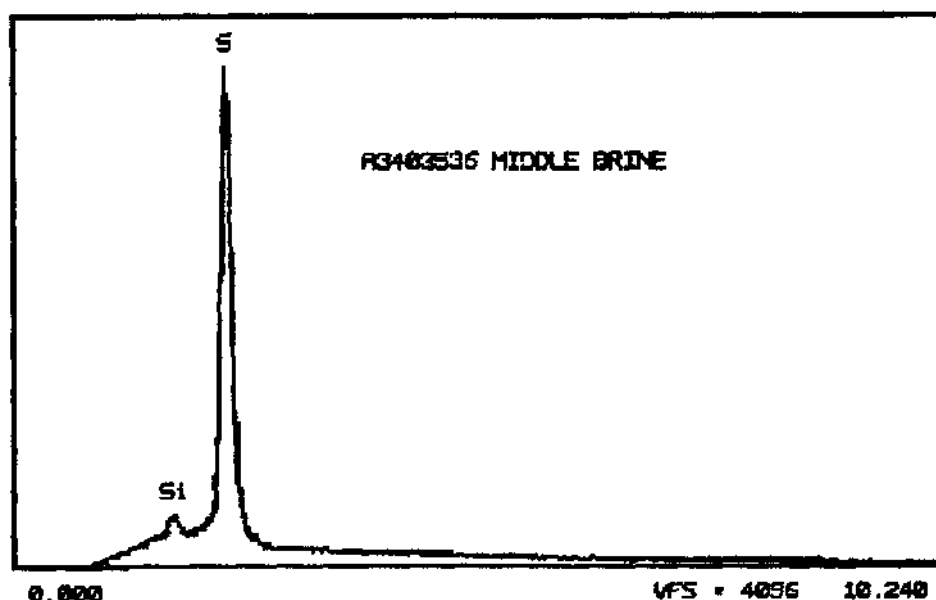


Figure 7. Energy dispersive X-ray spectrograph of RO membrane treated with polymer B.

membrane. In contrast, the sulfur peak for the control membrane (see Figure 5) could not be seen due to the large quantity of silicon present. Thus, it can be concluded that polymer B had a significant impact on minimizing silica fouling.

7. CONCLUSION

As water demands continue to increase, waters that were previously considered marginal at best will be brought into service. This will require that the current limits imposed by water treatment programs be expanded. One such limit is that silica levels be kept below 150 ppm as SiO_2 in order to avoid the formation of silicate deposits which are very difficult to remove safely and economically. The usage of polymeric antiscalants such as the ones described in this paper offer one potential water treatment method. As more of these polymeric silica antiscalants become available to the end-user, there will be increasing needs to do comparative studies such as are described in this article to determine under what conditions they will, and will not, adequately perform. Usage of these polymers will enable higher cycles of concentration and RO recovery rates resulting in increased water savings. More research is needed to expand on this method as well as to develop other methods for achieving this highly desirable goal.

REFERENCES

1. Byrne W, *Reverse Osmosis: A Practical Guide for Industrial Users*, Tall Oaks Publishing, Inc., Littleton, Colorado, 1995.

2. Dubin L, "Silica Inhibition in Cooling Water", In *Surface Reactive Peptides and Polymers*, American Chemical Society Symposium Series, Volume 444, 1991,
3. Dubin L, Dammeier RL, and Hart RA, "Deposit Control in High Silica Water", *Corrosion/85*, Paper No. 131, 1985.
4. Iler RK, *The Chemistry of silica*, John Wiley & Sons, New York, 1979.
5. Iler RK, *The Colloid Chemistry of Silica and silicates*, Cornell University Press, Ithaca, 1955.
6. Liebau F, *Structural Chemistry of Silicates*, Springer - Verlag, New York, 1985.
7. Hann WM and Robertson ST, "Control of Iron and Silica With Polymeric Dispersants", *Industrial Water Treatment* 1991;23(6):12-24.
8. McBride D and Mukhopadhyay D, "Higher Water Recovery and Solute Rejection Through a New RO Process", *Ultrapure Water*, 1997;3:24-29.
9. McBride D and Mukhopadhyay D, "450 ppm Silica Sustained in Innovative Reverse Osmosis Technology", *International Water Conference*, Paper No. 96-16, 1996.
10. Amjad Z, and Yorke M, "Carboxylic Functional Polyampholytes as Silica Polymer Retardants and Dispersants", U.S. Patent No. 4,510,059. 1985.
11. Amjad Z, Zibrida JF, and Zuhl RW, "A New Antifoulant for Controlling Silica Fouling in Reverse Osmosis Systems". *International Desalination Association. World Congress on Desalination and Water Reuse*, 1997.
12. Brooke M, "Magnesium Silicate Scale in Circulating Cooling Systems", *Corrosion/84*, Paper No. 327, 1984.
13. Freese DT, "Inhibition of Silica and Silicate Deposition in Cooling Water Systems", U.S. Patent No. 5,271,862. 1993.
14. Gill JS, Rey SP, and Wiernik JH, "Method for Controlling Silica/Silicate Deposition in Aqueous Systems Using Phosphonobutane Tricarboxylic Acid and Anionic Polymers", U.S. Patent No. 5,078,879. 1992.
15. Kronmiller DL, "Controlling Silicates in RO Water Systems", *Ultrapure Water*, 1992;2:42-43.
16. Meier DA and Fulks KE, "Water Treatment Options and Considerations for Water Re-Use", *Corrosion/90*, Paper No. 351. 1990.
17. Meier DA and Dubin L, "A Novel Approach to Silica Inhibition", *Corrosion/87*, Paper No. 334. 1987.
18. Miller JR, Ondyak JM, and Dubos TJ, "Silica Stabilization Helps Reduce Cooling Tower Blowdown", *Power* 1989;133(10):47-8.
19. Momozaki K, Kira M, Murano Y, Okamoto M, and Kawamura F, "Polyacrylamide Based Treatment Program for Open Recirculating Cooling Water System with High Silica Content", *International Water Conference*, Paper No. 92-11. 1992.
20. Smith CW, "Usage of a Polymeric Dispersant for Control of Silica", *Industrial Water Treatment*, 1993;4:20-26.
21. Weng PF, "Silica Scale Inhibition and Colloidal Silica Dispersion for Reverse Osmosis Systems", *Membrane and Desalting Technologies Biennial Conference and Exposition*, 1994.
22. Nicholas P, and Amjad Z, "Method for Inhibiting the Deposition of Silica and Silicate Compounds in Water Systems", US Patent 5,658,465. 1997.

INHIBITION OF GYPSUM SCALE FORMATION ON HEAT EXCHANGER SURFACES BY POLYMERIC ADDITIVES

Zahid Amjad

The B.F. Goodrich Company
Advanced Technology Group
9921 Brecksville Road
Brecksville, Ohio 44141

1. ABSTRACT

The formation and adherence of calcium sulfate dihydrate, hemihydrate, and anhydrite scales is a problem in many heat exchanger applications where the equipment is fed with waters containing high levels of calcium and sulfate. Industrial processes are affected by the deposition of sulfate scales including cooling, boiler, desalination (i.e., flash distillation), and oil recovery. Historically, polymeric and non-polymeric additives have been used in these processes to prevent the formation and deposition of scaling salts. In the present study, the influence of polymeric additives on gypsum ($\text{CaSO}_4 \cdot 2\text{H}_2\text{O}$) scale on heat exchanger surfaces has been investigated. It has been observed that polymer composition, molecular weight, ionic charge and charge density, and polymer dosage have a significant impact on the performance of the polymeric additive.

2. INTRODUCTION

The crystallization and adherence of scale-forming minerals (i.e., calcium sulfate, calcium carbonate, calcium phosphate, calcium phosphonate, etc.) on heat exchanger surface continues to present performance limitations for industrial water systems (i.e., cooling tower, boiler, flash distillation, etc.). In cooling water systems, gypsum (calcium sulfate dihydrate) is the most commonly encountered calcium sulfate scale whereas calcium sulfate hemihydrate and calcium sulfate anhydrite are the most frequently formed salts in high temperature processes (i.e., high temperature boilers, multistage flash distillation). The deposits that form can markedly reduce heat transfer causing energy losses or material damage, especially when coupled with corrosion. Various factors such as bubble

formation, suspended matter, and water chemistry have been shown to play role on the crystallization and deposition of calcium sulfates on the metal surfaces.

The effectiveness of a number of inhibitors in preventing or reducing the crystallization of gypsum has been investigated. Smith and Huilin¹ have examined the effect of number of polyelectrolytes on the growth rate of gypsum. Polymers containing carboxyl groups, such as poly(acrylic acid), PAC, and formulated products containing PAC were shown to be particularly effective as gypsum growth inhibitors. Amjad² in a study using the seeded growth method, reported that trace amounts of low molecular weight PAC can stabilize supersaturated solutions and lengthen the induction time before the onset of crystallization. The duration of induction times observed in the presence of polymers was found to be greatly influenced by the polymer concentration, solution temperature, pH, and the amount of gypsum seed crystals added.

In other studies involving the influence of phosphorous containing additives,³⁻⁵ it was shown that certain phosphonates are effective in inhibiting gypsum growth in aqueous solutions compared to polyphosphates. Amjad,^{6,7} in studies on the evaluation of polymers as gypsum scale inhibitors, showed that polymer composition, molecular weight, and ionic charge of the polymer play important roles in imparting the inhibitory activity to the polymer. Among the homopolymers evaluated, poly(acrylic acid) showed the best performance whereas neutral and cationic charged polymers were the least effective inhibitors.

Recently, due to environmental concerns such as toxicity and synthetic polymers as nutrients for microorganisms, there has been an increasing interest in the development and application of scale inhibitors derived from natural resources. Campbell and coworkers⁸ in their study on the influence of polyelectrolytes on the crystal growth of calcium oxalate monohydrate (COM) showed that poly(aspartic acid) and poly(glutamic acid) are effective COM growth inhibitors. The efficacy of poly(aspartic acid) as growth inhibitors for scale forming salts has been recently reported. The results of this study⁹ suggest that poly(aspartic acid) exhibits good inhibitory activity for calcium sulfate, calcium phosphate, and calcium oxalate and the performance of poly(aspartic acid) is comparable with the currently employed scale inhibitors.

In the present study we have investigated the formation of gypsum scale on the heat exchanger surfaces from calcium sulfate supersaturated solutions. The performance of polymeric additives containing different functional groups and ionic charges (i.e., poly(aspartic acid), PAS; poly(acrylic acid), PAC; poly(2-acrylamido-2-methylpropane sulfonic acid), PSA; poly(diallyldimethyl ammonium chloride), PDAC; and poly(vinyl pyrrolidone), PVP) as gypsum scale inhibitors was evaluated. In addition, scanning electron microscopy was used to study morphology of the gypsum crystals grown on the heat exchanger surface in the presence and absence of scale inhibitors.

3. EXPERIMENTAL

Grade A glassware, reagent grade chemicals, and double-deionized, distilled, and nitrogen purged and blanketed water were used. Calcium chloride solutions were standardized by ethylenediaminetetraacetic acid (EDTA) method. Sodium sulfate solutions were standardized by ion exchange method. The poly(acrylic acid), poly(2-acrylamido-2-methylpropane sulfonic acid), and poly(diallyldimethyl ammonium chloride) used in this study were commercial and experimental samples from The BFGoodrich Company. Poly(aspartic acid) was obtained from Sigma Chemicals Company. Poly(vinyl pyrrolidone) was obtained from ISP and was used without further purification.

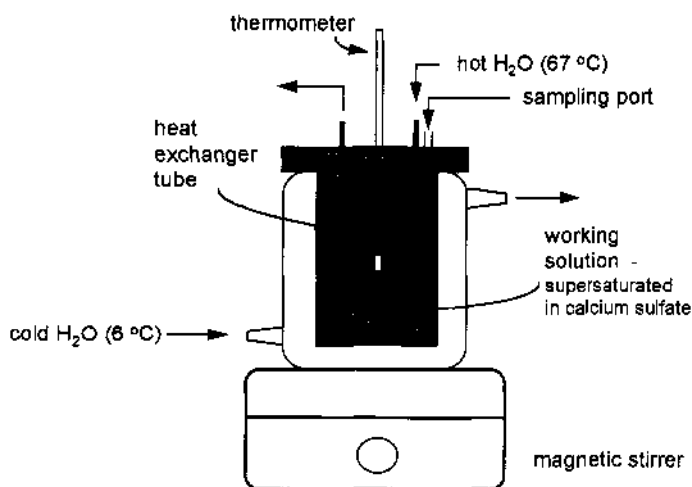


Figure 1. Experimental set-up used to study gypsum scale deposition on heat exchanger surfaces.

Supersaturated solutions of calcium sulfate were prepared in a double-walled, water jacketed crystallization cell of about 950 ml capacity. The heat exchanger tubes (40 cm long, 1.0 cm outer diameter) were used. These tubes were suspended from the lid of the crystallization cell and immersed in the supersaturated solution. The total metal surface area in contact with the calcium sulfate solution was typically about 80 cm². The tubes were chemically cleaned and rinsed thoroughly with distilled water to avoid any surface imperfections and impurities.

Scale deposition experiments were initiated by immersing the metal tube in the calcium sulfate supersaturated solutions. A temperature differential was provided by circulating hot water, maintained at 67 ± 0.5 °C, through the tube, and cold water, 6 ± 0.4 °C, through the outside of the crystallization cell. The experimental set-up is illustrated in Figure 1. Within ~ 5 minutes, a steady-state temperature was reached and the bulk solution temperature remained at a constant value. To minimize corrosion of the brass and copper heat exchanger during scale deposition, an azole-based corrosion inhibitor was used. During the scale deposition experiment solution samples were withdrawn from time to time and filtered through 0.22 micron filter paper, and soluble calcium was analyzed by EDTA titration. In addition, during the experiment solution temperature was also monitored as a function of time. In addition, gypsum crystals grown on heat exchanger surfaces in the presence and absence of inhibitors were also examined by scanning electron microscopy. Table 1 lists the structures and the molecular weights of the polymers evaluated in this study.

4. RESULTS AND DISCUSSION

Concentrations of the ionic species in the calcium sulfate supersaturated solutions at any instant during the gypsum growth experiments were calculated from the measured calcium ion concentrations using the successive approximation methods described previously.¹⁰ Allowance was made for the presence of the ion pair, CaSO₄, and calcium-inhibitor com-

Table 1. Inhibitors tested in the present study

Inhibitor	Structure	Molecular Weight	Acronym
Poly (aspartic acid)	$\begin{array}{c} \text{-(NH-CH-CO)-}_n \\ \\ \text{CH}_2\text{COOH} \end{array}$	6000	PAS
Poly (acrylic acid)	$\begin{array}{c} \text{-(CH}_2\text{-CH)-}_n \\ \\ \text{COOH} \end{array}$	5800	PAC
Poly (vinyl pyrrolidone)	$\begin{array}{c} \text{-(CH}_2\text{-CH)-}_n \\ \\ \text{C}_4\text{H}_7\text{O} \end{array}$	8000	PVP
Poly (diallyldimethyl ammonium chloride)	$\begin{array}{c} \text{-(CH}_2\text{CH-CHCH}_2\text{)-}_n \\ \qquad \qquad \\ \text{H}_2\text{C} \qquad \qquad \text{CH}_2 \\ \diagdown \qquad \diagup \\ \text{N}^+ \\ \diagup \qquad \diagdown \\ \text{H}_2\text{C} \qquad \qquad \text{CH}_2 \\ \text{Cl}^- \end{array}$	6000	PDAC
Poly (2-acrylamido-2-methylpropane sulfonic acid)	$\begin{array}{c} \text{-(CH}_2\text{-CH)-}_n \\ \\ \text{CO} \\ \\ \text{NH} \\ \\ \text{CH}_3\text{-C-CH}_3 \\ \\ \text{CH}_2\text{SO}_3\text{H} \end{array}$	6000	PSA

plexes. The driving force for gypsum scale formation can be expressed in terms of a Gibbs free energy of transfer, given in Table 2, from a supersaturated to an assumed saturated solution at the metal surface by equation 1.

$$\text{DG} = -RT \ln (\text{IP}/K_{\text{sp}}) \quad (1)$$

In equation 1, IP is the concentration product of free calcium and sulfate ions at time t and K_{sp} is the corresponding solubility constant. The ΔG values in Table 2 refer to the initial values, calculated for a temperature of 35 °C.

Experimental conditions and the gypsum growth data is summarized in Table 2. Typical curves for the calcium concentrations against time for gypsum deposition experiments on brass tubes in the absence of inhibitor (exp. 5, 8) are illustrated in Figure 2. It can be seen in Figure 2 that, following an induction period (~ 15 min), gypsum scale formation takes place on the heated brass surface. The reproducibility of the scale growth experiments is shown by the excellent agreement between the results of experiments 5 and 8 (Table 2).

Table 2. Results of gypsum growth experiments

Experiment	Inhibitor	Inhibitor concentration (ppm)	Mass of gypsum deposited (g)
1	none	0.0	1.77
5	none	0.0	1.81
8	none	0.0	1.72
10	none	0.0	1.62 ^b
11	none	0.0	1.45 ^c
13	PAS	0.05	1.58
15	PAS	0.10	1.41
16	PAS	0.20	0.78
17	PAS	0.50	0.42
18	PAS	1.00	0.12
19	PAC	0.075	1.35
20	PAC	0.10	1.02
21	PAC	0.20	0.6
22	PAC	0.50	0.15
23	PAC	1.00	NA
24	PSA	0.50	1.78
25	PSA	1.00	1.74
26	PDAC	0.50	1.84
27	PDAC	1.00	1.77
28	PVP	0.50	1.75
29	PVP	1.00	1.70

^aTotal calcium = sulfate = 3.45×10^{-2} M, brass heat exchanger, surface area = 78 cm², 6 hr, $\Delta G = -10.7$ KJ mo⁻¹

The temperature–time profiles for gypsum growth experiments in the absence of additives are also shown in Figure 2. It is worth noting that, as the concentration of calcium decreases (or the amount of gypsum deposited on the heat exchanger increases), the calcium sulfate solution temperature in the cell decreases. This observed decrease in solution temperature reflects the thermal loss of the heat exchanger. To verify that spontaneous precipitation did not occur during the scale deposition experiment, unfiltered samples were also analyzed for calcium ion and found to be within $\pm 0.5\%$ of the filtered sample.

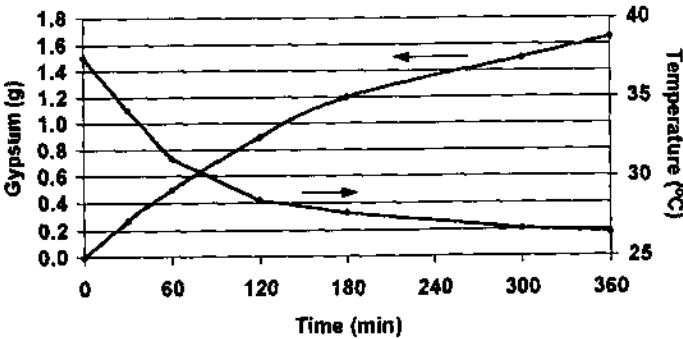


Figure 2. Gypsum growth on brass heat exchanger.

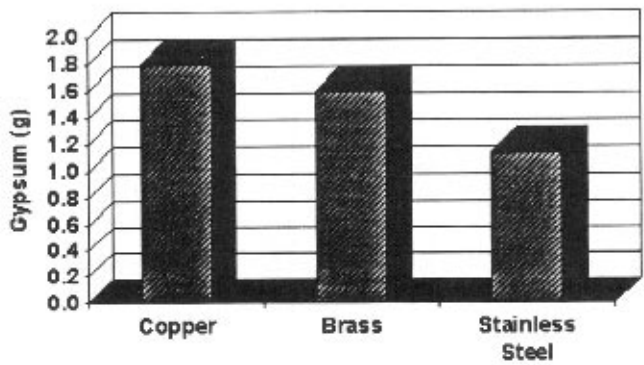


Figure 3. Growth of gypsum on heat exchangers of different metallurgy.

The influence of the nature of the heat exchanger surface (i.e., brass, copper, stainless steel, etc.) on the amount of gypsum scale formation was also investigated. Results, summarized in Table 2, are illustrated in Figure 3. It can be seen the amount of gypsum deposited strongly depends upon the metallurgy of the heat exchanger. For example, the amount of gypsum deposited in 6 hr is 1.8, 1.6, and 1.4 grams for copper, brass, and stainless steel, respectively. It should be noted that the amount of the gypsum deposited is consistent with the thermal conductivity characteristics i.e., copper, brass, and stainless steel.

Figure 4 shows calcium concentration–time profiles for scale deposition experiments in the presence of varying concentration of poly(aspartic acid), PAS. It can be seen that the addition of 0.20 ppm (parts per million) of PAS to the calcium sulfate supersaturated solution exhibits a marked reduction in gypsum growth. Figure 4 also shows that an increase in PAS concentration from 0.20 to 0.50 ppm results in a 50% decrease in the amount gypsum deposited on the heat exchanger and at 1.00 ppm PAS concentration, the gypsum growth is completely inhibited for at least 6 hours.

It has been previously reported that the influence of polymeric and non-polymeric additives as gypsum growth inhibitors fall into two categories: those inhibitors that affect the induction period and those that show no significant effect on the induction period preceding the gypsum crystal growth. The calcium–time profiles for the first type were ob-

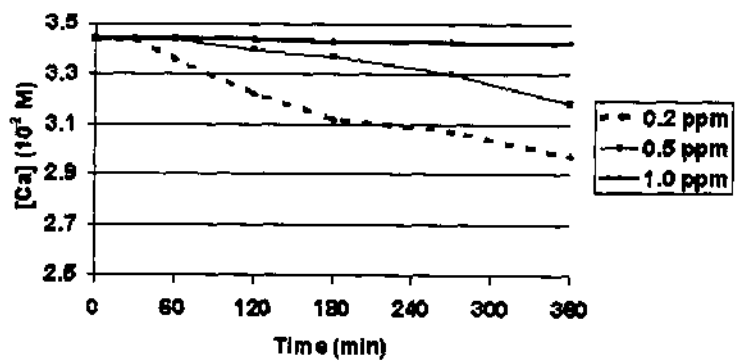


Figure 4. Inhibition of gypsum by poly (aspartic acid).

served for the better inhibitors while profiles for the second type were obtained for less effective inhibitors. In both cases the decrease in calcium ion concentration from solutions with increasing reaction time was found to follow a second-order rate law. To accommodate both types of behavior, in the present study we have selected, for comparing inhibitors performance, the amount of calcium ion remaining in solution after 6 hours of gypsum scale growth on the heat exchanger. When expressed as a fraction of the total calcium ion present at the beginning of the scale formation experiment, the difference between the initial and 6-hr residual calcium ion concentrations becomes a measure of the amount of gypsum scale deposited on the heat exchanger in the presence of inhibitors. The choice of a six hour growth time is arbitrary and, although the selection of different growth time would lead to a change of absolute amounts of gypsum scale deposited, it would not affect the relative ranking of the inhibitors effectiveness.

The results of gypsum growth experiments in which PAC, poly(acrylic acid), was used are summarized in Table 2. Calcium concentration-time profiles for experiments conducted in the presence of varying concentration of PAC are illustrated in Figure 5. As can be seen in Table 2 (expts 19–23), the amount of gypsum deposited strongly depends on PAC concentration. For example, amount of gypsum deposited in the presence of 0.10 ppm is 1.02 g compared to 0.15 g obtained in the presence of 0.50 ppm PAC concentration. Thus, a five fold increase in PAC concentration results in ~ six fold decrease in gypsum growth.

To study the influence of ionic charge of the polymers in preventing gypsum growth on brass heat exchanger, several experiments were conducted with polymers containing different charges i.e., anionic, neutral, and cationic. Results are summarized in Table 2 and illustrated in Figure 6. It can be seen that polymers containing neutral or cationic charge are ineffective gypsum growth inhibitors. For example, the amount of gypsum deposited on the heat exchanger in the presence of 1.0 ppm PDAC (cationic polymer), PVP (neutral), and PSA (anionic containing -sulfonic group) are 1.77, 1.70, and 1.74 g respectively, compared to 1.78 g obtained in the absence of polymer. The data presented in Figure 6 also shows that carboxyl containing polymers exhibit inhibitory power to a varying degree. It is worth noting that even though PSA is a stronger acid than PAS and PAC, its activity as a gypsum growth inhibitor is essentially insignificant thus suggesting that carboxyl group in the polymer plays an important role in providing the inhibitory activity.

The role of gas–solid–liquid interface has been reported to play an important role in the nucleation and subsequent attachment of scale crystals on heat transfer surfaces.

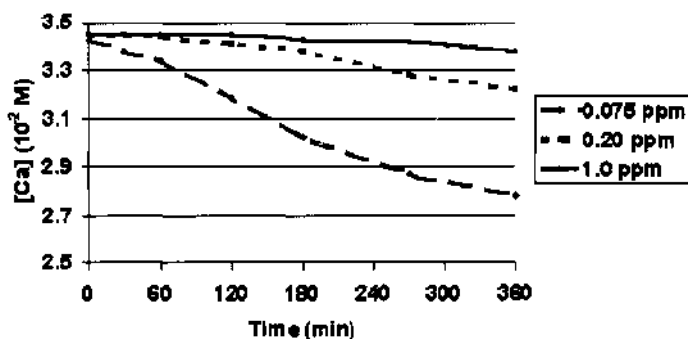


Figure 5. Inhibition of gypsum by poly(acrylic acid).

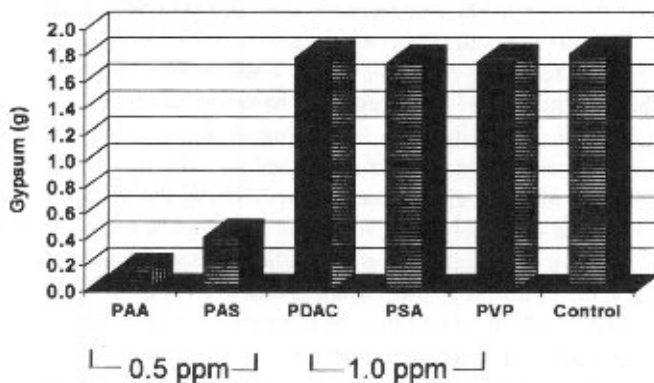


Figure 6. Comparison of gypsum growth on heat exchanger surface in the presence of various polymeric inhibitors.

Bramson et al.¹² proposed that the existence of gas bubbles at the heat transfer surface leads to anomalous results. They concluded that the surface-temperature gradient could only be partly responsible for the large variations in nucleation rate along a heated tube, and proposed an unsteady state nucleation mechanism to account for the observed phenomena. In their study, they attempted to remove air from the saturated solution of calcium sulfate before it was circulated through the annular heated tube exchanger. It is clear from the results of the present study that gas-liquid interface created by bubble formation plays an important role in the nucleation of gypsum scale crystals. This has been observed by other workers and may partly be due to surface-temperature gradients in the presence of the bubbles. Nancollas and Klima¹³ and Amjad,^{14,15} in their studies on the deposition of gypsum on Admiralty brass, suggested that gypsum crystals formed preferentially at the perimeters of the gas bubbles.

REFERENCES

1. Smith BR and Huilin Y, "Influence of Various Factors on the Performance of Gypsum Scaling Retardants", *Water Treatment*, 1992;7:51-46.
2. Amjad Z, "Kinetics of Crystal Growth of Calcium Sulfate Dihydrate: The Influence of Polymer Composition, Molecular Weight, and Solution pH", *Can. J. Chem.*, 1988;66: 1529-1536.
3. Liu ST and Nancollas GH, "The Crystal Growth of Calcium Sulfate Dihydrate in the Presence of Additives," *J. Colloid Interface Sci.*, 1973;44:422-429.
4. Amjad Z, "Applications of Antiscalants to Control Calcium Sulfate Scaling in Reverse Osmosis Systems", *Desalination*, 1985;54:263-276.
5. Lin ML, Ekis EW, Mouche RJ and Nassos PA, "Effective Gypsum Scale Inhibitors for Flue Gas Desulfurization Applications", *CORROSION/88* Paper No. 427, National Association of Corrosion Engineers, Houston, Texas, 1988.
6. Amjad Z and Masler WF, "The Inhibition of Calcium Sulfate Dihydrate Crystal Growth by Polyacrylates and the Influence of Molecular Weight", *CORROSION/85*, Paper No. 357, National Association of Corrosion Engineers, Houston, Texas, 1985.
7. Amjad Z and Hooley J, "Influence of Polyelectrolytes on the Crystal Growth of Calcium Sulfate Dihydrate", *J. Colloid and Interface Sci.*, 1986;111:496-503.
8. Campbell AA, Ebrahimpour A, Perez L, Smesko AA, and Nancollas GH, "The Dual Role of Polyelectrolytes and Proteins as Mineralization Promoters and Inhibitors of Calcium Oxalate Monohydrate", *Calcific Tissue Int.*, 1989;45:122-128.

9. Ross RJ, Low KC and Shannon JE, "Polyaspartate Scale Inhibitors Biodegradable Alternatives to Polyacrylates", CORROSION/96, Paper No. 162, National Association of Corrosion Engineers, Houston, Texas 1996.
10. Nancollas GH, *Interactions in Electrolyte Solution*, Elsevier, Amsterdam, 1966.
11. Gill JS and Nancollas GH, "Kinetics of Growth of Calcium Sulfate Heated Metal Surfaces", *J. Crystal Growth*, 1980;48:340.
12. Bramson D, Hasson D and Semiat R, "The Roles of Gas Bubbling, Wall Crystallization and particulate Deposition in CaSO_4 Scale Formation", *Desalination*, 1995; 100: 105–113.
13. Klima W, Nancollas GH, "The Growth of Gypsum", American Institute of Chemical Engineers Symposium Series on Crystallization and Precipitation Prevention, 1982.
14. Amjad Z, "Calcium Sulfate Dihydrate (Gypsum) Scale Formation on Heat Exchanger Surfaces. The Influence of Scale Inhibitors", *J. Colloid Interface Sci.*, 1988;123:523–36
15. Amjad Z, "Calcium Sulfate Dihydrate Scale Formation on Heat Exchanger Surfaces in the Presence of Inhibitors", Paper 178, CORROSION '78, National Association of Corrosion Engineers, Houston, TX 1989.

This page intentionally left blank.

APPLICATIONS OF STRUCTURED CATIONIC POLYELECTROLYTES IN WASTEWATER TREATMENTS

Haunn-Lin T. Chen

Cytec Industries Inc.
1937 West Main Street
Stamford, Connecticut 06904

1. ABSTRACT

High molecular weight water-soluble topologically structured copolymers of acrylamide (AMD) and 2-(acryloyloxy)ethyltrimethylammonium chloride (AETAC) were synthesized by inverse emulsion polymerization process. Copolymers with various structures were attained by introducing appropriate amounts of branching and chain-transfer agent in the monomer feed. Polymer structure was characterized by solution rheological properties comprising the measurements of the viscosity of a 0.2% polymer solution in de-ionized water (Bulk Viscosity, BV) and the viscosity of a 0.1% polymer solution in 1.0 N NaCl (Standard Viscosity, SV). The synthesized polymers were then subject to flocculation test with several types of sludge. De-watering rate, filtrate turbidity, and percent cake solids were used to ascertain the efficiency of flocculation. It was found that the polymer with a high BV and a low SV had exceptional performance on certain types of sludges. A statistically designed experiment was conducted to reveal the quantitative relationships between the structure parameters (BV and SV) and the performance characteristics.

2. INTRODUCTION

For decades high molecular weight cationic polyelectrolytes have been utilized as flocculants for isolation and separation of colloidal particles. Typical applications include treatments of wastewater sludge generated from city sewer systems and industries,¹ as paper retention aids,² in mineral processing,³ etc. Taking wastewater treatment as an example, the enormous volumes of city sewer and industrial wastewater generated each day are typically processed in treating plants through bio-digestion, either aerobic or anaerobic, to

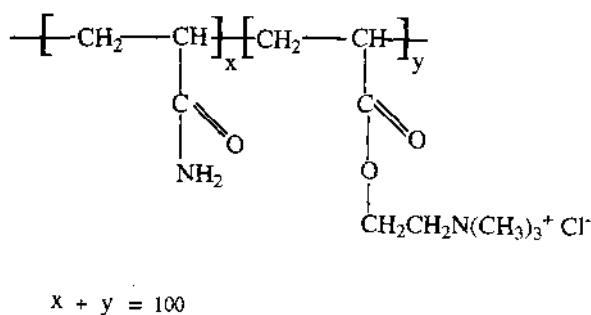


Figure 1. The structure of AMD-co-AETAC polymer where Y is the percent charge in the polymer.

transform both soluble and particulate pollutants into sludge solids. The sludge solids are then separated from water through de-watering or sedimentation process. Although bacteria are capable of forming flocs through their extracellular polymers (bio-flocculation⁴), the floc sizes are in general too small (ranging from submicron to millimeters) to afford an effective solid-liquid separation. Flocculation of these small flocs by water-soluble cationic polymers is therefore extremely desirable for high speed de-watering process. The basic mechanism of flocculation has been the subject of extensive investigations⁵ and is commonly described by charge neutralization and bridging mechanism.^{6,7}

Among all the commercial cationic flocculants, copolymers of acrylamide and 2-(acryloyloxy)ethyltrimethylammonium chloride (AMD-co-AETAC, see chemical structure in Figure 1) have been the choice due to their high performance and reasonable cost.

Since ultra high molecular weight (generally 5–15 millions Dalton) and high polymer concentration (to lower the shipping cost) are required, the production of these polymers by solution polymerization process is impractical due to their extremely high viscosities. As a consequence, commercial flocculants are generally produced in either inverse emulsion, inverse microemulsion, and solid (gel or bead) forms. The most commonly used products available on the market to date are plain linear copolymers of AMD and AETEC of various charge contents. Although those linear copolymers are easy to manufacture, they do however, not always meet the performance demands owing to the complex and unsettled nature of wastewater sludge. For instance, it is not unusual to find out that a flocculant works remarkably well for sludge A yet performs poorly on sludge B. This performance discrepancy can generally be attributed to the inadequate match of the sludge characteristics with charge density, molecular weight, and the least understood topological structure of the flocculant. Moreover, mixing intensity is also playing a decisive role on flocculation. Both insufficient conditioning or over shearing will result in poor flocculation. Obviously, these factors are interrelated. For instance, the requirement of a flocculant molecular weight goes up as the mixing intensity increases. Therefore, the investigation of the relationships among these factors is more appropriate by using statistically designed experiments conducted with well-characterized polymers. A separate paper conveying this issue is currently in preparation by the author.

To overcome the shortfall of linear polymers, branched and lightly crosslinked cationic copolymers, also known as "structured" polymers, have been introduced in the past several years. Some performance advantages of those structured flocculants over linear ones have been reported.^{8,9} No detailed information, however on the molecular structures of these polymers as well as their relationships to the flocculation effectiveness was re-

vealed. The difficulty of characterizing the structure of these polycationics may have been one of the major obstacles for detailed examination. In this paper, a rather simple method using rheological properties of polyelectrolytes to discriminate the structure variations in structured polymers has been developed. With this method, the relationships between polymer structure and the effectiveness on sludge flocculation has been investigated. The results has led to the discovery of a new type of flocculants that exhibit superior performances.

3. EXPERIMENTAL

3.1. Preparation of Structured AMD-Co-AETAC Polymers

These copolymers were prepared by the general inverse emulsion polymerization process as described in the following, using a 34.2% AETAC/65.8% AMD copolymer as an example. An aqueous phase containing 192.65 grams of a 52.64% acrylamide, 179.5 grams of a 80% AETAC, 82 grams of de-ionized water, 4.2 grams of ammonium sulfate, 29.4 grams of a 50% glutaric acid, 4.9 grams of a 5% ethylenediaminetetraacetic acid (disodium salt), 1 grams of 2-isopropanol (chain transferring agent), 0.01 grams of N,N'-methylenebisacrylamide (branching agent), and 2.5 gram of a 2% ammonium persulfate was prepared. The pH of the aqueous phase was adjusted to 3.5 with a diluted sulfuric acid. The oil phase contained a 173.4 grams of a low odor paraffin oil and 21 grams of so-bitan monooleate. To prepare the emulsion, the aqueous phase was poured slowly into the oil phase and homogenized for several minutes to afford a water-in-oil inverse emulsion. The monomer emulsion was then transferred into a three-necked flask. It was sparged with nitrogen and polymerized at 40°C for about 4 hours with a 1% sodium bisulfite solution added slowly to avoid overheating by the polymerization exotherm.

3.2. Characterization of Copolymers

A 0.2% polymer solution was prepared by dissolving the emulsion in de-ionized water containing 0.06% nonylphenol ethoxylate and its viscosity was measured with a Brookfield viscometer to obtain the Bulk Viscosity (BV). The 0.1% polymer solution in 1.0 N NaCl was prepared from the 0.2% solution by adding equal amount of 2.0 N NaCl solution. Its viscosity was measured with a Brookfield viscometer (UL adapter) at 60 rpm to give the Standard Viscosity (SV).

3.3. Flocculation Experiment

The experiment setup consists of a 500 ml square beaker fitted with an overhead variable speed stirrer which has a digital stirring speed readout. The stirring blade is a flat paddle with a dimension of 2.5 cm × 6.5 cm. The stirring time is controlled by a timer. To conduct the experiment, 300 g of wastewater sludge was placed in the square beaker. A dose amount of the 0.2% polymer solution, diluted to a constant volume of 45 ml with water, was added to the sludge and the stirrer was started with the timer. When the stirrer stopped, 3.5 ml of the flocculated sludge was collected for capillary suction time (CST) measurement. The flocculated sludge was then poured quickly into a funnel fitted with a belt press screen. The filtrate was collected in the graduated cylinder which was standing on a top-load balance. The balance was connected to a data-acquisition computer for re-

cording the drainage rate (the weight of filtrate versus time). For the sake of simplicity, we had used the drainage volume (converted from weight) collected at 10 seconds as a measurement of the de-watering efficiency and called it drainage@10 sec (in ml unit). The turbidity of the filtrate, in NTU unit, was determined with a Hach RX/RATIO turbidimeter. The wet cake in the funnel was transferred to a press device (TetraPress) and was processed with sequential increments in pressure up to 15 psi to simulate the process in belt press. The processed cake was then dried in a 105°C oven to a constant weight to determine the percent cake solids. Note that the polymer dosage had been converted from volume to pounds of polymer per dry ton of sludge (lbs/dton) with the conversion factor calculated from solids content in sludge.

4. RESULTS AND DISCUSSION

Flocculation of wastewater sludge with cationic polymer is a rather complicated process. To study the relationships between polymer structure and flocculation efficiency, one has to understand both the sludge characteristics and the polymer structure and properties. Sludge by itself is a very complex matter that consists of a variety of microorganisms such as bacteria, fungi, protozoa, and inorganic and organic particulates. The size of “bio-floc” in sludge can range from a single bacteria of about 0.5 micron to large aggregates of more than 1 mm. The floc shape can also vary from compact spheres (pin floc) to filamentous network (the so called “bulking”). Due to its “living” nature, sludge may change its properties the moment it leaves the “digester”. This change in characteristics has been found very often contributing to the inconsistency in the laboratory flocculation test. Fortunately, each wastewater treating plant seems to produce its own characteristic sludge that has “fairly consistent quality”, providing that neither the process nor the wastewater source has drastic changes. When conducting laboratory sludge flocculation test, running control experiments using a ratified flocculant is the safest way to ensure the sludge “quality”.

As mentioned earlier, characterization of structures has presented some impediments for studying the correlations between the structure and the performance of flocculants. For example, in the characterization of polymer molecular weight and hydrodynamic size, high performance size exclusion chromatography (HPSEC), light scattering, and viscometry are the most commonly used methods. These methods have been showing good results for low to medium molecular weight polyelectrolytes. For ultra high molecular weight cationic polymers, they are however, either very time-consuming or are subject to artifacts or interferences.^{10,11} Problems in GPC often arise from the adsorption of cationic polymer in the column. In light scattering methods, processes to prevent interferences such as dust, and preferential solvation are tedious and prone to artifacts. Intrinsic viscosity has been proven a convenient method to assess the information on molecular weight. For ultra high molecular weight polymers, breaking down of polymeric molecules by the shear generated in the capillary is always a concern. Although this problem can be curtailed by using four-bulb viscometer to allow zero-shear extrapolation, the interpretation of the results is still under debate.

In addition to the molecular weight, we are also interested in characterizing the topological structure of polyelectrolytes, especially in low to medium salt solutions that are typically the concentrations found in wastewater. Although scattering methods such as x-ray scattering and neutron scattering; and spectroscopy methods such as fluorescence, NMR, IR, and Raman have been applied to reveal polymer structure, they require exper-

tise, equipment, and experiments that are usually time consuming. In light of these difficulties, a quick method to assess the structure and properties of a flocculant is certainly desirable, either for researchers in the lab or application specialists in the field. Through the statistical analysis of experimental data, we have found, somewhat unexpectedly, that simple measurements of the solution rheological properties are capable of differentiating quantitatively the variances in the polymer structure. It should be pointed out that, although not perceived as well-defined as other complicated methods, viscosity measurement has been widely used in the flocculant industry for years.

The rheological properties we have employed in this study were the solution viscosity of a 0.2% polymer in de-ionized water and the viscosity of a 0.1% polymer in 1.0 M NaCl. For convenience, the former has been termed the Bulk Viscosity (BV) and the latter named the Standard Viscosity (SV). With linear AMD-co-AETAC polymers, BV of the same charge is almost linearly proportional to SV, as shown in Figure 2. By contrast, the ratio of BV to SV has been found reflecting well to the variations in the topological structure of nonlinear polyelectrolytes.

As mentioned in the experimental section, the structured AMD-co-AETAC copolymers were prepared by adding a chain-transferring agent and a branching agent in the monomer solution. Depending on the level of the chain-transferring agent and the branching agent, polymers with various structures can be produced. In this work, the preparation of these copolymers followed a CCI statistical design that gave a sixteen-run worksheet.

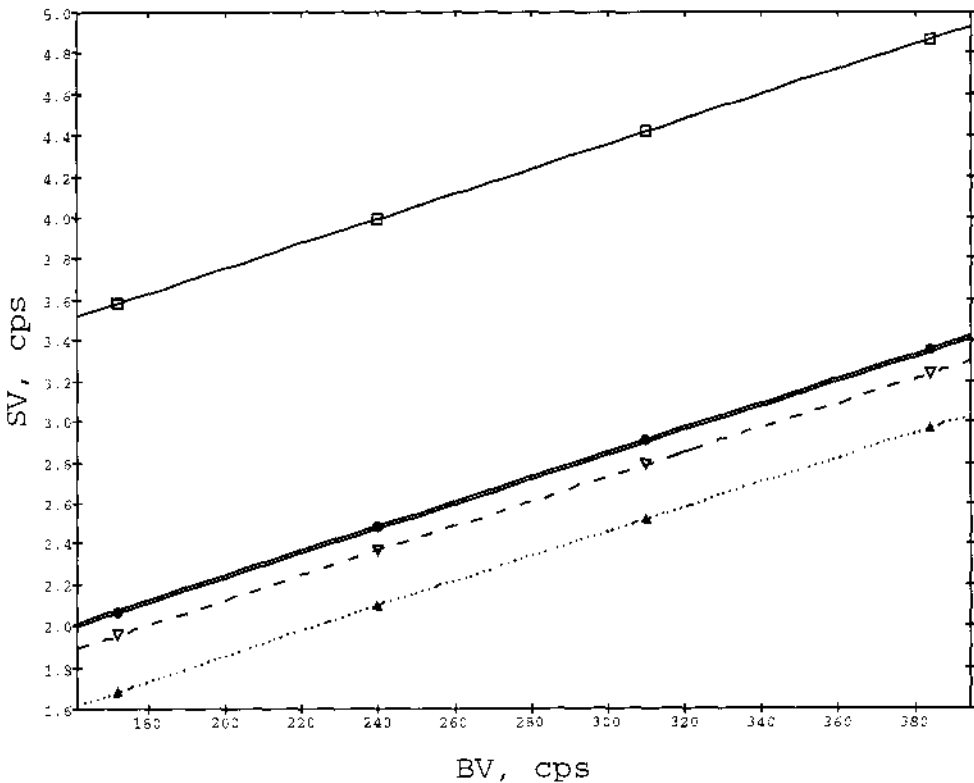


Figure 2. Predictions for mean responses of SV as a function of BV for linear AMD-co-AETAC polymers with various percent AETAC (□-5%; ●-25%; ▲-40%; ▽-55%).

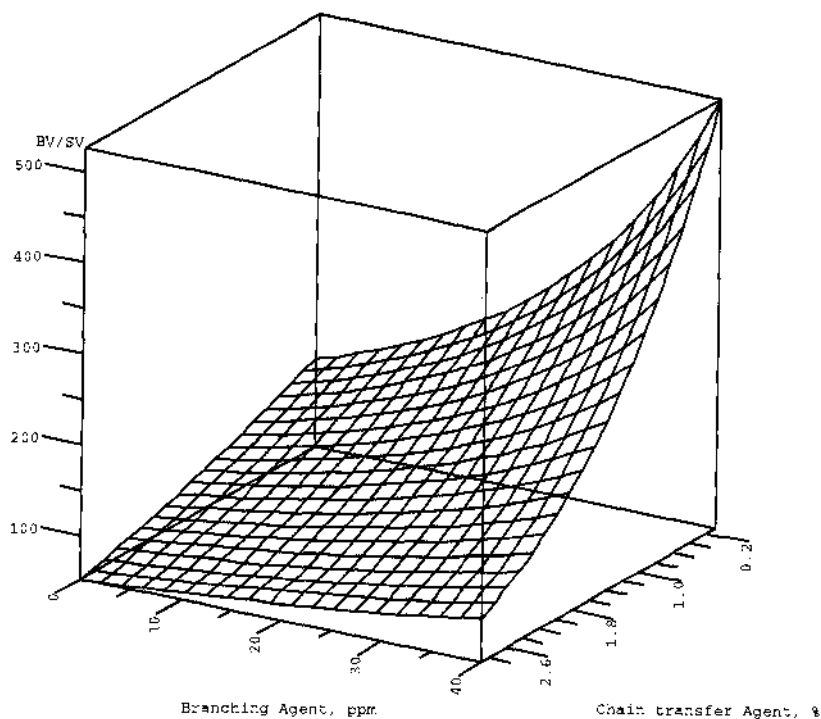


Figure 3. BV/SV ratio as a function of chain-transferring agent and branching agent for AMD-co-AETAC polymers with 40% AETAC.

After preparing these sixteen copolymers and measuring their bulk viscosities and standard viscosities, we had generated a statistical model to describe the relationship between the predictors (chain transferring agent and branching agent) and the response (BV/SV). Figure 3 is a three-dimensional plot delineating this relationship.

The copolymer with a distinctively high (BV/SV) ratio presents a very interesting case. These high (BV/SV) polymers, besides having high BV values, generally have Standard Viscosities below 2 cps. Remember that BV is the measurement of viscosity in very low salt conditions. For such a high molecular weight polyelectrolyte under this low salt condition, its 0.2% solution has already passed the semi-dilute critical concentration (c^*) and polymer chains are overlapping strongly.¹² On the other hand, due to the screening effect of salt, SV is more of a reflection of the polymer hydrodynamic mass in a compact structure. As a consequence, when salt concentration increases from near zero to 1.0 N, the polymer with a high (BV/SV) ratio must have proceeded some kinds of structural changes that yields a SV which is lower than its linear counterpart. This viscosity reversing phenomenon is illustrated in Figures 4 and 5, using copolymers with 55 % AETAC as the examples. As depicted in Figure 4, the percent decrease of BV of the linear polymer is greater than that of the structured polymer when NaCl concentration is below 0.5 N. Figure 5 shows that, as the NaCl concentration increases beyond 0.5 N, the structured polymer has a higher percent decrease in BV that leads to a lower final viscosity than its linear counterpart.

This (BV/SV) dependency on the polymer structure may be understandable considering that polyelectrolytes with different topological structures and especially, with differ-

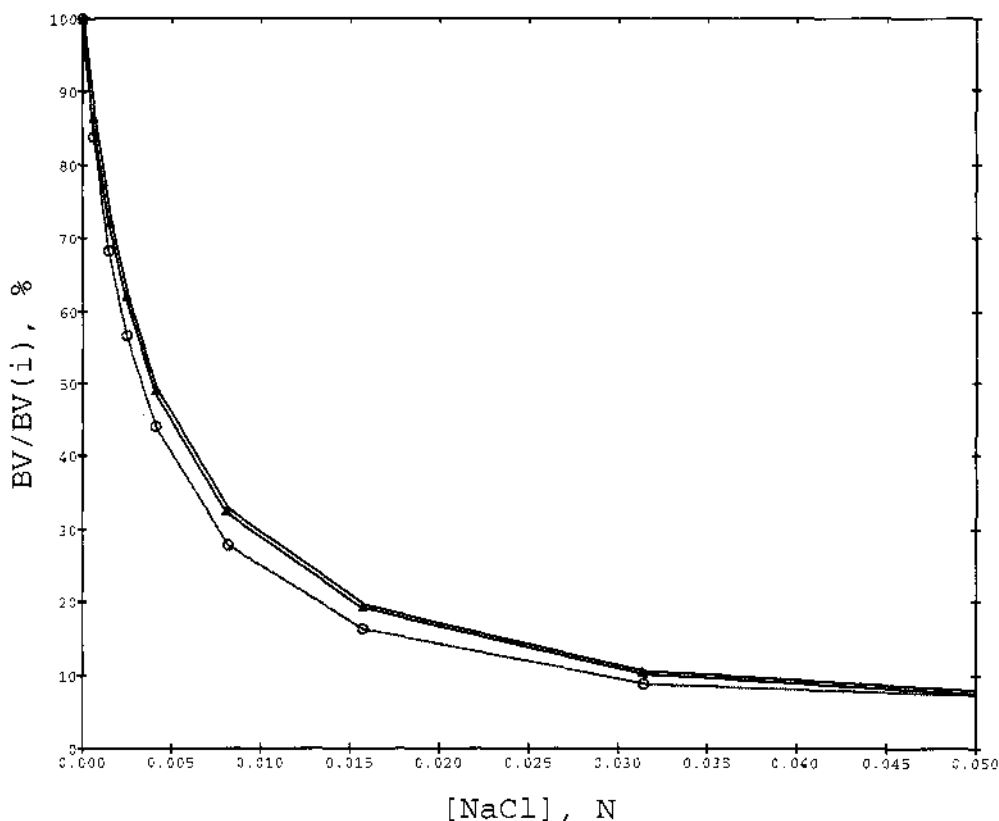


Figure 4. Effect of sodium chloride concentration, up to 0.05N, on BV/BV_i ratio for linear (O) and structured (▲) AMD-co-AETAC polymers with 55% AETAC.

ent charge distributions are having different inter-chain interactions. According to the kinetic model of free radical crosslinking polymerization proposed by Tobita and Hamielec using mean-field theory,¹³ the structures generated in our polymerization system are likely to vary from long-branched, short-branched, to nearly networked structure. The amounts of branching agent and chain-transferring agent are conceivably affecting the number and the chain length of the branches, respectively.

Another interesting behavior of polyelectrolytes is the so-called “ordinary-extraordinary” transition under low salt concentrations.¹⁴ In the extraordinary regime, a slow diffusive mode has been observed in quasielastic light scattering that has been attributed to the formation of clusters or multiple chain domains.¹⁵ The ordered clusters had also been observed by small angle neutron scattering of sodium polystyrenesulfonate and the cluster size was estimated to be around 400 to 1000 Angstrom.¹⁶ Although the current scientific investigations on this subject are mostly limited to linear polyelectrolytes, the explication may be extended to structured polyelectrolytes as well. Our perception is that long-range interactions or entanglements of branches would possibly affect the formation of these clusters. As a consequence, BV may be a reflection of branch chain length and number of branches in the polymer. More precise analytical methods such as determination of the number of branches by NMR,¹⁷ identification of clusters structure and size by light, x-ray,

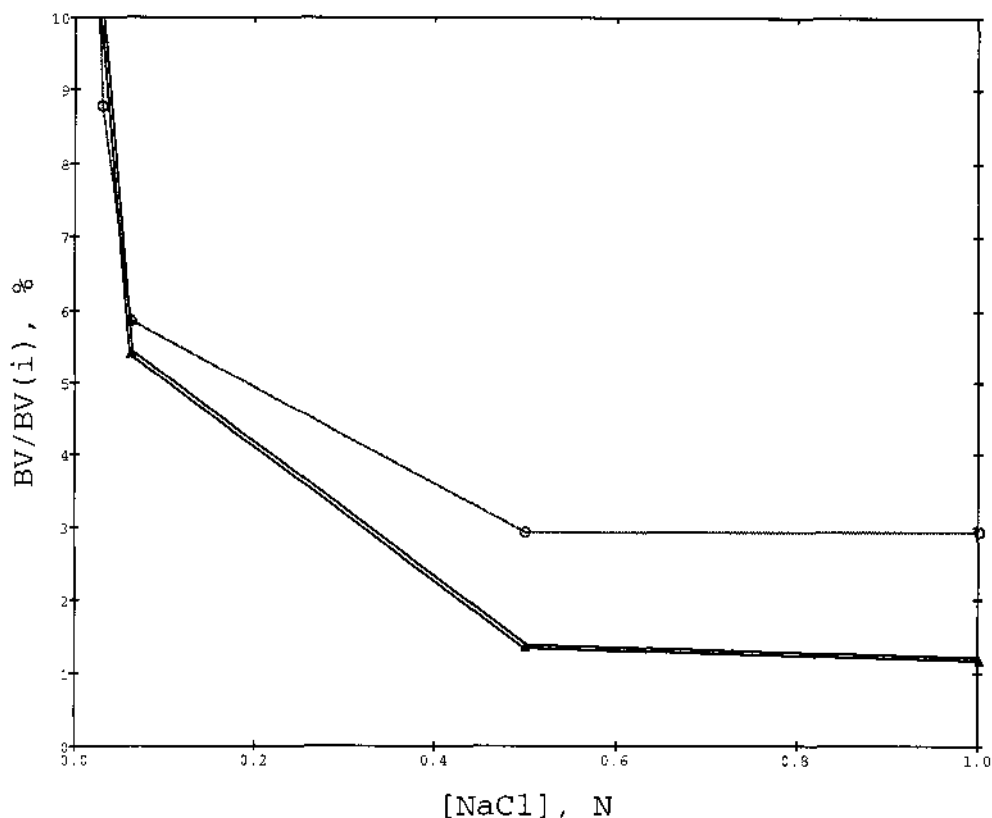


Figure 5. Effect of sodium chloride concentration, up to 1.0N, on BV/BVi ratio for linear (O) and structured (▲) AMD-co-AETAC polymers with 55% AETAC.

and neutron scatterings, and possible isolation and fractionation of branched portions by preparative ultracentrifugation, followed by HPSEC and NMR analysis, are under investigation.

Let us now switch to the subject of the correlations between flocculation behavior and polymer structure. In wastewater treatment technology, the flocculation efficiency is generally determined by a combination of numerous parameters such as free drainage rate, total filtrate volume, filtrate turbidity, suspended solids in filtrate, capillary suction time (CST), floc size, cleanliness of the filter screen, easiness of cake release from the screen, percent cake solids in the flocculated sludge, etc. In laboratory performance tests, free drainage, CST, filtrate turbidity, and percent cake solids are the typical parameters for defining the flocculation efficiency. An excellent flocculant implies having a high free drainage rate, which in most cases, will also have a high percent cake solids, a low filtrate turbidity, and a low -CST number. Our results indicate that CST behaves very similar to filtrate turbidity therefore it is not included in the discussion of this paper. Figure 6 shows a typical curve of free drainage versus polymer dose. The dose at which the maximum drainage is reached is called optimum dose which in this case is 19 lbs/dton. The drainage at this dose is the drainage at optimum dose. Either under or over dose will result in a lower drainage, a higher turbidity, and a lower percent cake solids. Obviously, the optimum dose depends on the type of

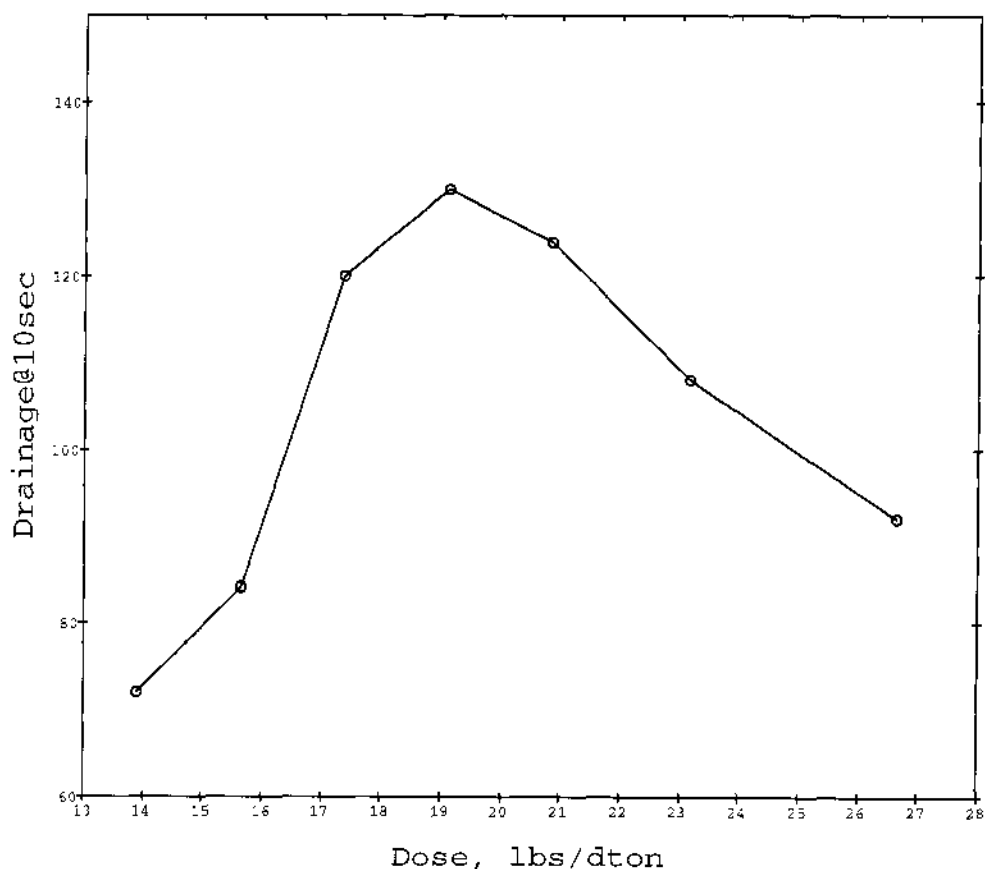


Figure 6. Typical response curve of drainage (@10 sec) to flocculant dosage.

sludge, the charge and structure of the flocculant, and mixing intensity. From performance point of view, the polymer that delivers the best flocculation efficiency at the lowest dose is definitely the ideal choice. It is however, not unusual that satisfactory performance can only be obtained at the expense of dose. Moreover, as we will find below, in some cases that the performance can not even be achieved in spite of heavy doses.

Table 1 presents a summary of the flocculation results of several structured and linear AMD-co-AETAC polymers with different charges on an aerobically digested sludge. The mixing condition was set at 300 rpm for 20 seconds. This sludge has been considered "difficult" because no ideal flocculant giving consistent performance has been identified. As we can see from Table 1, the structured polymer S34-1 with a SV of 1.9 cps, a BV of 488 cps, gave the highest free drainage, the highest percent cake solids, and the lowest turbidity among all the polymers. Polymer S34-3, which represented another type of structure, gave on the other hand very poor results. Polymer S34-2, although prepared as a structured polymer, had a (BV/SV) ratio very similar to the linear polymers L-40 and L-5. Its flocculation performance was also similar to the linear polymers. When the mixing condition was increased to 600 rpm and 60 seconds, as shown in Table 2, the structured polymer S34-1 stood out as the only performer among all, indicating that the structured flocculant is more shear resistant.

Table 1. Performance of linear and structured cationic polymers on an aerobically digested sludge, 300 rpm, 20 sec conditioning

Polymer	Charge (mole %)	SV (cps)	BV (cps)	Dose (#/dton)	Drainage (ml)	Turbidity (NTU)	Cake solids (%)
L-40	40	3.5	355	11.2	90	27	11.8
L-55	55	2.2	252	10.96	78	28	12.61
S34-1	34	1.9	488	12	160	16	14.3
S34-2	34	3.1	344	11.16	84	18	11.2
S34-3	34	2.5	367	11.16	68	42	11.3

These intriguing results prompted us to investigate in detail the structure effect on the flocculation. A series of structured copolymers with varying BV, SV and charge content (% AETAC) were prepared. Sludge flocculation experiments were conducted on a local primary/waste-activated mixed sludge according to an experimental design using response surface methodology. The mixing condition was set at 300 rpm and 20 seconds. Experimental results were analyzed to generate mathematical models describing the relationships between the predictors (BV, SV and % AETAC) and the responses (optimum dose, drainage, and % cake solids). Figure 7 illuminates the free drainage of the flocculated sludge as a function of BV and SV, at a polymer charge of 55% AETAC. The upper right hand corner of this three-dimensional plot clearly indicates that the polymer with a high BV and a low SV will have an extremely high free drainage. This outcome coincides remarkably with our initial testing results in Table 1. Note that at very high BV regime, polymer structure changes sharply as SV increases from 1.6 cps to 3.0 cps, resulting in a severe drop in drainage.

The polymers on the other two corners of the plot, namely, either a low BV and a low SV or a high BV and a high SV, perform very poorly. The (BV/SV) ratios of these two classes of polymers are, as compared with high BV and low SV copolymers, close to that of linear polymers. We may therefore expect their performance trend to be somewhat follows that of linear polymers. With this rationale, we may explain that the former case (low BV and low SV) is in an over shearing condition and the latter case (high SV and high BV) is simply not enough mixing. Finally, the polymer with a high SV and a low BV may represent the structure with short branches. Its flocculation effectiveness is close to or slightly better than that of a linear polymer.

Table 2. Performance of linear and structured cationic polymers on an aerobically digested sludge, 600 rpm, 60 sec conditioning

Polymer	Charge (mole %)	SV (cps)	BV (cps)	Dose (#/dton)	Drainage (ml)	Turbidity (NTU)	Cake solids (%)
L-40	40	3.5	355	20.16	46	black filtrate	N/A
L-55	55	2.2	252	20.16	54	black filtrate	N/A
S34-1	34	1.9	488	25.92	110	48	13.9
S34-2	34	3.1	344	17.28	52	black filtrate	N/A
S34-3	34	2.5	367	23	48	black filtrate	N/A

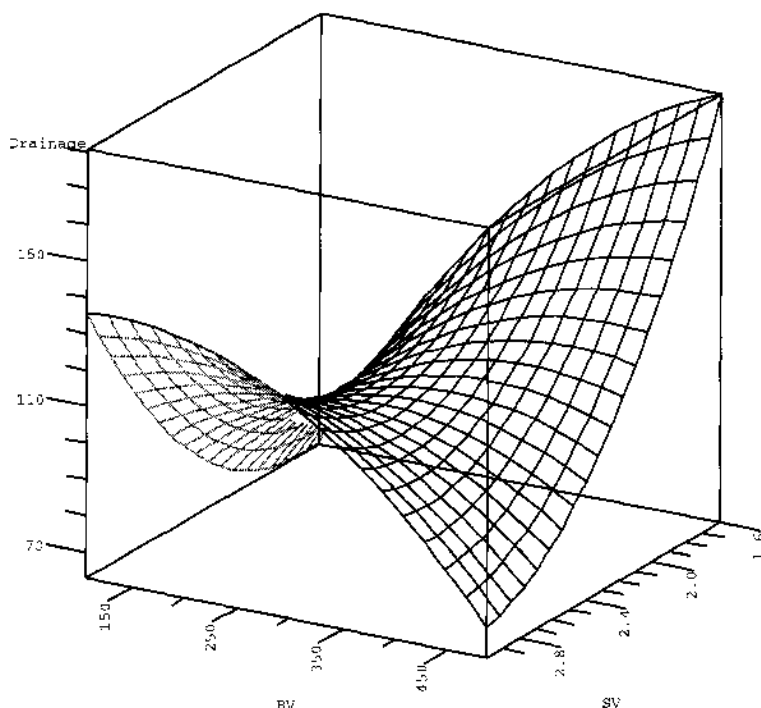


Figure 7. Drainage (@10 sec) as a function of BV and SV of structured AMD-co-AETAC polymers with 55% AETAC.

The second performance parameter that needs consideration is the charge content of the flocculant. As shown in Figure 8, using percent cake solids as the performance indicator, the charge requirement for this particular sludge is around 85%. When combining the effects of (BV/SV) ratio and % AETAC, we can see from Figure 9 that a copolymer with 85% AETAC and a (BV/SV) ratio of 300 will have the best performance in this experimental regime. Figure 10 denotes the relationship between optimum dose and the structure. The polymer with a (BV/SV) ratio around 120 will need the least amount of dose (about 9 lbs/dton) to flocculate the sludge suspended solids. It should be pointed out that this polymer flocculated unsatisfactorily with the sludge even at its optimum dose. When (BV/SV) is greater than 120, the dose demand will increase as the (BV/SV) ratio increases. Moreover, as polymer charge content increases from 25% to 85%, the dose demand decreases. The optimum dose for the best performance polymer in this series (85% AETAC with a (BV/SV) ratio of 300) was around 15 lbs/dton. One should not be mistaken that the introduction of structure to enhance the flocculation performance comes with a dose penalty. On the contrary, the remarkable improvement of performance/price ratio by the structured polymers, especially on those difficult-to-treat sludges, surpasses its requirement of a higher dose.

After this series of experiments, several local as well as distant wastewater sludges were also tested with those structured AMD-co-AETAC polymers. The structured polycationics with high (BV/SV) values have been observed to have the most significant performance improvement over linear and other structured cationic polymers on waste-activated (or aerobically digested) sludges.

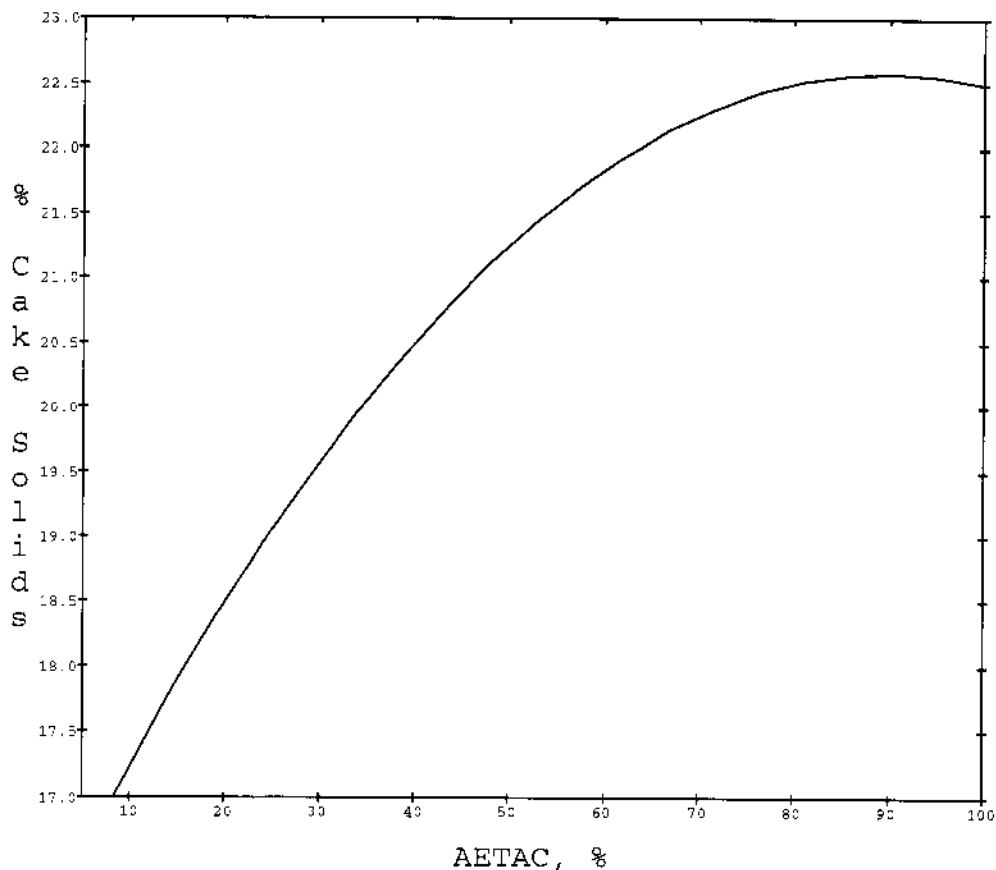


Figure 8. Effect of charge content of AMD-co-AETAC polymers on percent cake solids.

5. CONCLUSION

In this paper we have demonstrated the preparation and characterization of the structured AMD-co-AETAC polymers. The variation of structures in the copolymers was effected by varying the amounts of the chain-transferring agent and the branching agent in the monomer feed. The viscosities of the polyelectrolytes in low salt and in 1.0 N sodium chloride solutions were employed to ascertain the variance in their topological structures. The polymer with a very high (BV/SV) ratio was found to exhibit superior flocculating and de-watering properties on certain types of sludges. The benefit of using this type of polymers over its linear analogs on those difficult wastewater sludge exceeds its demand of a higher polymer dose.

ACKNOWLEDGMENT

Special thanks to J. Kozakiewicz and L. Rosati for their technical inspiration and C. Brady and R. Fogerty for their laboratory supports. Proof reading of this paper by D. Lipp is gratefully acknowledged.

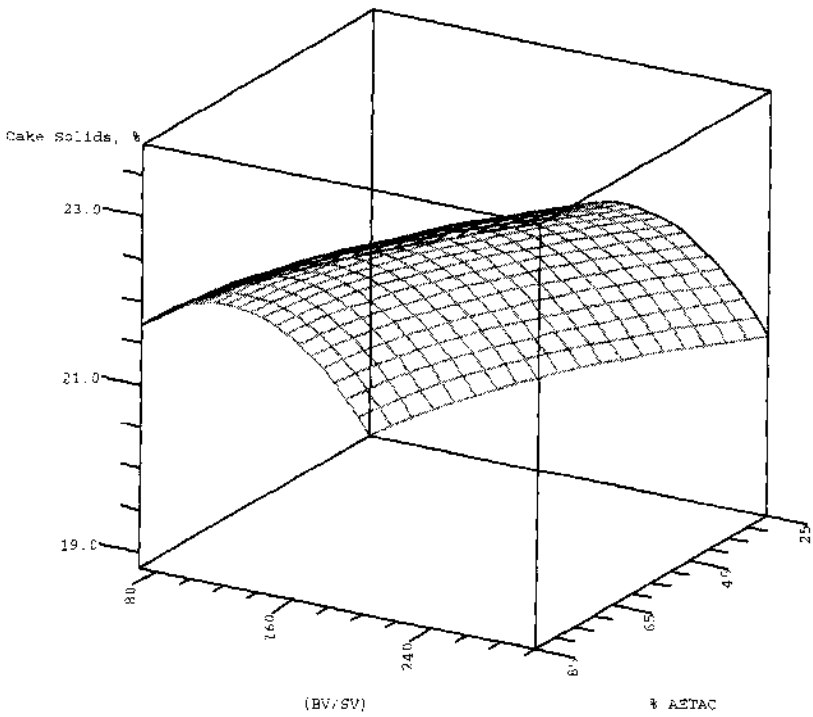


Figure 9. Percent cake solids as a function of BV/SV ratio and percent AETAC of AMD-co-AETAC polymers.

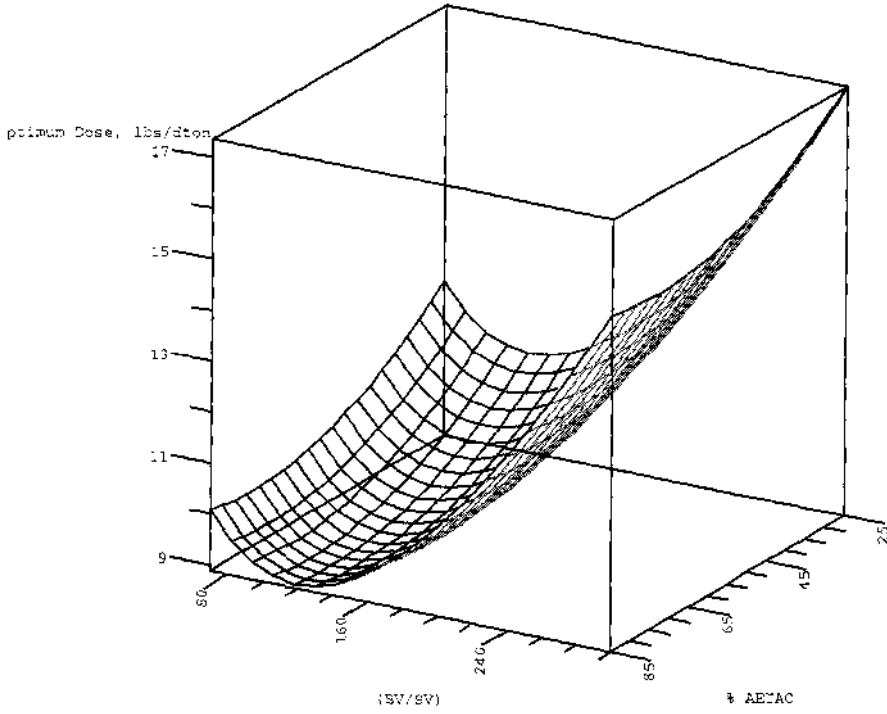


Figure 10. Optimum dose as a function of BV/SV ratio and percent AETAC of AMD-co-AETAC polymers.

REFERENCES

1. Schwoyer LK (Ed.), *Polyelectrolytes for Water and Wastewater Treatment*, CRC Press, 1981.
2. Halverson F, "Retention Aids, Drainage Aids, and Flocculants", In *Chem. Processing Aids in Papermaking: A Practical Guide*, K. Hipolit (Ed.), TAPPI PRESS, 1992.
3. Heiner HI, "Flocculating Agents", In *Kirk-Othmer Encyclopedia of Chemical Technology*, 4th ed. Vol. 11, 1994.
4. Pavoni JL, Tenney MW, and Echelberger Jr WT, "Bacterial Exocellular Polymers and Biological Flocculation," *J. Water Polln. Control Fedn.*, 1972;44:414
5. Dobias B (ed.), *Coagulation and Flocculation, Theory and Applications*, Surfactant Science Ser Vol. 47, Marcel Dekker, 1993.
6. Healy TW and La Mer VK, "The Energetics of Flocculation and Redispersion by Polymers", *J. Coll. Sci.*, 1964;19:323-332.
7. Pelssers EGM, Cohen Stuart MA, and Fleer GJ, "Kinetics of Bridging Flocculation", *J. Chem. Soc. Faraday Trans.*, 1990;86:1355.
8. Neff RE and Ryles RG, "Water Soluble Highly Branched Polymeric Microparticles", US Pat. 5,354,481 1994.
9. Morgan JE and Boothe JE, "Emulsion Polymerization of Cationic Monomers", US Pat. 3,698,037 1976.
10. Hunkeler D, Hamielec AE, and Baade W, "The Polymerization of Quaternary Ammonium Cationic Monomers with Acrylamide", In *Polymers In Aqueous Media*, J. E. Glass (Ed.), ACS Sym. Ser. 223, 1989.
11. Griebel T and Kulicke WM, "Molecular Characterization of Water-Soluble Cationic Polyelectrolytes", *Makromol. Chem.*, 1992;193:811-821.
12. Daoud M, Cotton JP, Famoux B, Jannink G, Sarma G, Benoit H, Duplessix R, Picot C, and de Gennes PG, "Solutions of Flexible Polymers. Neutron Experiments and Interpretation", *Macromolecules*, 1975;8:804.
13. Tobita H and Hamielec AE, "Modeling of Network Formation in Free Radical Polymerization, Macromolecules", 1989;22:3098.
14. Lin SC, Lee W, and Schurr JM, "Brownian Motion of Highly Charged Poly(L-lysine). Effects of Salt and Polyion Concentration", *Biopolymers* 1978;17:1041.
15. Sedlak M, Konak C, Stepanek P, and Jakes J, "Semidilute Solutions of Poly(Methacrylic Acid) in the Absence of Salt: Dynamic Light-Scattering Study", *Polymer*, 1978;28:873.
16. Matsuoka, Schwahn D, and Ise N, "Determination of Cluster Size in Polyelectrolyte Solutions by Small-Angle Neutron Scattering", In *Macro-ion Characterization*; ACS Sym. Ser. 548, K. S. Schmitz (ed.), 1994.
17. Lovell PA, private communication.

OPTIMIZATION OF COOLING WATER TREATMENT FORMULATIONS FOR USE IN RECYCLED WATERS

Paul J. Forbes

Garratt-Callahan Company
111 Rollins Road
Millbrae, California 94030

1. ABSTRACT

The drive for increased water conservation in industrial plants has expanded the use of non-traditional sources of makeup water for cooling towers. Studies of the use of recycled wastewater for tower makeup usually focus on process changes, but the focus of this paper is on the design process of custom water treatment programs for many kinds of water sources. Special problems unique to each type of non-traditional source water are identified and discussed. The use of computer software in guiding the formulation process is also discussed in detail. The components of cooling water formulations, including water soluble polymers, must be selected to deal with the unique set of problems presented by each type of water. Formulations must also be compatible with process changes, and not interfere with other processes downstream. As with other more traditional programs, cost and performance factors are critical.

2. INTRODUCTION

The need to conserve water and maintain equipment has forced us to deal with an increasingly difficult problem: How to control scale and corrosion in waters of lessening quality. Much of the existing literature deals with very large facilities where economies of scale allow for process changes. For many facilities, this is not economically feasible and other methods have to be found. Cooling towers are water saving devices, therefore, they are a natural place to look for additional water savings. Product formulators are continually asked to improve scale control and increase cycles of concentration. Developing a single product or treatment program for a variety of applications is extremely difficult,

given the variety of sources and the constantly changing character of these makeup sources.

Alternate sources of water, and sources previously discarded as unusable must be included as possible sources of makeup for cooling towers. Economical ways need to be created to help all consumers of water to achieve greater water savings. Custom formulations can easily be created using software and expertise. Water soluble polymers are being increasingly utilized in formulation for stressed conditions. Being aware of potential interactions with the source water, and available software, one can design formulations for every water consumer to meet their needs quickly and easily. This approach is much less costly and much better for some smaller consumers that are unable to make large process changes.

3. WATER CONSERVATION

3.1. Motivation for Water Savings

Water use in the United States and particularly in the arid Southwest, is rapidly increasing. Continued industrial growth, population growth, and power consumption all place demands on the finite quantity of water. Current large dependence on ground water is not sustainable. As there are no new sources of water, we must reallocate or conserve existing sources. Although irrigation, livestock, commercial and domestic use represent some of the largest consumers of water, the focus of this paper is on the thermoelectric power generation and industrial segments of water use. In these segments the non-consumptive use of water for cooling represents a potential for savings.

Steam electrical generation is the major consumer of water for cooling, but it has traditionally relied upon once-through cooling, rather than the use of wet cooling towers.

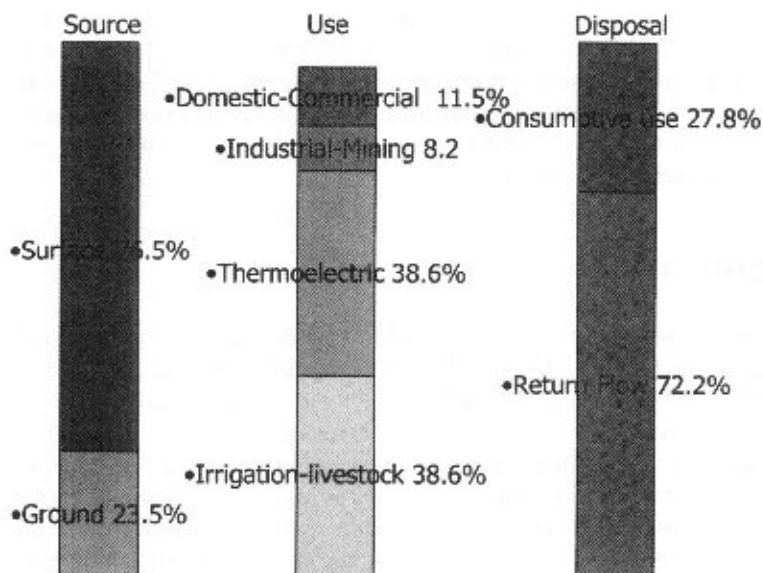


Figure 1. US. water utilization.

Domestic use	Water for household needs such as washing clothes, bathing and watering lawns (also called residential water use).
Commercial use	Water for hotels, restaurants, office buildings and other commercial facilities.
Irrigation use	Water for irrigation of crops, watering of parks and golf courses
Industrial use	Water for industrial purposes such as fabrication processing, washing and cooling.
Livestock use	Water for livestock watering, feed lots, dairies, fish farms and other farm needs.
Mining use	Water for the extraction of minerals and in the processing of ore at the mine site, or for mine operations.
Public use	Public water supplies such as firefighting street washing municipal parks and swimming pools
Rural use	Water for suburban or farm areas for domestic and livestock needs, which is generally self supplied.
Thermoelectric power use	Water for the process of the generation of thermoelectric power.

Figure 2. Water use definitions.

This percentage has shrunk rapidly from 80% once-through in 1975 to a projected 60% in 2000.¹ The conversion to wet cooling towers and to dry cooling towers has had a major impact on water use for steam electrical generation. In the industrial segment, four industries consume the majority of water: pulp and paper, chemical processing, oil refining and primary metal manufacturing. Together, these segments represent 96% of all industrial water use. Greater than 70% of water demand was for cooling.

Conservation of water is motivated by economics, and by the ways in which water is viewed. Resource usage is highly cultural, and perceptions of water use and water savings are highly subjective.² Engineers look for engineering solutions; chemists look for chemical solutions; and environmentalists look for environmental solutions. A much more common sense approach is warranted for serious conservation to occur. We must revisit previously “unworkable” solutions. Chemists need to be aware of process changes that can save water, and engineers must be aware of chemical solutions. Chemists and engineers must work together with environmentalists to provide economical environmental solutions.

3.2. Water Savings in the Design Phase, Process Changes, and External Tower Treatment for Water Conservation

Water conservation methods used by industry are manifold. Many process changes have allowed for the use of alternate sources, and the reuse of streams formerly sent to

waste. Complete reuse of blowdown has even allowed a steel mill to operate in a desert with no access to fresh water.³ Conservation methods are limited only by costs and creativity, however, conservation methods must be economically justified. Cost savings are often better than expected, since the perception is that water is cheap and plentiful. When costs are examined objectively, the return on investment is often greater than expected.⁴

Various pretreatment schemes are available to improve the quality or usability of otherwise unusable water. Sometimes several methods may be combined to optimize water quality and water savings. Often the blowdown or a sidestream is treated and returned back to the tower, which is not technically "pretreatment" but included here for convenience. Water savings should be included in the design phase for optimum benefit. Input from water conservation consultants should occur from plant design, through final construction and initial operation.⁵ The use of vapor compression evaporation, reverse osmosis (R.O.) and ultrafiltration, filtration, electrodialysis, steam stripping, and air cooling for water conservation are reported elsewhere.⁶

3.2.1. Wet Dry Cooling Towers. Wet dry cooling towers can be used to reduce water consumption with little alteration in chemical treatment. Unfortunately, the increase in efficiency comes with very high capital costs. Figure 3 shows a typical wet dry setup where air is heated and liquid is cooled via dry cooling. The heated air then contacts cooler water, enhancing efficiency and reducing fogging, due to the lower saturation.

3.2.2. Side-Stream Softening. Side-stream softening involves taking blowdown from a tower and removing hardness and returning it back to the system. Scale is controlled by removing all of the scale forming elements.⁷ There are two methods with many variations, both requiring much operator attention and careful control.⁸ The chemistry of side-stream softening is well documented in other papers.⁹⁻¹² Sludge created by cold lime-soda softening must be disposed of, which may become more difficult over time. Side-stream lime-soda softening only works if removable solids are limiting cycles of concentration. Once solids have been removed, further evaporation leads to high TDS waste. This can then be evaporated in zero blowdown schemes, or treated by electrodialysis or R.O. for even further concentration before disposal. Figure 4 shows a possible setup for sidestream lime soda softening coupled with sidestream R.O. Other methods substituting acid generated cation exchange resins for R.O. and cold lime soda softening also exist.

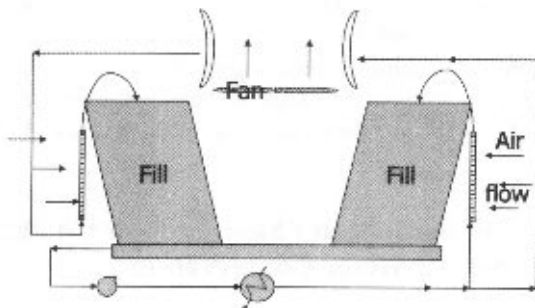


Figure 3. Wet dry cooling tower.

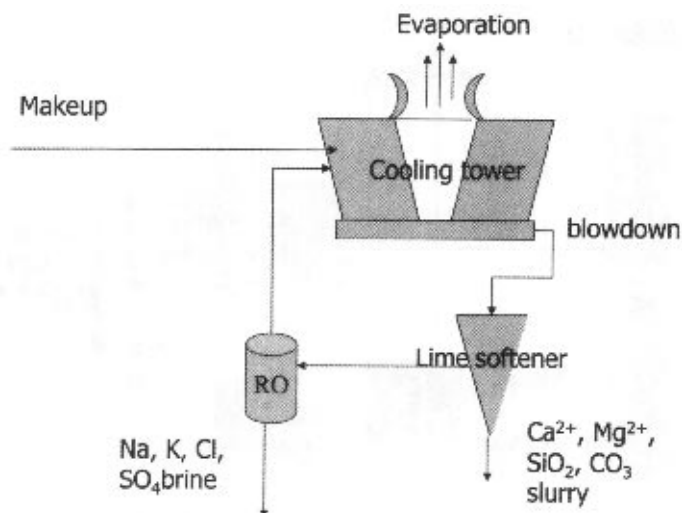


Figure 4. Side stream softening with R.O.

Lime-soda softening or reverse osmosis are usually favored over ion exchange in water conservation schemes since they do not require excessive amounts of backwash, which would defeat any water savings. Lime-soda softening or sodium cycle anion exchange zeolites are used for carbonate hardness and non-carbonate hardness removal. Anion exchange (demineralization) can be used for sulfate and phosphate removal. Lime-soda is usually preferred because it removes all precipitating elements, leaving the non-precipitating elements (like some corrosion inhibitors and biocides) behind. Lime-soda softening is also more amenable to zero blowdown schemes than other softening methods, since it removes the dissolved solids in solid form, rather than as a brine which must be further concentrated. This can be less energy intensive (or space intensive if solar evaporators are used) but generates more solids.

3.2.3. Separation of Waste Streams. Instead of having all processes utilize fresh water, systems can be engineered to alternate between various streams based on quality and availability. The best quality water is not needed for every application. Pickle water can be reclaimed for the tower in some installations. Lower quality boiler and tower blowdown can be used for slagging. There are substantial design and implementation costs to separate piping and lots of maintenance.¹³ Figure 5 shows how plant water supplies can be separated for various uses. This option may not be practical for many existing plants. Recovery and utilization schemes are popular, as is cascading water streams from one use to another.¹⁴ This involves taking condensate or pure water from process and putting it into towers. If tower control is difficult, tower blowdown may be used in another tower, rather than blowing it down or losing it.¹⁵

3.2.4. Good Housekeeping. Good housekeeping is important. One must watch for leaks, drift, and must optimize the mechanical operation of the cooling tower. All systems must be run at peak operation if water savings are important. Even with automated controls, monitoring is essential to prevent too much or too little bleed.¹⁶

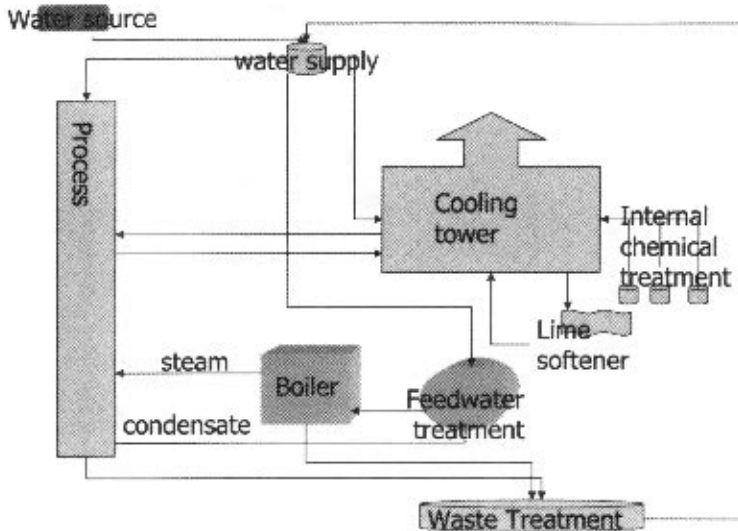


Figure 5. Plant water utilization.

3.2.5. Increase of Cycles to Eliminate Bleed or “Zero Blowdown”. Increasing cycles is related to good housekeeping. Sometimes very high cycles are achievable with little or no pretreatment. Very good quality makeup must be available. In many cases zero blowdown is achievable at 15 to 20 cycles.¹⁷ Studies of zero discharge or very low blowdown are numerous.^{18,19,20}

3.2.6. Reuse of Tower Blowdown. In addition to the above process changes affecting water savings, tower blowdown can be reused at a site for other purposes. There are many possible uses for tower blowdown, which can contribute to overall water conservation, and reduce disposal costs.

Some common uses are: deep well injection in oil fields, industrial wastewater reclamation for organics removal or stripping.²¹ Where electrical costs are low and/or waste heat for evaporation is available, concentration of tower blowdown reduces disposal cost, or reduces capital costs of construction of evaporation ponds for zero blowdown schemes.²² Situations where towers do not produce highly concentrated blowdown make the economics favorable. Figure 6 shows a possible setup. Either dilute water is used in tower 1, which is cycled up in tower 2, or concentrated blowdown in tower 1 is treated with acid, and tower 2 is made from corrosion resistant materials. This second option only works for scales that are controlled by reducing the pH, such as carbonate or calcium phosphate based scales. This option can also be very capital intensive.

4. TYPES OF RECYCLED WATER USED IN COOLING SYSTEMS

4.1. R.O. Reject

When R.O. use picked up in the early 1980’s, everyone wanted to use the R.O. reject in the cooling system, not in the best interest of water savings or cooling system operation, but due to discharge restrictions. There was simply nowhere else to put it. Once it was re-

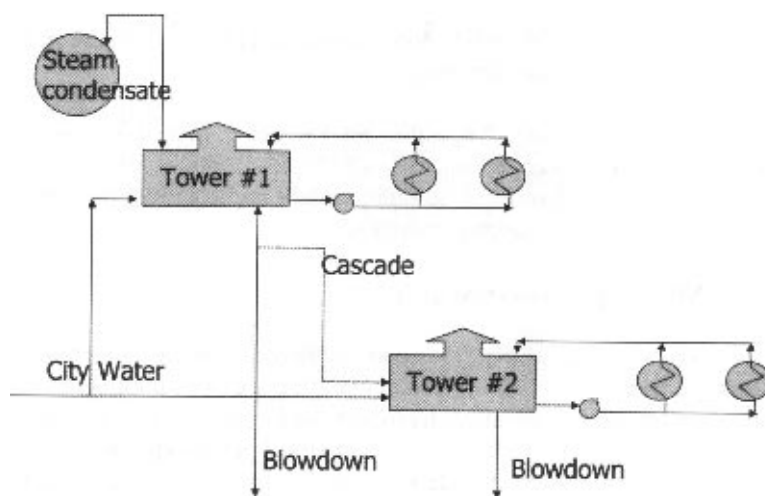


Figure 6. Cascading tower setup.

alized how detrimental this was to tower operation, the procedure was discontinued in favor of adding pH control and disposing of it to sewer, or concentrating it further and removing the solids.

4.2. Demineralizer Fast-Rinse

Demineralizer (DI) fast-rinse water is high in dissolved solids, but otherwise of good quality for use in cooling systems. High chlorides can cause the water to be very aggressive. Proper material selection for marine applications can alleviate potential problems. Hydrogen cycle cation effluent and 40% demineralized water have been used as tower makeup with zero bleedoff.

4.3. Storm Runoff

Parking lots and roofs are good collection sites for relatively good quality water. Some filtration for removal of organics and suspended solids is usually all that is required. On large sites, ponding basins, or cisterns can be created to accumulate runoff. Water may thus be provided for irrigation, industrial use, or groundwater recharge.

4.4. Agricultural Waste

Agricultural irrigation waste is high in suspended solids during rainy periods. Changes will have to be made to make agricultural wastewater more available for industrial use. Typically high in salts and fertilizers, agricultural waste can cause potential biological fouling. High phosphate levels could also cause problems in unsoftened waters. Cold lime-soda softening can, once again, be used for hardness and alkalinity removal.²³

4.5. Other Process Waters

4.5.1. Scrubbers and Air Washers. Blowdown from scrubbers usually has high levels of organics and very low pH. Adjustment of the pH, or mixture with other alkaline sources

can create relatively good quality water. Nitrification and pH adjustment can be used to remove ammonia, or other volatile elements.

4.5.2. Vegetable Wash-Water: Vegetable wash-water is high in suspended solids and dirt. It is suitable for use if flocculation, followed by filtration, or settling followed by filtration, can be done. Wash water can be more widely implemented in sugar plants using sugar beets if adequate pretreatment is developed.

4.6. Treated Municipal Wastewater

The reuse of municipal sewage waste in cooling towers was once more widespread. Municipal sewage wastewater is a large component of non-consumptive water use and the largest problem in terms of economical treatment. Since cooling towers represent some of the largest non-potable use of water and municipalities are looking for ways of disposal, the early consideration and current wide scale use of wastewater in cooling towers was a natural fit. Treatment programs were easier to run and less costly in the days of chromate corrosion inhibitors. Increasingly stringent regulations have limited the choices of corrosion inhibitors, scale inhibitors and biocides, making the use of this resource more costly. Figure 7 illustrates the cost differential experienced when the switch was made from chromate chemistry. Past cases with non-chromate inhibitors gave poor results. Chromates worked well with sidestream softening and zero blowdown schemes.^{24,25} Economics of recycling water are changing, however, as fresh water sources become limited. Restrictions or increased fees on discharge also help with the cost savings of recycling water. More costly inhibitors can now be justified.^{26,27}

Treated municipal wastewater has to have certain characteristics in order for it to work. Better quality water is available in most areas. There may be health concerns about people in the immediate area, however. Coliform bacteria and various other disease causing organisms must be monitored and controlled.²⁸ Biological control is the most difficult problem. Wastewaters have high dissolved solids, silica, alkalinity and hardness—1.5 to 3 times higher than “normal” waters.²⁹ Wastewaters also have high levels of ammonia, phosphate, suspended solids, heavy metals and organics. Removal of metals from waste waters for use in cooling systems must not compromise the corrosion or scale control downstream.³⁰

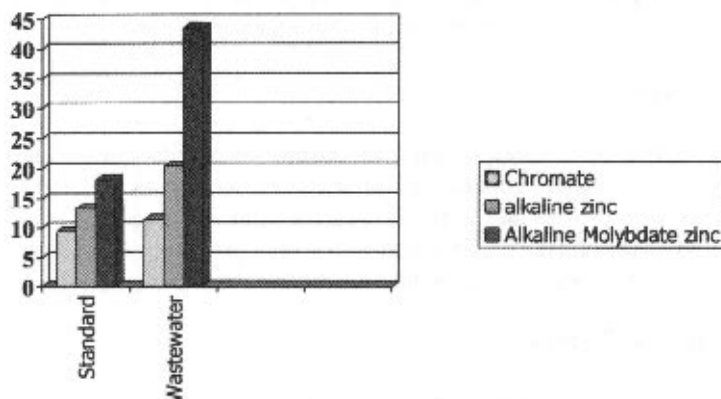


Figure 7. Projected costs for chemical treatment (\$/100,000 gal blowdown).

Extensive pretreatment is usually required prior to use in cooling systems. Filtration, nitrification, and trickling filters can be used to lower BOD and COD. The keys to successful use of wastewater are making sure that it meets requirements and a proper biocide program is in use. Procedures must be in place to substitute alternate water sources if qualifications aren't met. Foaming can also be a problem. Chemical defoamers may be required, unless there are mechanical ways of dealing with foam.^{31,32}

4.7. Biologically Treated Wastewater (Less BOD and COD)

Biologically treated wastewaters have lower BOD and COD than municipal wastewaters. Even with biological pretreatment, problems can still develop. There is a widely held perception that internal treatment should deal with everything. Massive calcium phosphate, biological sliming and foaming problems can occur without adequate external pretreatment. If only internal treatment is used, very high chlorine dosages and very high levels of inhibitor are required to make the program work.³³

4.8. Sea Water

Cooling towers can be run using seawater. Luckily, there is a lot of data on the use of seawater for cooling. The number of cycles is limited, but in marine locations, water quality is the issue, not quantity. Proper pretreatment and biological control along with proper materials selection make this a viable option. Sodium cycle cation exchange water would have many of the same characteristics, and therefore, the same precautions would apply.

Parameter	Recommended Limit
Cl	500 mg/l
SO ₄	200 mg/l
HCO ₃	24 mg/l
PO ₄	4.0 mg/l
Silica	80 mg/l
Al	0.1 mg/l
Fe	2.0 mg/l
Mn	0.5 mg/l
Hardness	600 mg/l
Calcium	600 mg/l
Magnesium	150 mg/l
Total Alkalinity	600 mg/l
PH	6.5-9.0
TDS	1000 mg/l
COD	40 mg/l
BOD	15 mg/l
Organics	1.0 mg/l
Ammonia	40 mg/l
Turbidity	50 NTU
TSS	10 mg/l

Figure 8. Recommended cooling water quality criteria for makeup water to recirculating systems.

4.9. Low TDS Water

Corrosivity can be controlled with proper chemical treatment. It can be mixed with other water streams to achieve better results.³⁴

4.10. Boiler Blowdown

Boiler blowdown is usually too high in solids for use as tower water, but under the right circumstances, it may be used to augment sidestream softening. It has phosphate and alkalinity, which would help precipitate hardness. Since in most cases boiler blowdown is already soft, it makes sense to include it when side stream softening is in use. High phosphate can be a problem unless polymers are used to prevent calcium phosphate dropout. Because boilers tend to be fairly tight systems, it is unusual to have enough blowdown for cooling needs.

4.11. Boiler Condensate

Boiler condensate would appear to be good quality water for cooling systems. It makes much more sense however to return it back to the boiler. If it is contaminated and cannot therefore be returned, it may be better to use it to dilute tower solids and achieve higher cycles than return it to the boiler. Contaminants would be iron, hardness, and amines. Since limits on hardness and iron are much tighter for boilers than for cooling systems, it is unlikely that a condensate would be unsuitable as tower makeup unless the water in the tower were already low in TDS and hardness. As with boiler blowdown, quantities are usually limited.

5. FORMULATION OF PRODUCTS FOR RECYCLED WATER

The primary goals of water treatment are to control scale, corrosion and biological fouling. This involves addition of chemicals. The quantity added and other factors related to use are gathered from system monitoring. How chemicals are being fed, and the conditions that exist within the system are often more important to the success of the overall program than the choice of product. If service is not included with the chemicals purchased, then in-plant monitoring of the program by qualified personnel is essential.

5.1. Scale Inhibition

5.1.1. K_{sp} and Simple Indices. K_{sp} values and simple indices have given way to complex computer models that incorporate solubility product, Gibbs free energy and multiple ion pair solutions. Most of the heavy mathematics can be discarded. Towers are non-ideal environments. Multivariate equations and constantly changing conditions make prediction of tower chemistry similar to weather prediction. Flow conditions, CO_2 from the atmosphere, sunlight, and temperature flux can all simultaneously affect conditions. So much data would be required so frequently as to make calculations pointless. It is not possible to measure all of the important parameters even if we wanted to.³⁵ Multiple page equations exist simply for predicting pH, therefore it is not a simple matter to calculate scaling indices for every possible ion pair.³⁶

Precipitation of solids has more to do with kinetics than with solubility products. Long retention times are just as critical as high levels of scale forming elements. It is eas-

ier to prevent scale in systems with high levels of scaling potential, if bleed is high, than moderate levels in systems with 3-week retention times. Many studies have been done on supersaturated solutions. Some calcium carbonate and calcium sulfate supersaturation models have been created.³⁷ Traditional indices do not accurately predict scaling tendencies at very high cycles of concentration. In contrast, non-equilibrium conditions of towers limit effectiveness of predictive models based on thermodynamics. Therefore, precise prediction of scaling must be based on pilot studies or field test. In most studies done, scaling was much more related to kinetics than to equilibrium conditions. Scales formed under very high cycle conditions will precipitate as mixed scales.³⁸

5.1.2. Software. Software is helpful from the standpoint of incorporating many different indices, incorporating complex ion pairs, and position relative to supersaturation. Field experience and knowledge of chemical application allows modern water chemists much more freedom to design programs. Due to the complexity of the calculations, computer programs are now used almost exclusively. Their use has been especially prevalent in smaller water treatment companies. These computer programs are useful in that they graphically illustrate scaling indices and potential. It is important to make sure K_{sp} alone is not used and that kinetics, and/or pilot studies are also used to make final adjustments to the program.

5.1.3. Phosphonates and Polymers. In order to extend the range of the predicted solubility limits, various scale inhibitors are used. Scale inhibition is usually achieved with a blend of phosphonates and water soluble polymers. Phosphonate and polymer selection is critical to the success of the program.

Phosphonates sequester calcium and provide scale control in hard water through a phenomenon known as threshold inhibition. A blend of phosphonates is usually better for controlling scale under a variety of conditions.³⁹ Generally only small quantities are required. Phosphonates containing nitrogen are less stable in the presence of chlorine. Zinc and alkanolamines are implicated in protection of some phosphonates from attack by chlorine. Bis-phosphonates containing nitrogen such as amino-*tris*-methylene phosphonic acid, AMP, effectively inhibit calcium salts and are widely used but are suitable only where chlorine is not used.

Formulation work based on other phosphonates show that 1,1-hydroxyethylidene-1-disphosphonic acid, HEDP, works well where chlorine precludes the use of AMP. Under non-stressed conditions, HEDP is superior in its cost/performance ratio to 2-phosphonobutane-1,2,4-tricarboxylic acid, PBTC. HEDP has poor hydrolytic stability with long retention times, or high concentrations of chlorine. Furthermore, HEDP should not be used in systems with soft water, as it can accelerate the corrosion of copper and zinc. Zinc is implicated in stabilizing aggressiveness on copper.

A blend of polymaleic acid and PBTC forms the base of most "stressed condition" formulations. PBTC is not considered a true phosphonate, due to the presence of only one phosphonic group, and is more like a polycarboxylic acid, such as gluconic or heptonic acid. This gives enhanced solubility under very high calcium (stressed) conditions. PBTC formulations are recommended where the Ryzner scaling index (RSI) values are below 4.5.

A wide variety of water soluble polymers are used in water treatment. Polyacrylates are used for calcium carbonate and general suspended solids dispersion. Polymaleates, and polyacrylic/polymaleic blends have higher calcium tolerance. Where hardness is removed, other types of scale such as silica and iron phosphate can occur. These must be dealt with using specialized polymers. These polymers have a variety of functional groups and are

commonly referred to as terpolymers. Terpolymers have the ability to prevent a wide variety of scales and are routinely added in small amounts to all formulations. Terpolymers become critical in reuse situations where high levels of many different ions exist and many types of scale must be inhibited simultaneously.⁴⁰ Some terpolymers exhibit good performance on silica, iron, and phosphate scales. Maleic anhydride polymers work the best for side-stream softening applications. The low charge density allows it to be recycled and prevents interference with the side-stream softening process.⁴¹

A blend of polymers is usually used to balance the formulation's ability to handle both calcium scale and phosphate stabilization. As more deposit forming elements such as zinc, silica, iron, silt and others are present, more types of polymer are needed. For simplicity, one polymer that has the greatest ability to handle the most elements is desirable.

5.1.4. Selection and Dosage. The amount of treatment chemical used depends on the amount of scale forming elements in solution. It is best to start with a 2:1 ratio of polymer to phosphonate.⁴² The higher the calcium, the more polymer is required, even up to a 3:1 ratio. As the RSI approaches 4.5 a switch from HEDP to PBTC and a switch from straight polyacrylate to a polyacrylate-polymaleate blend is recommended. In systems running high cycles, the HTI (Holding Time Index) is much greater, and HEDP can break down. This can aggravate calcium control, and since HEDP contains phosphonate group, it can contribute to phosphonate scale. In such situations, more polymer could be used, or a switch to PBTC, a more stable phosphonate is recommended.⁴³ Also as the HTI increases, conditions in the tower approach equilibrium, and kinetics are less important, therefore higher dosages of all scale inhibitors are required. Generally 20 ppm polymer is sufficient for the most rigorous conditions, making water soluble polymers very cost effective. Special terpolymers for control of silica up to 350 ppm as SiO_2 should be fed at up to 40 ppm.

5.2. Corrosion Inhibitors

A good corrosion control program makes the best of the given conditions. External pretreatment should be used in conjunction with internal treatment to provide the most favorable conditions for protection of all metals in the system. Internal treatment attempts to inhibit corrosion of all metals over the widest possible range of conditions.

5.2.1. Alkaline vs. Acid Programs. Historically, it was common to control scale by using pH control, and adding inexpensive corrosion inhibitors such as zinc, phosphate and chromate to control corrosion. This has been replaced in many locations by "alkaline programs". Alkaline programs allow the natural alkalinity to cycle up and aid in passivation and protection of metal components. Sometimes no direct corrosion inhibitors are added to alkaline programs. Under very alkaline pH >9.0 conditions, only phosphonate and polymer are required.⁴⁴ Small amounts of phosphate or molybdenum can be added to prevent pitting and as a tracer. Good corrosion control is usually achieved by adding corrosion inhibitors that work at both the anode and the cathode; thus most cooling formulations will contain both anodic and cathodic inhibitors.

5.2.2. Selection and Dosage. Molybdate/zinc and molybdate/phosphonate programs work well for alkaline programs. They combine anodic and cathodic protection of ferrous metals. The reduction in the use of acid will occur independently from water conservation trends.⁴⁵ Zinc/Molybdate inhibitors with BCDMH as a biocide work well with high pH corrosive water.⁴⁶

Zinc is a cathodic inhibitor that is very cost effective, however, there are restrictions on its use. If a method can be found to recover the zinc, such as in lime-soda softening, it could be used more widely. It works very well in conjunction with other inhibitors such as molybdenum and phosphonate. It is not effective in alkaline programs above pH 8.3.

Orthophosphate is usually combined with polyphosphate for corrosion control. The combination is very cost effective and combines both cathodic and anodic protection of system metallurgy. The drawback of this formulation is controlling the ratio of phosphate, calcium, and pH. A high performance polymer must be used to prevent the unwanted precipitation of the calcium phosphate. The less calcium present, the more orthophosphate is required to control corrosion. If water hardness is subject to change, feeding the orthophosphate and polyphosphate in separate product allows the ratio to be controlled at will.

Organic azole is added to formulations for the protection of copper and copper alloys. Some aromatic azoles have been developed for the protection of aluminum, and steel as well. Generally small amounts are required. The presence of copper ion in solution and high levels of chlorine increases demand.⁴⁷ Azoles are recommended in all formulations even if no copper is present, for the prevention of copper plating out on mild steel, which can cause galvanic corrosion of ferrous metals.

Inhibitor type and dosage is dictated by the corrosiveness of the program and the pH. The higher the pH and alkalinity, the less corrosive the water is. At very high cycles, the trend reverses itself as high TDS interferes with corrosion inhibition mechanisms. Regulations also affect choice, as there are restrictions on use of molybdenum, zinc and phosphate. Stabilized phosphate programs are generally the most cost effective, while molybdenum phosphonate programs give the best results. The wide dosage range of molybdates and phosphonates allows them to be used under a variety of conditions without fear of interaction or precipitation.

5.3. Bio-Control

Control of algae, bacteria, fungi and other organisms is essential for efficient cooling system operation. This is usually not possible in a dirty system. Frequent manual cleanings, and/or filtration are required.

5.3.1. Slug or Continuous Chemical Feed. Biocides can be fed continuously to maintain a constant level, or slug fed to provide shock treatment. Continuous feed gives tighter control, but is much more expensive than slug feeding. The goal is to prevent growths that would interfere with the normal operation of the system, not maintain crystal clear, germ free water.

5.3.2. Selection and Dosage. A variety of biocides are available. Usually an oxidizing and non-oxidizing biocide is recommended. Chemical interactions are of primary concern with oxidizing biocides. Anything oxidizable will create a demand for more biocide. Unless filtration and organics removal are incorporated, biological control can be difficult in systems with high cycle of concentration or high levels of organics. Continuous chlorination is the most common biocide program. Isothiazolone and shock chlorination have been shown to work well.⁴⁸

Widespread use of chlorine, once the rule, has been affected by regulatory concerns over chlorine and chlorinated organics. It is not as effective as other biocides but is much less expensive.⁴⁹ The pH should be below 7.5 for effective chlorination, otherwise addition of bromine, or non-oxidizing biocides is recommended.

5.4. Contaminants That Affect Water Reuse

5.4.1. Stable Organics. Stable organics can exist which will not be broken down by biological or chemical action. Foaming can be the largest problem encountered. ABS (alkylbenzene sulfonate) surfactants are still in use. These and other non-biodegradable surfactants can cause problems. At the time of their widespread use, no mechanical designs were available to help with foam. The only solution was an expensive chemical one.⁵⁰

5.4.2. Degradable Organics. Degradable organics are easier to deal with but they create chlorine demand, BOD, and COD. Where chlorine is not used continuously, biological growth, foaming and odors are a problem. Chlorine is the most common method for dealing with organics. There is a concern however with formation of chlorinated organics. Foaming and odors can still be a problem. SRB's (sulfate reducing bacteria) and other damaging anaerobic bacteria are more common in tower heavily laden with suspended solids and organics. Organics can foul ion exchange columns, but organics can also be removed by ion exchange since most organics are ionic. This process is best coupled with high molecular weight adsorption/exchange with granular activated carbon downstream. In such streams a 93–95% reduction of TOC is possible.⁵¹ Bioaugmentation is probably the most effective method for breaking down high levels of organics, but requires large areas for aeration and is subject to odor problems. Large capital costs may make this unworkable.

5.4.3. Ammonia. Ammonia or chloramines can cause SCC (stress corrosion cracking) in admiralty, even in the presence of azole.⁵² Ammonia is both a nutrient and a corrosive agent. Nitrification eliminates chlorinated organics and associated regulatory and odor concerns. Nitrification also eliminates corrosion potential of ammonia and potential chlorine demand. It requires lots of space and operator attention, however. The more ammonia there is to remove, the larger the capital costs involved.

5.4.4. Phosphate. Phosphate is a nutrient, but unlike ammonia, it is also a corrosion inhibitor. Too much phosphate can cause problems by precipitating with iron or calcium. Precipitation of phosphates is controlled in most cases by water soluble polymers. Side stream softening can be used for phosphate removal in high calcium waters. The perception in the industry is that softening is easier than pH or chemical control. This is not always the case. In most cases, it is better to leave the calcium and phosphate in and control the pH. Under these conditions, water soluble polymers perform an excellent role as calcium phosphate inhibitors. In systems using a phosphate based corrosion inhibitor it is important to keep the amount of phosphate contributed by the makeup in mind.

5.4.5. Potassium. Potassium is a nutrient. It has excellent solubility and is therefore used in a lot of formulations. In systems with very high cycles, potassium salts can build up and cause biological problems. Lower concentration sodium based formulations may be required, or increased biological control may be necessary. Like phosphate, it may act as a nutrient for biological growth downstream.

5.4.6. Hardness. Hardness can be much higher in recycled water. The water can be softened before going into the tower, mixed with a stream of lower hardness, or the entire system could have side-stream softening.

5.4.7. Silica. Silica is a problem in some waters and can greatly reduce the available cycles of concentration. R.O. and some types of deionization can remove silica, but everything else is removed as well. Side-stream softening using the cold lime-soda method works well if there is enough magnesium present. If not, it can be added in the form of magnesium hydroxide or magnesium chloride. Control of silica can also be achieved by the use of terpolymers. These water soluble polymers have extended the normal operation range of cooling systems. Under non-alkaline conditions the industry standard was 150 ppm as SiO_2 . Under alkaline cooling system conditions, this could be extended to 180 ppm as SiO_2 . Current technology allows steady trouble free operation at 350 ppm silica. High levels of polymer coupled with PBTC have removed existing silica deposits on-line without the need for ammonium bifluoride and hydrochloric acid cleaning.

5.4.8. Metals. Some of the largest users of industrial water are metals producers. A variety of metals can be contaminants in wastewaters. Aluminum and steel production require large quantities of water for production. Aluminum can precipitate to form aluminum sulfate or hydrated aluminum silicate deposits. Copper can aggravate corrosion problems on mild steel, but helps with algae control. Copper has been used for years as an algaecide. Iron is the most common metal found in cooling systems. It is the most common in towers using recycled water as well. Because corrosion of steel in cooling systems produced lots of iron, cooling systems have been developed over the years to deal with high iron levels. Polyphosphates or phosphonates can work in the absence of calcium. If phosphonates are being fed for calcium control, more must be fed in the presence of iron since iron can "poison" some polymers and tie up available phosphonate.

5.4.9. Suspended Solids. Suspended solids are a problem in cooling towers due to the large volumes of air processed. Anything contained in the air will be washed out and transferred to the tower. Conditions favorable to the growth of microorganisms can generate much material of biological origin. There is no way to remove solids from the system except for periodic physical cleaning, filtration or blowdown. In water savings schemes, blowdown is minimized. Unless frequent manual cleanings are performed or filters are installed, fouling problems or decreasing cycles are the consequence.

Suspended solids drop out in low flow areas, which causes anaerobic conditions. A type of corrosion called under-deposit corrosion is the result. If biofilms exist, suspended solids stick and rapidly insulate heat transfer surfaces, which reduces energy efficiency and can cause equipment shutdowns.

5.4.10. Dissolved Solids. Dissolved solids are the primary concern where side-stream softening is used. All precipitating solids are gone, and all that is left are organics and TDS (total dissolved solids). A problem with high TDS is staining or crust formation on tower fill, cars, or any structure nearby. High TDS also increases the potential for corrosion. Only titanium or A1-6x was found to be corrosion resistant to TDS at very high cycles.⁵³ Mild steel is unacceptable for use in marine or high TDS applications. For some applications using recycled water, new cooling tower designs are required.

5.4.11. Chlorides. High chlorides from softener or demineralizer fast rinse, seawater, or high TDS water can aggravate corrosion control. Chlorides, as low as 200 ppm, enhance SCC (stress corrosion cracking) of stainless steels. Increased corrosion of mild steel is a concern as well.

5.4.12. Surfactants. Surfactants are surface active agents that alter the wetting properties of water. High levels of surfactants can cause foaming problems. They can be broken down by the use of chlorine or other oxidizing biocides. Environmentally friendly surfactants can be broken down organically. Foaming can be controlled with the use of a commercial antifoam, but these can be difficult to use and can be very expensive.

5.4.13. Oil or Grease. Oil or grease can cause foaming problems as well. High alkalinity can contribute to foaming problems. They can also act as nutrients. Microorganisms can break down hydrocarbons. This can cause fouling problems, and high chlorine and oxygen demand. Where anaerobic conditions develop SRB's can proliferate. They can be dispersed with organic solvents, such as glycols or alcohols or broken down by microorganisms. The best way to eliminate problems is by tracking down the source and eliminating it, or pre-treating the water with microorganisms to remove it prior to use.

5.4.14. VOC's. Volatile organic carbons, or VOC's are usually flashed off from cooling towers. If odors or regulatory concerns are a problem, adsorption onto activated carbon and incineration are required.

5.5. Process Compatibility

All of the chemicals used for internal treatment should be compatible with materials used upstream, as well as downstream. In cascading systems or reuse systems, many chemicals are added and many contaminants are picked up. The formulations used must be selected to minimize interaction. All of the contaminants listed above and all of the inhibitors listed in the formulation section should be cross-checked to see if there are any potential problems.

5.5.1. Upstream. In towers where makeup is from process or a treated waste stream, all chemicals added upstream must not interfere with chemicals used for corrosion control, biological control or scale control. An example is where a cationic waste treatment polymers was fed at high levels to reduce heavy metals, but precipitated with anionic components added as scale inhibitors.

5.5.2. Downstream. Internal chemical treatment must not interfere with downstream processes. Scale inhibitors selected for use in the cooling system can interfere with the lime-soda softening process. Zinc used for corrosion control and biocides used for biological control can cause problems downstream due to toxicity. Alternate choices are usually available.

5.6. Cost Comparison of Various Programs

Oxidizing biocides have the advantage of relatively low cost, and quick action. There are many disadvantages however, including, chemical interaction with organics and organic inhibitors, formation of hazardous compounds, increased corrosion of system components, short shelf life, inactivation by ammonia, stripping by air at lower pH, and inactivation at higher pH.

Non-oxidizing are more expensive, but more specialized in their action. In general they are less reactive to system components and chemical treatments, and more amenable to use in a variety of recycled waters.

In general zinc and phosphate are inexpensive programs, while molybdate and all organic programs are more expensive. Use of certain types of waters, cycles limitations, or

regulatory constraints may make some programs more attractive. It is important to consider all costs, so that a valid comparison between process changes and internal treatment changes can be made.

5.7. Monitoring

All aspects of the program need to be monitored to insure success. Any tests performed under a “normal” treatment program should be done at an increased frequency in systems using recycled water.

5.7.1. Bio-Monitoring. The biological program can be monitored through visual observation, plate counts, dip slides, specific tests for SRB's, and condenser approach temperatures. Deposition monitors, that inferred fouling with pressure drop through the unit, are no longer available. Testing by this method gave mixed results.⁵⁴ The other methods are readily available and easy to perform. Newer tests utilizing ATP enzymes are usually not recommended for towers due to their poor accuracy at low levels of biogrowth, and their inability to differentiate between viable and non-viable cells.

Any changes anticipated to affect the biological control program should be accompanied by an increase in testing frequency. It is especially important to focus on sessile bacteria, which can form slimes.

5.7.2. Corrosion. Corrosion monitoring should focus on the materials used in the system and a good baseline should be established before starting any new treatment program, or process change. Both test strips (corrosion coupons) and instantaneous monitors should be used.

5.7.3. Scale. Scale can be monitored with the use of a deposition monitor. Visual observation of a heated probe gives indications of relative scale thickness on condenser tubes. This method of scale monitoring only works with scales with inverse solubility. Silica scale monitors are not commercially available. Frequent visual observation and rapid analysis of any samples are usually sufficient.

5.7.4. Inhibitors. Scale and corrosion inhibitors must contain something that is easy to test for. An easy to use test kit or on-line monitor is not necessary, but greatly increases the comfort level of most customers. Mathematical calculations are usually not sufficient to assure accurate dosing so some testing is required. The frequency of testing should be as often as necessary to assure enough chemical is present. It is not necessary to test for slug fed biocide levels, since the contact time is usually limited, and levels are changing constantly over time. An important aspect of testing is that the thing you are testing for must not add cost and must not interfere with other tests or processes.

6. TWO CASE STUDIES

6.1. Outline of the Optimization Process

Two cooling water formulations were created using the principles discussed so far. The process consisted of the following steps:

1. Analysis of the water proposed for use in the system
2. Survey of pretreatment and post treatment to evaluate any potential interactions
3. Entering data into computer program and generating scale forming tendency graphs
4. Survey of monitoring and pretreatment equipment and suggesting necessary improvements.
5. Creation of formulation based on corrosion, scale and biological fouling potential, and chemical interaction potential
6. Bench testing of formulation to test for stability and suitability
7. Field trial

6.2. Product Development

The product development model outlined here for synthetic or recycled waters differs from the standard development model in several important ways. The important differences are the emphasis on avoiding potential interaction, monitoring, and the use of computer software to predict potential for multiple chemical interactions.

6.3. Case Studies

The first case illustrates the differing scaling potential of two well waters for which one formulation had to be created. In well #2 water silica is limiting cycles. Well #1 water

Parameter	Well Water 1	Well Water 2
pH, as pH units:	7.26	7.73
Phenolphthalein Alkalinity as CaCO ₃	0.0	0.0
Total Alkalinity as CaCO ₃ :	100.0	68.0
Chloride, as Cl	51.0	9.0
Sulfate as SO ₄ :	13.0	8.0
Silica, as SiO ₂	44.0	89.0
Total Hardness as CaCO ₃ :	72.0	42.0
Calcium Hardness as CaCO ₃ :	49.0	28.0
Magnesium Hardness as CaCO ₃ :	23.0	14.0
Specific conductance, μ mhos:	488.0	192.0
Orthophosphate as PO ₄ :	13.0	<0.2
Nitrate as NO ₃ :	42.0	4.5
Appearance:	Clear and Colorless	Clear and colorless

Figure 9. Case study #1, two well waters. Note the high levels of silica in well #2 and nitrate and phosphate in well #1.

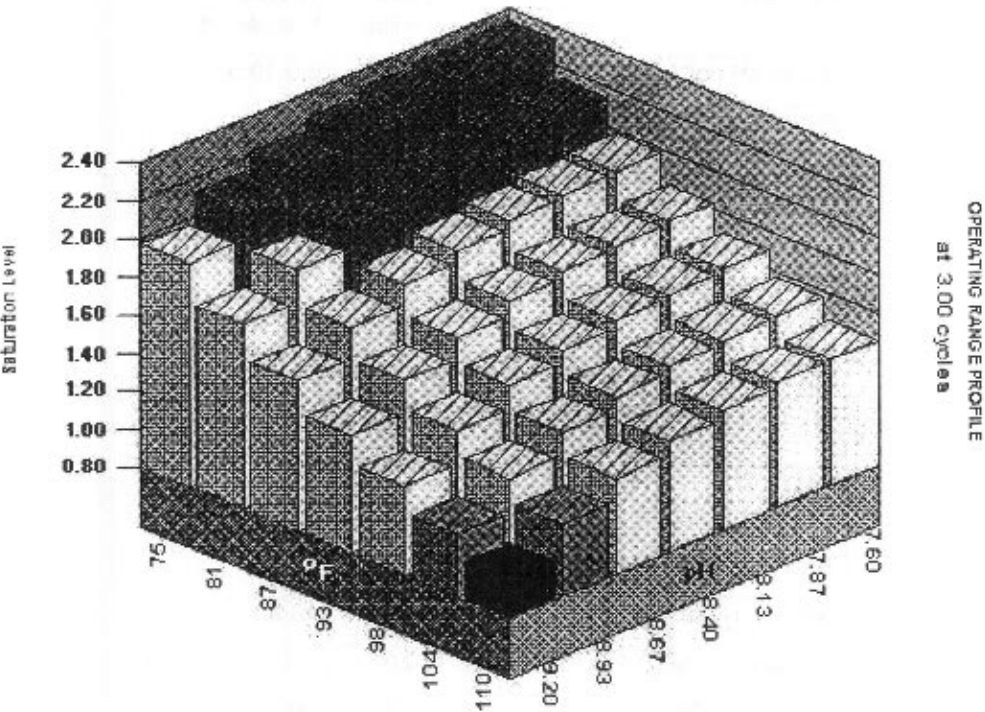


Figure 10. Silica saturation level.

had moderate levels of silica, but was high nitrate and phosphate, indicating a potential for calcium phosphate scale. In this case high silica dictated the use of a silica control polymer. Excellent calcium and silica control was provided by PBTC and terpolymer. Three years later, silica is still being removed and between 250 and 300 ppm of silica is maintained in the system.

The second case study illustrates the scaling potential of a well water and recycled wastewater for which one formulation had to be created. The first water is well water with high silica, and no phosphate. The second water is a synthetic water. It is a combination of acidic process water and city water R.O. reject. A product could be designed for either water, but the logistics of feeding one product for each type of makeup were deemed to difficult to handle. Additionally, there was the potential for the two waters to mix within the tower.

A single product had to be created to handle corrosion and scale of the individual water as well as potential mixtures of each. The most difficult problem was preventing high levels of phosphate in the synthetic water from combining with the high levels of calcium in the well water. Since calcium phosphate rather than silica was the concern here, a polymer with better calcium phosphate inhibition properties was selected. It was theorized that the difference in structure would only moderately affect the formulations ability to control silica scale while gaining a great cost performance advantage over the traditional silica control polymer. High levels of ammonia in the wastewater dictated much higher levels of triazole to control corrosion of copper alloys. Because wastewaters are more variable, flexible programs had to be developed. Much more monitoring and much more

Parameter	Well water	Treated Wastewater
pH, as pH units:	7.27	6.0-10.0
Phenolphthalein Alkalinity as CaCO ₃	0.0	0-40
Total Alkalinity as CaCO ₃ :	70.0	60-90
Chloride, as Cl	10.0	10-900
Sulfate as SO ₄ :	63.0	200-1200
Silica, as SiO ₂	52.0	10-70
Total Hardness as CaCO ₃ :	92.0	10-30
Calcium Hardness as CaCO ₃ :	73.0	6-24
Magnesium Hardness as CaCO ₃ :	19.0	2-12
Specific conductance, μ mhos:	291.0	2000-4000
Total Organic Carbon (TOC)	0.0	15-90
Orthophosphate as PO ₄ :	0.1	10-80
Ammonia as NH ₃	0.0	0-100
Nitrate as NO ₃ :	2.4	10-30
Appearance:	Clear	Clear

Figure 11. Case study #2, well water and treated wastewater. Note the high levels of phosphate in the wastewater and moderate levels of alkalinity and calcium in the city water. The mixture results in a high potential for calcium phosphate scale formation.

field evaluation had to take place. The more variables are encountered, the more difficult prediction becomes.

6.4. Discussion

It was important to know what the various scale forming elements were, and what to incorporate in the formulation to control both ends of the spectrum. For brevity, not all of the tables and graphical output are included here. It is important to include any chemicals added (i.e., phosphate) in the calculations. In both cases process changes were recommended to optimize the corrosion and scale control process. Biocide programs changed at both locations as a result of changes in the water chemistry. The most critical step in the process is to start with good data. Multivariate graphs are much more reliant on good data than simple indices.⁵⁵ The focus on data collection, and the use of computer software in these predictions was instrumental to the success of the programs.

Such computer software provides a distinct advantage over traditional methods as a tool to reduce costs and optimize treatment. Because conditions are rarely the same, a dynamic model must be set up to optimize water savings and optimize program parameters.

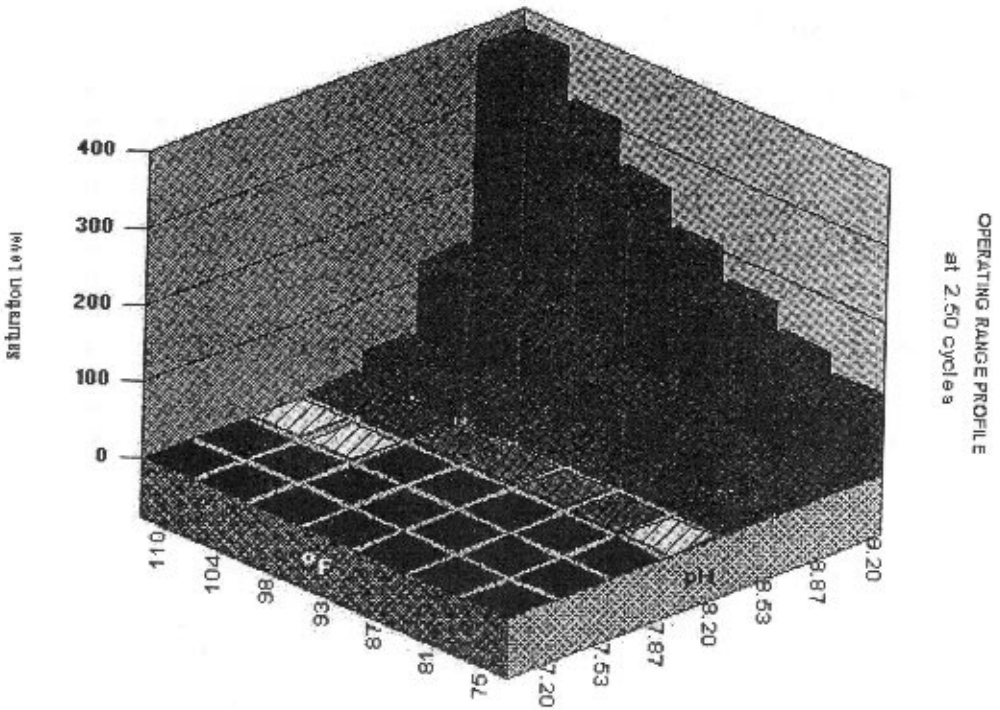


Figure 12. Calcium phosphate saturation.

In addition to simple indices and ion pair solutions, there is always a potential for interactions. Simply plugging numbers into a computer program does not guarantee good results. Field experience must be utilized to get the most out of any software package. The need to constantly recalculate and change the program is not a problem. Chemical formulations can be changed relatively easily.

7. SUMMARY

Industry has implemented many changes to increase conservation of water. Alternate sources of water are acceptable if process changes are made. The improvements in scale inhibitor technology, and system monitoring have largely been ignored or underexploited, and in many instances, alternate sources are usable simply with optimization of internal treatment. Computer software and knowledge of cooling water chemistry allow for the development of many kinds of formulations to meet the need for constantly changing conditions. Knowledge of various sources and their potential problems allows selection of appropriate corrosion, scale and biological growth inhibitors. Compatibility with process changes and equipment both upstream and downstream is important for product selection. An increased emphasis on monitoring, awareness of interactions and use of software is necessary for optimization of internal treatment programs. Costs of internal treatment optimization need to be compared with process changes in order to find the proper choice for the maximum return on investment.

8. CONCLUSION

There is very little information available on internal treatment for cooling systems using recycled water. The focus in the literature was on process changes. The only papers on internal treatment dealt specifically with either zero blowdown or the reuse of municipal wastewater in cooling systems. Most of the literature was written during the era of chromate and acid use. The switch to more alkaline treatment programs and the recent technological innovations in the use of water treatment polymers for scale control were not mentioned anywhere. The time was right to revisit the topic and look at the data objectively.

Cultural ideas, or individual or corporate perceptions (our world view) affect our responses to questions asked. We must be aware of these faults and constantly challenge our ideas and make sure that they are achieving our goals. Older paradigms die slowly. We must ask the question "is it now better to use internal treatment to increase cycles of concentration or spend money on process changes? This type of inquiry is rarely done. A large variety of water soluble polymers has exploded onto the scene. Are they really allowing significant water savings, and if they are, why aren't they being utilized? If they are they must be quickly integrated, and reevaluated as conditions and technology change.

REFERENCES

1. Brewer R, and McAuley PH. "The National Assessment Of Water Resources: Implications for the Cooling Tower Industry" Cooling Tower Institute Technical Paper 179-A, January, 1978.
2. Goldblatt M. "Innovative Thinking in Water Conservation" Cooling Tower Institute Technical Paper 94-09 February, 1994.
3. Stanton FP. "Water conservation from the standpoint of private industry" Cooling Tower Institute Technical Paper 54-A, January, 1968.
4. Owens A. "Water Reuse Programs can be Self Supporting" Industrial Water Treatment, November, 1993.
5. Webber BM and Owens AD. "The Importance of Water Management in Plant Design" Cooling Tower Institute Technical Paper 84-2, February, 1984.
6. Holiday A. "Conserving and Reusing Water", Chemical Engineering, 1982;4.
7. Perry MI and Matson JV. "Complete Reuse of Cooling Tower Blowdown" Cooling Tower Institute Technical Paper 145-A, January, 1975.
8. Hennings J, Misenheimer C and Templet H. "Side-Stream Softening of Cooling Tower Blowdown" Cooling Tower Institute Technical Paper 166-A, January, 1977.
9. Knight JT. "Chemistry of Sidestream Softening and Silica Reduction" Cooling Tower Institute Technical Paper 234-A, January, 1981.
10. Perry MI and Matson JV. "Complete Reuse of Cooling Tower Blowdown" Cooling Tower Institute Technical Paper 145-A, January, 1975.
11. Matson JV and Mouche WG. "Demonstration of a Maximum Recycle Sidestream Softening System at a Petrochemical Plant" Cooling Tower Institute Technical Paper 85-5, January, 1985.
12. Bydalek H, Hass KF, Mann CR and Le Page LR. "Use of Brackish Water in a Zero Discharge Cooling System" Cooling Tower Institute Technical Paper 223-A, January, 1980.
13. Stanton FP. "Water conservation from the standpoint of private industry" Cooling Tower Institute Technical Paper 54-A, January, 1968.
14. Weston RF and Sitman WD. "In-Plant Water Conservation in the Pollution Abatement Program" Proceedings of the International Water Conference #24, October, 1963.
15. Goldblatt M. "Innovative Thinking in Water Conservation" Cooling Tower Institute Technical Paper 94-09, February, 1994.
16. Farris CA Jr. "Proper and Efficient Operation of a Cooling Tower Water System" Cooling Tower Institute Technical Paper 79-A, January, 1970.
17. Geiger GE, Off F and Hatch MR. "Chemical Approaches to Zero Blowdown Operation" Cooling Tower Institute Technical Paper 93-05, February, 1993.

18. Goldblatt M. "Industrial Water Conservation – Zero Discharge or Partial Wastewater Reuse" Industrial Water Treatment, March, 1995.
19. Alfano S. "Water Conservation via New Cooling Water Technology" Cooling Tower Institute Technical Paper 95-05, February, 1995.
20. Bydalek H, Hass KF, Mann CR and Le Page LR. "Use of Brackish Water in a Zero Discharge Cooling System" Cooling Tower Institute Technical Paper 223-A, January, 1980.
21. Chapman, Cornell, Howland, Hays and Merryfield. "Water Reclamation at Lake Tahoe" Cooling Tower Institute Technical Paper 52-A, June, 1968.
22. Fosberg TM. "Industrial Waste Water Reclamation" Cooling Tower Institute Technical Paper 106-A, November, 1971.
23. Bydalek H, Hass KF, Mann CR and Le Page LR. "Use of Brackish Water in a Zero Discharge Cooling System" Cooling Tower Institute Technical Paper 223-A, January, 1980.
24. Fowlkes CC. "Corrosion Rates to be Expected at Zero Blowdown of Recirculating Water", Materials Performance, 1974;10.
25. Fowlkes CC. "Softening of Cooling Water Blowdown for Reuse", Cooling Tower Institute Technical Paper 112-A, January, 1973.
26. Gray HJ, McGuigan CV, and Rowland HW. "Sewage Plant Effluent as Cooling Tower Makeup --- A Case History" Cooling Tower Institute Technical Paper 116-A, January, 1973.
27. Strauss S. "Water management for Reuse/Recycle" Power, 1991;5.
28. Crook J. "Water Reclamation and reuse" In *Water Resources Handbook*, L. Mays (ed), McGraw Hill, New York, 1996.
29. Puckorius PR and Hess RT. "Wastewater Reuse for Industrial Cooling Water Systems" Industrial Water Treatment, September, 1991.
30. Kwong H and Woods G. "Reuse of Industrial Wastewater in Plant Cooling Towers" Industrial Water Treatment, May, 1994.
31. Cummings RO. "The Use of Municipal Sewage Effluent In Cooling Towers" Cooling Tower Institute Technical Paper 14-A, June, 1964.
32. Johnson WH. "Treatment of Sewage Plant Effluent for Industrial Reuse" Proceedings of the International Water Conference #25, September, 1964.
33. Gray HJ, McGuigan CV and Rowland HW. "Sewage Plant Effluent as Cooling Tower Makeup --- A Case History" Cooling Tower Institute Technical Paper 116-A, January, 1973.
34. Grobmyer WP, Brown JW and Butcher G. "Low T.D.S Makeup Water – A Problem?" Cooling Tower Institute Technical Paper 85-7, January, 1985.
35. Chen L, Freese DT and Snyder WR. "The Role of computer Calculated Supersaturation Ratios in Assessing Scaling Tendencies" Corrosion 82 March, 1982.
36. Ballard CW and Matson JV. "Precise Prediction of Cooling Water pH", CTI Journal, 1991;2.
37. Chen L, Freese DT and Snyder WR. "The Role of computer Calculated Supersaturation Ratios in Assessing Scaling Tendencies" Corrosion 82 March, 1982.
38. Gill JS and Varsanik RG. "Study of Cooling Water at High Cycles" Cooling Tower Institute Technical Paper 85-15, January, 1985.
39. Cavano RR. "The Phosphonates – Lore and Legend" Association of Water Technologies Spring Meeting, April, 1991.
40. Amjad Z. "Calcium Sulfate Dihydrate Scale Formation on Heat Exchanger Surfaces in the Presence of Inhibitors" Materials Performance, 1989;11.
41. Matson JV and Mouche WG. "Demonstration of a Maximum Recycle Sidestream Softening System at a Petrochemical Plant" Cooling Tower Institute Technical Paper 85-5, January, 1985.
42. Cavano RR. "Paths In Formulation" Association of Water Technologies Spring Meeting, April 1990.
43. Geiger GE, Off F and Hatch MR. "Chemical Approaches to Zero Blowdown Operation" Cooling Tower Institute Technical Paper 93-05, February, 1993.
44. Cavano RR. "Paths In Formulation" Association of Water Technologies Spring Meeting, April 1990.
45. Chemical Processing Staff "Alkaline Cooling Water Treatment Systems" Chemical Processing, 1991; 12.
46. Colturi TF and Kozelski KJ. "Corrosion and Biofouling Control in a Cooling Tower System" Materials Performance, 1984;8.
47. Cavano RR. "The Phosphonates – Lore and Legend" Association of Water Technologies, April, 1991.
48. Wykowski JC, Delaunay J and Franco RJ. "Reuse of Biologically Treated Wastewater as Cooling Tower Makeup" Corrosion/78 March, 1978.
49. Chemical Processing Staff, "Alkaline Cooling Water Treatment Systems" Chemical Processing, 1991; 12.
50. Cummings RO. "The Use of Municipal Sewage Effluent In Cooling Towers" Cooling Tower Institute Technical Paper 14-A, June, 1964.

51. Gottlieb MC. "Ion Exchange the reversible removal of naturally occurring organics using resins regenerated with sodium chloride" *Ultrapure Water*, 1996; 11.
52. Puckorius P. "Monitoring Requirements for Refinery Cooling System Reuse Water", *Materials Performance*, 1997;5:42-47.
53. Bydalek H, Hass KF, Mann CR and Le Page LR. "Use of Brackish Water in a Zero Discharge Cooling System" *Cooling Tower Institute Technical Paper 223-A*, January, 1980.
54. Matson JV and Characklis WG. "Biofouling Control in Recycled Cooling Water with Bromochlorodimethylhydantoin" *Cooling Tower Institute Technical Paper 250-A*, February, 1982.
55. Ferguson R. "Computer Aided Proposal Writing" *Association of Water Technologies Spring Meeting*, April, 1991.

WATER-SOLUBLE POLYMERS IN HAIR CARE

Prevention and Repair of Damage during Hair Relaxing

Ali N. Syed, Wagdi W. Habib, and Anna M. Kuhajda

Avlon Industries
5401 W. 65th Street
Bedford Park, Illinois 60638

1. ABSTRACT

Alkaline hair relaxers used to straighten excessively curly hair, usually African-American hair, often cause considerable hair damage. One of the effects of straightening the hair with relaxers is a loss in tensile strength due mainly to breakage of disulfide and hydrogen bonds. This loss in tensile strength leaves the hair more susceptible to breakage and cuticle erosion from subsequent grooming. The damaging effects of relaxer treatment are not limited to disulfide bond breakage alone. Another cause of hair damage during relaxing is swelling of hair fibers during the highly alkaline treatment. During a conventional hair relaxer treatment, the hair swells by 50% or higher, and another 20% upon rinsing. When hair swelling is not controlled, the hair develops radial and longitudinal cracks again rendering the hair susceptible to breakage from combing and brushing. This study presents results on the application of cationic polymers to strengthen hair during relaxing, and non-ionic polymers which control hair swelling.

2. INTRODUCTION

Water-soluble and water-dispersible polymers are widely used in the cosmetics industry in general, and in hair-care products in particular. Natural water-soluble polymers such as starches and gums have been used in hairstyling products for thousands of years.¹ Early formulations used for setting and styling hair were generally aqueous solutions or hydroalcoholic gels of polymers such as Gum Arabic, Karaya gum, shellac, and alginates. These early mucilage-based concoctions were heavy and became tacky when exposed to humidity in the atmosphere.

Today, chemists in the cosmetic industry have a large number of new, synthetic polymers to select from. Modern hair care formulations utilize polymers, copolymers, and terpolymers made from a large variety of functional groups. Polymers in the hair care industry are broadly classified based on their ionic charge into cationic, anionic, non-ionic, and amphoteric categories. Utilization of these polymers in combination with other additives in the cosmetic industry provides almost unlimited possibilities of conditioning, repairing, strengthening, forming, and overall enhancing the properties of the hair. Hair products containing conditioning polymers help prevent mechanical damage, and thus maintain the strength and integrity of hair by reducing the force required to comb through the hair.² In addition to preventing damage from combing, attempts have been made to reduce damage during chemical treatment.³ We have found applications and uses of a class of cationic polymers which strengthen the hair during relaxing, and non-ionic polymers which reduce the swelling that the hair undergoes during a highly alkaline chemical treatment. Before discussing the cationic and non-ionic polymers of particular interest, the following are examples and applications of anionic and amphoteric polymers.

3. LITERATURE REVIEW

3.1. Examples of Anionic Polymers

Figure 1 shows an example of an anionic polymer, polyacrylic acid. B.F. Goodrich (Cleveland, OH) manufactures a series of carbomers (molecular weight approximately 450,000 to 4,000,000 daltons) sold under the trade name Carbopol.⁴ These polymers are used as thickeners and emulsifiers in cosmetic preparations as well as for styling and holding the hair. Table 1 shows a prototype formulation of a hair styling gel utilizing polyacrylic acid.⁵ CTFA is the acronym for the Cosmetic, Toiletry, and Fragrance Association.

Another example of a commonly used anionic polymer includes copolymer of vinyl acetate and crotonic acid. Figure 2 shows the chemical structure vinyl acetate (VA)/Crotonates copolymer. In cosmetic formulations, it is a partially or completely neutralized copolymer used as a hair fixative in hair sprays. An example of a formulation containing this polymer is shown in Table 2.⁶

3.2. Examples of Amphoterics

An example of an amphoteric polymer is shown in Figure 3 (Amphomer®, National Starch). This polymer is used as a hair conditioner and fixative to provide more body, style, and manageability.⁷ An example of a formulation containing this polymer is shown in Table 3.⁸

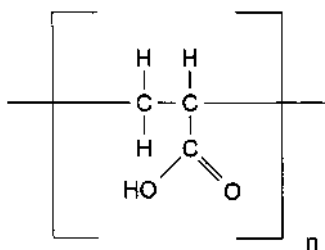


Figure 1. Homopolymer of acrylic acid (CTFA name: Carbomer).

Table 1. Prototype hair styling gel with poly(acrylic acid)

Ingredient	Percentage
Water	94.6
Methylparaben	0.2
Imidazolidinyl urea	0.3
Carbomer	1.0
Triethanolamine	1.3
Hydrolyzed animal protein	0.5
Fragrance	0.1

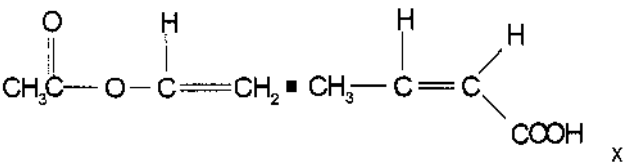


Figure 2. Copolymer of vinyl acetate and crotonic acid (CTFA name: VA/Crotonates copolymer).

3.3. Examples of Cationic Polymers

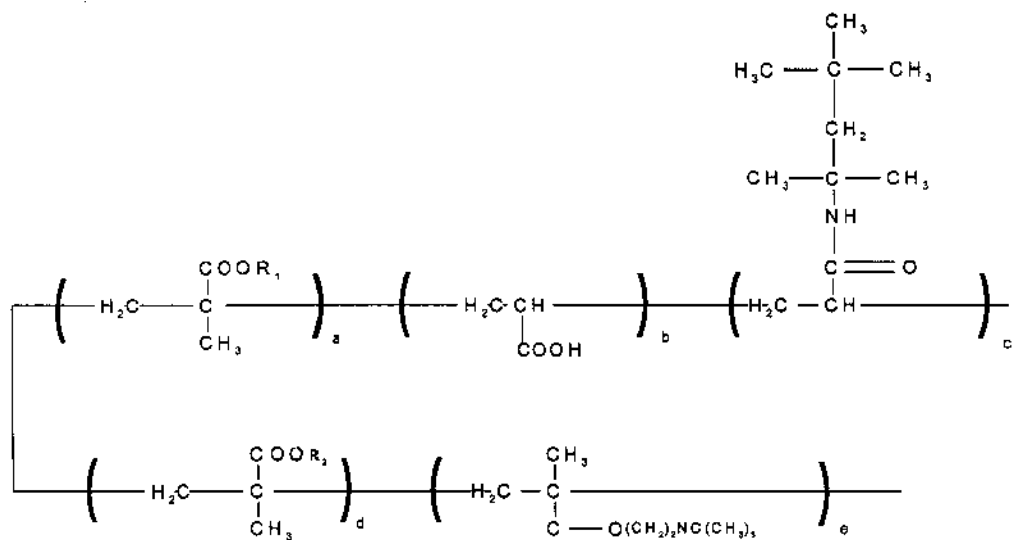
Figures 4 and 5 illustrate examples of a class of cationic polymers, quaternary ammonium polymers, commonly used in hair care formulations. Polyquaternium-6 is a highly substantive polymer for conditioners, while Polyquaternium-7 possesses film-forming and conditioning properties.⁹ Both polymers have been utilized for their mildness in shampoos as well as for their conditioning properties.¹⁰ An example of a patented conditioning relaxer formula is shown in Table 4.¹¹

Figure 6 shows another example of a commonly used cationic polymer called Polyquaternium-10. This polymer is a substantive conditioner for personal care products which is compatible in a wide range of anionic, amphoteric, nonionic, or cationic systems.¹² This polymer, when incorporated into conditioners, has been shown to significantly reduce combing force, thus reducing the mechanical damage to the hair from grooming.¹³ A patented formula of a detangling shampoo with Polyquaternium-10 is shown in Table 5.¹⁴

The following examples of cationic and non-ionic water-soluble polymers have been the focus of our study. Figure 7 illustrates a cationic polyamine, which is a secondary amine polymerized with epihalohydrin and further cross-linked with the addition of a small amount of ethylenediamine to form a polymer of the structure shown below (mo-

Table 2. Pump hair spray with VA / Crotonates copolymer

Ingredient	Percentage
VA/Crotonates copolymer	5.00
AMP	0.40
Quatemium-6	0.15
SDA 40	94.45
Fragrance	q.s.



Where R_1 & R_2 = (hydroxyl) alkyl

Figure 3. Acrylic resins with both cationic and carboxylic groups (CTFA name: Octylacrylamide/acrylates /butylaminoethyl methacrylate polymer).

Table 3. Non-aerosol styling spritz with amphomer

Ingredient	Percentage
Amphomer ^R	8.00
AMP	1.38
Dimethicone	0.20
Fragrance	qs.
Ethanol	90.42

lecular weight approximately 1,000,000 daltons). In our study, this cationic polyamine is shown to enhance the elasticity and strength of the hair.¹⁵

3.4. Examples of Nonionic Polymers

Figure 8 shows an example of a hydrogenated starch hydrolysate that we have found reduces damage during relaxing by reducing hair swelling.¹⁶

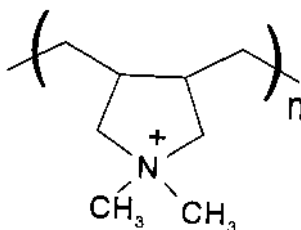


Figure 4. Dimethyl diallyl ammonium chloride homopolymer (CTFA name: Polyquaternium-6).

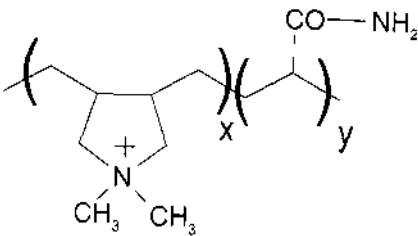


Figure 5. Dimethyl diallyl ammonium chloride with propanamide copolymer (CTFA name: Polyquaternium-7).

Table 4. Conditioning relaxer containing Polyquaternium 6 or 7

Ingredients	Percentage
Petrolatum	23.0
Mineral oil	14.0
Fatty alcohol	7.0
Ceteth 20	2.0
PEG 60 lanolin	1.5
Simethicone	0.1
Deionized water	44.4
Propylene glycol	2.0
Polyquaternium 6 or 7	1.0
Calcium hydroxide	5.0

3.5. Simplified Illustration of the Physical Structure of the Hair

Human hair consists of highly organized, keratinized cells. A cross-section of a hair fiber shows three main sections: cuticle, cortex, and medulla as shown in Figure 9. Scanning electron micrographs are shown illustrating cuticle and cortex in Figures 10 and 11, respectively (Reproduced with permission from Avlon Industries).

Hair can be damaged from chemical, environmental, or mechanical forces. The focus of our study is prevention of chemical damage from a commonly used procedure to straighten excessively curly hair called lanthionization. Damaged hair can be “repaired” by application of cationic polymers which attach to negatively charged damaged sites restoring the hair’s sheen, feel, and appearance.¹⁸ However, this procedure is temporary and does not address the problem of preventing tensile strength loss and breakdown of the internal structure of the hair.

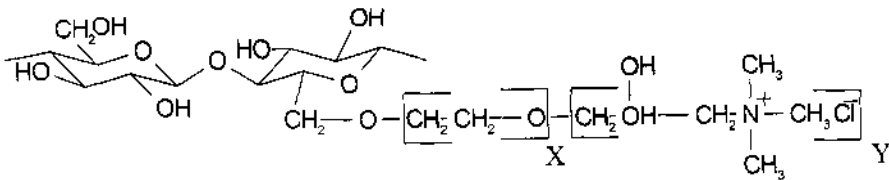


Figure 6. Hydroxyethyl cellulose with trimethyl ammonium substituted epoxide (CTFA name: Polyquaternium-10).

Table 5. Detangling shampoo with Polyquatemium- 10

Ingredients	Percentage
Deionized water	75.00
Methylparaben	0.20
Imidazolidinyl urea	0.30
Disodium EDTA	0.20
Polyquatemium- 10	1.50
Sodium lauryl sulfate	3.50
Disodium cocoamphodipropionate	8.00
Trideceth-7 carboxylic acid	7.00
Lauramide DEA	3.00
Glycol stearate	1.00
Fragrance	0.30

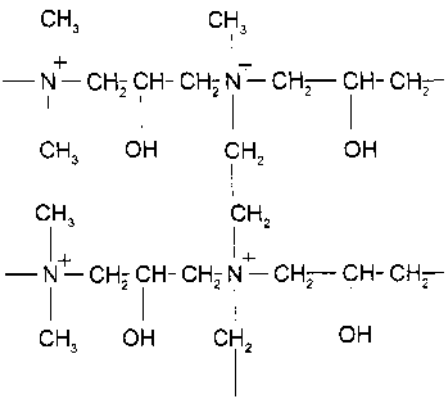


Figure 7. Cationic polyamine.

Hair relaxers change one-third of the disulfide bonds to lanthionine bonds using 2.0 to 2.4 percent sodium hydroxide in oil-in-water emulsion.¹⁹ The chemical changes that take place in the hair lead to a decrease in tensile strength by approximately 50% in the wet state.²⁰ Hair damage during relaxing is not restricted to disulfide bond breakage alone. The alkaline hair relaxer leads to an increase in hair swelling intensified by concurrent

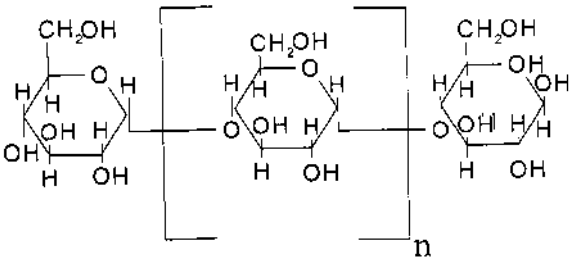


Figure 8. Hydrogenated starch hydrolysate.

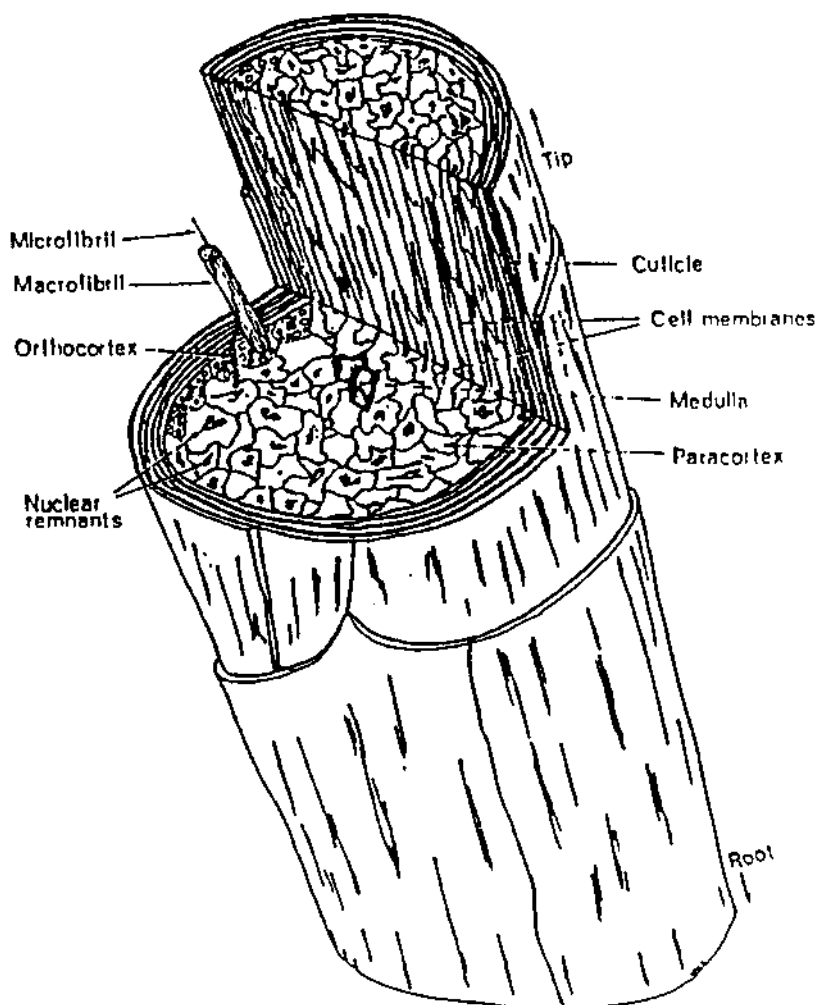


Figure 9. Cross section of hair fiber.

breakdown of disulfide bonds.²¹ Rinsing with water produces additional swelling due to osmotic forces, because there is a lower salt concentration outside the fibers at this stage of a chemical process.²² It has been the objective of our study to utilize water-soluble polymers to prevent or repair damage in relaxed hair by increasing the tensile strength and reducing swelling during relaxing.

4. EXPERIMENTAL AND RESULTS

4.1. Increasing the Strength of Relaxed Hair with a Cationic Polymer

The tensile strength loss of hair fibers treated with a hair straightening formula containing a cationic polyamine, such as the polyamine shown in Figure 7, versus a control

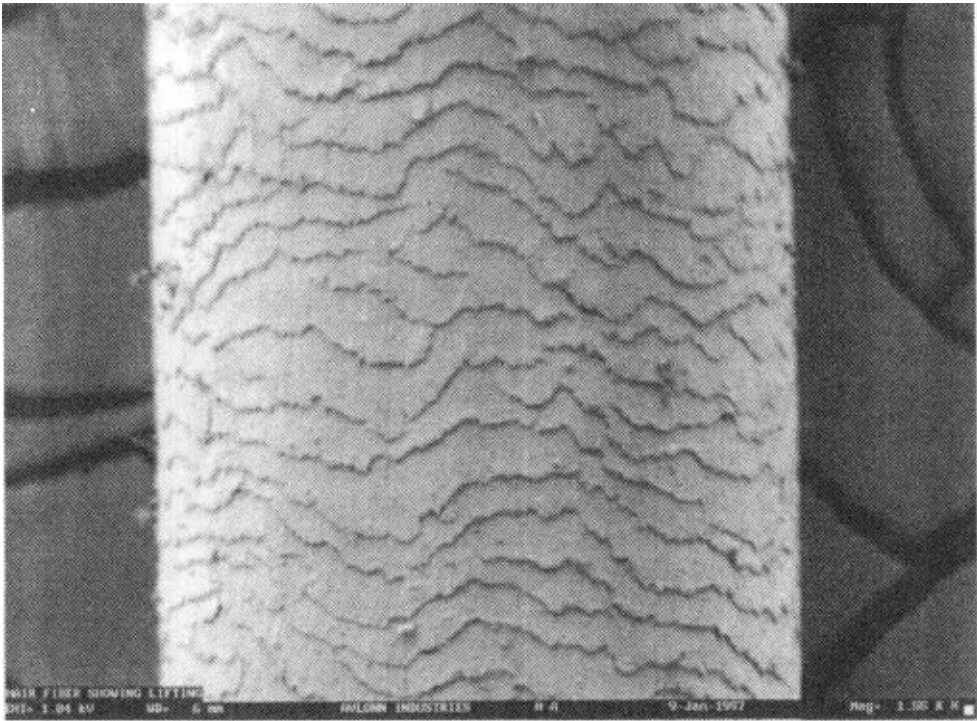


Figure 10. Cuticles of the hair.



Figure 11. Cortex of the hair.

relaxer without polymer was tested. Twelve inch long, dark brown European hair was obtained from DeMeo Brothers, New York. The hair fibers were washed with a 10% solution of ammonium lauryl sulfate, rinsed thoroughly, and allowed to dry overnight. Fibers of close diameter (71–80 microns) were selected for this study. Each fiber was cut in half and crimped into 30 mm sections using a Dia-Stron Crimp Press. The hair section closest to the root was designated as the control, and the section downstream was used for the experimental relaxer. The tensile strength of the untreated hair fibers under wet conditions was measured utilizing a Dia-Stron Miniature Tensile Tester, Dia-Stron, Ltd., U.K. The strength was determined by the amount of work required to extend the fibers 20% of their original length at a rate of 10.0 mm/min. The hair fibers were then allowed to restore overnight in water. The following day, the fibers were dried at 65% relative humidity and 21°C prior to treating with relaxers.

The control group was treated with hair relaxer without polymer, and the experimental group was treated with relaxer containing a cationic polyamine. Both sets were processed identically for 18 minutes, followed by rinsing, and then shampooing with a mild, acidic shampoo. The following day, the tensile strength of treated fibers was determined same as above using Dia-Stron MTT. The F20 index loss was then calculated.

Table 6 shows that hair treated with Control Relaxer without Polymers exhibited an F20 index loss of 50.94%, whereas, hair treated with Relaxer containing cationic Polyamine exhibited an F20 index loss of 45.11 %.-a statistically significant difference.

Table 7 shows a prototype formulation of a hair relaxer containing cationic strengthening ingredients.

4.2. Minimizing Swelling during Hair Relaxing

In addition to strengthening the hair while relaxing by forming a complex in the hair, we have discovered that water-soluble polymers, especially non-ionic polymers such as starch hydrolysates, reduce the swelling of the hair during relaxing. During the process of relaxing, the hair swells up to 50% or more of its original diameter. Upon rinsing with water, the hair suddenly swells another 20 to 30% because of a sudden surge of osmotic pressure inside the hair fibers. Much of the damage from swelling occurs during rinsing because the swelling is very rapid. The hair fibers develop radial and longitudinal cracks when swelling is not controlled. Figure 12 shows radial cracks and Figure 13 shows longitudinal cracks in hair fibers caused by swelling in an alkaline solution.

The swelling studies were performed using a LaserMike laser micrometer which measures the major and minor axis of the fiber simultaneously. LaserMike laser micrometer was purchased from LaserMike in Dayton, Ohio. European hair, available from DeMeo Brothers, with a uniform diameter of 71–80 microns was selected for this study. The original diameter of dry hair was measured under controlled conditions of 65% relative humidity and 21°C. Fibers were then immersed in relaxer for 18 minutes. After 18 minutes, excess relaxer was gently removed and the diameter again measured. The diameter measurements were continued through the rinsing phase. Figure 14 shows a graph comparing hair fiber swelling in relaxer without polymer versus with non-ionic polymer starch hydrolysate. Hair fibers treated with the control relaxer exhibited swelling of 45.21% at 18 minutes in relaxer, and peaked at 80.82% when rinsed with water.

Hair fibers using cream relaxer with polymer swelled to 19.78% before rinsing, and 38.46% upon rinsing. Therefore, hair fibers treated with relaxer containing non-ionic polymer exhibit significantly less swelling compared to relaxers without polymers.

An example of a relaxer with deswelling ingredients is shown in Table 8.

Table 6. Effect of cationic polymers in hair relaxer

Control fibers treated with relaxer without polymer				Experimental fibers treated with relaxer containing polyamine			
Hair fiber #	Initial work*	Work* after	F20 loss %	Hair fiber #	Initial work*	Work* after	F20 loss %
1	1.15	0.54	53.04	1	1.04	0.51	50.67
2	1.39	0.69	50.58	2	1.64	0.95	42.07
3	1.50	0.71	52.40	3	1.44	0.82	43.13
4	1.47	0.66	54.97	4	1.19	0.67	43.87
5	1.47	0.79	46.12	5	1.43	0.84	41.12
6	1.37	0.61	55.69	6	1.29	0.64	50.70
9	1.27	0.60	53.15	9	1.27	0.71	44.41
10	1.40	0.77	45.00	10	1.25	0.76	39.44
11	0.94	0.43	53.99	11	0.82	0.43	47.43
12	1.18	0.46	60.93	12	1.11	0.56	49.37
13	1.09	0.52	52.39	13	1.01	0.59	41.68
14	1.43	0.69	51.47	14	1.37	0.77	44.01
15	1.17	0.61	47.61	15	1.07	0.68	36.92
16	1.30	0.73	43.62	16	1.16	0.65	44.31
17	0.92	0.41	55.05	17	0.96	0.45	52.51
18	0.99	0.50	49.50	18	0.99	0.62	38.00
19	1.29	0.68	47.52	19	1.21	0.66	45.54
20	1.22	0.63	48.20	20	1.24	0.69	44.52
22	1.17	0.61	48.29	22	1.10	0.62	43.91
23	1.41	0.73	48.58	23	1.09	0.51	52.94
25	1.12	0.54	51.61	25	1.05	0.52	50.76
Average			50.94				45.11
Standard deviation			4.10				4.64
Coeff. of variance			8.05				10.28

*Work done is in millijoules

When used in combinations, relaxers containing combinations of deswelling and strengthening polymers leave the hair visibly and measurably healthier. Table 9 shows tensile strength results of hair treated with relaxer containing polymers versus a control relaxer without polymer. Figure 15 shows a scanning electron micrograph of a hair fiber treated with relaxer containing strengthening and deswelling polymers (reproduced with permission from Avlon Industries). The cuticles lay flat, and there are no visible cracks in the structure.

Table 7. Hair relaxer formulation containing cationic strengthening polymers

Ingredient	Percentage
Petrolatum and/or mineral oil	30.0 to 35.0
Fatty alcohols and/or emulsifying wax	6.0 to 10.0
Emulsifiers	2.5 to 4.0
Simethicone	0.1
Lanolin	0.5
Deionized water	46.4 to 56.9
Propylene glycol	5.0
Cationic polyamine (50%)	2.0
Sodium hydroxide	2.2

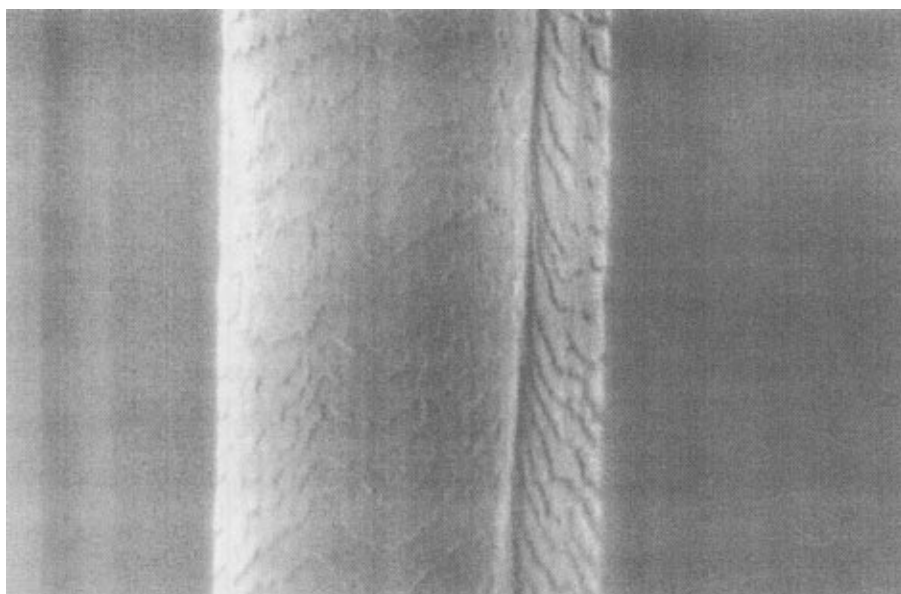


Figure 12. Radial cracks in hair fiber. (Reproduced with permission from Avlon Industries. All rights reserved.)

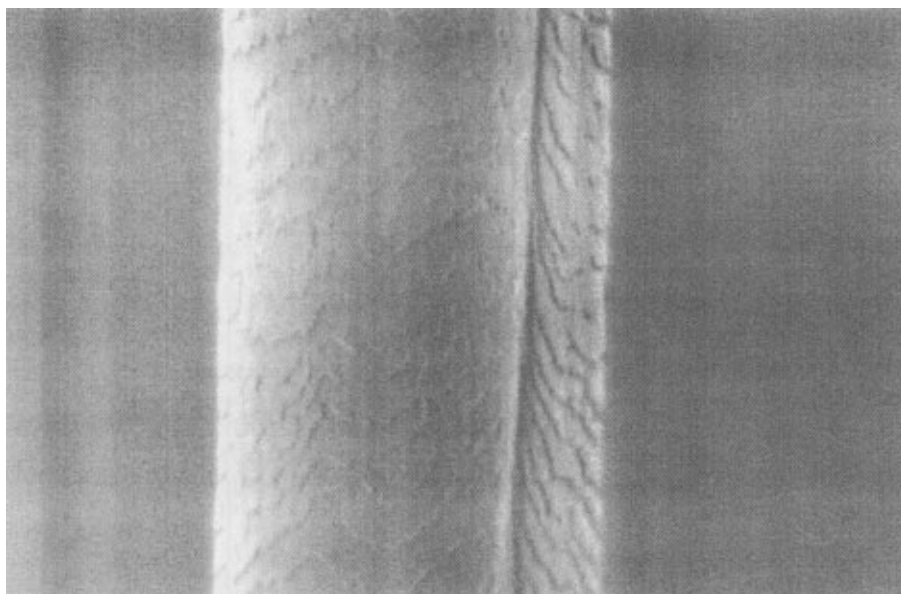


Figure 13. Longitudinal cracks in hair fiber. (Reproduced with permission from Avlon Industries. All rights reserved.)

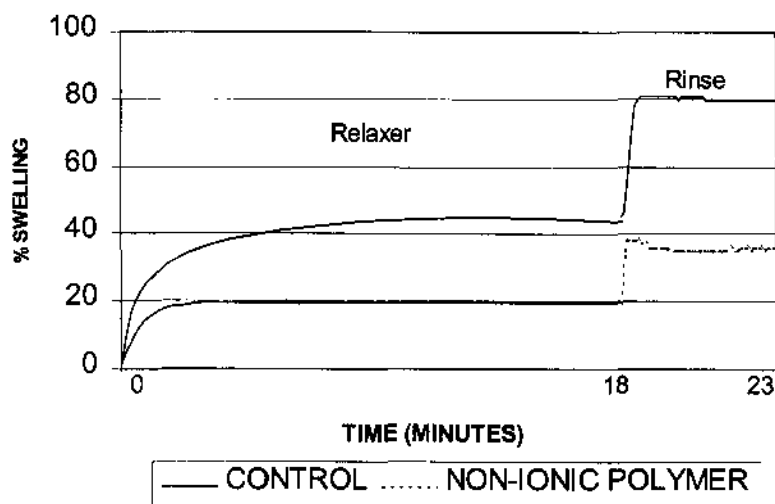


Figure 14. Hair swelling by relaxer with nonionic polymer.

5. CONCLUSIONS

A series of cationic polyamines and starch hydrolysates, when used at certain levels separately and in combinations, control the swelling and enhance the strength of relaxed hair. The theory is that during the relaxing process, hair is swollen to a maximum degree and the cuticle layers are widely open at this stage. The cationic polyamines are able to penetrate into the cortex. Upon rinsing the hair with water, as the hair deswells, the cationic polyamines are trapped in the cortex of the hair, as well as ionically bonded to the negative sites on the surface of the hair. Since cationic polyamines are very elastic, they improve the elasticity and tensile strength of the relaxed hair fibers. While cationic polyamines are penetrating inside the hair, the polymeric starch hydrolysates present in high concentration around and outside the hair fiber are able to reduce the osmotic pressure inside the hair, thereby reducing the swelling of hair fibers significantly. This reduction in swelling helps to prevent longitudinal and radial cracks in the hair fibers. The combination of deswelling and strengthening polymers results in healthier relaxed hair.

Table 8. Relaxer formulation with polymeric deswelling agent

Ingredient	Percentage
Petrolatum and/or mineral oil	30.0 to 35.0
Fatty alcohols and/or emulsifying wax	6.0 to 10.0
Emulsifiers	2.5 to 4.0
Simethicone	0.1
Lanolin	0.5
Deionized water	46.4 to 56.9
Propylene glycol	5.0
Hydrogenated starch hydrolysate	2.0
Sodium hydroxide	2.2

Table 9. Tensile strength of hair treated with relaxers containing polymers

Control no-base relaxer without polymers				Experimental no-base relaxer with polyamine and starch hydrolysate			
Hair	Initial work*	Work* after	%F20 loss	Hair	Initial work*	Work* after	%F20 loss
2	1.24	0.65	47.82	2	1.24	0.66	46.45
5	1.16	0.61	47.59	5	1.18	0.68	42.80
6	1.33	0.70	47.22	6	1.24	0.69	44.19
7	0.87	0.37	58.05	7	0.77	0.41	46.36
8	1.10	0.60	45.82	8	0.99	0.61	38.38
9	0.80	0.41	48.25	9	0.81	0.49	39.83
12	1.27	0.73	42.91	12	1.23	0.83	32.85
15	1.36	0.68	49.85	15	1.40	0.81	42.43
16	1.33	0.64	51.58	16	1.39	0.80	42.45
20	1.08	0.54	50.37	20	1.13	0.68	40.00
21	0.98	0.57	41.78	21	0.97	0.55	43.45
22	1.03	0.46	55.34	22	0.98	0.64	34.55
23	1.29	0.58	55.43	23	1.16	0.69	40.52
25	1.07	0.44	59.07	25	0.93	0.47	49.84
Average			50.08				41.72
Standard deviation			5.29				4.56
Coeff. of variance			10.57				10.93

*Work done is in millijoules

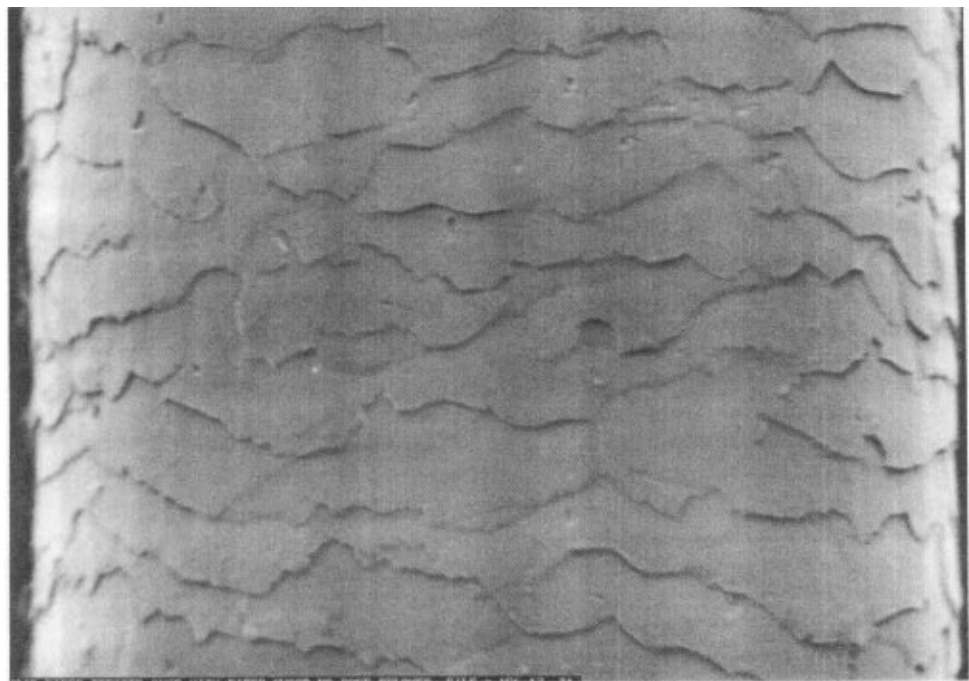


Figure 15. Hair fiber treated with relaxer containing deswelling and strenghtening polymers.

REFERENCES

1. Zviak C. *The Science of Hair Care* Marcel Dekker, Inc., New York, 1986.
2. Syed AN. "Composition for Decreasing Combing Damage to Hair and Method", U.S. Patent Application 08/267,829. 1993.
3. Syed AN. "Hair Strengthening Composition", U.S. Patent 5,639,449. 1997.
4. Carbopol Product Information Sheet, B.F. Goodrich, Brecksville OH.
5. Syed AN. *Hair and Hair Care*. D. H. Johnson (Ed), Marcel Dekker, Inc., New York, 1997.
6. Resyn 28-1310 Product Information Sheet, National Starch and Chemical Corporation, Specialty Polymers, Bridgewater NJ.
7. Amphomer® Product Information Sheet, National Starch and Chemical Corporation, Specialty Polymers, Bridgewater NJ.
8. National Starch and Chemical Corporation Formulary, National Starch and Chemical Corporation, Specialty Polymers, Bridgewater NJ.
9. Zviak C. *The Science of Hair Care* Marcel Dekker, Inc., New York, 1986.
10. Syed AN and Khalil EN, "Low Irritant Conditioning Shampoo Composition", U.S. Patent 4,205,063. 1980.
11. Syed AN and Khalil EN, Stable Hair Relaxer, U.S. Patent 4,390,033. 1983.
12. UCARE Polymer Product Information Sheet, Amerchorp Corporation, Edison NJ.
13. Syed AN, "Composition for Decreasing Combing Damage to Hair and Method", U. S. Patent Application No. 08/267/829. 1994.
14. Gerstein T, U.S. Patent 3,990,991. 1976.
15. Syed AN and Ahmad K, Hair Strengthening Composition and Method, U.S. Patent 5,639,449. 1997.
16. Syed AN and Ahmad K, "Composition and Process for Decreasing Hair Fiber Swelling". US. Patent 5,348,737. 1994.
17. Robbins CR, *Chemical and Physical Behavior of Human Hair*, 3rd Edition Springer Verlag, New York, 1994.
18. Swift JA, "A Course on Advanced Structure and Chemistry of Hair", Society of Cosmetic Chemists Continuing Education Program, Elizabeth NJ, 1996.
19. Epps J and Wolfram LJ, Letter to the Editor. Journal of the Society of Cosmetic Chemists, 1983;34:213-214.
20. Syed AN, "Ethnic Hair Care: History, Trends and Formulation". *Cosmetics & Toiletries*, 1993; 108:99-107.
21. Wolfram LJ, *Hair Research: Status and Future Aspects*, C. E. Orfanos, W. Montagna, and G. Stüttgen (Eds), Springer-Verlag, New York, 1981,
22. Robbins CR, *Chemical and Physical Behavior of Human Hair*, 3rd Edition Springer Verlag, New York, 1994.

APPLICATION OF ULTRA-HIGH MOLECULAR WEIGHT AMPHOTERIC ACRYLAMIDE COPOLYMERS TO DETERGENTS

Yoshiyuki Hayashi,¹ Danian Lu,¹ and Nobuo Kobayashi²

¹Faculty of Engineering and Design
Kyoto Institute of Technology
Matsugasaki, Kyoto 606 Japan
²Espo Co. Ltd., 1-280-2 Takeishi
Hanamigawa-ku, Chiba 262 Japan

1. ABSTRACT

Ultra-high molecular weight ($5\text{--}17 \times 10^6$ daltons) amphoteric copolymers prepared from acrylamide, acrylic acid, N-(dialkylaminomethyl)- and/or N-(trialkylammoniomethyl)-acrylamide are shown to be excellent finishing agents for natural fibers and superior to the finishing agents prepared from natural resources such as hyaluronate and xanthan gum. The detergents containing the copolymer, inorganic builders and a small amount of penetrating agent showed detergency comparable to commercial detergents.

2. INTRODUCTION

The envelopes of bacteria are extremely complex. The innermost layer of the envelope is always a phospholipid bilayer into which many functionally distinct proteins are inserted. Surrounding this “cytoplasmic facing membrane” is a rigid shell of covalently linked peptidoglycan.¹ From the glycans, a variety of carbohydrates are isolated and used for finishing agents of fibers, such as hyaluronic acid, xanthan gum and chitosan.

Ultra-high molecular weight amphoteric copolymers have been reported to be excellent deodorant components.² Other polymers which have been used as components in deodorants include natural anionic polymers such as hyaluronic acid and xanthan gum. In the last few years, a large variety of hydrophilic polymers have been evaluated as builders for detergent formulations but only a few (notably carboxymethyl cellulose, CMC, polyacrylic acid, PAA, and acrylic acid/maleic acid based copolymers) are used commercially.

Table 1. Properties of the polymer solution

Copolymer	A	B	C
Nonvolatile	0.47	0.50	1.00
PH	9.7	8.9	6.7

Ultra-high molecular weight amphoteric acrylamide copolymers are excellent finishing agents for fabrics. Thus, these polymers can be added to softening ingredients for laundering. In this study, we have examined the detergency of formulations containing ultra-high molecular weight amphoteric polymers.

3. EXPERIMENTAL

3.1. Preparation of the Polymers

Acrylamide and acrylic acid were free-radically copolymerized in water and the solution was neutralized with an aqueous solution of sodium hydroxide. The Mannich reaction of a copolymer was carried out in an aqueous solution with formaldehyde and dimethylamine, affording N-(dimethylaminomethyl) cationic radical. Three different polymer solutions (A,B,C: the ratio of acrylamide: acrylic acid: dimethylaminomethylacrylamide, 80: 15:5, 80: 10: 10 and 90: 10:0, respectively) were prepared and properties of the solution are shown in Table 1. Although the exact molecular weight or molecular weight distribution of the polymer was not available, the estimated molecular weight (calculated from viscosity data) was more than ten million daltons.

3.2. Deodorant Textiles Treated with an Aqueous Solution of Copolymer B

Contamination of the textiles with cigarette smell was carried out in an artificial smoking device. Cat urine / ethanol solution was sprayed on the textile in a sealed bottle.

Table 2. Antismelling effect of several polymers to tobacco smell on absorbed wool serge suiting (0.0 1 % owf as solid)

Polymer	Oscillator count difference
Untreated fabrics absorbed tobacco smell	18
High molecular weight polyvinyl alcohol (M.W.: 123,000)	31
Sodium salt of polyacrylic acid	22
Nonionic polyacrylamide (M.W.: 17,000,000)	17
Crude amphoteric polyacrylamide	16
Anionic polyacrylamide (M.W.: 6,000,000)	16
Cationic polyacrylamide (M.W.: 3,000,000)	12
Anionic polyacrylamide (M.W.: 17,000,000)	12
Sodium hyaluronate (M.W.: 3,000,000)	10
Xanthan gum	8
Amphoteric polyacrylamide B	4
Fabrics scoured	0

After the contaminated textiles were dried in a fresh air for four hours, the textile was placed in a sealed bottle, where the concentration of the volatile organic compounds was estimated using a biomimetic sensor. The results are shown in Tables 2 to 4.

3.3. MnO₂ Dispersion

Dispersion of MnO₂ (0.04g) in a 0.05% builder aqueous solution (100 mL) was shaken vigorously for 5 minutes. After letting stand for 1hour, the concentration of MnO₂ in the upper aqueous layer was analyzed. The results are shown in Table 5.

3.4. Detergency

Swatches were soaked with an artificial soil aqueous suspension consisting of channel carbon black (5g), tomato ketchup (30g), mayonnaise (30g) in a Aerosol OT (5g) and dried. The soiled swatches were washed in a home laundry machine.

4. RESULTS AND DISCUSSION

Consumer concerns about the use of synthetic compounds prompted us to develop new finishing agents from natural resources. We found that well-designed synthetic polymers can exhibit excellent properties as deodorant and coagulant, comparable or superior to that of natural polymers.² The deodorancy efficiency shown by amphoteric acrylamide copolymers was found to be highly dependant on the molecular weight. An average molecular weight of less than 100,000 daltons resulted in minimal deodorizing effect. Those having a viscosity of at least 3,000 centipoises (corresponding to greater than 10⁶ daltons) showed an excellent deodorizing effect. The number-average molecular weight was determined by measuring the viscosity of the 1% aqueous solution of the polymer with a Brookfield viscometer using a No.2 rotor, at 20°C. Viscosities of at least 1,000 centipoise roughly correspond to number average molecular weight of at least 1,000,000 dalton. Although high molecular weight polymers show excellant deodorizing power, optimal performance can be achieved by combining the polymers with other ingredients such as low molecular weight organic acids, hypochlorite, carbonates, surfactants, etc.

Deodorant swatches have been examined on the basis of: a) rate of absorption of malodorous compounds, b) weight of absorbed malodors, c) rate of release of the absorbed malodors, d) weight of malodors released after leaving the malodorous environment by a definite time, and e) rate and/or weight of deposition of malodors. Immobilized vesicle bilayers deposited on quartz crystal oscillator adsorbed malodors and adsorbability is comparable to that of biological organs. The adsorbability of the artificial bilayer is highly dependent on humidity of the environment. Under strictly defined conditions, the oscilla-

Table 3. Deodorant effects on silk fabrics (Tirimen)

	Tobacco smell emitted	Cat urine smell emitted	Sexually excited male cat smell emitted
Untreated fabrics	29	16	25
Polymer B*	5	6	8

Table 4. Deodorant effects on the exhaust gas from a city sewage plant (ppm by volume)

	NH ₃	(CH ₃) ₃ N	CH ₃ SH	H ₂ S	Panel
At 20 °C					
Untreated malodorous gas	17	19	12.0	11	9800
Spraying fresh water	0	0	7.8	6.2	5800
Spraying the polymer soli	0	0	0.5	0.2	1740
At 28 °C					
Untreated malorodrous gas	65	74	15	15	
Spraying fresh water	18	21	4	13	
Spraying of the polymer sol ^a	2	0	0	0	

tor showed to be an excellent counter for determination of the very dilute concentration of malodors.

Recently, the Japan Chemical Fiber Association (JCFA) issued tentative procedure for the estimation of deodorancy using malodors (such as ammonia, hydrogen sulfide and acetic acid). According to the the JCFA protocol, our polymer based deodorant formulations did not show positive results. After exposing the fabrics to a malodorous atmosphere, the apparels should not release malodors when removed to fresh air for 4 hours. The results are shown in Tables 2 to 4.

The data in Tables 2 and 3 show the oscillator count differences between the smell-absorbed fabrics and control fabrics. We found that the oscillator count difference data was in fair agreement with those of the JEPA recognized triangle method of odor determination.³ Spraying a dilute solution of the amphoteric polyacrylamide containing a small amount of surfactants and inorganic salts showed superior deodorant effects (Table 4).

Spraying the dilute polymer solution into a suspension of soot from combustion of styrene flocculated the soot. These results suggest that the amphoteric polymer trapped malodors and kept them in the film of the polymer. Toxicity tests of the polymers showed none of mutagenic activity, dermal irritation, and germinative and growth influence. The polymers were easily decomposed by bacteria in a aqueous solution, while silk and cotton fabrics treated with the polymer above 0.3% owf completely suppressed growth of bacteria.

Antistatic property of PET (tropical) fabrics treated with the polymer B is shown in Table 5, and the polymer C is clearly shown to be good antistatic agent for polyester.

As mentioned above, a small amounts of the polymers gave favorable effects on the treated fabrics. We examined the effects of the polymer in the presence of detergents. It is well known that washing efficiencies of detergents containing builders correlate with Ca²⁺ sequestering capacities and dispersing power for MnO₂. The overall suspending power of surfactants and builders is a function of the concentration and generally shows at least one optimum and varies with the presence of other ions.⁴⁻⁶ The suspending power for MnO₂ of the polymer A and C is shown in Table 6.

Table 5. Antistatic property of PET

	JIS L 1094 A method (half-value period, s)	JIS L 1094 B method (frictional voltage, v)
Control	38	-326
Polymer C (0.02% owf)	24	-230
Polymer C (0.2% owf)	3	-111

Table 6. The suspending power of MnO₂ (ppm)

Builder	Conc. of builder(ppm)						
	200	150	100	50	25	10	5
No builder							8
Polymer A	18	20	22	27	24	15	13
Polymer C	24	38	33	32	30	23	21
Sodium acrylate				11			
Sodium tripolyphosphate				13			

Table 7. A new detergent recipe

Ingredient	Chemicals weight (g)
Sodium Metasilicate	579
Copolymer C 0.3% aq. Sol.	50
Sodium Sulfate (+ polymer C 0.15g)	250
Sodium Percarbonate	100
Zeolite	10
Megafack F 179*	1
Sodium Oxalate	8
EDTA	2

*A fluorocarbon penetrating agent (Dic. Co.)

The dispersancy of polymer C is slightly better than that obtained with polymer A but the suspension of the either polymer is considerably better than the conventional builder.⁴ The polymers may act as a flocculant at high concentrations (500 ppm) but the optimum concentration for deodorancy is several orders of magnitude lower and, at these concentrations, the suspending power is superior to conventional builders. Additionally, the Ca²⁺ sequestering capacity of the polymer was found to be very low but the calcium suspension was stable compared to conventional sequestering agents.

We examined several recipes of detergents containing the polymers and inorganic builders. A starting recipe (Table 7) without conventional anionic surfactants showed good detergency compared to that of commercial laundry detergents (Table 8).

Incorporation of enzymes and fatty soaps in the detergent also improved the detergency. The prevention of soil redeposition is a critical factor for a good detergent.⁷ The redeposition may be prevented by the stabilization of solid soil particle in aqueous phase or by changing the hydrophilic of the soiled surface. The ultra-high molecular weight polymer

Table 8. Detergency of the new recipe detergent

Laundry temp. (°C)	Recovery of whiteness (%)	
	New detergent	Commercial*
20	45	52
60	62	60
80	82	68

*Attack (Kao Co.)

was a good suspension-stabilizer and soil-releasing agent on fabrics. Thus, both properties improve the overall performance of the detergent. When an aqueous solution of the polymer was mixed with anhydrous sodium sulfate powder, it was absorbed into the powder. Thus it is possible to formulate a powdered detergent containing the polymer (Table 7).

REFERENCES

1. J.D. Watson et al. (ed.), "Molecular Biology of The Gene", The Benjamin, 1987; 1: 104.
2. USP4,909,986 (Mar. 20, 1990).
3. Iwasaki Y, "Olfactory Malodor Determination Method", J. Pollution Control Society, 1978; 13:246.
4. Yoshio Abe et al., YUKAGAKU, 1981; 30:757.
5. T. Fujimoto (ed.), *Introduction to Polymer Chemicals* (in Japanese), Sanyou Chemical Ind., Kyoto, 1992:765.
6. Schwartz AM, and Perry JW, *Surface Active Agents*, Interscience, 1949.
7. Schwartz AM et al., *Surface Active Agents and Detergents*, Interscience, 1958.

Index Terms	Links
AA: <i>see</i> Acrylic acid	
AA/AHPSE/PEGAE	
calcium phosphate scale inhibition and	151
as clay dispersant agent	159
Acrylamide, wastewater treatments and	193
Acrylic acid	5
characteristics of	5
interfacial adsorption kinetics	20
poly: <i>see</i> Poly(acrylic acids)	
2-(Acryloyloxy)ethyltrimethylammonium	
chloride, wastewater treatments and	193
Activation free energy	55
Additives, crystallization kinetics and	51
Adsorption	
activation energy and	15
alumina powder	24
diffusion control of	15
electrostatic resistance to	19
hydroxyapatite and	66
hydroxyapatite crystal growth and	71
hydroxypropylcellulose, on HAP	105
kinetics of	11
polyacrylic acid	25
polymer: <i>see</i> Polymer adsorption	
of polyvinyl pyrrolidone on alumina	26
of SDS on HAP	108
of SPVPA to hydroxyapatite beads	97
water-soluble macromolecules	59
AIBN: <i>see</i> Azobisisobutyronitrile	
Alkaline hair relaxers	231
Alumina, polyacrylic acid adsorption on	25
Alumina powder adsorption	24
Aluminum separation	42
AMD-co-AETAC polymers	194
characterization of	195
flocculation experiments	195
preparation of	195
wastewater treatments and	194
Amorphous silica	175
Amphoteric acrylamide copolymers	
application to detergents	245
preparation of	246
Amphoterics	232
Anhydrite scales, formation on heat exchanger	
surfaces	183
Anionic polymers, examples of	232
Antiscalants, silica	176
Arrhenius expression	17
Azobisisobutyronitrile	91

Index Terms	Links
Bacteria, attachment to saliva-coated beads	95
Benzene hexacarboxylic acid, hydroxyapatite crystal growth and	77
Boltzmann's constant	18
Borate–carbazole reaction, uronic acid and	64
Boric acid, poly(vinyl alcohol) solubility and	34
1-Bromonaphthalene, surface tension of	58
Brownian diffusion coefficient	5
Calcite crystal growth	124
Calcium carbonate	136
formation in natural water	132
inhibition by maleic acid copolymers	117
Calcium carbonate crystal growth	119
kinetic inhibition of	131
organic inhibitors of	131
relative inhibition of	122
Calcium phosphate inhibitors, efficacy of	150
Calcium phosphate nucleation	
on FEP	59
on PMMA	59
radiofrequency glow discharge and	59
on silicone rubber	59
Calcium phosphate scale, novel inhibitor of	149
Calcium sulfate dihydrate scale, formation on heat exchanger surfaces	183
Calculus, dental: <i>see</i> Dental calculus	
Capillary suction time	200
Cationic polymers	
hair care and	233
performance on sludge	202
Cations, crystallization in presence of	58
Chlorides, recycled water and	221
Chondroitin sulphate, hydroxyapatite adsorption and	71
Chromatography, high performance size exclusion	196
Citric acid, hydroxyapatite crystal growth inhibition and	84
Clay dispersant, AA/AHPSE/PEGAE as	159
Colloidal particles, isolation/separation of	193
Concentrated particulate suspensions	23
Conformation: <i>see</i> Polymer concentration	
Constant composition	56
Contact angle	57
Cooling tower	
agricultural waste in	214
biologically treated wastewater in	215
boiler blowdown in	216
boiler condensate in	216

Index Terms	Links
Cooling tower (cont.)	
low TDS water	216
municipal wastewater in	214
reuse of blowdown	212
scale formation in	118
scrubber blowdown in	214
seawater and	215
side-stream softening	210
wet dry	210
Cooling water treatment	
calcium phosphate scale	149
optimization in recycled waters	207
Copolymers	
of acrylic acid	5
characterization of	195
HMPAAs and	4
maleic acid	120
of pyreneacrylamide	5
Corrosion	
control in recycled water	207
control of	149
Corrosion inhibitors	218
molybdate/phosphonate	218
molybdate/zinc	218
orthophosphate	219
zinc	219
Cosmetics industry, water-soluble polymers in	231
Crosslink density, in HMPAAs	20
Crystal growth	
calcite	136
hydroxyapatite: <i>see</i> Hydroxyapatite crystallization	
impurities and	52
organophosphonate inhibition of	78
polyelectrolytes and	120
in pure solution	52
pyrophosphate inhibition of	78
of SPVPA	92
Crystalline structure, of poly(vinyl alcohol) gels	35
Crystallinity	
optimal freezing times and	37
of poly(vinyl alcohol)	36
Crystallization	
cations and	58
of gypsum	183
hydroxyapatite: <i>see</i> Hydroxyapatite crystallization	
of hydroxyapatite	65
in presence of additives/impurities	54
PVA gels and	32
thermodynamics of	52

Index Terms	Links
Crystallization kinetics	56
additives/impurities influence on	51
constant composition method and	56
dosigraph and	56
potentiometer and	56
stoichiometrics and	56
Cyclohexane, interfacial adsorption kinetics	20
Cyclohexane/water interface	
dynamic interfacial tension data	13
HMPAA adsorption and	20
hydrophobically modified poly(acrylic acids) and	1
Decane, surface tension of	58
Dental calculus	
etiology of	92
sodium polyvinylphosphonic acid inhibition of	92
Dental calculus formation	91
SPVPA effects	95 100
Dental plaque	
etiology of	92
sodium polyvinylphosphonic acid inhibition of	92
SPVPA effects on	96
Dental plaque formation	91
SPVPA effects on	100
Deodorant textiles, copolymer treatment effects	246
Detergents, amphoteric acrylamide copolymers	245
Dialysis equilibrium, SDS concentration	
determination and	107
Dicalcium phosphate dihydrate, crystal	
growth inhibition	78
Dicarboxylic acid, hydroxyapatite crystal	
growth and	78
Diffusion coefficient	17
Diiodomethane, surface tension of	58
Dimethyl sulfoxide, as poly(vinyl alcohol) solvent	32
Dissolution studies	34
Disulfide bonds, hair relaxers and	231
DMSO: <i>see</i> Dimethyl sulfoxide	
Dodecaine, surface tension of	58
Dosigraph, crystallization kinetics and	56
Drop volume, Kruss Drop Volume Tensiometer and	13
Drop volume technique	12
Drop volume tensiometry	16
DuNouy ring method	10
Dynamic interfacial tension	
cyclohexane/water interface and	13
determination of	12 16

Index Terms	Links	
Electrolytes, inorganic	54	
Electrosteric stabilization	8	
Endochondral ossification, hydroxyapatite and	63	
Energy, activation	15	
Energy dispersive x-ray spectroscopy	179	
Energy production, scale formation in	118	
Enzymatic degradation, kinetics of	41	
Enzymes		
guar galactomannans and	41	
guar gum solutions and	43	
guar solution viscosity and	44	
Epton method, of SDS concentration determination	107	
Equilibrium interfacial tension	9	
determination of	10	
DuNouy ring method and	10	
Equilibrium swelling	34	
crystallinity of poly(vinyl alcohol) and	36	
Ethylene glycol, surface tension of	58	
Feed water, mineral scale formation	132	
FEP: <i>see</i>		
Poly(tetrafluoroethylene-co-hexafluoro-propylene)		
Flocculation		
AMD-co-AETAC polymers and	195	
cake solids and	200	
capillary suction time and	200	
filtrate turbidity an	200	
free drainage rate and	200	
wastewater sludge and	196	
Fluorescence spectroscopy		
polymer conformation and	23	
polymer interaction and	23	
Food additives, guar gum and	42	
Formamide, surface tension of	58	
Freezing/thawing, poly(vinyl alcohol) solubility	31	
Fulvic acid		
calcium carbonate formation	132	
hydroxyapatite crystal growth and	77	81
Galactomannans, as food additives	42	
Galactosamine, hydroxyapatite adsorption and	71	
α -Galactosidase, guar hydrolysis and	46	
Gas production		
guar use in	42	
inhibitor needs	170	
Gelation		
DMSO as poly(vinyl alcohol) solvent	32	
phase separation and	33	
Gelation rates, poly(vinyl alcohol)	32	

Index Terms	Links
Geothermal wells, calcium carbonate scale formation in	117
Gingivitis	92
Glucosamine, hydroxyapatite adsorption and	71
Glucose, hydroxyapatite crystal growth inhibition and	84
Glycerol, surface tension of	58
Glycolic acid, hydroxyapatite crystal growth inhibition and	84
Glycosaminoglycans	
hydroxyapatite crystal growth and	67
hydroxyapatite crystal growth inhibition and	63
Goniometer, direct contact angle measurements	57
Guar galactomannans, enzymatic modification of	41
as food additive	42
Guar gum	
enzymatic degradation of	43
gas production and	42
hydraulic fracturing of	42
mining industry and	42
oil production and	42
paper production and	41
Guaran	42
Guar hydrolysis, α -galactosidase and	46
Guar solutions	
degradation time and	41
enzymatic hydrolysis of	43
enzyme concentration and	41
molecular/rheological property changes	43
rheology of enzymatic degradation	41
SEC and	41
viscosity of	41 44
Gypsum crystallization	
inhibition on heat exchanger surfaces	183
temperature–time profiles of	187
Hair	
physical structure of	235
relaxed	
increasing strength of	237
minimizing swelling of	239
tensile strength of	231
water-soluble polymers in	231
Hair care	
amphoterics in	232
anionic polymers and	232
cationic polymers in	233
nonionic polymers in	234
HAP: <i>see</i> Hydroxyapatite	
Hair relaxers, cationic polymer effects in	240

Index Terms	Links
Hair swelling, hydrogenated starch hydrolysate and	234
Heat exchanger surfaces, gypsum scale inhibition on	183
Hemihydrate scales, formation on heat exchanger surfaces	183
Heptane, surface tension of	58
Hexacarboxylic acid, hydroxyapatite crystal growth and	78
Hexadecane, surface tension of	58
HMPAA: <i>see</i> Poly(acrylic acid), hydrophobically modified	
HPC: <i>see</i> Hydroxypropylcellulose	
HSA: <i>see</i> Human serum albumin	
Human serum albumin, adsorption on PMMA	59
Humic acid, calcium carbonate formation	132
Humic compounds, hydroxyapatite crystal growth and	77
Hydraulic fracturing	42
Hydrogen bonding	27
Hydrogen bonds, hair relaxers and	231
Hydrogenated starch hydrolysate, hair swelling and water solubility and	234 31
Hydrogen bonds, hair relaxers and	231
Hydrogenated starch hydrolysate, hair swelling and	234
Hydrolysis	
of guar solutions	43
water solubility and	31
Hydrophobes	
content in HMPAAs	21
oil/water interface and	9
Hydroxyapatite	
adsorption by hydroxypropylcellulose	109
adsorption isotherms	66
calcium phosphate nucleation and	60
desorption of hydroxypropylcellulose after dilution	110
desorption of SDS after dilution	110
growth inhibition by glycosaminoglycans	63
hydroxypropylcellulose adsorption on	105
mammalian hard tissue formation and	114
SDS adsorption on	108
surface complex formation effects on stability	112
Hydroxyapatite beads	
bacterial attachment to	95
SPVPA adsorption to	97
Hydroxyapatite crystallization	63
benzene hexacarboxylic acid and	77
citric acid inhibition of	84
dental calculus formation and	91
dicarboxylic acid influence on	78
fulvic acid and	77
glucose inhibition of	84
glycolic acid inhibition of	84

Index Terms	Links
Hydroxyapatite crystallization (cont.)	
hexacarboxylic acid influence on	78
humic compound influence on	77
inhibition of	67
kinetics of	96
magnesium inhibition of	84
mellitic acid inhibition of	84
phytic acid inhibition of	84
plaque formation and	91
poly(acrylic acid) and	77
poly(acrylic acid) inhibition of	84
pyrophosphate inhibition of	84
SPVPA adsorption and	93
tannic acid and	77
tricarboxylic acid influence on	78
zinc inhibition of	84
Hydroxyapatite disks, saliva-coated,	
bacterial attachment to	95
Hydroxyapatite suspension, stability	105
Hydroxypropylcellulose	
adsorption on hydroxyapatite	105
binding of SDS by	109
desorption of	110
mammalian hard tissue formation and	114
surface complex formation and	111
Impurities	
crystal growth and	52
crystallization kinetics and	51
nucleation and	52
Industrial water systems, scale formation and	183
Interfacial adsorption, kinetics of	20
Interfacial tension, <i>see also</i> Dynamic interfacial	
tension; Equilibrium interfacial tension	
contact angle measurement determination of	57
drop volume technique determining	12
Kinetics	
of adsorption studies	11
crystallization	51
of crystallization	56
hydrophobically modified poly(acrylic acids)	1
hydroxyapatite crystal growth	96
hydroxyapatite crystal growth rate and	84
of interfacial adsorption	20
Kruss Drop Volume Tensiometer	13
Kruss Processor Tensiometer K12	10
Langmuir adsorption isotherm curves	60

Index Terms	Links
Light scattering studies	5
Lime-soda softening	211
Macromolecules	
hydroxyapatite and	66
mineralization in presence of	59
water-soluble	59
Magnesium, hydroxyapatite crystal growth	
inhibition and	84
Magnesium silicate	175
Maleic acid copolymers	
affinity constants of	126
calcium carbonate inhibition and	117
chemical composition of	120
crystal growth and	120
Mammalian hard tissues, formation of	114
Mellitic acid, hydroxyapatite crystal growth	
inhibition and	84
Melting point, of poly(vinyl alcohol)	36
Metals, recycled water and	221
Methanolysis, of poly(vinyl acetate)	32
Methylene blue diphasic titration, SDS	
concentration determination and	107
Mineral scale formation	131
hydroxyapatite crystallization and	77
inhibition by polymers	163
precipitation inhibition of	164
semi-empirical inhibition model	165
Mineralization, macromolecules and	59
Mining industry, guar gum and	42
Molecular weight	
acrylic acids	5
pyreneacrylamide	5
water solubility and	31
Molybdate/phosphonate, corrosion inhibition and	218
Molybdate/zinc, corrosion inhibition and	218
Nonionic polymers, hair care and	234
Nucleation	
impurities and	52
on polymer surfaces	59
scale inhibitors and	169
Octane, surface tension of	58
Oil production	
guar use in	42
inhibitor needs	170
Oil-in-water emulsions	1
HMPAAs and	1
Oil/water interface, hydrophobes and	9

Index Terms	Links
Organic azole, corrosion inhibition and	219
Organic inhibitors, calcium carbonate crystal growth and	131
Organophosphonates, crystal growth inhibition	78
Orthophosphate, corrosion inhibition and	219
Osmosis, reverse	211
Paper production, guar gum and	41
Periodontitis	92
pH, effects, polyethylene oxide adsorption on silica	26
pH trigger, HMPAA and	8
Phase separation, gelation and	33
Phosphonates, recycled water and	217
Photo Correlation spectroscopy	23
Phytic acid, hydroxyapatite crystal growth inhibition and	84
Plaque, dental: <i>see</i> Dental plaque	
PMMA: <i>see</i> Poly(methyl methacrylate)	
Polyacrylic acid	232
Poly(acrylic acid)	
hydrophobically modified	1
adsorption efficiency in	19
crosslink density and	20
hydrophobe content in	21
low pressure region in	15
material characterization and	4
pH trigger and	8
hydroxyapatite crystal growth and	77
hydroxyapatite crystal growth inhibition and	84
neutralized	6
Polyacrylic acid adsorption, solids concentration effects on	25
Poly(aspartic acid), scale deposition experiments and	188
Polyelectrolytes	
cationic, in wastewater treatments	193
crystal growth experiments and	120
ordinary–extraordinary transition of	199
topological structure of	196
Polyethylene oxide, adsorption on silica	26
Polymer adsorption	23
density	29
methods of	25
solid concentration effect on	23
fluorescence spectroscopy and	23
pyrene labeled polyethylene oxide	25
solid concentration effect on	23
at solid/liquid interface	23
Polymer surfaces, nucleation on	59
Polymeric antiscalants, silica and	173

Index Terms	Links
Polymer conformation	23
Polymers	
alumina surface and	26
characterization of	5
concentrated particulate suspensions and	23
electrosteric stabilization of	8
in hair care	231
nonionic	234
recycled water and	217
structured	194
Poly(methyl methacrylate)	
calcium phosphate nucleation on	59
crystallization kinetics and	51
human serum albumin adsorption on	59
interfacial tension of	59
Polyquaternium-6	233
Polyquaternium-7	233
Polyquaternium-10	233
Poly(tetrafluoroethylene-co-hexafluoropropylene)	
calcium phosphate nucleation on	59
crystallization kinetics	51
Poly(vinyl acetate), methanolysis of	32
Poly(vinyl alcohol)	
aqueous solutions of	33
boric acid and	34
dimethyl sulfoxide as solvent	32
dissolution studies	34
equilibrium swelling studies	34
long-term stability of	32
melting point of	36
poly(vinyl acetate) and	32
retrogradation of	32
solidification of	32
stability of	34
temperature of	32
water solubility characteristics of	31
Poly(vinyl alcohol) gels	
biomedical applications of	32
crystalline structure of	35
freeze-dried	32
heat-treated	32
mechanical stability of	38
optimal freezing/thawing cycles	37
organic solvents and	32
rapid cycling conditions and	37
rapid freeze/thaw cycles and	37
stability of	37
synthesis of	33
water solubility of	31
Poly(vinyl alcohol) hydrogels:	
<i>see</i> Poly(vinyl alcohol) gels	

Index Terms	Links
Polyvinyl pyrrolidone, adsorption on alumina and	26
Potentiometer, crystallization kinetics and	56
Precipitation inhibition, mechanistic aspects of	164
Precipitation techniques	77
Pre-exponential factor	55
PVA: <i>see</i> Poly(vinyl alcohol)	
PYA: <i>see</i> Pyreneacrylamide	
Pyrene labeled polyethylene oxide, fluorescence at silica/water interface	23
Pyreneacrylamide	5
characteristics of	5
interfacial adsorption kinetics	20
Pyrophosphate	
crystal growth inhibition	78
hydroxyapatite crystal growth inhibition and	84
Radiofrequency glow discharge, crystallization kinetics and	51
RFGD: <i>see</i> Radiofrequency glow discharge	
Rheology	
guar solution enzymatic degradation	41
of guar solution hydrolysis	43
suspension	23
Scale formation	131
calcium carbonate	117
control in recycled water	207
maleic acid copolymers and	120
SDS: <i>see</i> Sodium dodecylsulfate	
SEC, guar solution enzymatic degradation	41
Shear viscosity, guar solutions and	41
Silica	
amorphous	175
antiscalants for	176
polyethylene oxide adsorption on	26
polymeric	175
polymeric antiscalants and	173
problems with	175
recycled water and	221
solubility in water systems	173
water treatment systems and	175
Silicate salts	173
Silica/water interface, pyrene labeled polyethylene oxide fluorescence at	23
Silicone rubber, calcium phosphate nucleation on	59
Sodium dodecylsulfate	
adsorption on HAP	108
binding by hydroxypropylcellulose	109

Index Terms	Links
Sodium dodecylsulfate (cont.)	
desorption of	110
dialysis equilibrium method of	
concentration determination	107
Epton method of concentration determination	107
hydroxypropylcellulose adsorption and	105
mammalian hard tissue formation and	114
methylene blue diphasic titration	107
surface complex formation and	111
total concentration of	107
Sodium polyvinylphosphonic acid	91
adsorption to hydroxyapatite beads	97
bacterial attachment assay	94
bacterial cultures and conditions	94
dental calculus/plaque inhibition	92
effect, calculus formation	95
effects, short-term plaque formation	96
seeded crystal growth	92
synthesis of	92
Solid/liquid interface	
polymer adsorption and	23
polymer conformation at	23
Solids, recycled water and	221
Solids concentration	
adsorption effects of	29
polyacrylic acid adsorption and	25
polyethylene oxide adsorption on silica and	27
Spectroscopy	
fluorescence	23
Photon Correlation	23
SPVPA: <i>see</i> Sodium polyvinylphosphonic acid	
StoichiometricsW crystallization kinetics and	56
Surface complex formation, biological significance of	114
Suspension pH, polyacrylic acid adsorption and	25
Suspension rheology	23
Swelling studies, of poly(vinyl alcohol)	34
Tannic acid, hydroxyapatite crystal growth and	77
Tensiometry, drop volume	16
Terpolymers	151
AA/AHPSE/PEGAE	151
calcium phosphate scale formation and	149
Tetradecaine, surface tension of	58
Thermodynamic characteristics, of poly(vinyl alcohol)	32
Thermoelectric power generation, water	
conservation and	208
Thermogram, of poly(vinyl alcohol) gels	35
Tricarboxylic acid, hydroxyapatite crystal growth and	78
Trypticase labeling media	94

Index Terms	Links
Uronic acid, borate–carbazole reaction determination of	64
Vinyl phosphonyl dichloride	91
Viscometry	196
Viscosity	
recycled	
of guar solutions	44
time-dependent behavior of	44
Wastewater	
Waste streams separation	211
biologically treated	215
municipal	214
recycled	207
Wastewater sludge, flocculation of	196
Wastewater treatments, cationic polyelectrolyte applications in	193
Water	
recycled	
agricultural waste	213
bio-control of	219
biologically treated wastewater	215
boiler blowdown	216
boiler condensate	216
contaminants that affect	220
cooling water treatment optimization in	207
corrosion inhibitors	218
demineralizer fast-rinse	213
low TDS water	216
monitoring	222
municipal wastewater	214
phosphonates and	217
polymers and	217
process compatibility and	222
product formulation	216
program cost comparison	222
R.O. reject	212
scale inhibition in	216
scrubber blowdown	213
seawater	215
silica and	221
software and	217
storm runoff	213
types in cooling systems	212
surface tension of	58

Index Terms	Links
Water conservation	208
cooling water treatment optimization and	207
in design phase	209
lime-soda softening	211
motivation for	208
reverse osmosis and	211
side-stream softening	210
thermoelectric power generation and	208
Water cooling systems	
scale formation in	118
steam electrical generation	208
Water solubility	
hydrogen bonding and	31
hydrolysis and	31
molecular weight and	31
of poly(vinyl alcohol)	31
Water treatment, silica and	175
 Zeldovich factor	 55
Zinc	
corrosion inhibition and	218
hydroxyapatite crystal growth inhibition and	84

Chemsoft®

Química Orgánica

Recopilación

José A. - UHMMBCH



2009

Química Orgánica

Recopilación

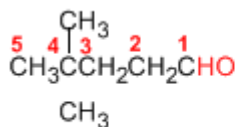
Índice.

- i. Nomenclatura de Aldehídos y Cetonas*
- ii. Preparación de Aldehídos y Cetonas*
- iii. Formación de Hidratos*
- iv. Formación de Hemiacetales*
- v. Formación de Acetales*
- vi. Formación de Acetales Cíclicos*
- vii. Acetales Como Grupos Protectores*
- viii. Formación de Iminas*
- ix. Formación de Oximas*
- x. Formación de Hidrazonas*
- xi. Formación de Azinas*
- xii. Formación de Semicarbazonas*
- xiii. Ensayo de la 2,4 - Dinitrofenilhidrazina*
- xiv. Formación de Cianhídrinas*
- xv. Reacción de Wittig*
- xvi. Oxidación de Baeyer Villiger*
- xvii. Problemas Nomenclatura Aldehídos y Cetonas*
- xviii. Problemas Resueltos de Aldehídos y Cetonas*
- xix. Teorías de Enoles y Enolatos*

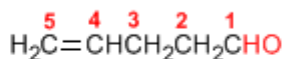
Nomenclatura de Aldehídos y Cetonas

Los aldehídos se nombran reemplazando la terminación **-ano** del alcano correspondiente por **-al**. No es necesario especificar la posición del grupo aldehído, puesto que ocupa el extremo de la cadena (localizador 1).

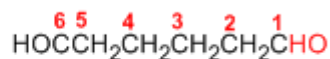
Cuando la cadena contiene dos funciones aldehído se emplea el sufijo **-dial**.



4,4-Dimetilpentanal

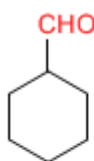


Hex-4-enal

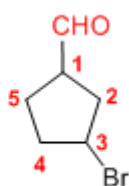


Pentanodial

El grupo **-CHO** unido a un ciclo se llama **-carbaldehído**. La numeración del ciclo se realiza dando localizador 1 al carbono del ciclo que contiene el grupo aldehído.



Ciclohexanocarbaldehído

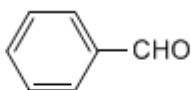


3-Bromociclopentanocarbaldehído

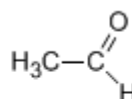
Algunos nombres comunes de aldehídos aceptados por la IUPAC son:



Formaldehído
(Metanal)

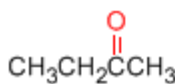


Benzaldehído
(Bencenocarbaldehído)

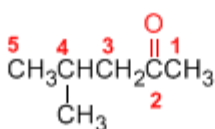


Acetaldehído
(Etanal)

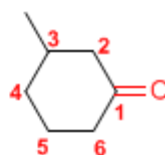
Las cetonas se nombran sustituyendo la terminación **-ano** del alcano con igual longitud de cadena por **-ona**. Se toma como cadena principal la de mayor longitud que contiene el grupo carbonilo y se numera para que éste tome el localizador más bajo.



Butanona

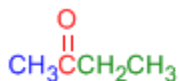


4-Metil-2-pentanona

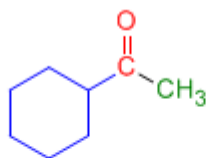


3-Metilciclohexanona

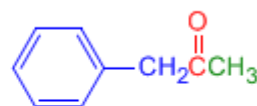
Existe un segundo tipo de nomenclatura para las cetonas, que consiste en nombrar las cadenas como sustituyentes, ordenándolas alfabéticamente y terminando el nombre con la palabra **cetona**.



Etil metil cetona



Ciclohexil metil cetona



Fenil metil cetona

[Siguiete >](#)

[\[Volver\]](#)

Charles Friedel (1832 - 1899)



Origen: Químico frances..

Lugar de nacimiento: Estrasburgo.

Formación: estudió química en la Universidad de Berlín entre 1895 y 1899, consiguiendo el doctorado este año.

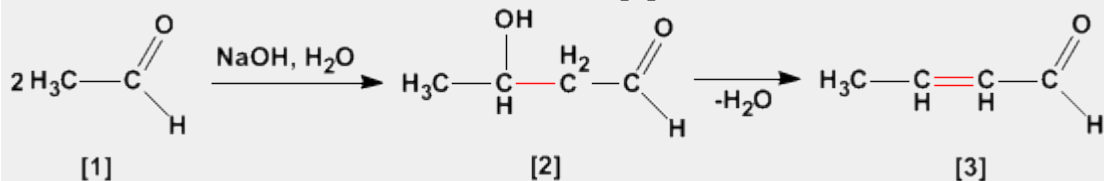
Docencia: Profesor en la Universidad de la Sorbona.

Investigación: Obtuvo el alcohol propílico. En 1877, Friedel y Crafts describieron por primera vez la reacción del benceno con un haloalcano en presencia de un ácido de Lewis. Esta reacción produce la alquilación del benceno y se conoce como alquilación de Friedl-Crafts.

Premio Nobel:

Aldólica (Condensación)

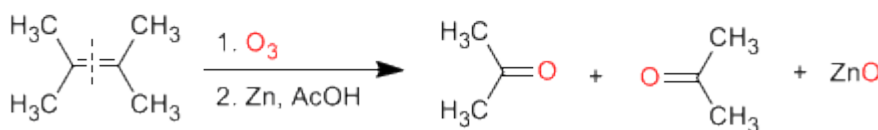
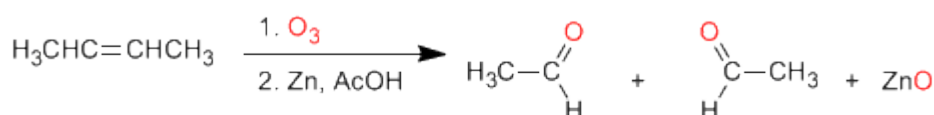
La condensación aldólica es una reacción de aldehídos o cetonas **[1]** que forma 3-hidroxicarbonilos (aldoles) **[2]**. El 3-hidroxialdehído **[2]** bajo condiciones de deshidratación por calentamiento rinde un aldehído alfa,beta-insaturado **[3]**.



Preparación de aldehídos y cetonas

Los aldehídos y cetonas pueden ser preparados por oxidación de alcoholes, ozonólisis de alquenos, hidratación de alquinos y acilación de Friedel-Crafts como métodos de mayor importancia.

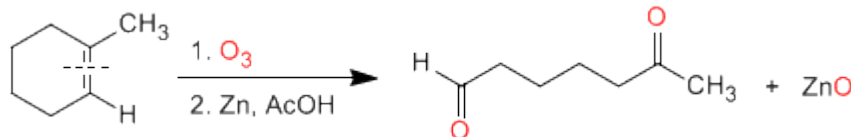
a) **Ozonólisis de alquenos:** Los alquenos rompen con ozono formando aldehídos y/o cetonas. Si el alqueno tiene hidrógenos vinílicos da aldehídos. Si tiene dos cadenas carbonadas forma cetonas.



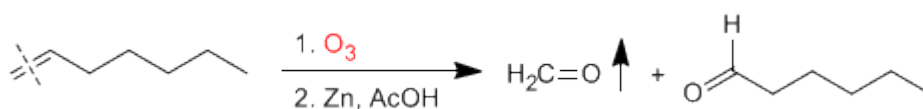
Ozonólisis

Los alquenos simétricos y terminales permiten la preparación de carbonilos mediante ozonólisis

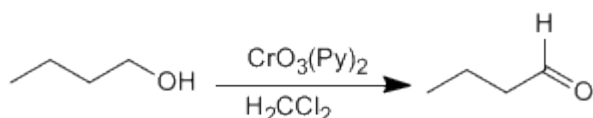
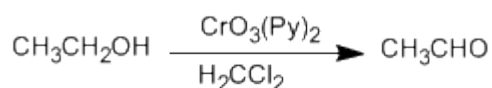
La ozonólisis de alquenos cíclicos produce compuestos dicarbonílicos:



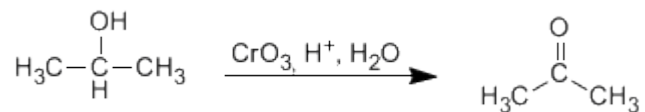
Los alquenos terminales rompen formando metanal, que separa fácilmente de la mezcla por su bajo punto de ebullición.



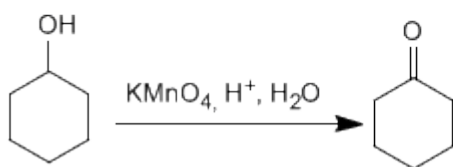
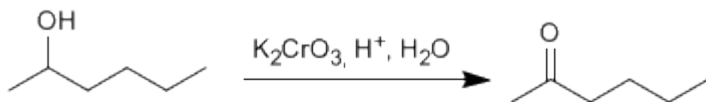
b) **Oxidación de alcoholes:** Los alcoholes primarios y secundarios se oxidan para dar aldehídos y cetonas respectivamente. Deben tomarse precauciones en la oxidación de alcoholes primarios, puesto que sobreoxidan a ácidos carboxílicos en presencia de oxidantes que contengan agua. En estos caso debe trabajarse con reactivos anhidros, como el clorocromato de piridino en diclorometano (PCC), a temperatura ambiente.



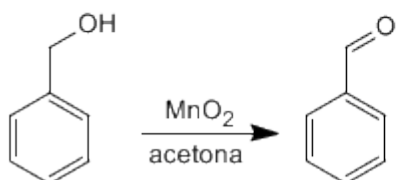
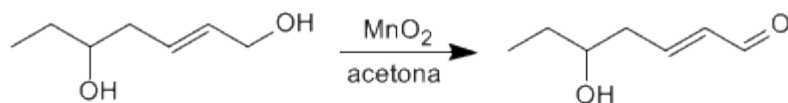
Los alcoholes secundarios dan cetonas por oxidación. Se emplean como oxidantes permanganato, dicromato, trióxido de cromo.



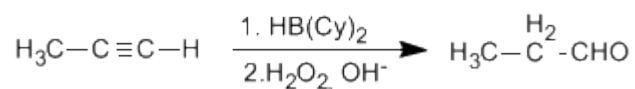
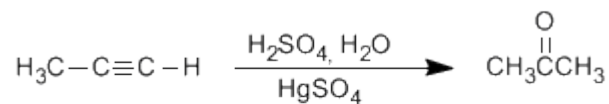
La oxidación supone la pérdida de dos hidrógenos del alcohol. Los alcoholes terciarios no pueden oxidar puesto que carecen de hidrógeno sobre el carbono.



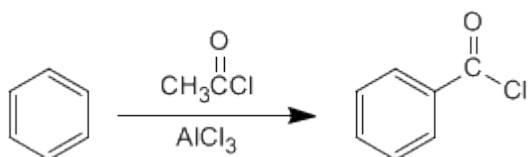
Los alcoholes alílicos y bencílicos se transforman en aldehídos o cetonas por oxidación con dióxido de manganeso en acetona. Esta reacción tiene una elevada selectividad y no oxida alcoholes que no se encuentren en dichas posiciones.



c) **Hidratación de alquinos:** Los alquinos se pueden hidratar Markovnikov, formando cetonas, o bien antiMarkovnikov, para formar aldehídos.



d) **Acilación de Friedel-Crafts:** La introducción de grupos acilo en el benceno permite la preparación de cetonas con cadenas aromáticas.



Otto Paul Hermann Diels (1876 - 1954)



Origen: Químico alemán.

Lugar de nacimiento: Königshütte (hoy Chorzów, Polonia).

Formación: estudió química en la Universidad de Berlín entre 1895 y 1899, consiguiendo el doctorado este año.

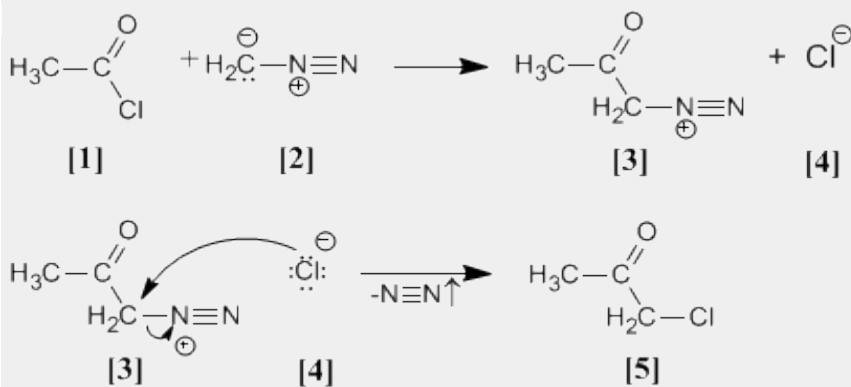
Docencia: profesor y jefe del departamento de química en la Universidad de Berlín. En 1916, tomó el puesto de profesor de Química en la Universidad de Kiel, cargo que no dejó hasta su jubilación en 1945.

Investigación: En 1906 descubrió el anhídrido malónico. Investigó en reacciones de deshidrogenación con selenio. Síntesis de α -dicetonas. Pero su trabajo más importante es la reacción de Diels - Alder.

Premio Nobel: En 1950 recibió el Premio Nobel junto a Kurt Alder

Arndt Eistert (Síntesis)

Cloruro de acetilo [1] se trata con diazometano [2] rindiendo la sal de diazonio [3]. El cloruro [4] producido reacciona con la sal de diazonio para dar la α -clorocetona [5].

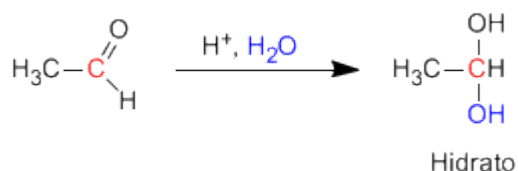


Síntesis de Arndt Eistert

Esta reacción permite transformar haluros de alcanoilo en cetonas halogenadas en su posición alfa.

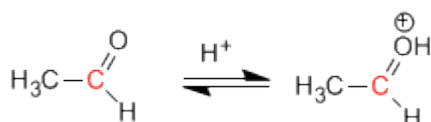
Formación de Hidratos

Los aldehídos y cetonas reaccionan en medio ácido acuoso para formar hidratos. El mecanismo consta de tres etapas. La primera y más rápida consiste en la protonación del oxígeno carbonílico. Esta protonación produce un aumento de la polaridad sobre el carbono y favorece el ataque del nucleófilo. En la segunda etapa el agua ataca al carbono carbonilo, es la etapa lenta del mecanismo. En la tercera etapa se produce la desprotonación del oxígeno formándose el hidrato final.

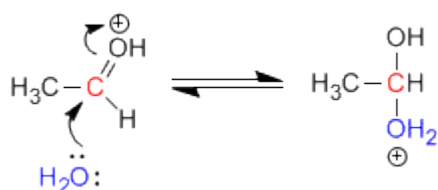


Mecanismo de la reacción

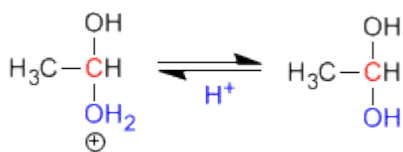
Etapa 1. Protonación del oxígeno carbonílico.



Etapa 2. Ataque nucleófilo del agua al carbonilo protonado.



Etapa 3. Desprotonación del hidrato





Origen: Químico estadounidense.

Lugar de nacimiento: Budapest

Formación: Se doctoró en la Universidad de Budapest en 1949

Docencia: Trabajó en el departamento de química orgánica de la Academia de Ciencias de Hungría y posteriormente en la Universidad de Cleveland.

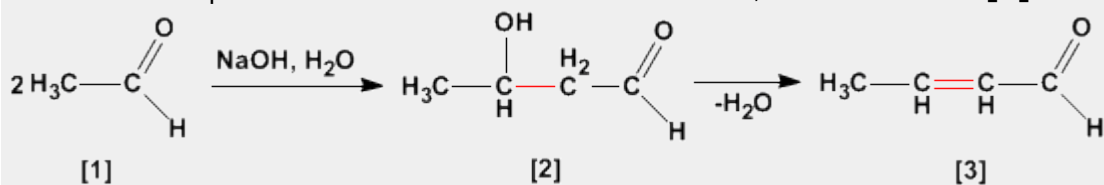
Industria: Trabajó en los laboratorios de la Dow Chemical de Ontario

Investigación: Olah consiguió preparar carbocationes estables utilizando componentes extremadamente ácidos.

Premio Nobel: En 1994 obtuvo el premio Nobel de Química por sus investigaciones sobre los carbocationes

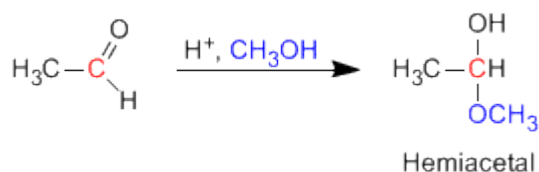
Aldólica (Condensación)

La condensación aldólica es una reacción de aldehídos o cetonas **[1]** que forma 3-hidroxicarbonilos (aldoles) **[2]**. El 3-hidroxialdehído **[2]** bajo condiciones de deshidratación por calentamiento rinde un aldehído alfa,beta-insaturado **[3]**.



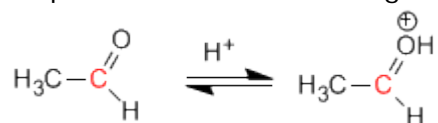
Formación de Hemiacetales

Los hemiacetales se forman por reacción de un equivalente de alcohol con el grupo carbonilo de un aldehído o cetona. Esta reacción se cataliza con ácido y es equivalente a la formación de hidratos.

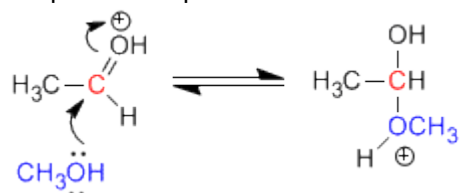


Mecanismo de la reacción:

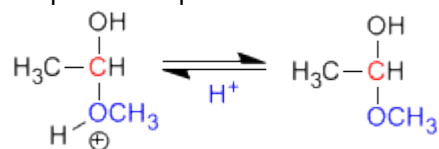
Etapas 1. Protonación del oxígeno carbonílico.



Etapas 2. Ataque nucleófilo del metanol al carbonilo protonado.



Etapas 3. Desprotonación del hemiacetal



Otto Paul Hermann Diels (1876 - 1954)



Origen: Químico alemán.

Lugar de nacimiento: Königshütte (hoy Chorzów, Polonia).

Formación: estudió química en la Universidad de Berlín entre 1895 y 1899, consiguiendo el doctorado este año.

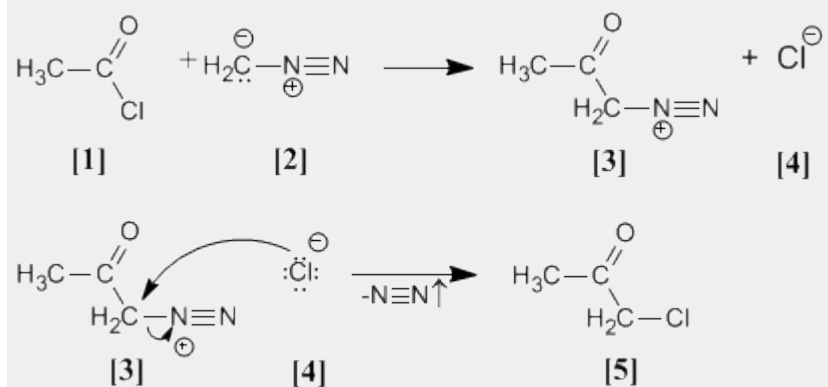
Docencia: profesor y jefe del departamento de química en la Universidad de Berlín. En 1916, tomó el puesto de profesor de Química en la Universidad de Kiel, cargo que no dejó hasta su jubilación en 1945.

Investigación: En 1906 descubrió el anhídrido malónico. Investigó en reacciones de deshidrogenación con selenio. Síntesis de α -dicetonas. Pero su trabajo más importante es la reacción de Diels - Alder.

Premio Nobel: En 1950 recibió el Premio Nobel junto a Kurt Alder

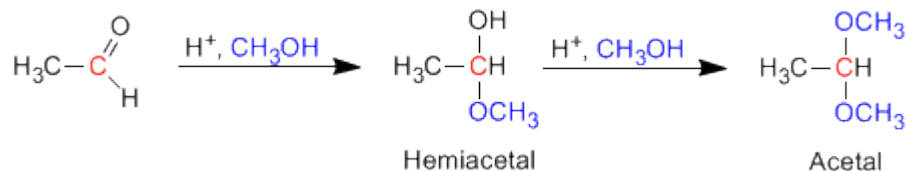
Arndt Eistert (Síntesis)

Cloruro de acetilo **[1]** se trata con diazometano **[2]** rindiendo la sal de diazonio **[3]**. El cloruro **[4]** producido reacciona con la sal de diazonio para dar la α -clorocetona **[5]**.



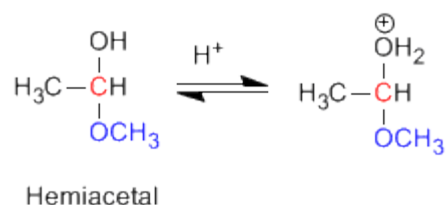
Formación de Acetales

Los aldehídos y cetonas reaccionan con alcoholes bajo condiciones de catálisis ácida, formando en una primera etapa hemiacetales, que posteriormene evolucionan por reacción con un segundo equivalente de alcohol a acetales.

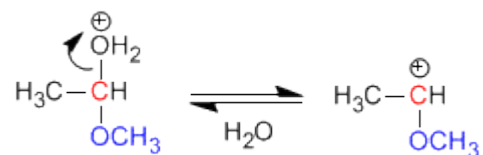


Mecanismo para la formación de acetales

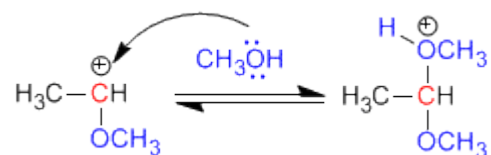
Etapa 1. Protonación del grupo hidroxilo



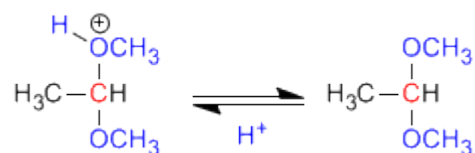
Etapa 2. Pérdida de agua.



Etapa 3. Ataque del alcohol al carbocatión



Etapa 4. Desprotonación del acetal



Otto Paul Hermann Diels (1876 - 1954)



Origen: Químico alemán.

Lugar de nacimiento: Königshütte (hoy Chorzów, Polonia).

Formación: estudió química en la Universidad de Berlín entre 1895 y 1899, consiguiendo el doctorado este año.

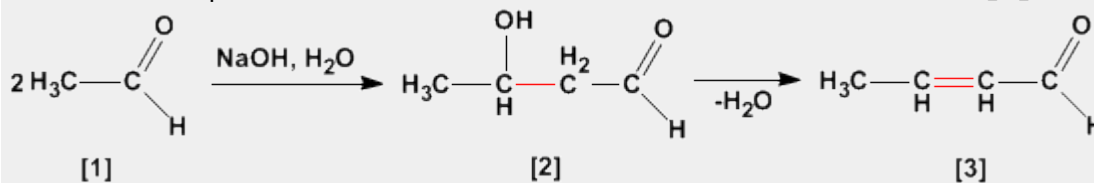
Docencia: profesor y jefe del departamento de química en la Universidad de Berlín. En 1916, tomó el puesto de profesor de Química en la Universidad de Kiel, cargo que no dejó hasta su jubilación en 1945.

Investigación: En 1906 descubrió el anhídrido malónico. Investigó en reacciones de deshidrogenación con selenio. Síntesis de α -dicetonas. Pero su trabajo más importante es la reacción de Diels - Alder.

Premio Nobel: En 1950 recibió el Premio Nobel junto a Kurt Alder

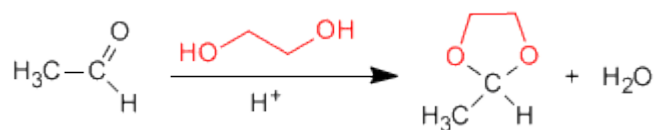
Aldólica (Condensación)

La condensación aldólica es una reacción de aldehídos o cetonas **[1]** que forma 3-hidroxicarbonilos (aldoles) **[2]**. El 3-hidroxialdehído **[2]** bajo condiciones de deshidratación por calentamiento rinde un aldehído alfa,beta-insaturado **[3]**.



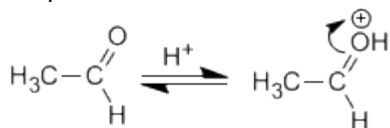
Formación de acetales cíclicos

Los 1,2- y 1,3-dioles reaccionan con aldehídos y cetonas formando acetales cíclicos. Los equilibrios se desplazan hacia el producto final eliminando el agua formada por destilación azeotrópica con benceno o tolueno.

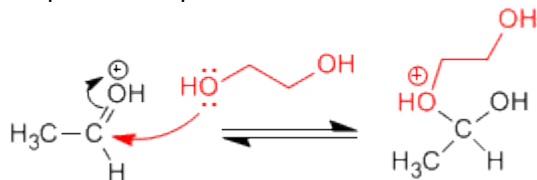


Mecanismo para la formación de acetales cíclicos:

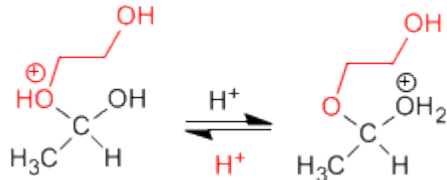
Etapa 1. Protonación del carbonilo



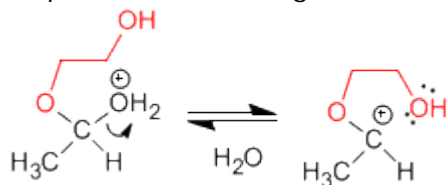
Etapa 2. Ataque nucleófilo del diol al carbonilo.



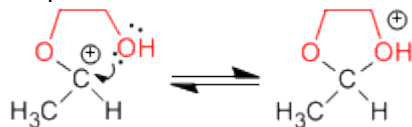
Etapa 3. Equilibrio ácido base entre el éter y el alcohol



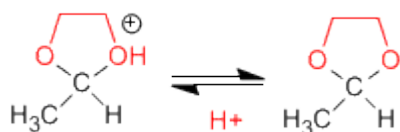
Etapa 4. Pérdida de agua



Etapa 5. Ciclación



Etapa 6. Desprotonación del acetal cíclico



Kurt Alder (1902 - 1958)



Origen: Químico alemán.

Lugar de nacimiento: Königshütte (hoy Chorzów, Polonia).

Formación: estudió en la Universidad de Kiel. Bajo la supervisión del químico alemán Otto Diels, su jefe e instructor en Kiel.

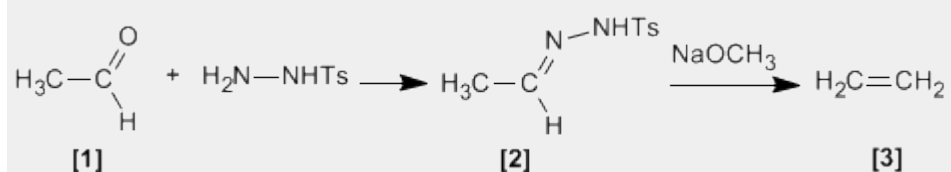
Docencia: Alder ejerció como profesor de química en las universidades de Kiel y Colonia.

Investigación: Alder se especializó en la síntesis diénica (conocida más tarde como la reacción Diels - Alder) que consiste fundamentalmente en el análisis y formación de compuestos orgánicos complejos. Ya en 1928 ambos fueron coautores de un ensayo sobre este proceso.

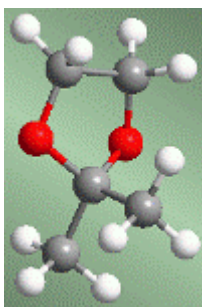
Premio Nobel: En 1950 recibió el Premio Nobel junto a Diels

Bamford Stevens (Reacción)

Tosilhidrazonas [2] de aldehídos o cetonas alifáticos [1] reaccionan con bases fuertes para dar alquenos [3].

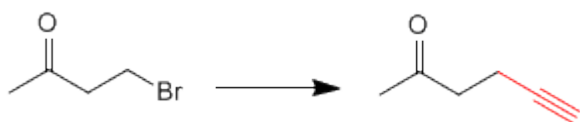


Acetales como grupos protectores

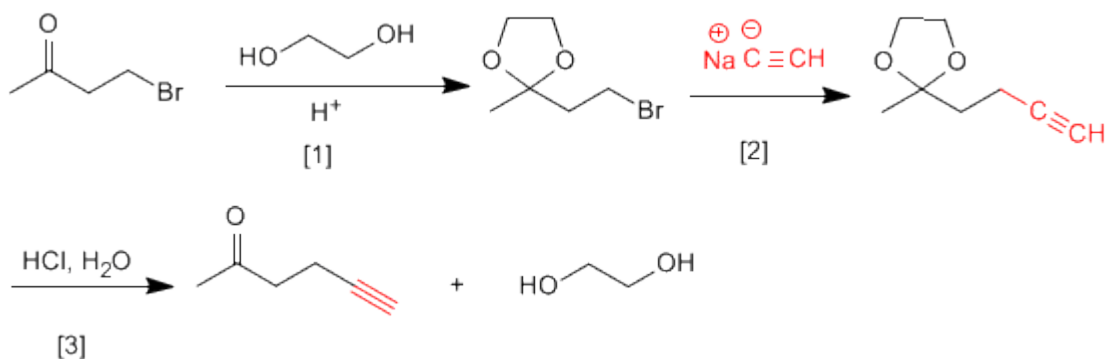


Los acetales pueden emplearse, por su estabilidad, como grupos protectores del carbonilo. El acetal es un éter, muy estable en medios básicos, aunque rompe en presencia de medios ácidos. En muchos procesos de síntesis el grupo carbonilo es incompatible con el reactivo utilizado. En estos casos debe protegerse para evitar que reaccione. La inestabilidad del acetal en medio ácido puede emplearse para desproteger el carbonilo.

Veamos algunos ejemplos:



Esta transformación requiere una sustitución, empleando como nucleófilo un acetiluro de sodio. El nucleófilo puede atacar también al grupo carbonilo, para evitarlo vamos a protegerlo.

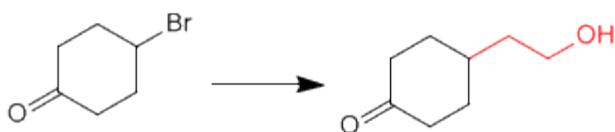


[1] Protección de la cetona.

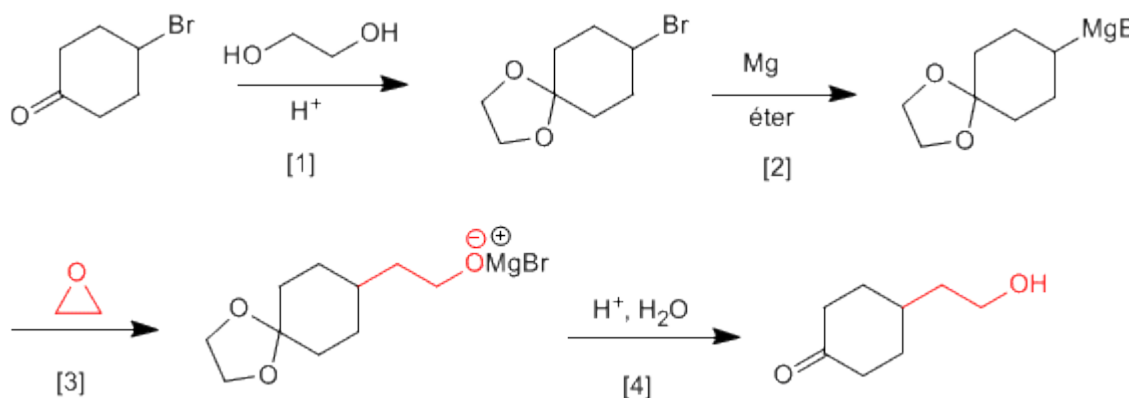
[2] Ataque del acetiluro al carbono del bromo.

[3] Desprotección del carbonilo

Veamos un segundo ejemplo:



Es necesario proteger la cetona antes de formar el organometálico para evitar la dimerización del compuesto.



- [1] Protección de la cetona.
 [2] Formación del magnesiano.
 [3] Apertura del oxaciclopropano.
 [4] Desprotección y protonación del alcóxido.

Otto Paul Hermann Diels (1876 - 1954)



Origen: Químico alemán.

Lugar de nacimiento: Königshütte (hoy Chorzów, Polonia).

Formación: estudió química en la Universidad de Berlín entre 1895 y 1899, consiguiendo el doctorado este año.

Docencia: profesor y jefe del departamento de química en la Universidad de Berlín. En 1916, tomó el puesto de profesor de Química en la Universidad de Kiel, cargo que no dejó hasta su jubilación en 1945.

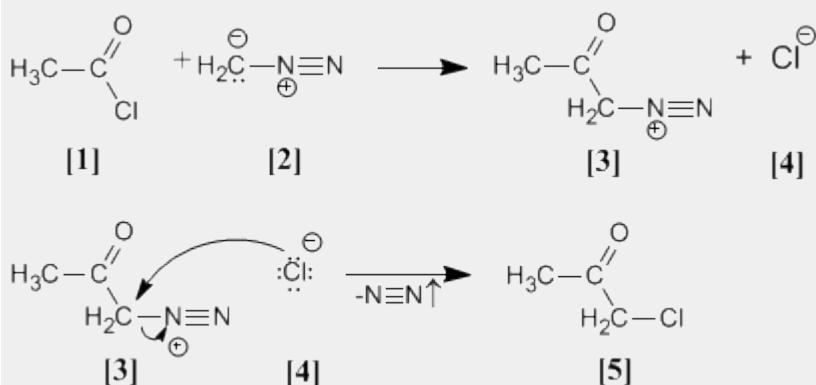
Investigación: En 1906 descubrió el anhídrido malónico.

Investigó en reacciones de deshidrogenación con selenio. Síntesis de α-dicetonas. Pero su trabajo más importante es la reacción de Diels - Alder.

Premio Nobel: En 1950 recibió el Premio Nobel junto a Kurt Alder

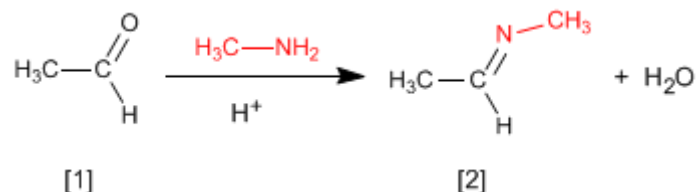
Arndt Eistert (Síntesis)

Cloruro de acetilo **[1]** se trata con diazometano **[2]** rindiendo la sal de diazonio **[3]**. El cloruro **[4]** producido reacciona con la sal de diazonio para dar la α-clorocetona **[5]**.



Formación de Iminas

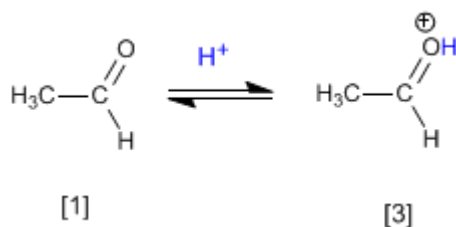
La reacción de aldehídos o cetonas **[1]** con aminas primarias genera iminas **[2]**. La reacción se favorece en un medio ligeramente ácido (pH=4.5).



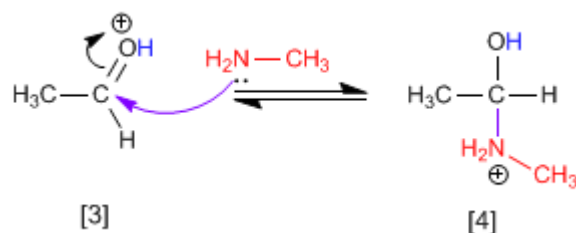
El control del pH es fundamental, puesto que se requiere la protonación del oxígeno del carbonilo para favorecer el ataque nucleófilo.

Mecanismo:

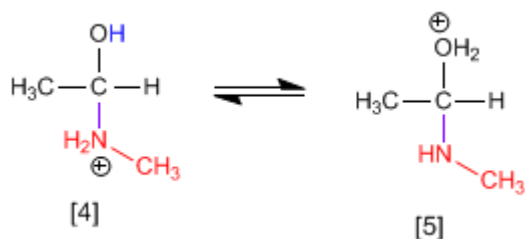
Etapla 1. Protonación del grupo carbonilo que aumenta la polaridad positiva sobre el carbono y favorece el ataque nucleófilo.



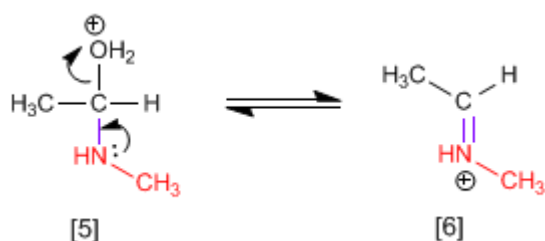
Etapla 2. Ataque nucleófilo de la amina primaria al carbono carbonilo.



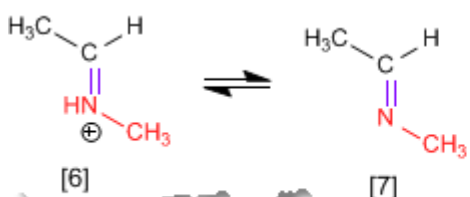
Etapla 3. Protonación del grupo hidroxilo para transformarlo en buen grupo saliente.



Etapla 4. Pérdida de agua y formación de la imina protonada.



Etapa 5. Desprotonación del catión.



George A. Olah (1927 -)



Origen: Químico estadounidense.

Lugar de nacimiento: Budapest

Formación: Se doctoró en la Universidad de Budapest en 1949

Docencia: Trabajó en el departamento de química orgánica de la Academia de Ciencias de Hungría y posteriormente en la Universidad de Cleveland.

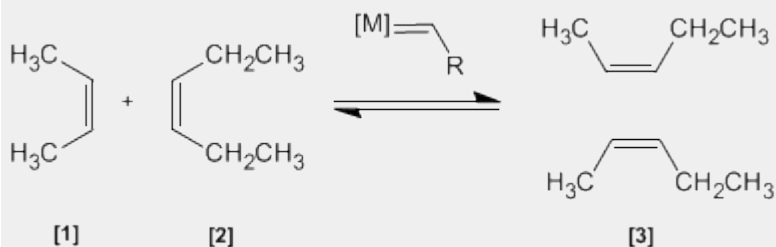
Industria: Trabajó en los laboratorios de la Dow Chemical de Ontario

Investigación: Olah consiguió preparar carbocationes estables utilizando componentes extremadamente ácidos.

Premio Nobel: En 1994 obtuvo el premio Nobel de Química por sus investigaciones sobre los carbocationes

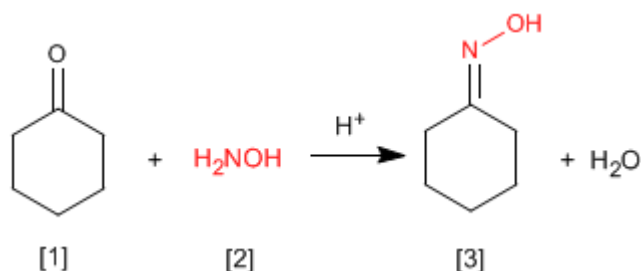
Metátesis de Alquenos

En esta reacción dos alquenos **[1]** y **[2]** son tratados con un metal de transición que actúa como catalizador, dando una mezcla de alquenos **[3]** (incluyendo isómeros Z/E). Este productos se obtiene por intercambio de grupos alquilideno.

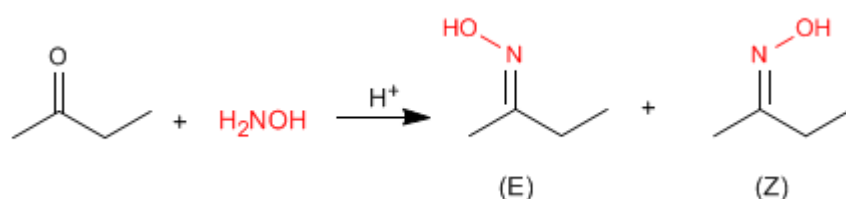


Formación de Oximas

Las oximas [3] se obtienen por reacción de aldehídos o cetonas [1] e hidroxilamina [2] en un medio débilmente ácido. El mecanismo es análogo al de formación de iminas.



Las oximas de aldehídos y cetona asimétricas presentan isomería Z/E dependiendo de la posición del hidroxilo.



Las iminas e hidrazonas (que comentaremos a continuación) también presentan esta característica.

George A. Olah (1927 -)



Origen: Químico estadounidense.

Lugar de nacimiento: Budapest

Formación: Se doctoró en la Universidad de Budapest en 1949

Docencia: Trabajó en el departamento de química orgánica de la Academia de Ciencias de Hungría y posteriormente en la Universidad de Cleveland.

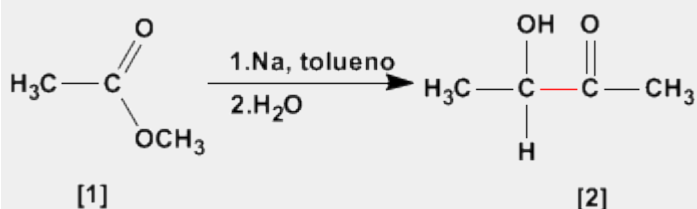
Industria: Trabajó en los laboratorios de la Dow Chemical de Ontario

Investigación: Olah consiguió preparar carbocationes estables utilizando componentes extremadamente ácidos.

Premio Nobel: En 1994 obtuvo el premio Nobel de Química por sus investigaciones sobre los carbocationes

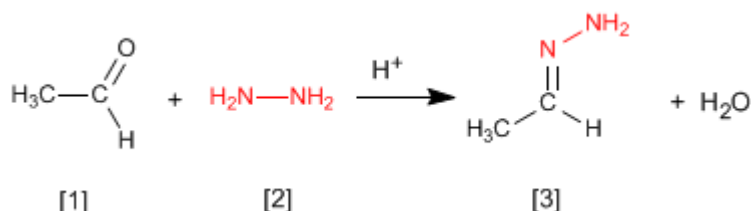
Aciloinica (Condensación)

La condensación aciloinica transforma ésteres [1] en alfa-hidroxicetonas [2]. Esta reacción se realiza con sodio metal en disolvente inerte.

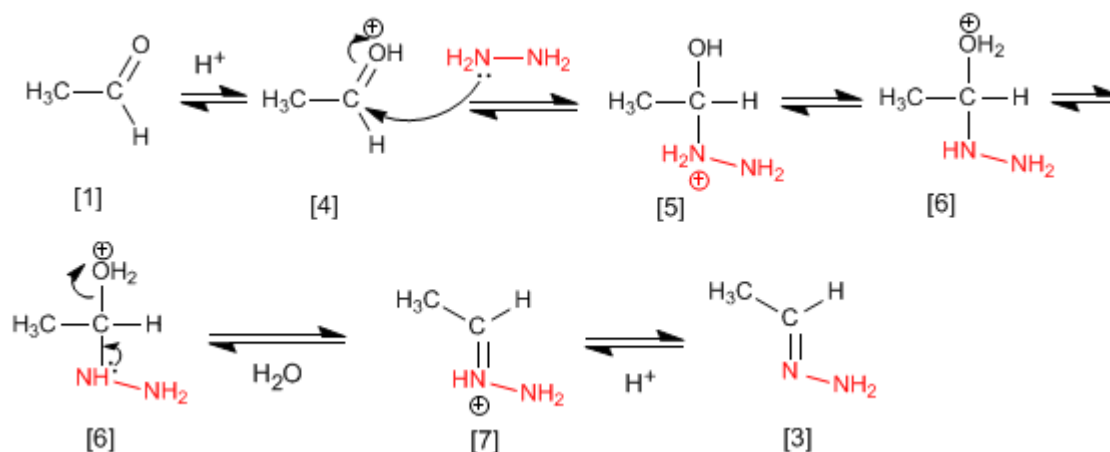


Formación de Hidrazonas

Las hidrazonas [3] se obtienen por reacción de aldehídos o cetonas [1] con hidrazina [2]. Igual que en el caso de las iminas y oximas requiere pH=4.



Aunque el mecanismo es análogo al de formación de iminas, comentaremos de nuevo los pasos.



El etanal [1] se protona formando su ácido conjugado [4]. La importante polaridad del carbono carbonilo de [4] favorece el ataque de la hidrazina [2] para formando el intermedio [5]. El compuesto [5] intercambia un protón entre el nitrógeno y el oxígeno, transformando el grupo hidroxilo en agua (buen grupo saliente). El intermedio [6] pierde una molécula de agua transformándose en [7], cuya desprotonación da la hidrazona final [3].

Kurt Alder (1902 - 1958)



Origen: Químico alemán.

Lugar de nacimiento: Königshütte (hoy Chorzów, Polonia).

Formación: estudió en la Universidad de Kiel. Bajo la supervisión del químico alemán Otto Diels, su jefe e instructor en Kiel.

Docencia: Alder ejerció como profesor de química en las universidades de Kiel y Colonia.

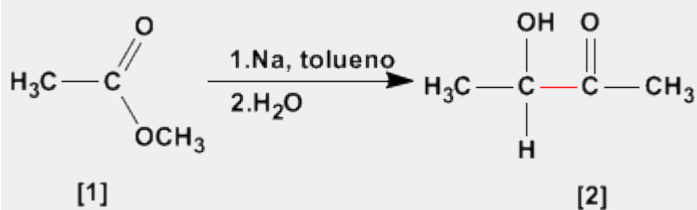
Investigación: Alder se especializó en la síntesis diénica (conocida más tarde como la reacción Diels - Alder) que consiste fundamentalmente en el análisis y formación de compuestos orgánicos complejos.

Ya en 1928 ambos fueron coautores de un ensayo sobre este proceso.

Premio Nobel: En 1950 recibió el Premio Nobel junto a Diels

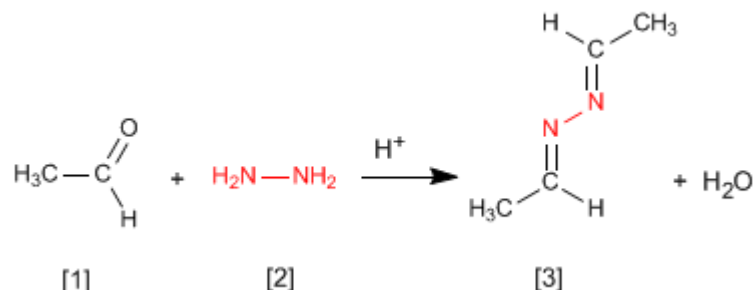
Aciloínica (Condensación)

La condensación aciloínica transforma esteres [1] en alfa-hidroxicetonas [2]. Esta reacción se realiza con sodio metal en disolvente inerte.



Formación de Azinas

La hidrazina [2] reacciona con dos moléculas de aldehído [1] para formar azinas [3].



El mecanismo es análogo al de formación de iminas, oximas e hidrazonas.

George A. Olah (1927 -)



Origen: Químico estadounidense.

Lugar de nacimiento: Budapest

Formación: Se doctoró en la Universidad de Budapest en 1949

Docencia: Trabajó en el departamento de química orgánica de la Academia de Ciencias de Hungría y posteriormente en la

Universidad de Cleveland.

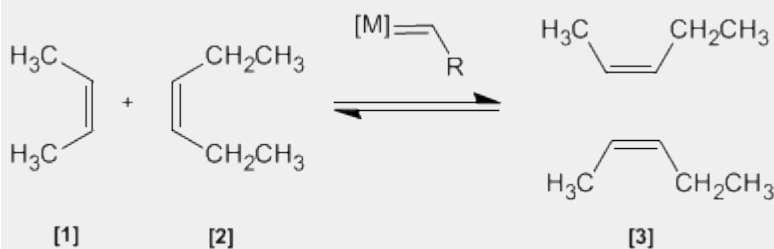
Industria: Trabajó en los laboratorios de la Dow Chemical de Ontario

Investigación: Olah consiguió preparar carbocationes estables utilizando componentes extremadamente ácidos.

Premio Nobel: En 1994 obtuvo el premio Nobel de Química por sus investigaciones sobre los carbocationes

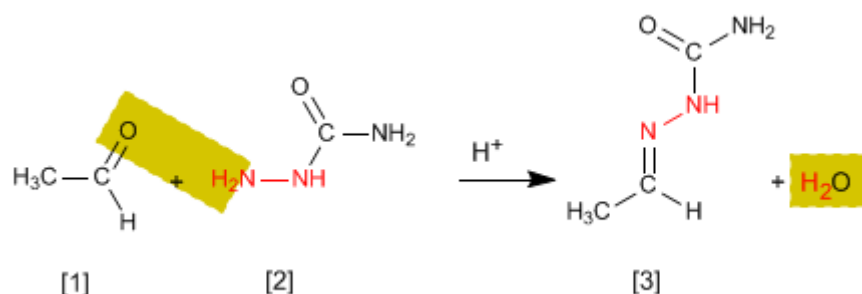
Metátesis de Alquenos

En esta reacción dos alquenos [1] y [2] son tratados con un metal de transición que actúa como catalizador, dando una mezcla de alquenos [3] (incluyendo isómeros Z/E). Este producto se obtiene por intercambio de grupos alquilideno.



Formación de Semicarbazonas

Las semicarbazonas [3] se obtienen por reacción de aldehídos o cetonas [1] con semicarbazida [2]. Veamos un ejemplo:



El mecanismo es análogo al de formación de iminas, oximas e hidrazonas.

Charles Friedel (1832 - 1899)



Origen: Químico frances..

Lugar de nacimiento: Estrasburgo.

Formación: estudió química en la Universidad de Berlín entre 1895 y 1899, consiguiendo el doctorado este año.

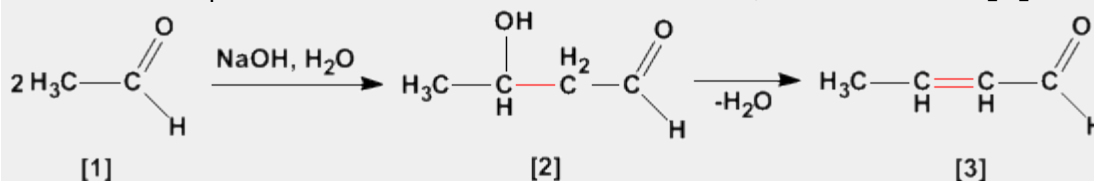
Docencia: Profesor en la Universidad de la Sorbona.

Investigación: Obtuvo el alcohol propílico. En 1877, Friedel y Crafts describieron por primera vez la reacción del benceno con un haloalcano en presencia de un ácido de Lewis. Esta reacción produce la alquilación del benceno y se conoce como alquilación de Friedl-Crafts.

Premio Nobel:

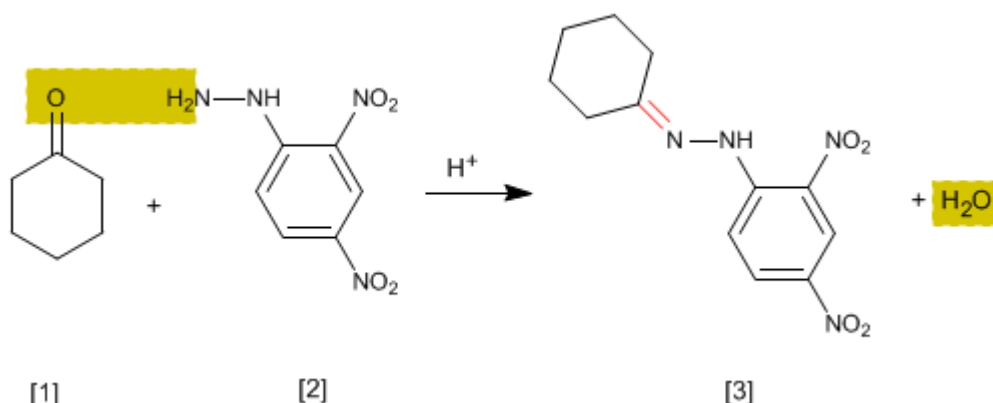
Aldólica (Condensación)

La condensación aldólica es una reacción de aldehídos o cetonas [1] que forma 3-hidroxicarbonilos (aldoles) [2]. El 3-hidroxialdehído [2] bajo condiciones de deshidratación por calentamiento rinde un aldehído alfa,beta-insaturado [3].



Ensayo de la 2,4-Dinitrofenilhidrazina

Se trata de un ensayo analítico específico de aldehídos y cetonas. Los carbonilos **[1]** reaccionan con 2,4-Dinitrofenilhidrazina **[2]** formando fenilhidrazonas **[3]** que precipitan de color amarillo. La aparición de precipitado es un indicador de la presencia de carbonilos en el medio.



El mecanismo de la reacción es análogo al de formación de iminas.

Kurt Alder (1902 - 1958)



Origen: Químico alemán.

Lugar de nacimiento: Königshütte (hoy Chorzów, Polonia).

Formación: estudió en la Universidad de Kiel. Bajo la supervisión del químico alemán Otto Diels, su jefe e instructor en Kiel.

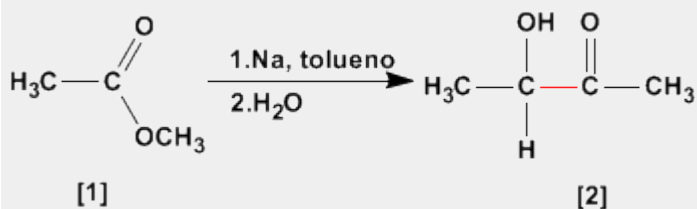
Docencia: Alder ejerció como profesor de química en las universidades de Kiel y Colonia.

Investigación: Alder se especializó en la síntesis diénica (conocida más tarde como la reacción Diels - Alder) que consiste fundamentalmente en el análisis y formación de compuestos orgánicos complejos. Ya en 1928 ambos fueron coautores de un ensayo sobre este proceso.

Premio Nobel: En 1950 recibió el Premio Nobel junto a Diels

Aciloinica (Condensación)

La condensación aciloinica transforma esteres **[1]** en alfa-hidroxicetonas **[2]**. Esta reacción se realiza con sodio metal en disolvente inerte.



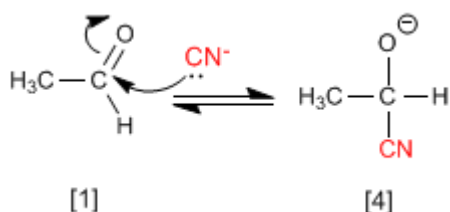
Formación de Cianhidrinas

Las cianhidrinas **[3]** se forman por reacción de aldehídos o cetonas **[1]** con ácido cianhídrico **[2]** y son compuestos que contienen un grupo ciano y un hidroxilo sobre el mismo carbono.

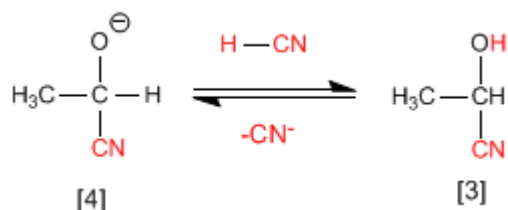


El mecanismo de la reacción transcurre en dos etapas:

Etapla 1. Los iones cianuro actúan como nucleófilos atacando al carbono carbonilo. El ácido cianhídrico es demasiado débil para generar cantidades importantes de cianuro, por ello, se añade cianuro de sodio o potasio al medio, garantizando la cantidad suficiente de cianuro para que la reacción transcurra en buen rendimiento.



Etapla 2. En este paso el ión alcóxido **[4]** se protona arrancando hidrógenos al ácido cianhídrico. En esta etapa se regeneran los iones cianuro.



Kurt Alder (1902 - 1958)



Origen: Químico alemán.

Lugar de nacimiento: Königshütte (hoy Chorzów, Polonia).

Formación: estudió en la Universidad de Kiel. Bajo la supervisión del químico alemán Otto Diels, su jefe e instructor en Kiel.

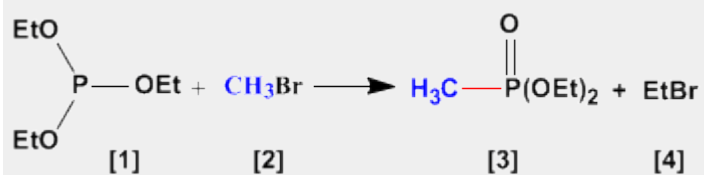
Docencia: Alder ejerció como profesor de química en las universidades de Kiel y Colonia.

Investigación: Alder se especializó en la síntesis diénica (conocida más tarde como la reacción Diels - Alder) que consiste fundamentalmente en el análisis y formación de compuestos orgánicos complejos. Ya en 1928 ambos fueron coautores de un ensayo sobre este proceso.

Premio Nobel: En 1950 recibió el Premio Nobel junto a Diels

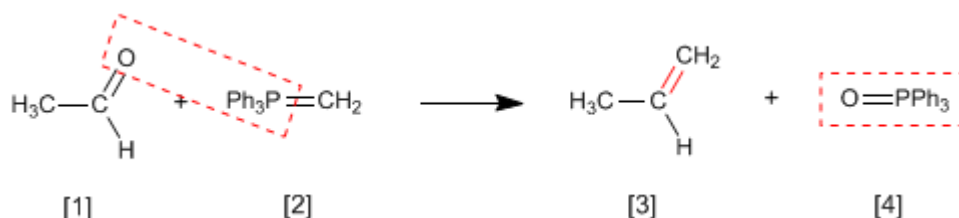
Arbuzov (Reacción)

La reacción de Arbuzov se emplea en la síntesis de fosfonatos **[3]** a partir de fosfitos **[1]**. Los fosfonatos obtenidos en la síntesis de Arbuzov se emplean como materiales de partida en la síntesis de Horner-Wittig.



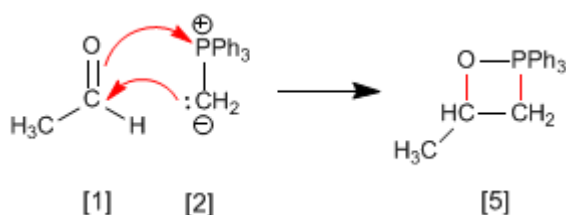
Reacción de Wittig

La reacción de Wittig emplea iluros de fósforo [2] para transformar aldehídos y cetonas [1] en alquenos [3]. Como subproducto se obtiene el óxido de trifenilfosfina [4].

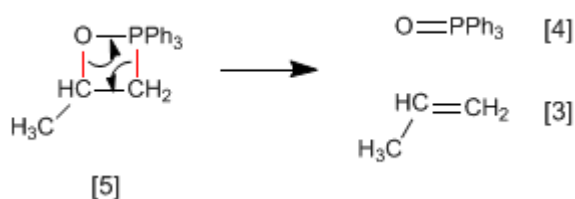


En el mecanismo de la reacción el iluro y el carbonilo se combinan para formar un oxafosfetano que rompe dejando libre el alqueno final.

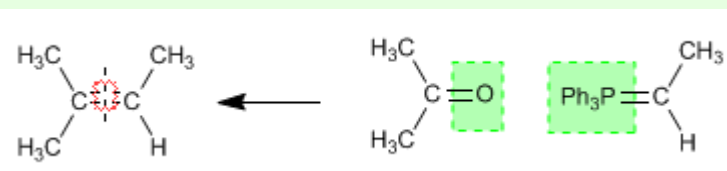
Etapas 1. El etanal y el iluro se combinan formando el fosfetano.



Etapas 2. El fosfetano rompe formando el alqueno y óxido de trifenilfosfina.

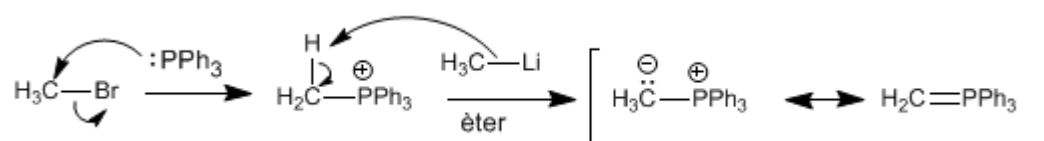


Ejemplo - Obtener mediante Wittig el 2-Metilbut-2-eno



Se rompe el alqueno por el doble enlace y a cada carbono se le agrega el grupo encerrado en verde.

Los **iluros de fósforo** se preparan mediante reacción de haloalcanos y trifenilfosfina, seguido de desprotonación del carbono con base fuerte (organometálicos de litio).



Charles Friedel (1832 - 1899)



Origen: Químico frances..

Lugar de nacimiento: Estrasburgo.

Formación: estudió química en la Universidad de Berlín entre 1895 y 1899, consiguiendo el doctorado este año.

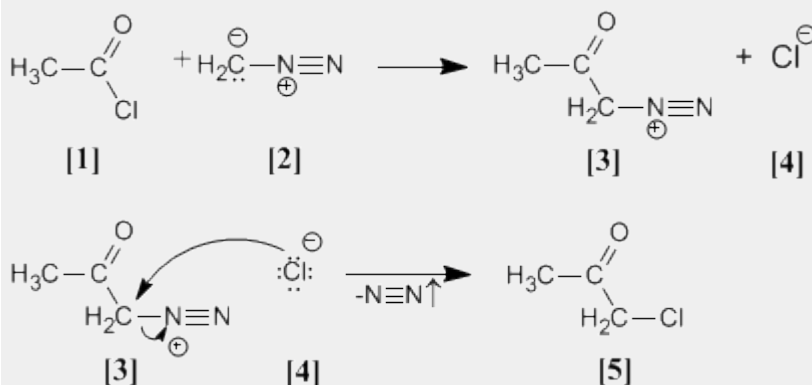
Docencia: Profesor en la Universidad de la Sorbona.

Investigación: Obtuvo el alcohol propílico. En 1877, Friedel y Crafts describieron por primera vez la reacción del benceno con un haloalcano en presencia de un ácido de Lewis. Esta reacción produce la alquilación del benceno y se conoce como alquilación de Friedl-Crafts.

Premio Nobel:

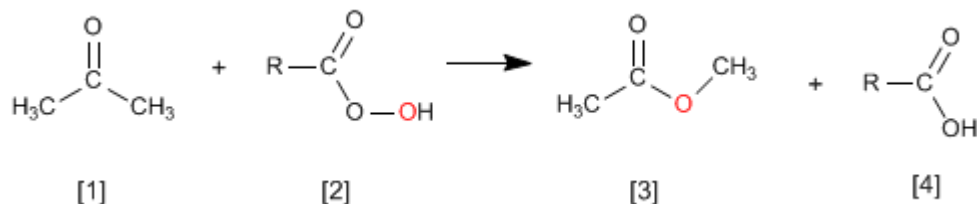
Arndt Eistert (Síntesis)

Cloruro de acetilo **[1]** se trata con diazometano **[2]** rindiendo la sal de diazonio **[3]**. El cloruro **[4]** producido reacciona con la sal de diazonio para dar la α -clorocetona **[5]**.

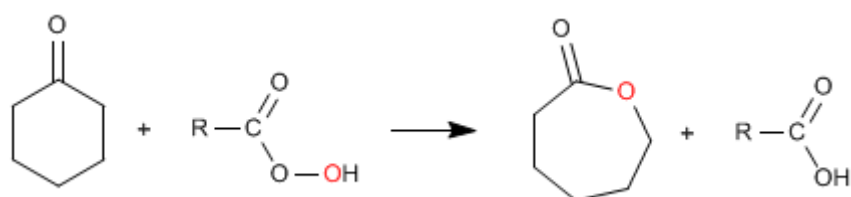


Oxidación de Baeyer Villiger

La reacción de cetonas **[1]** con perácidos **[2]** produce ésteres **[3]**. El oxígeno del perácido se inserta entre el carbono carbonilo y el carbono alfa de la cetona. Esta reacción fue descrita por Adolf von Baeyer y Victor Villiger in 1899.

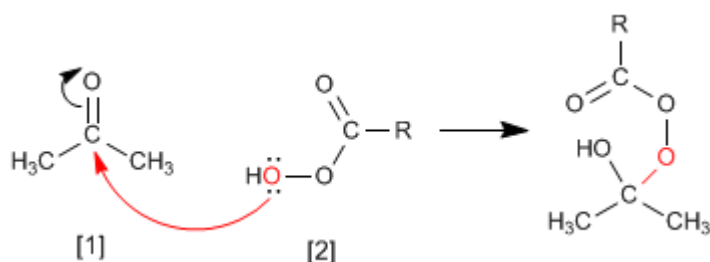


A partir de cetonas cíclicas se obtienen ésteres cíclicos (lactonas)

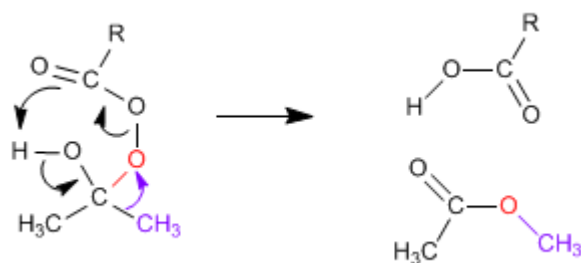


El mecanismo de Baeyer Villiger comienza con el ataque nucleófilo del perácido sobre el carbonilo, seguido de la migración del sustituyente desde el grupo carbonilo al oxígeno del perácido.

Etapas 1. Adición del perácido al carbonilo

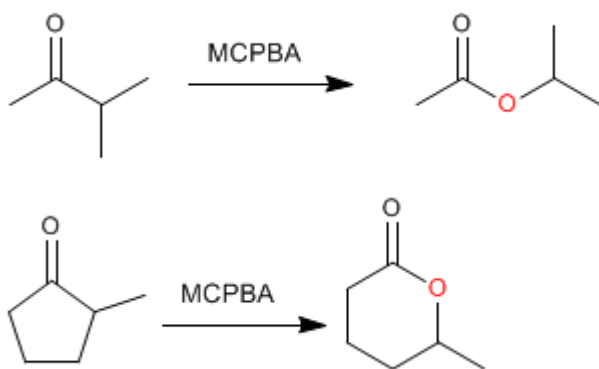


Etapas 2. Migración del sustituyente desde carbono carbonilo hacia el oxígeno (rojo)



Cuando la cetona tiene dos sustituyentes diferentes migra mejor el más sustituido. Existe un orden de migración que nos ayuda a decidir que sustituyente pasa a unirse al oxígeno del perácido.

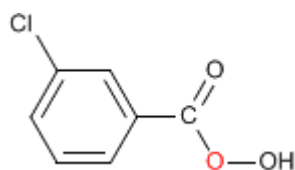
Orden de migración: H > carbono terciario > ciclohexilo > carbono secundario » fenilo > carbono primario > metilo



Como puede observarse en el orden de migración, el grupo que mejor migra, por su pequeño tamaño, es el hidrógeno, por ello, al tratar aldehídos con perácidos se produce la migración del hidrógeno formándose ácidos carboxílicos.



El **MCPBA** (Ácido meta-cloroperoxibenzoico) es un perácido ampliamente utilizado en la epoxidación de alquenos y también en Baeyer-Villiger. La fórmula del MCPBA se muestra a continuación.



Charles Friedel (1832 - 1899)



Origen: Químico frances..

Lugar de nacimiento: Estrasburgo.

Formación: estudió química en la Universidad de Berlín entre 1895 y 1899, consiguiendo el doctorado este año.

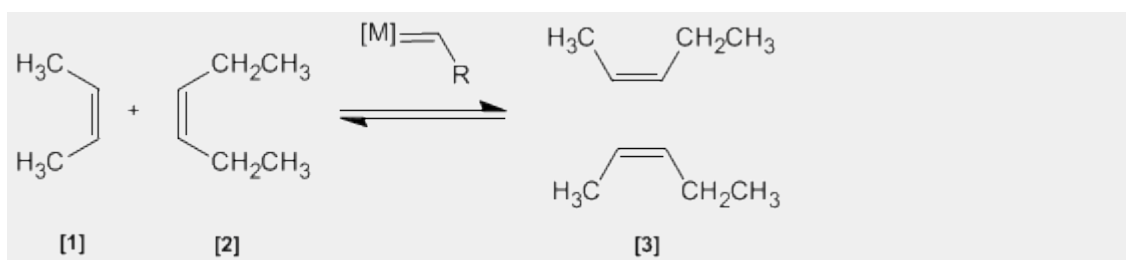
Docencia: Profesor en la Universidad de la Sorbona.

Investigación: Obtuvo el alcohol propílico. En 1877, Friedel y Crafts describieron por primera vez la reacción del benceno con un haloalcano en presencia de un ácido de Lewis. Esta reacción produce la alquilación del benceno y se conoce como alquilación de Friedl-Crafts.

Premio Nobel:

Metátesis de Alquenos

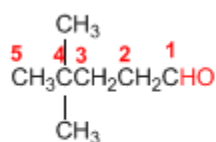
En esta reacción dos alquenos **[1]** y **[2]** son tratados con un metal de transición que actúa como catalizador, dando una mezcla de alquenos **[3]** (incluyendo isómeros Z/E). Este productos se obtiene por intercambio de grupos alquilideno.



Nomenclatura de Aldehídos y Cetonas - Reglas IUPAC

Regla 1. Los aldehídos se nombran reemplazando la terminación **-ano** del alcano correspondiente por **-al**. No es necesario especificar la posición del grupo aldehído, puesto que ocupa el extremo de la cadena (localizador 1).

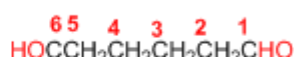
Cuando la cadena contiene dos funciones aldehído se emplea el sufijo **-dial**.



4,4-Dimetilpentanal

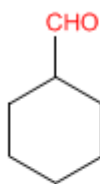


Hex-4-enal

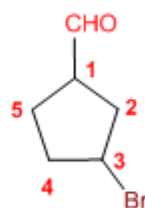


Hexanodial

Regla 2. El grupo **-CHO** se denomina **-carbaldehído**. Este tipo de nomenclatura es muy útil cuando el grupo aldehído va unido a un ciclo. La numeración del ciclo se realiza dando localizador 1 al carbono del ciclo que contiene el grupo aldehído.

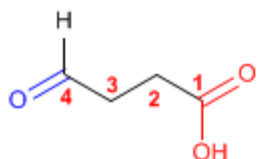


Ciclohexanocarbaldehído

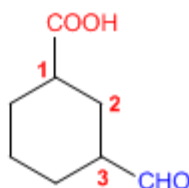


3-Bromociclopentanocarbaldehído

Regla 3. Cuando en la molécula existe un grupo prioritario al aldehído, este pasa a ser un sustituyente que se nombra como oxo- o formil-.



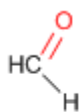
Ácido 4-oxobutanoico



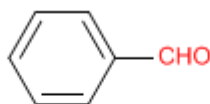
Ácido 3-formilciclohexanocarboxílico

Tanto **-carbaldehído** como **formil-** son nomenclaturas que incluyen el carbono del grupo carbonilo. **-carbaldehído** se emplea cuando el aldehído es grupo funcional, mientras que **formil-** se usa cuando actúa de sustituyente.

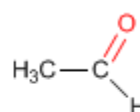
Regla 4. Algunos nombres comunes de aldehídos aceptados por la IUPAC son:



Formaldehído
(Metanal)

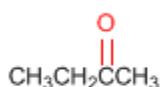


Benzaldehído
(Benceno**carbaldehído**)

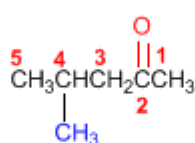


Acetaldehído
(Etanal)

Regla 5. Las cetonas se nombran sustituyendo la terminación **-ano** del alcano con igual longitud de cadena por **-ona**. Se toma como cadena principal la de mayor longitud que contiene el grupo carbonilo y se numera para que éste tome el localizador más bajo.



Butan**ona**

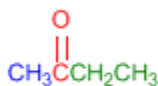


4-Metil-2-pentan**ona**

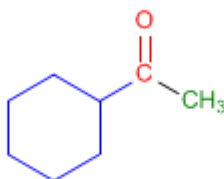


3-Metilciclohexan**ona**

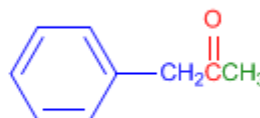
Regla 6. Existe un segundo tipo de nomenclatura para las cetonas, que consiste en nombrar las cadenas como sustituyentes, ordenándolas alfabéticamente y terminando el nombre con la palabra cetona.



Etil metil **cetona**

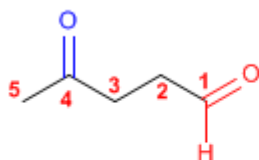


Ciclohexil metil **cetona**

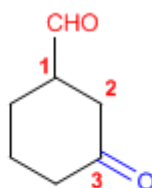


Fenil metil **cetona**

Regla 7. Cuando la cetona no es el grupo funcional de la molécula pasa a llamarse **OXO-**.



4-Oxopentan**al**

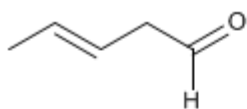


3-Oxociclohexano**carbaldehído**

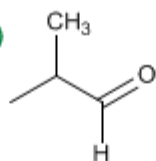
Nomenclatura de Aldehídos y Cetonas - Problema 9.1

Nombra los siguientes aldehídos y cetonas:

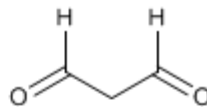
a)



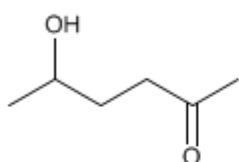
b)



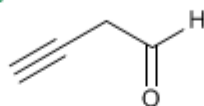
c)



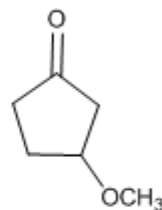
d)



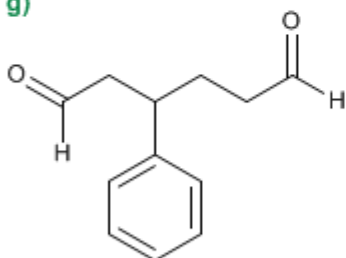
e)



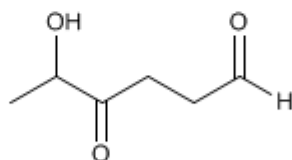
f)



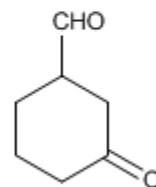
g)



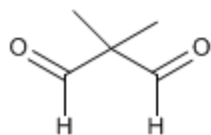
h)



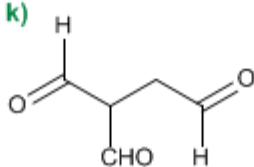
i)



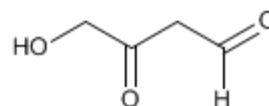
j)



k)

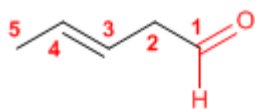


l)

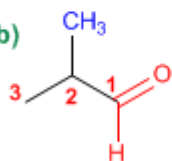


Solución

a)



b)



1. Cadena principal: 5 carbonos (pentano)

2. Numeración: comienza en el aldehído (grupo funcional)

Grupo funcional: aldehído

3. Nombre: Pent-3-enal

1. Cadena principal: 3 carbonos (propano)

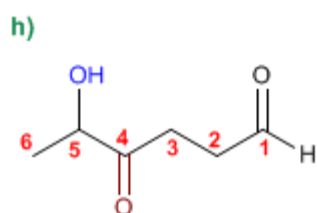
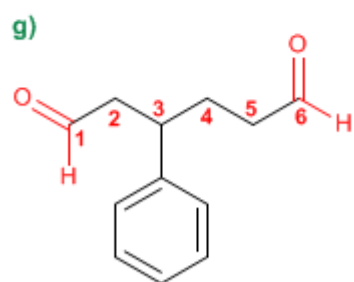
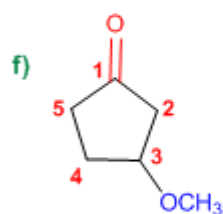
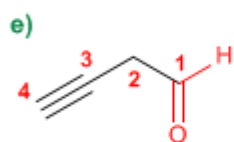
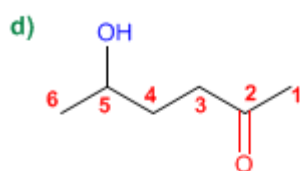
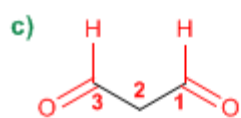
2. Numeración: localizador más bajo al aldehído.

3. Grupo funcional: aldehído

4. Sustituyentes: metilo en 2.

5. Nombre: 2-Metilpropanal

Los aldehídos y cetonas son prioritarios sobre alquenos y alquinos, y se numeran otorgándoles el localizador más bajo



1. Cadena principal: 3 carbonos (propano)
2. Grupo funcional: aldehído (dialdehído)
3. Nombre: Propanodial

1. Cadena principal: 6 carbonos (hexano)
2. Grupo funcional: cetona
3. Numeración: asignar el menor localizador a la cetona
4. Sustituyentes: hidroxí en 5.
5. Nombre: 5-Hidroxihexan-2-ona

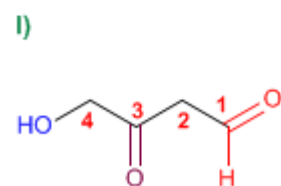
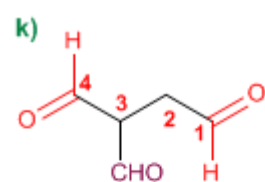
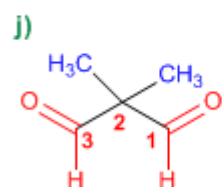
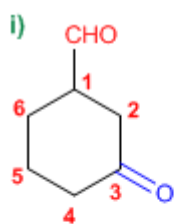
1. Cadena principal: 4 carbonos (butano)
2. Grupo funcional: aldehído
3. Numeración: asignar el menor localizador al aldehído
4. Nombre: But-3-inal

1. Cadena principal: ciclo de 5 miembros (ciclopentano)
2. Grupo funcional: cetona
3. Numeración: comienza en la cetona y prosigue hacia el sustituyente
4. Sustituyentes: metoxi en 3.
5. Nombre: 3-Metoxiciclopentanona

1. Cadena principal: 6 carbonos (hexano)
2. Grupo funcional: aldehído (dialdehído)
3. Numeración: comienza en el extremo que otorga al fenilo el localizador más bajo.
4. Sustituyentes: fenilo en 3.
5. Nombre: 3-Fenilhexanodial

1. Cadena principal: 6 carbonos (hexano)
2. Grupo funcional: aldehído
3. Numeración: asignar el menor localizador al aldehído
4. Sustituyentes: hidroxí en 5 y oxo en 4.
5. Nombre: 5-Hidroxí-4-oxohexanal

Los aldehídos son prioritarios sobre las cetonas que pasan a nombrarse como sustituyentes (oxo-)



1. Cadena principal: ciclo de 6 miembros (ciclohexano)
2. Grupo funcional: aldehído (-carbaldehído)
3. Numeración: menor localizador al grupo -CHO (este no se numera)
4. Sustituyentes: cetona (oxo-) en 3
5. Nombre: 3-Oxociclohexanocarbaldehído

1. Cadena principal: 3 carbonos (propano)
2. Grupo funcional: aldehído (dialdehído)
3. Sustituyentes: metilos en 2,2.
4. Nombre: 2,2-Dimetilpropanodial

1. Cadena principal: 4 carbonos (butano)
2. Grupo funcional: aldehído
3. Sustituyentes: formil en 3
4. Nombre: 3-Formilbutanodial

1. Cadena principal: 4 carbonos (butano)
2. Grupo funcional: aldehído
3. Numeración: asignar el menor localizador al aldehído
4. Sustituyentes: hidroxil en 4 y oxo en 3.
5. Nombre: 4-Hidroxil-3-oxobutanal

Nomenclatura de Aldehídos y Cetonas - Problema 9.2

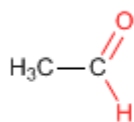
PRINT EMAIL

Dibuja la estructura de los siguientes aldehídos y cetonas:

- | | |
|---|----------------------------------|
| a) Etanal (acetaldehído) | g) 2,5-Dioxooctanodial |
| b) 3-Metilbutanal | h) 1,3-Ciclohexanodiona |
| c) Benzaldehído | i) 3-Metil-3-pental |
| d) 4-Hidrox ciclohexanocarbaldehído | j) 3-Oxobutanal |
| e) 3-Hidroxi-4-metil-5-oxociclohexanocarbaldehído | k) 3-Hidrox ciclopentanona |
| f) 2-Metil-2,5-octanodiona | l) 4-Etoxi-5-fenil-3-oxoheptanal |

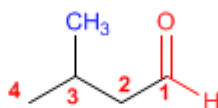
Solución

a)



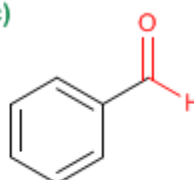
Etanal (acetaldehído)

b)

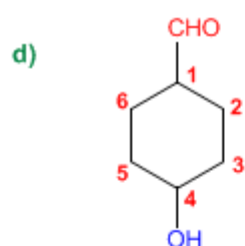


3-Metilbutanal

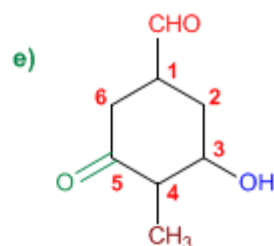
c)



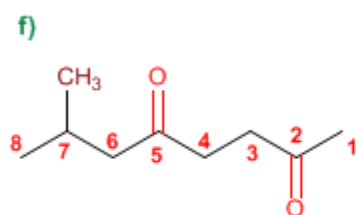
Benzaldehído



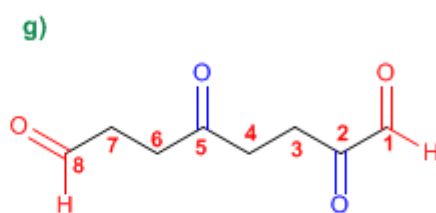
4-Hidroxiciclohexanocarbaldehído



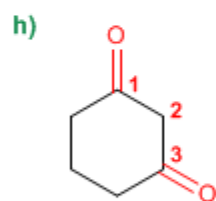
3-Hidroxi-4-metil-5-oxociclohexanocarbaldehído



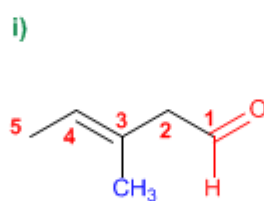
7-Metil-2,5-octanodiona



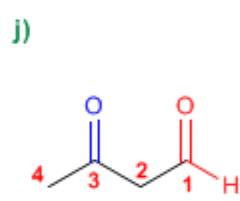
2,5-Dioxooctanodial



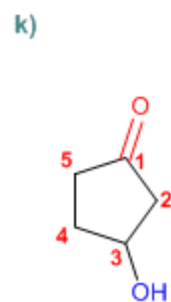
1,3-Ciclohexanodiona



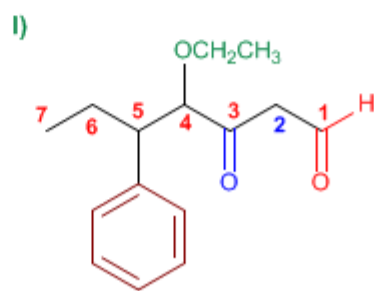
3-Metil-3-pentenal



3-Oxobutanal



3-Hidroxiciclopentanona

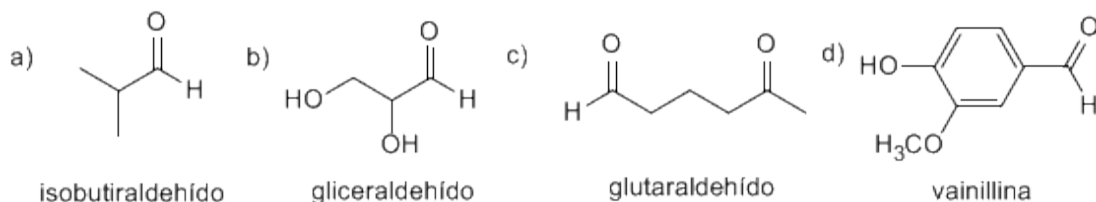


4-Etoxi-5-fenil-3-oxoheptanal

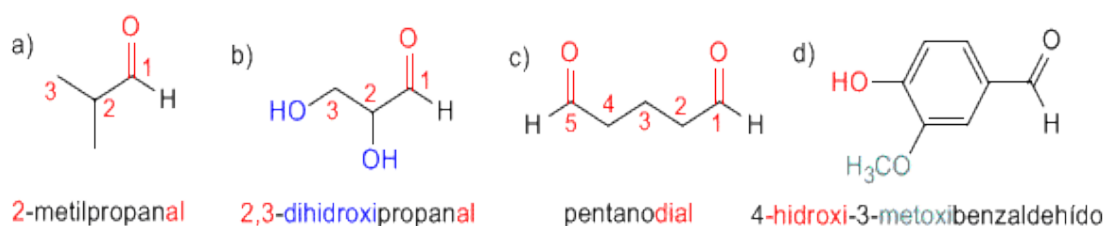
PROBLEMAS RESUELTOS DE ALDEHÍDOS Y CETONAS

Aldehídos y Cetonas: Problema 1

1) A continuación se dan nombres comunes y las fórmulas estructurales de algunos compuestos carbonílicos. Indique el nombre correspondiente según la IUPAC.



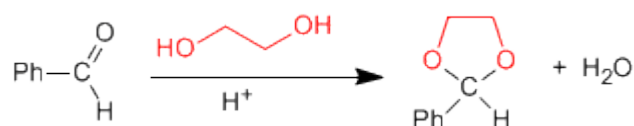
Solución



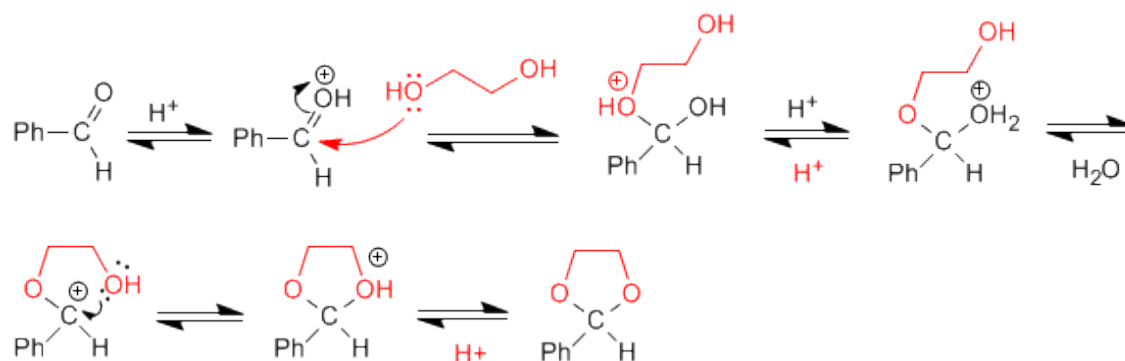
Aldehídos y cetonas: Problema 2

Dibuje la estructura del acetal que se forma cuando el benzaldehído se calienta con 1,2-etanodiol en medio ácido. Escriba un mecanismo detallado que justifique su formación. Describa paso a paso la hidrólisis de este acetal en medio ácido acuoso.

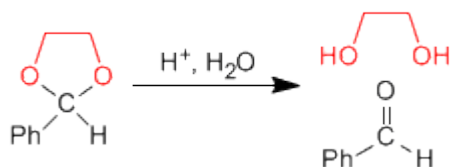
SOLUCIÓN



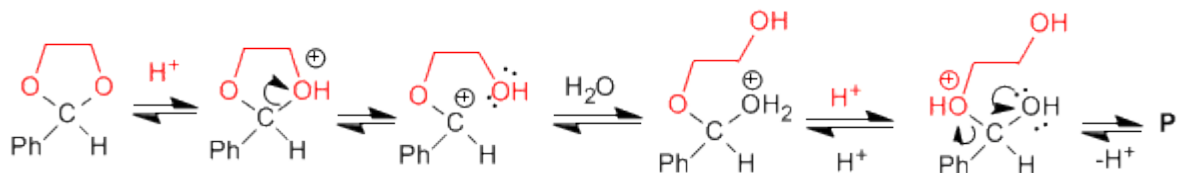
Mecanismo de formación del acetal:



La hidrólisis del acetal en medio ácido acuoso sigue es etapas inversas a la síntesis.



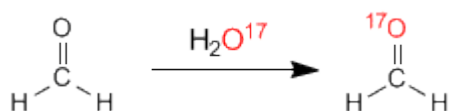
Mecanismo de hidrólisis del acetal cíclico.



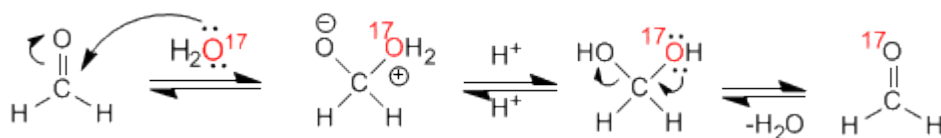
Aldehídos y Cetonas: Problema 3

Cuando se disuelve formaldehído en agua marcada con ^{17}O , se observa que después de unas horas tanto el hidrato del formaldehído como el formaldehído han incorporado el isótopo ^{17}O . Sugiera una explicación razonable de este hecho.

SOLUCION



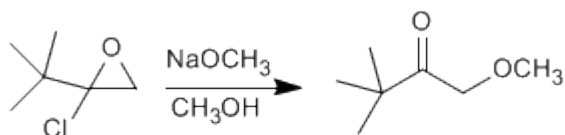
Mecanismo:



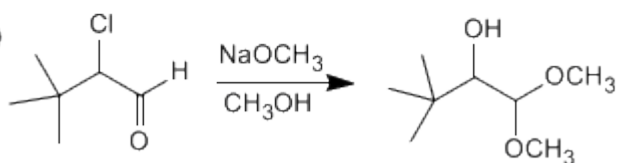
Aldehídos y Cetonas: Problema 4

Sugiera un mecanismo razonable para una de las siguientes reacciones:

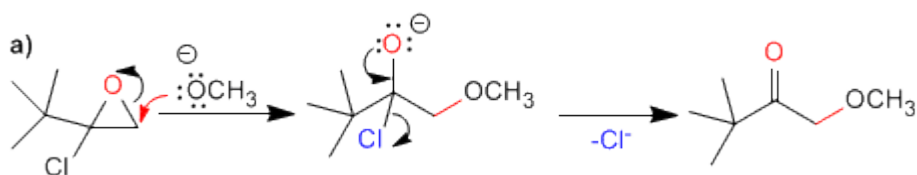
a)



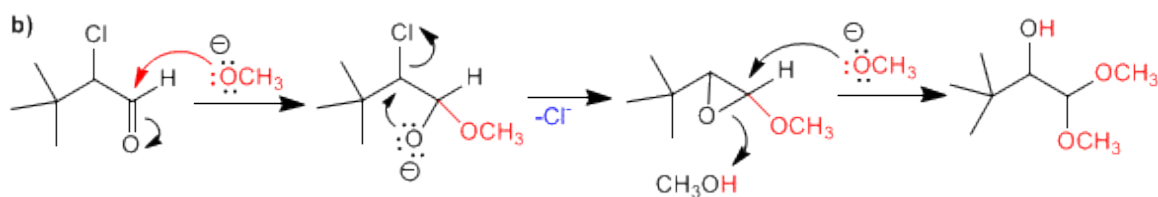
b)



SOLUCION



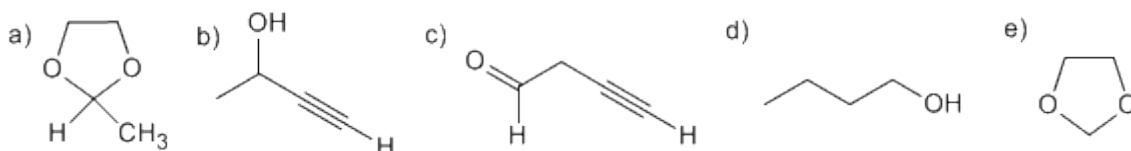
La primera etapa consiste en la apertura del oxaciclopropano sobre el carbono menos sustituido. En la segunda etapa, la cesión del par del oxígeno elimina el cloro, formándose un carbonilo.



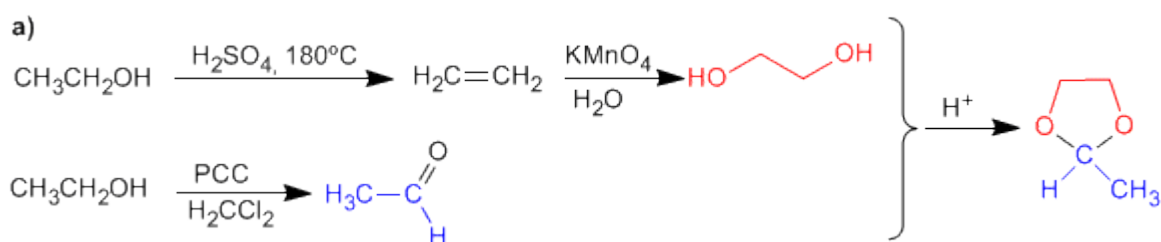
En el primer paso hay dos posibles posiciones de ataque; el carbono carbonilo y el carbono del cloro. Como el producto final no tiene metóxido en el carbono del cloro, atacamos al carbonilo. En la segunda etapa se produce una sustitución nucleófila intramolecular. Para terminar el metóxido abre el epóxido.

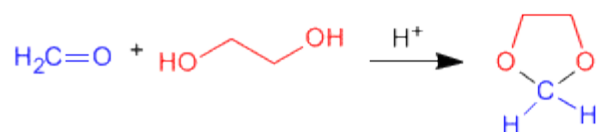
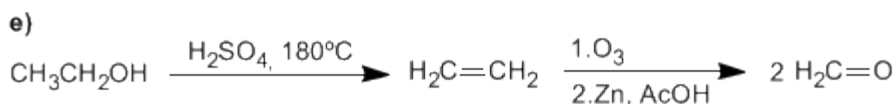
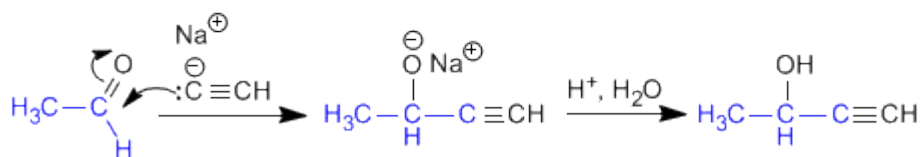
Aldehídos y Cetonas: Problema 5

Usando etanol como fuente de todos los átomos de carbono y los reactivos que necesite, describa una síntesis eficiente de cada una de las sustancias siguientes:

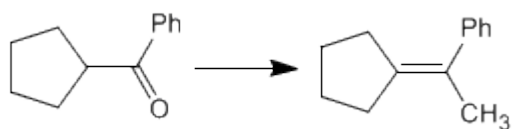


SOLUCIÓN





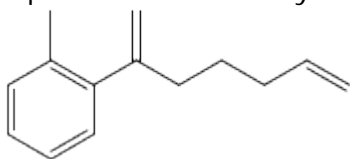
Utilizando los reactivos necesarios, indicar las etapas que permiten realizar la siguiente transformación:



[2] Isomerización en medio ácido, impulsada por la mayor estabilidad del alqueno interno.

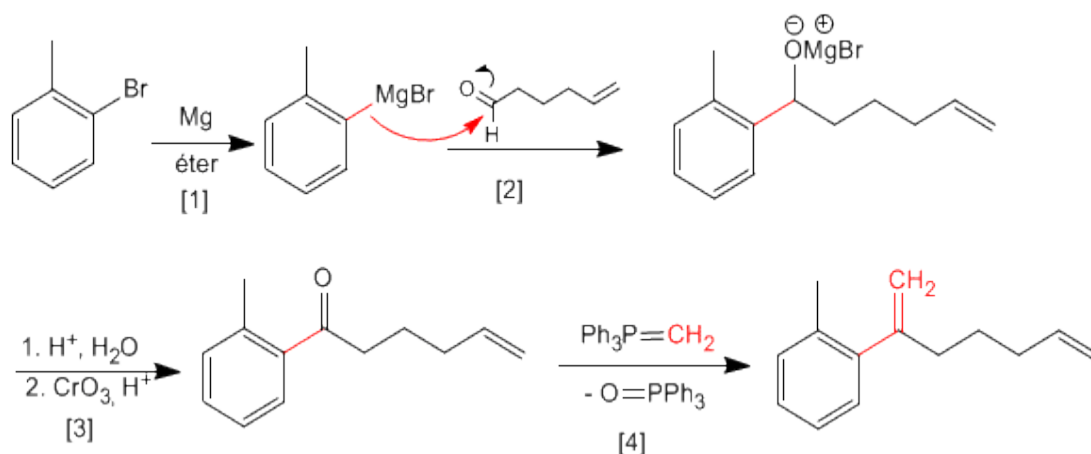
Aldehídos y Cetonas: Problema 7

A partir de 5-hexenal y o-bromotolueno obtener el siguiente producto.



Pueden ser necesarios reactivos orgánicos e inorgánicos adicionales.

SOLUCIÓN



[1] Formación del magnesiano

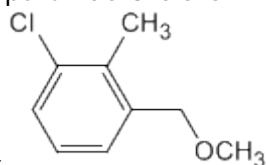
[2] Ataque nucleófilo del magnesiano al carbonilo.

[3] Hidrólisis y posterior oxidación del alcohol secundario.

[4] Reacción de Wittig entre la cetona y el trifenilmetilenfosforano.

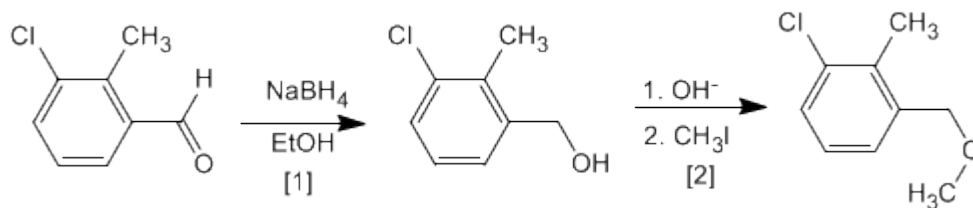
Aldehídos y Cetonas: Problema 8

Obtener a partir de 3-cloro-2-metilbenzaldehído y de los reactivos



necesarios
el compuesto siguiente:

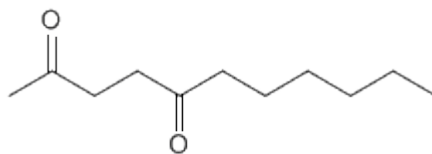
SOLUCIÓN



[1] Reducción del aldehído a alcohol

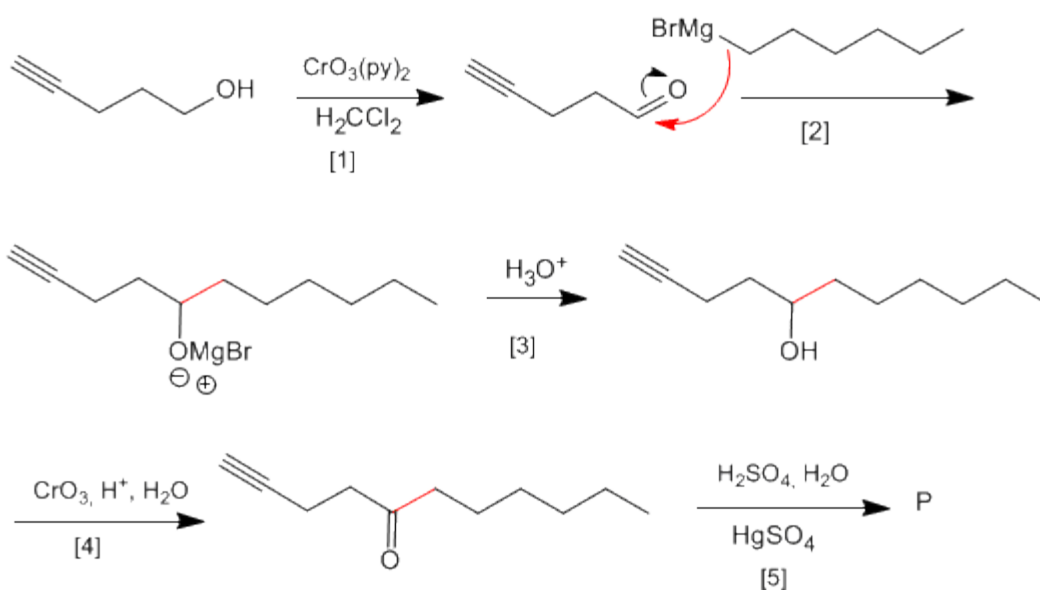
[2] Síntesis de Williamson de éteres.

Aldehídos y Cetonas: Problema 9



A partir de 4-pentin-1-ol obtener:

SOLUCIÓN

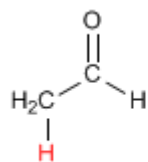


- [1] Oxidación del alcohol a aldehído
- [2] Formación del enlace carbono-carbono mediante organometálicos de magnesio
- [3] Protonación del alcohol
- [4] Oxidación del alcohol con Jones (Puedes utilizar también $\text{CrO}_3(\text{py})_2$)
- [5] Hidratación Markovnikov del alquino, para formar cetonas

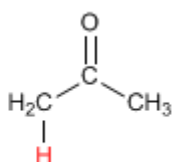
TEORÍA DE ENOLES Y ENOLATOS

Formación de Enolatos

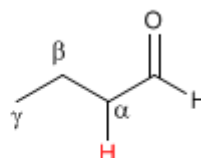
Los aldehídos y cetonas presentan hidrógenos ácidos en la posición vecina al grupo carbonilo, conocida como posición alfa. Estos hidrógenos presentan un pKa comprendido entre 18 y 21.



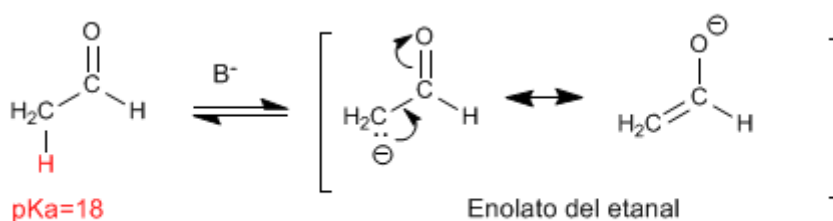
pKa=18



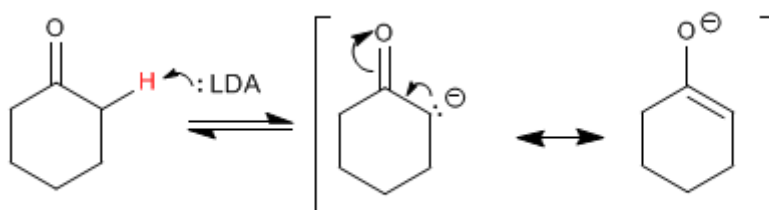
pKa=20-21



La acidez de los hidrógenos α es debida a la estabilización de la base conjugada (enolato) por resonancia.



Enolato del etanal

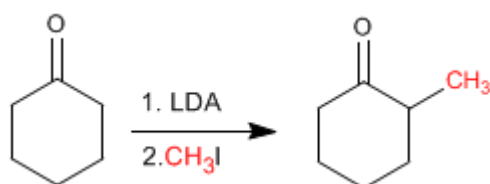


Enolato de la ciclohexanona

Alquilación de Enolatos

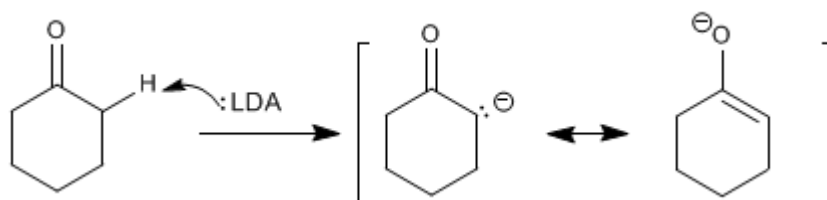
Los enolatos actúan como nucleófilos a través del carbono atacando a un gran número de electrófilos (haloalcanos, epóxidos, carbonilos, ésteres.....). En este punto nos fijaremos en la reacción entre enolatos y haloalcanos, que permite añadir cadenas carbonadas a la posición α de la cadena.

La Ciclohexanona se convierte en 2-Metilciclohexanona por tratamiento con LDA seguido de yoduro de metilo.

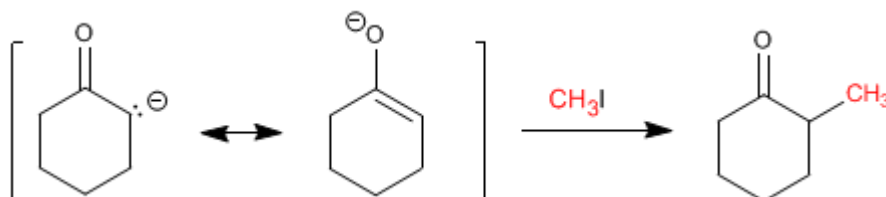


Etapas del mecanismo por el que se alquila la ciclohexanona:

Etapas 1. Formación del enolato

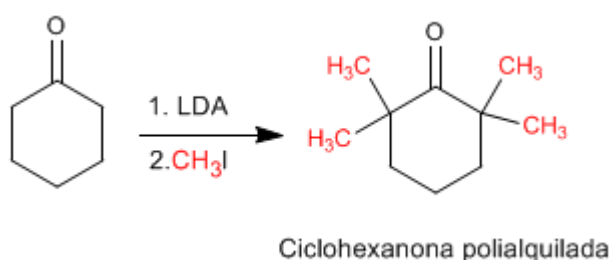


Etapas 2. Ataque nucleófilo del enolato sobre el haloalcano (Reacción de tipo S_N2)



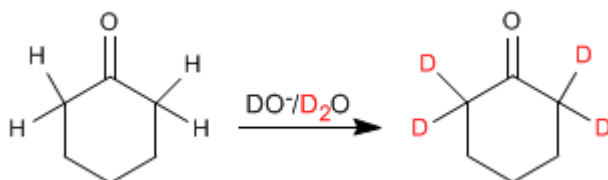
Las reacciones de alquilación tienen dos importantes problemas.

1. Competencia con la condensación aldólica. Los carbonilos en medio básico tienden a condensar para formar aldoles.
2. La reacción es difícil de controlar y tiende a polialquilar el carbonilo.



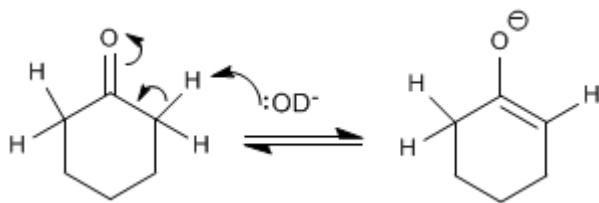
Intercambio hidrógeno - Deuterio

Los aldehídos y cetonas intercambian sus hidrógenos α por deuterios cuando se tratan con $\text{DO}^-/\text{D}_2\text{O}$ o con $\text{D}^+/\text{D}_2\text{O}$. En medios básicos la reacción transcurre a través de enolatos y en medios ácidos los intermediarios formados son enoles.

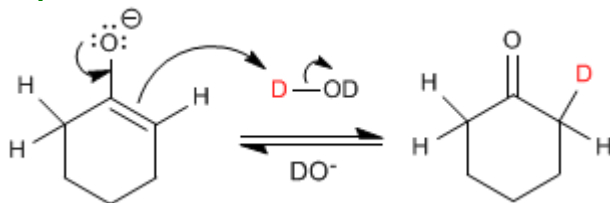


El mecanismo del intercambio hidrógeno-deuterio transcurre en los siguientes pasos:

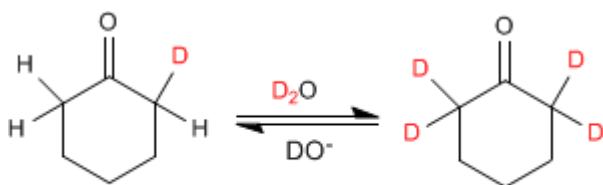
Etapas 1. Formación del enolato



Etapas 2. Transferencia del deuterio al enolato



Etapas 3. Sustitución del resto de hidrógenos



Halogenación de aldehídos y cetonas

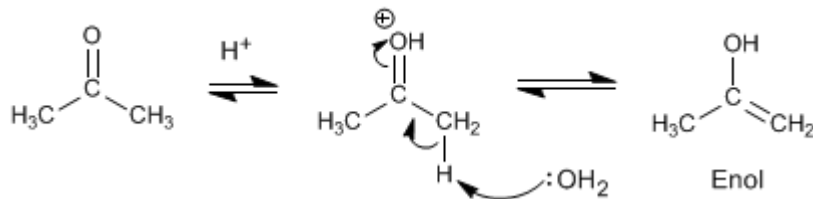
Los aldehídos y cetonas reaccionan con halógenos en medios ácidos o básicos produciéndose la sustitución de hidrógenos α por halógenos.

Halogenación de la propanona en medio ácido:

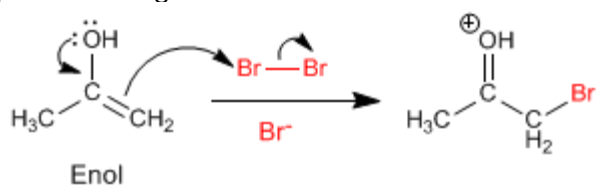


El mecanismo de halogenación en **medio ácido** tiene las siguientes etapas:

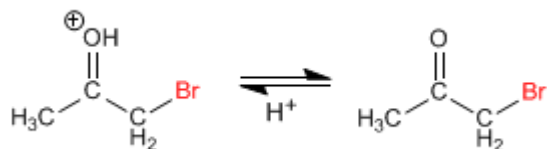
Etapas 1. Formación del enol



Etapas 2. Ataque nucleófilo del enol sobre el halógeno ayudado por la cesión del para del oxígeno.

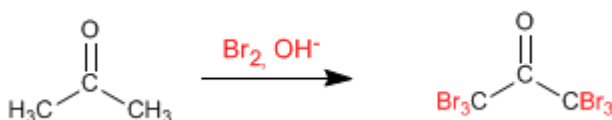


Etapa 3. Desprotonación



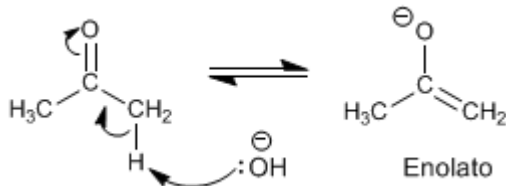
Trabajando con un equivalente de reactivo la halogenación para en una primera adición y no ocurren polihalogenaciones. El paso clave del mecanismo es la formación del enol y esta etapa requiere protonar el oxígeno del carbonilo. Una vez halogenada la posición α al oxígeno se vuelve menos básico, debido al efecto electronegativo del bromo, protonándose peor.

Halogenación de la propanona en **medio básico**:

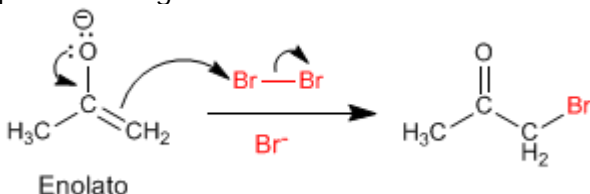


La halogenación en medio básico tiene el siguiente mecanismo:

Etapa 1. Formación del enolato



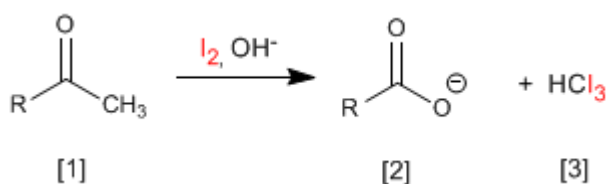
Etapa 2. Ataque nucleófilo del enolato sobre el halógeno ayudado por la cesión del par del oxígeno.



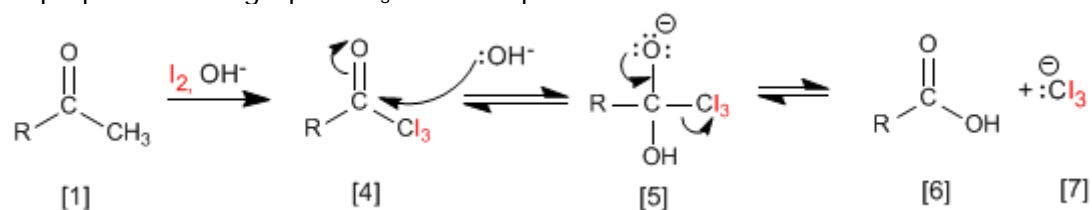
Este mecanismo se repite otras 5 veces sustituyendo todos los hidrógenos α por halógenos. En este caso la reacción no para puesto que el producto halogenado es más reactivo que la propanona de partida. La base arranca mejor los hidrógenos en el producto halogenado (son más ácidos), haciendo imposible parar la reacción.

Reacción del Haloformo (Yodoformo)

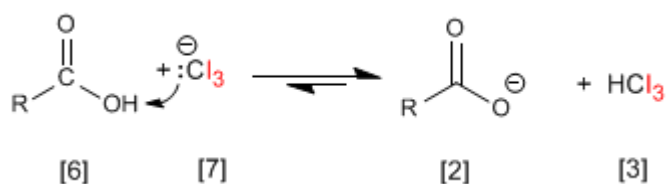
Las cetonas metílicas **[1]** reaccionan con halógenos en medios básicos generando carboxilatos **[2]** y haloformo **[3]**.



El mecanismo consiste en halogenar completamente el metilo, sustituyendo en una etapa posterior el grupo -CX₃ formado por -OH.



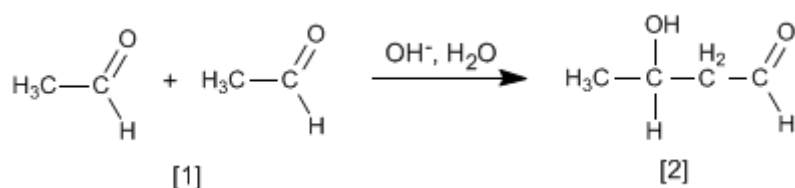
El grupo Cl₃⁻ es muy básico y desprotona el ácido carboxílico formándose yodoformo y el carboxilato.



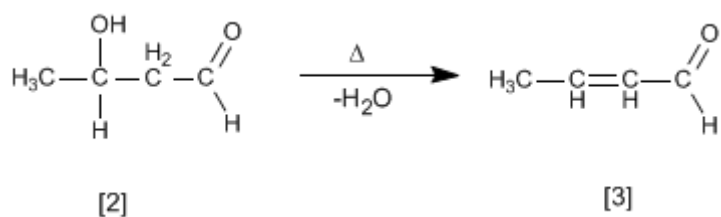
Esta reacción (con yodo) puede emplearse como ensayo analítico para identificar cetonas metílicas aprovechando que el yodoformo precipita de color amarillo.

Condensación Aldólica

Aldehídos y cetonas **[1]** condensan en medios básicos formando aldoles **[2]**. Esta reacción se denomina condensación aldólica.

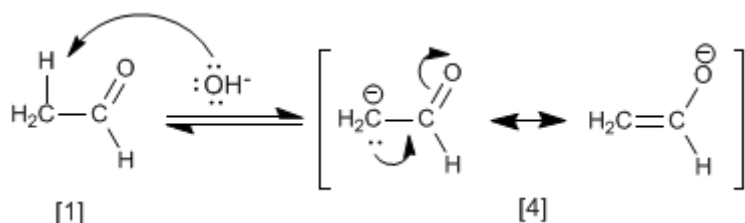


El aldol **[2]** formado deshidrata en el medio básico por calentamiento para formar un α,β-insaturado **[3]**.



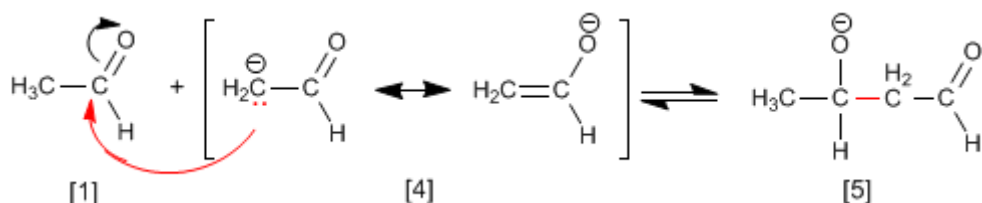
El mecanismo de la condensación aldólica transcurre con formación de un enolato, que ataca al carbonilo de otra molécula. En esta condensación se forma un enlace carbono-carbono entre el carbonilo de una molécula y el carbono α de la otra.

Etapas 1. Formación del enolato

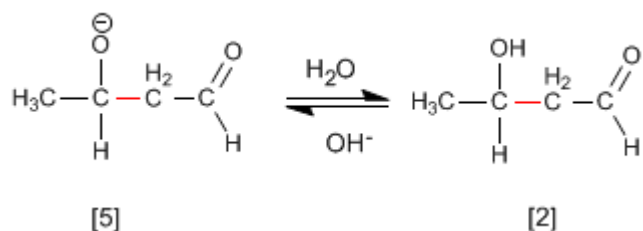


La base desprotona el carbono alfa del etanal [1] generando el enolato [4] estabilizado por resonancia.

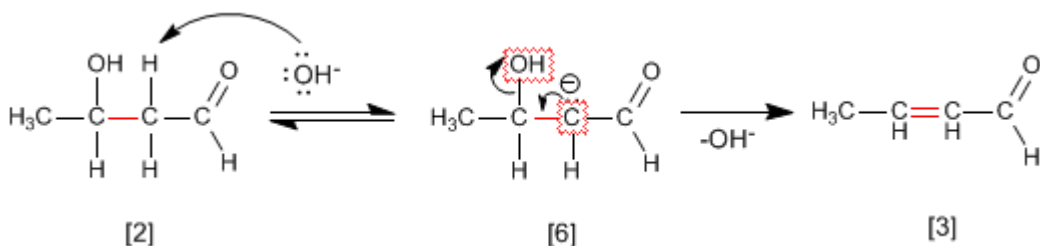
Etapas 2. Ataque nucleófilo del enolato sobre el carbonilo



Etapas 3. Protonación

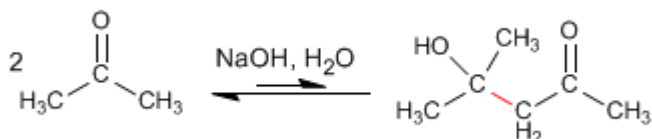


Etapas 4. Deshidratación del aldol

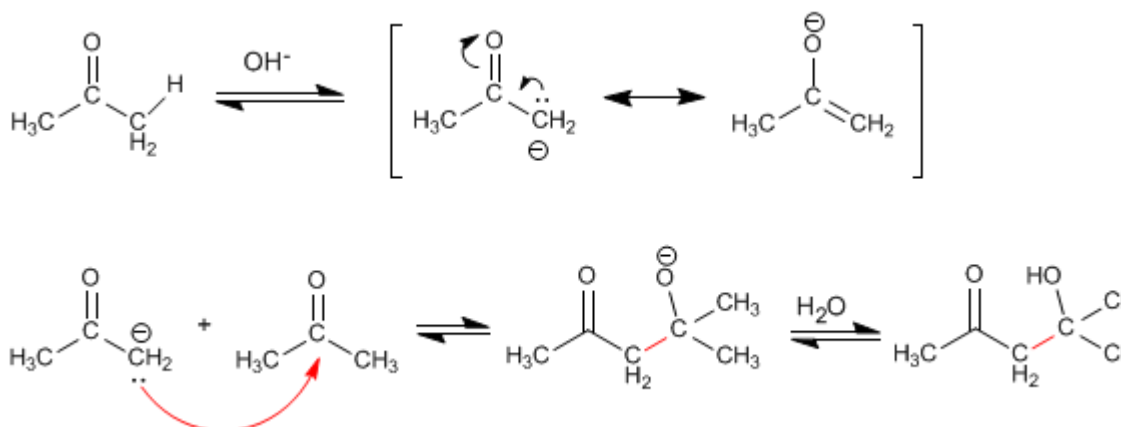


Condensación aldólica con cetonas

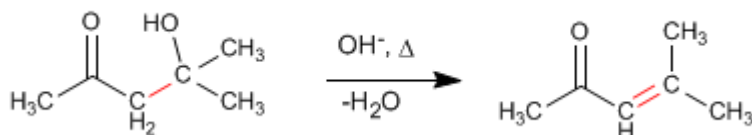
Las cetonas son menos reactivas que los aldehídos y dan un rendimiento muy bajo en la condensación aldólica. Así, dos moléculas de propanona condensan para formar el aldol correspondiente con un rendimiento del 2%. Se pueden conseguir porcentajes elevados del producto separándolo del medio de reacción según se va formando, o bien, calentando para deshidratarlo. De ambas formas los equilibrios de la aldólica se desplazan hacia el producto final.



Mecanismo de la reacción:

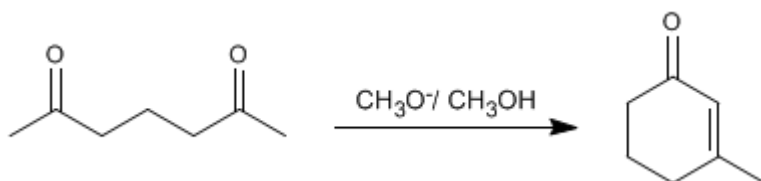


La deshidratación final permite el desplazamiento de los equilibrios. También se puede realizar una extracción del aldol del medio de reacción para favorecer la reacción.



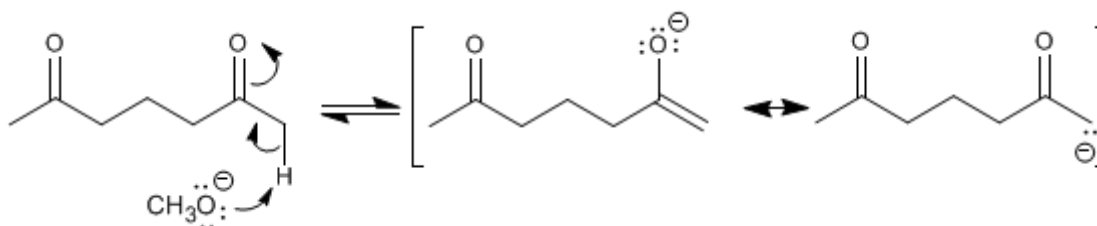
Condensación aldólica intramolecular

Los compuestos dicarbonílicos condensan mediante la aldólica intramolecular en medios básicos. En esta reacción se obtienen ciclos de cinco o seis miembros. Así, la 2,6-heptanodiona condensa con metóxido en metanol para formar el 3-metilciclohex-2-enona.

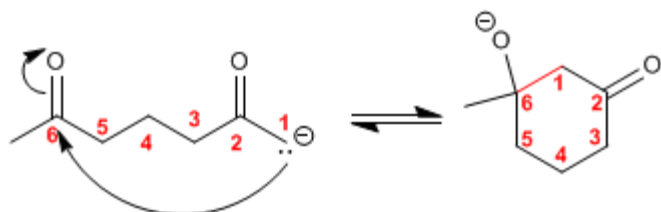


El mecanismo de la reacción transcurre a través de las siguientes etapas:

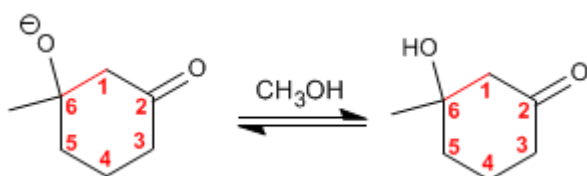
Etapa 1. Formación del enolato.



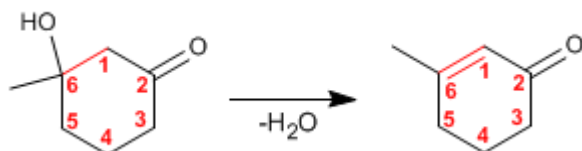
Etapa 2. Adición nucleófila intramolecular



Etapa 3. Protonación de la base del aldol



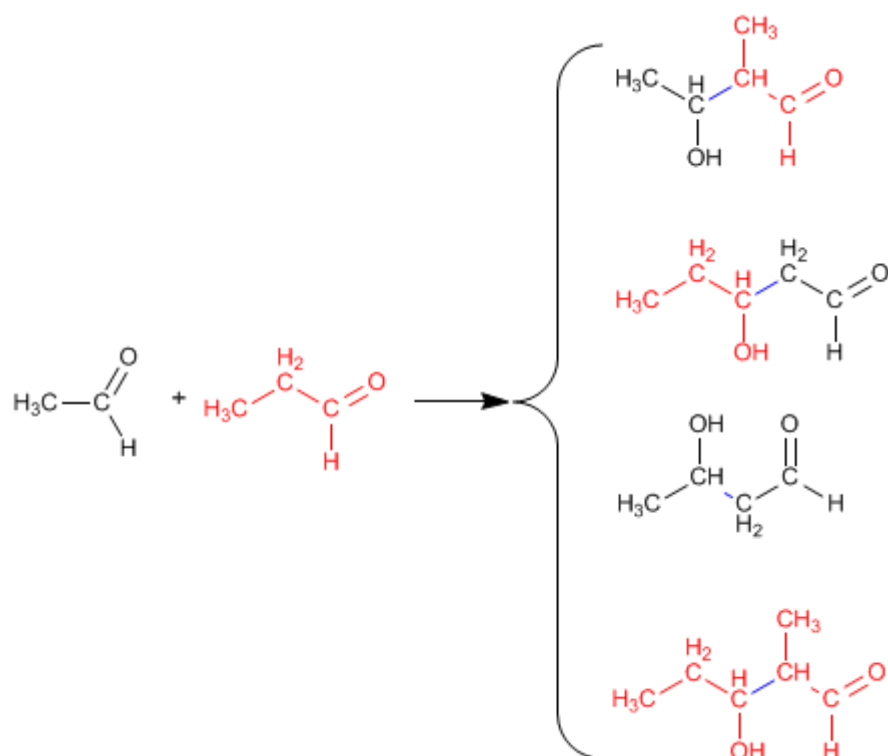
Etapa 4. Deshidratación del aldol



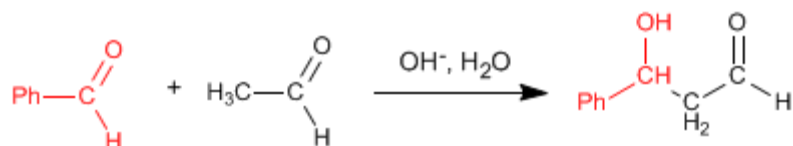
Condensación aldólica cruzada o mixta

La reacción entre dos carbonilos diferentes se llama aldólica cruzada o mixta. Esta reacción sólo tiene utilidad sintética en dos casos:

1. Sólo uno de los carbonilos puede formar enolatos.
 2. Uno de los carbonilos es mucho más reactivo que el otro.
- En el resto de situaciones la aldólica mixta genera mezclas de cuatro productos. Veamos como ejemplo la condensación del etanal y propanal.

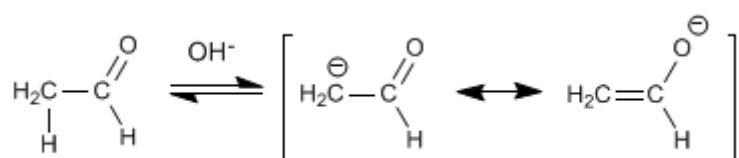


La condensación aldólica mixta del etanal con el benzaldehído genera un producto, cuando se trabaja en exceso de benzaldehído, debido a que el benzaldehído carece de hidrógenos en el carbono alfa y no puede formar enolatos.



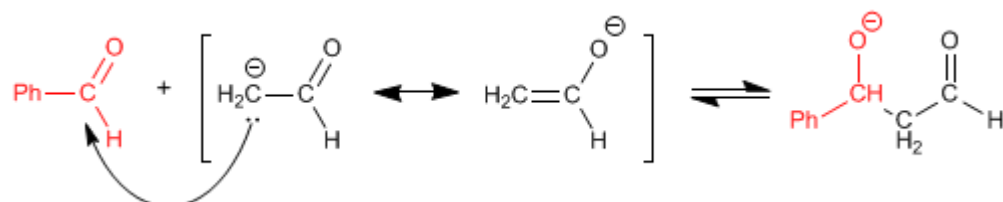
El mecanismo de esta reacción tiene lugar en las siguientes etapas:

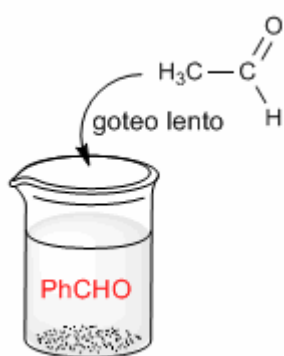
Etapas 1. Enolización del etanal



La formación de enolatos sólo puede tener lugar con el etanal, puesto que el benzaldehído carece de hidrógenos ácidos en el carbono alfa.

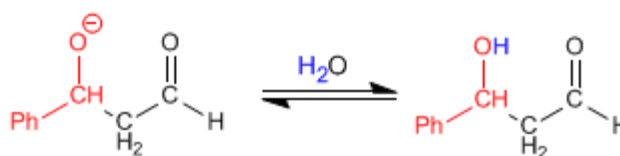
Etapas 2. Ataque nucleófilo del enolato al benzaldehído.





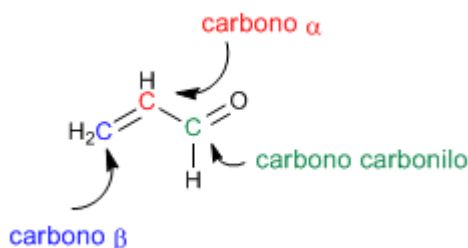
En esta etapa puede ocurrir el ataque del enolato de etanal sobre si mismo. Para evitarlo debe trabajarse en exceso de benzaldehído. Un procedimiento experimental muy usado para evitar la condensación del etanal consigo mismo es gotear lentamente el etanal sobre una disolución básica de benzaldehído

Etapa 3. Protonación



Síntesis de carbonilos alfa,beta-insaturados

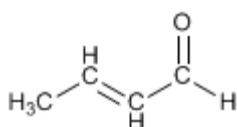
Los carbonilos α,β -insaturados son compuestos orgánicos que tienen un doble enlace entre las posiciones α,β de un aldehído o cetona.



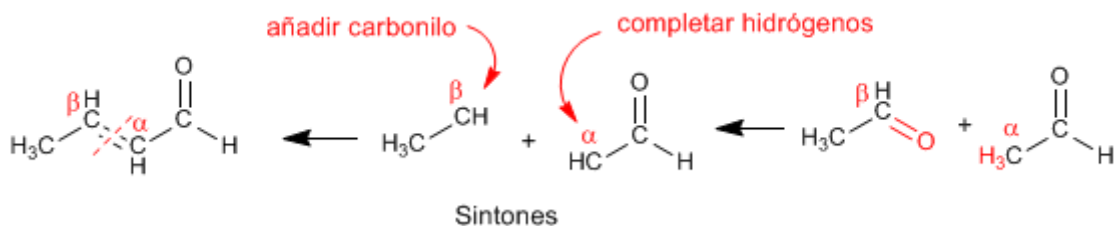
El propenal o acroleína es un carbonilo α,β -insaturado. Sus dos dobles enlaces conjugados le confieren una reactividad especial.

Existen 4 métodos importantes para la preparación de α,β -insaturados: condensación aldólica, halogenación del carbono α seguida de eliminación, oxidación de alcoholes alílicos y Wittig.

Método 1. Preparar mediante la condensación aldólica el siguiente compuesto.

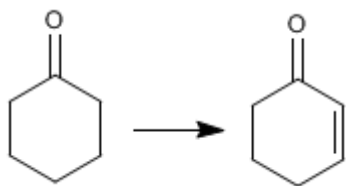


Empleamos la retrosíntesis para preparar el compuesto. Al ser de la familia de los α,β -insaturados se puede obtener mediante la condensación aldólica.

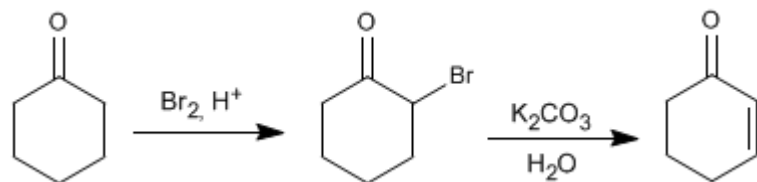


Para obtener los reactivos que forman el α,β -insaturado se rompe por el doble enlace, obteniéndose los sintones (equivalentes sintéticos). Los reactivos se obtienen añadiendo al carbono β un carbonilo y completando los hidrógeno que faltan en el carbono α .

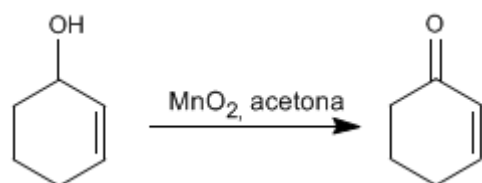
Ejemplo 2. Indicar como se puede realizar las siguiente transformación.



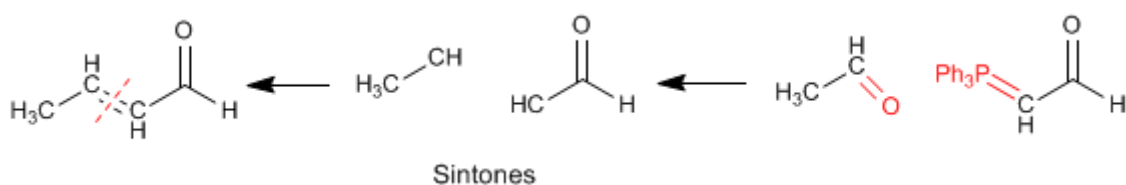
En una primera etapa se halogena la posición α del carbonilo. En la segunda etapa se realiza una eliminación que nos deja el producto final.



Método 3. La oxidación de alcoholes alílicos con dióxido de manganeso en acetona produce α,β -insaturados

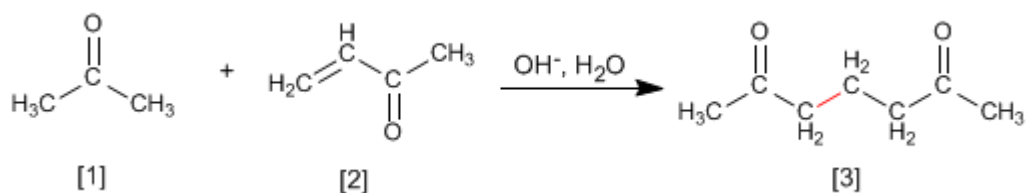


Método 4. Reacción de Wittig



Adición de Michael y anelación de Robinson

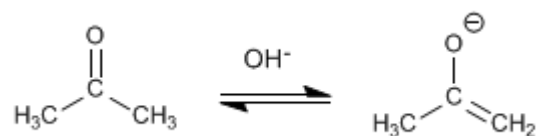
Los enolatos de aldehídos o cetonas se adicionan a los α,β -insaturados para formar 1,5-dicarbonilos. Esta reacción se denomina adición de Michael.



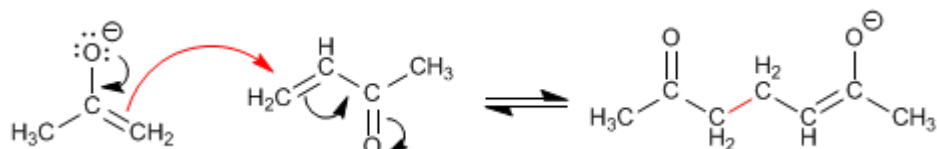
La propanona [1] reacciona con el α,β -insaturado [2] para formar el 1,5-dicarbonilo [3]

Mecanismo de la Adición de Michael:

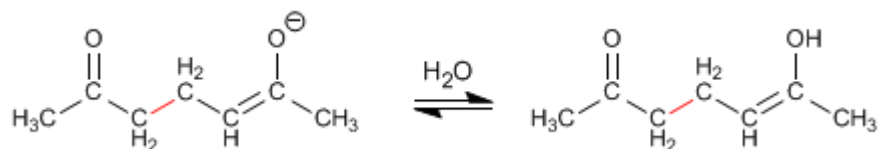
Etapla 1. Formación del enolato.



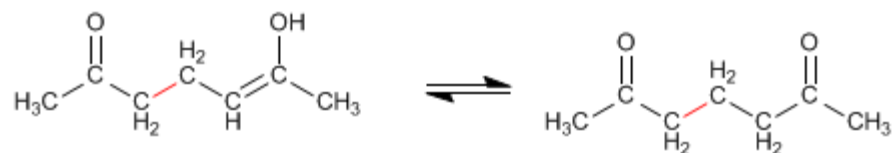
Etapla 2. Ataque nucleófilo del enolato al carbono β del α,β -insaturado.



Etapla 3. Equilibrio ácido-base



Etapla 4. Tautomería ceto-enol



El producto de Michael puede condensar mediante una aldólica intramolecular, formando un α,β -insaturado. El conjunto de la adición de Michael y la aldólica final se conoce como reacción de Robinson

Chemsoft ®

Química Orgánica

Recopilación : 2da Edición - 2009

José A.

Química Orgánica

Recopilación: 2da Edición

Diciembre 2009

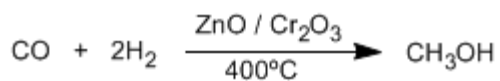
Índice:

- i. Alcoholes*
- ii. Éteres*
- iii. Aldehídos y Cetonas*
- iv. Enoles y Enolatos*
- v. Benceno*

SÍNTESIS Y REACTIVIDAD DE ALCOHOLES

Alcoholes - características generales

Los alcoholes son compuesto orgánicos que contienen el grupo hidroxilo (-OH). El metanol es el alcohol más sencillo, se obtiene por reducción del monóxido de carbono con hidrógeno.

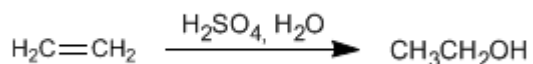


El metanol es un líquido incoloro, su punto de ebullición es 65°C, miscible en agua en todas las proporciones y venenoso (35 ml pueden matar una persona)

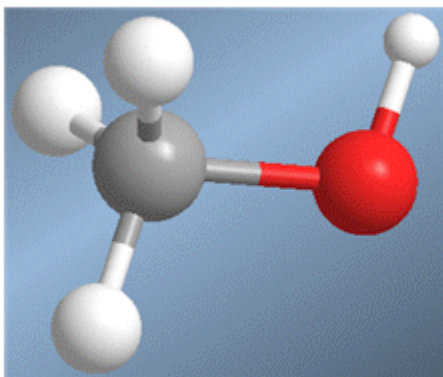
La mitad del metanol producido se oxida a metanal (formaldehído), material de partida para la fabricación de resinas y plásticos.

El etanol se obtiene por fermentación de materia vegetal, obteniéndose una concentración máxima de 15% en etanol. Por destilación se puede aumentar esta concentración hasta el 98%.

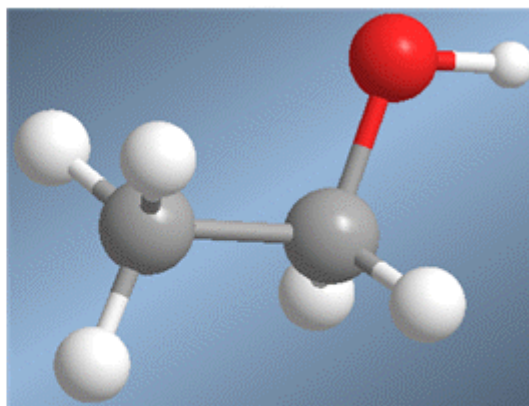
También se puede obtener etanol por hidratación del etileno (eteno) que se obtiene a partir del petróleo.



El etanol es un líquido incoloro, miscible en agua en todas proporciones, con punto de ebullición de 78°C. Es fácilmente metabolizado por nuestros organismos, aunque su abuso causa alcoholismo.



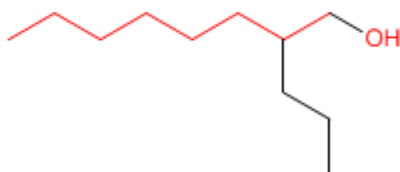
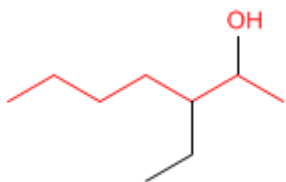
(metanol) CH_3OH



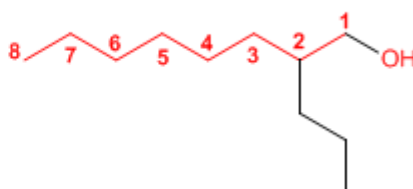
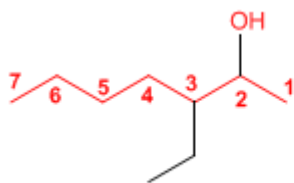
(etanol) $\text{CH}_3\text{CH}_2\text{OH}$

Nomenclatura de Alcoholes

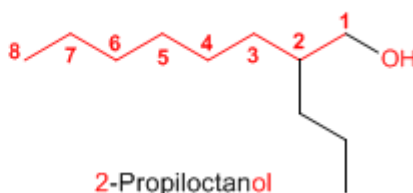
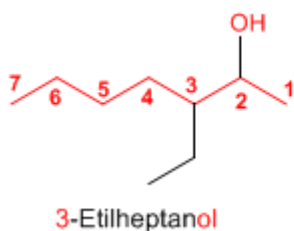
Regla 1. Se elige como cadena principal la de mayor longitud que contenga el grupo -OH.



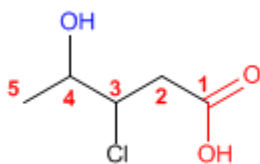
Regla 2. Se numera la cadena principal para que el grupo -OH tome el localizador más bajo. El grupo hidroxilo tiene preferencia sobre cadenas carbonadas, halógenos, dobles y triples enlaces.



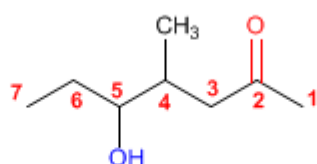
Regla 3. El nombre del alcohol se construye cambiando la terminación -o del alcano con igual número de carbonos por -ol



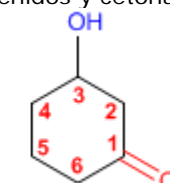
Regla 4. Cuando en la molécula hay grupos funcionales de mayor prioridad, el alcohol pasa a ser un mero sustituyente y se llama **hidroxi-**. Son prioritarios frente a los alcoholes: ácidos carboxílicos, anhídridos, ésteres, haluros de alcanoilo, amidas, nitrilos, aldehídos y cetonas.



Ácido 3-cloro-4-hidroxi-pentanoico

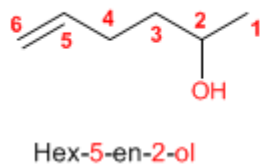


5-Hidroxi-4-metilheptanona

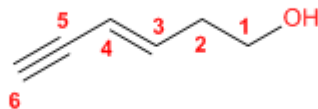


3-Hidroxiciclohexanona

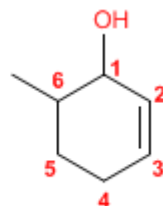
Regla 5. El grupo -OH es prioritario frente a los alquenos y alquinos. La numeración otorga el localizador más bajo al -OH y el nombre de la molécula termina en -ol.



Hex-5-en-2-ol



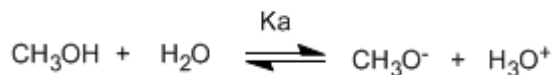
Hex-3-en-5-in-1-ol



6-Metilciclohex-2-en-1-ol

Acidez y basicidad de alcoholes

Los alcoholes son especies anfóteras (anfipróticas), pueden actuar como ácidos o bases. En disolución acuosa se establece un equilibrio entre el alcohol, el agua y sus bases conjugadas.



Escribiendo la constante del equilibrio (K_a)

$$K_a = \frac{[\text{H}_3\text{O}^+][\text{CH}_3\text{O}^-]}{[\text{CH}_3\text{OH}]} = 10^{-15.5}$$

El pequeño valor de la constante nos indica que el equilibrio está totalmente desplazado a la izquierda.


El logaritmo cambiado de signo de la constante de equilibrio nos da el pK_a del metanol, parámetro que indica el grado de acidez de un compuesto orgánico.

$$pK_a = -\log k_a = 15.5$$


El aumento del pK_a supone una disminución de la acidez. Así, el metanol con un pK_a de 15.5 es ligeramente más ácido que el etanol con pK_a de 15.9.

El pK_a de los alcoholes se ve influenciado por algunos factores como son el tamaño de la cadena carbonada y los grupos electronegativos

Al aumentar el tamaño de la cadena carbonada el alcohol se vuelve menos ácido.

CH_3OH	$pK_a = 15.5$	
$\text{CH}_3\text{CH}_2\text{OH}$	$pK_a = 15.9$	
$(\text{CH}_3)_2\text{CHOH}$	$pK_a = 17.1$	
$(\text{CH}_3)_3\text{COH}$	$pK_a = 18$	

Los grupos electronegativos (halógenos) aumentan la acidez de los alcoholes (bajan el pK_a)

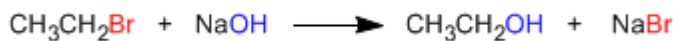
$\text{CH}_3\text{CH}_2\text{OH}$	$pK_a = 15.9$	
$\text{ClCH}_2\text{CH}_2\text{OH}$	$pK_a = 14.3$	
$\text{F}_3\text{CCH}_2\text{OH}$	$pK_a = 12.4$	

Síntesis de Alcoholes a partir de Haloalcanos

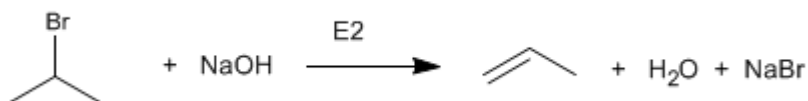
Los alcoholes se pueden obtener a partir de haloalcanos mediante reacciones S_N2 y S_N1

Síntesis de alcoholes mediante S_N2

Los haloalcanos primarios reaccionan con hidróxido de sodio para formar alcoholes. Haloalcanos secundarios y terciarios eliminan para formar alquenos.

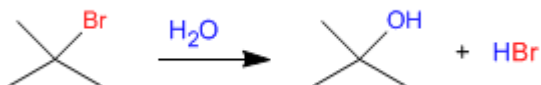


El bromuro de isopropilo (sustrato secundario) elimina al reaccionar con el ión hidróxido.



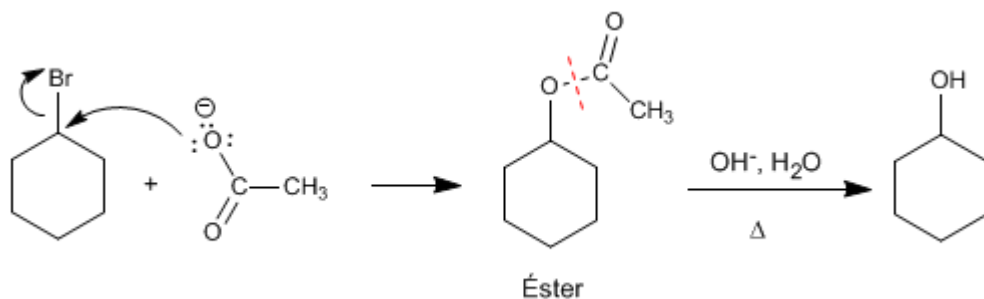
Síntesis de alcoholes mediante S_N1

Los sustratos secundarios y terciarios reaccionan con agua mediante mecanismo S_N1 para formar alcoholes.



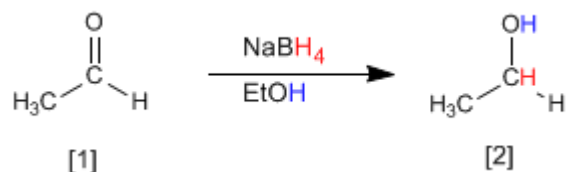
Hidrólisis de ésteres

Es un método interesante para preparar alcoholes a partir de haloalcanos secundarios. El haloalcano se convierte en éster por reacción con acetato de sodio, para después hidrolizarse en medio ácido o básico, obteniéndose el alcohol.



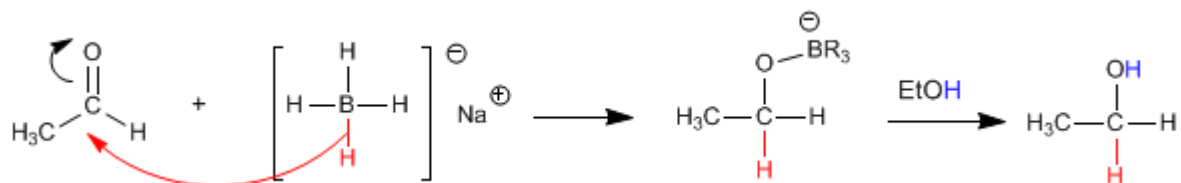
Síntesis de Alcoholes por reducción de carbonilos

Tanto el borohidruro de sodio (NaBH_4) como el hidruro de litio y aluminio (LiAlH_4) reducen aldehídos y cetonas a alcoholes.

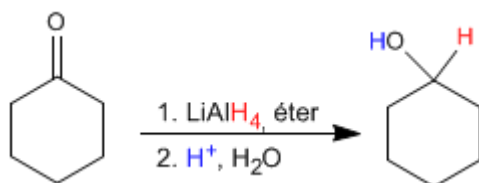


El etanal [1] se transforma por reducción con el borohidruro de sodio en etanol [2].

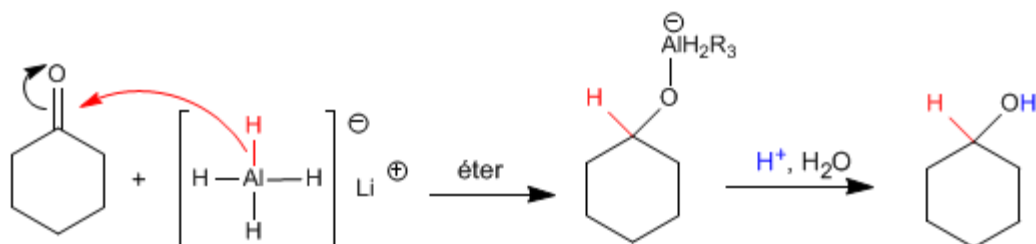
El mecanismo transcurre por ataque del hidruro procedente del reductor sobre el carbono carbonilo. En una segunda etapa el disolvente protona el oxígeno del alcóxido.



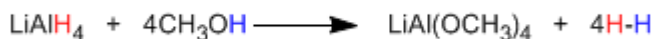
El hidruro de litio y aluminio trabaja en medio éter y transforma aldehídos y cetonas en alcoholes después de una etapa de hidrólisis ácida.



El mecanismo es análogo al del borohidruro de sodio.



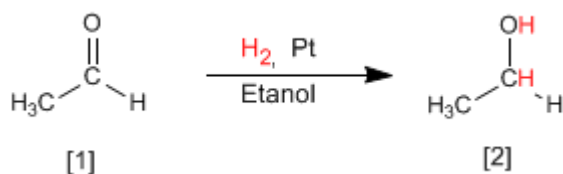
El reductor de litio y aluminio es más reactivo que el de boro, reacciona con el agua y los alcoholes desprendiendo hidrógeno. Por ello, debe disolverse en medios apróticos (éter).



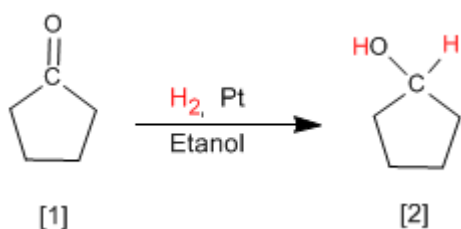
El reductor de boro, menos reactivo, descompone lentamente en medios próticos, lo que permite utilizarlo disuelto en etanol o agua.

Síntesis de Alcoholes por hidrogenación de Carbonilos

Otro método para preparar alcoholes consiste en la reducción de aldehídos o cetonas a alcoholes. El método más simple es la hidrogenación del doble enlace carbono-oxígeno, utilizando hidrógeno en presencia de un catalizador de platino, paladio, níquel o rutenio.



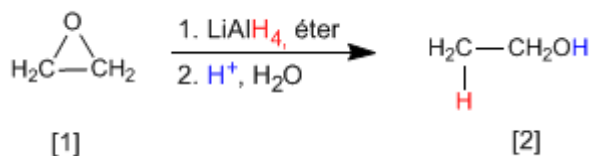
El etanal [1] se transforma por hidrogenación del doble enlace en etanol [2]



La ciclopentanona [1] se transforma por hidrogenación en ciclopentanol [2]

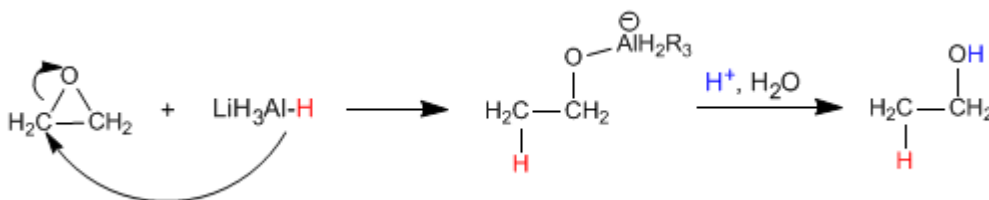
Síntesis de Alcoholes a partir de Epóxidos

Los alcoholes se pueden obtener por apertura de epóxidos (oxaciclopropanos). Esta apertura se puede realizar empleando reactivos organometálicos o el reductor de litio y aluminio.



El oxaciclopropano [1] se transforma por reducción con hidruro de litio y aluminio en etanol [2].

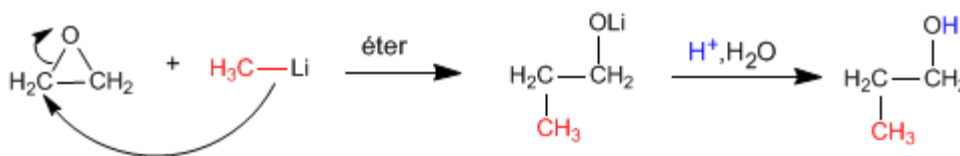
El mecanismo de la reacción comienza con el ataque del hidruro procedente del reductor sobre el carbono polarizado positivamente del epóxido, para terminar con la protonación del alcóxido.



Los reactivos de Grignard (organometálicos de magnesio) y los organolitílicos reaccionan con oxaciclopropano para dar un alcohol primario.



El metillitio ataca al oxaciclopropano [1] para formar propan-1-ol [2].

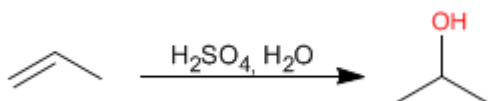


Síntesis de Alcoholes por Hidratación de Alquenos

Un método de síntesis para alcoholes, ya estudiado en la sección de alquenos, consiste en hidratar el alqueno. La adición del -OH puede ser en el carbono más sustituido del alqueno (Markovnikov), o bien, en el carbono menos sustituido (antiMarkovnikov).

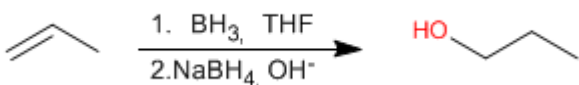
Hidratación Markovnikov

En esta hidratación el grupo hidroxilo va al carbono con más sustituyentes. Se emplea como reactivo sulfúrico acuoso, o bien, acetato de mercurio en agua, seguido de reducción con borohidruro de sodio.



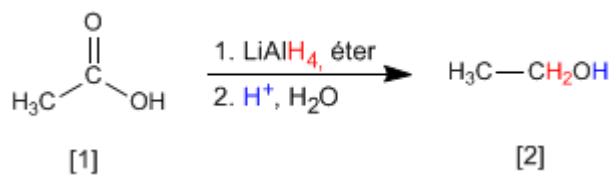
Hidratación antiMarkovnikov

El grupo hidroxilo se adiciona al carbono menos sustituido. El reactivo empleado es borano en THF seguido de oxidación con agua oxigenada en medio básico (hidroboración)

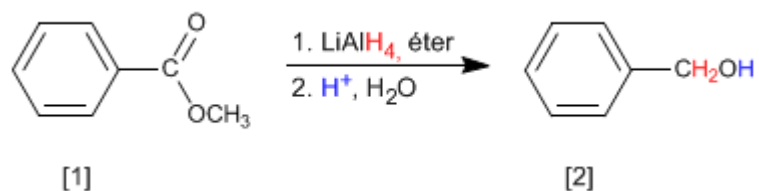


Síntesis de alcoholes por reducción de ácidos y ésteres

Los ácidos carboxílicos y los ésteres se reducen a alcoholes con el hidruro de litio y aluminio.
Reductores más suaves como el borohidruro de sodio son incapaces de reducir estos compuestos.



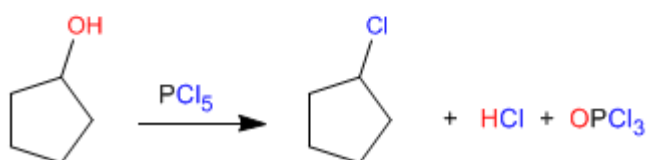
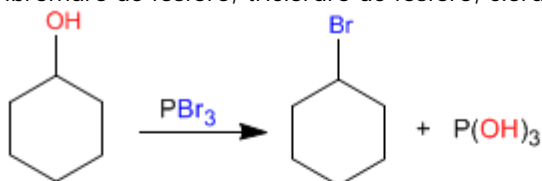
El ácido etanoico [1] se transforma por reducción con hidruro de litio y aluminio en etanol [2].



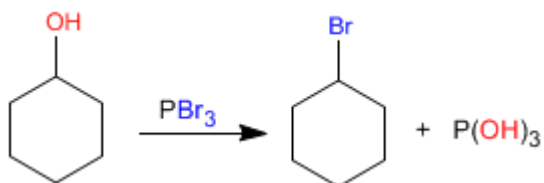
El benzoato de metilo [1] se transforma en alcohol bencílico [2] por reducción con hidruro de litio y aluminio.

Síntesis de Haloalcanos a partir de Alcoholes

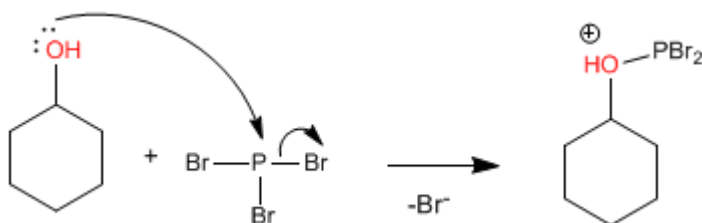
Los alcoholes primarios y secundarios pueden convertirse en haloalcanos con reactivos como: tribromuro de fósforo, tricloruro de fósforo, cloruro de tionilo y pentacloruro de fósforo.



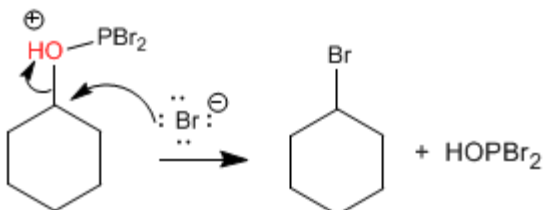
El mecanismo de estas reacciones es de tipo $\text{S}_{\text{N}}2$ y sólo los alcoholes primarios y secundarios reaccionan. Veamos el mecanismo de la primera reacción.



Etapas 1. Ataque del alcohol al tribromuro de fósforo



Etapas 2. Sustitución nucleófila bimolecular, actuando el bromuro como nucleófilo

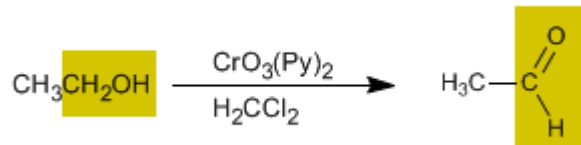


Todos los bromos del PBr_3 son reactivos y el mecanismo se repite dos veces más.

Oxidación de Alcoholes

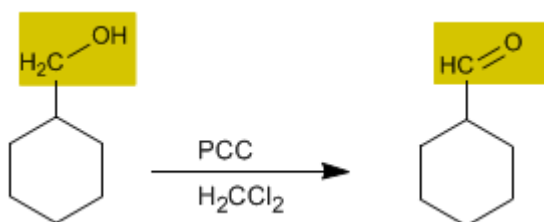
La oxidación de alcoholes forma compuestos carbonilos. Al oxidar alcoholes primarios se obtienen aldehídos, mientras que la oxidación de alcoholes secundarios forma cetonas.

Oxidación de alcoholes primarios a aldehídos



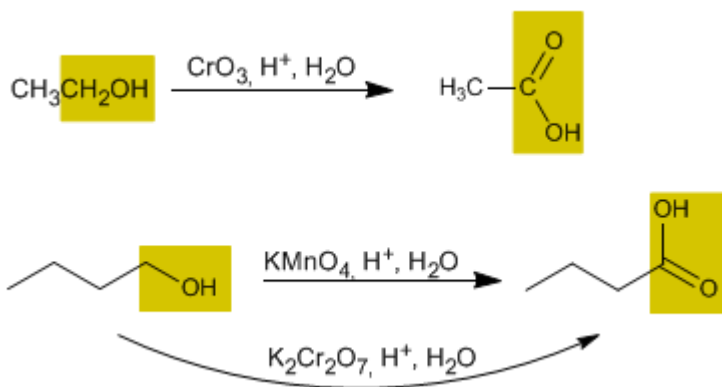
El trióxido de cromo con piridina en diclorometano permite aislar aldehídos con buen rendimiento a partir de alcoholes primarios.

Se conoce como PCC (clorocromato de piridinio) al trióxido de cromo con piridina y ácido clorhídrico en diclorometano. Este reactivo también convierte alcoholes primarios en aldehídos.



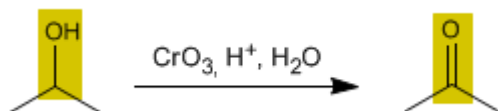
Oxidación de alcoholes primarios a ácidos carboxílicos

El trióxido de cromo en medio ácido acuoso (reactivo de Jones), el permanganato de potasio y el dicromato de potasio oxidan los alcoholes primarios a ácidos carboxílicos.



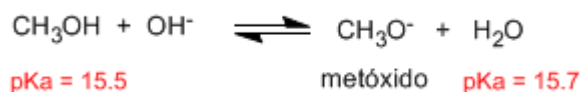
Oxidación de alcoholes secundarios a cetonas

Los oxidantes convierten los alcoholes secundarios en cetonas. No es posible la sobreoxidación a ácido carboxílico.

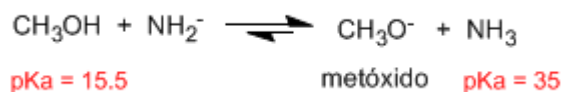


Formación de Alcóxidos a partir de Alcoholes

Los alcóxidos son las bases de los alcoholes, se obtienen por reacción del alcohol con una base fuerte.

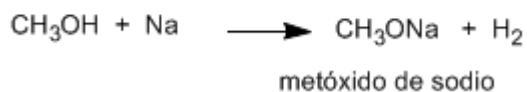
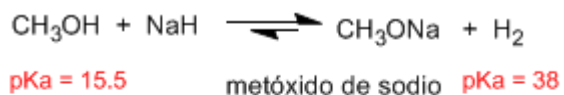


Los pK_a de los ácidos conjugados son similares y el equilibrio no se encuentra desplazado. El ión hidróxido es una base demasiado débil para formar el alcóxido en cantidad importante.



El amiduro es una base muy fuerte y desplaza el equilibrio a la derecha, transformando el metanol en metóxido.

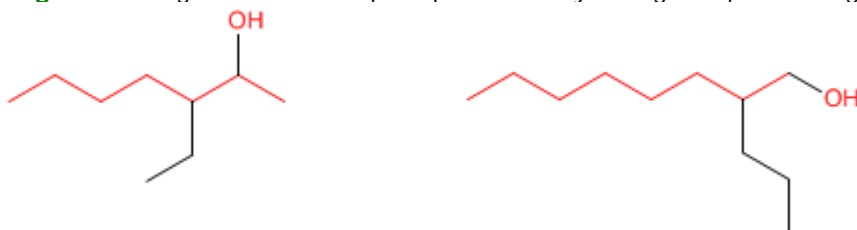
Otras bases fuertes que pueden ser usadas para formar alcóxidos son: hidruro de sodio, LDA, sodio metal.



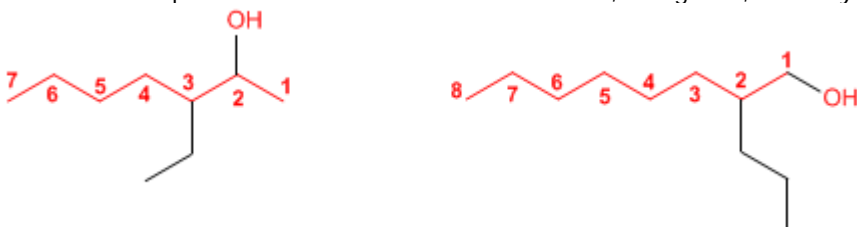
PROBLEMAS NOMENCLATURA - ALCOHOLES

Nomenclatura de Alcoholes - Reglas IUPAC

Regla 1. Se elige como cadena principal la de mayor longitud que contenga el grupo -OH.



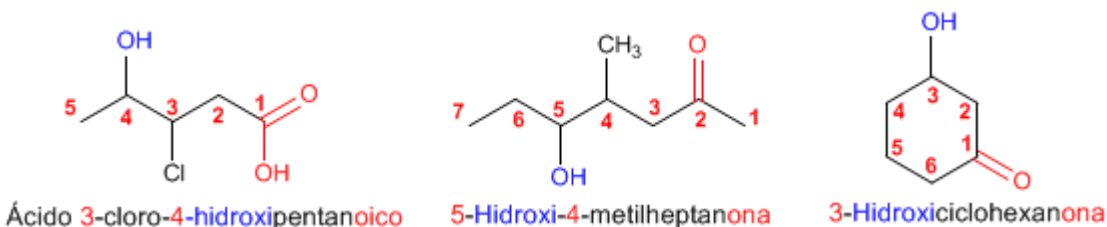
Regla 2. Se numera la cadena principal para que el grupo -OH tome el localizador más bajo. El grupo hidroxilo tiene preferencia sobre cadenas carbonadas, halógenos, dobles y triples enlaces.



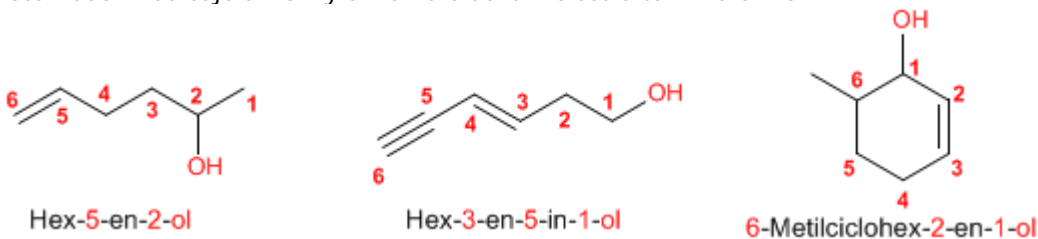
Regla 3. El nombre del alcohol se construye cambiando la terminación -o del alcano con igual número de carbonos por -ol



Regla 4. Cuando en la molécula hay grupos funcionales de mayor prioridad, el alcohol pasa a ser un mero sustituyente y se llama **hidroxi-**. Son prioritarios frente a los alcoholes: ácidos carboxílicos, anhídridos, ésteres, haluros de alcanoilo, amidas, nitrilos, aldehídos y cetonas.

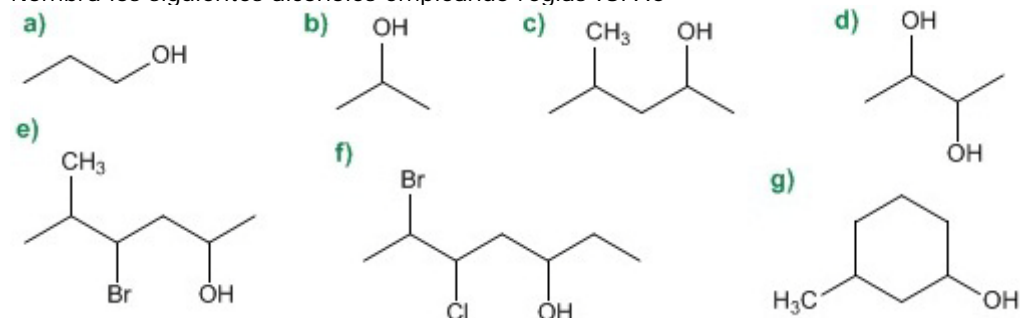


Regla 5. El grupo -OH es prioritario frente a los alquenos y alquinos. La numeración otorga el localizador más bajo al -OH y el nombre de la molécula termina en -ol.

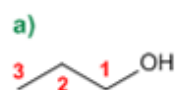


Nomenclatura de Alcoholes - Problema 0.1

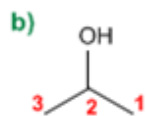
Nombra los siguientes alcoholes empleando reglas IUPAC



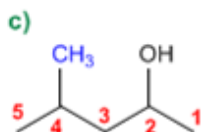
Solución:



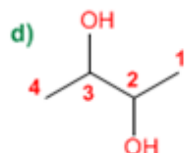
1. Cadena principal: la de mayor longitud que contenga el -OH (propano)
2. Numeración: otorga al -OH el localizador más bajo.
3. Sustituyentes: no
4. Nombre: Propan-1-ol



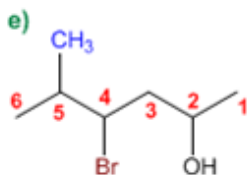
1. Cadena principal: la de mayor longitud que contenga el -OH (propano)
2. Numeración: indiferente.
3. Sustituyentes: no
4. Nombre: Propan-2-ol



1. Cadena principal: la de mayor longitud que contenga el -OH (pentano)
2. Numeración: otorga al -OH el localizador más bajo (-OH preferente sobre cadenas)
3. Sustituyentes: metilo en 4
4. Nombre: 4-Metilpentan-2-ol



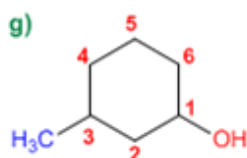
1. Cadena principal: mayor longitud (butano)
2. Numeración: comienza en uno de los extremos.
3. Sustituyentes: no
4. Nombre: Butano-2,3-diol



1. Cadena principal: mayor longitud (hexano)
2. Numeración: comienza en el extremo derecho, para otorgar al -OH el localizador más bajo.
3. Sustituyentes: bromo en posición 4 y metilo en 5.
4. Nombre: 4-Bromo-5-metilhexan-2-ol



1. Cadena principal: mayor longitud (heptano)
2. Numeración: comienza en extremo que otorga el localizador más bajo al -OH.
3. Sustituyentes: bromo en 6 y cloro en 5.
4. Nombre: 6-Bromo-5-cloroheptan-3-ol



1. Cadena principal: ciclo de seis miembros (ciclohexano)
2. Numeración: comienza en el carbono del -OH.
3. Sustituyentes: metilo en 3.
4. Nombre: 3-Metilciclohexanol

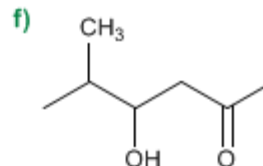
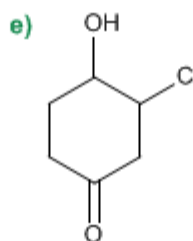
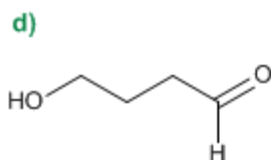
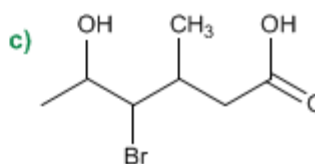
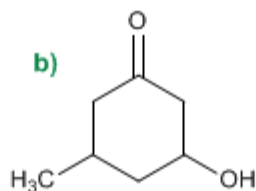
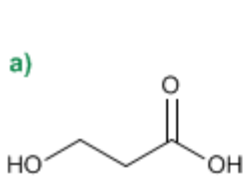
1. Cuando en una molécula hay más de un grupo -OH se pueden emplear los prefijos de cantidad di, tri, tetra, penta, hexa,..... La numeración debe otorgar los menores localizadores a los -OH.

2. El nombre del alcohol se construye comenzando por los sustituyentes, precedidos por sus respectivos localizadores, terminando en el nombre de la cadena principal. La terminación -o del alcano correspondiente se sustituye por -ol.

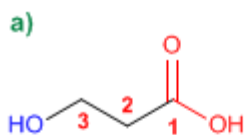
3. En el caso de alcoholes cíclicos no es necesario indicar la posición del grupo hidroxilo, puesto que siempre toma localizador 1.

Nomenclatura de Alcoholes - Problema 0.2

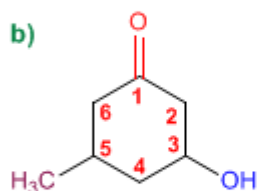
Nombra los siguientes moléculas, en las que el alcohol actúa como sustituyente.



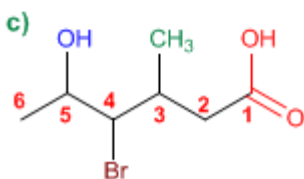
Solución



1. Cadena principal: más larga que contenga el grupo funcional (propano)
2. Grupo funcional: ácido carboxílico
3. Numeración: localizador más bajo al grupo ácido
4. Sustituyentes: grupo **hidroxi** en 3.
5. Nombre: **Acido 3-hidroxi**propanoico



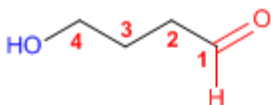
1. Cadena principal: ciclo de seis miembros (ciclohexano)
2. Grupo funcional: cetona
3. Numeración: localizador más bajo al grupo carbonilo
4. Sustituyentes: grupo **hidroxi** en 3 y **metilo** en 4.
5. Nombre: **2-Hidroxi-5-metilciclohexanona**



1. Cadena principal: más larga que contenga el grupo funcional (hexano)
2. Grupo funcional: ácido carboxílico
3. Numeración: asigna el localizador más bajo al grupo ácido.
4. Sustituyentes: **bromo** en 4, grupo **hidroxi** en 5 y **metilo** en 3
5. Nombre: **Acido 4-bromo-6-hidroxi-3-metilhexanoico**

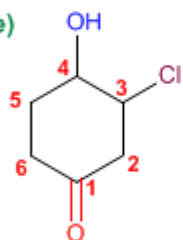
Los ácidos carboxílicos y las cetonas son prioritarios sobre los alcoholes.
El alcohol pasa a ser un sustituyente más de la molécula, ordenándose alfabéticamente con el resto de sustituyentes.

d)



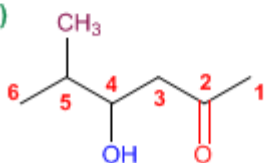
1. Cadena principal: más larga que contenga el grupo funcional (butano)
2. Grupo funcional: aldehído
3. Numeración: localizador más bajo al grupo carbonilo
4. Sustituyentes: grupo **hidroxi** en 4.
5. Nombre: **4-Hidroxibutanal**

e)



1. Cadena principal: ciclo de seis miembros
2. Grupo funcional: cetona
3. Numeración: localizador más bajo al carbonilo
4. Sustituyentes: **cloro** en 3 e **hidroxi** en 4.
5. Nombre: **3-Cloro-4-hidroxiciclohexanona**

f)



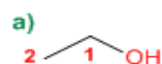
1. Cadena principal: más larga que contenga el grupo funcional (propano)
2. Grupo funcional: cetona
3. Numeración: localizador más bajo al grupo carbonilo
4. Sustituyentes: grupo **hidroxi** en 4 y **metilo** en 5.
5. Nombre: **3-Hidroxi-4-metilhexan-2-ona**

Nomenclatura de Alcoholes - Problema 0.3

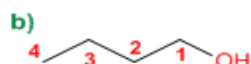
Dibujar la estructura de los siguientes alcoholes:

- | | |
|--------------------------|-----------------------------------|
| a) Etanol | i) Ciclopent-2-enol |
| b) Butanol | j) 2,3-Dimetilciclohexanol |
| c) 2-Metilpropan-1-ol | k) Octa-3,5-dien-2-ol |
| d) 2-Metilbutan-2-ol | l) Hex-4-en-1-in-3-ol |
| e) 3-Metilbutan-2-ol | m) 2-Bromohept-2-en-1,4-diol |
| f) 3-Metilbutan-1-ol | n) 2-Fenil-5-metilheptan-2-ol |
| g) 2,3-Pentanodiol | o) Alcohol bencílico |
| h) 2-Etil-pent-3-en-1-ol | p) 1,2,3-Propanotriol (glicerina) |

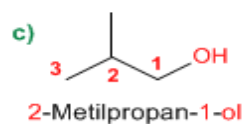
Solución:



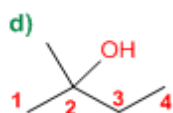
Etanol



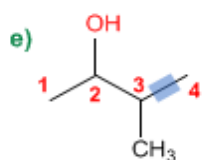
Butanol



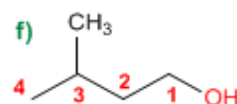
2-Metilpropan-1-ol



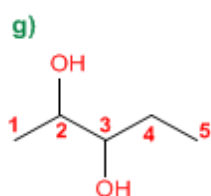
2-Metilbutan-2-ol



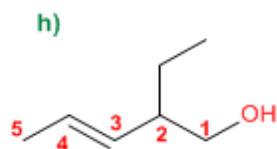
3-Metilbutan-2-ol



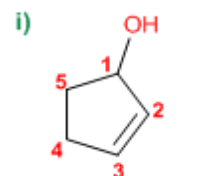
3-Metilbutan-1-ol



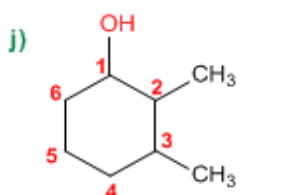
2,3-Pentanodiol



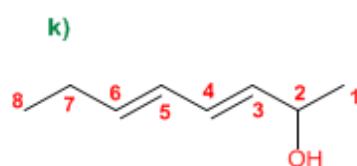
2-Etil-pent-3-en-1-ol



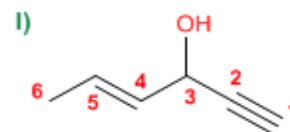
Ciclopent-2-enol



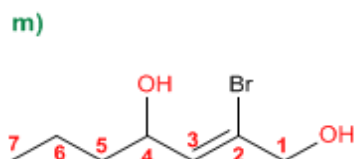
2,3-Dimetilciclohexanol



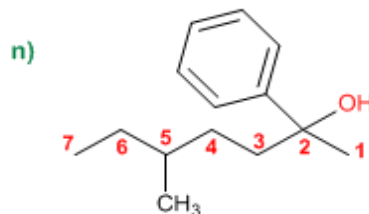
Octa-3,5-dien-2-ol



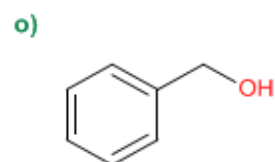
Hex-4-en-1-in-3-ol



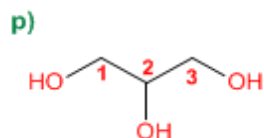
2-Bromohept-2-en-1,4-diol



2-Fenil-5-metilheptan-2-ol



Alcohol bencílico

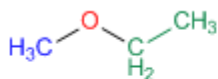


1,2,3-Propanotriol (glicerina)

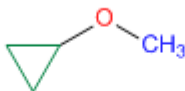
TEORÍA DE ÉTERES

Nomenclatura de éteres - epóxidos

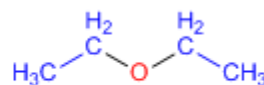
La nomenclatura de los éteres consiste en nombrar alfabéticamente los dos grupos alquilo que parten del oxígeno, terminando el nombre en éter. Veamos algunos ejemplos:



Etil metil éter

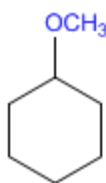


Ciclopropil metil éter

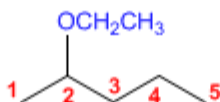


Dietil éter

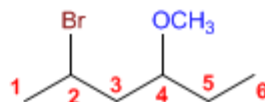
También se pueden nombrar los éteres como grupos alcoxi.



Metóxiciclohexano



2-Etoxi pentano

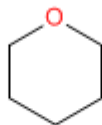


2-Bromo-4-metoxihexano

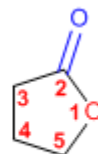
Los éteres cíclicos se forman sustituyendo $-CH_2-$ del ciclo por $-O-$. Este cambio se indica con el prefijo **oxa-**.



Oxaciclopropano



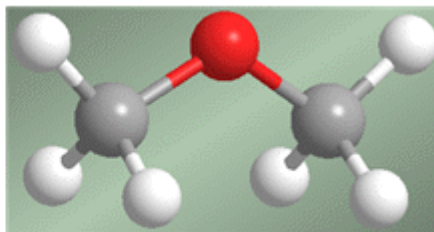
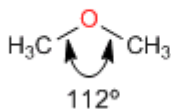
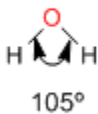
Oxaciclohexano



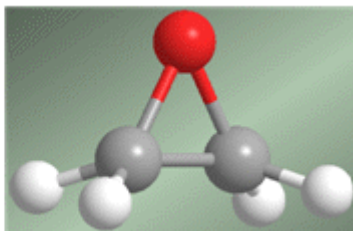
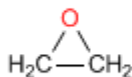
2-oxo-oxaciclopentano

Estructura y enlace en éteres y epóxidos

Los éteres son moléculas de estructura similar al agua y alcoholes. El ángulo entre los enlaces C-O-C es mayor que en el agua debido a las repulsiones estéricas entre grupos voluminosos.

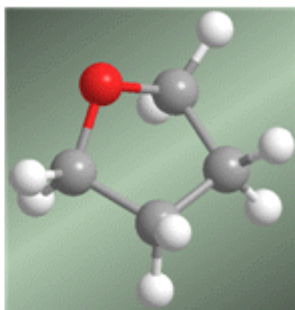
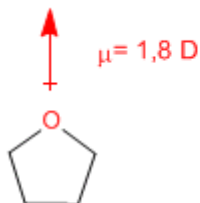


En el caso de los epóxidos la característica más relevante es la tensión del anillo, debida a ángulos de enlace muy distantes a los 109°.

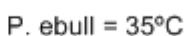


El enlace C-O-C presenta un ángulo de 61°.

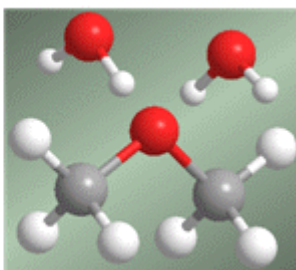
Los éteres son moléculas muy polares. Así, el Dietil éter presenta un momento dipolar de 1,2 D. Este momento dipolar es aún más importante en éteres cíclicos (oxaciclopropano, tetrahydrofurano) que presentan momentos dipolares sobre 1,8 D, similares al agua.



.....



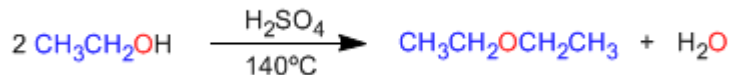
Dietil éter



Síntesis de éteres por condensación de alcoholes

1. Éteres a partir de alcoholes primarios

Los éteres simétricos pueden prepararse por condensación de alcoholes. La reacción se realiza bajo calefacción (140°C) y con catálisis ácida. Así, dos moléculas de etanol condensan para formar dietil éter.

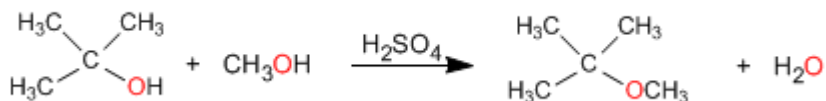


El mecanismo de la reacción transcurre en las siguientes etapas:



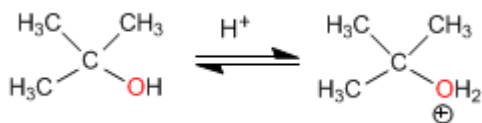
2. Uno de los alcoholes es secundario o terciario

En este caso la reacción transcurre en condiciones más suaves, a través de mecanismos $\text{S}_{\text{N}}1$.

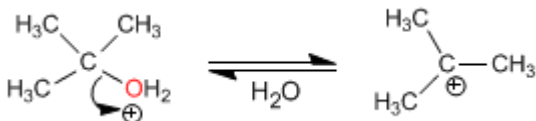


El mecanismo transcurre con formación de un carbocatión terciario de gran estabilidad

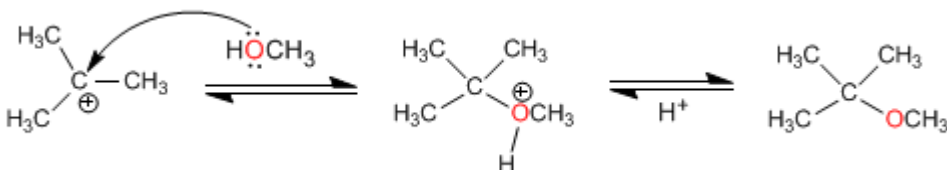
Etapa 1. Protonación del alcohol terciario



Etapa 2. Formación del carbocatión por pérdida de agua

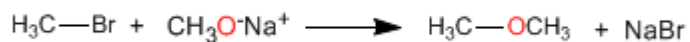


Etapa 3. Ataque nucleófilo del metanol



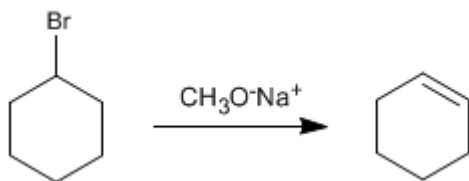
Síntesis de Williamson de los éteres

La reacción entre un haloalcano primario y un alcóxido (o bien alcohol en medio básico) es el método más importante para preparar éteres. Esta reacción es conocida como síntesis de Williamson.

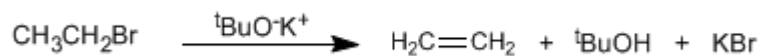


Esta reacción transcurre a través del mecanismo $\text{S}_{\text{N}}2$.

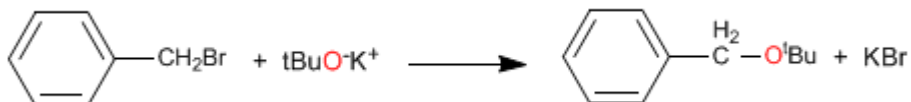
La importante basicidad de los alcóxidos produce reacciones de eliminación con sustratos secundarios y terciarios, formando alquenos en lugar de éteres.



Otra situación en la que Williamson no rinde éteres, es en el caso de emplear alcóxidos impedidos, como *tert*-butóxido de potasio. Debido a su gran tamaño el *tert*-butóxido elimina incluso con sustratos primarios.



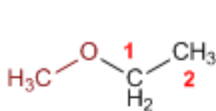
Con haloalcanos primarios y sobre todo con haloalcanos que carecen de hidrógenos β el rendimiento de Williamson es muy bueno.



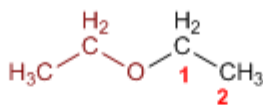
PROBLEMAS NOMENCLATURA - ÉTERES

Nomenclatura de Éteres - Reglas IUPAC

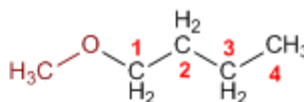
Regla 1. Los éteres pueden nombrarse como alcoxi derivados de alcanos (nomenclatura IUPAC sustitutiva). Se toma como cadena principal la de mayor longitud y se nombra el alcóxido como un sustituyente.



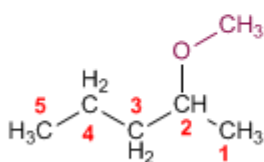
Metoxietano



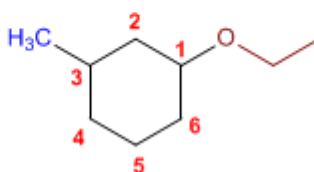
Etoxietano



1-Metoxibutano

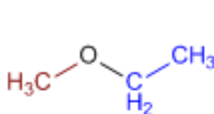


2-Metoxipentano

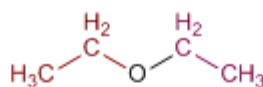


1-Etoxi-3-metilciclohexano

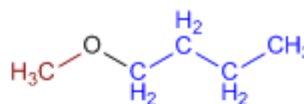
Regla 2. La nomenclatura funcional (IUPAC) nombra los éteres como derivados de dos grupos alquilo, ordenados alfabéticamente, terminando el nombre en la palabra éter.



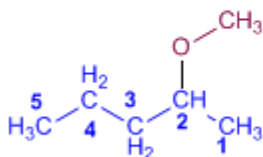
Etil metil éter



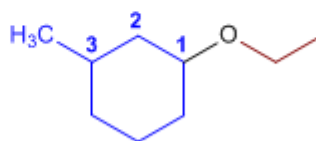
Dietil éter



Butil metil éter



Metil pent-2-il éter



Etil 3-metilciclohexil éter

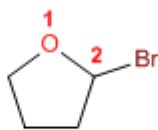
Regla 3. Los éteres cíclicos se forman sustituyendo un -CH₂- por -O- en un ciclo. La numeración comienza en el oxígeno y se nombran con el prefijo oxa- seguido del nombre del ciclo.



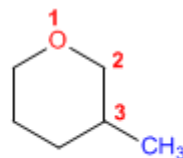
Oxaciclopropano



Oxaciclobutano



2-Bromooxaciclopentano

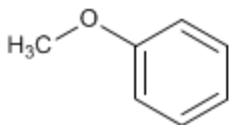


3-Metiloxaciclohexano

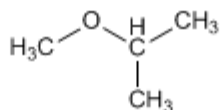
Nomenclatura de Éteres - Problema 0.1

Nombra los siguientes éteres:

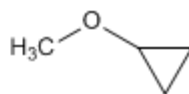
a)



b)



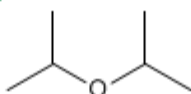
c)



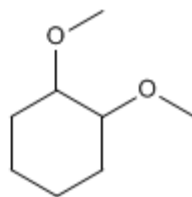
d)



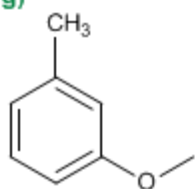
e)



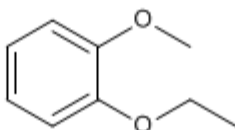
f)



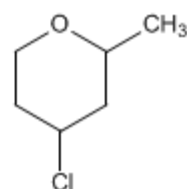
g)



h)

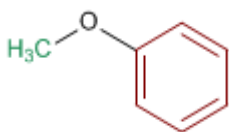


i)



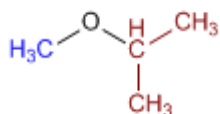
Solución:

a)



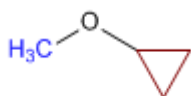
1. Sustituyentes: **fenil** y **metil**
2. Nombre: **Fenil metil** éter

b)



1. Sustituyentes: **isopropil** y **metil**
2. Nombre: **Isopropil metil** éter

c)



1. Sustituyentes: **ciclopropil** y **metil**
2. Nombre: **Ciclopropil metil** éter

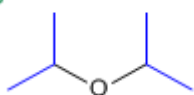
El nombre de los éteres se construye terminando en la palabra éter el nombre de las cadenas que parten del oxígeno. Estas cadenas se nombran como sustituyentes y se ordenan alfabéticamente. Obsérvese el espacio de separación entre las palabras.

d)



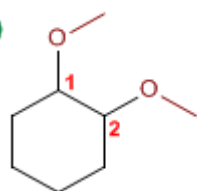
1. Sustituyentes: **etilo** y **propilo**
2. Nombre: **Etil propil** éter

e)



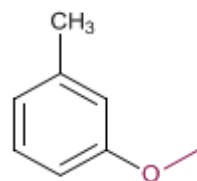
1. Sustituyentes: **isopropilos**
2. Nombre: **Diisopropil** éter

f)



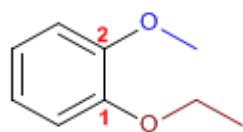
1. Cadena principal: ciclo de seis miembros (ciclohexano)
2. Numeración: otorga localizadores más bajos a sustituyentes
3. Sustituyentes: **metoxidos** en 1,2
4. Nombre: **1,2-Dimetoxiciclohexano**

g)



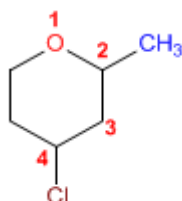
1. Cadena principal: Tolueno
2. Numeración: metilo y metóxido en meta.
3. Sustituyentes: **metoxido**
4. Nombre: **m-Metoxitolueno**

h)



1. Cadena principal: Benceno
2. Numeración: Comienza en el etoxi (antes alfabéticamente)
3. Sustituyentes: **etoxido** en 1 y **metoxido** en 2. (posición meta)
4. Nombre: **m-Etoximetoxibenceno**

i)



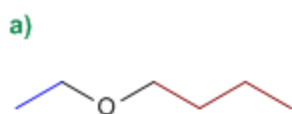
1. Cadena principal: ciclo de 6 miembros (oxaciclohexano)
2. Numeración: comienza en el oxígeno, prosigue a la derecha para otorgar a los sustituyentes los menores localizadores.
3. Sustituyentes: **cloro** y **metilo**
4. Nombre: **4-Cloro-2-metiloxaciclohexano**

Nomenclatura de Éteres - Problema 0.2

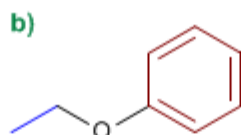
Dibuja las estructuras de los siguientes éteres:

- | | |
|--------------------------|----------------------------------|
| a) Butil etil éter | k) 2-Clorofenil fenil éter |
| b) Etil fenil éter | l) tert-butil isopropil éter |
| c) Difenil éter | m) 2-Metoxi-3-fenilbutan-1-ol |
| d) Divinil éter | n) Dietil éter |
| e) Isopropoxibutano | o) m-Etoxifenol |
| f) Bencil fenil éter | p) 2,3-Dimetiloxaciclopropano |
| g) Metoxiciclohexano | q) 3-Metoxioxaciclohexano |
| h) 4-Metoxipent-2-eno | r) 2-Etil-3-metiloxaciclopentano |
| i) 4-Etoxibut-1-ino | s) Ciclohexil ciclopropil éter |
| j) Ciclohexil fenil éter | t) 2-Metoxipentano |

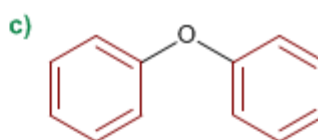
Solución



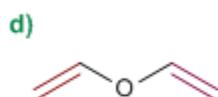
Butil etil éter



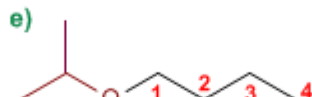
Etil fenil éter



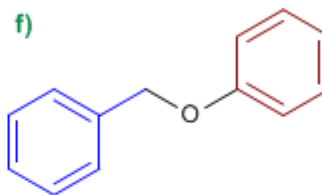
Difenil éter



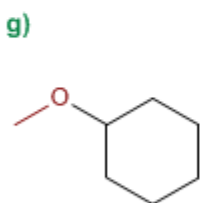
Divinil éter



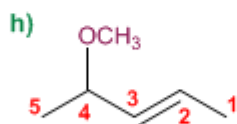
1-Isopropoxibutano



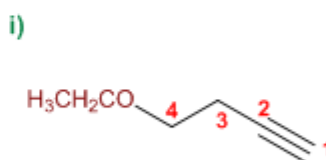
Bencil fenil éter



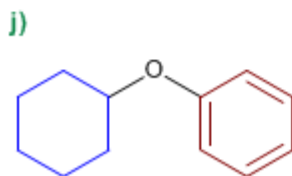
Metoxiciclohexano



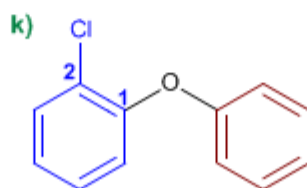
4-Metoxipent-2-eno



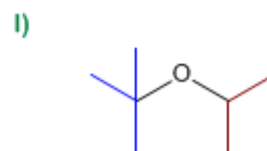
4-Etoxibut-1-ino



Ciclohexil fenil éter

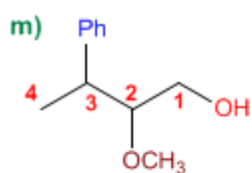


2-Clorofenil fenil éter

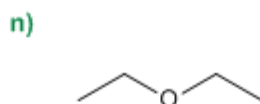


tert-butil isopropil éter

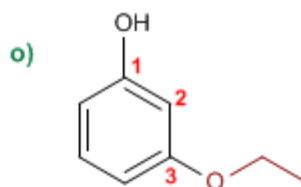
Los grupos alcóxido (metóxido, etóxido....) se ordenan alfabéticamente con los demás sustituyentes de la molécula y no tienen ninguna preferencia sobre ellos



2-Metoxi-3-fenilbutan-1-ol



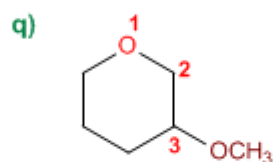
Dietil éter



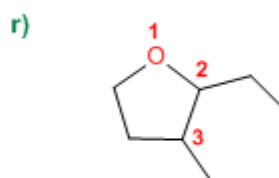
m-Etoxifenol



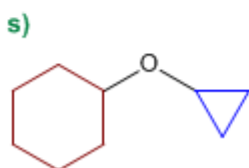
2,3-Dimetiloxa**c**ciclopropano



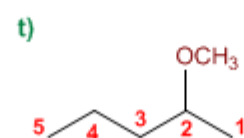
3-Metoxioxa**c**ciclohexano



2-Etil-3-metiloxa**c**ciclopentano



Ciclohexil ciclopropil éter

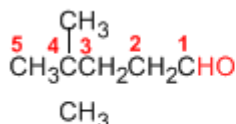


2-Metoxipentano

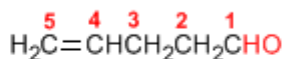
Nomenclatura de Aldehídos y Cetonas

Los aldehídos se nombran reemplazando la terminación **-ano** del alcano correspondiente por **-al**. No es necesario especificar la posición del grupo aldehído, puesto que ocupa el extremo de la cadena (localizador 1).

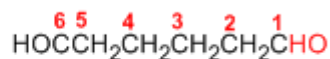
Cuando la cadena contiene dos funciones aldehído se emplea el sufijo **-dial**.



4,4-Dimetilpentanal

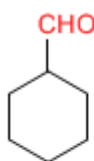


Hex-4-enal

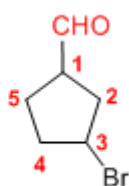


Pentanodial

El grupo **-CHO** unido a un ciclo se llama **-carbaldehído**. La numeración del ciclo se realiza dando localizador 1 al carbono del ciclo que contiene el grupo aldehído.



Ciclohexanocarbaldehído

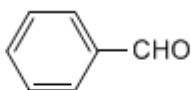


3-Bromociclopentanocarbaldehído

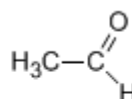
Algunos nombres comunes de aldehídos aceptados por la IUPAC son:



Formaldehído
(Metanal)

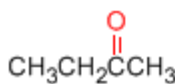


Benzaldehído
(Bencenocarbaldehído)

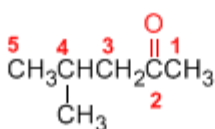


Acetaldehído
(Etanal)

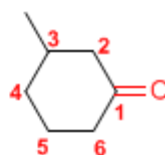
Las cetonas se nombran sustituyendo la terminación **-ano** del alcano con igual longitud de cadena por **-ona**. Se toma como cadena principal la de mayor longitud que contiene el grupo carbonilo y se numera para que éste tome el localizador más bajo.



Butanona

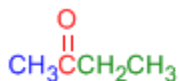


4-Metil-2-pentanona

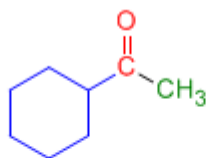


3-Metilciclohexanona

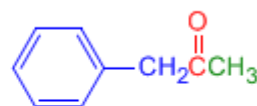
Existe un segundo tipo de nomenclatura para las cetonas, que consiste en nombrar las cadenas como sustituyentes, ordenándolas alfabéticamente y terminando el nombre con la palabra **cetona**.



Etil metil cetona



Ciclohexil metil cetona



Fenil metil cetona

[Siguiete >](#)

[\[Volver\]](#)

Charles Friedel (1832 - 1899)



Origen: Químico frances..

Lugar de nacimiento: Estrasburgo.

Formación: estudió química en la Universidad de Berlín entre 1895 y 1899, consiguiendo el doctorado este año.

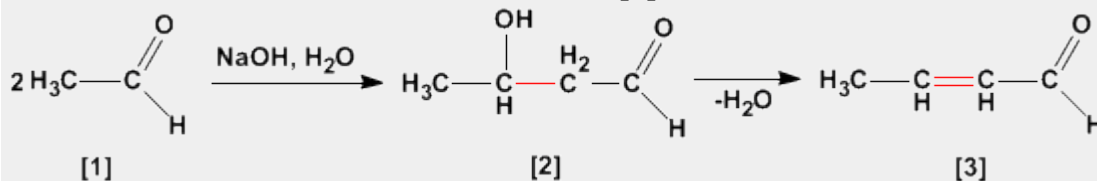
Docencia: Profesor en la Universidad de la Sorbona.

Investigación: Obtuvo el alcohol propílico. En 1877, Friedel y Crafts describieron por primera vez la reacción del benceno con un haloalcano en presencia de un ácido de Lewis. Esta reacción produce la alquilación del benceno y se conoce como alquilación de Friedl-Crafts.

Premio Nobel:

Aldólica (Condensación)

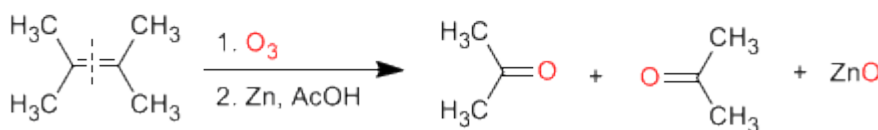
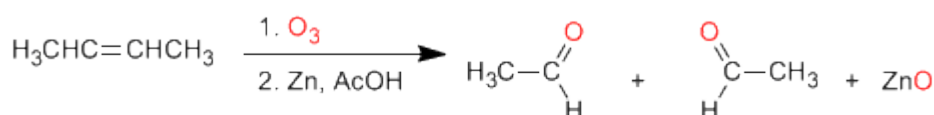
La condensación aldólica es una reacción de aldehídos o cetonas **[1]** que forma 3-hidroxicarbonilos (aldoles) **[2]**. El 3-hidroxialdehído **[2]** bajo condiciones de deshidratación por calentamiento rinde un aldehído alfa,beta-insaturado **[3]**.



Preparación de aldehídos y cetonas

Los aldehídos y cetonas pueden ser preparados por oxidación de alcoholes, ozonólisis de alquenos, hidratación de alquinos y acilación de Friedel-Crafts como métodos de mayor importancia.

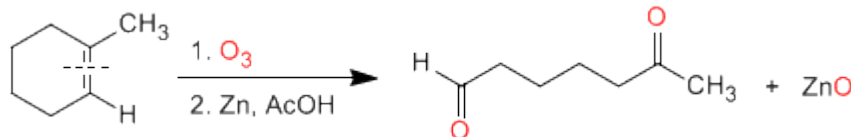
a) **Ozonólisis de alquenos:** Los alquenos rompen con ozono formando aldehídos y/o cetonas. Si el alqueno tiene hidrógenos vinílicos da aldehídos. Si tiene dos cadenas carbonadas forma cetonas.



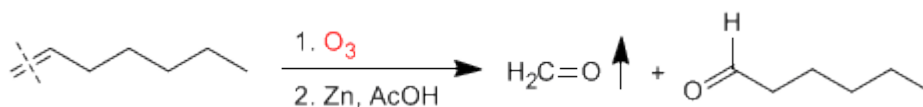
Ozonólisis

Los alquenos simétricos y terminales permiten la preparación de carbonilos mediante ozonólisis

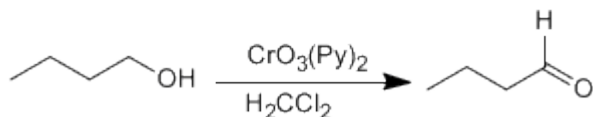
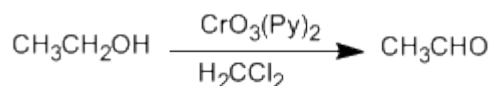
La ozonólisis de alquenos cíclicos produce compuestos dicarbonílicos:



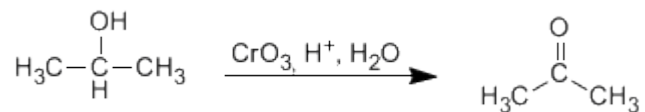
Los alquenos terminales rompen formando metanal, que separa fácilmente de la mezcla por su bajo punto de ebullición.



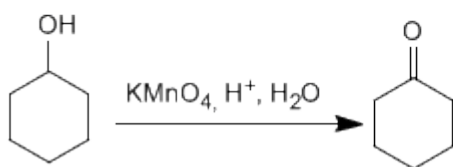
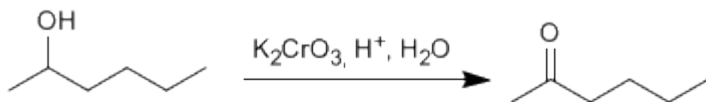
b) **Oxidación de alcoholes:** Los alcoholes primarios y secundarios se oxidan para dar aldehídos y cetonas respectivamente. Deben tomarse precauciones en la oxidación de alcoholes primarios, puesto que sobreoxidan a ácidos carboxílicos en presencia de oxidantes que contengan agua. En estos caso debe trabajarse con reactivos anhidros, como el clorocromato de piridino en diclorometano (PCC), a temperatura ambiente.



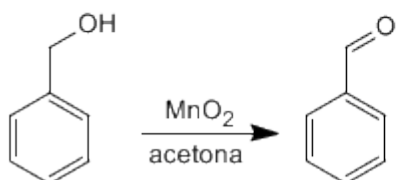
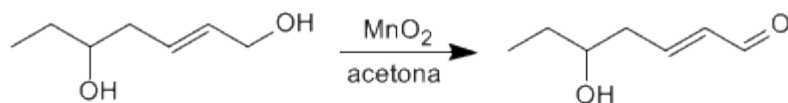
Los alcoholes secundarios dan cetonas por oxidación. Se emplean como oxidantes permanganato, dicromato, trióxido de cromo.



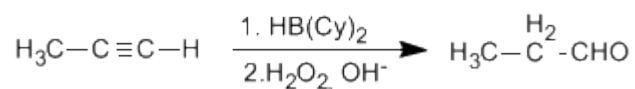
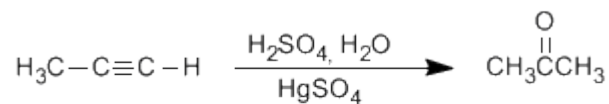
La oxidación supone la pérdida de dos hidrógenos del alcohol. Los alcoholes terciarios no pueden oxidar puesto que carecen de hidrógeno sobre el carbono.



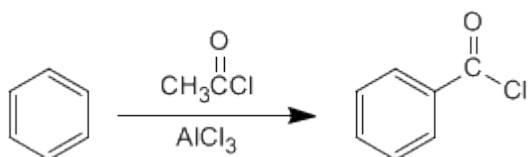
Los alcoholes alílicos y bencílicos se transforman en aldehídos o cetonas por oxidación con dióxido de manganeso en acetona. Esta reacción tiene una elevada selectividad y no oxida alcoholes que no se encuentren en dichas posiciones.



c) **Hidratación de alquinos:** Los alquinos se pueden hidratar Markovnikov, formando cetonas, o bien antiMarkovnikov, para formar aldehídos.



d) **Acilación de Friedel-Crafts:** La introducción de grupos acilo en el benceno permite la preparación de cetonas con cadenas aromáticas.



Otto Paul Hermann Diels (1876 - 1954)



Origen: Químico alemán.

Lugar de nacimiento: Königshütte (hoy Chorzów, Polonia).

Formación: estudió química en la Universidad de Berlín entre 1895 y 1899, consiguiendo el doctorado este año.

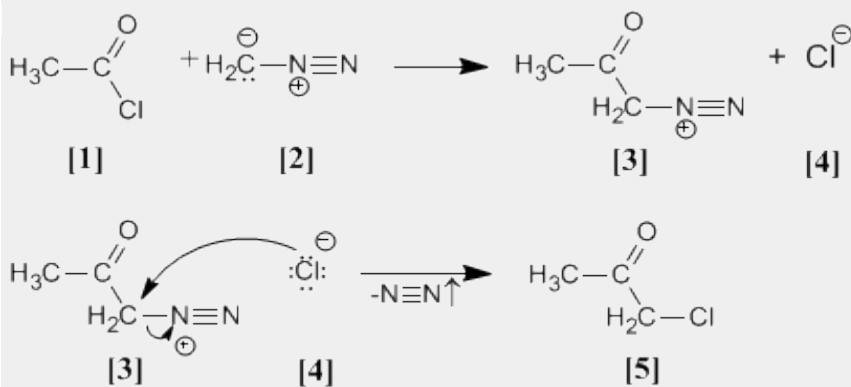
Docencia: profesor y jefe del departamento de química en la Universidad de Berlín. En 1916, tomó el puesto de profesor de Química en la Universidad de Kiel, cargo que no dejó hasta su jubilación en 1945.

Investigación: En 1906 descubrió el anhídrido malónico. Investigó en reacciones de deshidrogenación con selenio. Síntesis de α -dicetonas. Pero su trabajo más importante es la reacción de Diels - Alder.

Premio Nobel: En 1950 recibió el Premio Nobel junto a Kurt Alder

Arndt Eistert (Síntesis)

Cloruro de acetilo [1] se trata con diazometano [2] rindiendo la sal de diazonio [3]. El cloruro [4] producido reacciona con la sal de diazonio para dar la α -clorocetona [5].

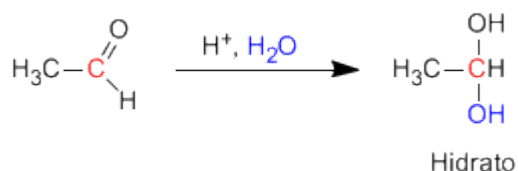


Síntesis de Arndt Eistert

Esta reacción permite transformar haluros de alcanoilo en cetonas halogenadas en su posición alfa.

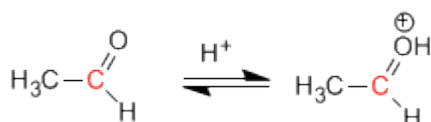
Formación de Hidratos

Los aldehídos y cetonas reaccionan en medio ácido acuoso para formar hidratos. El mecanismo consta de tres etapas. La primera y más rápida consiste en la protonación del oxígeno carbonílico. Esta protonación produce un aumento de la polaridad sobre el carbono y favorece el ataque del nucleófilo. En la segunda etapa el agua ataca al carbono carbonilo, es la etapa lenta del mecanismo. En la tercera etapa se produce la desprotonación del oxígeno formándose el hidrato final.

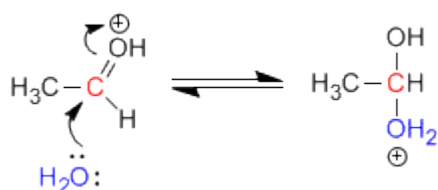


Mecanismo de la reacción

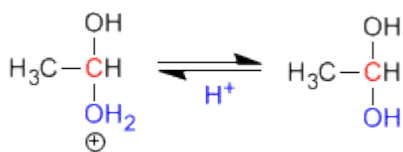
Etapa 1. Protonación del oxígeno carbonílico.



Etapa 2. Ataque nucleófilo del agua al carbonilo protonado.



Etapa 3. Desprotonación del hidrato





Origen: Químico estadounidense.

Lugar de nacimiento: Budapest

Formación: Se doctoró en la Universidad de Budapest en 1949

Docencia: Trabajó en el departamento de química orgánica de la Academia de Ciencias de Hungría y posteriormente en la Universidad de Cleveland.

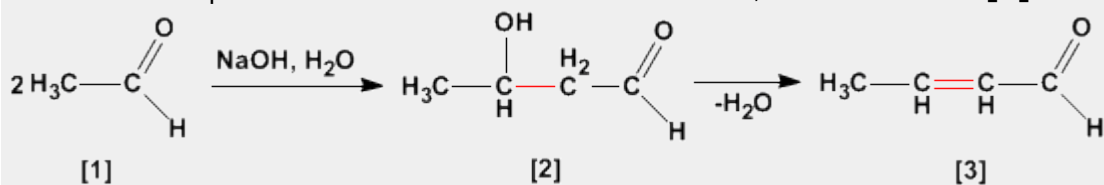
Industria: Trabajó en los laboratorios de la Dow Chemical de Ontario

Investigación: Olah consiguió preparar carbocationes estables utilizando componentes extremadamente ácidos.

Premio Nobel: En 1994 obtuvo el premio Nobel de Química por sus investigaciones sobre los carbocationes

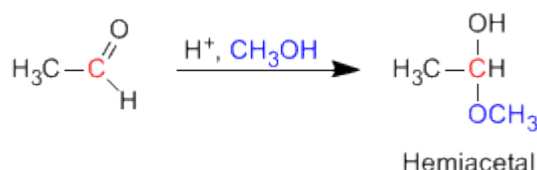
Aldólica (Condensación)

La condensación aldólica es una reacción de aldehídos o cetonas **[1]** que forma 3-hidroxicarbonilos (aldoles) **[2]**. El 3-hidroxialdehído **[2]** bajo condiciones de deshidratación por calentamiento rinde un aldehído alfa,beta-insaturado **[3]**.



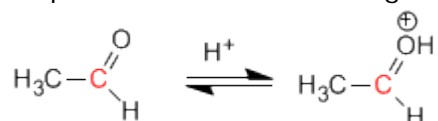
Formación de Hemiacetales

Los hemiacetales se forman por reacción de un equivalente de alcohol con el grupo carbonilo de un aldehído o cetona. Esta reacción se cataliza con ácido y es equivalente a la formación de hidratos.

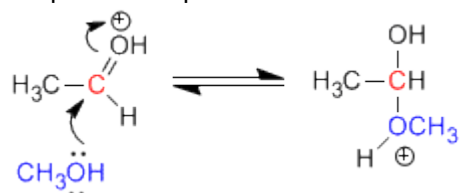


Mecanismo de la reacción:

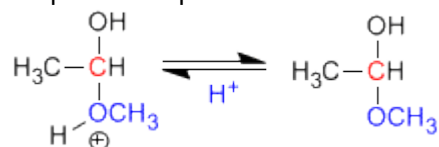
Etapas 1. Protonación del oxígeno carbonílico.



Etapas 2. Ataque nucleófilo del metanol al carbonilo protonado.



Etapas 3. Desprotonación del hemiacetal



Otto Paul Hermann Diels (1876 - 1954)



Origen: Químico alemán.

Lugar de nacimiento: Königshütte (hoy Chorzów, Polonia).

Formación: estudió química en la Universidad de Berlín entre 1895 y 1899, consiguiendo el doctorado este año.

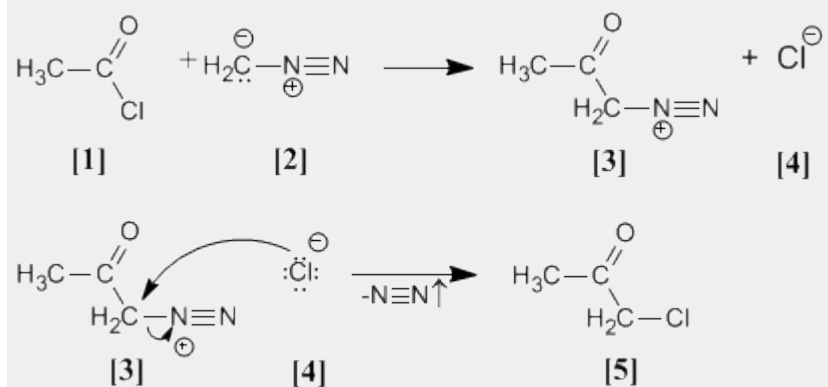
Docencia: profesor y jefe del departamento de química en la Universidad de Berlín. En 1916, tomó el puesto de profesor de Química en la Universidad de Kiel, cargo que no dejó hasta su jubilación en 1945.

Investigación: En 1906 descubrió el anhídrido malónico. Investigó en reacciones de deshidrogenación con selenio. Síntesis de α -dicetonas. Pero su trabajo más importante es la reacción de Diels - Alder.

Premio Nobel: En 1950 recibió el Premio Nobel junto a Kurt Alder

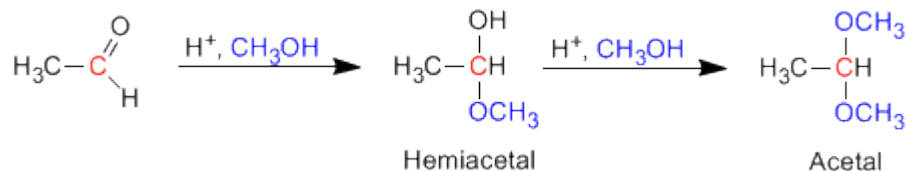
Arndt Eistert (Síntesis)

Cloruro de acetilo **[1]** se trata con diazometano **[2]** rindiendo la sal de diazonio **[3]**. El cloruro **[4]** producido reacciona con la sal de diazonio para dar la α -clorocetona **[5]**.



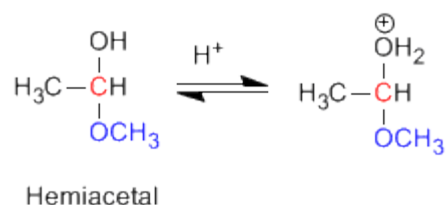
Formación de Acetales

Los aldehídos y cetonas reaccionan con alcoholes bajo condiciones de catálisis ácida, formando en una primera etapa hemiacetales, que posteriormene evolucionan por reacción con un segundo equivalente de alcohol a acetales.

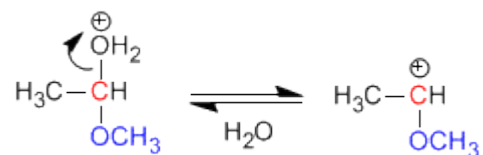


Mecanismo para la formación de acetales

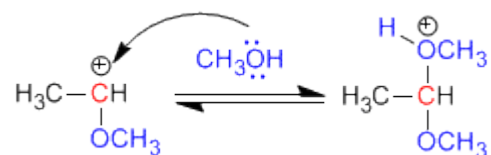
Etapa 1. Protonación del grupo hidroxilo



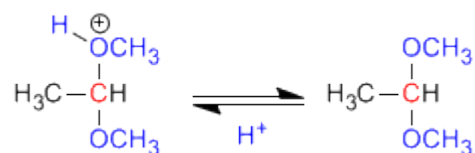
Etapa 2. Pérdida de agua.



Etapa 3. Ataque del alcohol al carbocatión



Etapa 4. Desprotonación del acetal



Otto Paul Hermann Diels (1876 - 1954)



Origen: Químico alemán.

Lugar de nacimiento: Königshütte (hoy Chorzów, Polonia).

Formación: estudió química en la Universidad de Berlín entre 1895 y 1899, consiguiendo el doctorado este año.

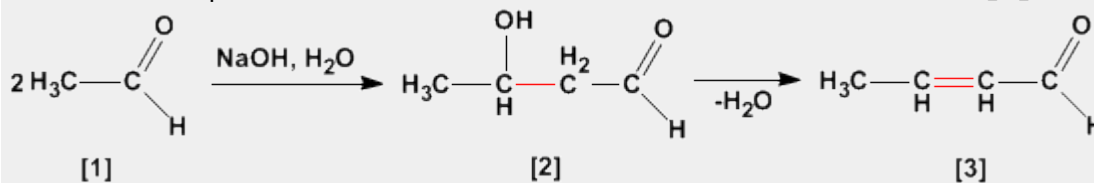
Docencia: profesor y jefe del departamento de química en la Universidad de Berlín. En 1916, tomó el puesto de profesor de Química en la Universidad de Kiel, cargo que no dejó hasta su jubilación en 1945.

Investigación: En 1906 descubrió el anhídrido malónico. Investigó en reacciones de deshidrogenación con selenio. Síntesis de α -dicetonas. Pero su trabajo más importante es la reacción de Diels - Alder.

Premio Nobel: En 1950 recibió el Premio Nobel junto a Kurt Alder

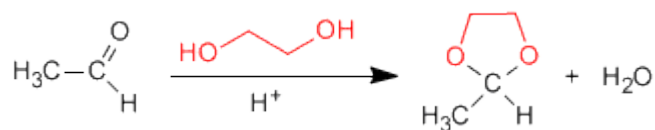
Aldólica (Condensación)

La condensación aldólica es una reacción de aldehídos o cetonas **[1]** que forma 3-hidroxicarbonilos (aldoles) **[2]**. El 3-hidroxialdehído **[2]** bajo condiciones de deshidratación por calentamiento rinde un aldehído alfa,beta-insaturado **[3]**.



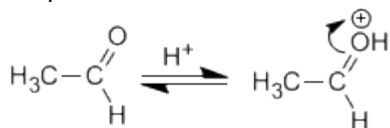
Formación de acetales cíclicos

Los 1,2- y 1,3-dioles reaccionan con aldehídos y cetonas formando acetales cíclicos. Los equilibrios se desplazan hacia el producto final eliminando el agua formada por destilación azeotrópica con benceno o tolueno.

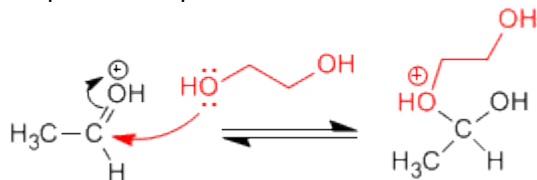


Mecanismo para la formación de acetales cíclicos:

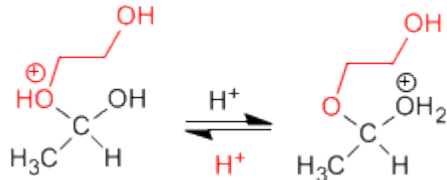
Etapa 1. Protonación del carbonilo



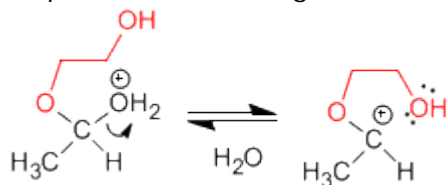
Etapa 2. Ataque nucleófilo del diol al carbonilo.



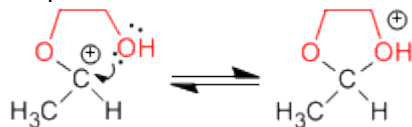
Etapa 3. Equilibrio ácido base entre el éter y el alcohol



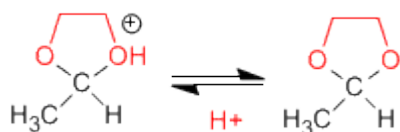
Etapa 4. Pérdida de agua



Etapa 5. Ciclación



Etapa 6. Desprotonación del acetal cíclico



Kurt Alder (1902 - 1958)



Origen: Químico alemán.

Lugar de nacimiento: Königshütte (hoy Chorzów, Polonia).

Formación: estudió en la Universidad de Kiel. Bajo la supervisión del químico alemán Otto Diels, su jefe e instructor en Kiel.

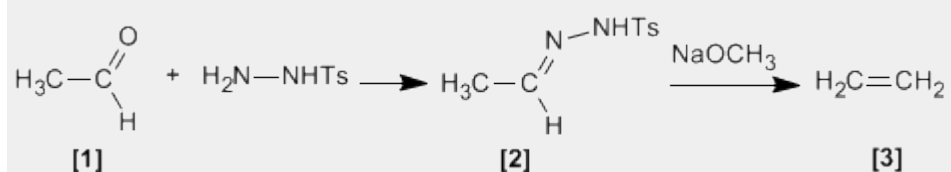
Docencia: Alder ejerció como profesor de química en las universidades de Kiel y Colonia.

Investigación: Alder se especializó en la síntesis diénica (conocida más tarde como la reacción Diels - Alder) que consiste fundamentalmente en el análisis y formación de compuestos orgánicos complejos. Ya en 1928 ambos fueron coautores de un ensayo sobre este proceso.

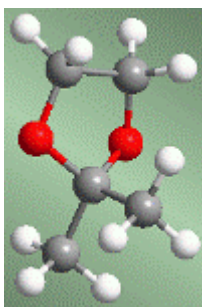
Premio Nobel: En 1950 recibió el Premio Nobel junto a Diels

Bamford Stevens (Reacción)

Tosilhidrazonas [2] de aldehídos o cetonas alifáticos [1] reaccionan con bases fuertes para dar alquenos [3].

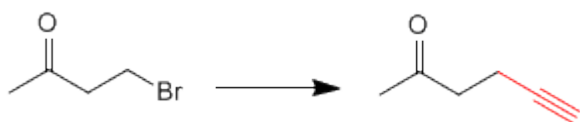


Acetales como grupos protectores

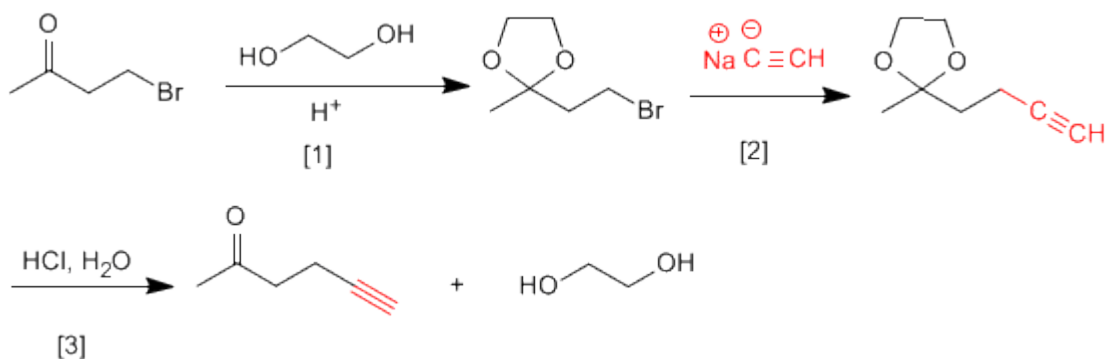


Los acetales pueden emplearse, por su estabilidad, como grupos protectores del carbonilo. El acetal es un éter, muy estable en medios básicos, aunque rompe en presencia de medios ácidos. En muchos procesos de síntesis el grupo carbonilo es incompatible con el reactivo utilizado. En estos casos debe protegerse para evitar que reaccione. La inestabilidad del acetal en medio ácido puede emplearse para desproteger el carbonilo.

Veamos algunos ejemplos:



Esta transformación requiere una sustitución, empleando como nucleófilo un acetiluro de sodio. El nucleófilo puede atacar también al grupo carbonilo, para evitarlo vamos a protegerlo.

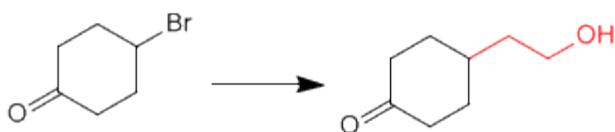


[1] Protección de la cetona.

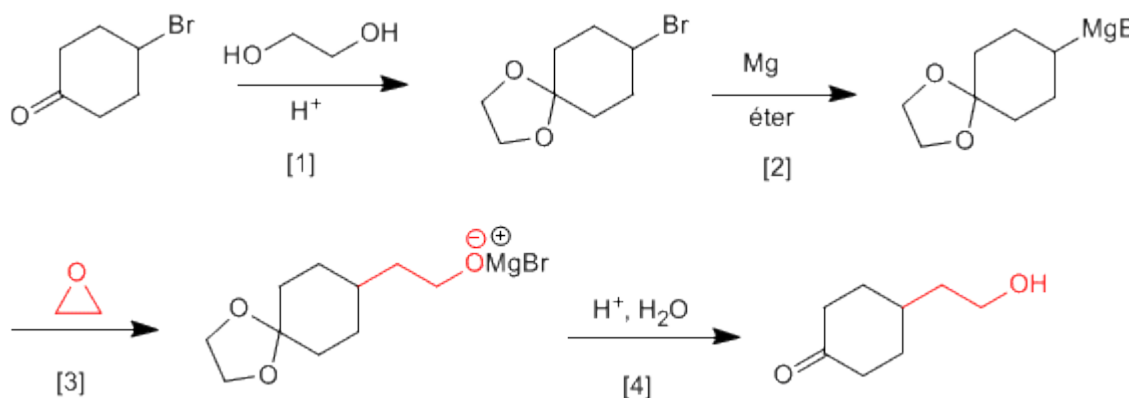
[2] Ataque del acetiluro al carbono del bromo.

[3] Desprotección del carbonilo

Veamos un segundo ejemplo:



Es necesario proteger la cetona antes de formar el organometálico para evitar la dimerización del compuesto.



- [1] Protección de la cetona.
 [2] Formación del magnesiano.
 [3] Apertura del oxaciclopropano.
 [4] Desprotección y protonación del alcóxido.

Otto Paul Hermann Diels (1876 - 1954)



Origen: Químico alemán.

Lugar de nacimiento: Königshütte (hoy Chorzów, Polonia).

Formación: estudió química en la Universidad de Berlín entre 1895 y 1899, consiguiendo el doctorado este año.

Docencia: profesor y jefe del departamento de química en la Universidad de Berlín. En 1916, tomó el puesto de profesor de Química en la Universidad de Kiel, cargo que no dejó hasta su jubilación en 1945.

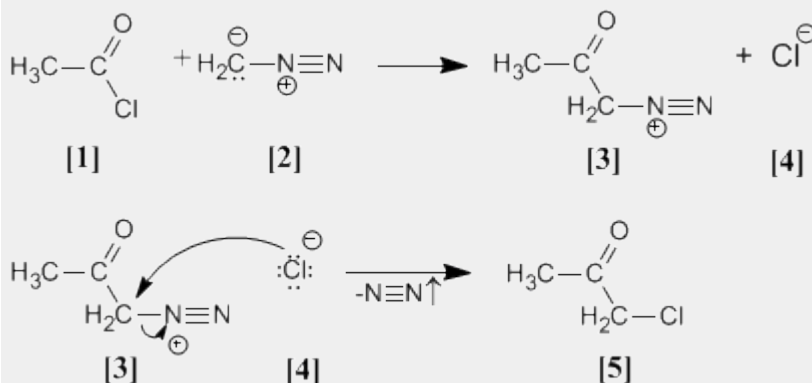
Investigación: En 1906 descubrió el anhídrido malónico.

Investigó en reacciones de deshidrogenación con selenio. Síntesis de α-dicetonas. Pero su trabajo más importante es la reacción de Diels - Alder.

Premio Nobel: En 1950 recibió el Premio Nobel junto a Kurt Alder

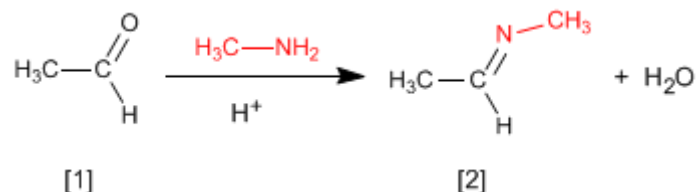
Arndt Eistert (Síntesis)

Cloruro de acetilo **[1]** se trata con diazometano **[2]** rindiendo la sal de diazonio **[3]**. El cloruro **[4]** producido reacciona con la sal de diazonio para dar la α-clorocetona **[5]**.



Formación de Iminas

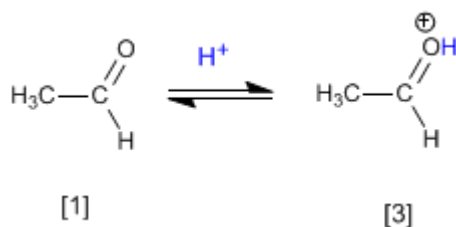
La reacción de aldehídos o cetonas **[1]** con aminas primarias genera iminas **[2]**. La reacción se favorece en un medio ligeramente ácido (pH=4.5).



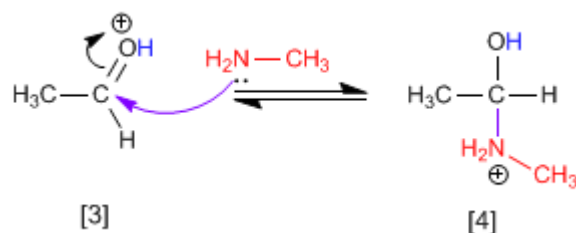
El control del pH es fundamental, puesto que se requiere la protonación del oxígeno del carbonilo para favorecer el ataque nucleófilo.

Mecanismo:

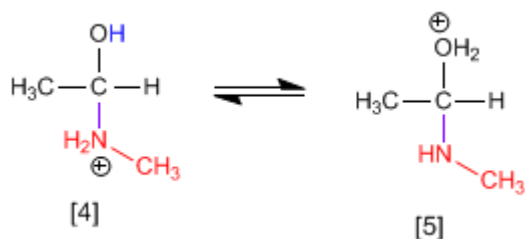
Etapas 1. Protonación del grupo carbonilo que aumenta la polaridad positiva sobre el carbono y favorece el ataque nucleófilo.



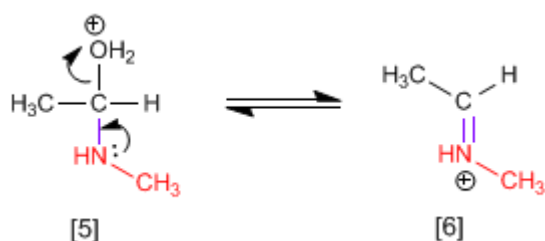
Etapas 2. Ataque nucleófilo de la amina primaria al carbono carbonilo.



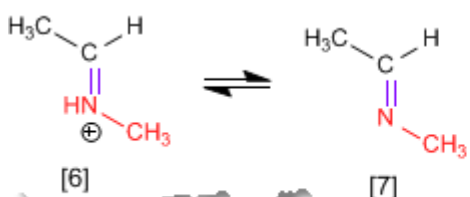
Etapas 3. Protonación del grupo hidroxilo para transformarlo en buen grupo saliente.



Etapas 4. Pérdida de agua y formación de la imina protonada.



Etapa 5. Desprotonación del catión.



George A. Olah (1927 -)



Origen: Químico estadounidense.

Lugar de nacimiento: Budapest

Formación: Se doctoró en la Universidad de Budapest en 1949

Docencia: Trabajó en el departamento de química orgánica de la Academia de Ciencias de Hungría y posteriormente en la Universidad de Cleveland.

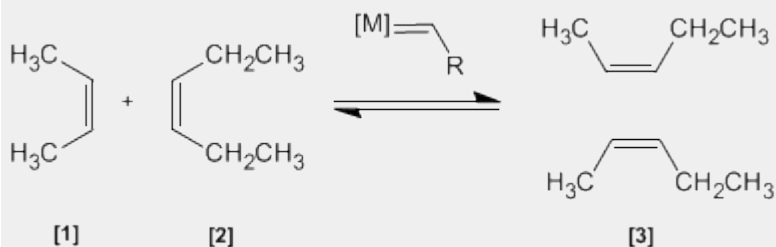
Industria: Trabajó en los laboratorios de la Dow Chemical de Ontario

Investigación: Olah consiguió preparar carbocationes estables utilizando componentes extremadamente ácidos.

Premio Nobel: En 1994 obtuvo el premio Nobel de Química por sus investigaciones sobre los carbocationes

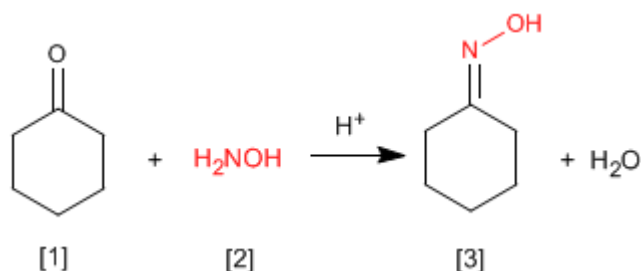
Metátesis de Alquenos

En esta reacción dos alquenos **[1]** y **[2]** son tratados con un metal de transición que actúa como catalizador, dando una mezcla de alquenos **[3]** (incluyendo isómeros Z/E). Este productos se obtiene por intercambio de grupos alquilideno.

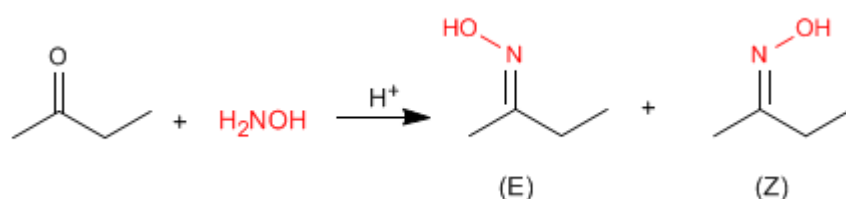


Formación de Oximas

Las oximas [3] se obtienen por reacción de aldehídos o cetonas [1] e hidroxilamina [2] en un medio débilmente ácido. El mecanismo es análogo al de formación de iminas.



Las oximas de aldehídos y cetona asimétricas presentan isomería Z/E dependiendo de la posición del hidroxilo.



Las iminas e hidrazonas (que comentaremos a continuación) también presentan esta característica.

George A. Olah (1927 -)



Origen: Químico estadounidense.

Lugar de nacimiento: Budapest

Formación: Se doctoró en la Universidad de Budapest en 1949

Docencia: Trabajó en el departamento de química orgánica de la Academia de Ciencias de Hungría y posteriormente en la Universidad de Cleveland.

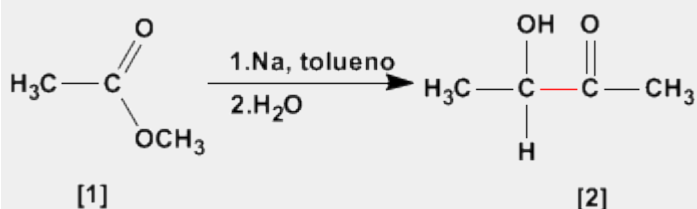
Industria: Trabajó en los laboratorios de la Dow Chemical de Ontario

Investigación: Olah consiguió preparar carbocationes estables utilizando componentes extremadamente ácidos.

Premio Nobel: En 1994 obtuvo el premio Nobel de Química por sus investigaciones sobre los carbocationes

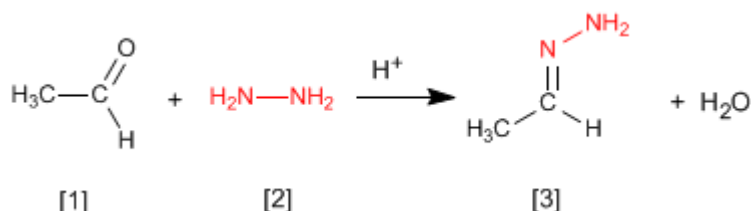
Aciloinica (Condensación)

La condensación aciloinica transforma ésteres [1] en alfa-hidroxicetonas [2]. Esta reacción se realiza con sodio metal en disolvente inerte.

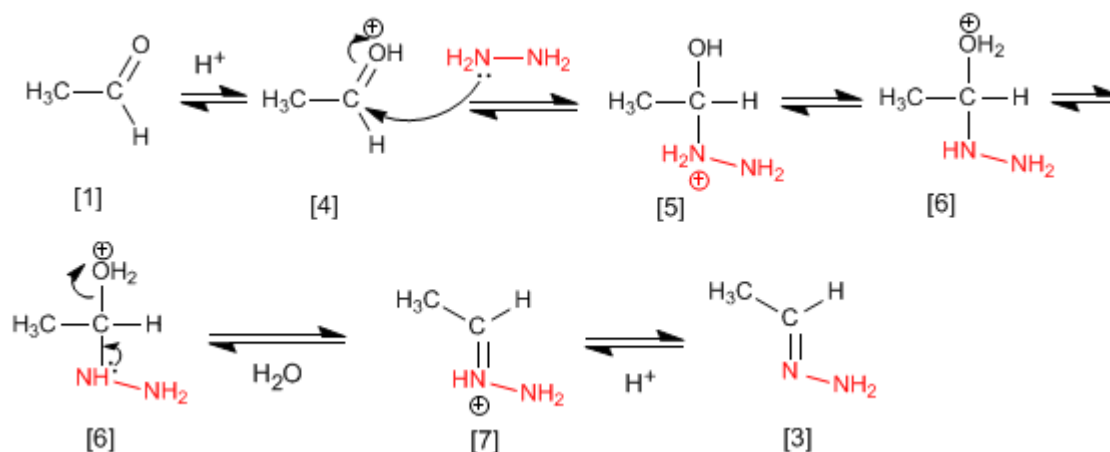


Formación de Hidrazonas

Las hidrazonas **[3]** se obtienen por reacción de aldehídos o cetonas **[1]** con hidrazina **[2]**. Igual que en el caso de las iminas y oximas requiere pH=4.



Aunque el mecanismo es análogo al de formación de iminas, comentaremos de nuevo los pasos.



El etanal **[1]** se protona formando su ácido conjugado **[4]**. La importante polaridad del carbono carbonilo de **[4]** favorece el ataque de la hidrazina **[2]** para formando el intermedio **[5]**. El compuesto **[5]** intercambia un protón entre el nitrógeno y el oxígeno, transformando el grupo hidroxilo en agua (buen grupo saliente). El intermedio **[6]** pierde una molécula de agua transformándose en **[7]**, cuya desprotonación da la hidrazona final **[3]**.

Kurt Alder (1902 - 1958)



Origen: Químico alemán.

Lugar de nacimiento: Königshütte (hoy Chorzów, Polonia).

Formación: estudió en la Universidad de Kiel. Bajo la supervisión del químico alemán Otto Diels, su jefe e instructor en Kiel.

Docencia: Alder ejerció como profesor de química en las universidades de Kiel y Colonia.

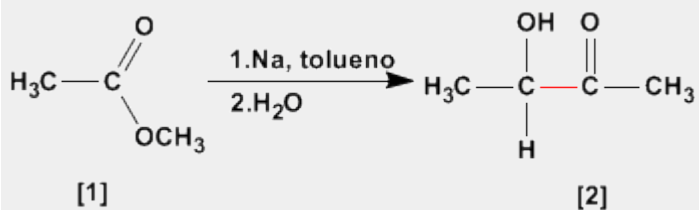
Investigación: Alder se especializó en la síntesis diénica (conocida más tarde como la reacción Diels - Alder) que consiste fundamentalmente en el análisis y formación de compuestos orgánicos complejos.

Ya en 1928 ambos fueron coautores de un ensayo sobre este proceso.

Premio Nobel: En 1950 recibió el Premio Nobel junto a Diels

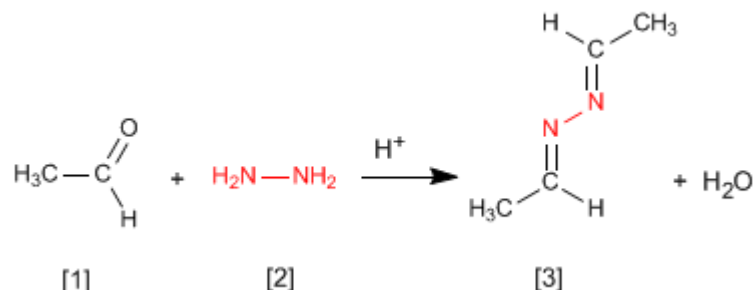
Aciloínica (Condensación)

La condensación aciloínica transforma esteres [1] en alfa-hidroxicetonas [2]. Esta reacción se realiza con sodio metal en disolvente inerte.



Formación de Azinas

La hidrazina [2] reacciona con dos moléculas de aldehído [1] para formar azinas [3].



El mecanismo es análogo al de formación de iminas, oximas e hidrazonas.

George A. Olah (1927 -)



Origen: Químico estadounidense.

Lugar de nacimiento: Budapest

Formación: Se doctoró en la Universidad de Budapest en 1949

Docencia: Trabajó en el departamento de química orgánica de la Academia de Ciencias de Hungría y posteriormente en la

Universidad de Cleveland.

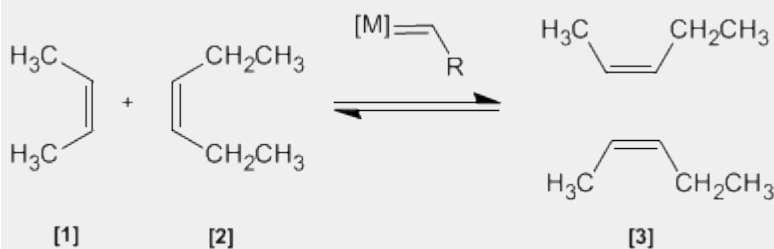
Industria: Trabajó en los laboratorios de la Dow Chemical de Ontario

Investigación: Olah consiguió preparar carbocationes estables utilizando componentes extremadamente ácidos.

Premio Nobel: En 1994 obtuvo el premio Nobel de Química por sus investigaciones sobre los carbocationes

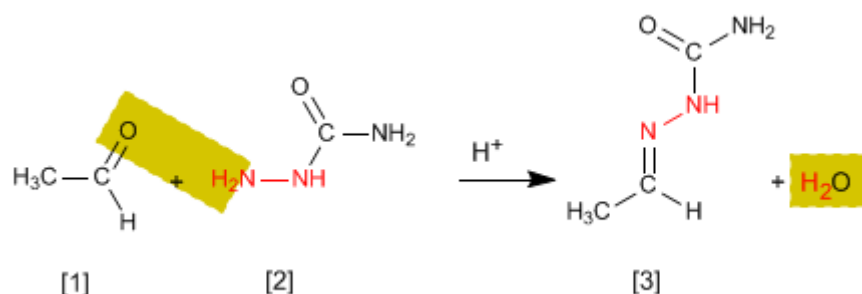
Metátesis de Alquenos

En esta reacción dos alquenos [1] y [2] son tratados con un metal de transición que actúa como catalizador, dando una mezcla de alquenos [3] (incluyendo isómeros Z/E). Este producto se obtiene por intercambio de grupos alquilideno.



Formación de Semicarbazonas

Las semicarbazonas [3] se obtienen por reacción de aldehídos o cetonas [1] con semicarbazida [2]. Veamos un ejemplo:



El mecanismo es análogo al de formación de iminas, oximas e hidrazonas.

Charles Friedel (1832 - 1899)



Origen: Químico frances..

Lugar de nacimiento: Estrasburgo.

Formación: estudió química en la Universidad de Berlín entre 1895 y 1899, consiguiendo el doctorado este año.

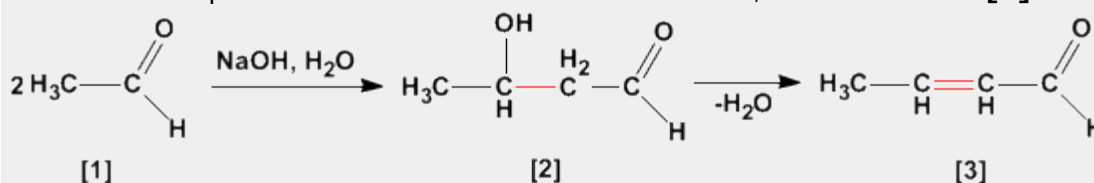
Docencia: Profesor en la Universidad de la Sorbona.

Investigación: Obtuvo el alcohol propílico. En 1877, Friedel y Crafts describieron por primera vez la reacción del benceno con un haloalcano en presencia de un ácido de Lewis. Esta reacción produce la alquilación del benceno y se conoce como alquilación de Friedl-Crafts.

Premio Nobel:

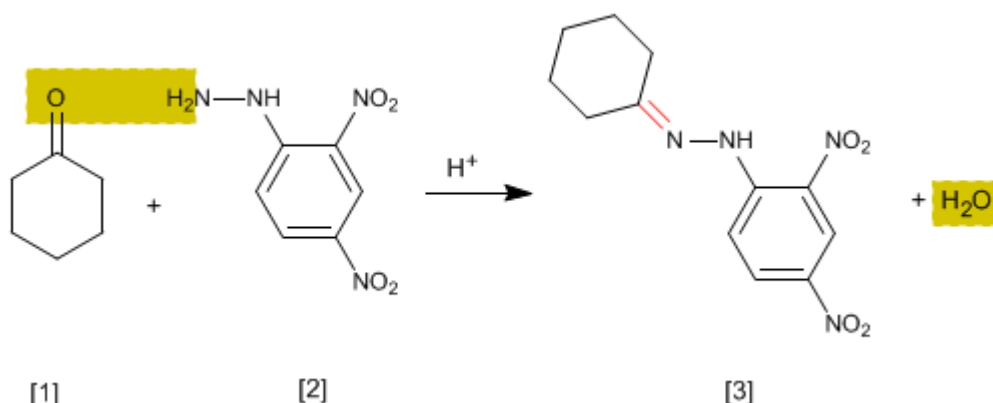
Aldólica (Condensación)

La condensación aldólica es una reacción de aldehídos o cetonas [1] que forma 3-hidroxicarbonilos (aldoles) [2]. El 3-hidroxialdehído [2] bajo condiciones de deshidratación por calentamiento rinde un aldehído alfa,beta-insaturado [3].



Ensayo de la 2,4-Dinitrofenilhidrazina

Se trata de un ensayo analítico específico de aldehídos y cetonas. Los carbonilos **[1]** reaccionan con 2,4-Dinitrofenilhidrazina **[2]** formando fenilhidrazonas **[3]** que precipitan de color amarillo. La aparición de precipitado es un indicador de la presencia de carbonilos en el medio.



El mecanismo de la reacción es análogo al de formación de iminas.

Kurt Alder (1902 - 1958)



Origen: Químico alemán.

Lugar de nacimiento: Königshütte (hoy Chorzów, Polonia).

Formación: estudió en la Universidad de Kiel. Bajo la supervisión del químico alemán Otto Diels, su jefe e instructor en Kiel.

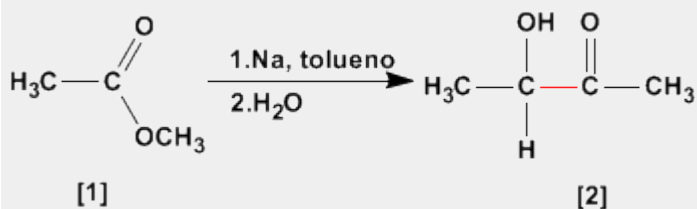
Docencia: Alder ejerció como profesor de química en las universidades de Kiel y Colonia.

Investigación: Alder se especializó en la síntesis diénica (conocida más tarde como la reacción Diels - Alder) que consiste fundamentalmente en el análisis y formación de compuestos orgánicos complejos. Ya en 1928 ambos fueron coautores de un ensayo sobre este proceso.

Premio Nobel: En 1950 recibió el Premio Nobel junto a Diels

Aciloinica (Condensación)

La condensación aciloinica transforma esteres **[1]** en alfa-hidroxicetonas **[2]**. Esta reacción se realiza con sodio metal en disolvente inerte.



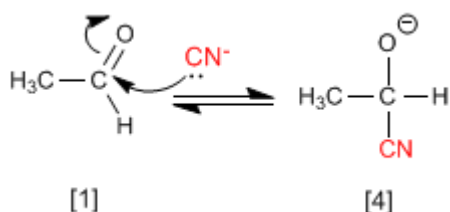
Formación de Cianhidrinas

Las cianhidrinas **[3]** se forman por reacción de aldehídos o cetonas **[1]** con ácido cianhídrico **[2]** y son compuestos que contienen un grupo ciano y un hidroxilo sobre el mismo carbono.

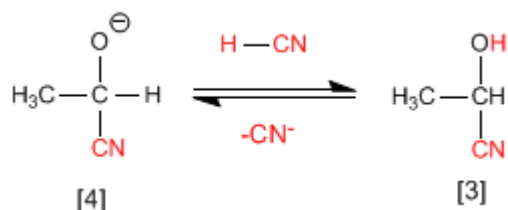


El mecanismo de la reacción transcurre en dos etapas:

Etapas 1. Los iones cianuro actúan como nucleófilos atacando al carbono carbonilo. El ácido cianhídrico es demasiado débil para generar cantidades importantes de cianuro, por ello, se añade cianuro de sodio o potasio al medio, garantizando la cantidad suficiente de cianuro para que la reacción transcurra en buen rendimiento.



Etapas 2. En este paso el ión alcóxido **[4]** se protona arrancando hidrógenos al ácido cianhídrico. En esta etapa se regeneran los iones cianuro.



Kurt Alder (1902 - 1958)



Origen: Químico alemán.

Lugar de nacimiento: Königshütte (hoy Chorzów, Polonia).

Formación: estudió en la Universidad de Kiel. Bajo la supervisión del químico alemán Otto Diels, su jefe e instructor en Kiel.

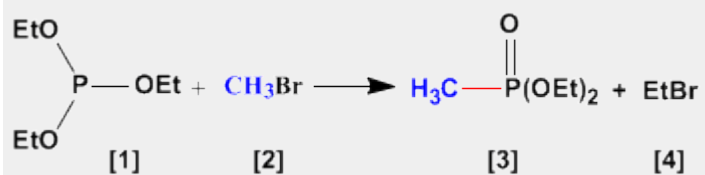
Docencia: Alder ejerció como profesor de química en las universidades de Kiel y Colonia.

Investigación: Alder se especializó en la síntesis diénica (conocida más tarde como la reacción Diels - Alder) que consiste fundamentalmente en el análisis y formación de compuestos orgánicos complejos. Ya en 1928 ambos fueron coautores de un ensayo sobre este proceso.

Premio Nobel: En 1950 recibió el Premio Nobel junto a Diels

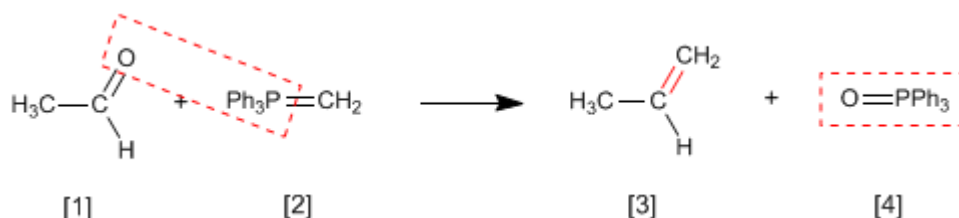
Arbuzov (Reacción)

La reacción de Arbuzov se emplea en la síntesis de fosfonatos **[3]** a partir de fosfitos **[1]**. Los fosfonatos obtenidos en la síntesis de Arbuzov se emplean como materiales de partida en la síntesis de Horner-Wittig.



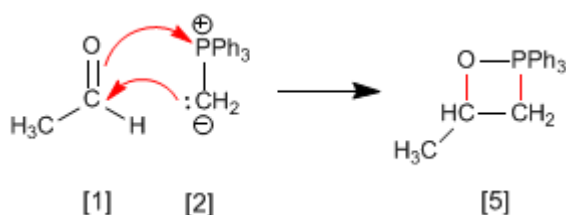
Reacción de Wittig

La reacción de Wittig emplea iluros de fósforo [2] para transformar aldehídos y cetonas [1] en alquenos [3]. Como subproducto se obtiene el óxido de trifenilfosfina [4].

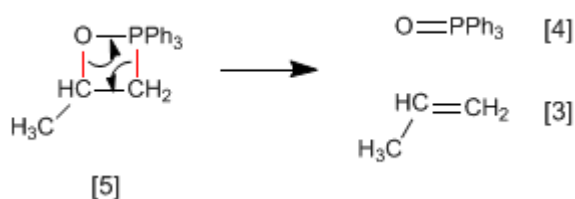


En el mecanismo de la reacción el iluro y el carbonilo se combinan para formar un oxafosfetano que rompe dejando libre el alqueno final.

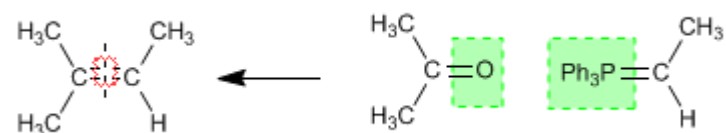
Etapas 1. El etanal y el iluro se combinan formando el fosfetano.



Etapas 2. El fosfetano rompe formando el alqueno y óxido de trifenilfosfina.

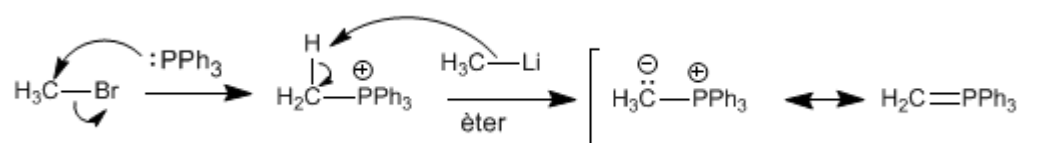


Ejemplo - Obtener mediante Wittig el 2-Metilbut-2-eno



Se rompe el alqueno por el doble enlace y a cada carbono se le agrega el grupo encerrado en verde.

Los **iluros de fósforo** se preparan mediante reacción de haloalcanos y trifenilfosfina, seguido de desprotonación del carbono con base fuerte (organometálicos de litio).



Charles Friedel (1832 - 1899)



Origen: Químico frances..

Lugar de nacimiento: Estrasburgo.

Formación: estudió química en la Universidad de Berlín entre 1895 y 1899, consiguiendo el doctorado este año.

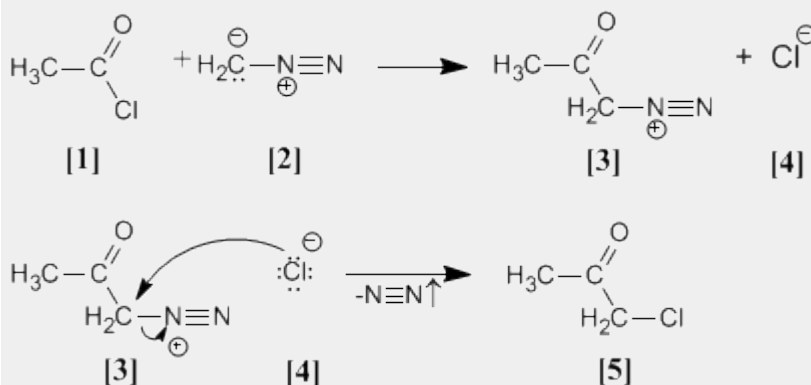
Docencia: Profesor en la Universidad de la Sorbona.

Investigación: Obtuvo el alcohol propílico. En 1877, Friedel y Crafts describieron por primera vez la reacción del benceno con un haloalcano en presencia de un ácido de Lewis. Esta reacción produce la alquilación del benceno y se conoce como alquilación de Friedl-Crafts.

Premio Nobel:

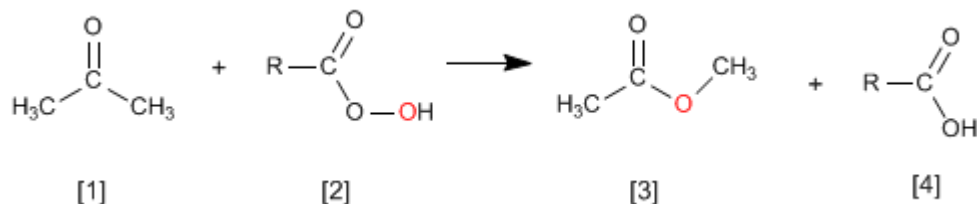
Arndt Eistert (Síntesis)

Cloruro de acetilo **[1]** se trata con diazometano **[2]** rindiendo la sal de diazonio **[3]**. El cloruro **[4]** producido reacciona con la sal de diazonio para dar la α -clorocetona **[5]**.

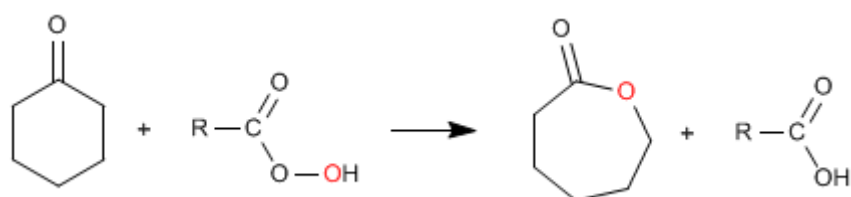


Oxidación de Baeyer Villiger

La reacción de cetonas **[1]** con perácidos **[2]** produce ésteres **[3]**. El oxígeno del perácido se inserta entre el carbono carbonilo y el carbono alfa de la cetona. Esta reacción fue descrita por Adolf von Baeyer y Victor Villiger in 1899.

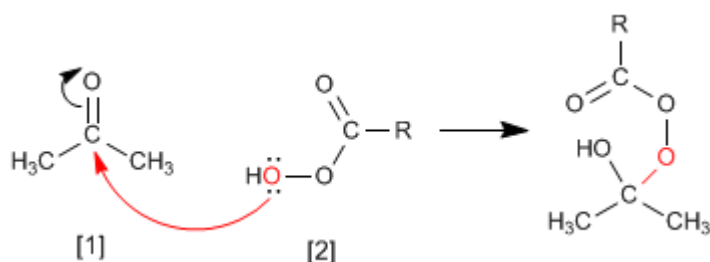


A partir de cetonas cíclicas se obtienen ésteres cíclicos (lactonas)

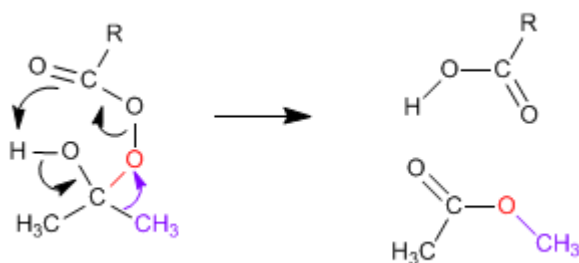


El mecanismo de Baeyer Villiger comienza con el ataque nucleófilo del perácido sobre el carbonilo, seguido de la migración del sustituyente desde el grupo carbonilo al oxígeno del perácido.

Etapas 1. Adición del perácido al carbonilo

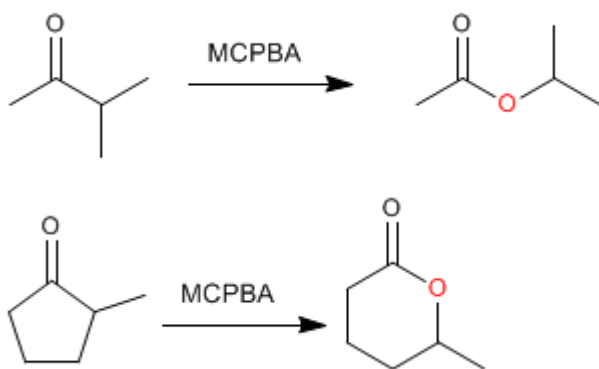


Etapas 2. Migración del sustituyente desde carbono carbonilo hacia el oxígeno (rojo)



Cuando la cetona tiene dos sustituyentes diferentes migra mejor el más sustituido. Existe un orden de migración que nos ayuda a decidir que sustituyente pasa a unirse al oxígeno del perácido.

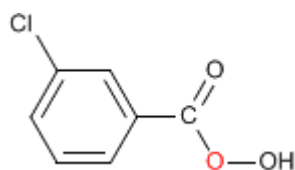
Orden de migración: H > carbono terciario > ciclohexilo > carbono secundario » fenilo > carbono primario > metilo



Como puede observarse en el orden de migración, el grupo que mejor migra, por su pequeño tamaño, es el hidrógeno, por ello, al tratar aldehídos con perácidos se produce la migración del hidrógeno formándose ácidos carboxílicos.



El **MCPBA** (Ácido meta-cloroperoxibenzoico) es un perácido ampliamente utilizado en la epoxidación de alquenos y también en Baeyer-Villiger. La fórmula del MCPBA se muestra a continuación.



Charles Friedel (1832 - 1899)



Origen: Químico frances..

Lugar de nacimiento: Estrasburgo.

Formación: estudió química en la Universidad de Berlín entre 1895 y 1899, consiguiendo el doctorado este año.

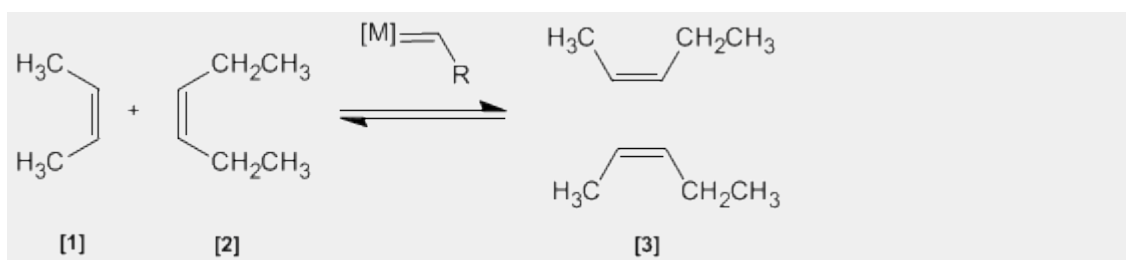
Docencia: Profesor en la Universidad de la Sorbona.

Investigación: Obtuvo el alcohol propílico. En 1877, Friedel y Crafts describieron por primera vez la reacción del benceno con un haloalcano en presencia de un ácido de Lewis. Esta reacción produce la alquilación del benceno y se conoce como alquilación de Friedl-Crafts.

Premio Nobel:

Metátesis de Alquenos

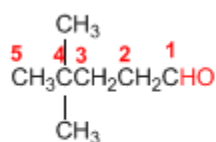
En esta reacción dos alquenos **[1]** y **[2]** son tratados con un metal de transición que actúa como catalizador, dando una mezcla de alquenos **[3]** (incluyendo isómeros Z/E). Este productos se obtiene por intercambio de grupos alquilideno.



Nomenclatura de Aldehídos y Cetonas - Reglas IUPAC

Regla 1. Los aldehídos se nombran reemplazando la terminación **-ano** del alcano correspondiente por **-al**. No es necesario especificar la posición del grupo aldehído, puesto que ocupa el extremo de la cadena (localizador 1).

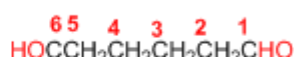
Cuando la cadena contiene dos funciones aldehído se emplea el sufijo **-dial**.



4,4-Dimetilpentanal

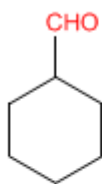


Hex-4-enal

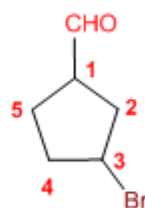


Hexanodial

Regla 2. El grupo **-CHO** se denomina **-carbaldehído**. Este tipo de nomenclatura es muy útil cuando el grupo aldehído va unido a un ciclo. La numeración del ciclo se realiza dando localizador 1 al carbono del ciclo que contiene el grupo aldehído.

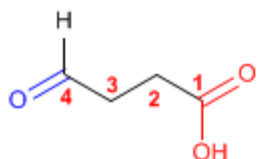


Ciclohexanocarbaldehído

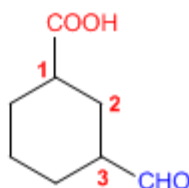


3-Bromociclopentanocarbaldehído

Regla 3. Cuando en la molécula existe un grupo prioritario al aldehído, este pasa a ser un sustituyente que se nombra como oxo- o formil-.



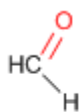
Ácido 4-oxobutanoico



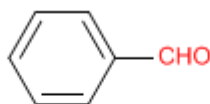
Ácido 3-formilciclohexanocarboxílico

Tanto **-carbaldehído** como **formil-** son nomenclaturas que incluyen el carbono del grupo carbonilo. **-carbaldehído** se emplea cuando el aldehído es grupo funcional, mientras que **formil-** se usa cuando actúa de sustituyente.

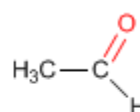
Regla 4. Algunos nombres comunes de aldehídos aceptados por la IUPAC son:



Formaldehído
(Metanal)

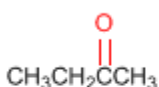


Benzaldehído
(Benceno**carbaldehído**)

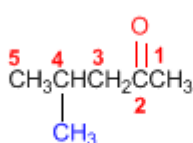


Acetaldehído
(Etanal)

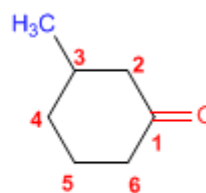
Regla 5. Las cetonas se nombran sustituyendo la terminación **-ano** del alcano con igual longitud de cadena por **-ona**. Se toma como cadena principal la de mayor longitud que contiene el grupo carbonilo y se numera para que éste tome el localizador más bajo.



Butan**ona**

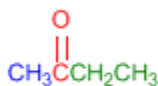


4-Metil-2-pentan**ona**

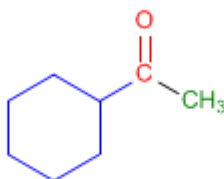


3-Metilciclohexan**ona**

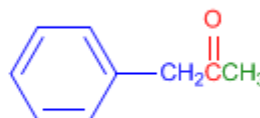
Regla 6. Existe un segundo tipo de nomenclatura para las cetonas, que consiste en nombrar las cadenas como sustituyentes, ordenándolas alfabéticamente y terminando el nombre con la palabra cetona.



Etil metil **cetona**

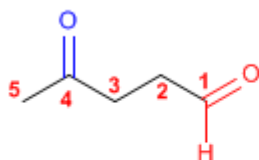


Ciclohexil metil **cetona**

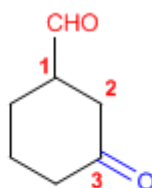


Fenil metil **cetona**

Regla 7. Cuando la cetona no es el grupo funcional de la molécula pasa a llamarse **OXO-**.



4-Oxopentan**al**

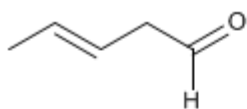


3-Oxociclohexano**carbaldehído**

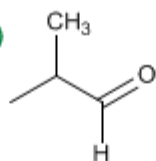
Nomenclatura de Aldehídos y Cetonas - Problema 9.1

Nombra los siguientes aldehídos y cetonas:

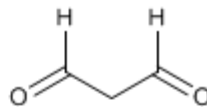
a)



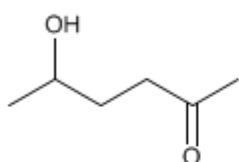
b)



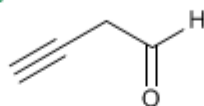
c)



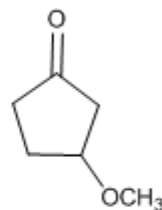
d)



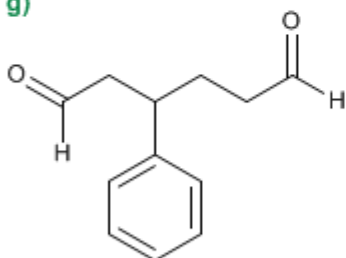
e)



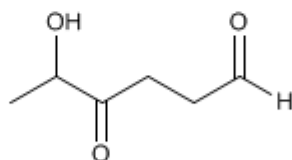
f)



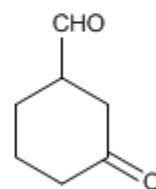
g)



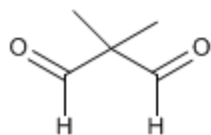
h)



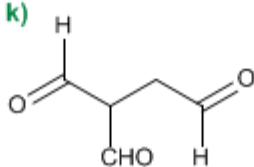
i)



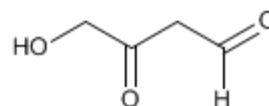
j)



k)

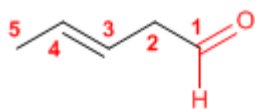


l)

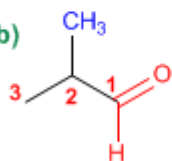


Solución

a)



b)



1. Cadena principal: 5 carbonos (pentano)

2. Numeración: comienza en el aldehído (grupo funcional)

Grupo funcional: aldehído

3. Nombre: Pent-3-enal

1. Cadena principal: 3 carbonos (propano)

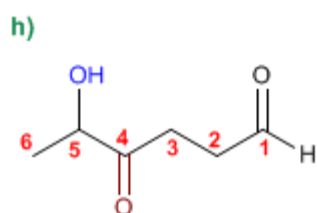
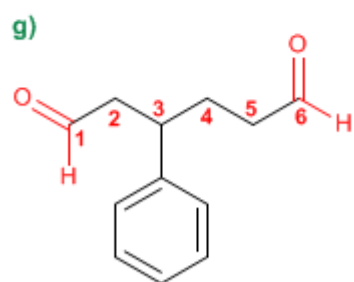
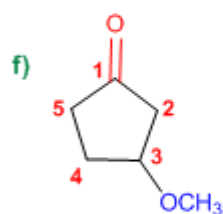
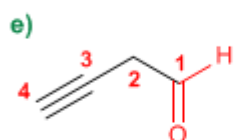
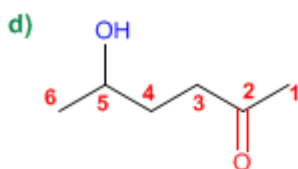
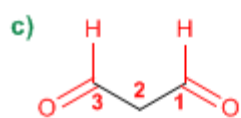
2. Numeración: localizador más bajo al aldehído.

3. Grupo funcional: aldehído

4. Sustituyentes: metilo en 2.

5. Nombre: 2-Metilpropanal

Los aldehídos y cetonas son prioritarios sobre alquenos y alquinos, y se numeran otorgándoles el localizador más bajo



1. Cadena principal: 3 carbonos (propano)
2. Grupo funcional: aldehído (dialdehído)
3. Nombre: Propanodial

1. Cadena principal: 6 carbonos (hexano)
2. Grupo funcional: cetona
3. Numeración: asignar el menor localizador a la cetona
4. Sustituyentes: hidroxí en 5.
5. Nombre: 5-Hidroxihexan-2-ona

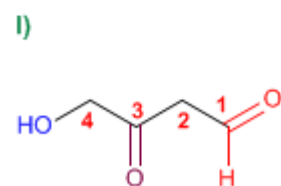
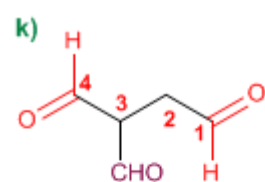
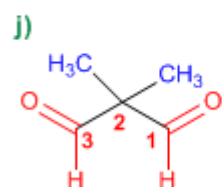
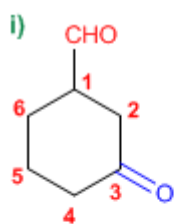
1. Cadena principal: 4 carbonos (butano)
2. Grupo funcional: aldehído
3. Numeración: asignar el menor localizador al aldehído
4. Nombre: But-3-inal

1. Cadena principal: ciclo de 5 miembros (ciclopentano)
2. Grupo funcional: cetona
3. Numeración: comienza en la cetona y prosigue hacia el sustituyente
4. Sustituyentes: metoxi en 3.
5. Nombre: 3-Metoxiciclopentanona

1. Cadena principal: 6 carbonos (hexano)
2. Grupo funcional: aldehído (dialdehído)
3. Numeración: comienza en el extremo que otorga al fenilo el localizador más bajo.
4. Sustituyentes: fenilo en 3.
5. Nombre: 3-Fenilhexanodial

1. Cadena principal: 6 carbonos (hexano)
2. Grupo funcional: aldehído
3. Numeración: asignar el menor localizador al aldehído
4. Sustituyentes: hidroxí en 5 y oxo en 4.
5. Nombre: 5-Hidroxí-4-oxohexanal

Los aldehídos son prioritarios sobre las cetonas que pasan a nombrarse como sustituyentes (oxo-)



1. Cadena principal: ciclo de 6 miembros (ciclohexano)
2. Grupo funcional: aldehído (-carbaldehído)
3. Numeración: menor localizador al grupo -CHO (este no se numera)
4. Sustituyentes: cetona (oxo-) en 3
5. Nombre: 3-Oxociclohexanocarbaldehído

1. Cadena principal: 3 carbonos (propano)
2. Grupo funcional: aldehído (dialdehído)
3. Sustituyentes: metilos en 2,2.
4. Nombre: 2,2-Dimetilpropanodial

1. Cadena principal: 4 carbonos (butano)
2. Grupo funcional: aldehído
3. Sustituyentes: formil en 3
4. Nombre: 3-Formilbutanodial

1. Cadena principal: 4 carbonos (butano)
2. Grupo funcional: aldehído
3. Numeración: asignar el menor localizador al aldehído
4. Sustituyentes: hidroxil en 4 y oxo en 3.
5. Nombre: 4-Hidroxil-3-oxobutanal

Nomenclatura de Aldehídos y Cetonas - Problema 9.2

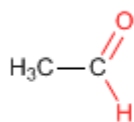
PRINT EMAIL

Dibuja la estructura de los siguientes aldehídos y cetonas:

- | | |
|---|----------------------------------|
| a) Etanal (acetaldehído) | g) 2,5-Dioxooctanodial |
| b) 3-Metilbutanal | h) 1,3-Ciclohexanodiona |
| c) Benzaldehído | i) 3-Metil-3-pental |
| d) 4-Hidroxyciclohexanocarbaldehído | j) 3-Oxobutanal |
| e) 3-Hidroxi-4-metil-5-oxociclohexanocarbaldehído | k) 3-Hidroxyciclopentanona |
| f) 2-Metil-2,5-octanodiona | l) 4-Etoxi-5-fenil-3-oxoheptanal |

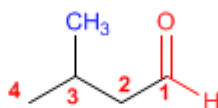
Solución

a)



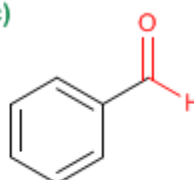
Etanal (acetaldehído)

b)

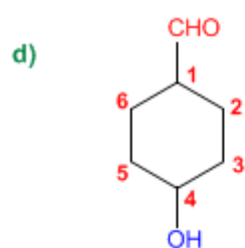


3-Metilbutanal

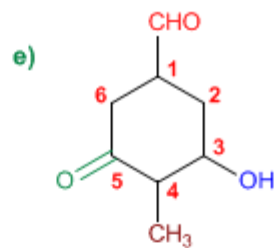
c)



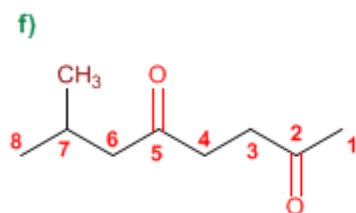
Benzaldehído



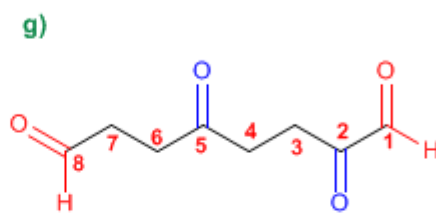
4-Hidroxiciclohexanocarbaldehído



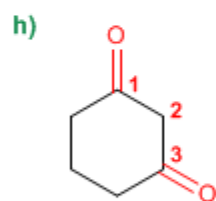
3-Hidroxi-4-metil-5-oxociclohexanocarbaldehído



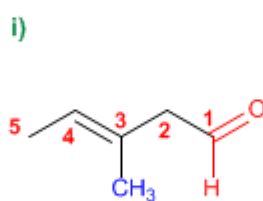
7-Metil-2,5-octanodiona



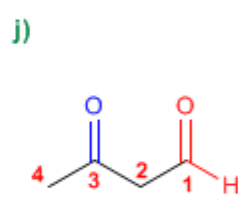
2,5-Dioxooctanal



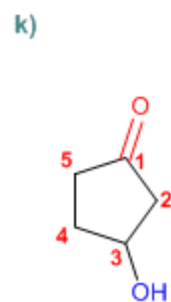
1,3-Ciclohexanodiona



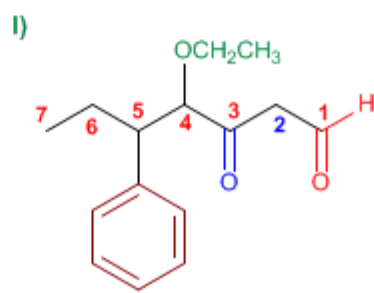
3-Metil-3-pentenal



3-Oxobutanal



3-Hidroxiciclopentanona

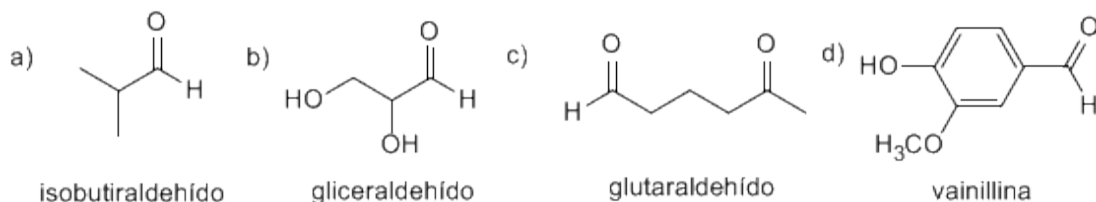


4-Etoxi-5-fenil-3-oxoheptanal

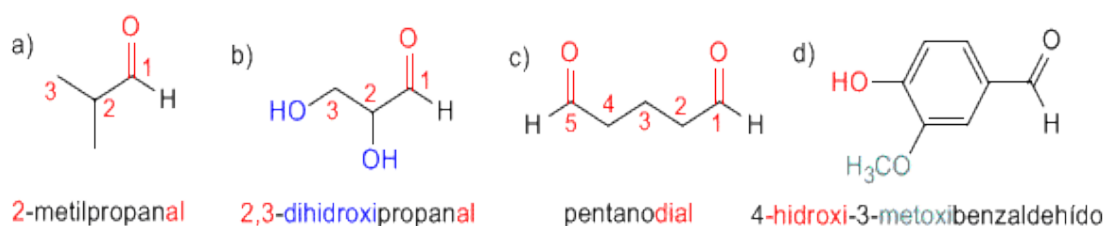
PROBLEMAS RESUELTOS DE ALDEHÍDOS Y CETONAS

Aldehídos y Cetonas: Problema 1

1) A continuación se dan nombres comunes y las fórmulas estructurales de algunos compuestos carbonílicos. Indique el nombre correspondiente según la IUPAC.



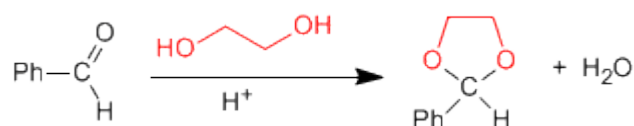
Solución



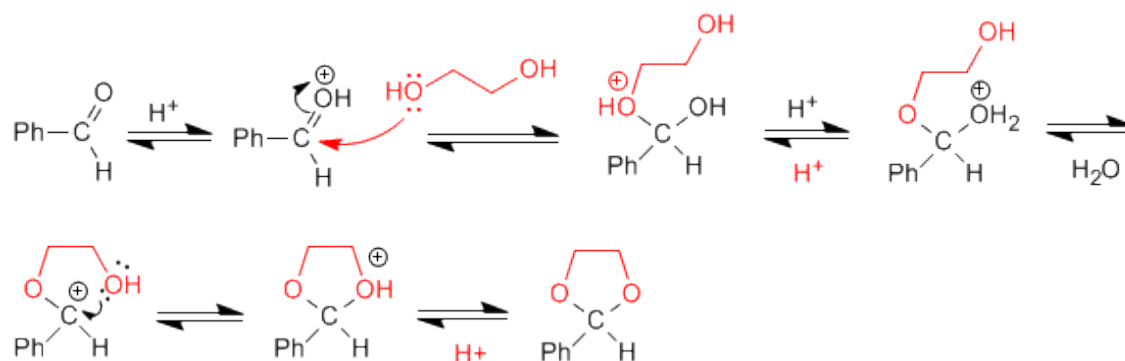
Aldehídos y cetonas: Problema 2

Dibuje la estructura del acetal que se forma cuando el benzaldehído se calienta con 1,2-etanodiol en medio ácido. Escriba un mecanismo detallado que justifique su formación. Describa paso a paso la hidrólisis de este acetal en medio ácido acuoso.

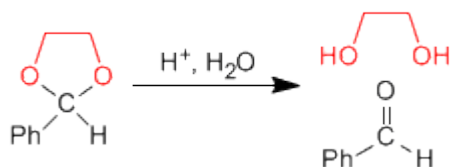
SOLUCIÓN



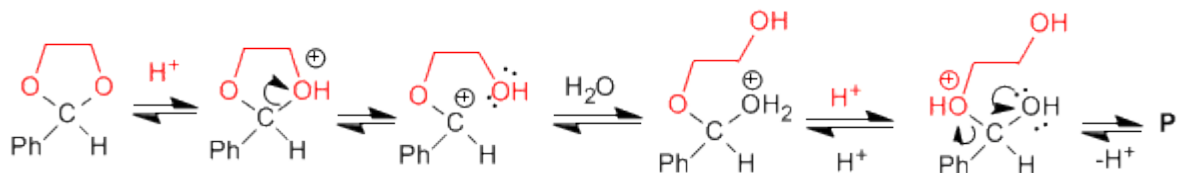
Mecanismo de formación del acetal:



La hidrólisis del acetal en medio ácido acuoso sigue es etapas inversas a la síntesis.



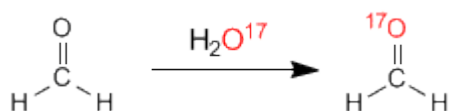
Mecanismo de hidrólisis del acetal cíclico.



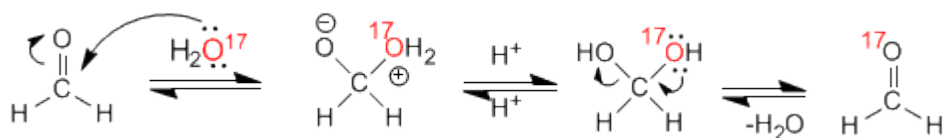
Aldehídos y Cetonas: Problema 3

Cuando se disuelve formaldehído en agua marcada con ^{17}O , se observa que después de unas horas tanto el hidrato del formaldehído como el formaldehído han incorporado el isótopo ^{17}O . Sugiera una explicación razonable de este hecho.

SOLUCION



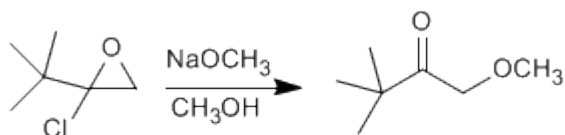
Mecanismo:



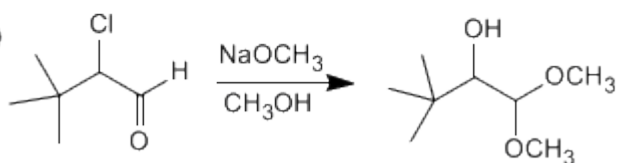
Aldehídos y Cetonas: Problema 4

Sugiera un mecanismo razonable para una de las siguientes reacciones:

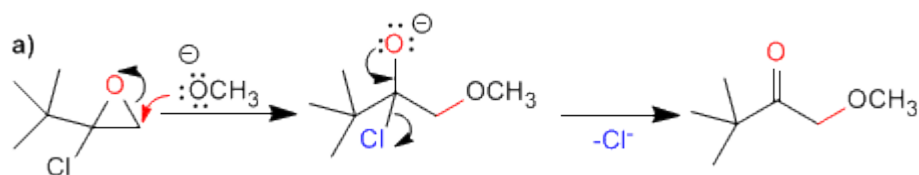
a)



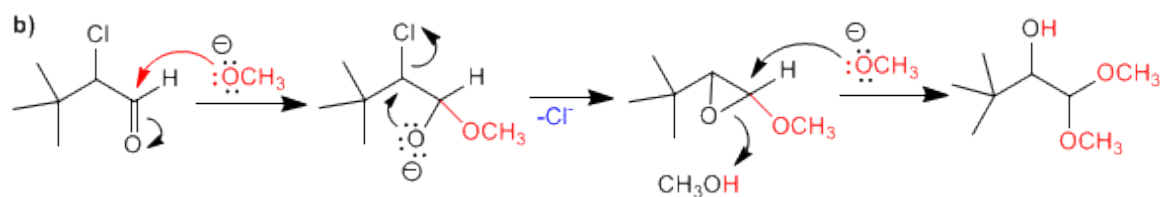
b)



SOLUCION



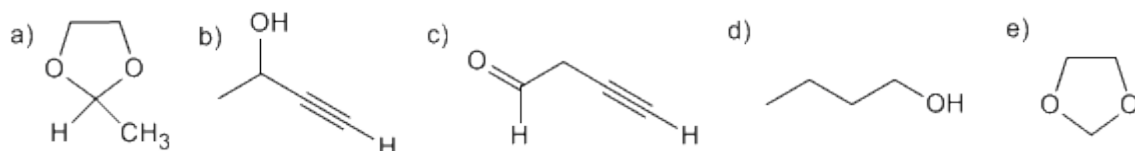
La primera etapa consiste en la apertura del oxaciclopropano sobre el carbono menos sustituido. En la segunda etapa, la cesión del par del oxígeno elimina el cloro, formándose un carbonilo.



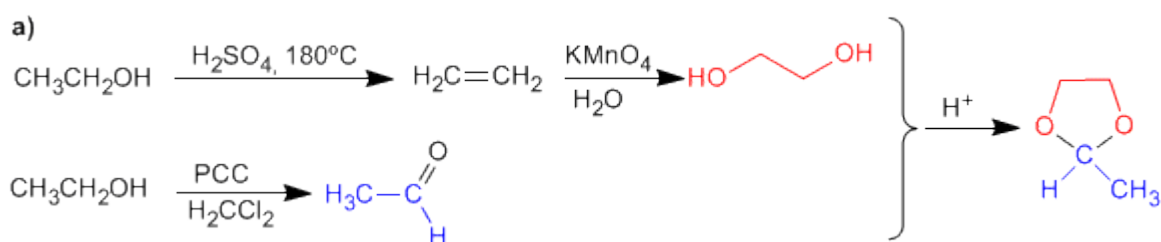
En el primer paso hay dos posibles posiciones de ataque; el carbono carbonilo y el carbono del cloro. Como el producto final no tiene metóxido en el carbono del cloro, atacamos al carbonilo. En la segunda etapa se produce una sustitución nucleófila intramolecular. Para terminar el metóxido abre el epóxido.

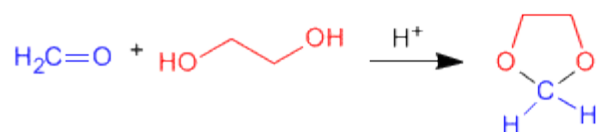
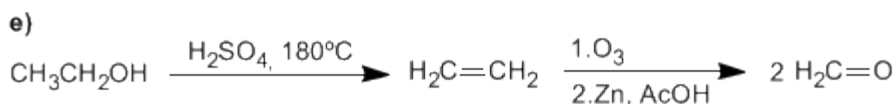
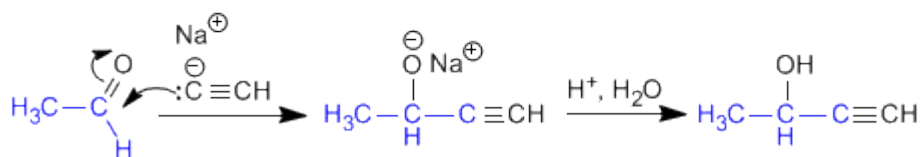
Aldehídos y Cetonas: Problema 5

Usando etanol como fuente de todos los átomos de carbono y los reactivos que necesite, describa una síntesis eficiente de cada una de las sustancias siguientes:

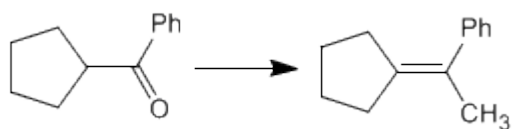


SOLUCIÓN

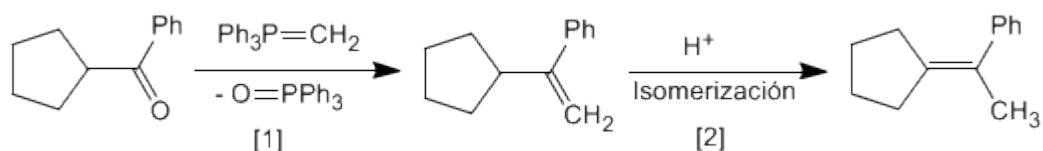




Utilizando los reactivos necesarios, indicar las etapas que permiten realizar la siguiente transformación:



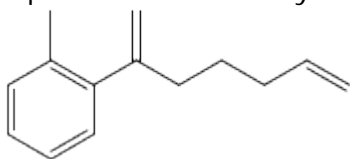
SOLUCIÓN



[2] Isomerización en medio ácido, impulsada por la mayor estabilidad del alqueno interno.

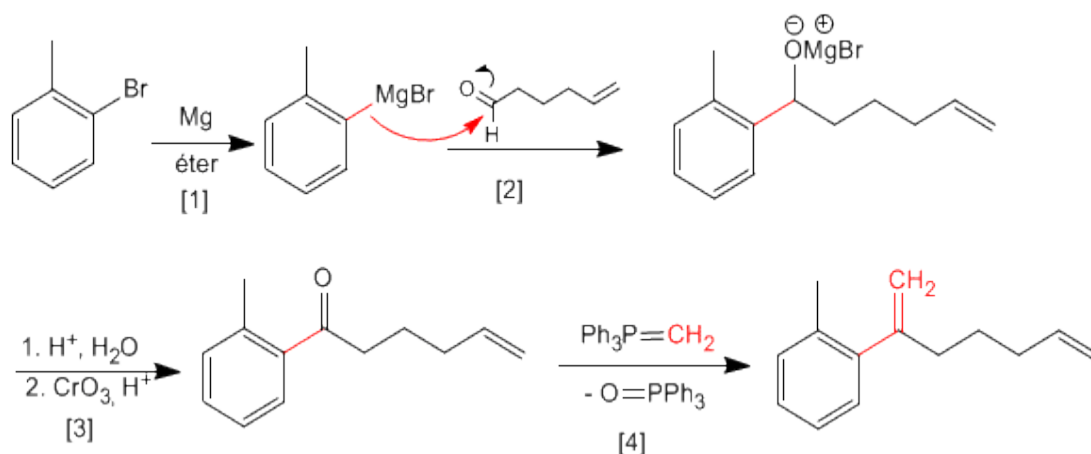
Aldehídos y Cetonas: Problema 7

A partir de 5-hexenal y o-bromotolueno obtener el siguiente producto.



Pueden ser necesarios reactivos orgánicos e inorgánicos adicionales.

SOLUCIÓN



[1] Formación del magnesiano

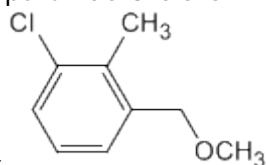
[2] Ataque nucleófilo del magnesiano al carbonilo.

[3] Hidrólisis y posterior oxidación del alcohol secundario.

[4] Reacción de Wittig entre la cetona y el trifenilmetilenfosforano.

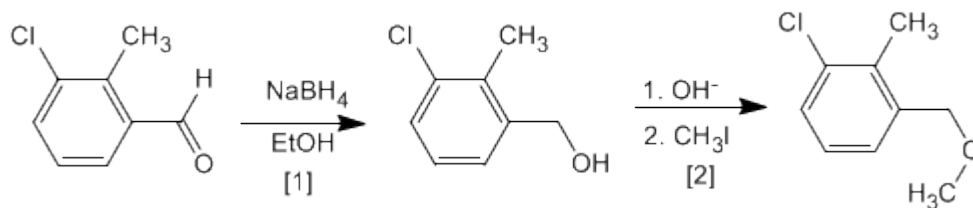
Aldehídos y Cetonas: Problema 8

Obtener a partir de 3-cloro-2-metilbenzaldehído y de los reactivos



necesarios
el compuesto siguiente:

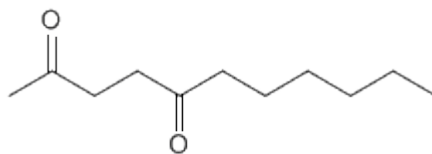
SOLUCIÓN



[1] Reducción del aldehído a alcohol

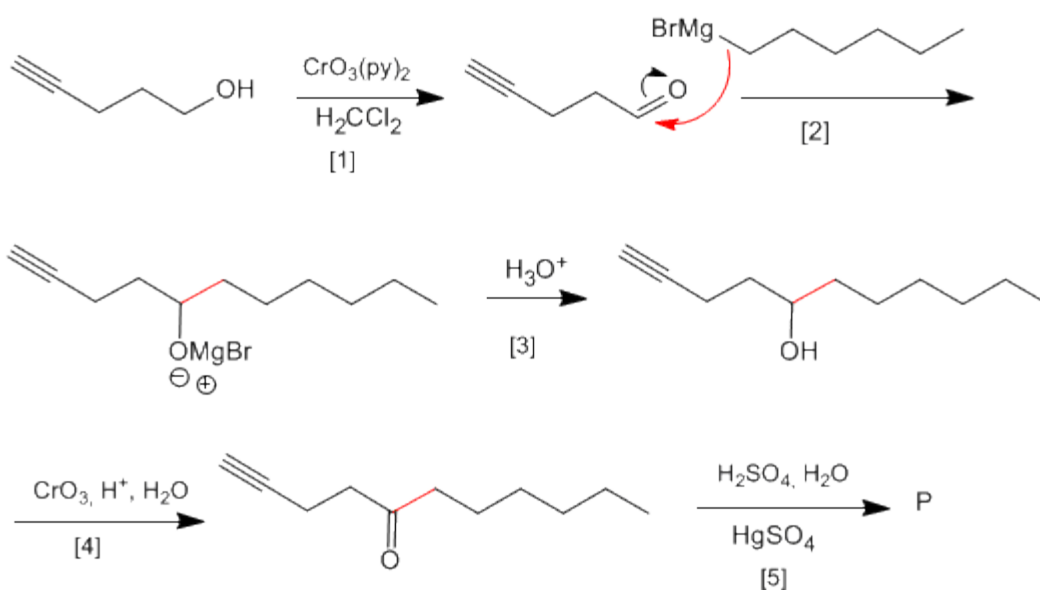
[2] Síntesis de Williamson de éteres.

Aldehídos y Cetonas: Problema 9



A partir de 4-pentin-1-ol obtener:

SOLUCIÓN

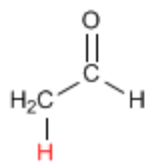


- [1] Oxidación del alcohol a aldehído
- [2] Formación del enlace carbono-carbono mediante organometálicos de magnesio
- [3] Protonación del alcohol
- [4] Oxidación del alcohol con Jones (Puedes utilizar también $\text{CrO}_3(\text{py})_2$)
- [5] Hidratación Markovnikov del alquino, para formar cetonas

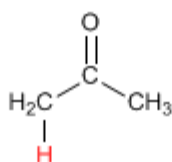
TEORÍA DE ENOLES Y ENOLATOS

Formación de Enolatos

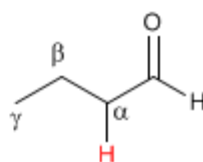
Los aldehídos y cetonas presentan hidrógenos ácidos en la posición vecina al grupo carbonilo, conocida como posición alfa. Estos hidrógenos presentan un pKa comprendido entre 18 y 21.



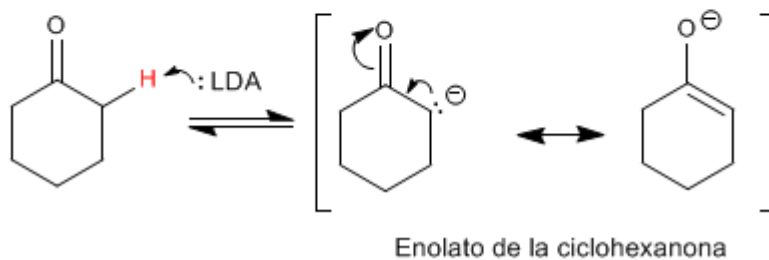
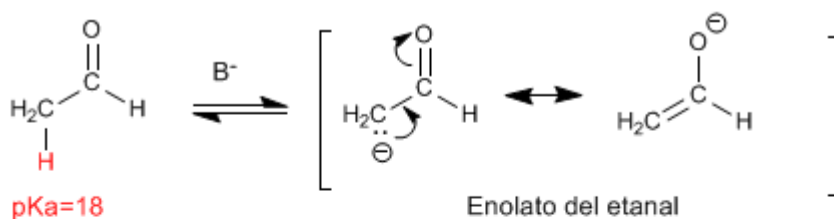
pKa=18



pKa=20-21



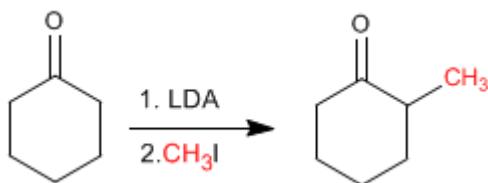
La acidez de los hidrógenos α es debida a la estabilización de la base conjugada (enolato) por resonancia.



Alquilación de Enolatos

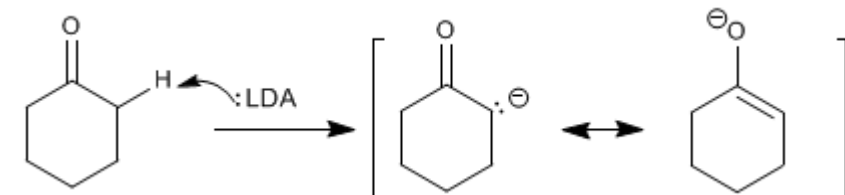
Los enolatos actúan como nucleófilos a través del carbono atacando a un gran número de electrófilos (haloalcanos, epóxidos, carbonilos, ésteres.....). En este punto nos fijaremos en la reacción entre enolatos y haloalcanos, que permite añadir cadenas carbonadas a la posición α de la cadena.

La Ciclohexanona se convierte en 2-Metilciclohexanona por tratamiento con LDA seguido de yoduro de metilo.

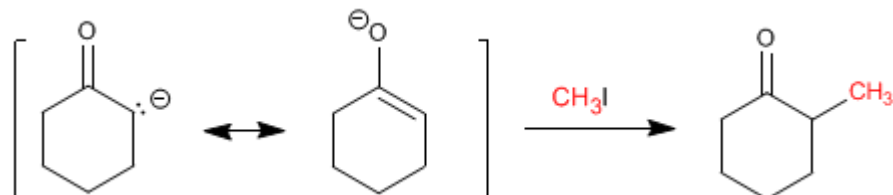


Etapas del mecanismo por el que se alquila la ciclohexanona:

Etapas del mecanismo

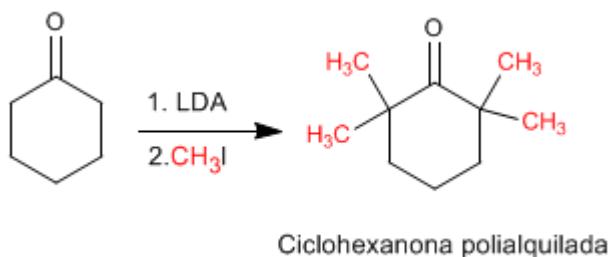


Etapas del mecanismo



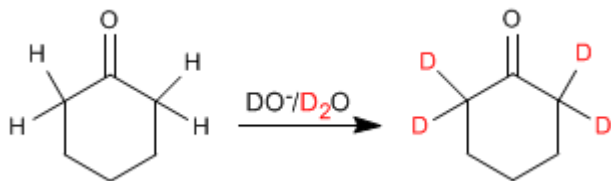
Las reacciones de alquilación tienen dos importantes problemas.

1. Competencia con la condensación aldólica. Los carbonilos en medio básico tienden a condensar para formar aldoles.
2. La reacción es difícil de controlar y tiende a polialquilar el carbonilo.



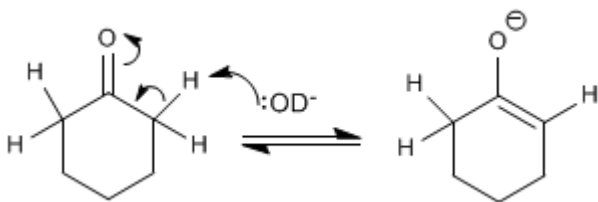
Intercambio hidrógeno - Deuterio

Los aldehídos y cetonas intercambian sus hidrógenos a por deuterios cuando se tratan con $\text{DO}^-/\text{D}_2\text{O}$ o con $\text{D}^+/\text{D}_2\text{O}$. En medios básicos la reacción transcurre a través de enolatos y en medios ácidos los intermediarios formados son enoles.

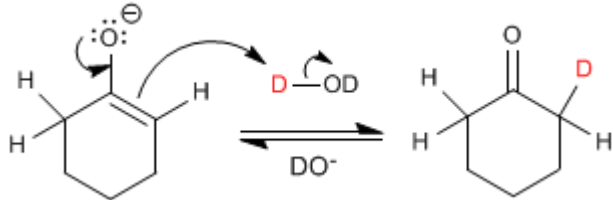


El mecanismo del intercambio hidrógeno-deuterio transcurre en los siguientes pasos:

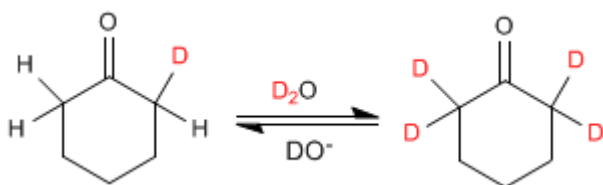
Etapas 1. Formación del enolato



Etapas 2. Transferencia del deuterio al enolato



Etapas 3. Sustitución del resto de hidrógenos



Halogenación de aldehídos y cetonas

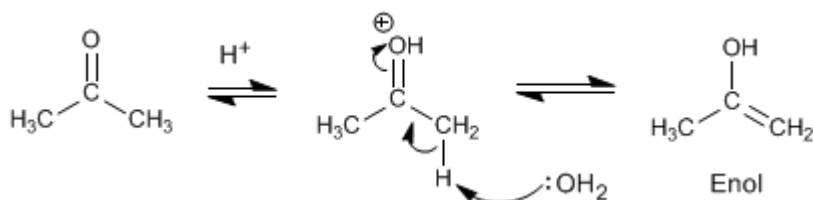
Los aldehídos y cetonas reaccionan con halógenos en medios ácidos o básicos produciéndose la sustitución de hidrógenos a por halógenos.

Halogenación de la propanona en medio ácido:

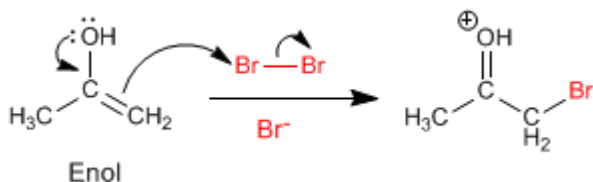


El mecanismo de halogenación en **medio ácido** tiene las siguientes etapas:

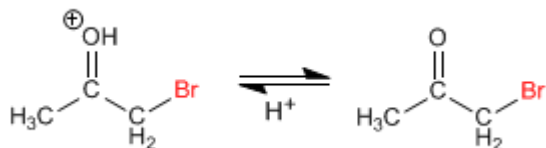
Etapas 1. Formación del enol



Etapas 2. Ataque nucleófilo del enol sobre el halógeno ayudado por la cesión del para del oxígeno.

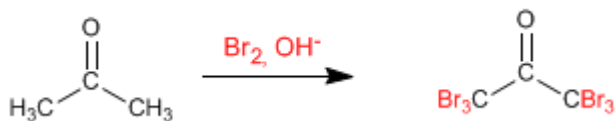


Etapas 3. Desprotonación



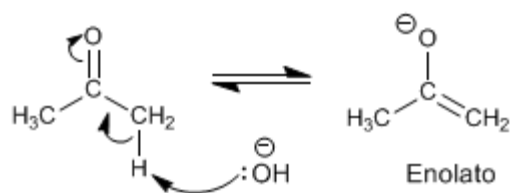
Trabajando con un equivalente de reactivo la halogenación para en una primera adición y no ocurren polihalogenaciones. El paso clave del mecanismo es la formación del enol y esta etapa requiere protonar el oxígeno del carbonilo. Una vez halogenada la posición α el oxígeno se vuelve menos básico, debido al efecto electronegativo del bromo, protonándose peor.

Halogenación de la propanona en **medio básico**:

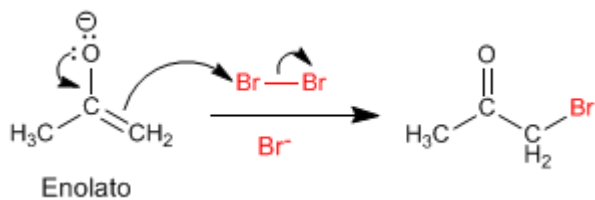


La halogenación en medio básico tiene el siguiente mecanismo:

Etapla 1. Formación del enolato



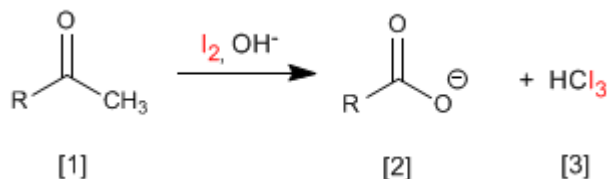
Etapla 2. Ataque nucleófilo del enolato sobre el halógeno ayudado por la cesión del para del oxígeno.



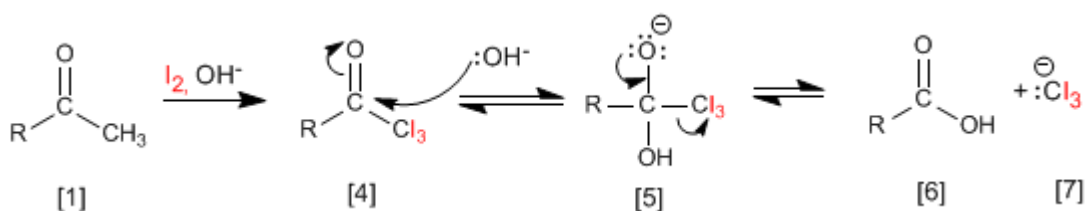
Este mecanismo se repite otras 5 veces sustituyendo todos los hidrógenos a por halógenos. En este caso la reacción no para puesto que el producto halogenado es más reactivo que la propanona de partida. La base arranca mejor los hidrógenos en el producto halogenado (son más ácidos), haciendo imposible parar la reacción.

Reacción del Haloformo (Yodoformo)

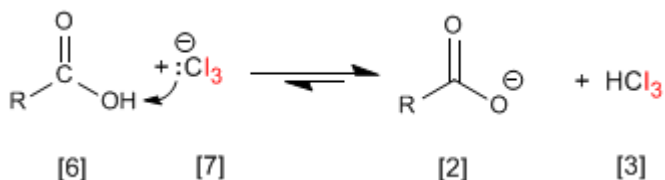
Las cetonas metílicas **[1]** reaccionan con halógenos en medios básicos generando carboxilatos **[2]** y haloformo **[3]**.



El mecanismo consiste en halogenar completamente el metilo, sustituyendo en una etapa posterior el grupo $-\text{CX}_3$ formado por $-\text{OH}$.



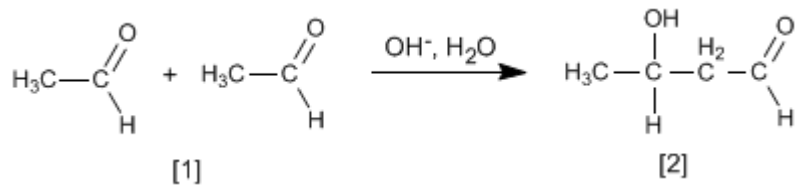
El grupo Cl_3^\ominus es muy básico y desprotona el ácido carboxílico formándose yodoformo y el carboxilato.



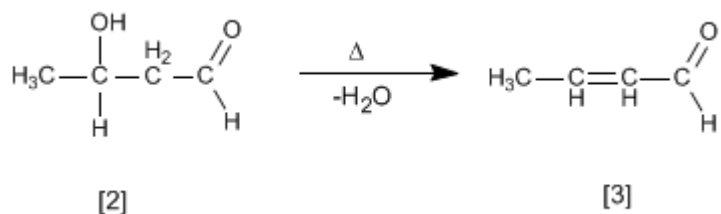
Esta reacción (con yodo) puede emplearse como ensayo analítico para identificar cetonas metílicas aprovechando que el yodoformo precipita de color amarillo.

Condensación Aldólica

Aldehídos y cetonas [1] condensan en medios básicos formando aldoles [2]. Esta reacción se denomina condensación aldólica.

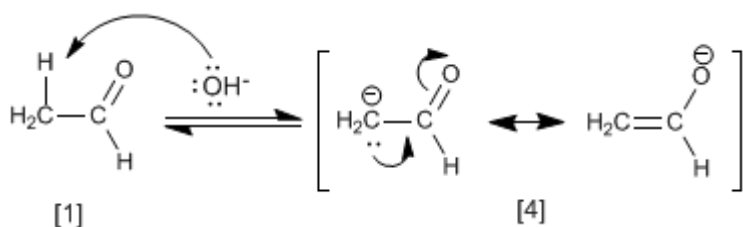


El aldol [2] formado deshidrata en el medio básico por calentamiento para formar un α,β -insaturado [3].



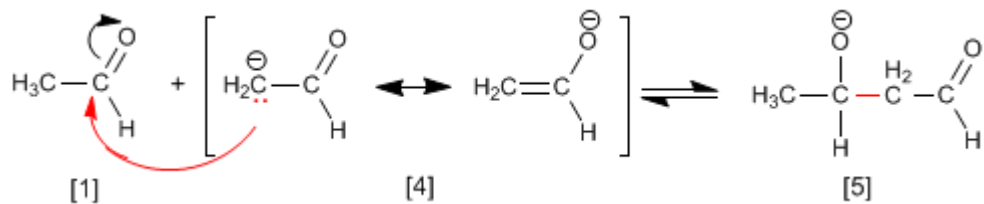
El mecanismo de la condensación aldólica transcurre con formación de un enolato, que ataca al carbonilo de otra molécula. En esta condensación se forma un enlace carbono-carbono entre el carbonilo de una molécula y el carbono α de la otra.

Etapas 1. Formación del enolato

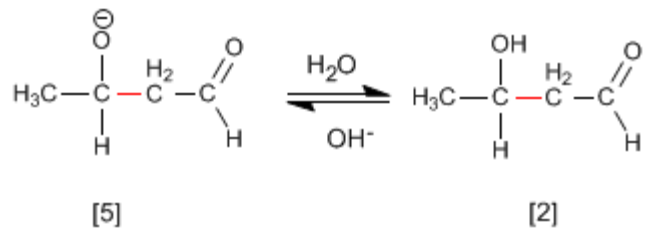


La base desprotona el carbono α del etanal [1] generando el enolato [4] estabilizado por resonancia.

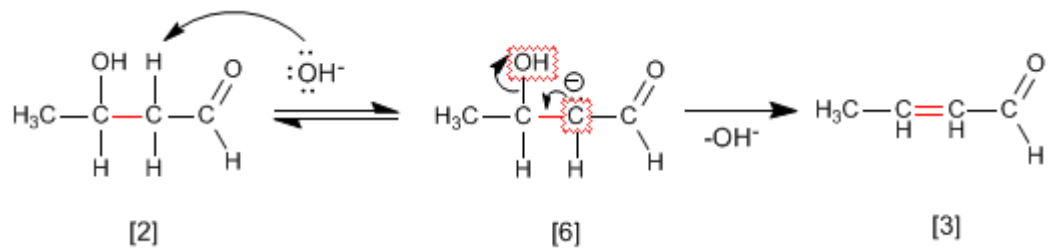
Etapas 2. Ataque nucleófilo del enolato sobre el carbonilo



Etapas 3. Protonación

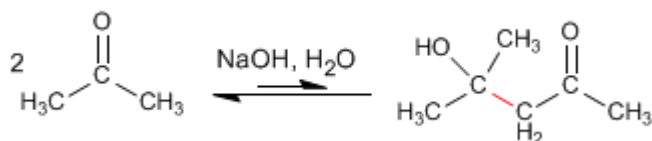


Etapas 4. Deshidratación del aldol

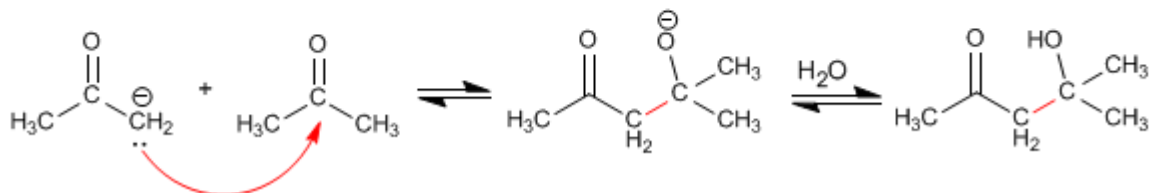
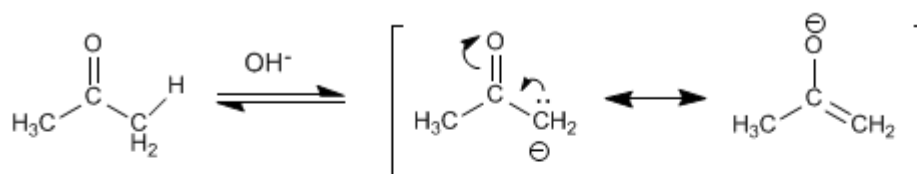


Condensación aldólica con cetonas

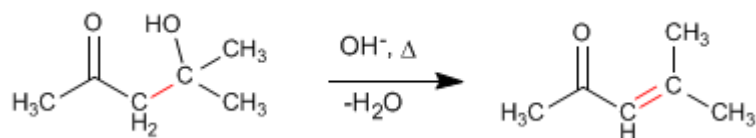
Las cetonas son menos reactivas que los aldehídos y dan un rendimiento muy bajo en la condensación aldólica. Así, dos moléculas de propanona condensan para formar el aldol correspondiente con un rendimiento del 2%. Se pueden conseguir porcentajes elevados del producto separándolo del medio de reacción según se va formando, o bien, calentando para deshidratarlo. De ambas formas los equilibrios de la aldólica se desplazan hacia el producto final.



Mecanismo de la reacción:



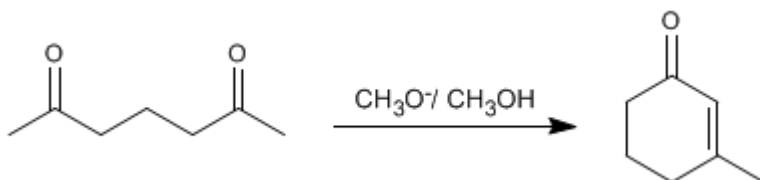
La deshidratación final permite el desplazamiento de los equilibrios. También se puede realizar una extracción del aldol del medio de reacción para favorecer la reacción.



Condensación aldólica intramolecular

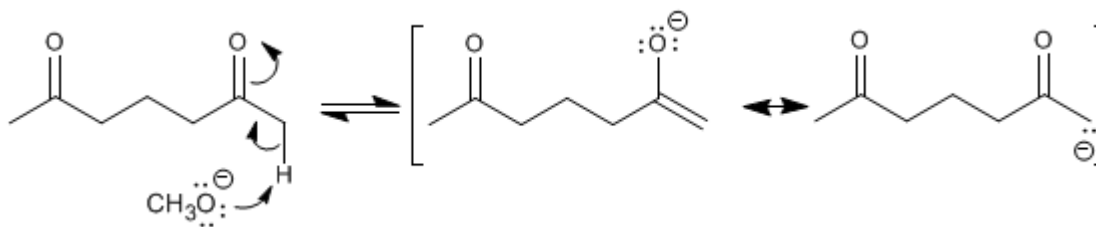
Los compuestos dicarbonílicos condensan mediante la aldólica intramolecular en medios básicos. En esta reacción se obtienen ciclos de cinco o seis miembros.

Así, la 2,6-heptanodiona condensa con metóxido en metanol para formar el 3-metilciclohex-2-enona.

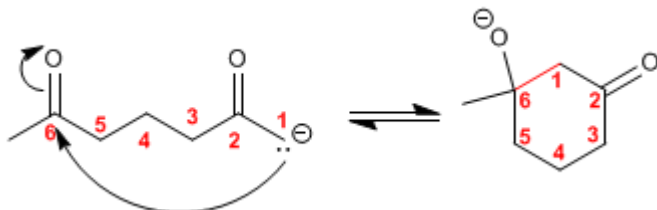


El mecanismo de la reacción transcurre a través de las siguientes etapas:

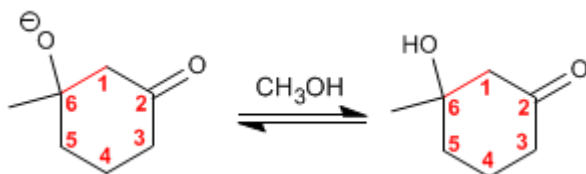
Etapla 1. Formación del enolato.



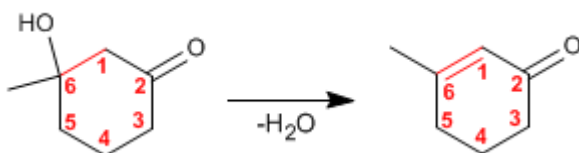
Etapla 2. Adición nucleófila intramolecular



Etapla 3. Protonación de la base del aldol



Etapla 4. Deshidratación del aldol

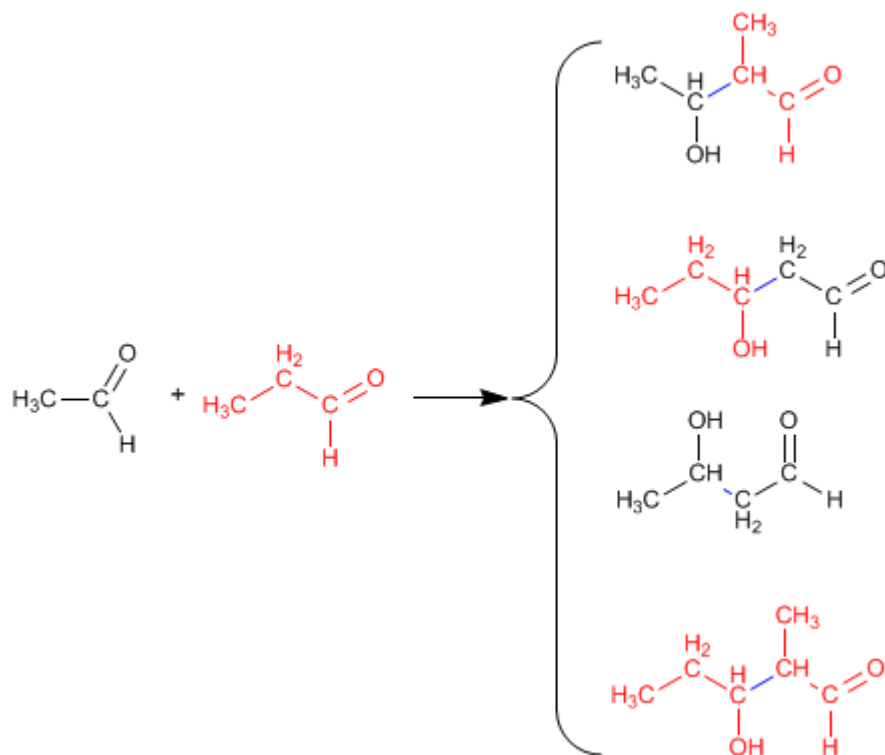


Condensación aldólica cruzada o mixta

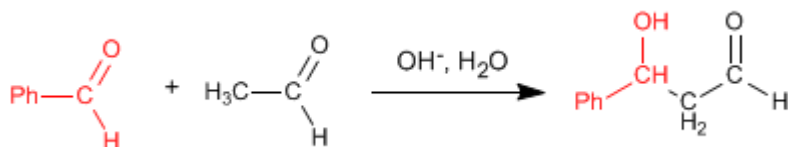
La reacción entre dos carbonilos diferentes se llama aldólica cruzada o mixta. Esta reacción sólo tiene utilidad sintética en dos casos:

1. Sólo uno de los carbonilos puede formar enolatos.
2. Uno de los carbonilos es mucho más reactivo que el otro.

En el resto de situaciones la aldólica mixta genera mezclas de cuatro productos. Veamos como ejemplo la condensación del etanal y propanal.

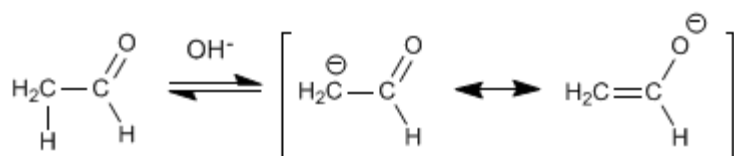


La condensación aldólica mixta del etanal con el benzaldehído genera un producto, cuando se trabaja en exceso de benzaldehído, debido a que el benzaldehído carece de hidrógenos en el carbono alfa y no puede formar enolatos.



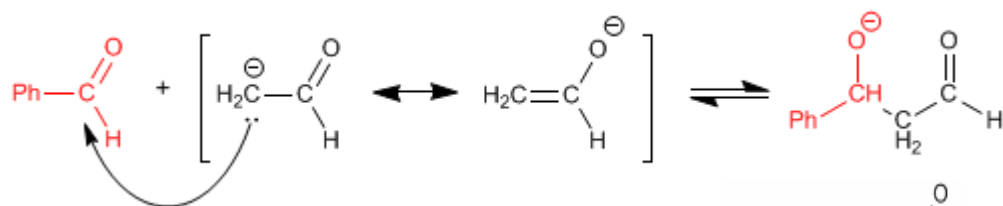
El mecanismo de esta reacción tiene lugar en las siguientes etapas:

Etapla 1. Enolización del etanal

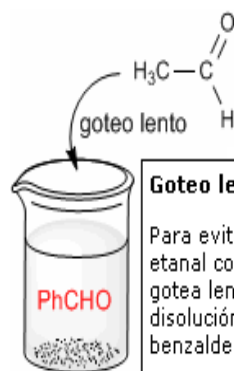


La formación de enolatos sólo puede tener lugar con el etanal, puesto que el benzaldehído carece de hidrógenos ácidos en el carbono alfa.

Etapla 2. Ataque nucleófilo del enolato al benzaldehído.



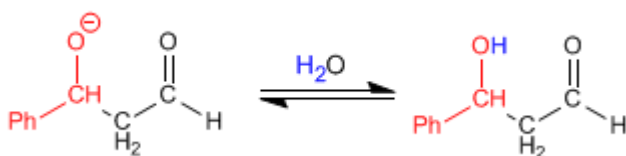
En esta etapa puede ocurrir el ataque del enolato de etanal sobre si mismo. Para evitarlo debe trabajarse en exceso de benzaldehído. Un procedimiento experimental muy usado para evitar la condensación del etanal consigo mismo es gotear lentamente el etanal sobre una disolución básica de benzaldehído



Goteo lento

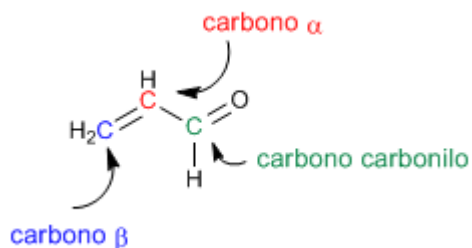
Para evitar la condensación del etanal consigo mismo, se gotea lentamente sobre una disolución básica de benzaldehído.

Etapla 3. Protonación



Síntesis de carbonilos alfa,beta-insaturados

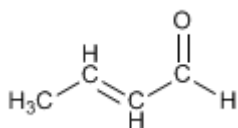
Los carbonilos α,β -insaturados son compuestos orgánicos que tienen un doble enlace entre las posiciones α,β de un aldehído o cetona.



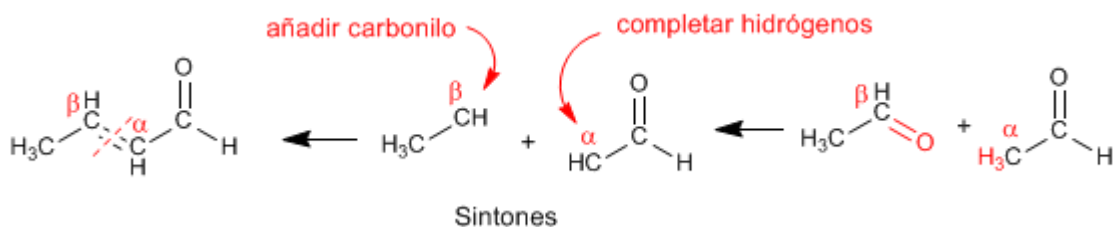
El propenal o acroleína es un carbonilo α,β -insaturado. Sus dos dobles enlaces conjugados le confieren una reactividad especial.

Existen 4 métodos importantes para la preparación de α,β -insaturados: condensación aldólica, halogenación del carbono α seguida de eliminación, oxidación de alcoholes alílicos y Wittig.

Método 1. Preparar mediante la condensación aldólica el siguiente compuesto.

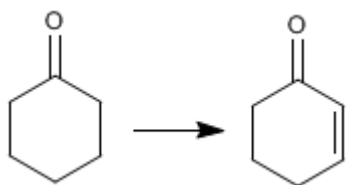


Empleamos la retrosíntesis para preparar el compuesto. Al ser de la familia de los α,β -insaturados se puede obtener mediante la condensación aldólica.

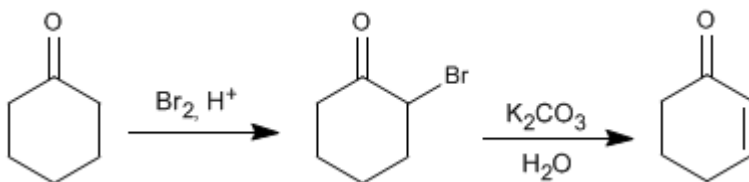


Para obtener los reactivos que forman el α,β -insaturado se rompe por el doble enlace, obteniéndose los sintones (equivalentes sintéticos). Los reactivos se obtienen añadiendo al carbono β un carbonilo y completando los hidrógenos que faltan en el carbono α .

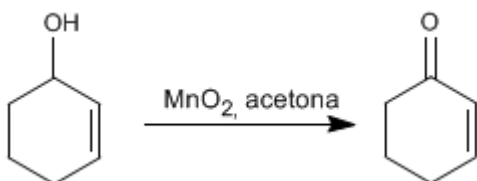
Ejemplo 2. Indicar como se puede realizar la siguiente transformación.



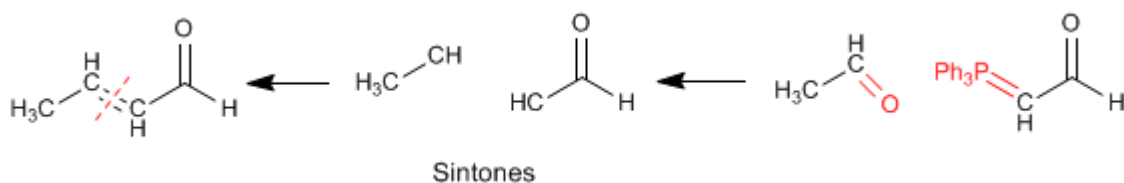
En una primera etapa se halogena la posición α del carbonilo. En la segunda etapa se realiza una eliminación que nos deja el producto final.



Método 3. La oxidación de alcoholes alílicos con dióxido de manganeso en acetona produce α,β -insaturados



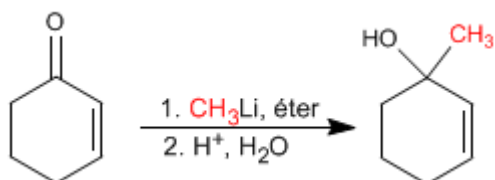
Método 4. Reacción de Wittig



Reactividad de carbonilos alfa,beta-insaturados

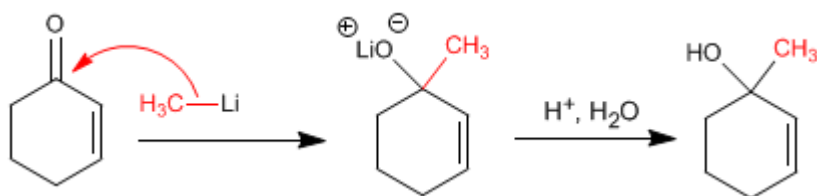
Los α,β -insaturados son compuestos que poseen dos posiciones electrófilas: el carbono carbonilo y el carbono β .

Adiciones 1,2. Los organometálicos de litio atacan al carbono carbonilo dando lugar a adiciones 1,2.



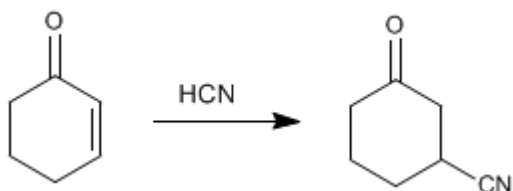
Los organometálicos de litio y magnesio atacan al carbono carbonilo de los α,β -insaturados

Mecanismo de la adición 1,2

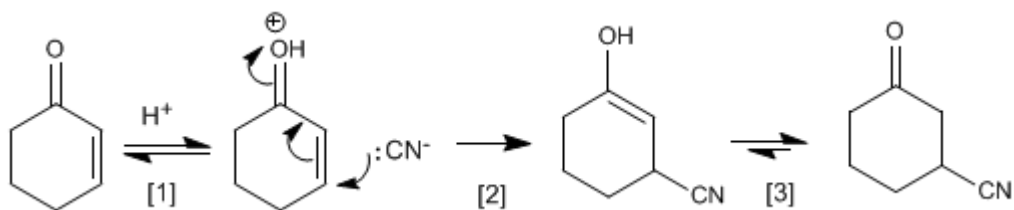


Adiciones 1,4. Los cupratos, cianuro y otros nucleófilos atacan al carbono β de los α,β -insaturados, dando adiciones 1,4.

El ácido cianhídrico da adiciones 1,4 con los α,β -insaturados. El ciano se une al carbono β .

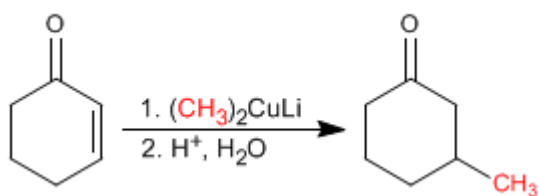


Mecanismo de adición del ácido cianhídrico a la Ciclohex-2-enona

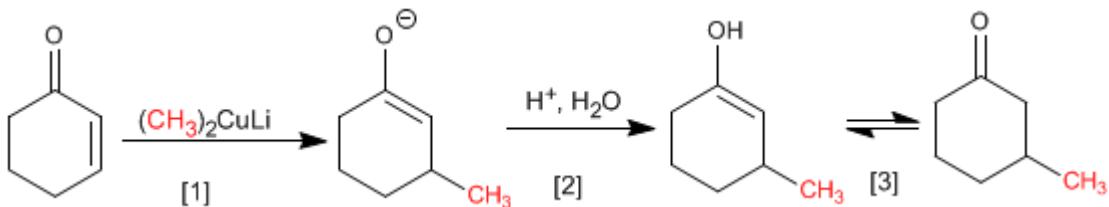


- [1] Protonación del carbonilo
- [2] Ataque nucleófilo del cianuro al carbono β .
- [3] Tautomería ceto-enol.

Los cupratos son organometálicos de cobre que se adicionan al carbono β de los α,β -insaturados.



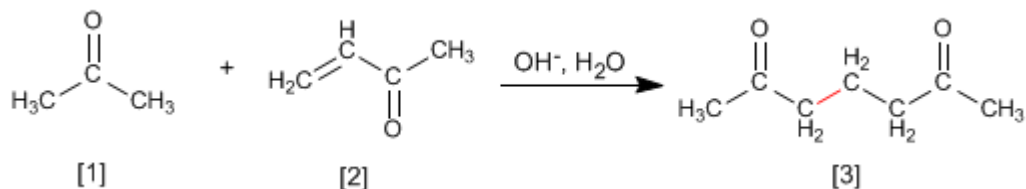
El mecanismo de la reacción comienza con el ataque nucleófilo del cuprato sobre el carbono β , formando un enolato, que se protona en la segunda etapa para dar un enol. El enol tautomeriza a cetona generando el producto final.



- [1] Adición nucleófila del cuprato.
- [2] Protonación del enolato
- [3] Tautomería ceto-enol

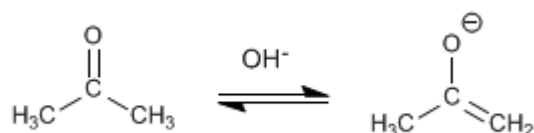
Adición de Michael y anelación de Robinson

Los enolatos de aldehídos o cetonas se adicionan a los α,β -insaturados para formar 1,5-dicarbonilos. Esta reacción se denomina adición de Michael.

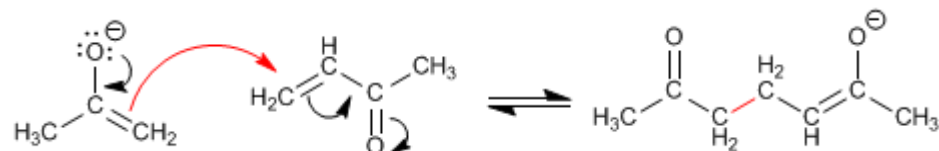


La propanona [1] reacciona con el α,β -insaturado [2] para formar el 1,5-dicarbonilo [3]
Mecanismo de la Adición de Michael:

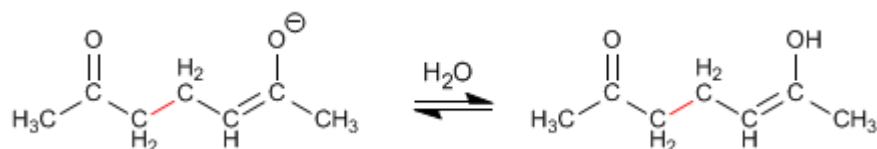
Etapla 1. Formación del enolato.



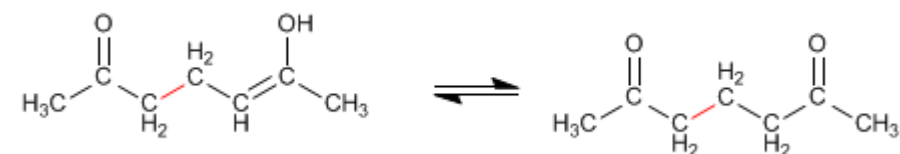
Etapla 2. Ataque nucleófilo del enolato al carbono β del α,β -insaturado.



Etapla 3. Equilibrio ácido-base



Etapla 4. Tautomería ceto-enol

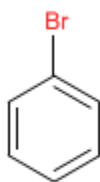


El producto de Michael puede condensar mediante una aldólica intramolecular, formando un α,β -insaturado. El conjunto de la adición de Michael y la aldólica final se conoce como reacción de Robinson

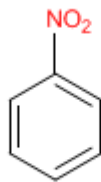
TEORÍA DEL BENCENO

Nomenclatura del Benceno

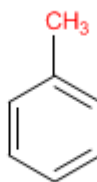
Los bencenos monosustituídos se nombran terminando el nombre del sustituyente en benceno.



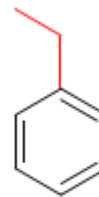
Bromobenceno



Nitrobenceno

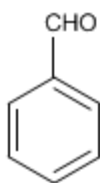


Metilbenceno

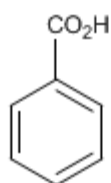


Etilbenceno

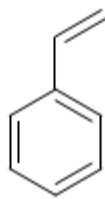
Algunos derivados monosustituídos del benceno tienen nombres comunes ampliamente aceptados.



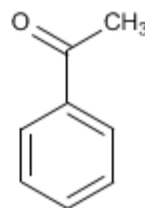
Benzaldehído



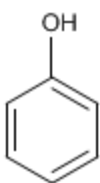
Ácido benzoico



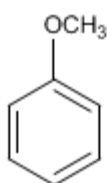
Estireno



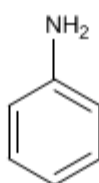
Acetofenona



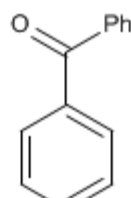
Fenol



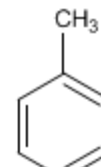
Anisol



Anilina

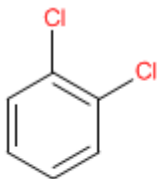


Benzofenona

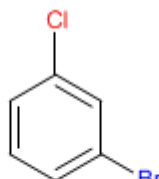


Tolueno

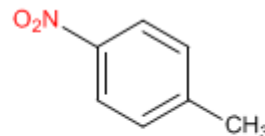
En bencenos disustituídos se emplean los prefijos *orto* (benceno 1,2-disustituído), *meta* (benceno 1,3-disustituído) y *para* (benceno 1,4-disustituído) para indicar la posición de los sustituyentes en el anillo.



o-Diclorobenceno
(1,2-Diclorobenceno)



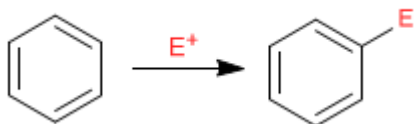
m-Bromoclorobenceno
(1-Bromo-3-clorobenceno)



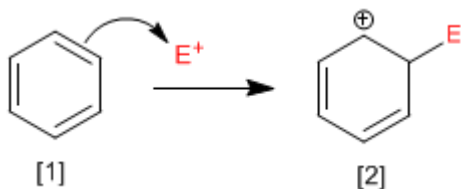
p-Nitrotolueno
(4-Nitrotolueno)

Sustitución Electrónica Aromática

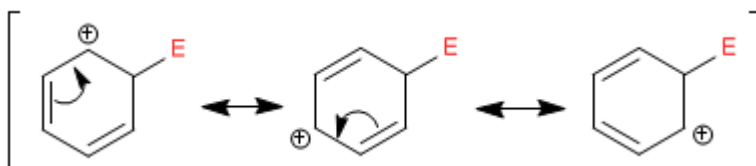
El benceno actúa como nucleófilo, atacando a un número importante y variado de electrófilos.



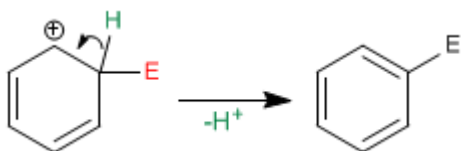
Etapas 1. En la primera etapa de la reacción el electrófilo acepta un par de electrones procedentes de la nube π del benceno, formándose un carbocatión estabilizado por resonancia.



El catión ciclohexadienilo [2] deslocaliza la carga positiva según las siguientes estructuras:

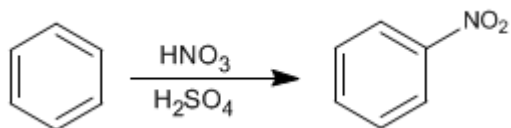


Etapas 2. En la segunda etapa el benceno recupera su aromaticidad por pérdida de un protón. Es una etapa rápida conocida como rearomatización del anillo.

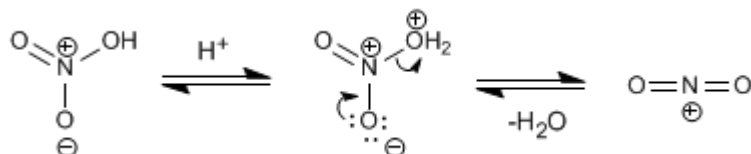


Nitración del Benceno

El benceno reacciona con la mezcla nítrico-sulfúrica adicionando grupos nitro.

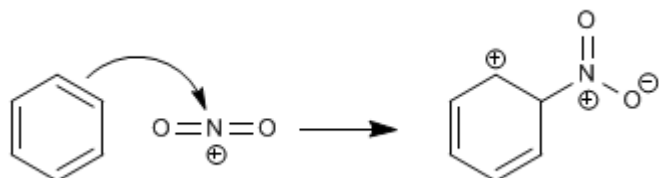


El electrófilo de esta reacción es el catión nitronio, NO_2^+ . Las concentraciones de este catión en el ácido nítrico son muy bajas para nitrar el benceno, por ello es necesario añadir ácido sulfúrico.

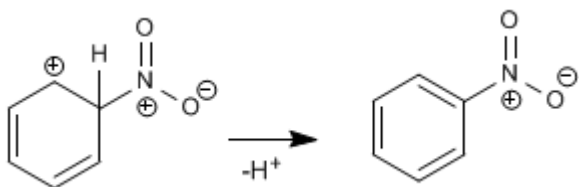


Mecanismo para la nitración del benceno:

Etapla 1. Ataque del benceno al catión nitronio

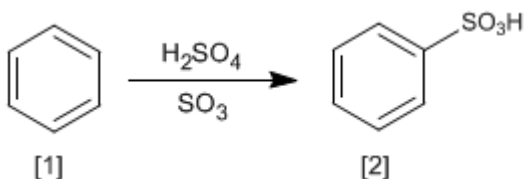


Etapla 2. Recuperación de la aromaticidad por pérdida de un protón



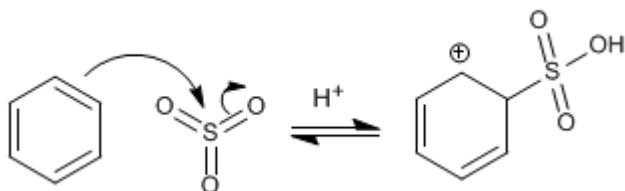
Sulfonación del Benceno

La reacción del benceno [1] con una disolución de trióxido de azufre en ácido sulfúrico produce ácidos bencenosulfónicos [2].

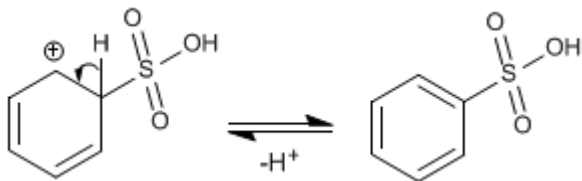


El mecanismo de la sulfonación tiene lugar con las siguientes etapas:

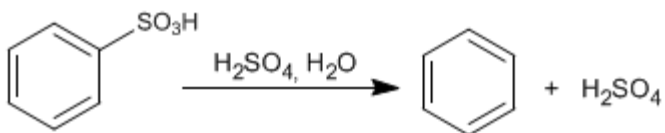
Etapas 1. Ataque del benceno al trióxido de azufre



Etapas 2. Recuperación de la aromaticidad por pérdida de un protón.

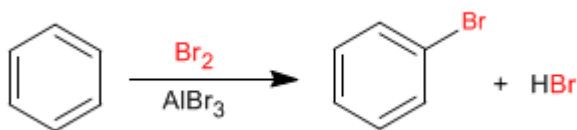


El mecanismo de la sulfonación es reversible, lo cual permite eliminar el grupo $-\text{SO}_3\text{H}$ por tratamiento con sulfúrico acuoso. Esta propiedad es utilizada para proteger posiciones del benceno, ocupándolas con el grupo $-\text{SO}_3\text{H}$.



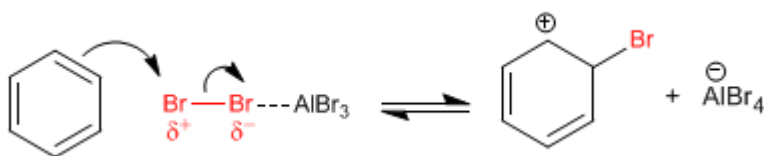
Halogenación del Benceno

El benceno reacciona con halógenos en presencia de ácidos de Lewis para formar derivados halogenados.

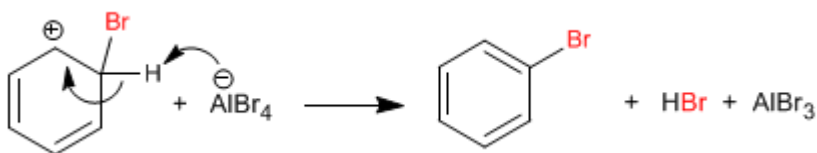


El mecanismo de la halogenación tiene lugar con las siguientes etapas:

Etapas 1. La molécula de bromo se polariza al interactuar con el ácido de Lewis. El benceno ataca al bromo polarizado positivamente para formar el catión ciclohexadienilo.



Etapas 2. Recuperación de la aromaticidad por pérdida de un protón.

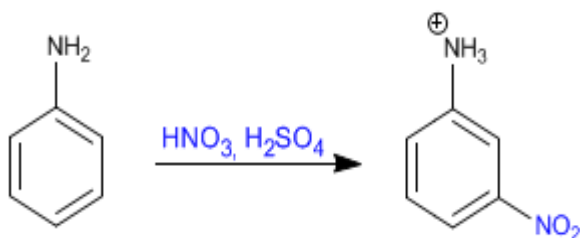


La cloración se puede llevar a cabo de forma similar a la bromación. La reacción con flúor y yodo se realiza muy poco frecuentemente. En el caso del flúor la reacción es difícil de controlar por su elevada reactividad. Por el contrario, el yodo reacciona lentamente y tiene un equilibrio desfavorable.

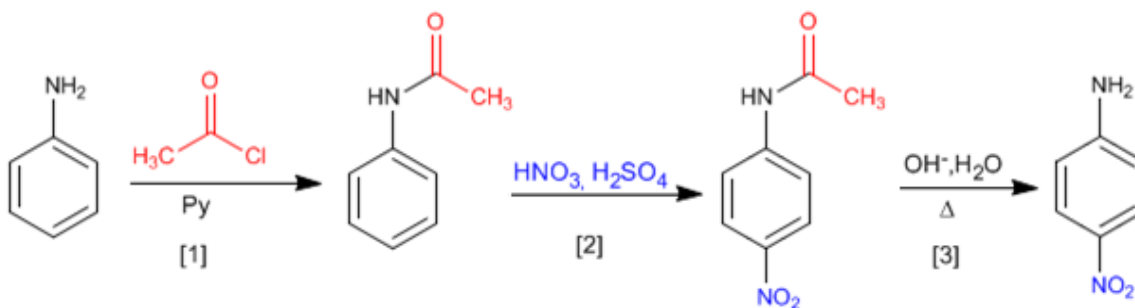
Benceno - Protección y desprotección del grupo amino

El grupo amino es un activante fuerte, que orienta a orto/para. Sin embargo, en medios ácidos se protona transformándose en un desactivante fuerte (sal de amonio) que orienta a posición meta. Se puede evitar la protonación del amino protegiéndolo con cloruro de etanoilo en piridina.

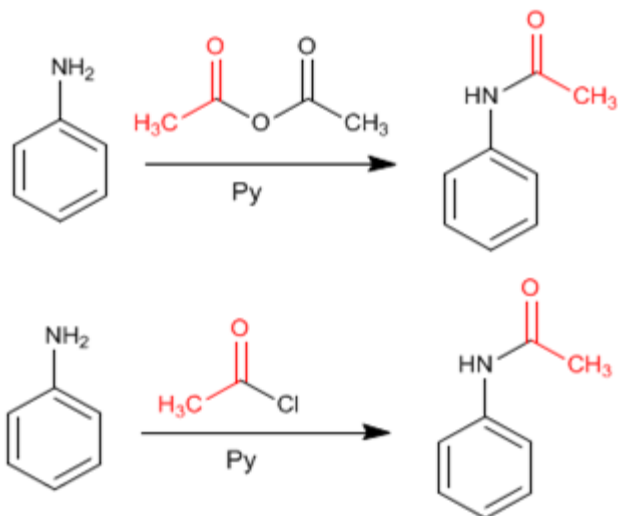
Nitración de la anilina sin protección del amino



Nitración de la anilina con protección del grupo amino, empleando cloruro de etanoilo

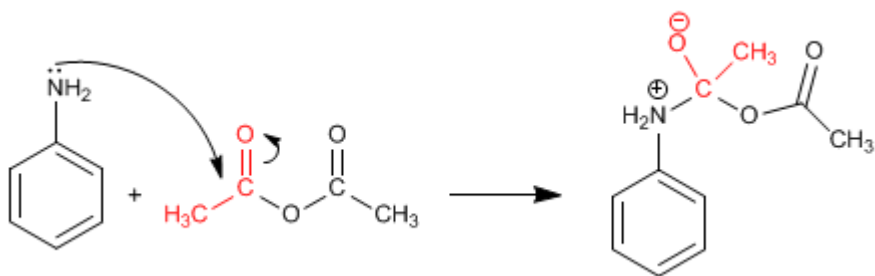


La protección del amino puede realizarse con anhídrido etanoico en piridina, o con cloruro de etanoilo en piridina

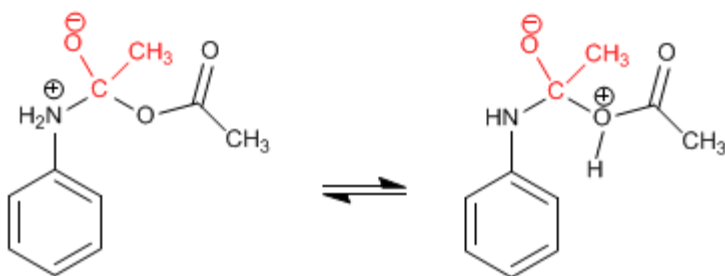


El producto final es una amida, mucho menos básica que la amina de partida y con menos tendencia a protonarse. El mecanismo de la reacción es el siguiente:

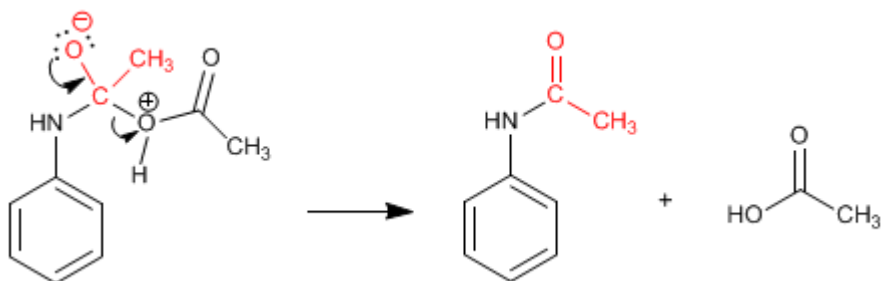
Etapla 1. Adición



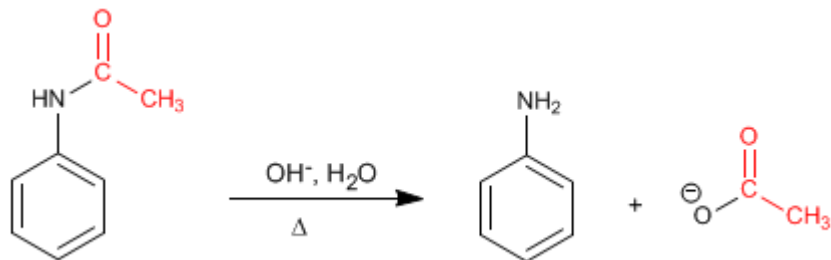
Etapla 2. Equilibrio ácido-base



Etapla 3. Eliminación

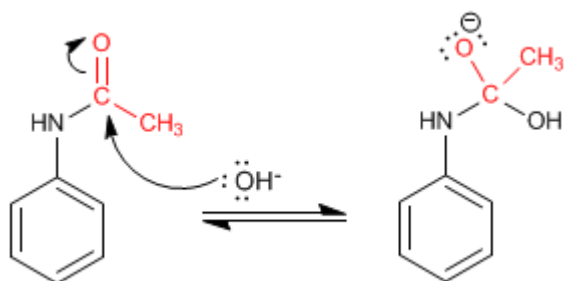


La amida formada se desprotege por hidrólisis ácida o básica, dejando libre la anilina.

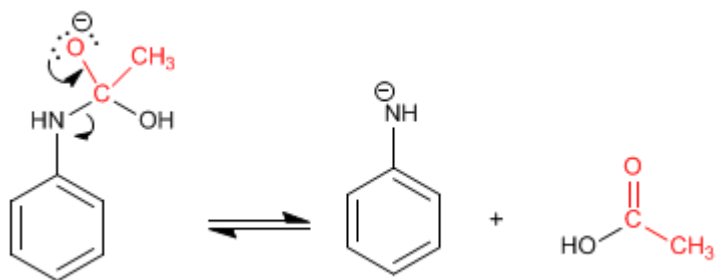


Mecanismo de desprotección en medio básico.

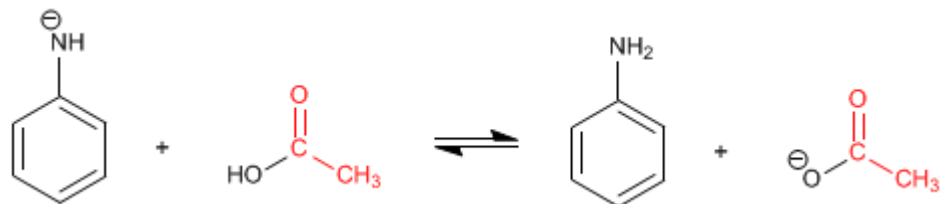
Etapla 1. Adición del grupo hidroxilo a la amida



Etapla 2. Eliminación

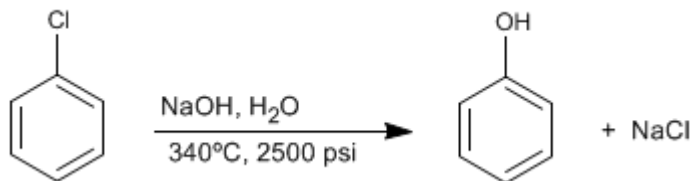


Etapla 3. Equilibrio ácido-base



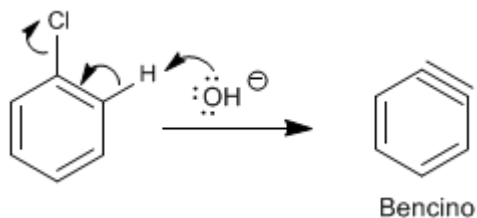
Sustitución nucleófila aromática: Bencino

Los bencenos halogenados reaccionan con sosa diluida en condiciones de alta presión y temperatura, para formar fenoles. Esta reacción no requiere grupos desactivantes en posición orto/para y sigue un mecanismo diferente al de la sustitución nucleófila aromática por adición-eliminación.

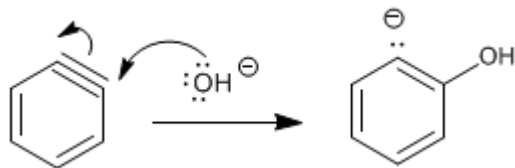


Esta reacción fue descubierta en 1928 por los químicos de la compañía Dow Chemical. El mecanismo consiste en la eliminación de HCl con formación de un intermedio inestable llamado bencino, el cual es atacado por los iones hidróxido del medio, para formar fenol.

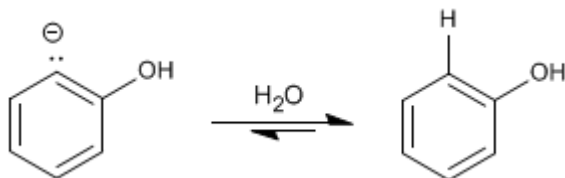
Etapas 1. Eliminación de HCl



Etapas 2. Adición del ion hidróxido al bencino



Etapas 3. Protonación



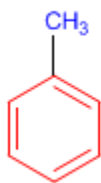
El mecanismo de esta reacción recibe el nombre de sustitución nucleófila aromática por eliminación-adición.

Cuando en el benceno existen sustituyentes produce mezclas, debido al ataque del nucleófilo sobre los dos carbonos del triple enlace.

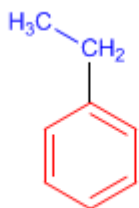
PROBLEMAS NOMENCLATURA - BENCENO

Nomenclatura de Benceno - Reglas IUPAC

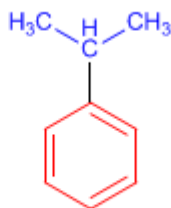
Regla 1. En bencenos monosustituídos, se nombra primero el radical y se termina en la palabra benceno.



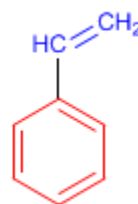
Metilbenceno



Etilbenceno

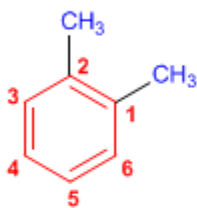


Isopropilbenceno



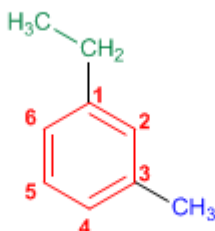
Vinilbenceno

Regla 2. En bencenos disustituídos se indica la posición de los radicales mediante los prefijos *orto-* (*o-*), *meta-* (*m-*) y *para-* (*p-*). También pueden emplearse los localizadores 1,2-, 1,3- y 1,4-.



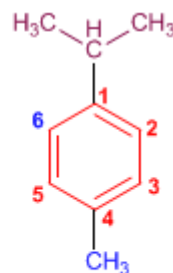
o-Dimetilbenceno

(1,2-Dimetilbenceno)



m-Etilmetilbenceno

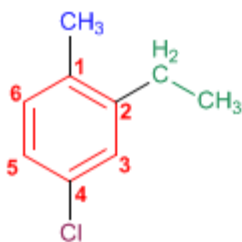
(1-Etil-3-metilbenceno)



p-Isopropilmetilbenceno

(1-Isopropil-4-metilbenceno)

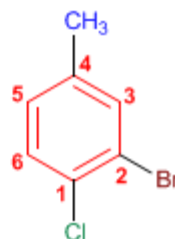
Regla 3. En bencenos con más de dos sustituyentes, se numera el anillo de modo que los sustituyentes tomen los menores localizadores. Si varias numeraciones dan los mismos localizadores se da preferencia al orden alfabético.



4-Cloro-2-etil-1-metilbenceno

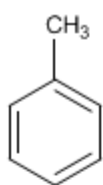


1,4-Dietil-2-metilbenceno

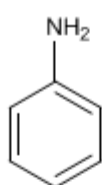


2-Bromo-1-cloro-4-metilbenceno

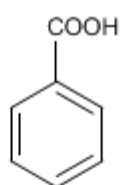
Regla 4. Existen numerosos derivados del benceno con nombres comunes que conviene saber:



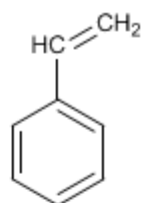
Tolueno



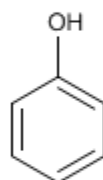
Anilina



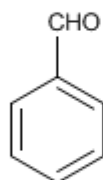
Ac. Benzoico



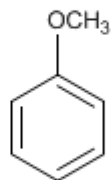
Estireno



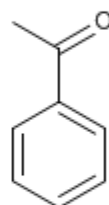
Fenol



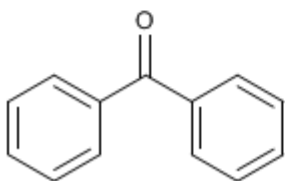
Benzaldehído



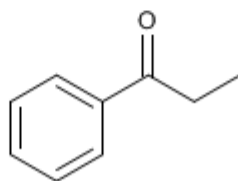
Anisol



Acetofenona



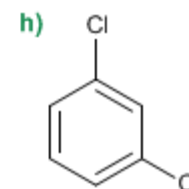
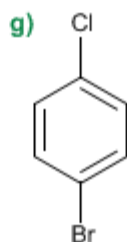
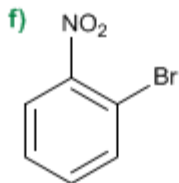
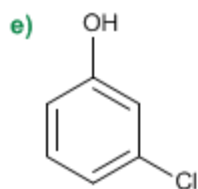
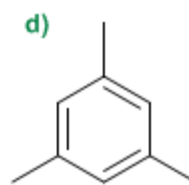
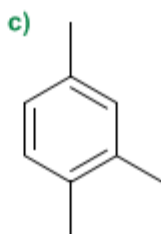
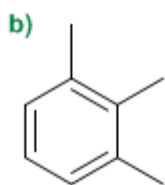
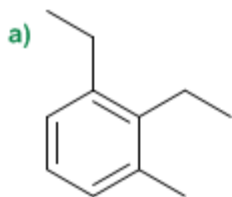
Benzofenona



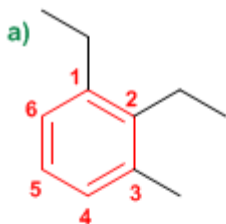
Propiofenona

Nomenclatura de Benceno - Problema 0.1

Nombra los siguientes derivados del benceno:



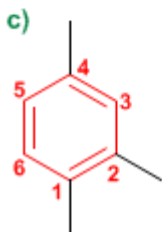
Solución



1. Cadena principal: benceno
2. Numeración: los sustituyentes deben tomar los menores localizadores, y además, se asignan los localizadores menores a los grupos que van antes en el orden alfabético (etilo antes que metilo)
3. Sustituyentes: etilos en 1,2 y metilo en 3.
4. Nombre: 1,2-Dietil-3-metilbenceno



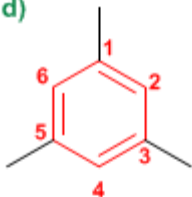
1. Cadena principal: benceno
2. Numeración: los sustituyentes deben tomar los menores localizadores.
3. Sustituyentes: metilos en posición 1,2,3.
4. Nombre: 1,2,3-Trimetilbenceno



1. Cadena principal: benceno
2. Numeración: los sustituyentes deben tomar los menores localizadores.
3. Sustituyentes: metilos en posición 1,2,4.
4. Nombre: 1,2,4-Trimetilbenceno

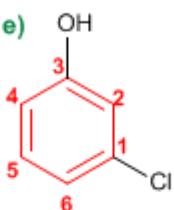
El anillo se numera para que los sustituyentes tomen los localizadores más bajos. En caso de empate se tiene en cuenta el orden alfabético

d)



1. Cadena principal: benceno
2. Numeración: se parte de un metilo y se numera en cualquier dirección.
3. Sustituyentes: metilos en 1,3,5.
4. Nombre: 1,3,5-Trimetilbenceno

e)



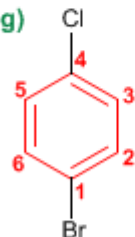
1. Cadena principal: benceno
2. Numeración: la numeración comienza en el cloro (va antes alfabéticamente) y prosigue por el camino más corto hacia el hidroxilo.
3. Sustituyentes: cloro en posición 1 e hidroxilo en posición 3 (posición meta)
4. Nombre: 1-Cloro-3-hidroxibenceno (*m*-Clorohidroxibenceno)

f)



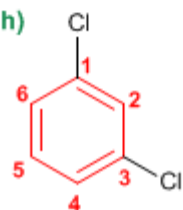
1. Cadena principal: benceno
2. Numeración: la numeración comienza en el bromo (preferencia alfabética)
3. Sustituyentes: bromo en posición 1 y nitro en posición 3 (posición orto)
4. Nombre: 1-Bromo-3-nitrobenzono (*o*-Bromonitrobenzono)

g)



1. Cadena principal: benceno
2. Numeración: comienza en el bromo (preferencia alfabética sobre el cloro)
3. Sustituyentes: bromo en 1 y cloro en 4 (posición para)
4. Nombre: 1-Bromo-4-clorobenceno (*p*-Bromoclorobenceno)

h)



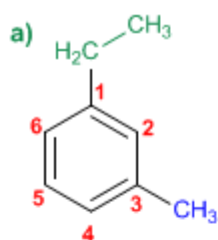
1. Cadena principal: benceno
2. Numeración: localizadores más bajos posibles a los cloros.
3. Sustituyentes: cloros en posición 1,3.
4. Nombre: 1,3-Diclorobenceno (*m*-Diclorobenceno)

Nomenclatura de Benceno - Problema 0.2

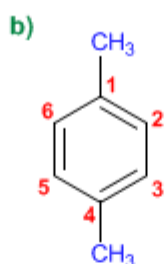
Formular los siguientes derivados del benceno:

- | | |
|---|---|
| a) 1-Etil-3-metilbenceno | k) 4,5-Difenil-1-octeno |
| b) <i>p</i> -Dimetilbenceno | l) 2-Fenil-4-metilhexeno |
| c) 1-Butil-3-etilbenceno | m) 1-(metiletil)-4-(2-metilpropil)benceno |
| d) <i>o</i> -Cloronitrobenceno | n) 6-Fenil-3-metilhexa-1,4-dieno |
| e) <i>m</i> -Bromoclorobenceno | o) <i>cis</i> -1-Fenil-1-buteno |
| f) <i>p</i> -Diisopropilbenceno | p) <i>trans</i> -2-Fenil-2-buteno |
| g) 1- <i>tert</i> -Butil-4-metilbenceno | q) 7-Etil-4,5-difenildec-5-en-1-ino |
| h) <i>o</i> -Alilvinilbenceno | r) <i>m</i> -Diciclohexilbenceno |
| i) <i>m</i> -Etilpropilbenceno | s) <i>p</i> -Ciclobutilciclobutilbenceno |
| j) 2-Etil-1,4-dimetilbenceno | t) 3-(1,1-Difeniletil)-3-metilhex-1-en-5-ino. |

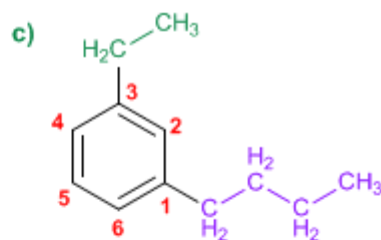
Solución



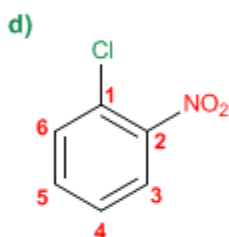
1-Etil-3-metilbenceno



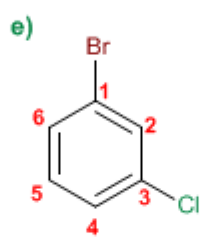
p-Dimetilbenceno



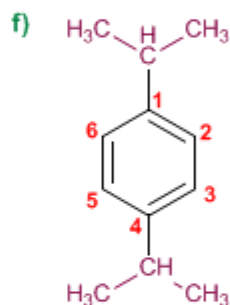
1-Butil-3-etilbenceno



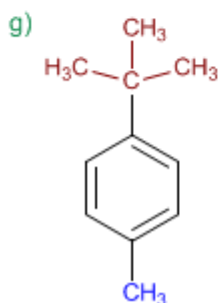
o-Cloronitrobenceno



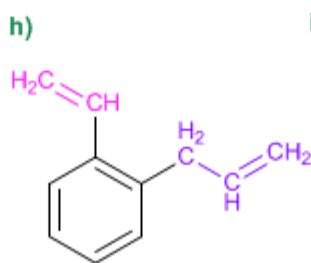
m-Bromoclorobenceno



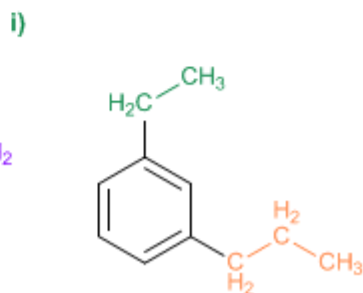
p-Diisopropilbenceno



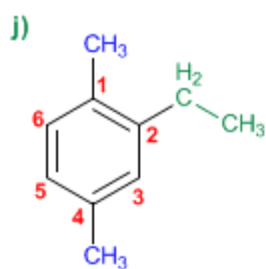
1-*tert*-Butil-4-metilbenceno



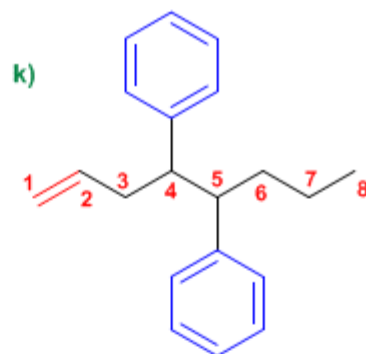
o-Alilvinilbenceno



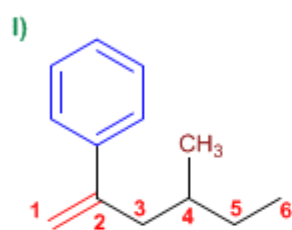
m-Etilpropilbenceno



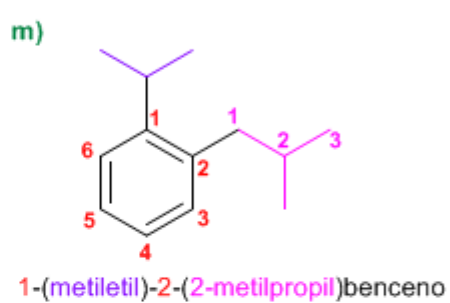
2-Etil-1,4-dimetilbenceno



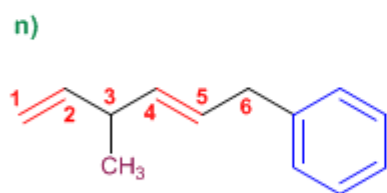
4,5-Difenil-1-eno



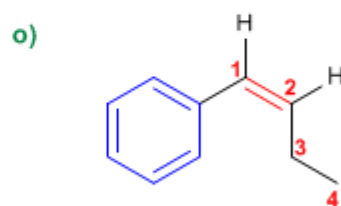
2-Fenil-4-metilhex-1-eno



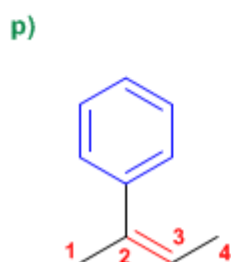
1-(metiletil)-2-(2-metilpropil)benceno



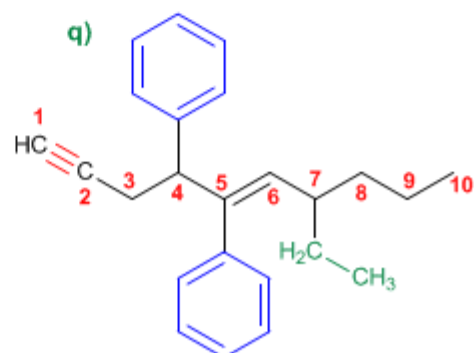
6-Fenil-3-metilhexa-1,4-dieno



cis-1-Fenil-1-butenó

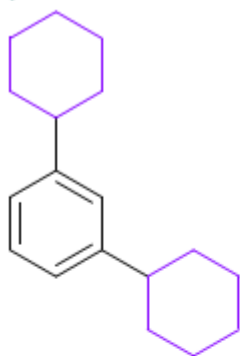


trans-2-Fenil-2-butenó



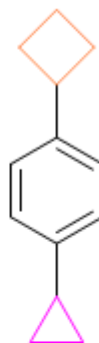
7-Etil-4,5-difenildec-5-en-1-ino

r)



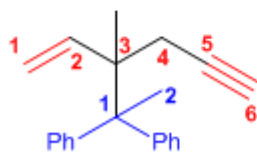
m-Diciclohexilbenceno

s)



p-Ciclobutilciclopropilbenceno

t)



3-(1,1-Difeniletil)-3-metilhex-1-en-5-ino.

Agradecimientos:

❖ <http://www.quimicaorganica.org>

❖ <http://www.taringa.net/perfil/jose07070012>

5ª edición

Química Orgánica



PEARSON
Prentice
Hall

L. C. Wade, Jr.

ÍNDICE DE CONTENIDOS

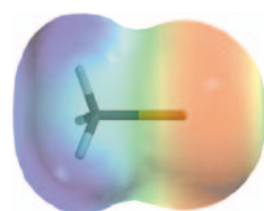
Prefacio xxii

Sobre el autor xxxvii

Capítulo 1

Introducción y revisión 1

- 1.1 Los orígenes de la química orgánica 1
- 1.2 Principios de la estructura atómica 3
- 1.3 La formación del enlace: la regla del octeto 6
- 1.4 Estructuras de Lewis 7
- 1.5 Enlace múltiple 8
 - Resumen: Modelos de enlace más frecuentes (sin carga) 9
- 1.6 La electronegatividad y la polaridad de enlace 9
- 1.7 Cargas formales 11
- 1.8 Estructuras iónicas 12
 - Resumen: Modelos de enlace más frecuentes en los compuestos e iones orgánicos 13
- 1.9 Resonancia 13
- 1.10 Fórmulas estructurales 17
- 1.11 Fórmulas moleculares y fórmulas empíricas 20
- 1.12 Ácidos y bases de Arrhenius 21
- 1.13 Ácidos y bases de Brønsted-Lowry 22
- 1.14 Ácidos y bases de Lewis 29
 - Glosario del Capítulo 1 32
 - Problemas 34

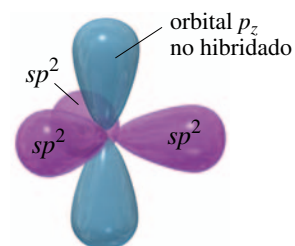


mapa del potencial electrostático del clorometano

Capítulo 2

Estructura y propiedades de las moléculas orgánicas 38

- 2.1 Propiedades ondulatorias de los electrones en los orbitales 38
- 2.2 Orbitales moleculares 40
- 2.3 Enlaces pi 43
- 2.4 Hibridación y geometría molecular 44
- 2.5 Representación de moléculas tridimensionales 47
- 2.6 Reglas generales de la hibridación y de la geometría 48
- 2.7 Rotación de enlaces 53
- 2.8 Isomería 54
- 2.9 Polaridad de enlaces y moléculas 57
- 2.10 Atracciones y repulsiones intermoleculares 60
- 2.11 Efecto de la polaridad en la solubilidad 64
- 2.12 Hidrocarburos 67
- 2.13 Compuestos orgánicos oxigenados 70
- 2.14 Compuestos orgánicos nitrogenados 72
 - Glosario del Capítulo 2 74
 - Problemas 76



átomo de carbono con hibridación sp^2 (vista lateral)

Capítulo 3

Estructura y estereoquímica de los alcanos 80

- 3.1 Clasificación de los hidrocarburos (revisión) 80
- 3.2 Fórmulas moleculares de los alcanos 81
- 3.3 Nomenclatura de los alcanos 82
Resumen: Reglas para la nomenclatura de los alcanos 87
- 3.4 Propiedades físicas de los alcanos 88
- 3.5 Aplicaciones y fuentes de los alcanos 90
- 3.6 Reacciones de los alcanos 92
- 3.7 Estructura y conformaciones de los alcanos 93
- 3.8 Conformaciones del butano 97
- 3.9 Conformaciones de los alcanos de cadena larga 99
- 3.10 Cicloalcanos 100
- 3.11 Isomería *cis-trans* en cicloalcanos 102
- 3.12 Estabilidad de los cicloalcanos: tensión de anillo 102
- 3.13 Conformaciones del ciclohexano 106
Estrategias para resolver problemas: Representación de las conformaciones de silla 109
- 3.14 Conformaciones de ciclohexanos monosustituídos 110
- 3.15 Conformaciones de ciclohexanos disustituídos 113
Estrategias para resolver problemas: Reconocimiento de isómeros *cis* y *trans* 115
- 3.16 Moléculas bicíclicas 117
Glosario del Capítulo 3 118
Problemas 122



Capítulo 4

El estudio de las reacciones químicas 124

- 4.1 Introducción 124
- 4.2 Cloración del metano 124
- 4.3 Reacción radicalaria en cadena 125
MECANISMO CLAVE: Halogenación radicalaria 127
- 4.4 Constantes de equilibrio y energía libre 129
- 4.5 Entalpía y entropía 131
- 4.6 Energías de disociación de enlace 133
- 4.7 Variación de entalpía en la reacción de cloración 135
- 4.8 Cinética y ecuación de velocidad 136
- 4.9 Energía de activación e influencia de la temperatura en la velocidad de reacción 138
- 4.10 Estados de transición 140
- 4.11 Velocidades en reacciones de varias etapas 141
- 4.12 Influencia de la temperatura en la reacción de halogenación 142
- 4.13 Halogenación de alcanos superiores 143
- 4.14 El postulado de Hammond 149
Estrategias para resolver problemas: Propuesta de un mecanismo de reacción 151
- 4.15 Inhibidores radicalarios 153
- 4.16 Intermedios reactivos 154
Resumen: Intermedios reactivos 160
Glosario del Capítulo 4 160
Problemas 163

Capítulo 5

Estereoquímica 167

- 5.1 Introducción 167
- 5.2 Quiralidad 168
- 5.3 Nomenclatura (*R*) y (*S*) de átomos de carbono asimétricos 174
- 5.4 Actividad óptica 178
- 5.5 Discriminación biológica de los enantiómeros 183
- 5.6 Mezclas racémicas 184
- 5.7 Exceso enantiomérico y pureza óptica 186
- 5.8 Quiralidad de sistemas conformacionalmente móviles 187
- 5.9 Compuestos quirales sin átomos asimétricos 189
- 5.10 Proyecciones de Fischer 191
 - Resumen: Las proyecciones de Fischer y su uso 195
- 5.11 Diastereómeros o diastereoisómeros 195
 - Resumen: Tipos de isómeros 197
- 5.12 Estereoquímica de las moléculas con dos o más carbonos asimétricos 198
- 5.13 Compuestos *meso* 199
- 5.14 Configuración absoluta y relativa 201
- 5.15 Propiedades físicas de los diastereómeros 202
- 5.16 Resolución de enantiómeros 204
 - Glosario del Capítulo 5 207
 - Problemas 209



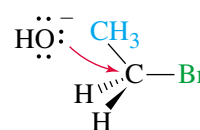
Capítulo 6

Haluros de alquilo: sustitución nucleofílica y eliminación 212

- 6.1 Introducción 212
- 6.2 Nomenclatura de haluros de alquilo 213
- 6.3 Aplicaciones y usos de los haluros de alquilo 215
- 6.4 Estructura de los haluros de alquilo 217
- 6.5 Propiedades físicas de los haluros de alquilo 218
- 6.6 Preparación de los haluros de alquilo 220
 - Resumen: Métodos de preparación de los haluros de alquilo 222
- 6.7 Reacciones de los haluros de alquilo: sustitución y eliminación 224
- 6.8 Sustitución nucleofílica bimolecular: la reacción S_N2 225
 - MECANISMO CLAVE: La reacción S_N2 225**
- 6.9 Generalidades sobre la reacción S_N2 227
 - Resumen: Reacciones S_N2 de haluros de alquilo 227
- 6.10 Factores que condicionan las reacciones S_N2 : fuerza de los nucleófilos 228
 - Resumen: Tendencias en la nucleofilia 230
- 6.11 Reactividad del sustrato en las reacciones S_N2 233
- 6.12 Estereoquímica de la reacción S_N2 236
- 6.13 Sustitución nucleofílica unimolecular: la reacción S_N1 238
 - MECANISMO CLAVE: La reacción S_N1 239**
- 6.14 Estereoquímica de la reacción S_N1 242
- 6.15 Reordenamientos en las reacciones S_N1 243
- 6.16 Comparación de las reacciones S_N1 y S_N2 246
 - Resumen: Sustituciones nucleofílicas 247



bromuro de etilo (1°)
el ataque es fácil



- 6.17 Eliminación unimolecular: la reacción E1 248
MECANISMO CLAVE: La reacción E1 248
Resumen: Reacciones mediadas por carbocationes 251
- 6.18 Eliminación bimolecular: la reacción E2 252
MECANISMO CLAVE: La reacción E2 252
- 6.19 Orientación en las reacciones de eliminación: la regla de Saytzeff 253
- 6.20 Estereoquímica de la reacción E2 255
- 6.21 Comparación de los mecanismos de eliminación E1 y E2 257
Resumen: Reacciones de eliminación 258
Estrategias para resolver problemas: Predicción de los productos resultantes de las sustituciones y eliminaciones 259
Resumen: Reacciones de los haluros de alquilo 261
Glosario del Capítulo 6 264
Problemas 267

Capítulo 7

Estructura y síntesis de alquenos 272

- 7.1 Introducción 272
- 7.2 Descripción de los orbitales del doble enlace en los alquenos 272
- 7.3 Elementos de insaturación 274
- 7.4 Nomenclatura de los alquenos 276
- 7.5 Nomenclatura de los isómeros *cis-trans* 278
Resumen: Reglas para nombrar los alquenos 280
- 7.6 Importancia comercial de los alquenos 281
- 7.7 Estabilidad de los alquenos 283
- 7.8 Propiedades físicas de los alquenos 289
- 7.9 Síntesis de alquenos mediante eliminación de haluros de alquilo 291
- 7.10 Síntesis de alquenos mediante deshidratación de alcoholes 300
MECANISMO CLAVE: Deshidratación de un alcohol catalizada por ácidos 300
- 7.11 Métodos industriales de síntesis de alquenos a alta temperatura 301
Estrategias para resolver problemas: Propuesta de mecanismos de reacción 303
Resumen: Métodos de síntesis de alquenos 306
Glosario del Capítulo 7 308
Problemas 310



Capítulo 8

Reacción de alquenos 314

- 8.1 Reactividad del doble enlace carbono-carbono 314
- 8.2 Adición electrofílica a alquenos 315
MECANISMO CLAVE: Adición electrofílica a alquenos 315
- 8.3 Adición de haluros de hidrógeno a alquenos 317
- 8.4 Adición de agua: hidratación de alquenos 322
- 8.5 Hidratación mediante oximercuriación-desmercuriación 324
- 8.6 Alcoximercuriación-desmercuriación 326
- 8.7 Hidroboración de alquenos 328
- 8.8 Hidrogenación catalítica de alquenos 333
- 8.9 Adición de carbenos a alquenos 336
- 8.10 Adición de halógenos a alquenos 338
- 8.11 Formación de halohidrinas 341
- 8.12 Epoxidación de alquenos 344
- 8.13 Apertura de epóxidos catalizada por ácidos 345
- 8.14 Hidroxilación de alquenos en *sin* 347
- 8.15 Ruptura oxidativa de alquenos 349

- 8.16 Polimerización de alquenos 352
[Estrategias para resolver problemas: Síntesis orgánica](#) 357
Resumen: Reacciones de alquenos 359
Glosario del Capítulo 8 363
Problemas 365

Capítulo 9

Alquinos 370

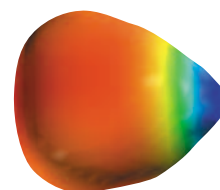
- 9.1 Introducción 370
9.2 Nomenclatura de alquinos 371
9.3 Propiedades físicas de los alquinos 372
9.4 Importancia comercial de los alquinos 372
9.5 Estructura electrónica de los alquinos 374
9.6 Acidez de los alquinos 375
9.7 Síntesis de alquinos a partir de acetiluros 378
9.8 Síntesis de alquinos mediante reacciones de eliminación 382
Resumen: Síntesis de alquinos 384
9.9 Reacciones de adición a alquinos 385
9.10 Reacciones de oxidación de alquinos 394
[Estrategias para resolver problemas: Síntesis en varias etapas](#) 396
Resumen: Reacciones de alquinos 397
Glosario del Capítulo 9 400
Problemas 401



Capítulo 10

Estructura y síntesis de alcoholes 405

- 10.1 Introducción 405
10.2 Estructura y clasificación de los alcoholes 405
10.3 Nomenclatura de los alcoholes y fenoles 407
10.4 Propiedades físicas de los alcoholes 411
10.5 Importancia comercial de los alcoholes 413
10.6 Acidez de los alcoholes y fenoles 415
10.7 Síntesis de alcoholes: introducción y revisión 418
Resumen: Síntesis previas de alcoholes 418
10.8 Reactivos organometálicos utilizados para la síntesis de alcoholes 420
10.9 Adición de reactivos organometálicos a compuestos carbonílicos 422
[MECANISMO CLAVE: Reacciones de Grignard](#) 423
Resumen: Reacciones de Grignard 429
10.10 Reacciones secundarias de compuestos organometálicos: reducción de haluros de alquilo 430
10.11 Reducción del grupo carbonilo: síntesis de alcoholes primarios y secundarios 432
Resumen: Reacciones de LiAlH_4 y NaBH_4 434
Resumen: Síntesis de alcoholes 435
10.12 Tioles (mercaptanos) 437
Glosario del Capítulo 10 440
Problemas 441



mapa de potencial
electrostático del metililitio

Capítulo 11

Reacciones de alcoholes 445

- 11.1 Estados de oxidación de los alcoholes y de los grupos funcionales relacionados 445
11.2 Oxidación de alcoholes 447
11.3 Métodos adicionales de oxidación de alcoholes 450

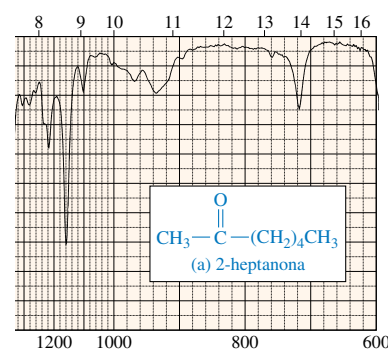
- 11.4 Oxidación biológica de alcoholes 452
- 11.5 Los alcoholes como nucleófilos y electrófilos: formación de tosilatos 454
Resumen: Reacciones S_N2 de tosilatos 456
- 11.6 Reducción de alcoholes 457
- 11.7 Reacciones de alcoholes con haluros de hidrógeno 457
- 11.8 Reacciones de alcoholes con haluros de fósforo 461
- 11.9 Reacciones de alcoholes con cloruro de tionilo 463
- 11.10 Reacciones de deshidratación de alcoholes 464
Estrategias para resolver problemas: Propuesta de mecanismos de reacción 468
- 11.11 Reacciones características de los dioles 472
- 11.12 Esterificación de alcoholes 474
- 11.13 Ésteres de ácidos inorgánicos 475
- 11.14 Reacciones de los alcóxidos 477
MECANISMO CLAVE: Síntesis de Williamson de éteres 478
Estrategias para resolver problemas: Síntesis en varias etapas 479
Resumen: Reacciones de alcoholes 482
Glosario del Capítulo 11 485
Problemas 486



Capítulo 12

Espectroscopía de infrarrojo y espectrometría de masas 490

- 12.1 Introducción 490
- 12.2 El espectro electromagnético 491
- 12.3 La región del infrarrojo 492
- 12.4 Vibraciones moleculares 493
- 12.5 Vibraciones activas e inactivas en el IR 495
- 12.6 Registro del espectro infrarrojo 496
- 12.7 Espectroscopía infrarroja de los hidrocarburos 499
- 12.8 Absorciones características de los alcoholes y las aminas 504
- 12.9 Absorciones características de los compuestos carbonílicos 505
- 12.10 Absorciones características de los enlaces C—N 511
- 12.11 Breve resumen de las frecuencias de tensión en el IR 513
- 12.12 Análisis e interpretación de los espectros de IR (problemas resueltos) 514
- 12.13 Introducción a la espectrometría de masas 519
- 12.14 Determinación de la fórmula molecular mediante espectrometría de masas 522
- 12.15 Modelos de fragmentación en la espectrometría de masas 526
Resumen: Modelos comunes de fragmentación de masas 530
Glosario del Capítulo 12 531
Problemas 533

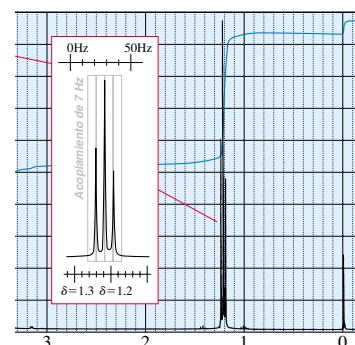


Capítulo 13

Espectroscopía de resonancia magnética nuclear 539

- 13.1 Introducción 539
- 13.2 Teoría de la resonancia magnética nuclear 539
- 13.3 Apantallamiento magnético por parte de los electrones 542
- 13.4 El espectrómetro de RMN 544
- 13.5 El desplazamiento químico 545
- 13.6 El número de señales 552
- 13.7 El área de los picos 553
- 13.8 Desdoblamiento espín-espín 556
Estrategias para resolver problemas: Representación de un espectro de RMN 561

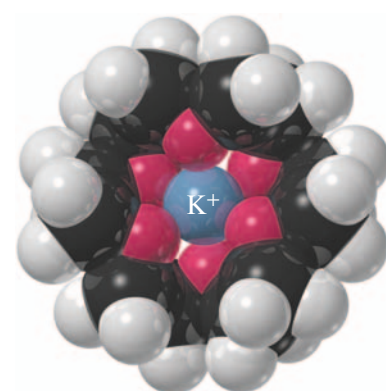
- 13.9 Acoplamientos complejos 565
- 13.10 Protones no equivalentes según la estequímica 568
- 13.11 Dependencia de la variable tiempo en la espectroscopía de RMN 571
Estrategias para resolver problemas: Interpretación de un espectro de RMN de protón 574
- 13.12 Espectroscopía de RMN de carbono-13 579
- 13.13 Interpretación de un espectro de RMN de carbono 584
- 13.14 Imágenes mediante resonancia magnética nuclear 587
Estrategias para resolver problemas: Problemas de espectroscopía 588
- Glosario del Capítulo 13 592
- Problemas 593



Capítulo 14

Éteres, epóxidos y sulfuros 600

- 14.1 Introducción 600
- 14.2 Propiedades físicas de los éteres 600
- 14.3 Nomenclatura de los éteres 605
- 14.4 Espectroscopía de los éteres 608
- 14.5 La síntesis de Williamson de éteres 610
- 14.6 Síntesis de éteres mediante alcoximercuriación-desmercuriación 612
- 14.7 Síntesis industrial: deshidratación bimolecular de alcoholes 612
Resumen: Síntesis de éteres 613
- 14.8 Ruptura de éteres con HBr y HI 613
- 14.9 Autooxidación de éteres 615
Resumen: Reacciones de éteres 616
- 14.10 Sulfuros (tioéteres) 616
- 14.11 Síntesis de epóxidos 619
Resumen: Síntesis de epóxidos 622
- 14.12 Apertura de epóxidos catalizada por ácidos 622
- 14.13 Apertura de epóxidos catalizada por bases 625
- 14.14 Orientación en la apertura de epóxidos 627
- 14.15 Reacciones de epóxidos con reactivos de Grignard y compuestos organolíticos 629
- 14.16 Resinas epoxi: el advenimiento de los pegamentos modernos 629
Resumen: Reacciones de epóxidos 631
- Glosario del Capítulo 14 632
- Problemas 634



éter 18-corona-6
solvatando el K^+

Capítulo 15

Sistemas conjugados, simetría orbital y espectroscopía ultravioleta 638

- 15.1 Introducción 638
- 15.2 Estabilidad de los dienos 638
- 15.3 Los sistemas conjugados según la teoría de orbitales moleculares 640
- 15.4 Los cationes alílicos 644
- 15.5 Adición 1,2 y 1,4 a dienos conjugados 645
- 15.6 Control cinético frente a control termodinámico en la adición de HBr a 1,3-butadieno 647
- 15.7 Radicales alílicos 649
- 15.8 Los orbitales moleculares del sistema alílico 651
- 15.9 Configuraciones electrónicas del radical, del catión y del anión alilo 652
- 15.10 Reacciones de sustitución S_N2 de haluros de alilo y de tosilatos 654
- 15.11 La reacción de Diels-Alder 655



MECANISMO CLAVE: La reacción de Diels-Alder 656

- 15.12 La reacción de Diels-Alder como ejemplo de una reacción pericíclica 663
- 15.13 Espectroscopía de absorción ultravioleta 666
- Glosario del Capítulo 15 672
- Problemas 675

Capítulo 16

Compuestos aromáticos 679

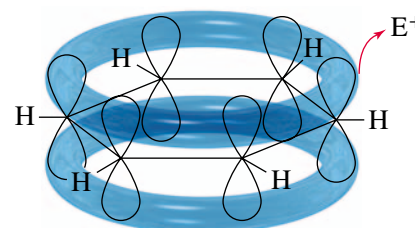
- 16.1 Introducción: el descubrimiento del benceno 679
- 16.2 Estructura y propiedades del benceno 679
- 16.3 Los orbitales moleculares del benceno 684
- 16.4 El ciclobutadieno según la teoría de orbitales moleculares 686
- 16.5 Compuestos aromáticos, antiaromáticos y no aromáticos 688
- 16.6 La regla de Hückel 689
- 16.7 Derivación de la regla de Hückel de la teoría de orbitales moleculares 691
- 16.8 Iones aromáticos 692
- 16.9 Compuestos aromáticos heterocíclicos 697
- 16.10 Hidrocarburos aromáticos polinucleares 702
- 16.11 Alótropos aromáticos del carbono 704
- 16.12 Compuestos heterocíclicos fusionados 706
- 16.13 Nomenclatura de los derivados del benceno 707
- 16.14 Propiedades físicas del benceno y de sus derivados 709
- 16.15 Espectroscopía de los compuestos aromáticos 710
- Glosario del Capítulo 16 713
- Problemas 715



Capítulo 17

Reacciones de compuestos aromáticos 722

- 17.1 Sustitución electrofílica aromática 722
- MECANISMO CLAVE: Sustitución electrofílica aromática 723**
- 17.2 Halogenación del benceno 723
- 17.3 Nitración del benceno 726
- 17.4 Sulfonación del benceno 726
- 17.5 Nitración del tolueno: efecto de la sustitución con grupos alquilo 728
- 17.6 Sustituyentes activadores *orto* y *para*-orientadores 730
- Resumen: Activadores *orto* y *para*-orientadores 733
- 17.7 Sustituyentes desactivadores *meta*-orientadores 734
- Resumen: Desactivadores *meta*-orientadores 737
- 17.8 Sustituyentes halogenados: desactivadores, pero *orto*, *para*-orientadores 737
- Resumen: Efectos orientadores de los sustituyentes 739
- 17.9 Efecto de múltiples sustituyentes sobre la sustitución electrofílica aromática 739
- 17.10 Alquilación de Friedel-Crafts 742
- 17.11 Acilación de Friedel-Crafts 746
- Resumen: Comparación de la alquilación y acilación de Friedel-Crafts 748
- 17.12 Sustitución nucleofílica aromática 750
- 17.13 Reacciones de adición de los derivados del benceno 754
- 17.14 Reacciones de las cadenas laterales de los derivados del benceno 757
- 17.15 Reacciones de los fenoles 761
- Resumen: Reacciones de los compuestos aromáticos 764
- Glosario del Capítulo 17 767
- Problemas 769



Capítulo 18

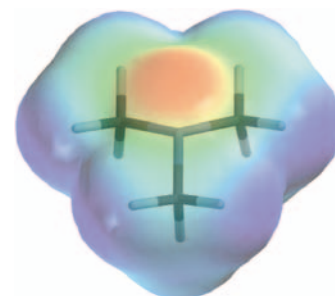
Cetonas y aldehídos 774

- 18.1 Compuestos carbonílicos 774
- 18.2 Estructura del grupo carbonilo 775
- 18.3 Nomenclatura de cetonas y aldehídos 775
- 18.4 Propiedades físicas de cetonas y aldehídos 778
- 18.5 Espectroscopía de cetonas y aldehídos 780
- 18.6 Importancia industrial de cetonas y aldehídos 787
- 18.7 Revisión de la síntesis de cetonas y aldehídos 787
- 18.8 Síntesis de cetonas y aldehídos a partir de 1,3-ditianos 791
- 18.9 Síntesis de cetonas a partir de ácidos carboxílicos 792
- 18.10 Síntesis de cetonas a partir de nitrilos 793
- 18.11 Síntesis de aldehídos y cetonas a partir de cloruros de ácido 793
Resumen: Síntesis de cetonas y aldehídos 795
- 18.12 Reacciones de cetonas y aldehídos: adición nucleofílica 797
MECANISMO CLAVE: Adiciones nucleofílicas a grupos carbonilo 800
- 18.13 La reacción de Wittig 800
- 18.14 Hidratación de cetonas y aldehídos 804
- 18.15 Formación de cianohidrinas 806
- 18.16 Formación de iminas 807
MECANISMO CLAVE: Formación de iminas 808
- 18.17 Condensaciones con hidroxilamina e hidrazinas 810
Resumen: Condensación de aminas con cetonas y aldehídos 811
- 18.18 Formación de acetales 811
MECANISMO CLAVE: Formación de acetales 812
Estrategias para resolver problemas: Propuesta de mecanismos de reacción 815
- 18.19 El uso de acetales como grupos protectores 817
- 18.20 Oxidación de aldehídos 818
- 18.21 Otras reducciones de cetonas y aldehídos 819
Resumen: Reacciones de cetonas y aldehídos 821
Glosario del Capítulo 18 824
Problemas 827

Capítulo 19

Aminas 836

- 19.1 Introducción 836
- 19.2 Nomenclatura de las aminas 837
- 19.3 Estructura de las aminas 839
- 19.4 Propiedades físicas de las aminas 841
- 19.5 Basicidad de las aminas 842
- 19.6 Efectos sobre la basicidad de las aminas 844
- 19.7 Sales de amonio 846
- 19.8 Sales de amonio y catalizadores de transferencia de fase 848
- 19.9 Espectroscopía de las aminas 849
- 19.10 Reacciones de las aminas con cetonas y aldehídos (revisión) 854
- 19.11 Sustitución aromática en arilaminas y piridina (revisión) 854
- 19.12 Alquilación de aminas con haluros de alquilo 858
- 19.13 Acilación de aminas con cloruros de ácido 859
- 19.14 Formación de sulfonamidas 861
- 19.15 Aminas como grupos salientes: la eliminación de Hofmann 862
- 19.16 Oxidación de aminas. La eliminación de Cope 865



mapa de potencial electrostático de la trimetilamina

- 19.17 Reacciones de aminas con ácido nitroso 868
- 19.18 Reacciones de las sales de diazonio aromáticas 870
- Resumen: Reacciones de las aminas 874
- 19.19 Síntesis de aminas 877
- Resumen: Síntesis de aminas 887
- Glosario del Capítulo 19 890
- Problemas 892

Capítulo 20

Ácidos carboxílicos 900

- 20.1 Introducción 900
- 20.2 Nomenclatura de los ácidos carboxílicos 900
- 20.3 Estructura y propiedades físicas de los ácidos carboxílicos 904
- 20.4 Acidez de los ácidos carboxílicos 906
- 20.5 Sales de ácidos carboxílicos 909
- 20.6 Fuentes comerciales de los ácidos carboxílicos 912
- 20.7 Espectroscopía de los ácidos carboxílicos 913
- 20.8 Síntesis de los ácidos carboxílicos 918
- Resumen: Síntesis de los ácidos carboxílicos 920
- 20.9 Reacciones de los ácidos carboxílicos y sus derivados. Sustitución nucleofílica en el grupo acilo 921
- 20.10 Condensación de los ácidos con los alcoholes: la esterificación de Fischer 922
- MECANISMO CLAVE: Esterificación de Fischer 923**
- 20.11 Síntesis y aplicaciones de los cloruros de ácido 925
- 20.12 Esterificación con diazometano 928
- 20.13 Condensación de ácidos con aminas: síntesis directa de amidas 928
- 20.14 Reducción de los ácidos carboxílicos 929
- 20.15 Alquilación de los ácidos carboxílicos para obtener cetonas 931
- Resumen: Reacciones de los ácidos carboxílicos 931
- Glosario del Capítulo 20 933
- Problemas 934

Capítulo 21

Derivados de los ácidos carboxílicos 940

- 21.1 Introducción 940
- 21.2 Estructura y nomenclatura de los derivados de ácido 941
- 21.3 Propiedades físicas de los derivados de ácidos carboxílicos 947
- 21.4 Espectroscopía de los derivados de ácidos carboxílicos 950
- 21.5 Interconversión entre los derivados de ácidos mediante sustitución nucleofílica en el grupo acilo 957
- MECANISMO CLAVE: Mecanismo de adición-eliminación en la sustitución nucleofílica en el grupo acilo 957**
- 21.6 Sustitución nucleofílica en el grupo acilo catalizada por ácidos 964
- Estrategias para resolver problemas: Propuestas de mecanismos de reacción 965**
- 21.7 Hidrólisis de los derivados de ácidos carboxílicos 968
- 21.8 Reducción de los derivados de ácidos 972
- 21.9 Reacciones de los derivados de ácidos con reactivos organometálicos 975
- 21.10 Resumen de la química de los cloruros de ácido 976
- 21.11 Resumen de la química de los anhídridos de ácido 978
- 21.12 Resumen de la química de los ésteres 981
- 21.13 Resumen de la química de las amidas 984
- 21.14 Resumen de la química de los nitrilos 987
- 21.15 Tioésteres 988

- 21.16 Ésteres y amidas del ácido carbónico 990
- Glosario del Capítulo 21 992
- Problemas 994

Capítulo 22

Sustituciones en alfa, y condensaciones de enoles y de iones enolato 1003

- 22.1 Introducción 1003
- 22.2 Enoles e iones enolato 1004
- 22.3 Halogenación en alfa de cetonas 1007
- 22.4 Bromación en alfa de ácidos: la reacción de HVZ (Hell-Volhard-Zelinsky) 1012
- 22.5 Alquilación de iones enolato 1013
- 22.6 Formación y alquilación de enaminas 1015
- 22.7 Condensación aldólica de cetonas y aldehídos 1017
- MECANISMO CLAVE: Condensación aldólica catalizada por una base 1018**
- 22.8 Deshidratación de aldoles 1020
- MECANISMO CLAVE: Deshidratación de un aldol 1021**
- 22.9 Condensaciones aldólicas cruzadas 1021
- Estrategias para resolver problemas: Propuesta de mecanismos de reacción 1022**
- 22.10 Ciclaciones aldólicas 1025
- 22.11 Diseño de síntesis utilizando condensaciones aldólicas 1026
- 22.12 La condensación de Claisen de ésteres 1027
- MECANISMO CLAVE: Condensación de Claisen 1028**
- 22.13 La condensación de Dieckmann: un tipo de ciclación de Claisen 1031
- 22.14 Condensaciones de Claisen cruzadas 1031
- 22.15 Síntesis empleando compuestos β -dicarbonílicos 1034
- 22.16 La síntesis malónica 1036
- 22.17 La síntesis acetilacética 1039
- 22.18 Adiciones conjugadas: la reacción de Michael 1042
- MECANISMO CLAVE: Adiciones 1,2 y 1,4 1043**
- 22.19 La anillación de Robinson 1046
- Estrategias para resolver problemas: Propuesta de mecanismos de reacción 1047**
- Resumen: Adiciones y condensaciones de enolatos 1049
- Glosario del Capítulo 22 1051
- Problemas 1052



Capítulo 23

Carbohidratos y ácidos nucleicos 1057

- 23.1 Introducción 1057
- 23.2 Clasificación de los hidratos de carbono 1058
- 23.3 Monosacáridos 1059
- 23.4 Diastereómeros *eritro* y *treo* 1062
- 23.5 Epímeros 1063
- 23.6 Estructura cíclica de los monosacáridos 1064
- 23.7 Anómeros de los monosacáridos. Mutarrotación 1068
- 23.8 Reacciones de los monosacáridos: reacciones secundarias en medio básico 1070
- 23.9 Reducción de los monosacáridos 1072
- 23.10 Oxidación de los monosacáridos. Los azúcares reductores 1073
- 23.11 Los azúcares no reductores: formación de glicósidos 1075
- 23.12 Formación de éteres y ésteres 1078
- 23.13 Reacciones con fenilhidrazina: formación de osazonas 1080
- 23.14 Acortamiento de la cadena: degradación de Ruff 1081

- 23.15 Alargamiento de la cadena: síntesis de Kiliani-Fischer 1081
Resumen: Reacciones de los azúcares 1083
- 23.16 La prueba de Fischer de la configuración de la glucosa 1085
- 23.17 Determinación del tamaño del anillo. Escisión de azúcares con ácido peryódico 1088
- 23.18 Disacáridos 1090
- 23.19 Polisacáridos 1095
- 23.20 Ácidos nucleicos: introducción 1098
- 23.21 Ribonucleósidos y ribonucleótidos 1100
- 23.22 La estructura del ácido ribonucleico 1102
- 23.23 La desoxirribosa y la estructura del ácido desoxirribonucleico 1102
- 23.24 Funciones adicionales de los nucleótidos 1106
Glosario del Capítulo 23 1108
Problemas 1111

Capítulo 24

Aminoácidos, péptidos y proteínas 1114

- 24.1 Introducción 1114
- 24.2 Estructura y estereoquímica de los α -aminoácidos 1115
- 24.3 Propiedades ácido-base de los aminoácidos 1119
- 24.4 Puntos isoeléctricos y electroforesis 1121
- 24.5 Síntesis de aminoácidos 1123
Resumen: Síntesis de aminoácidos 1127
- 24.6 Resolución de los aminoácidos 1128
- 24.7 Reacciones de los aminoácidos 1129
Resumen: Reacciones de aminoácidos 1131
- 24.8 Estructura y nomenclatura de péptidos y proteínas 1132
- 24.9 Determinación de la estructura de los péptidos 1136
- 24.10 Síntesis de péptidos en solución 1142
- 24.11 Síntesis de péptidos en fase sólida 1145
- 24.12 Clasificación de las proteínas 1151
- 24.13 Niveles de la estructura de las proteínas 1151
- 24.14 Desnaturalización de las proteínas 1154
Glosario del Capítulo 24 1156
Problemas 1158

Capítulo 25

Lípidos 1162

- 25.1 Introducción 1162
- 25.2 Ceras 1162
- 25.3 Triglicéridos 1163
- 25.4 Saponificación de grasas y aceites. Jabones y detergentes 1166
- 25.5 Fosfolípidos 1170
- 25.6 Esteroides 1171
- 25.7 Prostaglandinas 1174
- 25.8 Terpenos 1175
Glosario del Capítulo 25 1179
Problemas 1180



Capítulo 26

Polímeros sintéticos 1182

- 26.1 Introducción 1182
- 26.2 Polímeros de adición 1183
- 26.3 Estereoquímica de los polímeros 1189
- 26.4 Control estereoquímico de la polimerización. Catalizadores de Ziegler-Natta 1190
- 26.5 Gomas naturales y sintéticas 1190
- 26.6 Copolímeros de dos o más monómeros 1192
- 26.7 Condensación de polímeros 1192
- 26.8 Estructura y propiedades de los polímeros 1196
- Glosario del Capítulo 26 1198
- Problemas 1200

Apéndices

- 1A Posiciones de absorción de protones en RMN, en varios entornos estructurales 1204
- 1B Constantes de acoplamiento espín-espín 1205
- 1C Desplazamientos químicos de ^{13}C en los compuestos orgánicos 1205
- 2A Grupos de frecuencias características en el infrarrojo 1206
- 2B Absorciones en el infrarrojo características de los grupos funcionales 1209
- 3 Las reglas de Woodward-Fieser para predecir los espectros del ultravioleta-visible 1211
- 4A Métodos y sugerencias para proponer mecanismos 1215
- 4B Sugerencias para desarrollar síntesis de varios pasos 1218
- 5 Valores de $\text{p}K_{\text{a}}$ de compuestos representativos 1219

Esquemas de Mecanismos y Mecanismos clave

- CAPÍTULO 4 Halogenación vía radicales libres 127
- CAPÍTULO 6 Bromación alílica 221
 - La reacción $\text{S}_{\text{N}}2$ 225
 - Inversión de la configuración en las reacciones $\text{S}_{\text{N}}2$ 237
 - La reacción $\text{S}_{\text{N}}1$ 239
 - Racemización en las reacciones $\text{S}_{\text{N}}1$ 242
 - Transposición de hidruro en las reacciones $\text{S}_{\text{N}}1$ 244
 - Transposición de metilo en la reacción $\text{S}_{\text{N}}1$ 245
 - La reacción $\text{E}1$ 248
 - Reordenamientos en la reacción $\text{E}1$ 250
 - La reacción $\text{E}2$ 252
- CAPÍTULO 7 Deshidrohalogenación a través del mecanismo $\text{E}2$ 291
 - Estereoquímica de la reacción $\text{E}2$ 293
 - Dibromación $\text{E}2$ en la formación de un dibromuro vecinal 297
 - Deshidratación de un alcohol catalizada por un ácido 300
- CAPÍTULO 8 Adición electrofílica a alquenos 315
 - Adición iónica de HBr a un alqueno 316
 - Adición radicalaria de HBr a un alqueno 319
 - Hidratación de un alqueno catalizada por ácidos 323

	Oximercuriación de un alqueno	325
	Hidroboración de un alqueno	329
	Oxidación de un trialquilborano	332
	Adición de halógenos a alquenos	339
	Formación de halohidrinas	341
	Epoxidación de alquenos	344
	Apertura de epóxidos catalizada por ácidos	345
CAPÍTULO 9	Reducción de un alquino con un metal en amoniaco líquido	388
	Tautomería ceto-enólica catalizada por ácidos	392
CAPÍTULO 10	Reacciones de Grignard	423
	Reducción de un grupo carbonilo con hidruros	432
CAPÍTULO 11	Reacción de un alcohol terciario con HBr (S_N1)	458
	Reacción de un alcohol primario con HBr (S_N2)	458
	Reacción de alcoholes con PBr_3	462
	Revisión: Deshidratación de un alcohol catalizada por un ácido	464
	La transposición pinacolínica	472
	La síntesis de Williamson de éteres	478
CAPÍTULO 14	Ruptura de un éter con HBr	614
	Apertura de un epóxido catalizada por ácidos	622
	Apertura de un epóxido catalizada por ácidos en una solución alcohólica	623
	Apertura de un epóxido catalizada por bases	626
CAPÍTULO 15	Adición 1,2 y 1,4 a dienos conjugados	646
	Bromación alílica radicalaria	649
	La reacción de Diels-Alder	656
CAPÍTULO 17	Sustitución electrofílica aromática	723
	Bromación de benceno	723
	Nitración de benceno	726
	Sulfonación de benceno	727
	Alquilación de Friedel-Crafts	743
	Acilación de Friedel-Crafts	747
	Sustitución nucleofílica aromática (adición-eliminación)	751
	Sustitución nucleofílica aromática	753
	La reducción de Birch	756
CAPÍTULO 18	Adiciones nucleofílicas al grupo carbonilo	800
	La reacción de Wittig	802
	Hidratación de cetonas y aldehídos	804
	Formación de cianohidrinas	806
	Formación de iminas	808
	Formación de acetales	812
	Reducción de Wolff-Kishner	821
CAPÍTULO 19	Sustitución electrofílica aromática de la piridina	856
	Sustitución nucleofílica aromática de la piridina	857
	Acilación de una amina con un cloruro de ácido	859
	Eliminación de Hofmann	863
	Eliminación de Cope de un óxido de amina	867
	Diazoación de una amina	868
	Transposición de Hofmann	886
CAPÍTULO 20	Sustitución nucleofílica sobre el grupo acilo de un éster	922
	Esterificación de Fischer	923
	Esterificación con diazometano	928

CAPÍTULO 21	Mecanismo de adición-eliminación en la sustitución nucleofílica en el grupo acilo 957
	Transformación de un cloruro de ácido en un anhídrido 959
	Transformación de un cloruro de ácido en un éster 960
	Transformación de un cloruro de ácido en una amida 960
	Transformación de un anhídrido de ácido en un éster 961
	Transformación de un anhídrido de ácido en una amida 961
	Transformación de un éster en una amida (amonólisis de un éster) 962
	Transesterificación 967
	Saponificación de un éster 968
	Hidrólisis de una amida en medio básico 970
	Hidrólisis de una amida en medio ácido 971
	Hidrólisis catalizada por una base de un nitrilo 972
	Reducción de un éster por un hidruro 973
	Reacción de un éster con dos moles de un reactivo de Grignard 975
CAPÍTULO 22	Sustitución en alfa 1003
	Adición de un enolato a cetonas y aldehídos (condensación) 1003
	Sustitución de un enolato en un éster (condensación) 1004
	Tautomería ceto-enólica catalizada por una base 1004
	Tautomería ceto-enólica catalizada por un ácido 1005
	Halogenación promovida por una base 1008
	Pasos finales de la reacción del haloformo 1009
	Halogenación catalizada por un ácido 1011
	Condensación aldólica catalizada por una base 1018
	Condensación aldólica catalizada por un ácido 1020
	Deshidratación de un aldol 1021
	Condensación de Claisen 1028
	Adiciones 1,2 y 1,4 1043
CAPÍTULO 23	Formación de un hemiacetal cíclico 1064
	Epimerización de la glucosa catalizada por una base 1071
	Reordenamientos enodiol catalizados por una base 1072
CAPÍTULO 26	Polimerización radicalaria 1185
	Polimerización catiónica 1186
	Polimerización aniónica 1188

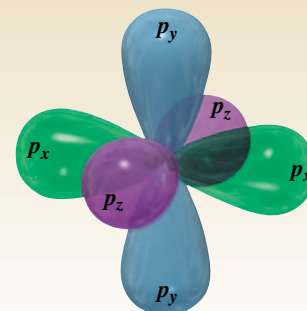
Soluciones de los problemas seleccionados A1

Créditos de las fotografías CF1

Índice I1

CAPÍTULO 1

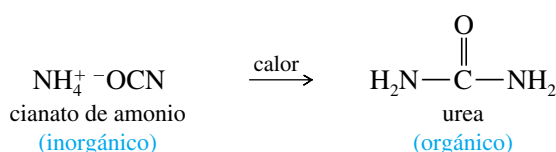
Introducción y revisión



La definición moderna de **química orgánica** es la *química de los compuestos de carbono*. ¿Qué tiene de especial el carbono que hay una rama de la química que se dedica a él? Al contrario que otros elementos, el carbono forma enlaces fuertes con otros átomos de carbono y con una gran variedad de otros elementos. Las cadenas y anillos de átomos de carbono son tan variadas que se puede formar una variedad interminable de moléculas. Esta diversidad de los compuestos de carbono es la base para la vida en la Tierra. Los seres vivos están formados de compuestos orgánicos complejos con funciones estructurales, químicas o genéticas.

El término **orgánico** literalmente significa «derivado de los organismos vivos». Originalmente, la ciencia de la química orgánica era el estudio de los compuestos que se extraían de los organismos vivos o productos naturales. Compuestos tales como azúcar, urea, levadura, ceras y aceites vegetales eran considerados «orgánicos» y se aceptó el **Vitalismo** como teoría que explicaba su origen: la creencia en que los productos naturales necesitaban una «fuerza vital» para ser creados. Por tanto, la química orgánica era el estudio de los compuestos que tenían esa fuerza vital. La química inorgánica era el estudio de los gases, rocas, minerales y de los compuestos que se podían obtener a partir de ellos.

En el siglo XIX, la experimentación demostró que los compuestos orgánicos se podían sintetizar a partir de compuestos inorgánicos. En 1828, el químico alemán Friedrich Wöhler convirtió el cianato de amonio, obtenido a partir de amoníaco y ácido ciánico, en urea simplemente calentando el cianato en ausencia de oxígeno.



La urea también proviene de los seres vivos y se creía que contenía la fuerza vital, a pesar de que el cianato de amonio es inorgánico y por tanto, según aquella creencia, no poseía la fuerza vital. Algunos químicos sostenían que esa fuerza vital provenía de las manos de Wöhler, pero la mayoría reconocieron la posibilidad de sintetizar compuestos orgánicos a partir de compuestos inorgánicos. También se llevaron a cabo otras síntesis, por lo que la teoría de la fuerza vital se descartó.

Desde que el Vitalismo se descartó a comienzos del siglo XIX, se podría pensar que esta idea habría ya desaparecido, pero estaríamos equivocados, ya que el Vitalismo hoy forma parte de la mentalidad de las personas que creen que los productos «naturales» (derivados de las plantas) son diferentes y más saludables que aquellos compuestos exactamente iguales, «artificiales», que han sido sintetizados.

Como químicos, sabemos que los compuestos derivados de las plantas y los compuestos sintetizados son idénticos. La única diferencia es el contenido en ^{14}C : los compuestos sintetizados a partir de derivados del petróleo tienen menor contenido del isótopo radioactivo ^{14}C ,

1.1

Los orígenes de la química orgánica



El corazón artificial Jarvik 7 está compuesto en gran parte de materiales orgánicos sintéticos.

ya que este isótopo ha ido desapareciendo con el tiempo. Los compuestos derivados de las plantas, al haber sido sintetizados recientemente a partir del CO_2 del aire, tienen un contenido más elevado en ^{14}C . Algunos suministradores importantes de productos químicos dan los análisis de los isótopos para confirmar que los «productos naturales» que distribuyen tienen mayor contenido en ^{14}C y son derivados de las plantas. Estos sofisticados análisis dan un aspecto de alta tecnología al Vitalismo del siglo XXI.

A pesar de que los compuestos orgánicos no necesitan una fuerza vital, todavía se diferencian de los compuestos inorgánicos. La característica que distingue a los compuestos orgánicos es que *todos* contienen uno o más átomos de carbono. Pero no todos los compuestos que contienen carbono son orgánicos, sustancias tales como: diamante, grafito, dióxido de carbono, cianato de amonio y carbonato de sodio son compuestos derivados de minerales, y tienen propiedades características de los compuestos inorgánicos. No obstante, la mayoría de los millones de compuestos que contienen carbono se clasifican como orgánicos.

Nosotros mismos estamos compuestos en gran parte por moléculas orgánicas y nos alimentamos de compuestos orgánicos. Las proteínas de nuestra piel, los lípidos de las membranas de nuestras células, el glucógeno de nuestro hígado y el DNA del núcleo de nuestras células son compuestos orgánicos. Nuestros cuerpos también están regulados y son defendidos por compuestos orgánicos complejos.

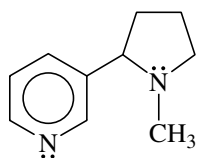
Los químicos han aprendido a diseñar y sintetizar muchas de estas moléculas complejas. Los productos sintéticos se utilizan como productos farmacéuticos, plásticos, pesticidas, pinturas y fibras. La mayoría de los avances más importantes en medicina se debe actualmente a los avances en química orgánica. Así, se sintetizan nuevos productos farmacéuticos para combatir enfermedades y se obtienen nuevos polímeros para elaborar dispositivos ortopédicos con los que sustituir órganos dañados. La química orgánica ha cerrado el ciclo, comenzó con el estudio de los compuestos derivados de «órganos» y ahora nos proporciona los productos farmacéuticos y materiales que necesitamos para salvar o reemplazar esos órganos.

Uno de los efectos de la nicotina es incrementar la concentración de una sustancia química en el sistema de estímulos cerebrales. La liberación de esta sustancia química hace que los fumadores se sientan bien y refuerza la necesidad de fumar.

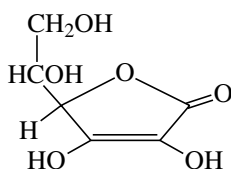
Una de las razones por las que los químicos sintetizan derivados de compuestos orgánicos complejos como la morfina es descubrir nuevas sustancias que mantengan sus propiedades útiles (analgésia) pero no las propiedades indeseables (adicción).



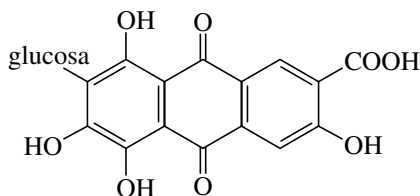
nicotina



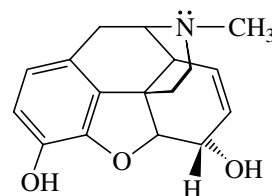
vitamina C



carmín



morfina



A continuación daré cuatro ejemplos de compuestos orgánicos aislados de organismos vivos: el tabaco contiene nicotina, un alcaloide que crea adicción; los escaramujos contienen vitamina C, esencial para prevenir el escorbuto; el carmín proviene de las cochinillas, insectos que suelen estar en las chumberas, y las adormideras contienen morfina, sustancia que mitiga el dolor pero provoca adicción.

Antes de comenzar el estudio de la química orgánica, se han de revisar algunos principios básicos. Muchos de los conceptos de estructura atómica y molecular son cruciales para entender la estructura y el enlace de los compuestos orgánicos.

1.2A Estructura del átomo

Los átomos están formados por protones, neutrones y electrones. Los protones están cargados positivamente y se encuentran, junto con los neutrones (sin carga), en el núcleo. Los electrones contienen una carga negativa de la misma magnitud que la carga positiva de los protones y se encuentran en el espacio que rodea al núcleo (Figura 1.1). Los protones y los neutrones tienen una masa parecida, aproximadamente unas 1800 veces la masa de un electrón. A pesar de que prácticamente toda la masa del átomo está concentrada en el núcleo, son los electrones los que participan en los enlaces químicos y en las reacciones.

Cada elemento se caracteriza por el número de protones que tiene en el núcleo (número atómico). El número de neutrones normalmente es parecido al número de protones, pero este número de neutrones puede variar. Los átomos que tienen el mismo número de protones pero diferente número de neutrones se llaman **isótopos**. Por ejemplo, el átomo de carbono más común es el que tiene seis protones y seis neutrones en el núcleo; su número másico (suma de protones y de neutrones) es 12, por lo que lo escribimos con el símbolo ^{12}C . Aproximadamente el 1% de los átomos de carbono tienen 7 neutrones y su número másico es 13, simbolizado por ^{13}C . Una fracción muy pequeña de átomos de carbono tiene ocho neutrones, por lo que su número másico es 14. El ^{14}C es un isótopo radioactivo, con un periodo de semidesintegración (tiempo que tarda una determinada masa de ese isótopo en desintegrarse y perder la mitad de su masa) de 5 730 años. Este tiempo de desintegración del ^{14}C se utiliza para determinar la edad de los materiales orgánicos de hasta unos 50 000 años de antigüedad.

1.2B Estructura electrónica del átomo

Las propiedades químicas de un elemento se determinan por el número de protones de su núcleo y el correspondiente número de electrones que hay alrededor del núcleo. Los electrones forman enlaces y determinan la estructura de las moléculas resultantes. Debido a que los electrones son muy pequeños y están en movimiento, se comportan simultáneamente como partículas y como ondas.

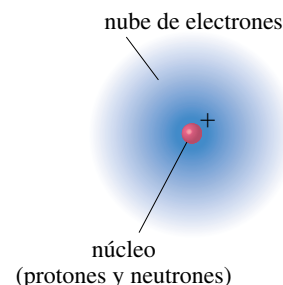
Los electrones que se encuentran moviéndose alrededor del núcleo se encuentran en **orbitales**. El principio de incertidumbre de Heisenberg dice que nunca se puede determinar con exactitud dónde se encuentra el electrón; sin embargo, se puede determinar la **densidad electrónica**, la probabilidad de encontrar al electrón en una determinada zona del orbital. Por tanto, un orbital es un estado de energía permitido para un electrón, con una función de probabilidad asociada que define la distribución de la densidad electrónica en el espacio.

Los orbitales atómicos se agrupan en «capas» o niveles diferentes a distintas distancias del núcleo. Cada capa se identifica por un número cuántico principal n , siendo $n = 1$ para la capa de menor energía (la que está más próxima al núcleo). Al aumentar n , las capas están más alejadas del núcleo, tienen una energía más alta y pueden contener más electrones. La mayoría de los elementos más comunes de los compuestos orgánicos se encuentran en las dos primeras filas (periodos) de la tabla periódica, lo que indica que sus electrones se encuentran en las dos primeras capas de electrones. La primera capa ($n = 1$) puede alojar dos electrones y la segunda capa ($n = 2$) puede alojar ocho.

La primera capa de electrones contiene solamente el orbital $1s$. Todos los orbitales s tienen simetría esférica, lo cual quiere decir que son no direccionales. La densidad electrónica del orbital $1s$ se representa en la Figura 1.2. Se puede observar que la densidad electrónica es más alta en las proximidades del núcleo y va disminuyendo exponencialmente según va aumentando la distancia al núcleo. Se podría comparar el orbital $1s$ con una cápsula de algodón, donde la semilla representaría el núcleo. La densidad del algodón es mayor en los lugares próximos a la semilla y su densidad va disminuyendo según se va alejando del núcleo.

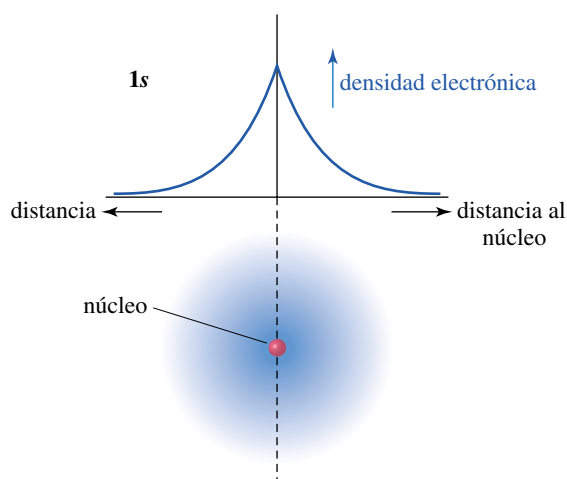
La segunda capa de electrones consta de orbitales $2s$ y $2p$. El orbital $2s$ posee simetría esférica igual que el $1s$, pero su densidad electrónica no es una simple función exponencial. El orbital $2s$ tiene una densidad electrónica más pequeña en las proximidades del

1.2 Principios de la estructura atómica



▲ Figura 1.1

El átomo tiene un denso núcleo, cargado positivamente, rodeado de una nube de electrones.

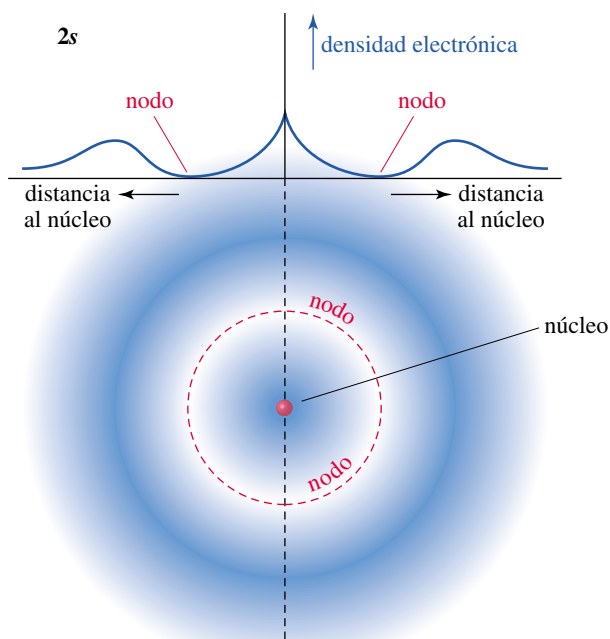


► Figura 1.2

Gráfico y diagrama del orbital atómico 1s. La densidad electrónica es más alta cerca del núcleo y disminuye exponencialmente al aumentar la distancia al núcleo en cualquier dirección.

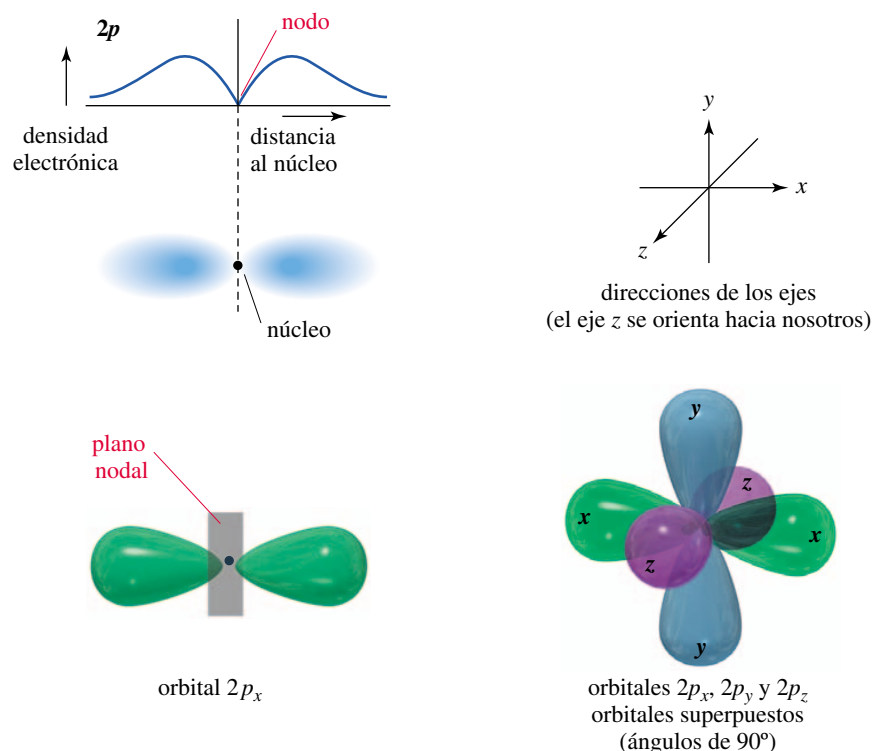
núcleo, ya que la mayor parte de la densidad electrónica está más alejada, más allá de una zona de densidad electrónica nula llamada **nodo**. Como la densidad electrónica del orbital 2s cerca del núcleo es menor que en el caso del orbital 1s, el orbital 2s tiene energía más alta. La Figura 1.3 muestra una representación gráfica del orbital 2s.

Además del orbital 2s, la segunda capa también contiene tres orbitales atómicos 2p, orientados cada uno de ellos en las tres direcciones del espacio. Estos tres orbitales reciben el nombre $2p_x$, $2p_y$ y $2p_z$, según su orientación a lo largo de los ejes x , y o z . Los orbitales 2p tienen una energía ligeramente superior a la de los orbitales 2s, debido a que la localización media de los electrones en los orbitales 2p se sitúa a una distancia más alejada del núcleo. Cada orbital p consta de dos lóbulos, uno a cada lado del núcleo, con un **plano nodal** en el núcleo. El plano nodal es una región (plana) del espacio que incluye el núcleo y tiene una densidad electrónica nula. Los tres orbitales 2p únicamente difieren en sus orientaciones espaciales, por lo que tienen la misma energía. Los orbitales que tienen la misma cantidad de energía reciben el nombre de **orbitales degenerados**. La Figura 1.4 muestra las formas de los tres orbitales atómicos 2p degenerados.



► Figura 1.3

Los orbitales 2s tienen una pequeña región de densidad electrónica elevada próxima al núcleo, pero la mayor parte de la densidad electrónica está alejada del núcleo, más allá del nodo o región de densidad electrónica cero.

◀ **Figura 1.4**

Orbitales $2p$. Hay tres orbitales $2p$, orientados unos con respecto a los otros perpendicularmente. Se nombran según su orientación a lo largo del eje x , y o z .

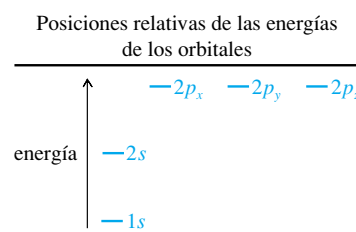
El *principio de exclusión de Pauli* dice que un orbital como máximo puede alojar dos electrones, de forma que sus espines estén apareados. La primera capa (un orbital $1s$) puede alojar dos electrones. La segunda capa (un orbital $2s$ y tres orbitales $2p$) puede alojar ocho electrones y la tercera capa (un orbital $3s$, tres orbitales $3p$ y cinco orbitales $3d$) puede alojar 18 electrones.

1.2C Configuraciones electrónicas de los átomos

Aufbau significa «construir» en alemán, y el *principio de aufbau* explica cómo establecer la configuración electrónica de un átomo en su estado fundamental (el de mayor estabilidad). Se comienza con el orbital de energía más baja y se van llenando ordenadamente de menor a mayor energía hasta que se han colocado todos los electrones. La Tabla 1.1 muestra las configuraciones electrónicas en estado fundamental de todos los elementos que forman parte de los dos primeros periodos de la tabla periódica.

TABLA 1.1 Configuraciones electrónicas de los elementos del primer y segundo periodo

Elemento	Configuración	Electrones de valencia
H	$1s^1$	1
He	$1s^2$	2
Li	$1s^2 2s^1$	1
Be	$1s^2 2s^2$	2
B	$1s^2 2s^2 2p_x^1$	3
C	$1s^2 2s^2 2p_x^1 2p_y^1$	4
N	$1s^2 2s^2 2p_x^1 2p_y^1 2p_z^1$	5
O	$1s^2 2s^2 2p_x^2 2p_y^1 2p_z^1$	6
F	$1s^2 2s^2 2p_x^2 2p_y^2 2p_z^1$	7
Ne	$1s^2 2s^2 2p_x^2 2p_y^2 2p_z^2$	8



► **Figura 1.5**

Primeras tres filas de la tabla periódica. La organización de la tabla periódica se debe al alojamiento de los electrones en los orbitales por orden creciente de energía. Para estos elementos representativos, el número de la columna corresponde al número de electrones de valencia.

El carbonato de litio, una sal de litio, es un antidepresivo que se utiliza para tratar el problema psiquiátrico conocido como manía. La manía está caracterizada por comportamientos tales como alteraciones del humor, sentimientos de grandeza, obsesiones y dificultad para dormir. No se sabe cómo actúa el carbonato de litio cuando estabiliza el humor de este tipo de pacientes.

Detalle de la tabla periódica

IA							gases nobles (VIII)
H	IIA	IIIA	IVA	VA	VIA	VIIA	He
Li	Be	B	C	N	O	F	Ne
Na	Mg	Al	Si	P	S	Cl	Ar

En la Tabla 1.1 se ilustran dos conceptos adicionales. Los **electrones de valencia** son los electrones que se encuentran en la capa más externa. El carbono tiene cuatro electrones de valencia, el nitrógeno cinco y el oxígeno seis. El helio tiene dos electrones de valencia y el neón tiene ocho, lo que corresponde, respectivamente, a la primera capa de valencia y a la segunda capa de valencia llenas. En general (para los elementos representativos), la columna o número de grupo de la tabla periódica corresponde al número de electrones de valencia (Figura 1.5). El hidrógeno y el litio tienen un electrón de valencia y los dos se encuentran en la primera columna (grupo IA) de la tabla periódica. El carbono tiene cuatro electrones de valencia y está en el grupo IVA de la tabla periódica.

Observad en la Tabla 1.1 que los electrones de valencia tercero y cuarto del carbono no están apareados, ocupan orbitales separados. A pesar de que el principio de exclusión de Pauli dice que dos electrones pueden ocupar el mismo orbital, los electrones se repelen uno a otro, y el apareamiento requiere energía adicional. La **regla de Hund** afirma que cuando hay dos o más orbitales de la misma energía, los electrones preferentemente se alojan en orbitales *diferentes* antes que aparearse en un mismo orbital. El primer electrón $2p$ (caso del boro) se coloca en un orbital $2p$, el segundo (caso del carbono) en un orbital diferente y el tercero (caso del nitrógeno) se coloca en el último orbital $2p$. El cuarto, quinto y sexto electrón $2p$ se aparearán, respectivamente, con los tres primeros electrones.

PROBLEMA 1.1

Escriba las configuraciones electrónicas de los elementos de la tercera fila que se muestra en la tabla periódica parcial de la Figura 1.5

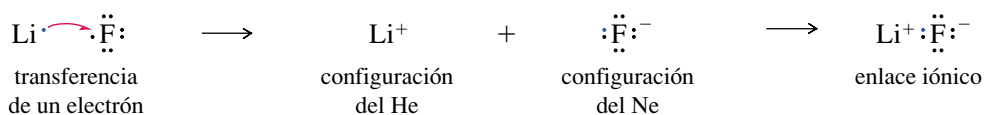
1.3

La formación del enlace: la regla del octeto

En 1915, G. N. Lewis propuso varias teorías nuevas para describir cómo se enlazaban los átomos unos a otros para formar moléculas. Una de esas teorías afirma que una capa llena de electrones es especialmente estable y que *los átomos transfieren o comparten electrones para que de esa forma las capas se llenen de electrones*. Una capa llena de electrones tiene la configuración de un gas noble como el He, Ne o Ar. A este principio se le dio el nombre de la **regla del octeto** porque una capa llena implica ocho electrones de valencia para los elementos de la segunda fila de la tabla periódica.

1.3A Enlace iónico

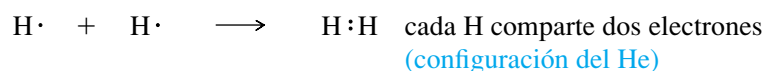
Hay dos formas en las que los átomos pueden interactuar para adquirir configuraciones de gas noble. Algunas veces los átomos adquieren configuraciones de gas noble transfiriendo electrones de un átomo a otro. Por ejemplo, el litio tiene un electrón más en su configuración que el helio, y el fluor tiene un electrón menos que la configuración del neón; el litio pierde fácilmente sus electrones de valencia y el fluor los gana fácilmente:



La transferencia de un electrón da a cada uno de los elementos la configuración de gas noble. Los iones resultantes tienen cargas opuestas y se atraen uno a otro formando un **enlace iónico**. El enlace iónico normalmente da lugar a la formación de grandes estructuras cristalinas en vez de moléculas individuales. El enlace iónico es muy frecuente en los compuestos inorgánicos, pero bastante inusual en los orgánicos.

1.3B Enlace covalente

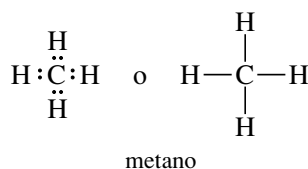
El **enlace covalente**, en el que se comparten electrones en lugar de transferirse, es la forma más habitual de enlace en los compuestos orgánicos. El hidrógeno, por ejemplo, necesita un segundo electrón para conseguir la configuración del gas noble helio. Si dos átomos de hidrógeno se unen y forman un enlace, «comparten» sus dos electrones y cada átomo tiene dos electrones en su capa de valencia.



El enlace covalente se estudiará con más detalle en el Capítulo 2.

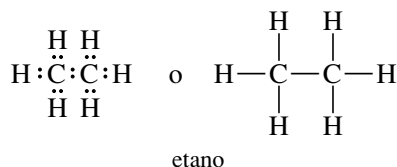
Una forma de simbolizar el enlace en una molécula covalente consiste en usar **estructuras de Lewis**. En una estructura de Lewis cada electrón de valencia se simboliza por un punto. Un par de electrones de enlace se simboliza por un par de puntos o por una línea (—). Se ha de intentar que todos los átomos tengan sus propias configuraciones de gas noble: dos electrones en el caso del hidrógeno y octetos para los elementos de la segunda fila de la tabla periódica.

Considere, por ejemplo, la estructura de Lewis del metano (CH_4):



El carbono contribuye con cuatro electrones de valencia y cada hidrógeno aporta uno, dando un total de ocho electrones. Todos estos ocho electrones rodean al carbono dando lugar a un octeto y cada átomo de hidrógeno comparte dos de los electrones.

La estructura de Lewis para el etano (C_2H_6) es más compleja:



Una vez más, se han colocado los electrones de valencia (14) y se han distribuido de forma que cada átomo de carbono quede rodeado por ocho electrones y cada hidrógeno por dos. La única estructura posible para el etano es la que se ha mostrado anteriormente, con los dos átomos de carbono compartiendo un par de electrones y cada átomo de hidrógeno compartiendo dos con uno de los carbonos. La estructura del etano muestra las características más importantes del carbono (su habilidad para formar enlaces fuertes carbono-carbono).

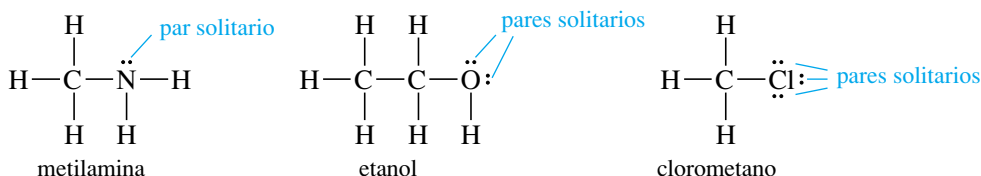
Los electrones de la capa de valencia que *no* son compartidos entre dos átomos reciben el nombre de **electrones no enlazantes**. Un par de electrones no enlazantes a menudo también es conocido como un **par solitario**. Los átomos de oxígeno, de nitrógeno y los halógenos (F, Cl, Br, I) normalmente tienen electrones no enlazantes en sus compuestos

1.4 Estructuras de Lewis

SUGERENCIA PARA RESOLVER PROBLEMAS

Las estructuras de Lewis son la forma de representar los enlaces en química orgánica. Aprender a representarlas de forma rápida y correctamente será muy útil a lo largo de este curso.

estables. Estos pares solitarios de electrones no enlazantes ayudan a determinar la reactividad de sus compuestos. Las estructuras de Lewis siguientes muestran un par solitario de electrones en el átomo de nitrógeno de la metilamina y dos pares solitarios en el átomo de oxígeno del etanol. Los átomos de los halógenos normalmente tienen tres pares solitarios, como se muestra en la estructura del clorometano.



Una estructura de Lewis correcta debería mostrar los pares solitarios de electrones. Los químicos orgánicos a menudo dibujan estructuras de Lewis omitiendo la mayoría o todos los pares solitarios de electrones. Estas no son estructuras correctas de Lewis porque uno se ha de imaginar el número de electrones no enlazantes.

PROBLEMA 1.2

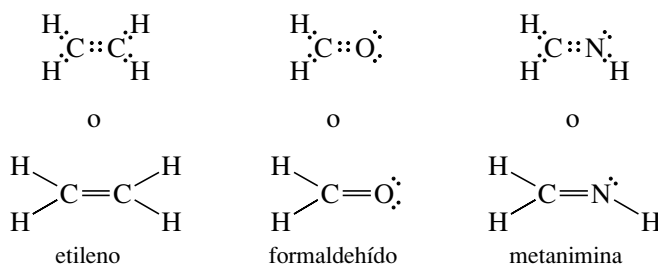
Dibuje las estructuras de Lewis de los siguientes compuestos:

- | | |
|--|--|
| (a) amoníaco, NH_3 | (b) agua, H_2O |
| (c) ión hidronio, H_3O^+ | (d) propano, C_3H_8 |
| (e) etilamina, $\text{CH}_3\text{CH}_2\text{NH}_2$ | (f) dimetil éter, CH_3OCH_3 |
| (g) fluoroetano, $\text{CH}_3\text{CH}_2\text{F}$ | (h) 2-propanol, $\text{CH}_3\text{CH}(\text{OH})\text{CH}_3$ |
| (i) borano, BH_3 | (j) trifluoruro de boro, BF_3 |

Explique qué es inusual en el enlace de los compuestos (i) y (j).

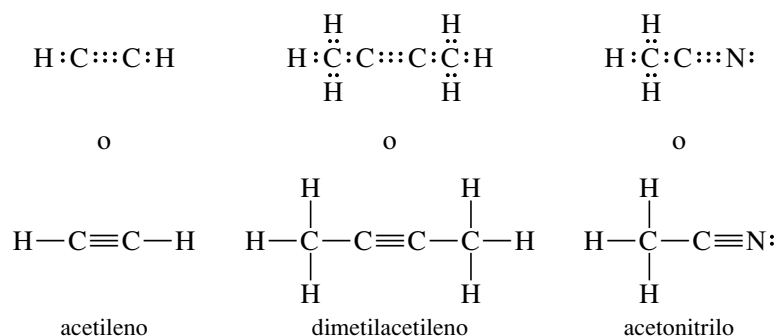
1.5 Enlace múltiple

Al representar las estructuras de Lewis en la Sección 1.4, se pusieron un par de electrones entre cada dos átomos. La compartición de un par de electrones entre dos átomos se conoce como **enlace sencillo**. Muchas moléculas comparten con sus átomos adyacentes dos o incluso tres pares de electrones; cuando se comparten dos pares se da el nombre de **enlace doble** y cuando se comparten tres pares se da el nombre de **enlace triple**. El etileno (C_2H_4) es un compuesto orgánico con un doble enlace. Cuando se representan las estructuras de Lewis para el etileno, la única forma de conseguir que los dos átomos de carbono tengan octetos es mediante la compartición de dos pares de electrones. El ejemplo siguiente muestra compuestos orgánicos con dobles enlaces. En cada caso, se comparten cuatro electrones (dos pares) entre dos átomos para formar octetos. Una doble línea ($=$) simboliza el doble enlace.



El acetileno, cuando se combina con el oxígeno, arde con una llama intensa que tiene diversas aplicaciones. Se puede utilizar para soldar las piezas de un puente bajo el agua o para reparar las tuberías de un oleoducto en Siberia.

El acetileno (C_2H_2) tiene un triple enlace. Su estructura de Lewis muestra los tres pares de electrones entre los dos átomos de carbono para que formen un octeto. Una línea triple (\equiv) simboliza el triple enlace.



Todas estas estructuras de Lewis muestran que el carbono normalmente forma cuatro enlaces en compuestos orgánicos neutros. El nitrógeno generalmente forma tres enlaces y el oxígeno dos. El hidrógeno y los halógenos normalmente forman un enlace. El número de enlaces que normalmente puede formar un átomo se conoce como **valencia**. El carbono es tetravalente, el nitrógeno trivalente, el oxígeno divalente, y el hidrógeno y los halógenos monovalentes. Si se recuerda el número usual de enlaces de estos elementos, se podrán escribir estructuras orgánicas con mucha facilidad. Si una estructura se representa de forma que cada átomo tenga el número de enlaces que le corresponden, la estructura de Lewis será correcta.

RESUMEN Modelos de enlace más frecuentes (sin carga)

	$\begin{array}{c} \\ -\text{C}- \\ \end{array}$	$\begin{array}{c} \cdot\cdot \\ -\text{N}- \\ \end{array}$	$\begin{array}{c} \cdot\cdot \\ -\text{O}- \\ \cdot\cdot \end{array}$	$-\text{H}$	$\begin{array}{c} \cdot\cdot \\ -\text{Cl}: \end{array}$
	carbono	nitrógeno	oxígeno	hidrógeno	halógenos
valencia:	4	3	2	1	1
pares solitarios:	0	1	2	0	3

SUGERENCIA PARA RESOLVER PROBLEMAS

Estos «números de enlaces usuales» pueden ser sencillos o estar combinados en dobles y triples enlaces. Por ejemplo, los tres enlaces del nitrógeno podrían corresponder a tres enlaces sencillos, a un enlace sencillo y uno doble, o a un triple enlace ($:\text{N}\equiv\text{N}:$). En los problemas hay que considerar todas las posibilidades.

PROBLEMA 1.3

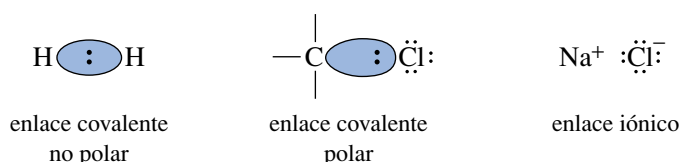
Escriba la estructura de Lewis para cada una de las siguientes fórmulas moleculares:

- | | | |
|---|---|----------------------------|
| (a) N_2 | (b) HCN | (c) HONO |
| (d) CO_2 | (e) H_2CNH | (f) HCO_2H |
| (g) $\text{C}_2\text{H}_3\text{Cl}$ | (h) HNNH | (i) C_3H_6 |
| (j) C_3H_4 (dos dobles enlaces) | (k) C_3H_4 (un triple enlace) | |

PROBLEMA 1.4

Rodee con un círculo los pares solitarios (pares de electrones no enlazantes) en las estructuras representadas en el Problema 1.3.

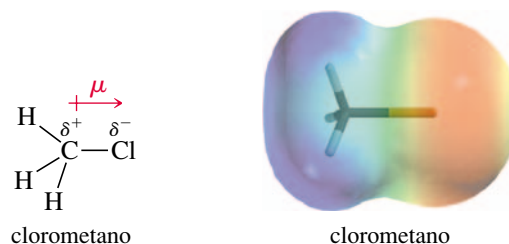
Un enlace cuyos electrones están igualmente compartidos por los dos átomos recibe el nombre de **enlace covalente no polar**. El enlace en la molécula de H_2 y el enlace $\text{C}-\text{C}$ en el etano son enlaces covalentes no polares. En la mayoría de enlaces entre dos elementos diferentes los electrones del enlace están atraídos de forma diferente por cada uno de los dos núcleos. Cuando la compartición del par de electrones del enlace no es igual para los dos átomos, a este enlace se le conoce como **enlace covalente polar**.



1.6 La electronegatividad y la polaridad de enlace

► **Figura 1.6**

El clorometano contiene un enlace polar carbono-cloro con una carga negativa parcial en el cloro y una carga positiva parcial en el carbono. El mapa de potencial electrostático muestra una región roja (rica en electrones) alrededor de la carga negativa parcial y una región azul (pobre en electrones) alrededor de la carga positiva parcial. El resto de colores indican valores intermedios de potencial electrostático.



Cuando el carbono se enlaza al cloro, por ejemplo, los electrones de enlace son atraídos más fuertemente hacia el átomo de cloro, por lo que el átomo de carbono adquirirá una pequeña carga positiva parcial y el átomo de cloro esa misma cantidad de carga pero de signo negativo. La Figura 1.6 muestra el enlace polar carbono-cloro del clorometano. Nosotros simbolizaremos la polaridad de enlace por una flecha que tenga como origen la carga positiva del enlace polar, y sobre este origen un signo positivo. La polaridad de un enlace se mide por su **momento dipolar** (μ), definido por el producto de la carga (separación de las cargas δ^+ y δ^-) y la longitud del enlace. El símbolo δ^+ significa «una pequeña cantidad de carga positiva» y el símbolo δ^- «una pequeña cantidad de carga negativa».

La Figura 1.6 también muestra un **mapa de potencial electrostático (MPE)** para el clorometano, que usa colores para representar la distribución de la carga calculada en una molécula. El rojo indica regiones ricas en electrones y el azul regiones pobres en electrones. El naranja, amarillo y verde indican niveles intermedios de potencial electrostático. En el clorometano, la región roja muestra la carga negativa parcial del cloro y la región azul indica la carga positiva parcial de los átomos de carbono y de hidrógeno.

A menudo se usan las **electronegatividades** como guía para predecir si un determinado enlace será polar y la dirección del momento dipolar. La escala de electronegatividad de Pauling, la que comúnmente utilizan los químicos orgánicos, se basa en las propiedades del enlace y es muy útil para predecir la polaridad de los enlaces covalentes. Los elementos con electronegatividades más altas atraen con más fuerza a los electrones de enlace. No obstante, en un enlace entre dos átomos diferentes, el átomo con la electronegatividad más alta es el extremo negativo del dipolo. La Figura 1.7 muestra las electronegatividades de Pauling para algunos de los elementos importantes de los compuestos orgánicos.

Obsérvese que la electronegatividad aumenta de izquierda a derecha a lo largo de la tabla periódica. El nitrógeno, el oxígeno y los halógenos son más electronegativos que el carbono; el sodio, el litio y el magnesio son menos electronegativos. La electronegatividad del hidrógeno es parecida a la del carbono, por lo que el enlace C—H normalmente se considera no polar. La polaridad de los enlaces y de las moléculas se tratará con más detalle en la Sección 2.9.

PROBLEMA 1.5

Haga uso de las electronegatividades para predecir los momentos dipolares de los siguientes enlaces:

- (a) C—Cl (b) C—O (c) C—N (d) C—S (e) C—B
(f) N—Cl (g) N—O (h) N—S (i) N—B (j) B—Cl

► **Figura 1.7**

Electronegatividades de algunos de los elementos que se encuentran en los compuestos orgánicos.

H 2.2						
Li 1.0	Be 1.6	B 1.8	C 2.5	N 3.0	O 3.4	F 4.0
Na 0.9	Mg 1.3	Al 1.6	Si 1.9	P 2.2	S 2.6	Cl 3.2
K 0.8						Br 3.0
						I 2.7

En los enlaces polares, las cargas parciales (δ^+ y δ^-) de los átomos del enlace son *reales*. Las **cargas formales** proporcionan un método de seguimiento de los electrones, pero pueden corresponder o no a cargas reales. En la mayoría de los casos, si la estructura de Lewis muestra que un átomo tiene una carga formal, quiere decir que tiene parte de esa carga. El concepto de carga formal ayuda a determinar qué átomos tienen mayor cantidad de carga en una molécula y ver que hay átomos cargados en moléculas que son neutras globalmente.

Para calcular las cargas formales, hay que contar cuántos electrones contribuyen a la carga de cada átomo y comparar ese número con el número de electrones de valencia que hay en el átomo neutro y aislado (dado por el número de grupo en la tabla periódica). Los electrones que contribuyen a la carga de un átomo son:

1. *Todos* sus electrones no compartidos (no enlazantes).
2. *La mitad* de los electrones (enlazantes) que comparte con otros átomos, o un electrón de cada par de enlace.

La carga formal de un átomo determinado puede ser calculada mediante la fórmula:

$$\text{carga formal (CF)} = [\text{número de grupo}] - [\text{electrones no enlazantes}] - \frac{1}{2}[\text{electrones compartidos}]$$

PROBLEMA RESUELTO 1.1

Calcule la carga formal (CF) de cada átomo de las estructuras siguientes:

(a) Metano (CH_4)

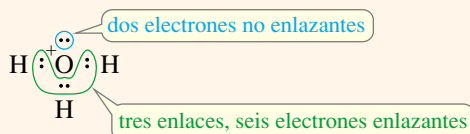


SOLUCIÓN

Cada átomo de hidrógeno del metano tiene un par enlazante de electrones (dos electrones compartidos). La mitad de los dos electrones compartidos es un electrón de valencia y es lo que el hidrógeno necesita para ser neutro. Los átomos de hidrógeno con un enlace son neutros formalmente: $\text{CF} = 1 - 0 - 1 = 0$.

El átomo de carbono tiene cuatro pares de electrones enlazantes (ocho electrones). La mitad de los ocho electrones compartidos, esto es, cuatro electrones son los que el carbono (grupo IVA) necesita para ser neutro. El carbono es formalmente neutro cuando tiene cuatro enlaces: $\text{CF} = 4 - 0 - \frac{1}{2}(8) = 0$.

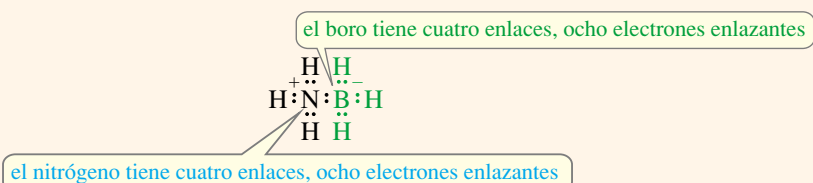
(b) Ión hidronio, H_3O^+



SOLUCIÓN

Cuando se representa la estructura de Lewis para este ión, se utilizan ocho electrones: seis del oxígeno y tres de los hidrógenos, menos uno porque el ión tiene una carga positiva. Cada hidrógeno tiene un enlace y es formalmente neutro. El oxígeno está rodeado por un octeto, con seis electrones enlazantes y dos electrones no enlazantes. La mitad de los electrones enlazantes más todos los electrones no enlazantes contribuyen a la carga: $6/2 + 2 = 5$; pero el oxígeno (grupo VIA) necesita seis electrones de valencia para ser neutro, por este motivo, el átomo de oxígeno tiene una carga formal de $+1$: $\text{CF} = 6 - 2 - \frac{1}{2}(6) = +1$.

(c) $\text{H}_3\text{N} - \text{BH}_3$



1.7 Cargas formales

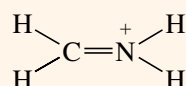
SOLUCIÓN

Éste es un compuesto neutro donde los átomos individuales están cargados formalmente. La estructura de Lewis muestra que tanto el nitrógeno como el boro tienen cuatro pares de electrones enlazantes. Los dos átomos, boro y nitrógeno, tienen $8/2 = 4$ electrones que contribuyen a sus cargas. El nitrógeno (grupo V) necesita cinco electrones de valencia para ser neutro, por lo que su carga formal es $+1$. El boro (grupo III) sólo necesita tres electrones de valencia para ser neutro, por lo que su carga formal es -1 .

$$\text{Nitrógeno: } CF = 5 - 0 - \frac{1}{2}(8) = +1$$

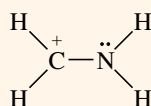
$$\text{Boro: } CF = 3 - 0 - \frac{1}{2}(8) = -1$$

(d) $[\text{H}_2\text{CNH}_2]^+$

**SOLUCIÓN**

En esta estructura, tanto el carbono como el nitrógeno tienen cuatro pares de electrones enlazantes. Con cuatro enlaces, el carbono es formalmente neutro; no obstante, el nitrógeno es del grupo V, por lo que su carga positiva formal es: $CF = 5 - 0 - 4 = +1$.

Este compuesto también podría ser representado con la siguiente estructura de Lewis:



En esta estructura, el átomo de carbono tiene tres enlaces con seis electrones enlazantes que, si se dividen entre dos, $6/2 = 3$, se observa que el carbono tiene un electrón menos de los cuatro que necesita para ser neutro formalmente: $CF = 4 - 0 - \frac{1}{2}(6) = +1$.

El nitrógeno tiene seis electrones enlazantes y dos electrones no enlazantes. Si se hace el cálculo $6/2 + 2 = 5$, se observa que el nitrógeno es neutro en esta segunda estructura:

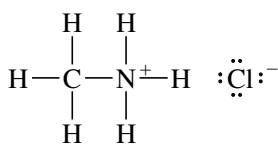
$$CF = 5 - 2 - \frac{1}{2}(6) = 0$$

El significado de estas dos estructuras de Lewis se discute en la Sección 1.9.

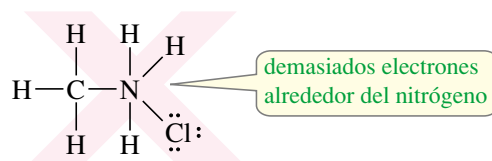
La mayoría de los compuestos orgánicos sólo contienen un número pequeño de elementos bastante comunes, normalmente con el octeto de electrones completo. La tabla resumen de la página siguiente indica la naturaleza de los enlaces más habituales, utilizando líneas para representar los pares de electrones enlazantes. Utilice estas reglas de cálculo de las cargas formales para comprobar las cargas que se dan en las estructuras. Si las estructuras se entienden bien, será fácil representar los compuestos orgánicos y sus iones de forma rápida y correcta.

1.8 Estructuras iónicas

Algunos compuestos orgánicos contienen enlaces iónicos. Por ejemplo, la estructura del cloruro de metilamonio ($\text{CH}_3\text{NH}_3\text{Cl}$) no se puede representar si solamente se utilizan enlaces covalentes; esto requeriría que el nitrógeno tuviese cinco enlaces, lo que implicaría diez electrones en la capa de valencia. La estructura correcta contiene un ión cloruro enlazado iónicamente al resto de la estructura.



cloruro de metilamonio



no se puede representar mediante enlaces covalentes

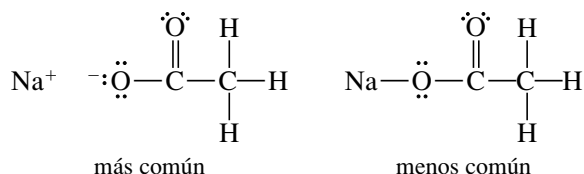
RESUMEN Modelos de enlace más frecuentes en los compuestos e iones orgánicos

Átomo	Electrones de valencia	Cargado positivamente	Neutro	Cargado negativamente
B	3		(no octeto) $\begin{array}{c} \text{—B—} \\ \end{array}$	$\begin{array}{c} \\ \text{—B—} \\ \end{array}$
C	4	$\begin{array}{c} + \\ \text{—C—} \\ \end{array}$ (no octeto)	$\begin{array}{c} \\ \text{—C—} \\ \end{array}$	$\begin{array}{c} \cdot\cdot \\ \text{—C—} \\ \end{array}$
N	5	$\begin{array}{c} \\ \text{—N}^+ \\ \end{array}$	$\begin{array}{c} \cdot\cdot \\ \text{—N—} \\ \end{array}$	$\begin{array}{c} \cdot\cdot \\ \text{—N—} \\ \end{array}$
O	6	$\begin{array}{c} \cdot\cdot \\ \text{—O}^+ \\ \end{array}$	$\begin{array}{c} \cdot\cdot \\ \text{—O—} \\ \end{array}$	$\begin{array}{c} \cdot\cdot \\ \text{—O—} \\ \end{array}$
halógeno	7	$\begin{array}{c} \cdot\cdot \\ \text{—Cl}^+ \\ \end{array}$	$\begin{array}{c} \cdot\cdot \\ \text{—Cl:} \end{array}$	$\begin{array}{c} \cdot\cdot \\ \text{:Cl:}^- \end{array}$

SUGERENCIA PARA RESOLVER PROBLEMAS

Esta tabla es muy importante. Haz un número de problemas suficientes como para familiarizarte con estos modelos de enlace, tal que puedas saber cuándo otros modelos son incorrectos o bien inusuales.

Algunas moléculas se pueden representar tanto en forma covalente como iónica. Por ejemplo, el acetato de sodio (NaOCOCH_3) se puede representar tanto con un enlace covalente como con un enlace iónico entre el sodio y el oxígeno. Como el sodio normalmente forma enlaces iónicos con el oxígeno (NaOH), la estructura con enlace iónico es la que se prefiere. En general, los enlaces entre átomos con gran diferencia de electronegatividad (2 o más) normalmente se representan como compuestos iónicos.


PROBLEMA 1.6

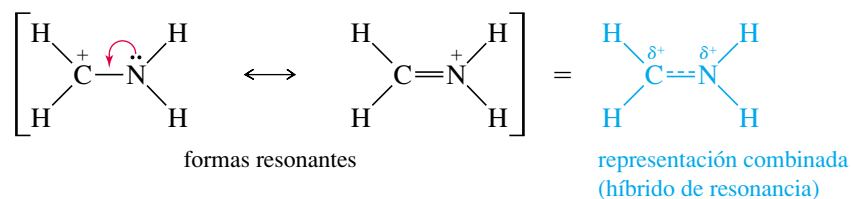
Dibuje las estructuras de Lewis de los siguientes compuestos e iones, diciendo cuál es su carga formal apropiada:

- | | |
|---|---------------------------------|
| (a) $[\text{CH}_3\text{OH}_2]^+$ | (b) NH_4Cl |
| (c) $(\text{CH}_3)_2\text{NH}_2\text{Cl}$ | (d) NaOCH_3 |
| (e) $^+\text{CH}_3$ | (f) $^-\text{CH}_3$ |
| (g) NaBH_4 | (h) NaBH_3CN |
| (i) $(\text{CH}_3)_2\text{O—BF}_3$ | (j) $[\text{HONH}_3]^+$ |
| (k) $\text{KOC}(\text{CH}_3)_3$ | (l) $[\text{H}_2\text{C=OH}]^+$ |

1.9A Híbridos de resonancia

Algunas de las estructuras de los compuestos no es adecuado representarlas mediante una sola estructura de Lewis. Cuando son posibles dos o más estructuras de enlace de valencia, que difieren sólo en la colocación de los electrones, la molécula suele mostrar características de las dos estructuras. A estas estructuras diferentes se las conoce como **estructuras de resonancia** o **formas resonantes**, ya que no son compuestos diferentes, sino formas diferentes de representar el mismo compuesto. La molécula real se dice que corresponde a un **híbrido de resonancia** de sus formas resonantes. En el Problema resuelto 1.1(d) se mostró cómo el ión $[\text{H}_2\text{CNH}_2]^+$ se podía representar por cualquiera de las siguientes formas de resonancia:

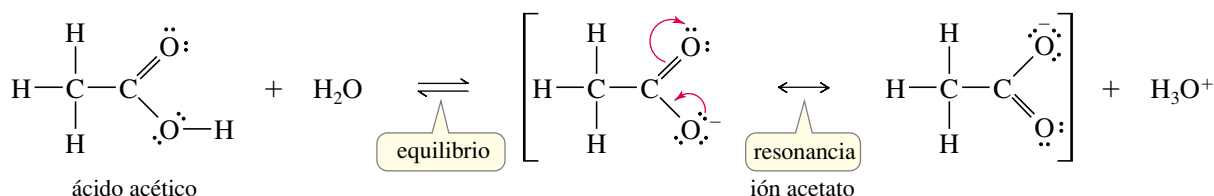
1.9 Resonancia



La estructura real de este ión es un híbrido de resonancia de las dos estructuras. En la molécula real, la carga positiva está **deslocalizada** (extendida) entre el átomo de carbono y el de nitrógeno. En la forma resonante de la izquierda, la carga positiva está en el carbono, pero el carbono no tiene un octeto. Los electrones no enlazantes del nitrógeno se pueden mover por el enlace (tal como indica la flecha roja) dando una segunda estructura con un doble enlace entre el nitrógeno que tiene carga positiva y el carbono que posee un octeto. La representación combinada de las dos formas de resonancia en una sola representación da lugar a una carga compartida entre el nitrógeno y el carbono.

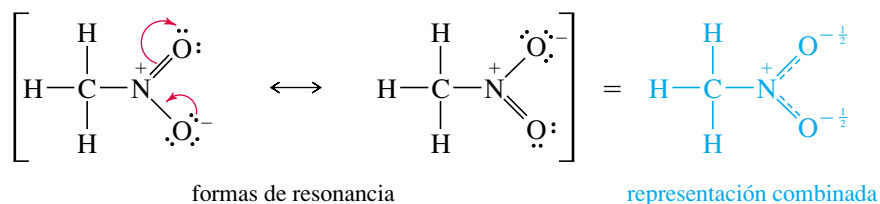
El extender la carga positiva sobre dos átomos hace que el ión sea más estable que en el caso de que la carga positiva estuviera localizada solamente sobre el carbono o sobre el nitrógeno. Se dice que este catión está **estabilizado por resonancia**. La resonancia es más importante cuando permite que una carga esté deslocalizada entre dos o más átomos, como en el ejemplo mencionado.

La estabilización por resonancia desempeña un papel crucial en la química orgánica, especialmente en la química de compuestos que tienen dobles enlaces. Se usará frecuentemente el concepto de resonancia a lo largo de este curso. Por ejemplo, la acidez del ácido acético (véase abajo) se incrementa por efecto de la resonancia. Cuando el ácido acético pierde un protón, el ión acetato resultante tiene una carga negativa deslocalizada sobre los dos átomos de oxígeno. Cada átomo de oxígeno posee la mitad de la carga negativa y su deslocalización estabiliza el ión. Cada uno de los enlaces carbono-oxígeno es intermedio entre un enlace doble y un enlace sencillo, por lo que se dice que su *orden de enlace* es de $1\frac{1}{2}$.



Se usará una sola flecha con doble punta entre las formas de resonancia (a menudo puestas entre corchetes) para indicar que la estructura real es un híbrido de las estructuras de Lewis representadas. Por otra parte, un equilibrio se representará por dos flechas con sentidos opuestos.

Algunas moléculas sin carga también tienen estructuras de resonancia estabilizadas con la misma carga formal positiva y negativa. Se pueden representar dos estructuras de Lewis para el nitrometano (CH_3NO_2), pero las dos estructuras tienen una carga positiva formal en el nitrógeno y una carga negativa en uno de los oxígenos. Por tanto, el nitrometano tiene una carga positiva en el átomo de nitrógeno y una carga negativa extendida por igual sobre los dos átomos de oxígeno. Los enlaces N—O están entre un enlace sencillo y uno doble, tal como se indica en la representación combinada siguiente:

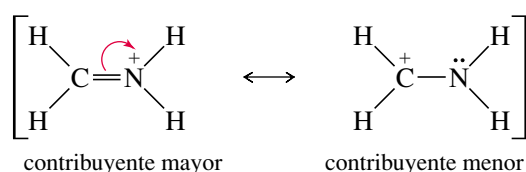


Recuerde que las formas de resonancia individuales no existen como especies químicas independientes. La molécula no «resuena» entre esas estructuras, es un híbrido con

características de ambas estructuras. Una analogía sería una mula, que es un híbrido de un caballo y un burro. La mula no «resuena» entre parecerse a un caballo o a un burro; simplemente es una mula, con el amplio dorso de un caballo y las grandes orejas de un burro.

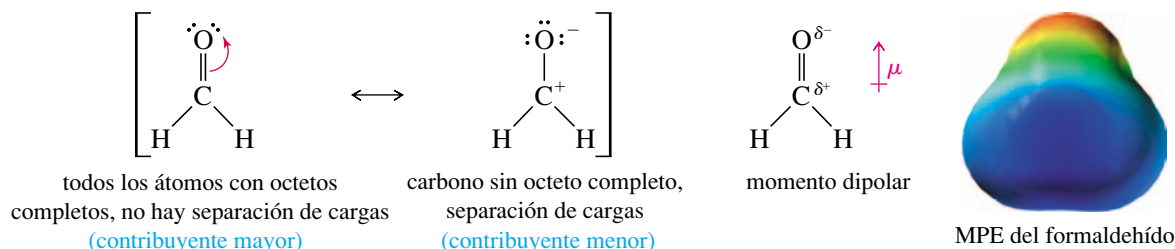
1.9B Contribución mayor o menor de las formas resonantes al híbrido de resonancia

Dos o más estructuras de Lewis correctas para un mismo compuesto pueden o no representar distribuciones de electrones de igual energía. A pesar de que formas de resonancia separadas no existen, se pueden estimar sus energías relativas como si existieran. La mayoría de las formas de resonancia estables son representaciones más cercanas de la molécula real que las menos estables. Las dos formas de resonancia del apartado anterior, para el ión acetato, tienen enlaces similares e idéntica energía. Lo mismo se puede decir para las dos formas de resonancia del nitrometano. Las formas de resonancia siguientes, por el contrario, tienen enlaces diferentes.



Las estructuras anteriores no tienen la misma energía estimada. La primera estructura tiene la carga positiva en el nitrógeno. La segunda tiene la carga positiva en el carbono, y el átomo de carbono no posee un octeto completo. La primera estructura es más estable ya que tiene un enlace adicional y todos los átomos tienen octetos completos. Muchos iones estables tienen una carga positiva en el átomo de nitrógeno con cuatro enlaces (*véase* la tabla resumen de la página 13). A la forma de resonancia más estable se la conoce como la **contribuyente mayor** y a la forma menos estable como la **contribuyente menor**. La estructura del compuesto real se parece más al contribuyente mayor que al contribuyente menor.

Muchas moléculas orgánicas tienen contribuyentes de resonancia mayor y menor. El formaldehído ($\text{H}_2\text{C}=\text{O}$) se puede representar con una carga negativa en el oxígeno, equilibrada por una carga positiva en el carbono. Esta forma de resonancia polar tiene mayor energía estimada que la estructura con doble enlace, porque tiene separación de cargas, menos enlaces y un átomo de carbono cargado positivamente con un octeto incompleto. La estructura con cargas separadas es solamente un contribuyente menor, pero ayuda a explicar por qué el enlace $\text{C}=\text{O}$ del formaldehído es muy polar, con una carga positiva parcial en el carbono y una carga negativa parcial en el oxígeno. El mapa de potencial electrostático (MPE) también muestra una región rica en electrones (rojo) alrededor del oxígeno y una región pobre en electrones (azul) alrededor del carbono en el formaldehído.



Cuando se representan las formas de resonancia, se intenta dibujar estructuras que sean lo más bajas posible en energía. Las mejores candidatas son las que tienen un número máximo de octetos y el máximo número de enlaces. Además, las estructuras tienen que tener la mínima cantidad de separación de cargas.

Sólo los electrones pueden estar deslocalizados. Al contrario que los electrones, los núcleos no pueden estar deslocalizados, deben permanecer en el mismo lugar, con las mismas distancias de enlace y los mismos ángulos en todos los contribuyentes a la resonancia. Las reglas generales siguientes serán útiles para representar estructuras de resonancias.

SUGERENCIA PARA RESOLVER PROBLEMAS

Para comparar las formas de resonancia se pueden utilizar los siguientes criterios, comenzando por el más importante:

1. Tantos octetos como sea posible.
2. Tantos enlaces como sea posible.
3. Si hay carga negativa se coloca en los átomos electronegativos.
4. La menor separación de cargas posible.

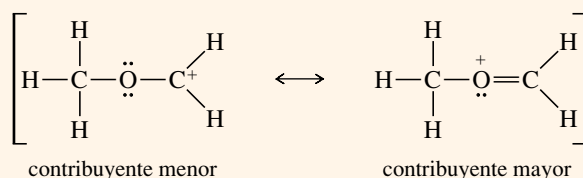
1. Todas las estructuras de resonancia deben ser estructuras de Lewis válidas para el compuesto.
2. Sólo se puede cambiar la posición de los electrones de una estructura a otra (los electrones de los dobles enlaces y pares solitarios son los que se cambian con más frecuencia). El núcleo no se puede cambiar de posición y los ángulos de enlace han de ser los mismos.
3. El número de electrones desapareados (si hay alguno) debe permanecer igual. La mayoría de los compuestos estables no tienen electrones desapareados y todos los electrones deben permanecer apareados en todas las estructuras de resonancia.
4. El contribuyente mayor a la resonancia es el que tiene menor energía.
Los buenos contribuyentes generalmente tienen todos los octetos satisfechos, con el máximo número de enlaces covalentes que sea posible y con una separación de cargas lo menor posible. Las cargas negativas son más estables en los átomos más electronegativos.
5. La estabilización por resonancia es más importante cuando sirve para deslocalizar una carga entre dos o más átomos.

PROBLEMA RESUELTO 1.2

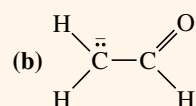
Para cada uno de los siguientes compuestos, represente las formas de resonancia importantes. Indique qué estructuras tienen contribuyentes mayores y menores, o si tienen la misma energía.

(a) $[\text{CH}_3\text{OCH}_2]^+$

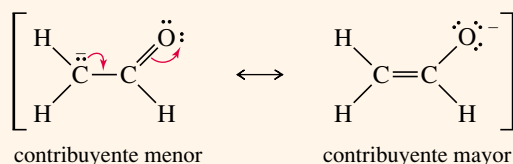
SOLUCIÓN



La primera estructura (menor) tiene un átomo de carbono con sólo seis electrones a su alrededor. La segunda estructura (mayor) tiene octetos en todos los átomos y un enlace adicional.



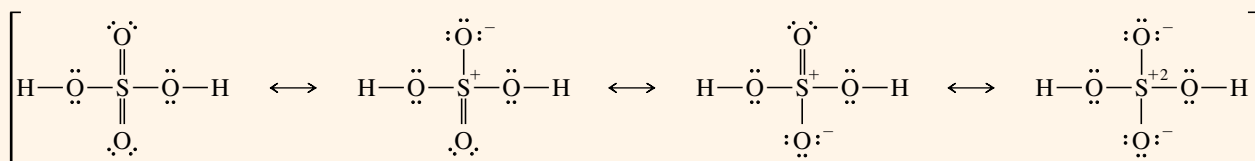
SOLUCIÓN



Las dos estructuras tienen octetos en el átomo de oxígeno y en el de carbono, y tienen el mismo número de enlaces. La primera estructura tiene la carga negativa en el carbono y la segunda la tiene en el oxígeno. El oxígeno es más electronegativo que el carbono, por lo tanto, la segunda estructura es el contribuyente mayor.

(c) H_2SO_4

SOLUCIÓN



La primera estructura, con más enlaces y menor separación de carga, es posible porque el azufre es un elemento de la tercera fila de la tabla periódica con orbitales *d* accesibles, lo que le da la posibilidad de expandir aparentemente su octeto. Por ejemplo, el SF_6 es un compuesto estable con 12 electrones alrededor del azufre. Sin embargo, algunos cálculos teóricos sugieren que la última estructura representada, con octetos en todos los átomos, podría ser la contribuyente mayor a la resonancia. No se puede predecir siempre el contribuyente mayor de un híbrido de resonancia.

PROBLEMA 1.7

Represente las formas de resonancia importantes de las siguientes moléculas e iones:

- (a) CO_3^{2-} (b) NO_3^- (c) NO_2^- (d) $\text{H}_2\text{C}=\text{CH}-\text{CH}_2^+$
 (e) $\text{H}_2\text{C}=\text{CH}-\text{CH}_2^-$ (f) SO_4^{2-} (g) $[\text{CH}_3\text{C}(\text{OCH}_3)_2]^+$

PROBLEMA 1.8

Para cada uno de los siguientes compuestos, represente las formas de resonancia importantes. Indique qué estructuras son las contribuyentes mayores y menores a la resonancia, o si tienen la misma energía.

- (a) $[\text{H}_2\text{CNO}_2]^-$ (b) $\text{H}_2\text{C}=\text{CH}-\text{NO}_2$ (c) $[\text{H}_2\text{COH}]^+$
 (d) H_2CNN (e) $[\text{H}_2\text{CCN}]^-$ (f) $\text{H}_2\text{N}-\overset{+}{\text{CH}}-\text{CH}=\text{CH}-\text{NH}_2$
 (g) $\text{H}-\overset{\text{O}}{\parallel}{\text{C}}-\overset{-}{\text{CH}}-\overset{\text{O}}{\parallel}{\text{C}}-\text{H}$ (h) $\text{H}-\overset{\text{O}}{\parallel}{\text{C}}-\text{NH}_2$

SUGERENCIA**PARA RESOLVER PROBLEMAS**

Quando se representan formas de resonancia para iones, observe cómo se puede deslocalizar la carga entre varios átomos. Intente colocar una carga negativa sobre elementos electronegativos como el oxígeno y el nitrógeno. Intente, así mismo, colocar una carga positiva sobre todos los carbonos que sea posible, pero especialmente sobre los átomos que puedan alojar la carga positiva y tener un octeto completo; por ejemplo, el oxígeno (con tres enlaces) o el nitrógeno (con cuatro enlaces).

Los químicos orgánicos utilizan varias clases de fórmulas para representar los compuestos orgánicos. Algunas de estas fórmulas incluyen una notación específica que requiere una explicación. Las **fórmulas estructurales** indican qué átomos están enlazados a otros. Hay dos tipos de fórmulas estructurales: las estructuras de Lewis completas y las fórmulas estructurales condensadas. Además, hay varias formas de representar fórmulas estructurales condensadas. Según se ha visto, una estructura de Lewis simboliza un par de electrones enlazantes como un par de puntos o como una línea (—). Los pares solitarios de electrones se muestran como pares de puntos.

1.10**Fórmulas estructurales****1.10A Fórmulas estructurales condensadas**

Las **fórmulas estructurales condensadas** (Tabla 1.2) se representan sin mostrar todos los enlaces individuales. En una estructura condensada, cada átomo central se representa junto a los átomos a los que está enlazado. Los átomos enlazados a un átomo central a menudo se escriben a continuación del átomo central (CH_3CH_3 en lugar de $\text{H}_3\text{C}-\text{CH}_3$) incluso aunque no sea el orden del verdadero enlace. En muchos casos, si hay dos o más grupos idénticos, se puede utilizar un paréntesis y un subíndice para representar a todos estos grupos. Los electrones no enlazantes raramente se representan en las fórmulas estructurales condensadas.

TABLA 1.2 Ejemplos de fórmulas estructurales condensadas

Compuesto	Estructura de Lewis	Fórmula estructural condensada
etano	$\begin{array}{c} \text{H} & \text{H} \\ & \\ \text{H}-\text{C} & -\text{C}-\text{H} \\ & \\ \text{H} & \text{H} \end{array}$	CH_3CH_3
isobutano	$\begin{array}{c} \text{H} & \text{H} & \text{H} \\ & & \\ \text{H}-\text{C} & -\text{C}- & \text{C}-\text{H} \\ & & \\ \text{H} & & \text{H} \\ & & \\ & \text{H}-\text{C}-\text{H} \\ & & \\ & \text{H} & \end{array}$	$(\text{CH}_3)_3\text{CH}$
n-hexano	$\begin{array}{c} \text{H} & \text{H} & \text{H} & \text{H} & \text{H} & \text{H} \\ & & & & & \\ \text{H}-\text{C} & -\text{C} & -\text{C} & -\text{C} & -\text{C} & -\text{C}-\text{H} \\ & & & & & \\ \text{H} & \text{H} & \text{H} & \text{H} & \text{H} & \text{H} \end{array}$	$\text{CH}_3(\text{CH}_2)_4\text{CH}_3$

(continúa en la página siguiente)

TABLA 1.2 (continuación)

Compuesto	Estructura de Lewis	Fórmula estructural condensada
dietil éter	$ \begin{array}{ccccccc} & \text{H} & \text{H} & & \text{H} & \text{H} & \\ & & & & & & \\ \text{H} & - \text{C} & - \text{C} & - \ddot{\text{O}} & - \text{C} & - \text{C} & - \text{H} \\ & & & & & & \\ & \text{H} & \text{H} & & \text{H} & \text{H} & \end{array} $	$\text{CH}_3\text{CH}_2\text{OCH}_2\text{CH}_3$ o $\text{CH}_3\text{CH}_2-\text{O}-\text{CH}_2\text{CH}_3$ o $(\text{CH}_3\text{CH}_2)_2\text{O}$
etanol	$ \begin{array}{ccccc} & \text{H} & \text{H} & & \\ & & & & \\ \text{H} & - \text{C} & - \text{C} & - \ddot{\text{O}} & - \text{H} \\ & & & & \\ & \text{H} & \text{H} & & \end{array} $	$\text{CH}_3\text{CH}_2\text{OH}$
alcohol isopropílico	$ \begin{array}{ccccc} & \text{H} & & \ddot{\text{O}} & - \text{H} & \text{H} \\ & & & & & \\ \text{H} & - \text{C} & - & \text{C} & - & \text{C} & - \text{H} \\ & & & & & \\ & \text{H} & & \text{H} & & \text{H} \end{array} $	$(\text{CH}_3)_2\text{CHOH}$
dimetilamina	$ \begin{array}{ccccc} & \text{H} & & \text{H} & \\ & & & & \\ \text{H} & - \text{C} & - & \ddot{\text{N}} & - \text{C} & - \text{H} \\ & & & & & \\ & \text{H} & & \text{H} & & \text{H} \end{array} $	$(\text{CH}_3)_2\text{NH}$

Cuando se escribe una fórmula estructural condensada para un compuesto que contiene enlaces dobles o triples, los enlaces múltiples con frecuencia se representan igual que en las estructuras de Lewis. La Tabla 1.3 muestra ejemplos de fórmulas estructurales condensadas que contienen enlaces múltiples. Observe que el grupo $-\text{CHO}$ de un aldehído y el grupo $-\text{COOH}$ de un ácido carboxílico se enlazan de forma diferente a como sugiere la notación condensada.

Como se puede observar en las Tablas 1.2 y 1.3, la diferencia entre una fórmula estructural de Lewis completa y una fórmula estructural condensada puede ser confusa. Los químicos con frecuencia representan las fórmulas con algunas partes condensadas y otras

TABLA 1.3 Fórmulas estructurales condensadas para dobles y triples enlaces

Compuesto	Estructura de Lewis	Fórmula estructural condensada
2-buteno	$ \begin{array}{ccccccc} & \text{H} & \text{H} & & \text{H} & & \\ & & & & & & \\ \text{H} & - \text{C} & - \text{C} & = \text{C} & - \text{C} & - \text{H} \\ & & & & & \\ & \text{H} & & \text{H} & \text{H} & \end{array} $	$\text{CH}_3\text{CHCHCH}_3$ o $\text{CH}_3\text{CH}=\text{CHCH}_3$
acetonitrilo	$ \begin{array}{ccc} & \text{H} & \\ & & \\ \text{H} & - \text{C} & - \text{C} \equiv \text{N} : \\ & & \\ & \text{H} & \end{array} $	CH_3CN o $\text{CH}_3\text{C}\equiv\text{N}$
acetaldehído	$ \begin{array}{ccc} & \text{H} & \ddot{\text{O}} \\ & & \\ \text{H} & - \text{C} & - \text{C} & - \text{H} \\ & & \\ & \text{H} & \end{array} $	CH_3CHO o $\text{CH}_3\overset{\text{O}}{\underset{ }{\text{C}}}\text{H}$
acetona	$ \begin{array}{ccccc} & \text{H} & & \ddot{\text{O}} & & \text{H} \\ & & & & & \\ \text{H} & - \text{C} & - & \text{C} & - & \text{C} & - \text{H} \\ & & & & & \\ & \text{H} & & \text{H} & & \text{H} \end{array} $	CH_3COCH_3 o $\text{CH}_3\overset{\text{O}}{\underset{ }{\text{C}}}\text{CH}_3$
ácido acético	$ \begin{array}{ccc} & \text{H} & \ddot{\text{O}} \\ & & \\ \text{H} & - \text{C} & - \text{C} & - \ddot{\text{O}} & - \text{H} \\ & & \\ & \text{H} & \end{array} $	CH_3COOH o $\text{CH}_3\overset{\text{O}}{\underset{ }{\text{C}}}-\text{OH}$ o $\text{CH}_3\text{CO}_2\text{H}$

completamente desarrolladas. El estudiante debería trabajar con las diferentes formas de representar las fórmulas para entender su significado.

PROBLEMA 1.9

Represente las estructuras de Lewis completas para las siguientes fórmulas estructurales condensadas:

- (a) $\text{CH}_3(\text{CH}_2)_3\text{CH}(\text{CH}_3)_2$ (b) $(\text{CH}_3)_2\text{CHCH}_2\text{Cl}$ (c) $\text{CH}_3\text{CH}_2\text{COCHCH}_2$
 (d) $\text{CH}_3\text{CH}_2\text{CHO}$ (e) CH_3COCN (f) $(\text{CH}_3)_3\text{CCOOH}$ (g) $(\text{CH}_3\text{CH}_2)_2\text{CO}$

1.10B Fórmulas lineoangulares

Otra forma de representar las estructuras orgánicas es la **fórmula lineoangular**, algunas veces llamada **estructura esquelética** o de barras. Las fórmulas lineoangulares con frecuencia se usan en los compuestos cíclicos y muy ocasionalmente en los lineales. En una fórmula lineoangular, los enlaces están representados por líneas y los átomos de carbono vienen dados por los vértices o puntos de encuentro de dos líneas, o el punto del principio o final de la línea en el caso de los extremos. Los átomos de nitrógeno, de oxígeno y los halógenos se escriben con su símbolo, pero los átomos de hidrógeno frecuentemente no se simbolizan a no ser que vayan unidos a elementos que se han simbolizado. Se supone que cada átomo de carbono tiene los suficientes átomos de hidrógeno para que el total de sus enlaces sea cuatro. Los electrones no enlazantes raramente se representan. La Tabla 1.4 muestra algunos ejemplos de estas representaciones lineoangulares.

TABLA 1.4 Ejemplos de representaciones lineoangulares

Compuesto	Estructura condensada	Fórmula lineoangular
hexano	$\text{CH}_3(\text{CH}_2)_4\text{CH}_3$	
2-hexeno	$\text{CH}_3\text{CH}=\text{CHCH}_2\text{CH}_2\text{CH}_3$	
3-hexanol	$\text{CH}_3\text{CH}_2\text{CH}(\text{OH})\text{CH}_2\text{CH}_2\text{CH}_3$	
2-ciclohexenona		
2-metilciclohexanol		
ácido nicotínico (vitamina, también llamada niacina)		

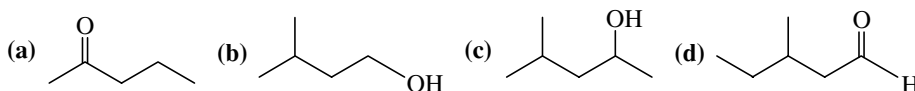
PROBLEMA 1.10

Escriba la estructura de Lewis correspondiente a las siguientes estructuras lineoangulares:

- (a)
- (b)
- (c)
- (d)
- (e)
- (f)
- (g)
- (h)

PROBLEMA 1.11

Represente las fórmulas estructurales condensadas correspondientes a las siguientes estructuras lineoangulares:



1.11

Fórmulas moleculares y fórmulas empíricas

Antes de poder escribir las posibles fórmulas estructurales de un compuesto, se necesita saber su fórmula molecular. La **fórmula molecular** simplemente informa del número de átomos de cada elemento que hay en una molécula de un compuesto. Por ejemplo, la fórmula molecular del 1-butanol es $C_4H_{10}O$.



1-butanol, fórmula molecular $C_4H_{10}O$

Cálculo de la fórmula empírica Las fórmulas moleculares se pueden determinar mediante un proceso que consta de dos pasos. El primer paso es la determinación de la **fórmula empírica**, o relación relativa entre los elementos presentes en la molécula. Suponga, por ejemplo, que en un compuesto desconocido, por análisis elemental cuantitativo, se encontró que contenía un 40.00% de carbono y un 6.67% de hidrógeno. La masa restante, 53.33%, se supone que era oxígeno. Para pasar esos números a una fórmula empírica, se puede seguir un procedimiento simple:

1. Suponga que la muestra contiene 100 g, por lo que los valores porcentuales dan el número de gramos de cada elemento. Dividiendo el número de gramos de cada elemento por la masa atómica se obtiene el número de moles de ese átomo en los 100 g de muestra.
2. Divida cada uno de los números de moles obtenidos en el paso anterior por el número más pequeño y redondee a la cifra entera más próxima. Este paso ha de conducir a la relación existente, expresada en números enteros, entre los elementos de la molécula.

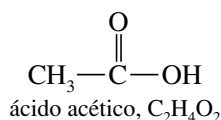
Para el compuesto desconocido, con los datos anteriores y siguiendo los pasos indicados, se obtendrían los siguientes resultados:

$$\begin{aligned} \frac{40.0 \text{ g C}}{12.0 \text{ g/mol}} &= 3.33 \text{ mol C}; & \frac{3.33 \text{ mol}}{3.33 \text{ mol}} &= 1 \\ \frac{6.67 \text{ g H}}{1.01 \text{ g/mol}} &= 6.60 \text{ mol H}; & \frac{6.60 \text{ mol}}{3.33 \text{ mol}} &= 1.98 \approx 2 \\ \frac{53.3 \text{ g O}}{16.0 \text{ g/mol}} &= 3.33 \text{ mol O}; & \frac{3.33 \text{ mol}}{3.33 \text{ mol}} &= 1 \end{aligned}$$

En el primer cálculo se divide el número de gramos de carbono por 12, el número de gramos de hidrógeno por 1 y el número de gramos de oxígeno por 16. Se comparan los resultados dividiendo todos los valores obtenidos por el número más pequeño, 3.33. El resultado final da una relación de un átomo de carbono por dos de hidrógeno y uno de oxígeno. Este resultado nos dice que la fórmula empírica es $C_1H_2O_1$ o CH_2O , que muestra solamente la relación de los elementos. La fórmula molecular puede ser un múltiplo cualquiera de la fórmula empírica, porque cualquier múltiplo también tiene la misma relación numérica entre los átomos de sus elementos. Fórmulas moleculares posibles son CH_2O , $C_2H_4O_2$, $C_3H_6O_3$, $C_4H_8O_4$, etc.

Cálculo de la fórmula molecular ¿Cómo se sabe cuál es la fórmula molecular correcta? Se puede elegir el verdadero múltiplo de la fórmula empírica cuando se conoce la masa molecular. Las masas moleculares de una sustancia se pueden determinar por métodos como el *descenso crioscópico* o el *aumento ebulloscópico* de un disolvente cuando contiene la sustancia desconocida a una concentración molar. Si el compuesto es volátil, se puede convertir en gas y utilizar su volumen para determinar el número de moles por la *ley de los gases ideales*. En la actualidad existen métodos entre los que se incluye la *espectrometría de masas*, que será tratada en el Capítulo 11.

Para el ejemplo anterior (fórmula empírica: CH_2O) supondremos que la masa molecular es aproximadamente 60. La masa de una unidad de CH_2O es 30, por lo que el compuesto contendrá el doble número de átomos. La fórmula molecular será $\text{C}_2\text{H}_4\text{O}_2$. Este compuesto podría ser el ácido acético.



En los Capítulos 12, 13 y 15 se usarán técnicas espectroscópicas para determinar la estructura completa de un compuesto una vez que se conozca su fórmula molecular.

PROBLEMA 1.12

Escriba la fórmula empírica y la fórmula molecular a partir de los análisis elementales siguientes. En cada caso, proponga al menos una estructura que corresponda a la fórmula molecular.

	C	H	N	Cl	PM(*)
(a)	40.0%	6.67%	0	0	90
(b)	32.0%	6.67%	18.7%	0	75
(c)	37.2%	7.75%	0	55.0%	64
(d)	38.4%	4.80%	0	56.8%	125

(*) Peso molecular.

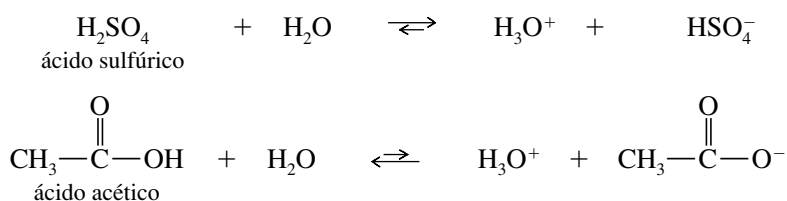
SUGERENCIA PARA RESOLVER PROBLEMAS

Si un análisis elemental no suma el 100%, el porcentaje que falta se supone que es de oxígeno.

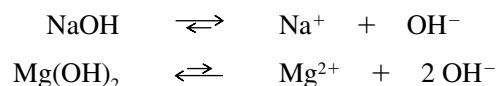
Las propiedades y la reactividad de los ácidos y de las bases son fundamentales para el estudio de la química orgánica. Hay que saber exactamente qué quieren decir los términos **ácido** y **base**. La mayoría de la gente estaría de acuerdo en que el H_2SO_4 es un ácido y el NaOH una base. ¿El BF_3 es un ácido o es una base? ¿El etileno ($\text{H}_2\text{C}=\text{CH}_2$) es un ácido o una base? Para responder a estas preguntas se necesitan entender las tres definiciones diferentes de los ácidos y de las bases: la definición de Arrhenius, la de Brønsted-Lowry y la de Lewis.

La primera clasificación de los compuestos ácidos se hizo basándose en su sabor agrio. Los términos latinos *acidus* (agrio) y *acetum* (vinagre) dieron lugar a los términos actuales de *ácido* y *ácido acético*. Los compuestos alcalinos (bases) eran sustancias que neutralizaban a los ácidos, tales como la caliza y las cenizas de las plantas (en árabe, *al kalai*).

La *teoría de Arrhenius* se desarrolló al final del siglo diecinueve y definía los ácidos como sustancias que se disocian en el agua para formar iones H_3O^+ . Se asumió que los ácidos más fuertes, tales como el ácido sulfúrico (H_2SO_4), se disociaban mucho más que los ácidos débiles, tales como el ácido acético (CH_3COOH).



Según la definición de Arrhenius, las bases son sustancias que se disocian en solución acuosa para formar iones hidroxilo. Por otra parte se consideró que las bases fuertes, tales como el NaOH , se disociaban más que las débiles o que aquellas que se disuelven moderadamente, como el $\text{Mg}(\text{OH})_2$.



La acidez o basicidad de una solución acuosa (agua) de una sustancia se mide por la concentración de H_3O^+ en dicha disolución. Este valor también permite conocer implícitamente la concentración de OH^- , ya que estas dos concentraciones están relacionadas entre sí por la constante de ionización del agua:

$$K_w = [\text{H}_3\text{O}^+][\text{OH}^-] = 1.00 \times 10^{-14} \quad (\text{a } 24^\circ\text{C})$$

1.12 Ácidos y bases de Arrhenius

En las soluciones neutras la concentración de $[\text{H}_3\text{O}^+]$ y de $[\text{OH}^-]$ son iguales,

$$[\text{H}_3\text{O}^+] = [\text{OH}^-] = 1.0 \times 10^{-7} \text{ M} \text{ en una solución neutra}$$

Las soluciones ácidas y básicas poseen un exceso de $[\text{H}_3\text{O}^+]$ o de $[\text{OH}^-]$, respectivamente.

$$\text{ácidas: } [\text{H}_3\text{O}^+] > 10^{-7} \text{ M} \text{ y } [\text{OH}^-] < 10^{-7} \text{ M}$$

$$\text{básicas: } [\text{H}_3\text{O}^+] < 10^{-7} \text{ M} \text{ y } [\text{OH}^-] > 10^{-7} \text{ M}$$

Como estas concentraciones pueden abarcar un amplio rango de valores, la acidez o basicidad de una solución normalmente se mide en escala logarítmica. El **pH** se define como el logaritmo (en base 10), cambiado de signo, de la concentración de H_3O^+ .

$$\text{pH} = -\log_{10}[\text{H}_3\text{O}^+]$$

Una solución neutra tiene un pH de 7, una solución ácida tiene un pH menor que 7 y una solución básica tiene un pH mayor que 7.

PROBLEMA 1.13

Calcule el pH de las siguientes soluciones:

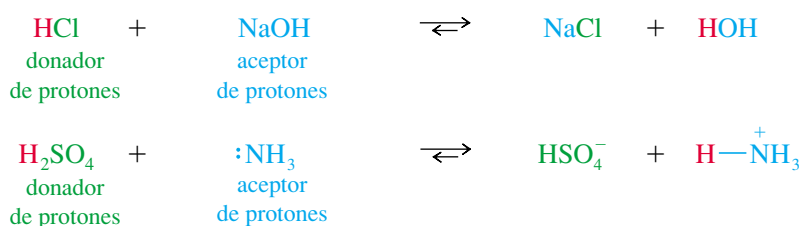
- (a) 5.00 g de HBr en 100 mL de solución acuosa.
- (b) 1.50 g de NaOH en 50 mL de solución acuosa.

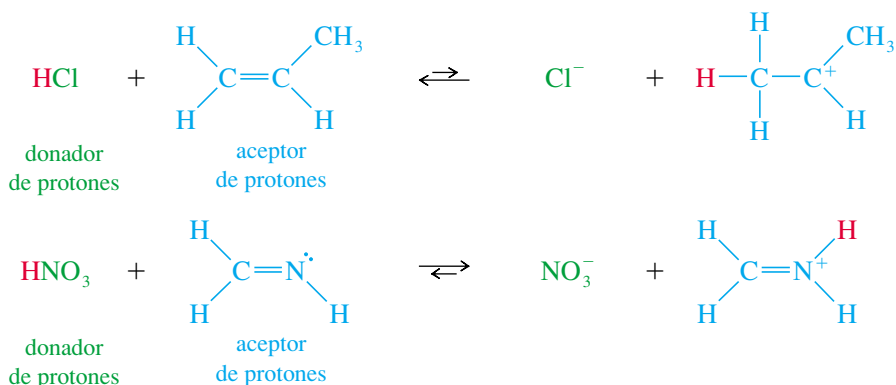
La definición de Arrhenius fue una contribución importante para poder entender muchos ácidos y muchas bases, pero no explica por qué un compuesto como el amoníaco (NH_3) neutraliza los ácidos, a pesar de no tener un ión hidróxido en su fórmula molecular. En la Sección 1.13 se explica una teoría más versátil de ácidos y bases que incluye al amoníaco y a una variedad más amplia de ácidos y bases orgánicos.

1.13 Ácidos y bases de Brønsted-Lowry

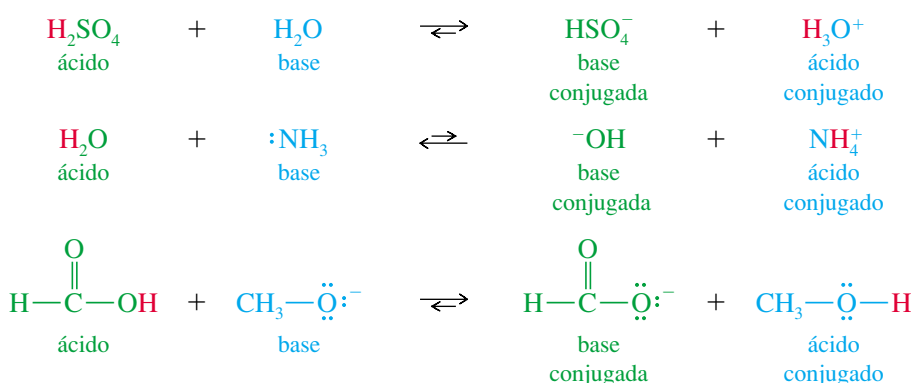
En 1923, Brønsted y Lowry definieron los ácidos y las bases teniendo en cuenta su capacidad de liberar o captar protones, respectivamente. Un **ácido de Brønsted-Lowry** es cualquier especie que puede donar un protón, y una **base de Brønsted-Lowry** es cualquier especie que puede aceptar un protón. Estas definiciones también incluyen todos los ácidos y bases de Arrhenius, ya que los compuestos que se disocian para dar H_3O^+ son donadores de protones y los compuestos que se disocian para dar OH^- son aceptores de protones (el ión hidróxido acepta un protón para formar H_2O).

Además de los ácidos y bases de Arrhenius, la definición de Brønsted-Lowry incluye también las bases que no tienen iones hidróxido, y que pueden aceptar protones. Observe los ejemplos siguientes de ácidos capaces de ceder protones a las bases. El NaOH es una base tanto si se considera la definición de Arrhenius o la de Brønsted-Lowry. Los tres ejemplos siguientes son bases de Brønsted-Lowry pero no bases de Arrhenius, ya que no tienen iones hidróxido.



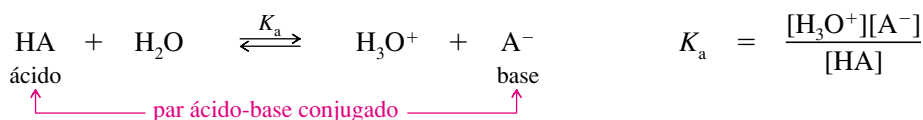


Cuando una base acepta un protón, se convierte en un ácido capaz de devolver ese protón. Cuando un ácido cede un protón, se convierte en una base capaz de aceptar de nuevo ese protón. Uno de los principios más importantes de la definición de Brønsted-Lowry es el concepto de **ácidos y bases conjugados**. Por ejemplo, el NH_3 y el NH_4^+ forman un par de ácido y base conjugados; el NH_3 es la base, cuando acepta un protón, se transforma en el ácido conjugado, NH_4^+ . Muchos compuestos (por ejemplo, el agua) pueden reaccionar como un ácido o como una base. A continuación se dan algunos ejemplos de pares ácido-base conjugados:



1.13A Fuerza de los ácidos

La fuerza de un ácido de Brønsted-Lowry se expresa de forma similar a la definición de Arrhenius, teniendo en cuenta su grado de ionización en agua. La reacción general de un ácido (HA) con agua es la siguiente:



A la K_a se la conoce con el nombre de *constante de disociación del ácido* y su valor indica la fuerza relativa del ácido. Cuanto más fuerte es el ácido, más se disocia, dando un valor de K_a mayor. Las constantes de disociación de un ácido varían en un intervalo amplio. Los ácidos fuertes se ionizan casi completamente en agua y sus constantes de disociación son superiores a 1. La mayoría de los ácidos orgánicos son ácidos débiles, con valores de K_a menores que 10^{-4} . Muchos compuestos orgánicos son ácidos extremadamente débiles; por ejemplo, el metano y el etano tienen un carácter ácido muy débil, su K_a es inferior a 10^{-40} .

Debido a este amplio margen de valores, las constantes de disociación ácida frecuentemente se expresan en escala logarítmica. El $\text{p}K_a$ de un ácido se define de forma parecida al pH: logaritmo (en base 10), con signo negativo, de la K_a .

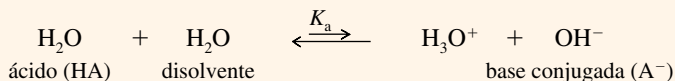
$$\text{p}K_a = -\log_{10} K_a$$

PROBLEMA RESUELTO 1.3

Calcule la K_a y el pK_a del agua.

SOLUCIÓN

El equilibrio que define la K_a del agua es:



El agua se comporta en esta disolución como ácido y como disolvente. La expresión del equilibrio es:

$$K_a = \frac{[\text{H}_3\text{O}^+][\text{A}^-]}{[\text{HA}]} = \frac{[\text{H}_3\text{O}^+][\text{OH}^-]}{[\text{H}_2\text{O}]}$$

Donde $[\text{H}_3\text{O}^+][\text{OH}^-] = 1.00 \times 10^{-14}$, constante del producto de ionización del agua.

La concentración de moléculas de H_2O en el agua simplemente es el número de moles de agua en 1 L (aproximadamente 1 kg).

$$\frac{1000 \text{ g/L}}{18 \text{ g/mol}} = 55.6 \text{ mol/L}$$

Haciendo la sustitución:

$$K_a = \frac{[\text{H}_3\text{O}^+][\text{OH}^-]}{[\text{H}_2\text{O}]} = \frac{1.00 \times 10^{-14}}{55.6} = 1.8 \times 10^{-16} \text{ M}$$

El logaritmo de 1.8×10^{-16} es -15.7 , por lo que el pK_a del agua es 15.7.

**SUGERENCIA
PARA RESOLVER PROBLEMAS**

En la mayor parte de los casos, el pK_a de un ácido coincide con el valor del pH de un ácido disociado en un 50%. A un pH menor (más ácido), el ácido estará menos disociado; a un pH mayor (más básico), el ácido estará más disociado.

Los ácidos fuertes generalmente tienen valores de pK_a próximos a 0 y los ácidos débiles, como la mayoría de los ácidos orgánicos, tienen valores superiores a 4. *Los ácidos más débiles tienen valores de pK_a más elevados.* La Tabla 1.5 recoge los valores de K_a y pK_a de algunos de los compuestos inorgánicos y orgánicos más habituales. Observa que los valores de pK_a aumentan cuando los valores de K_a disminuyen.

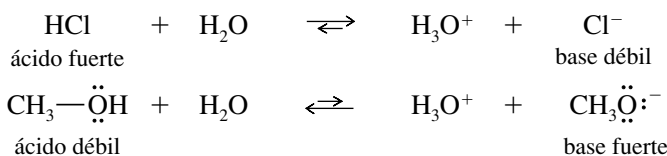
PROBLEMA 1.14

El amoníaco se encuentra en la Tabla 1.5 de dos formas, la forma básica y su ácido conjugado.

- Explique cómo el amoníaco puede actuar como base y como ácido. ¿Cuál de estas dos formas es más habitual en las soluciones acuosas?
- Explique por qué el agua puede actuar como ácido y como base.
- Explique por qué el metanol (CH_3OH) puede comportarse como ácido y como base. Escriba una ecuación para la reacción del metanol con el ácido sulfúrico.

1.13B Fuerza de las bases

La fuerza de un ácido es inversa a la fuerza de su base conjugada. Si un ácido (HA) es fuerte, su base conjugada (A^-) será débil, al ser estable en su forma aniónica; de lo contrario, el ácido HA no perdería fácilmente sus protones. Por lo tanto, la base conjugada de un ácido fuerte será una base débil. Por otra parte, si un ácido es débil, su conjugado es una base fuerte.

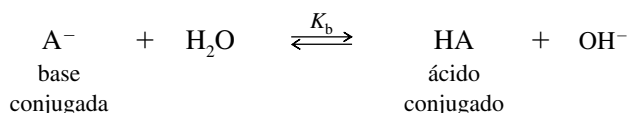


En la reacción de un ácido con una base, el equilibrio generalmente está desplazado hacia la formación de los ácidos y bases *débiles*. Por ejemplo, en las reacciones anteriores, el H_3O^+ es un ácido más débil que el HCl, pero un ácido más fuerte que el CH_3OH ; esto conlleva que el H_2O sea una base más fuerte que el Cl^- , pero más débil que el CH_3O^- .

TABLA 1.5 Fuerza relativa de algunos ácidos inorgánicos y orgánicos frecuentes, y sus bases conjugadas

	Ácido		Base conjugada	K_a	pK_a
ácidos fuertes	HCl ácido clorhídrico	$+ H_2O \rightleftharpoons H_3O^+ + Cl^-$	ion cloruro	1.6×10^2	-2.2
	HF ácido fluorhídrico	$+ H_2O \rightleftharpoons H_3O^+ + F^-$	ion fluoruro	6.8×10^{-4}	3.17
	$\begin{array}{c} O \\ \\ H-C-OH \end{array}$ ácido fórmico	$+ H_2O \rightleftharpoons H_3O^+ + \begin{array}{c} O \\ \\ H-C-O^- \end{array}$	ion formiato	1.7×10^{-4}	3.76
	$\begin{array}{c} O \\ \\ CH_3-C-OH \end{array}$ ácido acético	$+ H_2O \rightleftharpoons H_3O^+ + \begin{array}{c} O \\ \\ CH_3-C-O^- \end{array}$	acetano ion	1.8×10^{-5}	4.74
ácidos débiles	$H-C \equiv N:$ ácido cianhídrico	$+ H_2O \rightleftharpoons H_3O^+ + :C \equiv N:$	ion cianuro	6.0×10^{-10}	9.22
	$^+NH_4$ ion amonio	$+ H_2O \rightleftharpoons H_3O^+ + :NH_3$	amoniaco	5.8×10^{-10}	9.24
	CH_3-OH alcohol metílico	$+ H_2O \rightleftharpoons H_3O^+ + CH_3O^-$	metóxido ion	3.2×10^{-16}	15.5
	H_2O agua	$+ H_2O \rightleftharpoons H_3O^+ + HO^-$	ion hidróxido	1.8×10^{-16}	15.7
muy débil	NH_3 amoniaco	$+ H_2O \rightleftharpoons H_3O^+ + :\ddot{N}H_2$	ion amiduro	10^{-33}	33
no ácido	CH_4 metano	$+ H_2O \rightleftharpoons H_3O^+ + :\ddot{C}H_3$	anión metilo	$<10^{-40}$	>40

La fuerza de una base se mide de forma similar a la de los ácidos, usando la constante de equilibrio de la reacción de hidrólisis:



La constante de equilibrio (K_b) para esta reacción se conoce con el nombre de *constante de disociación de la base* para la base A^- . Debido a que esta constante tiene un amplio rango de valores, frecuentemente se expresa en forma logarítmica. El pK_b se define como el logaritmo (en base 10), cambiado de signo, de la K_b .

$$K_b = \frac{[HA][OH^-]}{[A^-]} \quad pK_b = -\log_{10} K_b$$

Cuando se multiplica K_a por K_b , se puede apreciar cómo la acidez de un ácido está relacionada con la basicidad de su base conjugada:

Las propiedades ácido-base de muchos productos naturales son importantes de cara a su aislamiento, a su distribución en el cuerpo y a justificar sus efectos terapéuticos. Por ejemplo, la morfina (p. 2), que se aísla de las adormideras (opio), llega al cerebro como base libre, en la que el nitrógeno no está cargado. Sin embargo, son sus especies cargadas las que actúan como analgésicas.

$$(K_a)(K_b) = \frac{[\text{H}_3\text{O}^+][\text{A}^-]}{[\text{HA}]} \frac{[\text{HA}][\text{OH}^-]}{[\text{A}^-]} = [\text{H}_3\text{O}^+][\text{OH}^-] = 1.0 \times 10^{-14}$$

constante del producto de ionización del agua

$$(K_a)(K_b) = 10^{-14}$$

Aplicando logaritmos:

$$\text{p}K_a + \text{p}K_b = -\log 10^{-14} = 14$$

El producto de K_a por K_b siempre es igual a la constante del producto iónico del agua, 10^{-14} . Si el valor de K_a es grande, el valor de K_b será pequeño; es decir, cuanto más fuerte es un ácido, más débil es su base conjugada. De forma similar, un valor pequeño de K_a (ácido débil) implica un valor grande de K_b (base fuerte).

Cuanto más fuerte es un ácido, más débil es su base conjugada.

Cuanto más débil es un ácido, más fuerte es su base conjugada.

Las reacciones ácido-base favorecen la formación de ácidos más débiles y/o bases más débiles.

SUGERENCIA PARA RESOLVER PROBLEMAS

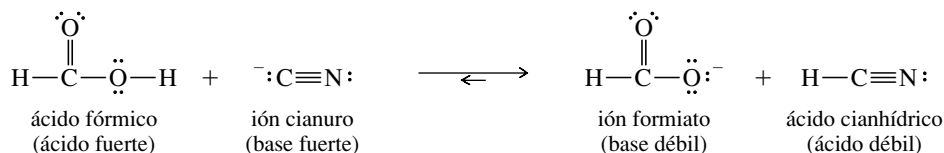
Un ácido donará un protón a la base conjugada de cualquier ácido que sea más débil (menor K_a o mayor $\text{p}K_a$).

PROBLEMA 1.15 (parcialmente resuelto)

Escriba las ecuaciones para las siguientes reacciones ácido-base. Utilice la información de la Tabla 1.5 para predecir si el equilibrio favorecerá a los reactivos o a los productos.

- (a) $\text{HCOOH} + ^-\text{CN}$ (b) $\text{CH}_3\text{COO}^- + \text{CH}_3\text{OH}$
 (c) $\text{CH}_3\text{OH} + \text{NaNH}_2$ (d) $\text{NaOCH}_3 + \text{HCN}$
 (e) $\text{HCl} + \text{H}_2\text{O}$ (f) $\text{H}_3\text{O}^+ + \text{CH}_3\text{O}^-$

Solución para (a): el ión cianuro es la base conjugada del HCN; puede aceptar un protón del ácido fórmico:



Observando la Tabla 1.5, se aprecia que el ácido fórmico ($\text{p}K_a = 3.76$) es un ácido más fuerte que el HCN ($\text{p}K_a = 9.22$) y que el cianuro es una base más fuerte que el formiato. Resultan favorecidos, pues, los productos ácido y base más débiles.

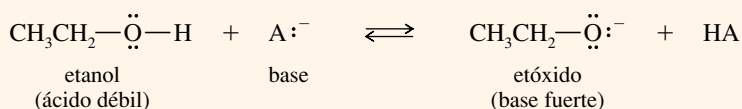
PROBLEMA RESUELTO 1.4

Cada uno de los compuestos siguientes puede actuar como un ácido. Escriba la reacción de cada compuesto con una base general (A^-) y la estructura de Lewis de la base conjugada que se obtiene.

- (a) $\text{CH}_3\text{CH}_2\text{OH}$ (b) CH_3NH_2 (c) CH_3COOH

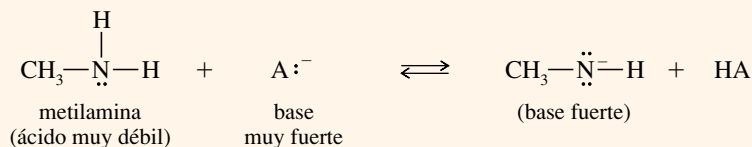
SOLUCIÓN

- (a) El etanol ($\text{CH}_3\text{CH}_2\text{OH}$) puede perder el protón del grupo $\text{O}-\text{H}$ para formar una base conjugada que es un ión orgánico análogo al ión hidroxilo.

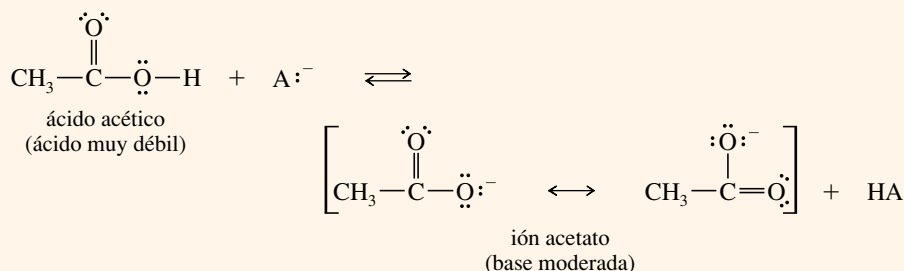


(Los protones del grupo $\text{C}-\text{H}$ son mucho menos ácidos que los protones del grupo $\text{O}-\text{H}$, porque el carbono es menos electronegativo que el oxígeno y, por lo tanto, la carga negativa es menos estable en el carbono.)

- (b) La metilamina (CH_3NH_2) es un ácido muy débil. Una base muy fuerte le puede sustraer un protón y dar lugar a una base conjugada fuerte.



- (c) El ácido acético (CH_3COOH) es un ácido moderadamente fuerte. Su base conjugada es el ión acetato que está estabilizado por resonancia.

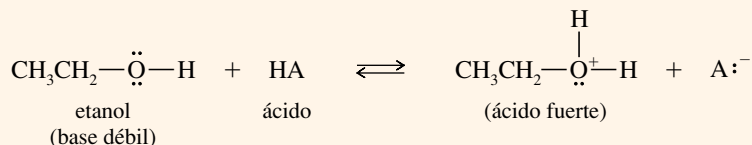


PROBLEMA RESUELTO 1.5

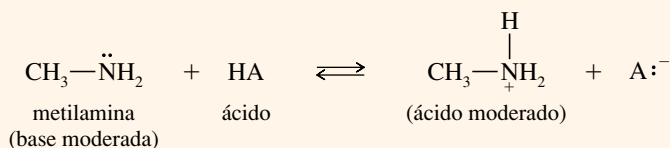
Cada uno de los compuestos del Problema resuelto 1.4 también pueden reaccionar como una base. Escriba la reacción de cada compuesto con un ácido general (HA) y las estructuras de Lewis del ácido conjugado que se obtiene.

SOLUCIÓN

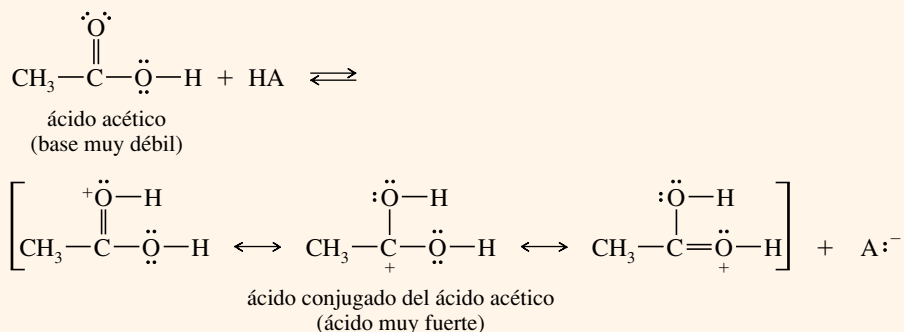
- (a) El etanol puede protonarse en su átomo de oxígeno. Observe que uno de los pares solitarios del oxígeno forma el nuevo enlace O—H.



- (b) El átomo de nitrógeno de la metilamina tiene un par de electrones que pueden enlazarse con un protón.



- (c) El ácido acético tiene electrones no enlazantes en los dos átomos de oxígeno. Cada uno de estos átomos de oxígeno podría protonarse, pero la protonación de oxígeno que forma parte del doble enlace está favorecida porque la protonación de este oxígeno da lugar a un ácido conjugado simétrico y estabilizado por resonancia.



PROBLEMA 1.16

El Problema resuelto 1.5(c) muestra la protonación del oxígeno con doble enlace del ácido acético. Escriba el producto obtenido de la protonación en el otro oxígeno (—OH). Explique por qué la protonación del oxígeno con doble enlace está favorecida.

PROBLEMA 1.17

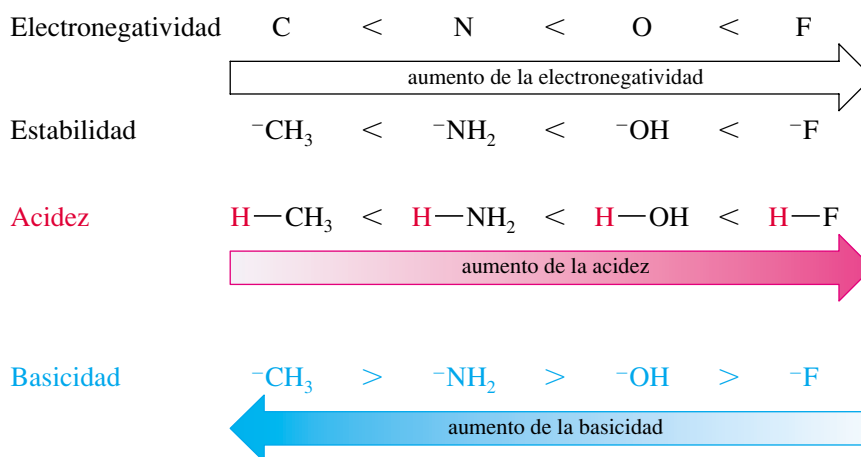
- (a) Ordene por orden decreciente de acidez el etanol, la metilamina y el ácido acético.
 (b) Ordene por orden decreciente de basicidad el etanol, la metilamina ($\text{p}K_b = 3.36$) y el ión etóxido ($\text{CH}_3\text{CH}_2\text{O}^-$). En cada caso, explique las razones de este orden.

1.13C Efectos estructurales en la acidez

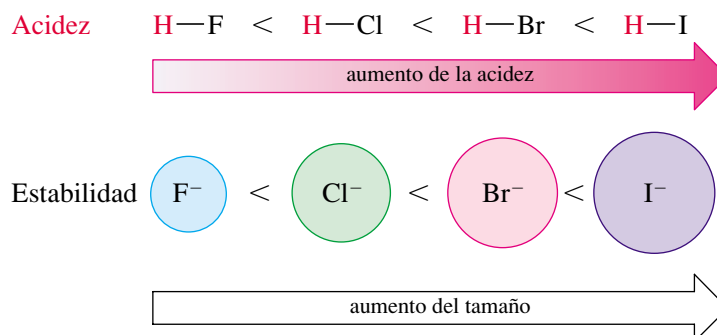
Cuando se observa una estructura, ¿cómo se puede predecir si el compuesto será un ácido fuerte o débil, o bien si no tendrá nada de carácter ácido? Según la teoría de Brønsted-Lowry, un ácido (HA) es un compuesto que ha de contener un átomo de hidrógeno que puede ser cedido como un protón. Un ácido fuerte debe formar una base conjugada estable (A^-) después de perder el protón.

La estabilidad de la base conjugada es una buena guía para conocer la fuerza del ácido. Los aniones más estables tienden a ser bases más débiles y sus ácidos conjugados tienden a ser ácidos más fuertes. Algunos de los factores que afectan a la estabilidad de las bases conjugadas son la electronegatividad, el tamaño y la resonancia.

Electronegatividad Cuanto más electronegativo sea un elemento, será capaz de adquirir una carga negativa con más facilidad, lo que dará lugar a una base conjugada más estable y a un ácido fuerte. La electronegatividad aumenta de izquierda a derecha en la tabla periódica.



Tamaño La carga negativa de un anión es más estable cuando se distribuye sobre una región del espacio más amplia. Si se considera una columna de la tabla periódica, la acidez aumenta hacia abajo, a medida que el tamaño de los elementos aumenta.



Estabilización por resonancia La carga negativa de una base conjugada puede estar deslocalizada entre dos o más átomos, y estabilizada por resonancia. Dependiendo de la electronegatividad que tengan esos átomos y de cómo se comparta esa carga, la deslocalización por resonancia con frecuencia es el efecto dominante que ayuda a la estabilización del anión. Observe las bases conjugadas siguientes:

Base conjugada	Ácido	pK _a
$\text{CH}_3\text{CH}_2-\ddot{\text{O}}:^-$ ión etóxido	$\text{CH}_3\text{CH}_2-\text{OH}$ etanol	15.9 (ácido débil)
$\left[\text{CH}_3-\overset{\text{O}}{\underset{\cdot\cdot}{\parallel}}\text{C}-\ddot{\text{O}}:^- \longleftrightarrow \text{CH}_3-\overset{\cdot\cdot}{\underset{\cdot\cdot}{\parallel}}\text{C}=\ddot{\text{O}}:^- \right]$ ión acetato	$\text{CH}_3-\overset{\text{O}}{\parallel}\text{C}-\text{OH}$ ácido acético	4.74 (ácido moderado)
$\left[\text{CH}_3-\overset{\text{O}}{\underset{\cdot\cdot}{\parallel}}\text{S}-\ddot{\text{O}}:^- \longleftrightarrow \text{CH}_3-\overset{\cdot\cdot}{\underset{\cdot\cdot}{\parallel}}\text{S}=\ddot{\text{O}}:^- \longleftrightarrow \text{CH}_3-\overset{\cdot\cdot}{\underset{\cdot\cdot}{\parallel}}\text{S}=\ddot{\text{O}}:^- \right]$ ión metanosulfonato	$\text{CH}_3-\overset{\text{O}}{\parallel}\text{S}-\text{OH}$ ácido metanosulfónico	-1.2 (ácido fuerte)

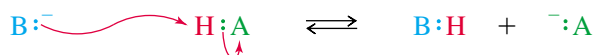
El ión etóxido es el más fuerte de las tres bases anteriores. El etóxido tiene una carga negativa localizada en un átomo de oxígeno; el ión acetato tiene una carga negativa compartida por dos átomos de oxígeno y el ión metanosulfonato tiene una carga negativa extendida sobre tres átomos de oxígeno. Los valores de los pK_a de los ácidos conjugados de esos aniones muestran que los ácidos son más fuertes si su desprotonación da lugar a bases conjugadas estabilizadas por resonancia.

PROBLEMA 1.18

Escriba las ecuaciones correspondientes a las reacciones ácido-base siguientes. Señale los ácidos y bases conjugados y justifique, si es el caso, su estabilización por resonancia escribiendo las posibles formas resonantes. Prediga si el equilibrio está desplazado hacia los reactivos o hacia los productos.

- (a) $\text{CH}_3\text{CH}_2\text{OH} + \text{CH}_3\text{NH}^-$ (b) $\text{CH}_3\text{CH}_2\text{COOH} + \text{CH}_3\text{NHCH}_3$
 (c) $\text{CH}_3\text{OH} + \text{H}_2\text{SO}_4$ (d) $\text{NaOH} + \text{H}_2\text{S}$
 (e) $\text{CH}_3\text{NH}_3^+ + \text{CH}_3\text{O}^-$ (f) $\text{CH}_3\text{O}^- + \text{CH}_3\text{COOH}$
 (g) $\text{CH}_3\text{SO}_3^- + \text{CH}_3\text{COOH}$

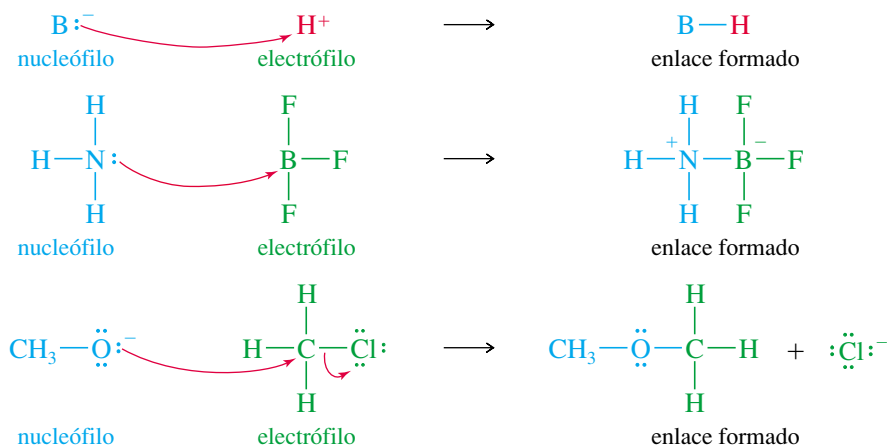
La definición de Brönsted-Lowry de ácidos y bases depende de la transferencia de un protón del ácido a la base. La base utiliza un par de electrones no enlazantes para formar un enlace con el protón. G. N. Lewis pensó que esta clase de reacciones no necesitaba obligatoriamente un protón para tener lugar. Una base podría usar su par solitario de electrones para enlazarse a algún otro átomo deficiente en electrones. En efecto, puede haber reacciones ácido-base desde el punto de vista de los *enlaces* que se forman y rompen, sin necesidad de que se transfiera un protón. La siguiente reacción muestra la transferencia del protón haciendo hincapié en los enlaces que se forman y que se rompen. Los químicos orgánicos utilizan de forma rutinaria flechas curvadas para mostrar el movimiento de los electrones que participan,



Las **bases de Lewis** son especies con electrones no enlazantes que pueden ser cedidos para formar nuevos enlaces. Los **ácidos de Lewis** son especies que pueden aceptar esos pares de electrones para formar nuevos enlaces. Debido a que un ácido de Lewis *acepta* un par de electrones, se le conoce como **electrófilo**, palabra derivada del griego, que significa «amante de electrones». A la base de Lewis se le llama **nucleófilo**, o «amante de los núcleos», ya que cede electrones a un núcleo que tenga un orbital vacío (o prácticamente vacío). En este libro, a veces se usan caracteres coloreados para enfatizar: azul para los nucleófilos, verde para los electrófilos y ocasionalmente rojo para los protones ácidos.

1.14 Ácidos y bases de Lewis

Las definiciones ácido-base de Lewis incluyen reacciones que no tienen ninguna relación con los protones. A continuación se muestran algunos ejemplos de reacciones ácido-base de Lewis. Observe que los ácidos y las bases de Brønsted-Lowry también están incluidos dentro de la definición de Lewis, siendo el protón un electrófilo. Las flechas curvadas (rojas) se usan para mostrar el movimiento de los electrones, generalmente desde el nucleófilo al electrófilo.

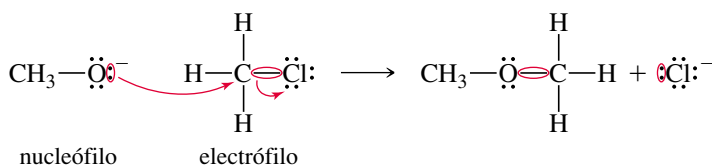


Algunos de los términos asociados con los ácidos y bases poseen significados específicos en química orgánica. Cuando un químico orgánico utiliza el término *base*, normalmente quiere decir «aceptor de protones» (una base de Brønsted-Lowry). De manera similar, el término *ácido* normalmente implica a un protón ácido (un ácido de Brønsted-Lowry). Cuando una reacción ácido-base implica la formación de un enlace con otro elemento (especialmente carbono), un químico orgánico denomina al donador de electrones *nucleófilo* (base de Lewis) y al aceptor de electrones, *electrófilo* (ácido de Lewis).

Las **flechas curvadas** se utilizan para mostrar el movimiento de un par de electrones desde el donador de electrones al aceptor de electrones. El movimiento de cada par de electrones implicado en formar o romper enlaces se indica por sus propias flechas separadas, como se muestra en las reacciones anteriores. En este libro, estas flechas curvadas se dibujan siempre en rojo. En la reacción anterior del CH₃O⁻ con CH₃Cl, una flecha curvada muestra el par solitario del oxígeno formando un enlace con el carbono; otra flecha curvada muestra que el par enlazante del C—Cl se separa del átomo de carbono y se transforma en un par solitario formando el ión Cl⁻.

SUGERENCIA PARA RESOLVER PROBLEMAS

Utilice una flecha curvada para cada par de electrones que participen en la reacción.



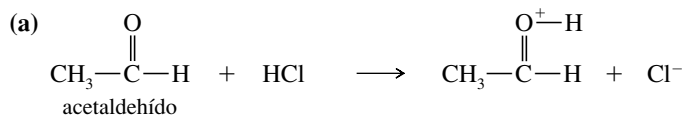
La flecha curvada se usa universalmente para seguir el camino del movimiento de los electrones en las reacciones; en este libro también se ha utilizado (en la Sección 1.9, por ejemplo) para seguir el movimiento de los electrones en las estructuras de resonancia, con objeto de representar el supuesto «flujo electrónico» cuando se pasaba de una estructura de resonancia a otra. Recuerde que los electrones no «fluyen» en las estructuras de resonancia, simplemente están deslocalizados. Este formalismo de las flechas nos ayuda, sin embargo, a comprender la interconversión entre las formas resonantes. Estas flechas curvadas se usan constantemente para seguir el camino de los electrones, tanto en el cambio de reactivos a productos como cuando imaginamos nuevas estructuras resonantes adicionales de un híbrido de resonancia.

PROBLEMA 1.19 (parcialmente resuelto)

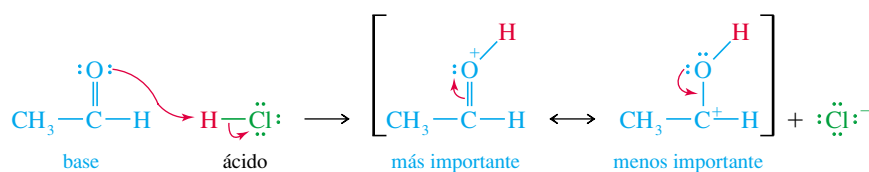
En las siguientes reacciones ácido-base:

- (1) Determine qué especies actúan como ácidos y cuáles como bases.
- (2) Utilice las flechas curvadas para mostrar el movimiento de los pares de electrones de las reacciones, así como el movimiento imaginario de electrones en los híbridos de resonancia de los productos.

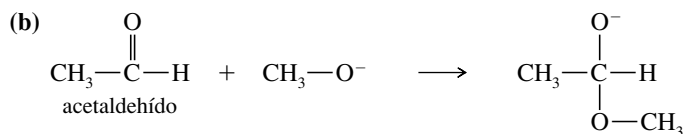
(3) Indique qué reacciones son las más apropiadas para poderlas incluir dentro de las reacciones ácido-base de Brønsted-Lowry.



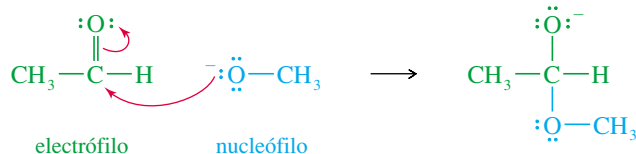
En esta reacción hay transferencia del protón del HCl al grupo C=O del acetaldehído, por tanto, es una reacción ácido-base de Brønsted-Lowry, donde el HCl actúa como ácido (donador de protones) y el acetaldehído actúa como base (aceptor de protones). Antes de dibujar una flecha curvada, recuerde que las flechas deben mostrar el movimiento de los electrones *desde* el donador del par de electrones (la base) *hasta* el aceptor del par de electrones (el ácido). Una flecha debe ir *desde* los electrones no enlazantes del acetaldehído *hasta* el átomo de hidrógeno del HCl y el enlace del ácido clorhídrico se ha de romper, con la formación del ión cloruro que ha captado los electrones del enlace H—Cl. Dibujar las flechas es fácil después de haber representado correctamente estructuras de Lewis de todos los reactivos y productos.



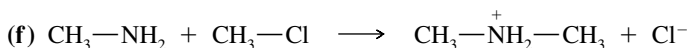
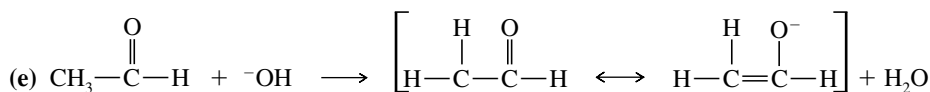
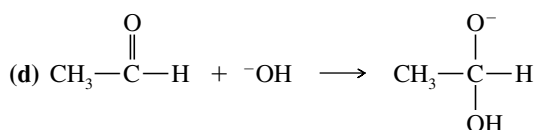
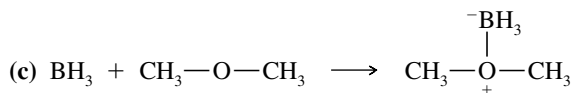
Las formas de resonancia del producto muestran que un par de electrones puede moverse entre el átomo de oxígeno y el enlace pi del C=O. La carga positiva está deslocalizada sobre los átomos de carbono y de oxígeno, con la mayor parte de la carga positiva sobre el oxígeno, ya que todos los octetos están completos en esa estructura de resonancia.



En este caso, ningún protón se ha transferido, por lo que no es una reacción ácido-base de Brønsted-Lowry. En su lugar, se ha formado un enlace entre el átomo de carbono del grupo C=O y el átomo de oxígeno del grupo CH₃—O[−]. Dibujar las estructuras de Lewis ayuda a ver que el grupo CH₃—O[−] (el nucleófilo en esta reacción) cede los electrones para formar el nuevo enlace con el acetaldehído (el electrófilo). Este resultado concuerda con la intuición de que un ión cargado negativamente es probablemente rico en electrones y por tanto un donador de electrones.



Observe que el acetaldehído actúa como nucleófilo (base) en (a) y como electrófilo en (b). Como la mayoría de los compuestos orgánicos, el acetaldehído puede ser tanto un ácido como una base. Actúa como una base si se le añade un ácido lo suficientemente fuerte para que ceda un par de electrones o capte un protón.



SUGERENCIA PARA RESOLVER PROBLEMAS

Las flechas curvadas se utilizan en los mecanismos para mostrar el *flujo de electrones* y no el movimiento de los átomos. Estas flechas curvadas se usarán constantemente a lo largo de este curso.

Glosario del Capítulo 1

Cada capítulo finaliza con un glosario que recoge los términos nuevos más importantes del capítulo. Estos glosarios son más que un diccionario en el que se buscan términos desconocidos conforme se los vaya encontrando (el índice sirve para este propósito). El glosario es una de las herramientas para revisar el capítulo, se puede leer cuidadosamente para saber si se entienden y se recuerdan todos los términos químicos mencionados. Cualquier concepto que no resulte familiar debería ser revisado volviendo a la página que aparece numerada en el mismo.

Ácido conjugado El ácido que resulta de la protonación de una base. (p. 23)

Ácido de Lewis, base de Lewis. Véase ácidos y bases.

Ácidos y bases (pp. 21-31)

(definiciones de Arrhenius)

Ácido: se disocia en agua para dar H_3O^+ .

Base: se disocia en agua para dar OH^- .

(definiciones de Brønsted-Lowry)

Ácido: donador de protones.

Base: aceptor de protones.

(definiciones de Lewis)

Ácido: aceptor de un par de electrones (electrófilo).

Base: donador de un par de electrones (nucleófilo).

Base conjugada La base que resulta de la pérdida de un protón de un ácido. (p. 23)

Cargas formales Método para hacer un seguimiento de las cargas, el cual permite mostrar qué carga habría en una determinada estructura de Lewis. (p. 11)

Densidad electrónica Probabilidad relativa de encontrar un electrón en una cierta región del espacio. (p. 3)

Electrófilo Aceptor de un par de electrones. (p. 29)

Electronegatividad Medida de la capacidad de un elemento para atraer electrones. Los elementos con electronegatividades más altas atraen a los electrones con más fuerza. (p. 10)

Electrones de valencia Electrones que se encuentran en la capa externa más alejada del núcleo. (p. 6)

Electrones no enlazantes Electrones de valencia que no se utilizan en el enlace. A un par de electrones no enlazantes con frecuencia se le denomina **par solitario**. (p. 7)

Enlace covalente Enlace que se forma por la compartición de electrones en la región que hay entre dos núcleos. (p. 7)

Enlace sencillo: enlace covalente en el que se comparte un par de electrones. (p. 8)

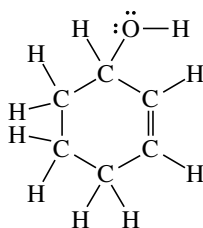
Enlace doble: enlace covalente en el que se comparte dos pares de electrones. (p. 8)

Enlace triple: enlace covalente en el que se comparte tres pares de electrones. (p. 8)

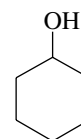
Enlace covalente polar Enlace covalente en el que los electrones se comparten de forma desigual. Cuando los electrones están igualmente compartidos se llama **enlace covalente no polar**. (p. 9)

Enlace iónico Enlace que se produce por la atracción de iones que tienen carga opuesta. El enlace iónico normalmente da lugar a la formación de una gran estructura cristalina en tres dimensiones. (p. 7)

Estructura de Lewis Fórmula estructural que muestra todos los electrones de valencia, con los enlaces simbolizados por líneas (—) o por pares de puntos, y los electrones no enlazantes simbolizados por puntos. (p. 7)



estructura de Lewis del 2-ciclohexenol



2-ciclohexenol
fórmula lineoangular equivalente

Flechas curvadas El dibujar flechas curvadas es un método que se utiliza para seguir el camino de los electrones cuando se mueven desde el nucleófilo al electrófilo (o dentro de una molécula) durante el transcurso de una reacción. (p. 30)

Fórmula empírica Relación numérica de los átomos en un compuesto. (p. 20). Véase también **fórmula molecular**.

Fórmula lineoangular (estructura esquelética o de barras) Fórmula estructural con enlaces representados por líneas; los átomos de carbono son los puntos de encuentro entre dos líneas o el final de la línea cuando está en el extremo de la cadena. Los átomos de nitrógeno, de oxígeno y los halógenos se representan, pero los átomos de hidrógeno no. Se supone que cada átomo de carbono tiene los hidrógenos suficientes para que en total tenga cuatro enlaces. (p. 19)

Fórmula molecular Número de átomos de cada elemento que forman parte de una molécula de un compuesto. La **fórmula empírica** simplemente da la relación de los átomos de los diferentes elementos. Por ejemplo, la fórmula molecular de la glucosa es $C_6H_{12}O_6$; su fórmula empírica es CH_2O . Ni la fórmula empírica ni la fórmula molecular dan información estructural. (p. 4)

Fórmulas estructurales Una **fórmula estructural completa** (tal como una estructura de Lewis) muestra todos los átomos y enlaces en la molécula. Una **fórmula estructural condensada** muestra cada átomo central y los átomos con los que está enlazado. Una **fórmula lineoangular** supone que hay un átomo de carbono donde dos líneas se encuentren, o donde la línea comience o termine. Véanse los ejemplos de la Sección 1.10. (p. 17)

Híbrido de resonancia Molécula o ión para el cual se pueden representar dos o más estructuras de Lewis válidas, diferenciándose solamente en la posición de los electrones de valencia. Estas estructuras de Lewis se conocen como **formas de resonancia** o **estructuras de resonancia**. Las formas de resonancia individuales no existen, pero se puede estimar sus energías relativas. A las estructuras más importantes (de energía más baja) se las conoce como **contribuyentes mayores**, y a las estructuras menos importantes (energía más alta), como **contribuyentes menores**. Cuando una carga se reparte entre dos o más átomos por resonancia, se dice que está **deslocalizada** y que la molécula está **estabilizada por resonancia**. (pp. 13-16)

Isótopos Átomos con el mismo número de protones pero diferente número de neutrones. Átomos del mismo elemento pero con diferentes masas atómicas. (p. 3)

Mapa de potencial electrostático (MPE) Representación molecular calculada por computador que utiliza colores para mostrar la distribución de carga en una molécula. En la mayoría de los casos, el MPE utiliza el color rojo para indicar las regiones ricas en electrones (potencial electrostático más negativo) y azul para indicar las regiones pobres en electrones (potencial electrostático más positivo). Los colores intermedios naranja, amarillo y verde indican regiones con potenciales electrostáticos intermedios. (p. 10)

Momento dipolar (μ) Medida de la polaridad de un enlace (o una molécula), proporcional al producto de la separación de cargas por la longitud de enlace. (p. 10)

Nodo Región de un orbital con densidad electrónica cero. (p. 4)

Nucleófilo Donador de par de electrones (base de Lewis). (p. 29)

Orbital Estado de energía permitida para un electrón que rodea a un núcleo; función de probabilidad que define la distribución de la densidad electrónica en el espacio. El *principio de exclusión de Pauli* afirma que un orbital sólo puede ser ocupado por dos electrones, como máximo, si los espines de éstos están apareados. (p. 3)

Orbitales degenerados Orbitales con energías idénticas. (p. 4)

Par solitario Par de electrones no enlazantes. (p. 7)

pH Medida de la acidez de una solución, definido como el logaritmo (en base 10), cambiado de signo, de la concentración de H_3O^+ . $pH = -\log_{10}[H_3O^+]$. (p. 22)

Plano nodal Región plana (plano) del espacio con densidad electrónica cero. (p. 4)

Química orgánica Definición nueva: química de los compuestos de carbono. Definición antigua: estudio de los compuestos derivados de los organismos vivos y sus productos naturales. (p. 1)

Regla de Hund Cuando hay dos orbitales o más con la misma energía (orbitales degenerados) vacíos, la configuración de energía más baja se consigue colocando los electrones en orbitales diferentes (con espines paralelos), mejor que colocándolos apareados en el mismo orbital. (p. 6)

Regla del octeto Los átomos generalmente se enlazan para que sus capas de valencia se completen con electrones (configuración de gas noble). Para los elementos de la segunda fila de la tabla periódica, esta configuración tiene ocho electrones de valencia. (p. 6)

Valencia Número de enlaces que normalmente forma un átomo. (p. 9)

Vitalismo Creencia en que la síntesis de compuestos orgánicos requiere la presencia de una «fuerza vital». (p. 1)

Pautas esenciales para resolver los problemas del Capítulo 1

1. Escribir e interpretar las fórmulas estructurales de Lewis, condensadas y lineoangulares. Indicar qué átomos tienen cargas formales.
2. Escribir formas de resonancia y usarlas para predecir la estabilidad.
3. Calcular fórmulas empíricas y moleculares de composiciones elementales.
4. Predecir la acidez y la basicidad relativa basada en la estructura, en el enlace y en la resonancia de los pares ácido-base conjugados.
5. Calcular, usar e interpretar los valores de K_a y pK_a .
6. Identificar nucleófilos (bases de Lewis) y electrófilos (ácidos de Lewis) y escribir ecuaciones de reacciones ácido-base de Lewis utilizando flechas curvadas para mostrar el flujo de los electrones.

Problemas

Es fácil engañarse a uno mismo pensando que se entiende la química orgánica cuando realmente no se entiende. Según se van leyendo a lo largo de este libro, todos los conceptos y las ideas pueden tener sentido, pero todavía no se ha aprendido a combinar y a usar esos conceptos e ideas. Un examen es un trance duro para darse cuenta de que realmente no se han entendido los contenidos.

La mejor forma de aprender química orgánica es aplicarla. Por supuesto se necesita leer y releer todo el material del capítulo, pero este nivel de entendimiento es justamente el comienzo. Se proponen problemas para poder trabajar con las ideas, aplicándolas a nuevos compuestos y reacciones que no se han visto con anterioridad. Al resolver problemas, uno se ve obligado a utilizar los conceptos y a entender lo que antes no se había comprendido, también se aumenta el nivel de autoestima y de habilidad para realizar los exámenes.

En cada capítulo se incluyen varias clases de problemas. Hay problemas dentro de los capítulos, que se introducen como ejemplos y explican cómo se han de resolver. Se ha de realizar ese tipo de problemas según se vaya leyendo el capítulo para asegurarse de que se han entendido los conceptos. Las soluciones de muchos de estos problemas se encuentran al final de libro. Los Problemas del final de cada capítulo proporcionan una experiencia adicional en el uso de los conceptos y obligan a pensar con detenimiento sobre las ideas expuestas en el texto. Para algunos de estos problemas se incluyen soluciones breves al final del libro, sin embargo, se pueden encontrar soluciones más detalladas de los mismos en el *Manual de Soluciones*.

Estudiar química orgánica sin resolver problemas es como lanzarse al aire sin paracaídas. Al principio parece divertido, pero después puede resultar duro para aquellos que carezcan de preparación.

1.20 Defina y ponga un ejemplo para cada término:

- | | | |
|------------------------------------|----------------------------|-------------------------------|
| (a) isótopos | (b) orbital | (c) nodo |
| (d) orbitales degenerados | (e) electrones de valencia | (f) enlace iónico |
| (g) enlace covalente | (h) estructura de Lewis | (i) electrones no enlazantes |
| (j) enlace sencillo | (k) enlace doble | (l) enlace triple |
| (m) enlace polar | (n) cargas formales | (o) formas de resonancia |
| (p) fórmula molecular | (q) fórmula empírica | (r) ácido y base de Arrhenius |
| (s) ácido y base de Brønsted-Lowry | (t) ácido y base de Lewis | (u) electrófilo |
| (v) nucleófilo | | |

1.21 Nombre el elemento que corresponda a cada configuración electrónica.

- (a) $1s^2 2s^2 2p^2$ (b) $1s^2 2s^2 2p^4$ (c) $1s^2 2s^2 2p^6 3s^2 3p^3$ (d) $1s^2 2s^2 2p^6 3s^2 3p^5$

1.22 Hay una pequeña sección de la tabla periódica que se debe conocer en química orgánica. Escriba de memoria esta parte, realizando los siguientes pasos:

- (a) Haga una lista, de memoria, de los elementos de las dos primeras filas de la tabla periódica, junto con su número de electrones de valencia.
 (b) Use esta lista para construir las dos primeras filas de la tabla periódica.
 (c) Los compuestos orgánicos a veces contienen azufre, fósforo, cloro, bromo y yodo. Añada estos elementos a la tabla periódica.

1.23 Para cada compuesto, diga si el enlace es covalente, iónico, o intermedio entre covalente e iónico.

- (a) NaCl (b) NaOH (c) CH_3Li (d) CH_2Cl_2 (e) NaOCH_3 (f) HCO_2Na (g) CF_4

1.24 (a) El PCl_3 y el PCl_5 son compuestos estables. Escriba la estructura de Lewis para los dos compuestos.

- (b) El NCl_3 es un compuesto conocido, pero todos los intentos de sintetizar el NCl_5 han fracasado. Escriba las estructuras de Lewis para el NCl_3 y una hipotética para el NCl_5 , y explique por qué el NCl_5 es una estructura improbable.

1.25 Escriba una estructura de Lewis para cada una de las especies.

- (a) N_2H_4 (b) N_2H_2 (c) $(\text{CH}_3)_4\text{NCl}$ (d) CH_3CN (e) CH_3CHO (f) $\text{CH}_3\text{S(O)CH}_3$
 (g) H_2SO_4 (h) CH_3NCO (i) $\text{CH}_3\text{OSO}_2\text{OCH}_3$ (j) $\text{CH}_3\text{C(NH)CH}_3$ (k) $(\text{CH}_3)_3\text{CNO}$

1.26 Escriba una estructura de Lewis para cada compuesto. Incluya todos los pares de electrones no enlazantes.

- (a) $\text{CH}_3\text{CHCHCH}_2\text{CHCHCOOH}$ (b) $\text{NCCH}_2\text{COCH}_2\text{CHO}$
 (c) $\text{CH}_2\text{CHCH(OH)CH}_2\text{CO}_2\text{H}$ (d) $\text{CH}_3\text{CH(CH}_3\text{)CH}_2\text{C(CH}_2\text{CH}_3\text{)}_2\text{CHO}$

1.27 Escriba la fórmula lineoangular de todos los compuestos del Problema 1.26.

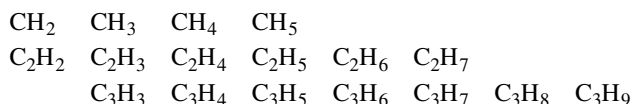
1.28 Escriba las estructuras de Lewis para:

- (a) dos compuestos de fórmula C_4H_{10} (b) dos compuestos de fórmula $\text{C}_2\text{H}_7\text{N}$
 (c) dos compuestos de fórmula $\text{C}_3\text{H}_8\text{O}_2$ (d) dos compuestos de fórmula $\text{C}_2\text{H}_4\text{O}$

1.29 Represente una fórmula estructural completa y una fórmula estructural condensada para:

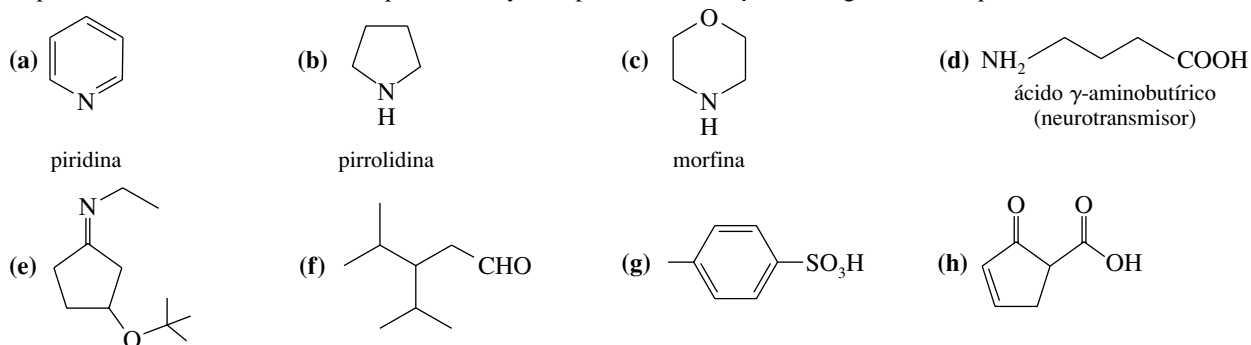
- (a) tres compuestos de fórmula $\text{C}_3\text{H}_8\text{O}$ (b) cinco compuestos de fórmula $\text{C}_3\text{H}_6\text{O}$

1.30 Alguna de las siguientes fórmulas moleculares corresponde a compuestos estables. Represente, cuando sea posible, una estructura estable para cada fórmula.



Proponga una regla general que dé el número de átomos de hidrógeno en los hidrocarburos estables.

1.31 Represente estructuras de Lewis completas, incluyendo pares solitarios, para los siguientes compuestos:



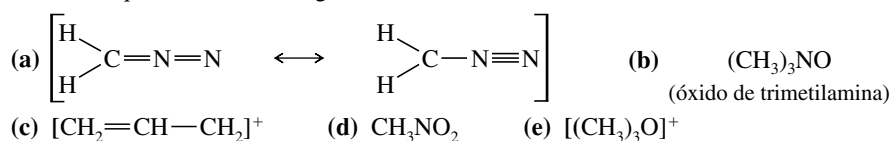
1.32 Escriba la fórmula molecular de todos los compuestos del Problema 1.31.

1.33 Un compuesto X, aislado de la lanolina (grasa de la lana de oveja), tiene un fuerte aroma a calcetines sucios sudados. Un análisis cuidadoso mostró que el compuesto X contenía un 62.0% de carbono y un 10.4% de hidrógeno. No se encontró nitrógeno ni halógenos.

- (a) Escriba la fórmula empírica del compuesto X.
 (b) La determinación del peso molecular mostró que el compuesto X tenía un peso molecular aproximadamente igual a 117; encuentre la fórmula molecular del compuesto X.
 (c) Hay muchas estructuras posibles que tienen esa fórmula molecular. Represente las fórmulas estructurales completas de cuatro de ellas.

1.34 Para cada una de las siguientes estructuras:

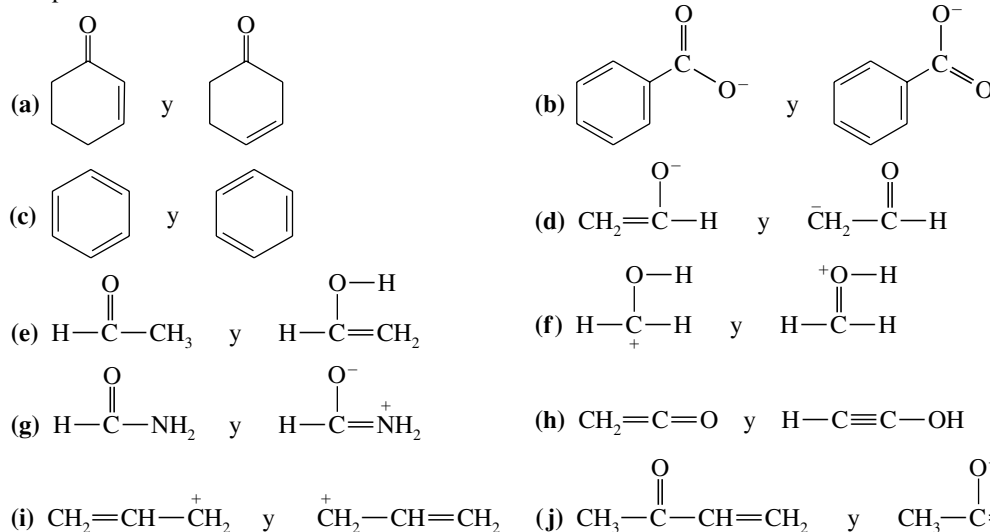
- (1) Represente una estructura de Lewis, poniendo también los electrones no enlazantes.
 (2) Calcule la carga formal de todos los átomos excepto del hidrógeno. Todos son eléctricamente neutros excepto aquellos en los que se indica su carga.



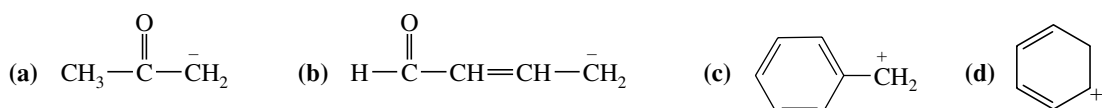
1.35 (1) Teniendo en cuenta la electronegatividad, establezca la dirección de los momentos dipolares de los siguientes enlaces.
 (2) En cada caso, prediga si el momento dipolar es relativamente grande o pequeño.

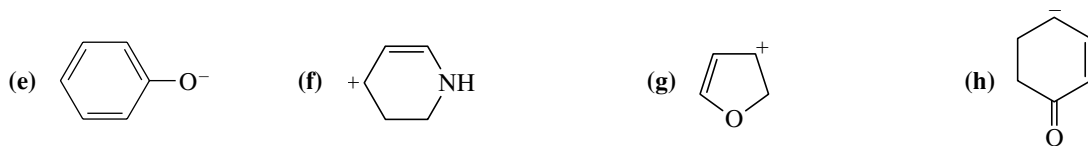
- (a) $\text{C}-\text{Cl}$ (b) $\text{C}-\text{H}$ (c) $\text{C}-\text{Li}$ (d) $\text{C}-\text{N}$ (e) $\text{C}-\text{O}$
 (f) $\text{C}-\text{B}$ (g) $\text{C}-\text{Mg}$ (h) $\text{N}-\text{H}$ (i) $\text{O}-\text{H}$ (j) $\text{C}-\text{Br}$

1.36 Determine si los siguientes pares de estructuras son diferentes compuestos o solamente formas de resonancia del mismo compuesto.



1.37 Represente las formas de resonancia importantes para mostrar la deslocalización de cargas en los iones siguientes:





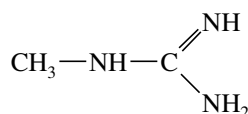
1.38

- (a) Represente las formas de resonancia para el SO_2 (conectividad $\text{O}-\text{S}-\text{O}$).
 (b) Represente las formas de resonancia para el ozono (conectividad $\text{O}-\text{O}-\text{O}$).
 (c) El dióxido de azufre tiene una forma de resonancia más que el ozono, explique por qué esa estructura no es posible para el ozono.

*1.39

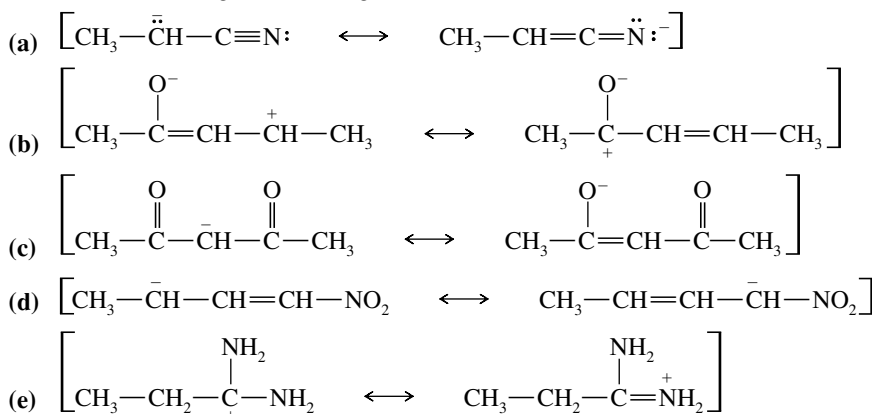
El compuesto siguiente puede protonarse en cualquiera de los átomos de nitrógeno, no obstante, uno de esos nitrógenos es mucho más básico que los otros.

- (a) Represente las formas de resonancia importantes de los productos de protonación de cada uno de los tres átomos de nitrógeno.
 (b) Determine qué átomo de nitrógeno es el más básico.



1.40

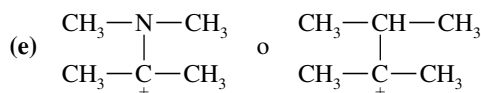
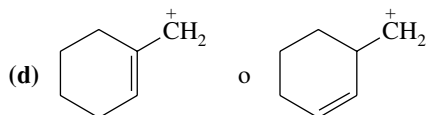
En los siguientes apartados de formas de resonancia, señale los contribuyentes mayor y menor, y diga qué estructuras tienen la misma energía. Si falta alguna forma de resonancia, añádala.



1.41

Para cada par de iones, determine cuál es más estable. Use formas de resonancia para explicar las respuestas.

- (a) $\text{CH}_3-\overset{+}{\text{CH}}-\text{CH}_3$ o $\text{CH}_3-\overset{+}{\text{CH}}-\text{OCH}_3$
 (b) $\text{CH}_2=\text{CH}-\overset{+}{\text{CH}}-\text{CH}_3$ o $\text{CH}_2=\text{CH}-\text{CH}_2-\overset{+}{\text{CH}}_2$
 (c) $\overset{-}{\text{CH}}_2-\text{CH}_3$ o $\overset{-}{\text{CH}}_2-\text{C}\equiv\text{N}:$



1.42

Ordene las siguientes especies por orden creciente de acidez, explicando las razones de este ordenamiento.



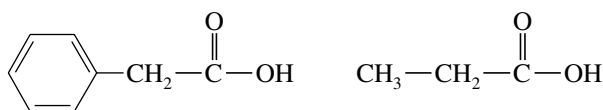
1.43

Ordene las siguientes especies por orden creciente de basicidad, explicando las razones de este ordenamiento.



1.44

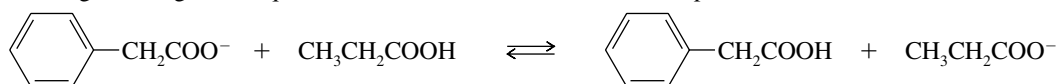
La K_a del ácido fenilacético es 5.2×10^{-5} y el pK_a del ácido propiónico es 4.87.

ácido fenilacético, $K_a = 5.2 \times 10^{-5}$ ácido propiónico, $pK_a = 4.87$

- (a) Calcule el pK_a del ácido fenilacético y la K_a del ácido propiónico.

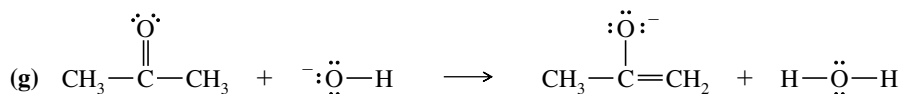
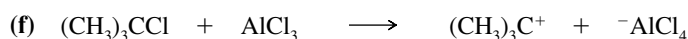
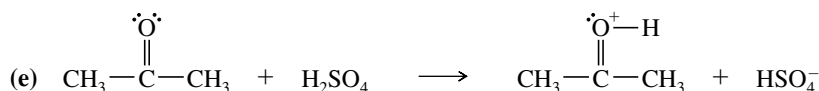
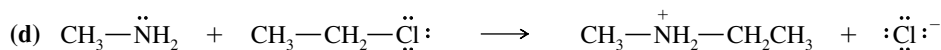
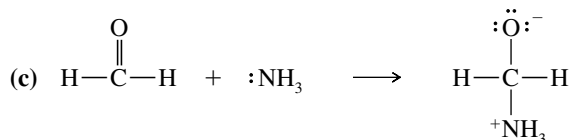
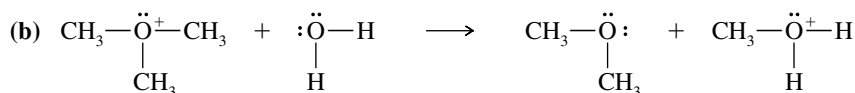
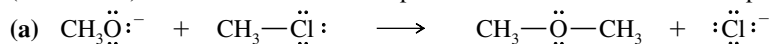
(b) ¿Cuál de los dos ácidos es el más fuerte? Calcule cuánto más fuerte es uno que otro.

(c) Prediga si el siguiente equilibrio favorecerá a los reactivos o a los productos.



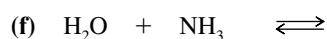
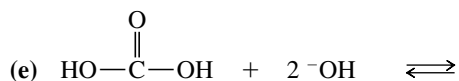
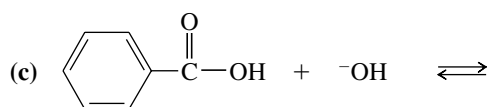
1.45

En las siguientes reacciones ácido-base clasifique los reactivos como ácidos de Lewis (electrófilos) o bases de Lewis (nucleófilos). Utilice flechas curvadas para indicar el movimiento de los pares de electrones en las reacciones.



1.46

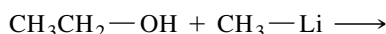
Prediga los productos de las siguientes reacciones ácido-base:



*1.47

El metilítio (CH_3Li) a menudo se usa como base en reacciones orgánicas.

(a) Prediga los productos de la siguiente reacción ácido-base:



(b) ¿Cuál es el ácido conjugado del CH_3Li ? ¿Qué es el CH_3Li ?, ¿una base fuerte o débil?

*1.48

En 1984, Edward A. Doisy de la Universidad de Washington extrajo 1 360 kg de ovarios de cerda para aislar unos pocos miligramos de estradiol puro, una potente hormona femenina. Doisy quemó 5.00 mg de esa preciada muestra en oxígeno y encontró que se obtenían 14.54 mg de CO_2 y 3.97 mg de H_2O .

(a) Determine la fórmula empírica del estradiol.

(b) La masa molecular del estradiol se determinó posteriormente y se encontró que era de 272. Determine la fórmula molecular del estradiol.